The Identification & Optimisation of Endogenous Signalling Pathway Modulators

This Thesis is Submitted for the Degree of Doctor of Philosophy

Matteo Gianella-Borradori

Wolfson College

Trinity Term 2013

Department of Chemistry

Oxford University

Acknowledgements

First and foremost I want to thank my parents for their support (financially, but mainly mentally), not only during the course of my DPhil, but throughout life. When life was a smooth ride they were encouraging and most importantly when times were tough they were even more supportive. I am not sure without some of their stern words and advice I would be at this stage now. Next, my brothers, Stine and Agg, wonderful company on a relaxing summer day, lightweight session in the gym and a "casual" night out in town. You cannot choose who your siblings are, but I could not be happier with the outcome. Finally, all other members of the Gianella/Borradori clan, in particular my grandmother and god-mother who sent a regular supply of swiss chocolate and cheese to feed me.

I would like to thank Angie (Dr. Angela Russell) for believing in me from the beginning and providing me with the opportunity to share knowledge, drive research and provide a good supply of banter to her group (which some enjoyed more than others). It has been a pleasure and privilege working for and with you.

The work environment has contributed very much to my success and drive throughout the years. The constant stream of wisdom from Boudry (Dr.Peter Sed"a"n) and his sometimes limited patience deepened my understanding of med chem and life. Matthew Benson, was fortunate enough to be exposed to my presence for nearly a year, however in this time he has taught me all I know about molecular biology. The fruitful collaborations with the Greaves lab and the Battacharya lab made my DPhil journey a life changing experience.

I would like to thank all the post and present Russell group members, in particular Banana (Gu Liu) for her help and reality checks, Poulet (Carole Bataille) for the support, Bob

Westwood for his infinite wisdom (and sports banter) and Camillo, Sam, Abby, Craig, Graham, Simon and Kristina.

Finally I could not have done all this without a constant stream of support from college friends. Wolfson college has gifted me with some unbelievable friends in the past years; Mole (Jon Halling and his wonderful wife), the ever-growing Estrada family, Gloworm (Matt), Teusz, Gido, Joe, Skwirtz (James), Microphone (Joel), Edwards, Alison, Washid (Huw) and Jarule (Jared). Last but not the least, my experience here in Oxford was seriously enriched with the friendships of Pietrolinus (Petr), Adam, Schlange (Matt), Panzer (Augustus) and my Habibti, Thank you for all the good times together, and stimulating conversations.

Abstract

Chapter 1 Provides an overview of drug discovery with particular emphasis on library selection and hit identification methods using virtual based approaches.

Chapter 2 Gives an outline of the bone morphogenetic protein (BMP) signalling pathway and literature BMP pathway modulators. The association between the regulation of BMP pathway and cardiomyogenesis is also described.

Chapter 3 Describes the use of ligand based virtual screening to discover small molecule activators of the BMP signalling pathway. A robust cell based BMP responsive gene activity reporter assay was developed to test the libraries of small molecules selected. Hit molecules from the screen were synthesised to validate activity. It was found that a group of known histone deacetylase (HDAC) inhibitors displayed most promising activity. These were evaluated in a secondary assay measuring the expression of two BMP pathway regulated genes, hepcidin and Id1, using reverse transcription polymerase chain reaction (RT-PCR). **188** was discovered to increase expression of both BMP-responsive genes.

Chapter 4 Provides an overview of existing cannabinoid receptor (CBR) modulating molecules and their connection to progression of atherosclerosis.

Chapter 5 Outlines the identification and optimisation of selective small molecule agonists acting at the cannabinoid 2 receptor (CB_2R). Ligand based virtual screen was undertaken and promising hits were synthesised to allow structure activity relationship (SAR) to be developed around the hit molecule providing further information of the functional groups tolerated at the active site. Subsequent studies led to the investigation and optimisation of physicochemical properties around **236** leading to the development of a suitable compound for *in vivo* testing. Finally, a CB_2R selective compound with favourable physicochemical properties was evaluated *in vivo* in a murine inflammation model and displayed reduced recruitment of monocytes to the site of inflammation.

Abbreviations

3D	three dimensional
Å	Ångstrom
Ac	acetyl
ADP	adenosine-5'-diphosphate
ala	alanine
AMP	adenosine-5'-monophosphate
AMPK	AMP-activated protein kinase
Ar	aromatic
AT_1	angiotensin II type 1 receptor
ATP	adenosine-5'-triphosphate
BMP	bone morphogenetic protein
Bn	benzyl
br	broad
BRE	BMP response element
BREluc	BMP response element driving luciferase
n-bu	normal (primary) butyl
t-butyl	tertiary butyl
°C	degrees Celsius
cAMP	cyclic AMP
CBR	cannabinoid receptor
CDI	carbonyldiimidazole
CDTA	1,2-diaminocyclohexanetetraacetic acid
CHD	coronary heart disease
CHO	chinese hamster ovary
ClogP	calculated partition coefficient between octanol and water
cm^{-1}	wavenumber(s)
COSY	proton-proton correlation spectroscopy
CMV	cytomegalovirus
CNS	central nervous system
CTR	carboxylic acid terminus
m-CPBA	*meta*-chloroperbenzoic acid

δ	chemical shift in parts per million downfield from tetramethylsilane
d	d(s), doublet (spectral)
Da	Daltons
DBU	1,8-diazabicyclo[5.4.0]undec-7-ene
dec.	decomposition
DEPT	distortionless enhancement by polarisation transfer
DMAP	4-dimethylaminopyridine
DMF	*N*,*N*-dimethylformamide
DMSO	dimethylsulfoxide
DNA	deoxyribonucleic acid
DNMT	DNA methyl transferases
DOS	diversity oriented synthesis
DTT	dithiothreitol
EC_{50}	concentration affecting 50% of specimens
EDG	electron donating group
EGCG	epigallocatechin gallate
EGFP	enhanced green fluorescent protein
EndoMT	endothelial to mesenchymal transition
eq.	equivalents
ESC	embryonic stem cells
ESI	electrospray ionisation
Et	ethyl
et al	et alia (Latin) and others
ES^+	electrospray ionisation, operating in positive mode
ES^-	electrospray ionisation, operating in negative mode
EWG	electron withdrawing group
FACS	fluorescence-activated cell sorting
FBDD	fragment based drug discovery
FGF	fibroblast growth factor
*Fli*1	friend leukemia integration 1
g	gram(s)
GPCR	G-protein coupled receptor
HBA	hydrogen bond acceptor

HBD	hydrogen bond donor
HDAC	histone deacetylase
HEK	human embryonic kidney
HMG CoA	3-hydroxy-3-methylglutaryl-coenzyme A
HMT	histone methyl transferases
h	hours
HPLC	high-performance liquid chromatography
HRMS	high-resolution mass spectrometry
Hz	hertz
IBMX	3-isobutyl-1-methylxanthine
IC_{50}	inhibition concentration affecting 50% of specimens
i. e.	id est (latin) that is
IP	intraperitoneal
IR	infrared
J	coupling constant (in NMR spectroscopy); joules
k	kilo
K_i	dissociation constant at 50% of unbound specimens
LE	ligand efficiency
LLE	lipophilic ligand efficiency
leu	leucine
lit.	literature
luc	luciferase
µ	micro
m	multiplet (spectral); metre(s); milli
M	molar (moles per litre)
M^+	parent molecular ion
MAP	mitogen activated protein
Me	methyl
MDCK	Madin-Darby canine kidney
MDR	multidrug resistance protein
MHC	major histocompatibility complex
MHz	megahertz
MIC	minimum inhibitory concentration
min	minute(s); minimum

MLM	mouse liver microsomes
mM	millimole
mmol	millimile(s)
MOA	mode of action
mol	mole(s)
Mp	melting point
MS	mass spectroscopy
MT	melatonin receptor
MTS	medium throughput screen
m/z	mass-to-charge ratio
Mw	molecular weight
n	nano
NADPH	nicotinamide adenine dinucleotide phosphate
NTR	amine terminus
Nu	nucleophile
PAOA	pimeloylanilide o-aminoanilide
PBS	phosphate buffered saline
PDE	phosphodiesterase
Ph	phenyl
PPA	polyphosphoric acid
ppm	part(s) per million
^{i}Pr	*iso*propyl
PRMT	protein arginine methyl transferases
Py	pyridine
q	quartet (spectral)
qt	quintet (spectral)
RLU	relative luminescence units
RMM	relative molecular weight
RNA	ribonucleic acid
ROCS	rapid overlay of chemical structures
ROS	reactive oxygen species
rt	room temperature
RT-PCR	reverse transcription polymerase chain reaction
RyR	ryanodine receptor

s	singlet (spectral); second(s)
SAHA	suberoylanilide hydroxamic acid
SAR	structure activity relationship
smad	small mother against decapentaplegic
SPR	surface plasmon resonance
t	triplet
Tbx20	T-box20
TFA	trifluoroacetic acid
TGF-β	transforming growth factor β
THC	tetrahydrocannabinol
THF	tetrahydrofuran
tlc	thin layer chromatography
Trb3	tribbles homolog 3
TSA	trichostatin A
$t_{1/2}$	half life
UpR	upregulation
ν	wavenumber, cm^{-1}
VPA	valproic acid
Wnt	wingless
wt	wild type

Table of Contents

Chapter 1: Introduction to the Drug Discovery Process

1.1 Drug Discovery

Without medicine, the world would not be what it is now and people would not live as long and as well as they currently do. The process of drug discovery is the fundamental method for discovering molecules and developing them to successful medicines. However, with increasing discovery activity, the number of molecules in development is very high, development is long and very costly and it is becoming increasingly difficult to discover molecules with improved properties over available agents.[1,2] The methods of drug discovery are very well established and all medicines on the market will have passed through the rigorous and tightly regulated processes of qualifying the drug for distribution to the public resulting in low attrition rates.

The drug discovery process for identifying valid hits can commence with two different biological screening methods: one phenotypic and the other target based.[3] A hit is defined as a compound with good biological activity that has the potential for structural elaboration to a more potent agent. The phenotypic based approach for discovering hits, analyses the effect that compounds have on cells, tissues or organisms. Whereas the target based hit discovery approach investigates the effect of compounds on a specific and often isolated target protein through *in vitro* assays. Target based approaches are focussed on measuring activity on an enzyme or alternatively modulating a signalling pathway modulated by the target.[4]

The first step after selecting a target and validating its biological activity, is to confirm that the hit acts through binding to the postulated target. The hit is then optimised with structural modifications to improve activity at the target and to optimise its physicochemical properties. A suitable candidate produced through the drug discovery process with the required activity, selectivity, pharmaco-kinetic and -dynamic properties will then progress to the drug development stage in which preclinical and clinical evaluation will determine its potential as a medicine (**Figure 1**).

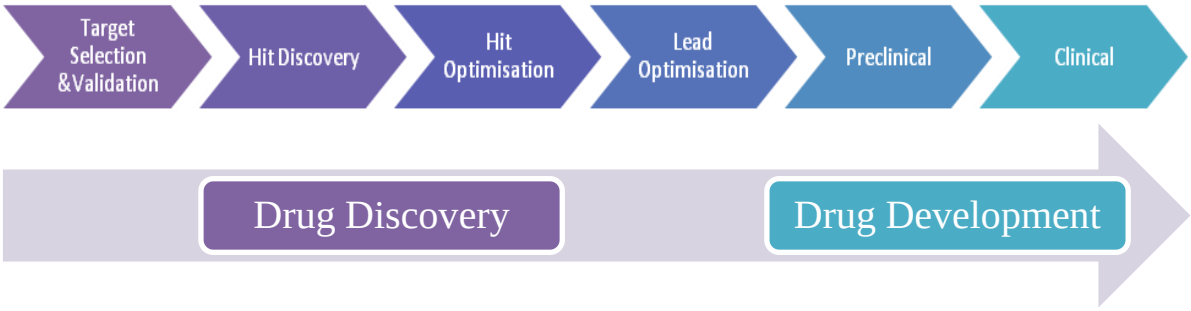

Figure 1 outline of the process of drug discovery and drug development

It is the process of finding the right hit molecules with potential for becoming a new medicine which is the most important stage in drug discovery. A large proportion of this piece of work uses ligand based virtual screening, one particular method of hit identification, to discover new starting molecules and subsequently moves into hit optimisation.

1.1.1 Library Selection in Drug Discovery

Different methods of hit identification can process different numbers of compounds. In high throughput screening (HTS), the selection criteria used can be very broad. Often millions of compounds can rapidly be screened and processed by robotics, and the general attitude is that increasing the number of screened compounds leads to a greater number of hits, although the overall hit rate remains the same.[5] In screens using a smaller library where only hundreds of compounds are processed, selecting suitable molecules and likely hits is of much greater importance for maintaining a high hit rate.

Filters can be used to reduce the size of the library without reducing the chances of discovering a drug molecule.[6] One such filter removes compounds with pharmacologically labile groups, based on previous stability studies or on the literature. An example where such a filter is useful are nitroaromatic groups since by binding to deoxyribonucleic acid (DNA) these have demonstrated carcinogenic and mutagenic effects.[7] The nitro group can also be reduced to the analine and converted to the aromatic hydroxylamine which, are all toxicophores in cells. Frequently appearing pharmacophores and functional groups in marketed drugs can be used as guidelines to identify suitable starting structures to design a library. A study was carried out by researchers at Vertex investigating the most and least common frameworks and functional groups used in drugs.[8,9] They showed that the range of cores used and functional groups is small. The most frequently present functionalities include carbonyl, methyl and hydroxyl groups. This study gives an indication of desirable functional groups in molecules to be included in the compounds in screening.

Further guidelines used in library selection are the famous Lipinski rule set of 5 (**Figure 2**). In a study by Lipinski *et al*, successful oral delivered drugs on the market were analysed by their chemical and physical properties resulting in the following general criteria for molecules to be drug-like, that is for greater likelihood of being orally bioavalable;[10,11]

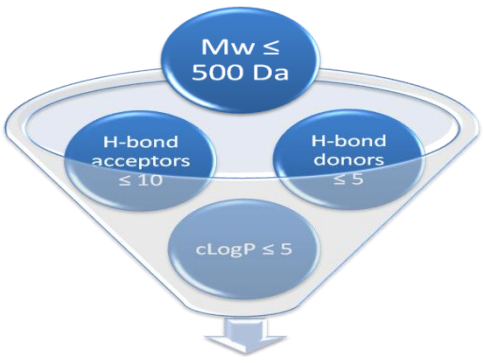

Figure 2 Lipinski's rules of 5 filters for compounds selection

The Lipinski rules provide a general overview of desired chemical properties rendering molecules more drug-like and increasing chances of developing a successful drug.

Molecular weight (Mw) in excess of 500 was shown to be correlated to low oral bioavailability. In addition, larger molecules generally increase the values of the calculated partition coefficient (ClogP) which has since been associated with toxicity and *in vitro* receptor promiscuity.[12,13] The final observation was the number of HBA and HBD a molecule holds should be limited. In Addition to Lipinski's rules, other parameters have been identified to be important in providing oral bioavailability.[14,15] Amongst them, Veber *et al* indicated that a limited number of rotatable bonds (≤ 10) and a limited surface area (≤ 140) increases the absorption across membranes into the blood.[16]More recently, a study by Gleeson *et al* emphasized the importance of Mw and LogP on a range of ADMET properties in determining the behaviour of the drug *in vivo*.[17]

Using these guidelines, large libraries can be scanned for suitable compounds. This set of rules however, applies primarily for orally administered drugs and does not consider active and carrier transport across membranes. Teague *et al* have also proposed additional properties of molecules rendering them more lead-like, based on the premise that lead optimisation and drug development almost always increases relative molecular mass (RMM).[18] Compounds should be of low Mw, polar and provide few simple synthetic step approaches to provide a diverse library of compounds.

The sources of compounds that can be used for screening are numerous and the total number of potential compounds very large (**Figure 3**). Commercial sources include libraries of natural products and synthetic combinatorial libraries.[19,20] Natural products tend to be complex molecules isolated from sponges, other marine organisms or terrestrial plants and fungi. These sources tend to yield low quantities of compound that often have high Mw, are complex and can be hard to synthesise on a large scale. Alternatively, molecules can be obtained from diversity orientated synthetic (DOS) libraries, which include compounds with vastly different chemical structures. DOS libraries consist of a

variety of pharmacophores and functional groups that cover a wide range of chemical space.[21] This allows for investigations into a wide range of core structures providing a general overview of what functionalities are tolerated. However, the downside is that there will be a limited number of examples with the same framework providing limited insight into a compound class. Purchasing custom made libraries can be very expensive and testing these is also expensive. Therefore, alternative approaches have been sought to increase the chance of finding hits with reduced costs and a smaller library size.

One recent development has been the use of computational methods to effectively screen for possible hits using virtual libraries.[22,23] A focussed virtual library with potentially higher chances of providing good hits, can also be generated by using published knowledge of compounds or targets. A further improvement in efficiency can be obtained by using existing compounds with active pharmacophores on the same or homologous receptors or alternatively distinct functional groups, extending from the core of the molecule, known from previously discovered molecules to be active at the receptor.

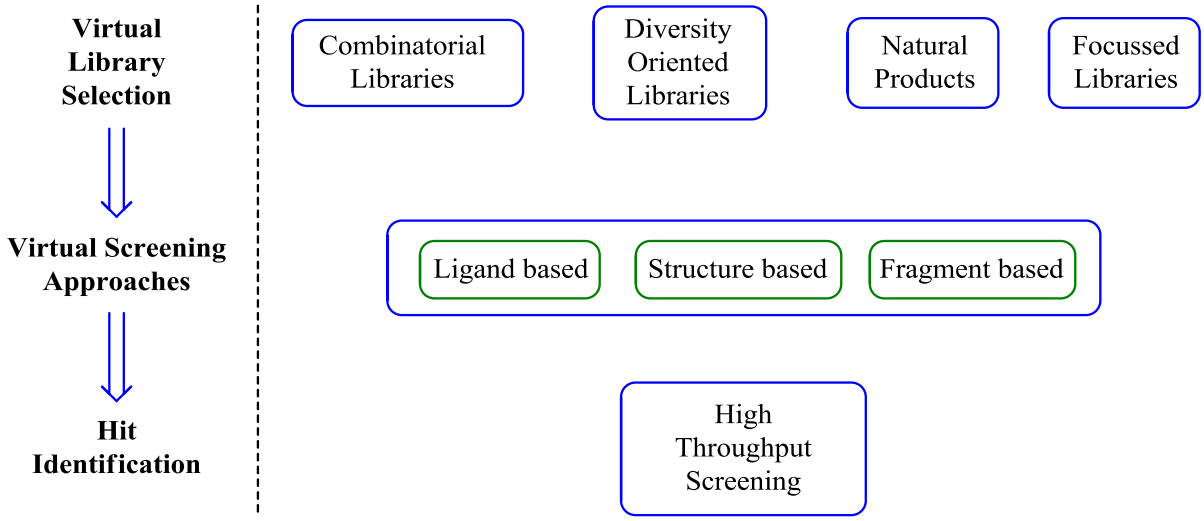

Figure 3 Outline of the possible methods of hit identification and choices of library selection

1.1.2 Hit Identification Methods

1.1.2.1 High Throughput Screening (HTS)

For the discovery of a hit, several approaches have been used in the past, to varying degrees of success. HTS is a method that has been used for many years for the discovery of hits. The method involves the use of compound libraries consisting of millions of compounds which, with the help of robotics and computational methods, are all pharmacologically tested in the biological system.[24] The first step is to screen the compounds in a primary assay, which can consist of two different methods; the first is to test the compounds directly against the drug target, which would be possible if the protein could be purified and produced on a large scale. Alternatively, a more complex cell based assay is required. However, the readout obtained from a cell based assay does not necessarily represent activation through the desired pathway (**Figure 4**).[25] Activity could result from modulation of a different pathway or from the targeted receptor activating an alternative pathway than the intended one, in a process called functional selectivity or biased agonism.[26] In this case, a secondary assay would be required to verify that the hit actually binds to the expected target.

Typical readouts from an HTS would be produced by the measurement of optical readouts such as fluorescence and luminescence. The variability could be measured using a statistical tool known as the z-score. [27] The output of the HTS will ultimately produce a measure of the potency of the compound.

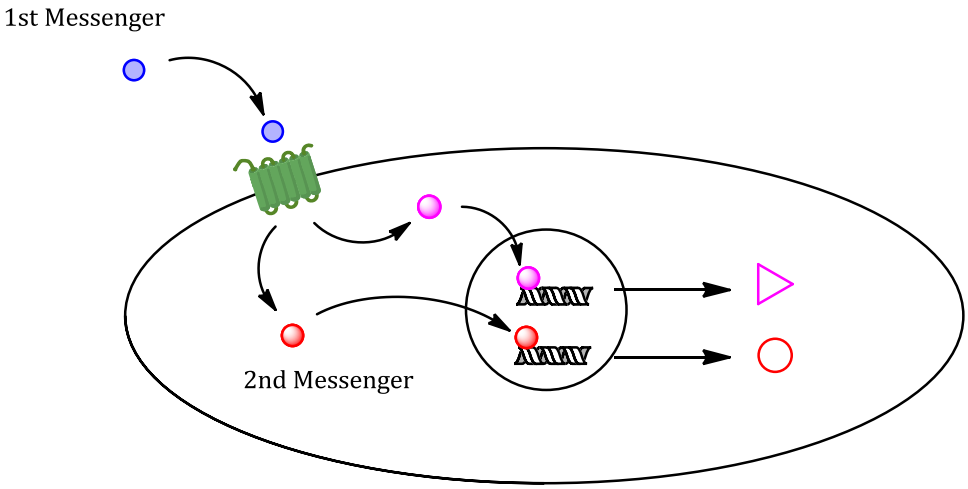

Figure 4 Outline of functional selectivity, ligand binding of 1st messenger to the receptor can activate different intracellular pathways and ultimately resulting in a different outcome

HTS allows researchers to have no prior knowledge of possible chemotypes that would modulate the activity on the desired target therefore allowing more flexibility in the compound selection. Compounds emerging from the HTS interact with the target either by activation or inhibition and are referred to as "hits". These can then be individually selected to provide a starting point for further chemical diversification, in a process called hit optimisation that will provide an understanding of the molecule's structure-activity relationships (SAR).

However, this method requires a readily available large compound collection, or funds to acquire one, and the costly equipment to carry out the procedure to established robust and reliable assays for compound screening. Therefore, HTS was almost exclusively used by large companies.[28] This method has achieved extensive success, in 2004 for example 43 laboratories running HTS generated 746 leads.[29] With continued improvements in computational methods, virtual screening is developing into a powerful tool for the refinement of large chemical libraries into focussed sets of compounds to be screened against a target.[30]

1.1.2.2 Virtual Screen in Drug Discovery

1.1.2.2.1 Structure and Ligand Based Approaches

Virtual screening is a different method used in the identification of novel active molecules in drug discovery. This differs from HTS in many ways and most importantly allows screenings when resources are either technically or financially more constrained.

In structure-based virtual screening the three dimensional (3D) biomolecular structure of the target is known and is used to screen a virtual library against.[31] For this method to be used, the 3D structure of the target has to be defined either using X-ray crystallography or nuclear magnetic resonance (NMR) techniques, or alternatively by generating a homology model of the target.[32,33] From the 3D structure, the active site can be identified by co-crystallisation with a high affinity ligand, substrate or cofactor, or if this is unavailable through predictive algorithms.[34] With this method a virtual library of millions of compounds can be screened against the target and virtual hits can be followed up. With successful hits, *i.e*. those that confirm in an appropriate assay, docking studies using the 3D structure of the target can be carried out attempting to identify areas of the molecule that can be "grown" to improve binding to the pocket.[35] An example where this method was implemented was for discovering a new neuramidase inhibitor for treatment of viral infections leading to the development of zanamivir (Relenza, **4**) (**Figure 5**).[36] *N*-acetylneuramic acid (NANA, **1**) a mild inhibitor of the enzyme provided a suitable starting point for further optimisation. The crystal structure of the neuramidase bound with a known inhibitor 2-deoxy-2,3-dehydro-*N*-acetylneuraminic acid (DANA, **2**) was resolved and computational studies identified possible exploitation of charged residue in the pocket.[37] The C(4) position was altered to a amine **3** and ultimately to a guanidine subunit **4** presenting the most potent influenza virus neuramidase inhibitors at the time.[38,39] However, in the absence of an X-ray crystal structure homology models provide reliable

information for computational studies on the desired target only if there is a high degree of similarity to another protein crystal structure. Therefore, a method that would not require 3D structures would present a desirable alternative for non crystallised targets.

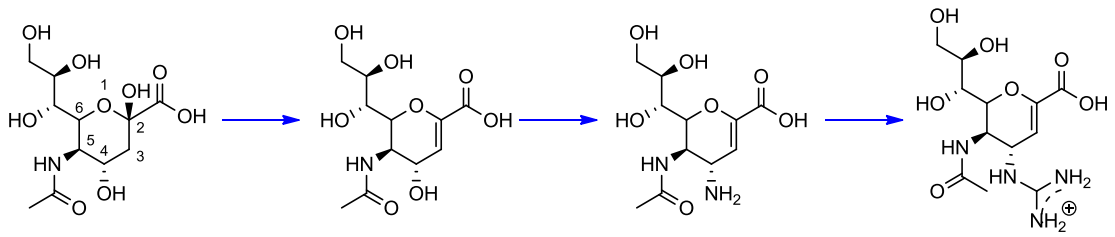

1 NANA | **2** DANA | **3** 4-amino DANA | **4** Zanamivir

Figure 5 Development of zanamivir (**4**) using structure based drug design

The second type of virtual screening method is ligand based design for identifying hit compounds. The concept of ligand-based design dates back to the 1960's with the discovery of propranolol (**9**), which is a β-adrenergic receptor antagonists (**Figure 6**).[40,41] Sir James Black used the structure of earlier adrenaline derivatives, isoprenaline (**6**), dichloroisoprenaline (**7**) and pronethalol (**8**), and with some slight chemical modifications discovered a new drug, propranol (**9**), pioneering work for which he was awarded the Nobel prize in medicine in 1988. Isoprenaline was the first selective β-adrenergic ligand discovered by a minor modification on adrenaline discovered by Konzett.[42] Modifications included the substitution of the diol to the chloro **7** and napthaleno **8** derivatives.[43] By identifying what groups in previously discovered molecules can be modified to improve physicochemical properties of compounds, Sir James Black managed to dramatically improve the biological and pharmacokinetic properties of prenethalol (**8**) by the inclusion of an oxymethylene group between the naphthyl and hydroxyallyl substituents to generate **9**, removing the carcinogenic effect of precursors.[44]

Black is much of a fatherly figure in the use of known drugs for specific targets to identify novel ones; "The most fruitful basis for the discovery of a new drug is to start with an old

drug".[45] This method can, in contrast to the structure-based approach, be used when 3D structures of protein targets are not defined. The method has evolved significantly from Sir James's days to make use of computational methods allowing the discovery of active molecules based on known activities.

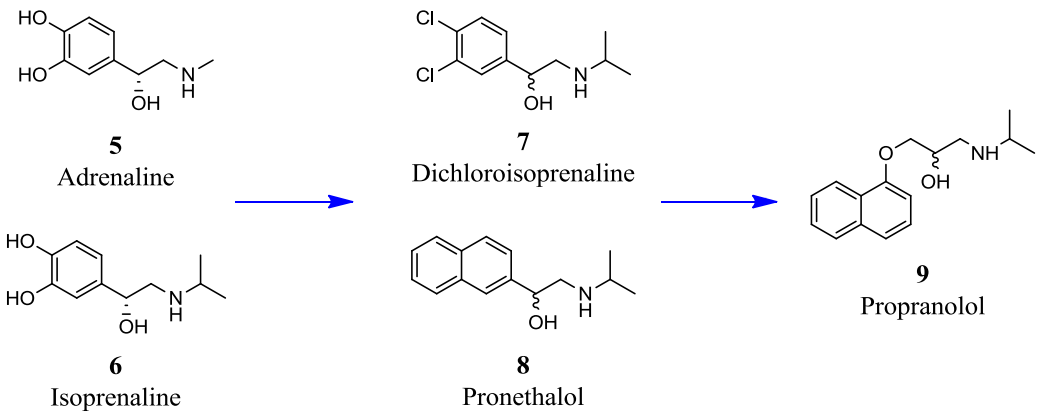

Figure 6 The development of a new β-adrenergic receptor antagonist's propranolol (**9**) from simple modifications from previously known drugs

1.1.2.2.2 Fragment Based Drug Discovery

A different approach is provided by the use of fragment based drug design (FBDD).[46] This technique can also make use of computational chemistry to identify hit molecules, however the main novelty is that the library used consists of fragments of compounds, i.e. low Mw (typically <300 Da).[47] Classical constraints for fragments in FBDD include the filters of the "rule of 3" (**Figure 7**).[48] These filters have some restrictions on the type of compounds which can be used in the screen against a certain target.

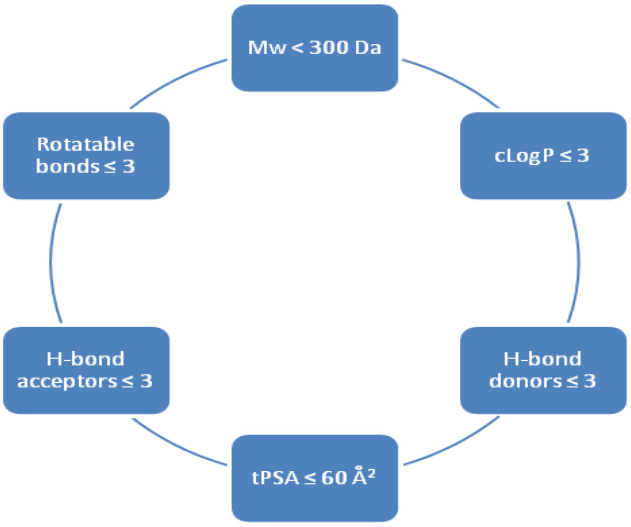

Figure 7 Summary of Rule of 3 applied to FBDD

These fragments are not the typical molecules used in HTS or structure-based virtual screening, they both possess a lower molecular weight and several points for future chemical diversification for hit optimisation. In methods described in previous sections, HTS compounds have usually high molecular weights that do not leave much room for modifications necessary in ligand optimisation. In contrast FBDD uses smaller starting points (fragments) that allow modifications by adding mass that may lead to more favourable pharmacochemical properties. This method could provide a better alternative when HTS does not yield positive result. It has been applied in a study aiming to identify inhibitors of DNA gyrase for antibacterial activity.[49] Using the characterised 3D X-ray structure of the target, a fragment based virtual screen, detecting mM activities of fragments, was carried out leading to the discovery of 3000 predicted binding molecules. Seven classes of compounds were ultimately validated as true inhibitors and some of the results of the dissociation constants in high sensitivity heteronuclear $^{1}H/^{15}N$ correlation NMR spectroscopy of the fragments are displayed in **Figure 8** (**10**-**14**).

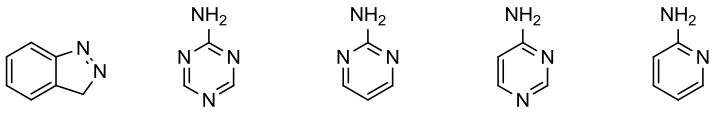

	10	**11**	**12**	**13**	**14**
K_D (mM)	10	60	60	200	200

Figure 8 Example of fragments identified using FBDD in a study by Boehm *et al* [49]

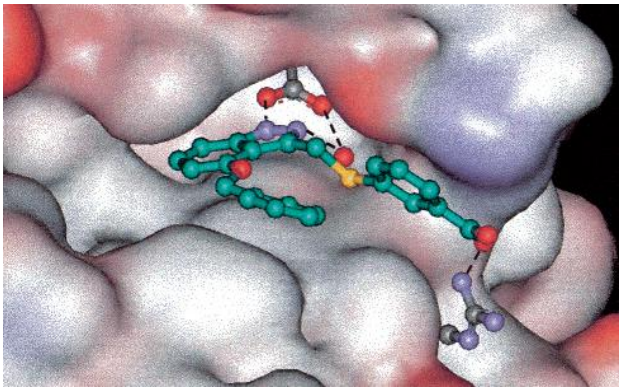

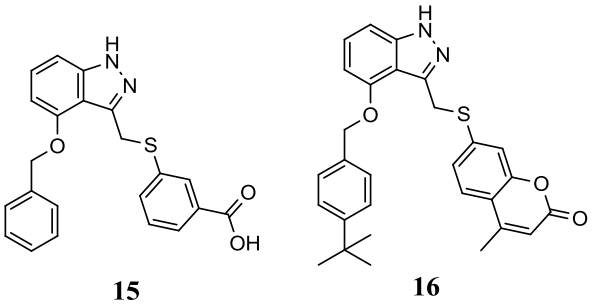

15 **16**

Figure 9 Example of a 3D X-ray crystal structure of DNA gyrase with indazole compound **15** bound in the active site leading to the development of compound **16** after optimisation[49]

The indazole fragment **10** displayed the most promising binding to the target active site and was used as a core for further optimisation. With the use of computational methods, side chains were added to improve the activity, leading to the generation of a crystal structure of **15** bound in the active site of the enzyme (**Figure 9**). Optimisation finally let to the synthesis of compound **16**, which displays 10 fold higher activity than novobiocin, an antibacterial drug marketed in the 1960's. This illustrated the possibility of a virtual screen using low molecular weight fragments to identify new chemical cores. These are small enough to allow extensive further function improvements by adding side chains. Limitations of FBDD includes the requirement of high sensitivity allowing the detection of compound potency in micromolar (mM) range (see **Figure 8**), additionally this method needs a solved crystal structure, NMR or surface plasmon resonance (SPR) method for binding analysis.

Nevertheless, the use of virtual screening in hit identification can indeed provide an efficient alternative way of screening large number of compounds in a more cost effective

manner. This allows smaller research groups to carry out drug discovery programs when they lack the facilities and the resources to embark on HTS.

1.1.3 Hit Classification

Hit identification is the first step of an often long process leading to a development of a successful drug molecule. In the initial stages of research, amongst other criteria, what makes a good hit is the observation of the desired effect within a cellular context or in a secondary assay for instance, following receptor binding, the cascade of intracellular responses can be extremely broad and variable (*vide infra*). Depending on the type of effect the molecule has on the receptor, the intracellular signalling pathway can be either enhanced or decreased. The first possible response that can be observed by ligands can be to produce a positive response.[50] Such target binding molecules are called full agonists and their purpose is to give after binding to the target a 100% response (**Figure 10**). A partial agonist provides a smaller response than a full agonist. An example of an exogenous full agonist is morphine (**17**), which is used as a mediator of the μ-opioid receptors. **17** mimics the activity of endogenous endorphins by binding to the active site of the receptors in the central nervous system (CNS). To neutralise the effect of morphine on the μ-opioid receptors another class of ligands can be used, namely antagonists. Naloxone (**18**) is an antagonist molecule used to counteract the morphine agonist effect on the μ-opioid receptors.[51] The downstream effect of an antagonist is to reduce the intracellular signalling caused by the activation of the receptor. Finally, there are inverse agonists that cause a negative response. This group of ligands leads to a level of activity lower than the basal level and this is obviously only possible for receptors that have some level of basal activation in the absence of agonist binding.

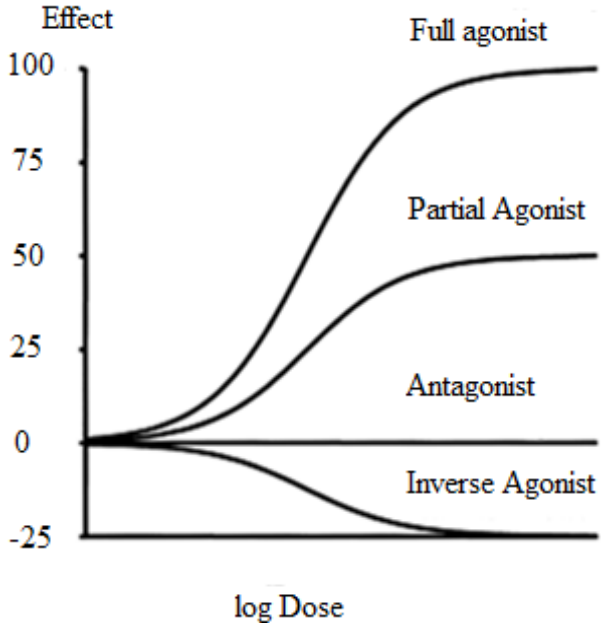

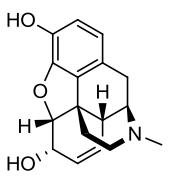

17
Morphine

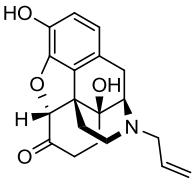

18
Naloxone

Type of Ligand	Efficacy (%)
Full agonist	100
Partial agonist	0 < E < 100
Antagonist	0
Inverse agonist	0

Figure 10 Graphs showing the effect of involvement of target binding ligands and their efficacy on the target. Morphine (**17**), a μ-opioid receptor agonist and naloxone (**18**) the antagonist.

Readings obtained from primary biological assays displaying potency of compounds on a particular target, as previously outlined, must be followed up by a secondary screen. Possible effects caused by the compound that are not related to target activation or inhibition can include for instance fluorescence quenching, compound aggregation and the presence of reactive functionalities.[52] These would influence the read-out of the assay without acting on the desired target but interfering with the assay procedure, and thus appear as false positives. Therefore, before proceeding with further studies, hit validation needs to be carried out, this is essential in order to eradicate the false positive hits.

1.1.4 Hit Optimisation

After identification of a hit that binds and gives the desired response on the target, the next challenge is to improve its potency. If the 3D structure of the target is known, optimisation can be efficiently achieved guided by computational methods. If this is not the case, a range of different compounds need to be made where each structural variant leads to an

increased understanding of the interactions between ligand and active site and the steric and electronic demands involved. Successful SAR development on a hit with increased potency on the desired target advances the molecule to become a lead. Further optimisation steps will address a range of other essentials parameters and will aim at further improving efficacy and optimise physicochemical and pharmacokinetic properties (**Figure 11**).

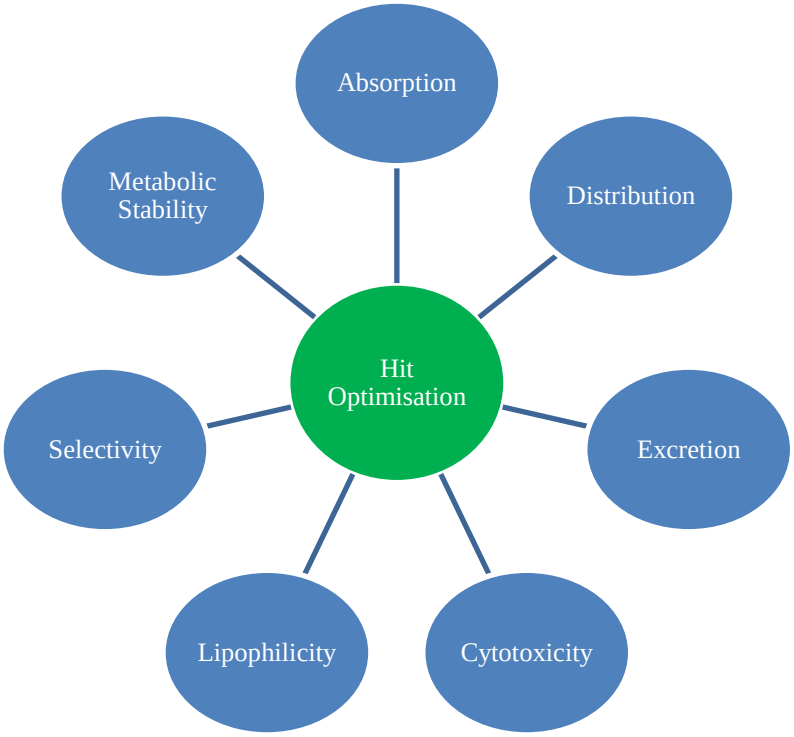

Figure 11 Properties to consider in hit optimisation of molecules in drug discovery

1.2 Overall Project Aims

The project aim is to discover novel agonist molecules on two different targets, one, is a molecular target, the other a target pathway. One is involved in regeneration of damaged heart muscle and the other in treatment of atherosclerosis. Deploying a ligand based virtual screening approach, published receptor binding compounds would be screened against the in-house compound collection for possible hits in a cellular assay. The target pathway is the bone morphogenetic protein (BMP) signalling pathway. Activation of this pathway has been demonstrated to influence lineage determination of stem cell and in particular to promote cardiomyogenesis. Molecules activating this pathway would provide a potential treatment for patients having suffered from myocardial infarction with the loss of functioning heart muscle cells, where the generation of new cardiomyocytes would restore heart function.

The molecular target is the cannabinoid 2 receptor (CB_2R) which is a transmembrane G-protein coupled receptor (GPCR). When activated it forms the $G_{i/o}$ complex and regulates the activity of adenyl cyclase. Activation of this pathway has been observed to reduce the progression of atherosclerotic plaque development *in vivo.* Agonists binding CB_2R could provide possible treatment for patients suffering from atherosclerosis, a chronic inflammatory condition affecting arterial walls.

Part I: The Discovery of a Novel Bone Morphogenic Protein Pathway Agonist

Chapter 2: Introduction to Bone Morphogenic Protein

2.1 Importance of Bone Morphogenic Protein Signalling in Myocardial Remodelling

The main cause of myocardial fibrosis is by a myocardial infarction, but can also be developed by other conditions including hypertension, and is associated with subsequent development of scarring in heart tissue.[53] Fibrosis is the process of excessive accumulation of adherant fibroblasts and deposition of connective tissue such as collagen, influencing the function and physiology of the heart. It contributes to 45% of deaths in the developed world as the disease affects major organs including lungs, liver, kidney and heart.[54] In the heart, the development of a fibrotic scar leads to impaired cardiac function and ultimately heart failure.

Methods of replacing the fibrotic scar tissue with functional cardiomyocytes would provide life changing improvements for patients suffering from this disease.[55] Stem cells provide a suitable tool for replacing damaged myocardium and reinstating cardiac function.[56] Stem cells are remarkable cells which retain the ability to differentiate into any cell type when provided with the correct stimulus. For their use in therapeutics, endogenous stem cells can in principle be differentiated *in situ* to the desired lineage, or alternatively an exogenous supply of cells can be administered to the site of injury. The latter is however limited by the supply of such cells and evidence of its effectiveness has yet to be demonstrated clinically.

Current *in situ* regenerative methods involve the addition of growth factors, such as thymosin β-4, promoting resident progenitor stem cell differentiation leading to the regeneration of damaged heart tissue.[57,58] However, this is currently limited by the number of resident stem cells, their low innate capacity to repair, limited effectiveness and

pleiotropic effects of current biological therapies with the use of expensive recombinant proteins. The Transforming growth factor β (TGF-β) superfamily has a key role in differentiation of stem cells to cardiomyocytes, in particular the bone morphogenic proteins (BMPs). It was discovered that endothelial to mesenchymal stem cell transition (EndoMT) leads to increased accumulation of fibroblasts following injury and activation by TGF-β led to the production of excessive ECM proteins resulting in cardiac fibrosis.[59] Additionally, TGF-β induced cardiac fibrosis, whereas BMP activation was observed to significantly reduce EndoMT and fibroblast recruitment. It is hypothesised that a small molecule agonist of the BMP pathway could help resolve current issues in reducing EndoMT in *vivo*, and possibly provide a new therapeutic possibility in reducing fibrotic tissue to improve cardiac function following myocardial infarction.

2.2 Myocardial Infarction

A myocardial infarction results from lack of sufficient blood supply, to a part of the heart, for the cells to survive. The most common cause of reduced or a complete block of blood flow to the heart is from the formation of a clot, an example of such is an atherosclerotic plaque formed as a result of chronic inflammation of the endothelium of the blood vessel. The plaque reduces the size of the pore of the blood vessel and in advanced stages of the disease can lead to complete blockage of blood vessel and death of the undersupplied part of the heart (coloured in blue, **Figure 1**). The heart has very limited regenerative potential and the affected area is converted to scar tissue leading to loss of myocardial function. The most promising approach to help the heart recover from such an incident is by exogenous cell delivery or endogenous cell activation to cardiomyocytes and other damaged tissues to restore cardiac function.

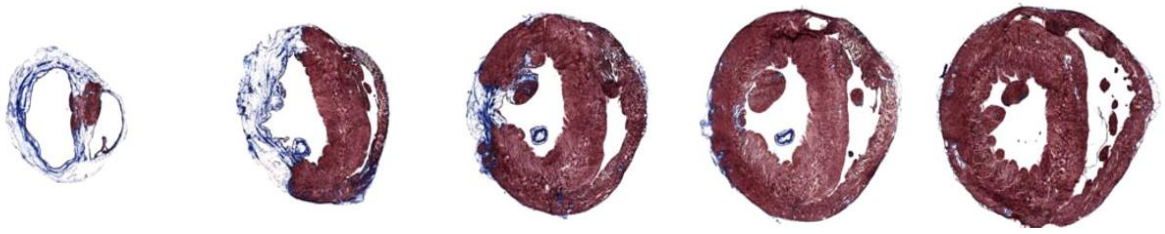

Figure 1 Ventricular cross section of post myocardial infarction stained with Masson's Trichrome where myocytes are stained in red and fibrotic tissues in blue REF

2.3 Stem Cell Differentiation

Stem cells could have enormous potential in the future of regenerative medicine. There are however, some major obstacles that need to be overcome to make the application of stem cells for therapeutic use possible. The first and foremost challenge is the inability to efficiently control the differentiation process of stem cells and often to unambiguously determine their terminal lineage. Secondly, the lack of a readily available supply of stem cells in adults limits opportunities of *in vivo* experiments without the supplement of exogenous cells. Adults still hold limited populations of stem cells in several tissues including neural stem cells within the brain which possess the ability to self-renew and differentiate, and haematopoietic stem cells in the bone marrow which can give rise to any blood cell. The heart however, has a very limited regenerative potential with very small number of cells to generate new myocytes.[60,61] The lack of a ready supply of resident stem cells presents a major challenge when the heart needs to recover from a myocardial infarction due to either the lack of cells to replace the developed fibrotic scar tissue or promote the natural regeneration process. In addition, there still exists indecision as to what defines an adult cardiac stem cell and the pathways responsible for its development. Several pathways have been discovered to participate in stem cell differentiation and self-renewal in the presence of exogenous growth factors and small molecule ligands, including the TGF-β and BMP pathways, which will be discussed in this chapter.

2.3.1 Small Molecules in Stem Cell Differentiation

Small molecules represent an attractive alternative to growth factors for the control of stem cell differentiation which have shown significant promise and are believed to hold huge potential for the treatment of diseases and injuries.[62,63,64] Currently control over differentiation of embryonic or adult stem cells to a desired cell type, is associated with several problems, including differentiation efficiency.[65,66] Small molecules can easily be administered and removed at precise concentrations and accurate time points. The accessibility of vast libraries of structurally diverse compounds provides unlimited options of starting materials displaying selective control over specific molecular targets, including epigenetic factors.[67] Finally, replacement of proteins and growth factors with small molecules provides a more cost-efficient, accessible and chemically stable alternative for control of stem cell fate.

Several examples have been reported with the administration of small molecules to enhance the yield of differentiated cells. Three structurally related small molecules, cardionogens (**19-21**), have recently been discovered to enlarge the size of the developing heart in zebrafish and induce differentiation of mouse embryonic stem cells *in vitro* to cardiomyocytes by inhibition of the Wnt signalling pathway (**Figure 2**).[68] The ability to regulate a signalling pathway using small molecules would allow convenient control of stem cell fate by addition and removal of a small molecule at various time points in the differentiation process. Thus, our interest lies in employing small molecules that selectively regulate the activity of the BMP signalling pathway, presenting a possible method for enhancing cardiomyogenesis, *i.e.* the inherent development of new cardiac muscle tissue, and replacing the developed fibrotic scar tissue with functioning cardiomyocytes.

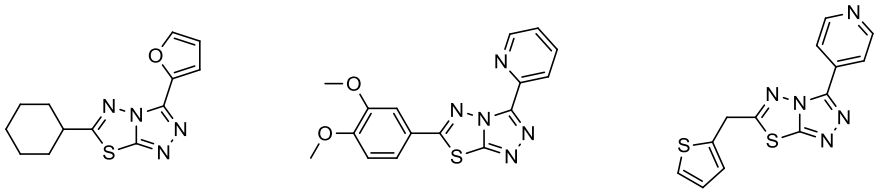

19 **20** **21**

Figure 2 Structures of three identified cardionogens (**19-21**)

2.3.2 Cardiomyogenesis

2.3.2.1 Overview of Cardiomyogenesis

The ability of differentiating stem cells to a cardiac lineage would be of tremendous use in regenerative medicine for the treatment of patients with cardiac malfunction or who have suffered a myocardial infarction. Regulation of the BMP pathway has been shown to be involved in cardiomyogenesis as well as osteogenesis, the formation of bone mass.[69] There are several transcriptional markers which identify whether a cell has become a functional cardiomyocyte. In a study using human embryonic stem cells, beating cardiomyocytes were observed in conditions promoting terminal differentiation. It was noted that with the addition of 5-aza-2'-deoxycytidine (**22**), which is a DNA-methyl transferase inhibitor, to the cell culture medium, the population of beating cardiomyocytes increased (**Figure 3**). Up to 70% of the cell population was confirmed to express the cardiac specific transcription factors GATA-4, Nkx2.5 and MEF-2.[70] Further research led to the observation that a known histone deacetylase (HDAC) inhibitor, trichostatin A (TSA, **23**) administered with **22** led to an increased number of cardiomyocytes in culture from rat mesenchymal stem cells.[71] However, the mechanism of action appears to be HDAC independent. Co-treatment of **22** and **23** displayed increased expression of cardiac gene markers, however only using **23** showed maximal inhibition of HDAC activity, but no effect on expression of cardiac genes.

The antioxidant, ascorbic acid (**24**) was also discovered to promote formation of cells of cardiac lineage from mouse embryonic stem cells.[72] In an 880 compound screen using embryonic stem cells with stably transfected muscle specific myosin heavy chain (MHC) expression-dependent enhanced green fluorescent protein (EGFP) reporter, **24** was identified to promote differentiation to cardiac cells also displaying expression of cardiac genes. In a separate study, treatment of cells with all-*trans* retinoic acid (**25**) was also shown to increase the number of cardiomyocytes in culture.[73] When grown in culture, embryonic stem cells spontaneously differentiate *via* embryoid bodies, into spontaneously beating functional cardiomyocytes. It was observed in this study that retinoic acid accelerates the formation of ventricular cardiomyocytes. However, these were amongst the select few antioxidants shown to promote cardiomyogenesis.

More recently a study by Russell *et al* described 3,5-disubstituted isoxazoles as stimulating ventricular function after myocardial infarction *in vivo*.[74] The mode of action was confirmed, by screening a range of different targets, to proceed *via* activation of an extracellular pH sensing GPR98 protein, which is a G-protein coupled receptor (GPCR). After myocardial infarction the first physiological change is lowering of pH due to anaerobic metabolism and lactic acid export. Activation of GPR98 by the small molecule promotes Ca^{2+} release and a stabilisation of the acidic conditions generated.

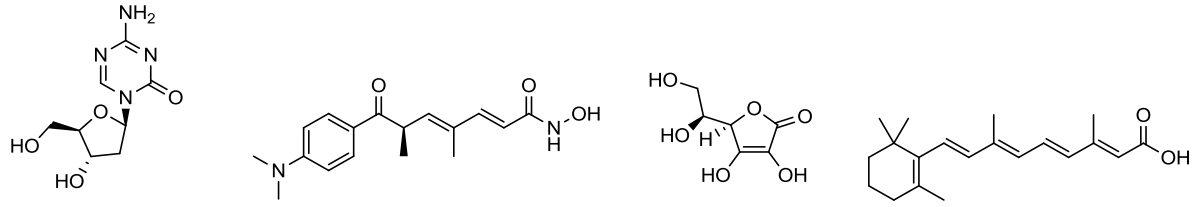

22 5-aza-2'-deoxycytidine

23 Trichostatin A

24 Ascorbic acid

25 Retinoic acid

Figure 3 Small molecules **22-25** shown to promote cardiac differentiation to terminal cardiomyocyte lineage expressing cardiac transcription markers GATA-4, Nkx2.5 and MEF-2

Calcium is also crucial in maintaining function of cardiomyocytes, where spontaneously beating cells are driven by a change in Ca^{2+} concentration in the cell. It was observed that

in cardiomyogenesis, as the cells progress to a terminally differentiated state, the spontaneous beating of the cell increases in rate. Ryanodine receptors (RyR) are known to be involved in the compartmentalisation of Ca^{2+} ions and possibly the spontaneous beating of the differentiated cells. In an study by Yang *et al*, RyR knockout systems were generated, and indeed the observation was a slowing of spontaneous beat.[75] Therefore, another influence contributing to the differentiation of embryonic stem cells to fully functioning cardiomyocytes is the presence of ryanodine.

The above mentioned compounds provide evidence that small molecules can replace current use of growth factors and provide a possible method of promoting and enhancing differentiation of stem cells to the cardiac lineage. The mechanism through which the small molecules act to promote cardiomyogenesis is not always known. However, the focus of this study will be on the development of selective BMP pathway regulating molecules to ultimately support the hypothesis that small molecule activation of the pathway of a TGF-β superfamily member, namely the BMP pathway, promotes cardiomyogenesis.

2.4 TGF-β Superfamily

The TGF-β superfamily consists of TGF-βs, BMPs and activin/inhibin/nodal subfamilies. These all bind to TGF-β type II receptor dimer which then recruits the type I receptor dimer to form a tetramer. The type II receptor is a serine/threonine kinase membrane receptor which phosphorylates intracellular smad proteins when activated by coupling to the type I receptor. Following phosphorylation, the phosphorylated smad (p-smad) complex translocates into the nucleus to regulate transcription of certain genes (**Figure 4**).[76] The TGF-β receptor ligands are known to be involved in many biological processes related to stem cell biology including proliferation and lineage determination.

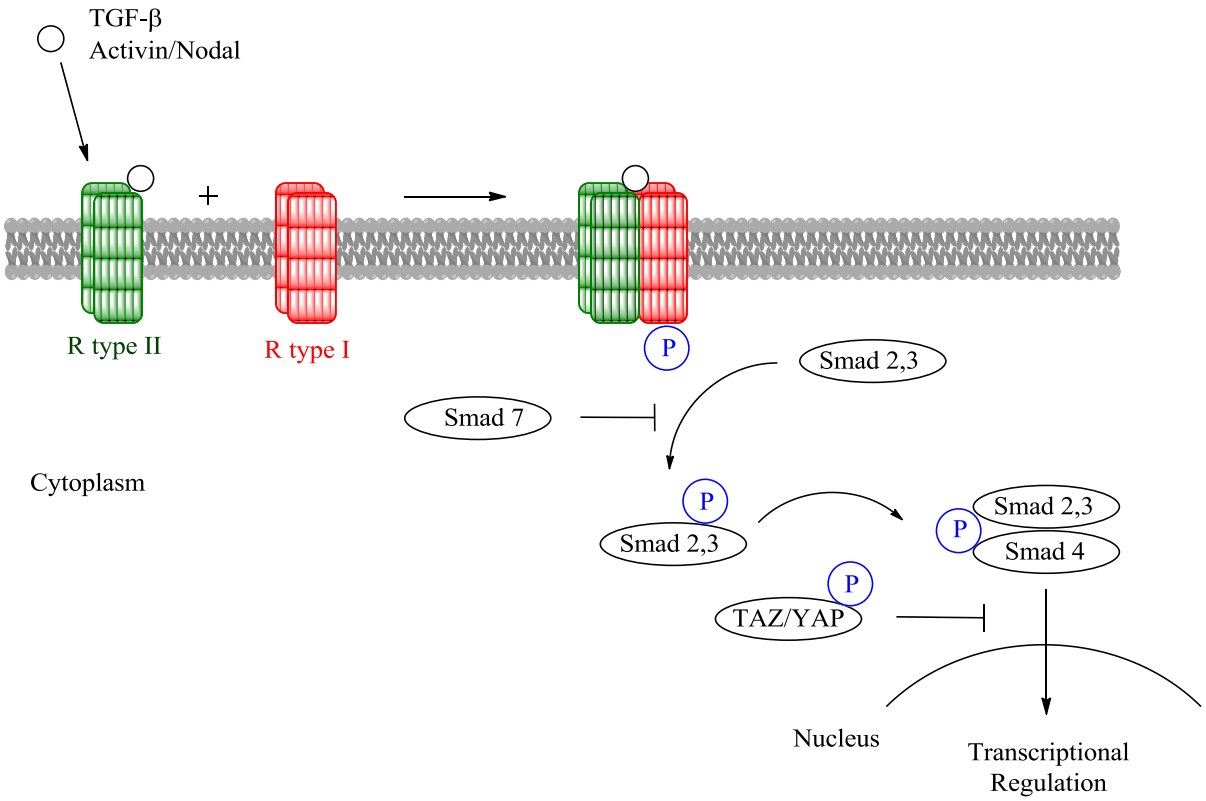

Figure 4 A simple outline of the smad dependent TGF-β pathway and phosphorylated TAZ/YAP complex inhibiting nuclear translocation of the smad complex

Using human embryonic stem cells (hESC) it was discovered that smad 2 and 3 were phosphorylated and subsequently translocated into the nucleus in undifferentiated hESC.[77] The activation of the TGF-β pathway was thought to regulate the expression levels of phosphorylated smads and maintenance of pluripotency, *i.e.* the ability to differentiate to all cell types representative of endogenous and adult tissue. The study additionally investigates the effect of a TGF-β pathway inhibiting molecule, SB431542 (**26**) (**Figure 5**).[78] In the presence of the small molecule, levels of phosphorylated smad 2 and 3 decreased and the number of differentiated cells increased. Expression levels of transcriptional regulator TAZ, was also identified to have an effect on pluripotency of hESC, by the regulation of the phosphorylated smads.[79] In the presence of transcriptional regulator TAZ, p-smad 2 and 3 were translocated into the nucleus. On the contrary in the absence of TAZ, nuclear translocation of the smad complex did not take place and differentiation was promoted.

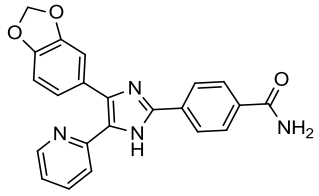

26
SB431542

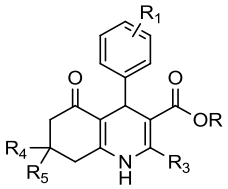

26a
1,4 Dihydropyridines

Figure 5 Structure of TGF-β antagonist SB431542 (**26**) and 1, 4 DHP

The most studied ligands of the TGF-β receptors are nodal and activin. These were found to have significant influences in the propagation and development of stem cells.[80,81,82] The regulation of the pathway with these TGF-β superfamily proteins was found to have an effect in mesoderm and endoderm formation, where knockout of the nodal gene suppressed mesoderm formation.[83,84] The regulation of the TGF-β signalling pathway has been shown to have an important effect in the regulation of early developmental stages of stem cell development and in the differentiation process. Additionally a recent study identified 1,4-dihydropyridines **26a** (1,4 DHP), a new class of TGF-β receptor inhibitors, to stimulate cardiomyocyte differentiation in murine ESC (**Figure 5**).[85] Interestingly, the mode of action of DHP's involves promotion of TGF-β receptor type II degradation by directing the receptor to proteosomes, which are responsible for protein breakdown. The strong TGF-β signalling inhibition led to the increased cardiogenic differentiation activity *in vitro*.

Within the family of the TGF-β there is the BMP subfamily, which will be the focus of the research in this project.

2.4.1 The BMP Signalling Pathway

The BMP signalling pathway is part of the TGF-β superfamily and has been identified to be crucial to the self-renewal and differentiation of embryonic stem cells.[86] The pathway which enables BMP to control cell fate, is activated by ligands binding to the heteromeric type I/type II serine/threonine receptor complex (**Figure 6**).[87] BMP does not have high binding affinity to the type I receptor and even less for the type II receptor.[88] It has been

discovered that a pre-assembled receptor complex of type I and type II is required to provide high binding affinity to the BMP ligands. Upon ligand binding to the receptor complex the type II receptor phosphorylates the type I receptor predominantly on serine and threonine residues which initiates a downstream response. The bound BMP receptor complex then phosphorylates intracellular regulatory smad (R-smad 1, 5 and 8) proteins which consequently bind to Co-smad-4. Another class of smad proteins can act as pathway inhibitors, these were named inhibitory smads (I-smads 6 and 7). Assembly of the p-smads and co-smad generate the heteromeric complex which subsequently translocates into the nucleus where it regulates transcription of target genes.[89] Regulation of smad signalling has been shown to have a significant effect on stem cell fate and the expression of differentiation 1 (Id1) gene.[90,91] Therefore, regulation of the BMP signalling pathway would lead to a control of stem cell lineage commitment.

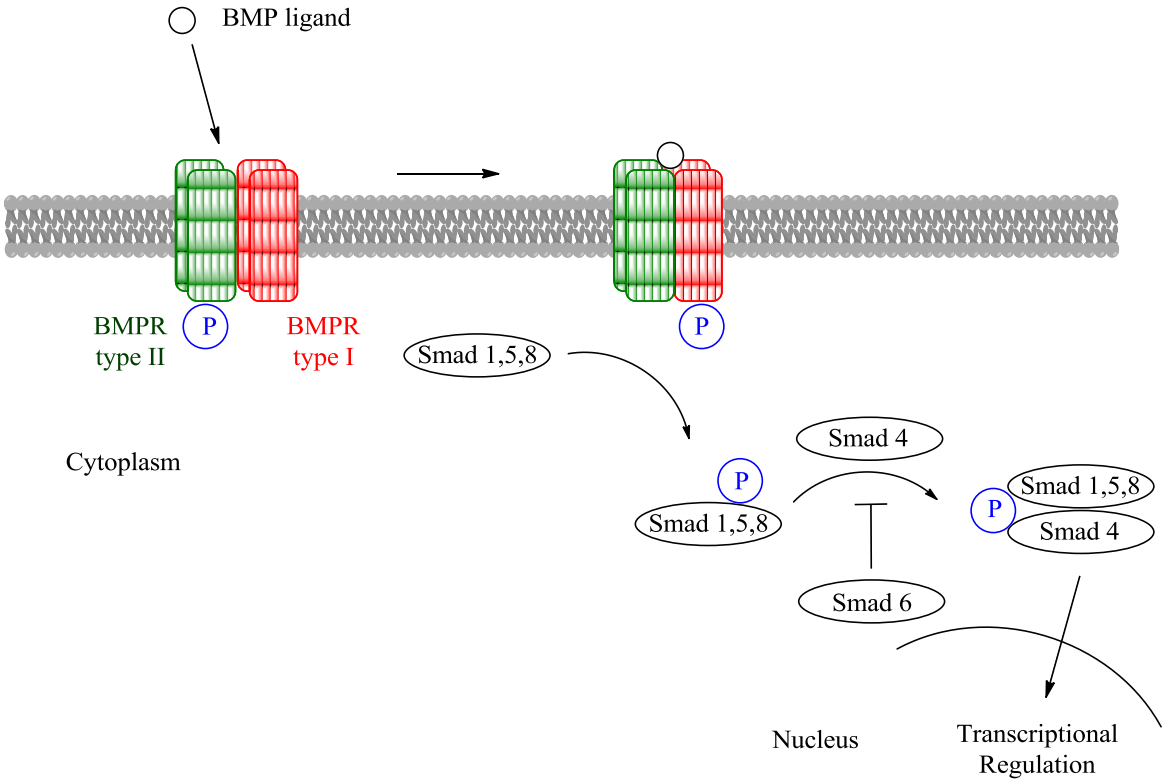

Figure 6 Outline of the signal transduction by BMPR. Heteromeric complex formation followed by high affinity ligand binding initiate's intracellular smad phosphorylation of R-smads 1, 5 or 8 and complexation to Co-smad4. The complex translocates into the nucleus to affect gene expression. I-smad 6/7 acts as a pathway inhibitor of smad complexation and subsequent nuclear migration

2.4.2 The BMPs in Stem Cell Differentiation

To date, a total of twenty different BMPs have been identified. Whilst most of them belong to the TGF-β superfamily, BMP-1 was recognized to function as a metalloprotease in the development of cartilage and does not belong to the TGF-β superfamily.[92] BMP-2 and BMP-4 were found to be expressed in osteoblasts and promote differentiation of bone formation during embryogenesis.[93,94] Addition of the small molecules, phenamil (**27**), was found to work in synergy with BMP-4 to induce osteogenesis in mesenchymal stem cells (**Figure 7**).[69] **27** was found to promote expression of tribbles homolog 3 (Trb3) which degraded the smad-ubiquitin regulatory factor 1 allowing for control of smad expression *via* the BMP pathway. Another class of small molecules discovered by Guo *et al* was found to increase expression of BMP-2 *in vitro*, these were benzothiophene and benzofuran derivatives.[95] After administration of benzofuran (**28**) and benzothiophene (**29**) in mice with osteoporosis, upregulation (UpR) of BMP-2 signalling and an increase in bone mass was observed.

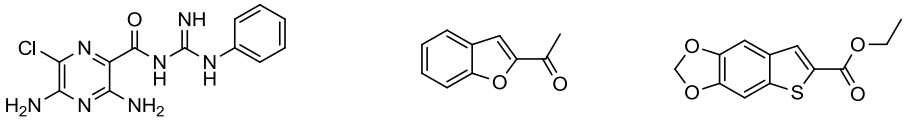

27 Phenamil

28 UpR 33.5 %

29 UpR 64.2 %

Figure 7 Phenamil (**27**) and examples of the benzofuran (**28**) and benzothiophene (**29**) derivatives which were found to upregulate BMP-2 expression

Additionally, the development of muscle tissue in vertebrates was also discovered to be dependent on BMP-4 activation.[96] This demonstrates the multifunctional nature of BMPs in regulating stem cell fate, which further extends from osteogenesis to have involvement in adipogenesis, development of fat cells, and cardiomyogenesis.

2.4.2.1 BMPs in Cardiomyogenesis

Activation of the BMP signalling pathway can either induce differentiation of stem cells, using BMP-4, or promote retention of pluripotency with the use of BMP-2.[97,98] In addition, regulation of BMP signalling controls cell proliferation and apoptosis.[99,100,86]

Cardiomyocyte development can either be promoted or inhibited depending on the time at which BMPs were added or removed. Inactivation of the gene encoding BMP, led to either death of the embryo or to a less developed embryonic mesoderm.[101] The mesoderm, the middle layer of the embryo, has been shown to differentiate to cardiac lineage and is responsible for heart formation. It was also noted that during mesodermal pattern formation in the embryonic development, BMP-4 and BMP-2 were expressed at high levels.[102] To verify the involvement of BMPs, noggin which exhibits antagonist activity by binding to BMP-2 and BMP-4, was incubated with the stem cells leading to inhibited growth of the mesoderm, strongly supporting the suspected involvement of BMP signalling in mesoderm formation.[103,104,97] Many biological studies to date have investigated the participation of BMP signalling in stem cell differentiation using BMP antagonists. Gremlin has been shown to also bind to BMP-2 and BMP-4 and prevent their receptor binding.[105] It was observed that BMP inhibition with the use of Gremlin was crucial in kidney and lung development. Another example of an antagonist of the BMP pathway is Chordin which similarly to Gremlin and Noggin, binds to the BMP protein and prevents its binding to the receptor complex.[106] The use of antagonists has provided a lot of insight into the importance of the activity of the BMP pathway in tissue formation and development.

2.4.3 Small Molecules Binding to the BMPR and Regulating Differentiation

The first reported selective small molecule acting as a BMP pathway inhibitor was identified in 2008 by Hong *et al*.[107] Compound C (dorsomorphin, **30**) was originally discovered as an AMP-activated protein kinase inhibitor (AMPK) in a high throughput screen and more recently used in cancer therapy.[108,109] The activity of **30** on BMP signalling was identified by measuring the growth of the dorsoventral axis of zebrafish, which has been found to be influenced by BMP signalling. Stunted development was observed with administration of **30** which was subsequently identified as a BMP antagonist.[64] Inhibition of BMP signalling results in dorsolization, which is the development of dorsal, tail, structures over ventral ones. The study also observed, supporting previous observations, that addition of dorsomorphin inhibits osteoblast differentiation which is mediated through the BMP pathway. Dorsomorphin was further studied in connection to the BMP pathway inducing myocardial differentiation.[62] During the early stages (24 h) of mouse embryonic stem cell development it was noticed that cardiomyogenesis was increased by 20-fold with the addition of the BMP inhibitor. Therefore, cardiomyogenesis appears to be controlled by the time point at which the addition of the ligand is made and type of response the ligand exhibits on BMP signalling. Having identified a BMP inhibitor molecule with the desired effects *in vivo* and *in vitro*, optimisation to a more active and efficient molecule was attempted.

SAR studies around dorsomorphin (**30**) were carried out by Cuny *et al*, identifying the pyrazolo pyrimidine core to be essential for BMP activity (**Figure 8**).[110] Optimisation at the C(4) position to a quinoline and the addition of a phenyl piperazine at the C(8) position led to the discovery of a more potent BMP inhibitor, LDN-193189 (**33**) (EC_{50} 4.9 nM). **33** yielded an activity over 100 fold more than that of dorsomorphin and was void of AMPK activity.

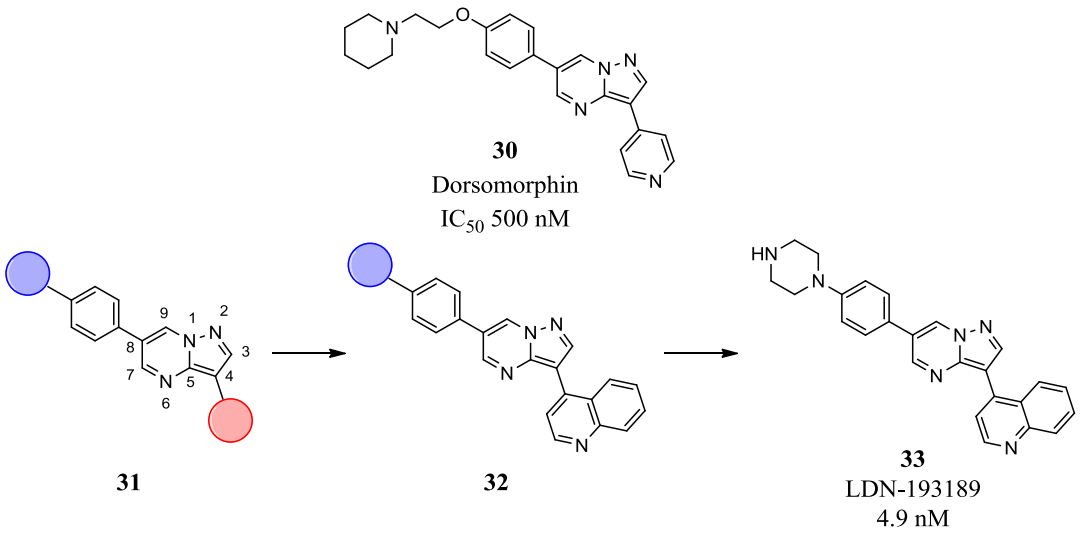

Figure 8 The structure of the parent compound, Dorsomorphin (**30**) and SAR progression, introducing the quinoline and phenyl piperazine onto the pyrazolo pyrimidine core led to the discovery LDN-193189 (**33**)

Experiments studying the effect of addition of LDN-193189 **33** displayed a similar effect to its parent compound dorsomorphin.[111] Phosphorylation of smad 1, 5 and 8 was inhibited and bone formation was reduced during treatment with the BMP inhibitor. It was observed that ectopic bone formation was nearly completely eliminated in mouse models when treated with LDN-193189 (**33**).[64,112]

While BMP antagonism at very early stages of ESC differentiation promotes cardiomyogenesis, it is well established that BMP stimulation is required at later stages to promote cardiac lineage formation, consistent with developmental cues present *in vivo* (*vide supra*).[324, 325]

To date several small molecule BMP antagonists such as **30** and **33** have been discovered, but BMP agonists have yet to be identified.[113,105,107] The current treatment involving the addition of recombinant BMP-4 protein is expensive and inefficient for scale up. As identified in multiple studies (*vide supra*) the role of BMP pathway activation is crucial at many stages in the development of mature cardiomyocytes (**Figure 9**).[114] Developing a BMP agonist would allow for the differentiation of stem cells to cardiomyocytes by the activation of the BMP pathway at the correct time point in the differentiation process and

provide for a novel therapy for formation regenerated cardiac tissue. The appeal in identifying a BMP agonist, lies in the application of such a molecule in regenerative medicine. Antagonists of the receptor have already been developed and studied, but not much research has been carried out using agonists. A reason for this is the lack of selective agonists, and the cost of the current standard, namely recombinant BMP. Identifying new BMP agonists would provide an interesting research area in terms of acessing a new domain in intellectual property and developing the first BMP selective agonists for the use in stem cell differentiation.

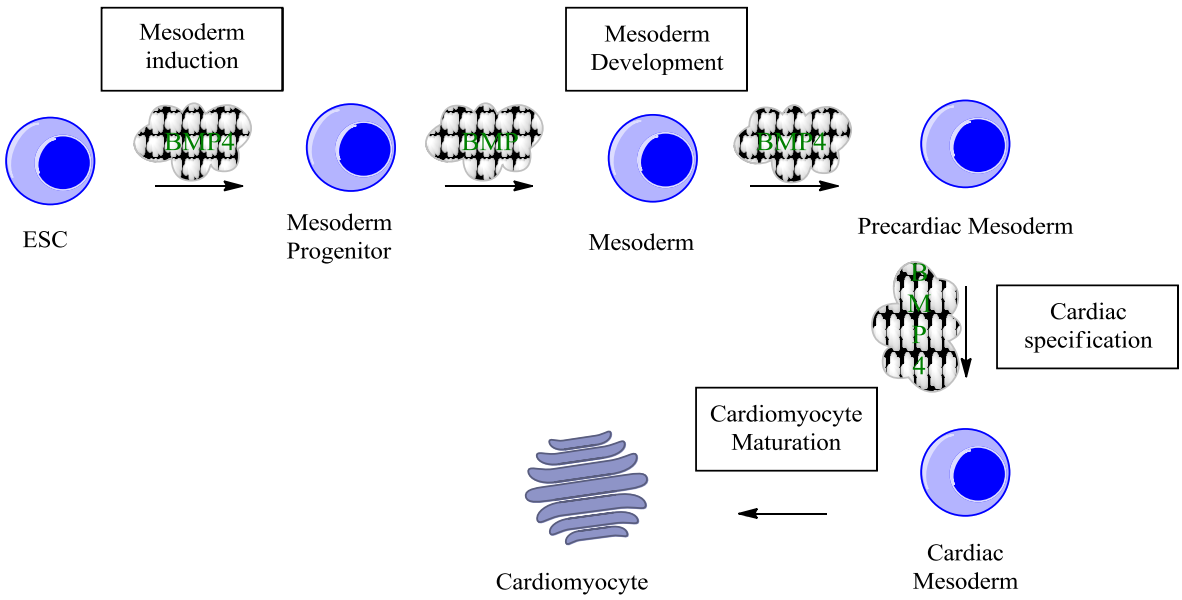

Figure 9 An outline of the steps involved in embryonic stem cells to terminally differentiated cardiomyocytes, indicating the many stages at which BMPs are responsible in directing stem cell fate

2.5 Cardiomyogenesis and Myocardial Infarcts

This frequent involvement of the BMP pathway in stem cell differentiation pattern makes it a very interesting target for identifying regulatory small molecules. Directing stem cells toward a cardiac muscle cell in regenerative medicine could be of huge value as the heart has a very limited ability to repair damaged or lost cardiomyocytes. A therapy to replace

fibrotic tissue in the heart would provide a life-changing opportunity to patients having suffered myocardial infarctions.

2.6 Project Aim

Activation of the BMP pathway was discovered to have an *in vivo* application to replace fibrotic scar tissue and improve heart efficiency after myocardial infarction. The vast involvement of the BMP pathway at multiple stages in the development process has made it an appealing target for future advances in regenerative medicine. Especially, with the use of ligands activating the BMP pathway and promoting differentiation of stem cells to beating exogenous cardiomyocytes. The replacement of growth factors with cost effective and accessible small molecules would allow for precise control of a stimulus at a desired time point in the differentiation process. The aim of this project is to establish a robust and reliable method of testing small molecules that influence expression of BMP pathway dependent gene markers. The small molecules could be controlling protein expression *via* the BMP pathway of alternatively influence different regulatory mechanism leading to effects on gene expression. Following the identification of an active small molecule, a method of stem cell differentiation to a cardiac lineage without the use of growth factors and recombinant BMP-4 protein would be evaluated. This in turn would potentially enable the culture of exogenous cardiomyocytes on a large scale and possible promotion of endogenous stem cells to cardiomyocytes in use for treatment of patients having suffered from myocardial infarction.

Chapter 3: The Discovery of new BMP Pathway Agonist

3.1 BMP and Myocardial Infarction

This following study aims at identifying novel agonist small molecules acting on the BMP pathway, which would allow for a cheaper and more efficient method of differentiating stem cells to cardiomyocytes and replacing current methods of *in vitro* lineage determination using growth factors. Ultimately, the goal is to translate the BMP pathway activation into promoting cardiomyogenesis of stem cells and applying this in the treatment of regenerating areas of the heart covered by fibrotic tissue. Using a range of screening tools, compounds influencing the BMP pathway were investigated to identify new agonists of the pathway. The first method employed was using the zebrafish embryos and observation of developmental gene expression levels *in vivo*.

3.2 Zebrafish Assay

The zebrafish (*Danio rerio*), is a small freshwater fish and provides a well studied model which has been used to investigate compound toxicity and embryonic development (**Figure 1**).[115] An example of a previous study employing zebrafish embryos to investigate gene expression, was of T-box (*Tbx*) 6 by Wnt and BMP pathway activation in embryonic development.[116] The embryos of the zebrafish are transparent and develop externally making them a suitable tool for a 96 well format and adaptive for miniaturisation. The zebrafish assay provides a cheap and fast method with a short reproductive cycle and low maintenance costs for rapid visual assessment of drug administration on development and gene expression of early stages of embryogenesis.

Using the zebrafish embryos, molecules identified as possible BMP activators were tested and the development of the dorsoventral axis and expression of three genes downstream of BMP was observed. *Fli*1, *Gata*1 and *Tbx*20, were found to be expressed after BMP activation however, not all are essential in the development of the heart. Friend leukemia integration 1 (*Fli*1) was identified to be crucial in haemangioblast formation.[117] *Gata*1 expression was identified to influence differentiation to erythroid specific lineage.[118] Finally, expression of *Tbx*20 was discovered to regulate cardiac stem cell development.[119] The degree of gene expression patterns was compared to BMP activated mutants (chordino mutants) (**Figure 1**). Chordin, a BMP antagonist was made unavailable in the chordino mutants by a loss-of-function mutation of the chordin gene, resulting in an increased level of BMP pathway activation and downstream gene expression.[120] Using a labelled complimentary RNA strand, the gene transcripts were visualised by antibody binding to the RNA probe. This method is called *in situ* hybridisation and allows for the visualisation of temporal and spatial gene expression patterns by detecting corresponding RNAs.

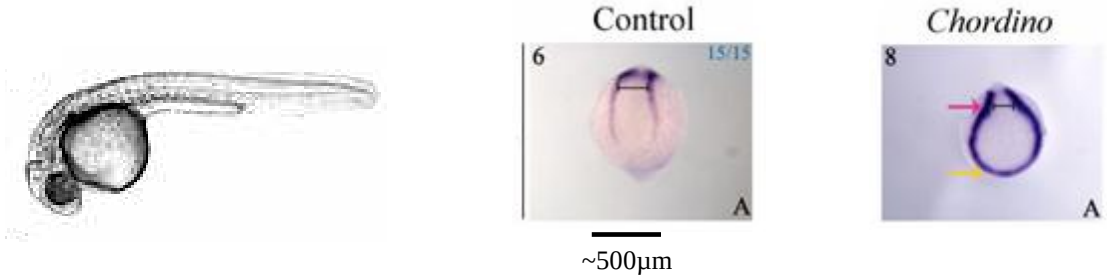

Figure 1 Zebrafish embryo, image on left hand. Pictures on right hand, embryos displaying *Fli1* gene expression patterns using in situ hybridisation method, in control (wt, embryo 15 of 15) and the positive BMP activated *chordino* mutant. Red and yellow arrows denote points of interest with BMP pathway activation displaying areas of increased *Fli1* expression. More pronounced staining signifies higher levels of mRNA expression levels[121]

Having identified an assay which would allow for the identification of molecules by the observed expression levels of BMP responsive genes, suitable compounds had to be selected for screening. By recognising what amino acid residues on the BMP ligand are essential in the binding to the BMP receptor target, structural mimetics could be generated

based on the spatial arrangement of the residues and subsequently used to search a compound database for similar compounds.

3.2.1 Generation of a Putative Peptidomimetic

Two amino acids on BMP-2 were identified to be crucial for binding at the BMPR type II as mutations at the alanine 34 (ala34) to aspartic acid (A34D) and leucine 90 (leu90) to alanine (L90A), showed reduced binding to the BMPR II (green in bold, **Figure 2** (**A**)).[122,123] These amino acids were used as a template in a ligand-based *in silico* screen using rapid overlay of chemical structures (ROCS).[124] ROCS uses a method of virtual screening of a target against a library of virtual compounds by shape comparison. It permits a quick and effective overlay of chemical structures to identify new potential lead molecules.[125,126]

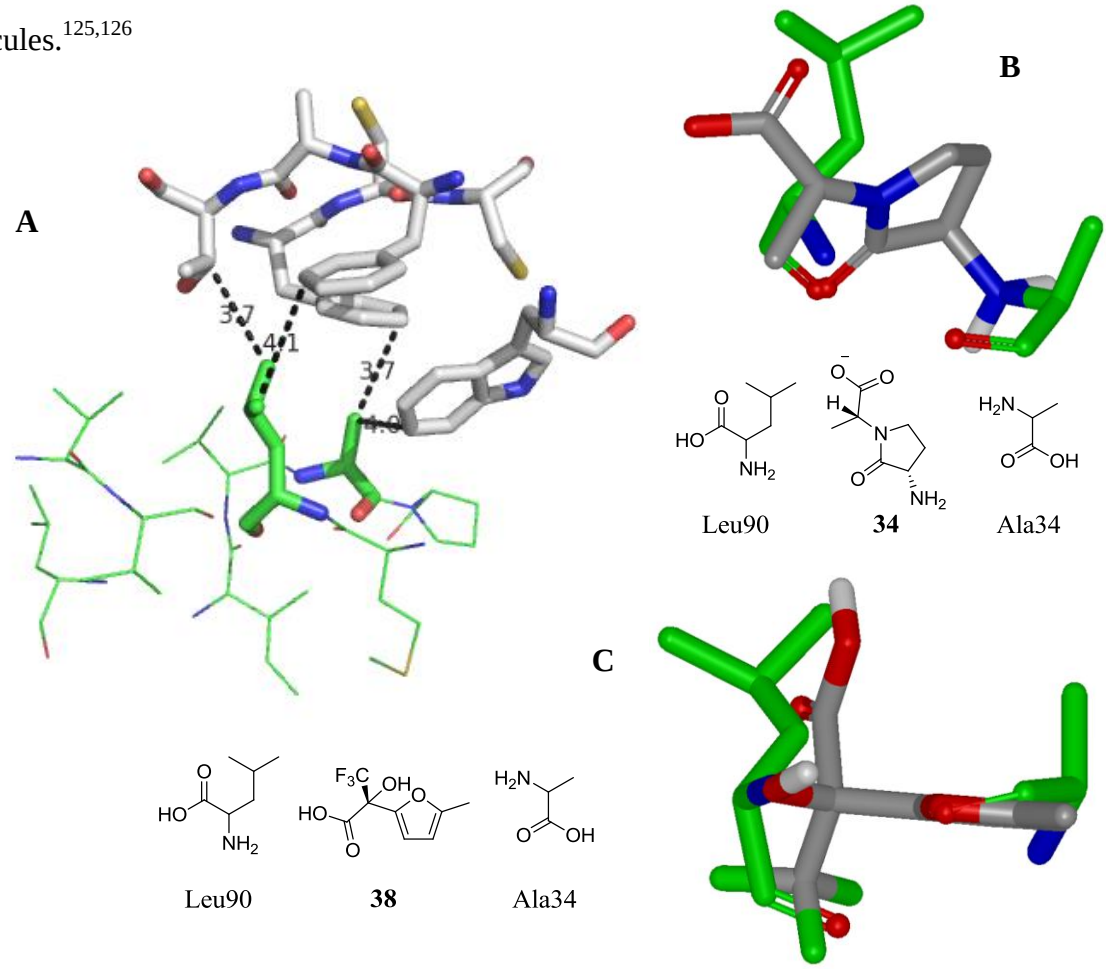

Figure 2 Crystal structure of the BMP-2 protein (green) with the ala34 and leu90 in bold. Interactions to the BMPR II receptor (grey) with the ligand indicated by the yellow dotted lines with distances in Å (**A**). Peptidomimetic (**34**) overlay with the two amino acid residues (**B**) and with the furan (**38**) (**C**)

After completing the ROCS *in silico* screen against a library of peptidomimetics, the pyrrolidinone **34** was identified to provide a good overlay against the two amino acid residues (**Figure 2** (**B**)). Although the overlay displays some mismatch, the polar residues of the amine of **34** and the alanine overlay. Additionally, the amide in **34** is in close proximity with the polar groups on leucine 90. This permits the hydrophobic side of **34** to be exposed to the solvent, which is exposed to hydrophobic residues on the BMP binding protein. Finally, the carboxylate mimics the features of the isopropyl on the leucine residue. Similarly the polar residues of (-)**38** overlay the ones of the BMPR binding site. The in-house library of 25,000 compounds was then screened against the peptide mimetic to identify small molecules with displaying good overlay.

The compounds were ranked by the combo score which is obtained by the addition of two calculated parameters; Tanimoto coefficient (shape Tanimoto score) and scaled colour (colour score) (**Figure 3**).[127,124] The colour score is a calculated parameter which assesses the chemical and pharmacophore matching of the molecules, while the Tanimoto score provides an overview of the shape alignment of the molecules.

Colour Score + **Shape Tanimoto Score** = **Combo Score**

Figure 3 Calculation of combo score by combination of colour and tanimoto score

Template	Rank	Cmpd #	Structure	Shape Tanimoto	Scaled colour	Combo score
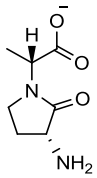 **34**	1	**35**	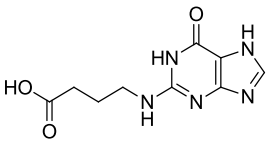	0.725	0.790	1.515
	2	**36**	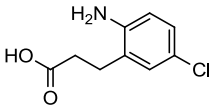	0.792	0.682	1.474
	3	**37**	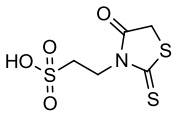	0.859	0.602	1.461
	4	(–)**38**	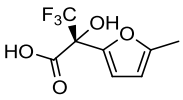	0.805	0.605	1.410

Table 1 Peptide mimetic (**34**) discovered and top four ranked compounds from the ligand type based virtual screen ranked on the basis of their combo score (shape tanimoto + scaled colour)

3.2.2 *In vivo* Testing of Hits

The top 15 compounds that emerged from the virtual screen were tested in the zebrafish assay and led to the identification of (–)3,3,3-trifluoro-2-hydroxy-2-(5-methylfuran-2-yl)propanoic acid ((–)**38**, 10 µM) as a potential enhancer of BMP signalling.[121] Overlay of (–)**38** with the peptidomimetic **34** displayed a close fit (**Figure 4**). The furan ring overlays onto the pyrrolidinone and both of the carboxylic acid moieties are virtually superimposable.

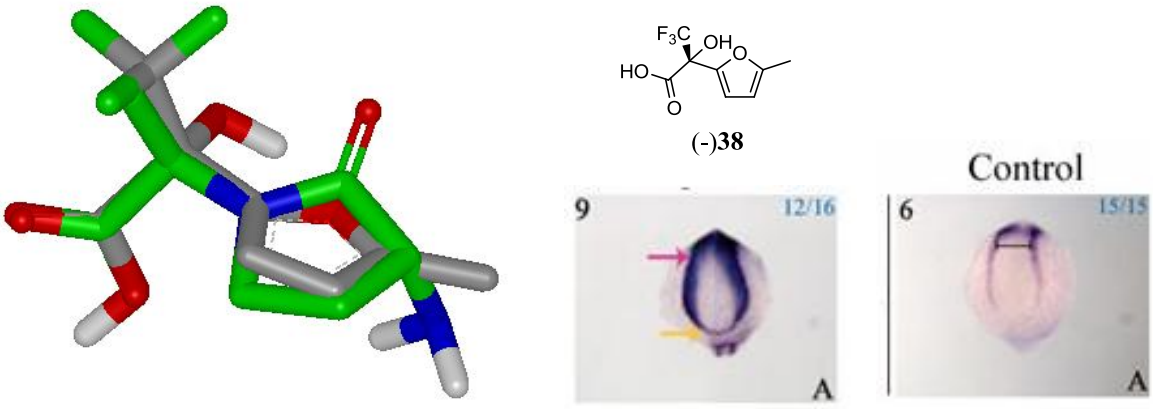

Figure 4 Overlay of the peptidomimetic **34** and compound (–)**38**, the *Fli*1 expression pattern in zebrafish embryos when treated with **38** (embryo 12 of 16), red and yellow arrow denote points of interest with BMP pathway activation displaying areas of increased *Fli*1 expression, and the control (wt, embryo 15 of 15).

However, the zebrafish assay does not provide conclusive data, in that an increase expression of *Fli*1 with the treatment of the racemic (–)**38**, is indeed exhibited due activation of the BMP pathway or *via* to binding to BMPR. A more precise assay measuring activity of the BMP pathway would be required to verify that the elevated gene expression is not caused by an off-target effect. Other pathways regulating expression of *Gata*1, *Tbx*1 and *Fli*1 such as the FGF and TGF-β pathway could be the target of the small molecule. To confirm the activity of **38**, a racemic solid sample was synthesised along with a range of structural analogues of **38** for preliminary SAR development and investigations into pathway specificity.

The synthesis of (±)**38** was carried out *via* a solvent free electrophilic substitution of 2-methyl furan (**39**) with 3,3,3-ethyl trifluoropyruvate to yield the ester (**40**).[128] Subsequent base mediated hydrolysis using sodium hydroxide yielded the sodium carboxylate salt **41** (**Scheme 1**).

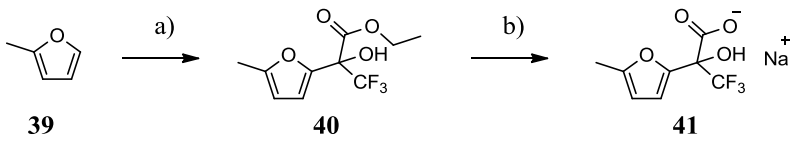

Scheme 1 Synthesis of a solid sample of (±)**38** a) ethyl 3,3,3-trifluoro-2-oxopropanoate, rt 16 h, 68% b) NaOH, MeOH, rt 16 h, 98%

3.3 Library Synthesis around (±)38

3.3.1 Possible SAR around (±)38

Having identified **38** to promote BMP-dependent gene markers, the molecule was dissected to investigate what functionalities could prove to be essential in providing the observed activity. **Figure 5** outlines the possible points of diversification on **42**. With changes affecting the H-bonding character and steric properties of the molecule, a library of compounds was developed to provide an understanding of the functionality involved in providing the observed activity in the zebrafish assay.

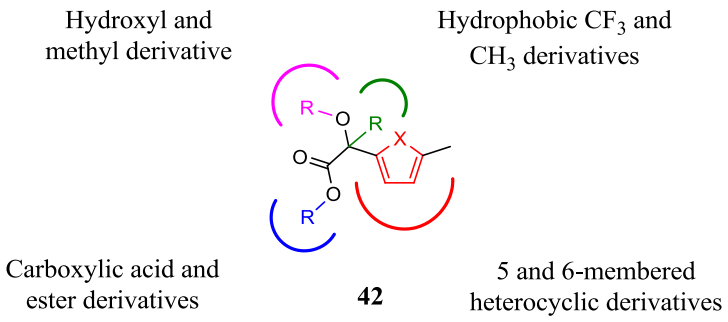

Figure 5 Possible points of diversification around the structure of **42**

3.3.2 5-Membered Ring Analogues

The first focus was to maintain the furan ring and vary the side chains (**Figure 5**, R-groups). The carboxylic acid functionality could be interacting with the receptor *via* hydrogen bonding. Using the synthesis previously established (*vide supra*), the ester **40** and the carboxylate salt **41** were prepared to investigate the importance of the free acid in providing activity.

Furthermore, the hydroxyl functionality at the C(6) position could also be participating in H-bonding to the receptor. Therefore, hydroxyl alkylation could provide some insight into the importance of this functional group in providing the observed activity and confirm possible receptor interactions. Methyl alkylation of the hydroxyl group was attempted using a range of different bases and solvents in an effort to produce the *O*-methylated

compound **43** (**Scheme 2**). The only successful procedure involved a mild base and methyl iodide to provide **43** in low yield. Finally, the trifluoromethyl group was replaced by another ethyl ester **44** to provide further possible H-bonding interactions with the active site. Attempting to use ethyl 2-oxopropanoate in the electrophilic substitution, **45** was not isolated from the complex mixture, illustrating the requirement of an electron withdrawing group to undergo the electrophilic substitution on the neighbouring carbonyl. The derivatives would allow investigations into crucial interactions of the functional groups of the C(5) position side chain of 2-methylfuran.

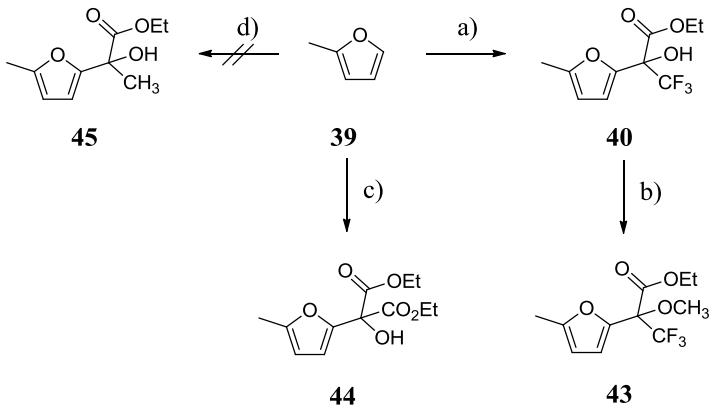

Scheme 2 Synthesis of 2-methylfurano derivatives a) ethyl 3,3,3-trifluoropyruvate, CH_2Cl_2, rt 16 h, 68% b) Et_3N, MeI, MeOH, rt 16 h, 28% c) diethyl 2-oxo malonate, 0 °C – rt 1.5 h, 71% d) ^nBuLi (2.5 M in hexanes), THF -78 °C – rt 1 h, ethyl pyruvate 1 h rt

Additionally, the furan ring was replaced with other 5-membered heterocycles to investigate the effect on size and electronic properties of the heterocyclic ring (**Scheme 3**). **47** was obtained by an electrophilic substitution with ethyl 3,3,3-trifluoro pyruvate, however required the addition of a Lewis acid, $SnCl_4$, to improve the yield. Subsequent base hydrolysis yielded **48** as the sodium carboxylate salt. The pyrrole **51** and methyl pyrrole **52** derivatives were synthesised *via* a catalyst and solvent free electrophilic substitution in high yield (**Scheme 4**).[129] Finally, base hydrolysis of the esters **51**, **52** provided the corresponding carboxylate salts **53**, **54** respectively.

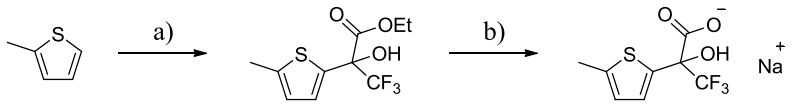

46 **47** **48**

Scheme 3 Synthesis of thiophene derivative **48** a) ethyl 3,3,3-trifluoro pyruvate, $SnCl_2$, CH_2Cl_2, rt 16 h, 78% b) NaOH, MeOH, rt 16 h, 96%

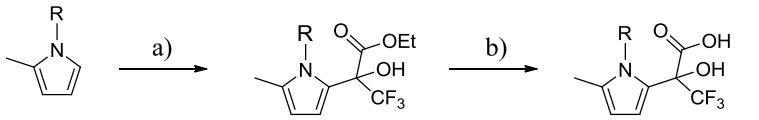

49 R = H
50 R = CH_3
51 R = H 89%
52 R = CH_3 92%
53 R = H 97%
54 R = CH_3 88%

Scheme 4 Synthesis of pyrolo derivatives a) ethyl 3,3,3-trifluoro pyruvate, rt 2 h b) NaOH, MeOH, rt 16 h

A small representative library of derivatives of (±)**38** was developed. Further modifications replacing the 5 with 6-membered rings were investigated.

3.3.3 6-Membered Ring Analogues

Using isosteres of furan and thiophene such as benzene and pyridine, would provide an overview whether size and presence of the heteroatom plays a crucial role in providing activity. 6-Membered ring derivatives were synthesised in good yield *via* Grignard reactions using either phenyl magnesium bromide (**55**) or 2-pyridyl magnesium bromide (**61**) (**Scheme 5 and 6**). **55** was treated with the corresponding ethyl esters to yield **57-60**. The pyridyl Grignard **61** was selected as it mimics the 2-substituted 5-membered heterocycles most and was prepared *in situ* with the addition of ^{i}PrMgCl to 2-bromopyridine (**56**), which was subsequently treated with ethyl 3,3,3-trifluoropyruvate to yield **62** (**Scheme 6**). The corresponding carboxylate salts **63-67** were obtained by base hydrolysis of esters **57-60** and **62**.

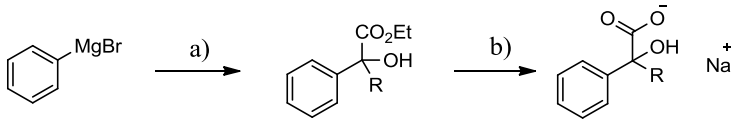

55

57 R = CF_3	73%	**63** R = CF_3	94%
58 R = CH_3	83%	**64** R = CH_3	97%
59 R = 2-thienyl	30%	**65** R = 2-thienyl	93%
60 R = Ph	41%	**66** R = Ph	91%

Scheme 5 Synthesis of phenyl derivatives **63-66** a) $RC(O)CO_2Et$, -78 °C - rt b) NaOH, MeOH, rt 16 h

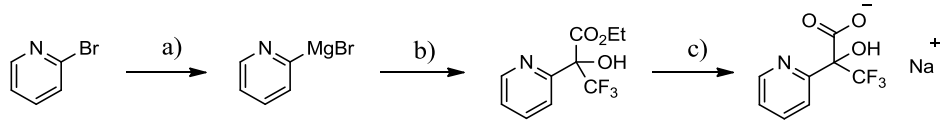

56 **61** **62** **67**

Scheme 6 Synthesis of **67** a) $^{i}PrMgCl$, Et_2O, -78 °C – rt 1 h b) Ethyl 3,3,3-trifluoro pyruvate, -78 °C - rt, 23% c) NaOH, MeOH, rt 16 h, 95%

The synthesis of an initial 19 compounds with structural variations would provide preliminary SAR into this compound series and the importance of the various functional groups. To test for activity of the compounds and for specificity for the BMP pathway, a suitable assay had to be developed.

3.4 Biological Assay Development

3.4.1 Protein Complimentary Assay

As outlined in the introduction, BMPR activation leads to the phosphorylation of intracellular receptor regulated mothers against decapentaplegic (R-smad) proteins. These phosphorylated proteins then couple to the common mediator smad 4 (Co-smad) protein to form a heterodimer complex which translocates into the nucleus. The first attempted method of measuring BMP activity was to establish a split luciferase protein complimentary assay (PCA) evaluating protein-protein interaction between R-Smad1, 5 or 8 and Co-Smad4. By covalent addition of one of the 2 parts of the renilla luciferase (RLuc) (8,1 or 8,2) one to the R-smad and the other half to the Co-smad, activity of the BMP pathway could be directly measured by bringing the two halves into close proximity,

generating the reconstituted protein complex, Rluc8. Rluc activity is measured through the oxidation of the Rluc substrate, coelenterazine, by the production of light (**Figure 6**). Renilla luciferase was the luciferase of choice due to its small size (36 kDa) and does not require addition of adenosine triphosphate (ATP) in the assay conditions. Examples in the literature have emphasised the potential of the split luciferase system in assessing protein-protein interactions, for example to measure association and dissociation of Rluc tagged proteins in protoblasts.[130]

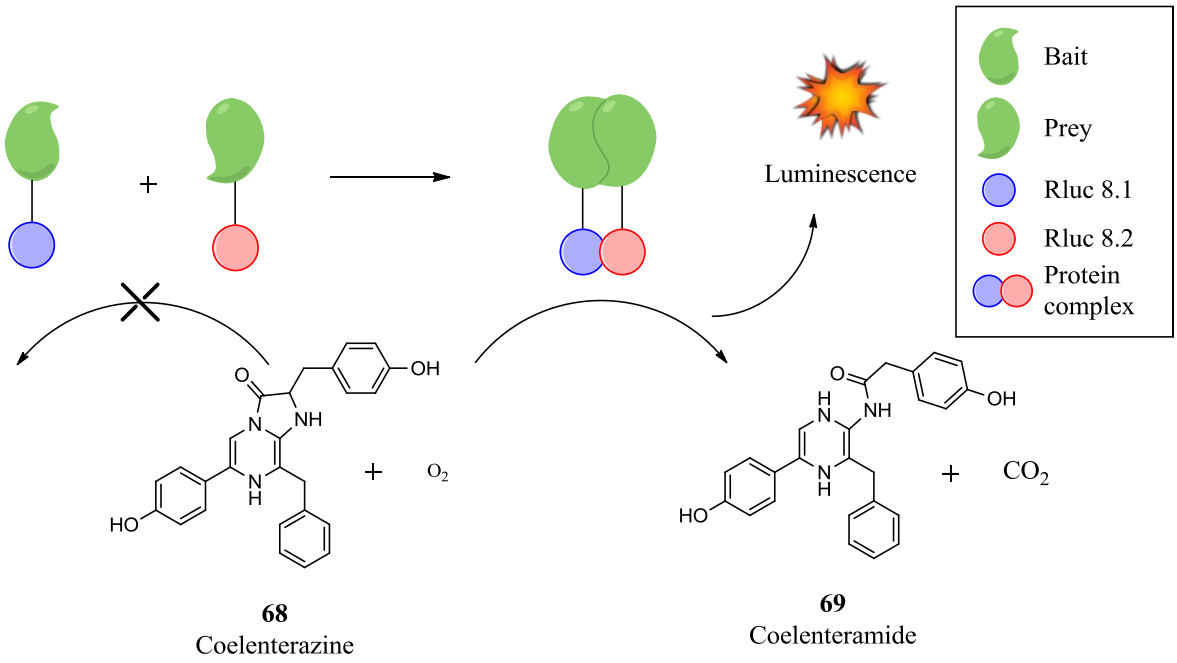

Figure 6 Overview of the PCA where the bait and the prey protein covalently linked to half of the Rluc 8 protein combine to generate the reconstituted renilla luciferase enzyme by protein dimerisation leading to oxidation of colelenterazine (**68**) to produce light and coelenteramide (**69**). No reaction takes place if proteins do not dimerise.

The expression vectors (**70**) containing half of the Rluc 8 subunits were assembled *via* a Gateway LR reaction using pCDNA3 entry vector containing a cytomegalovirus (CMV) promoter and two att R sites for the insertion of the fragment. Each entry vector also included in its sequence half of the Rluc 8 gene either at the amine terminus (NTR) or at the carboxylic acid terminus (CTR) of the protein produced by transcription and

subsequent mRNA translation (**Figure 7**). The combinations assembled are summarised in **Table 2**.

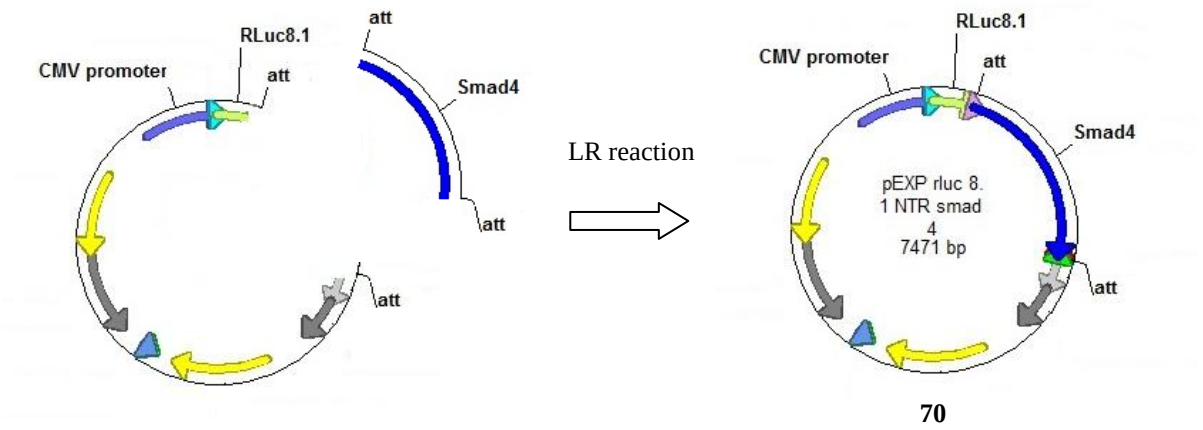

70

Figure 7 Example of a Gateway LR reaction combining the entry vector containing the CMV promoter and one half of Rluc 8 sequence. While the destination vector comprises of the smad gene sequence, together they generate the expression vectors (**70**) summarised in table 2

Co-smad	R-smad
Smad4 Rluc 8.1NTR	Smad1 Rluc 8.2NTR
	Smad1 Rluc 8.2CTR
Smad4 Rluc 8.1NTR	Smad5 Rluc 8.2NTR
	Smad5 Rluc 8.2CTR
Smad4 Rluc 8.1NTR	Smad8 Rluc 8.2NTR
	Smad8 Rluc 8.2CTR
Smad4 Rluc 8.2NTR	Smad1 Rluc 8.2NTR
	Smad1 Rluc 8.2CTR
Smad4 Rluc 8.2NTR	Smad5 Rluc 8.2NTR
	Smad5 Rluc 8.2CTR
Smad4 Rluc 8.2NTR	Smad8 Rluc 8.2NTR
	Smad8 Rluc 8.2CTR

Co-smad	R-smad
Smad4 Rluc 8.1CTR	Smad1 Rluc 8.2NTR
	Smad1 Rluc 8.2CTR
Smad4 Rluc 8.1CTR	Smad5 Rluc 8.2NTR
	Smad5 Rluc 8.2CTR
Smad4 Rluc 8.1CTR	Smad8 Rluc 8.2NTR
	Smad8 Rluc 8.2CTR
Smad4 Rluc 8.2CTR	Smad1 Rluc 8.2NTR
	Smad1 Rluc 8.2CTR
Smad4 Rluc 8.2CTR	Smad5 Rluc 8.2NTR
	Smad5 Rluc 8.2CTR
Smad4 Rluc 8.2CTR	Smad8 Rluc 8.2NTR
	Smad8 Rluc 8.2CTR

Table 2 Summary of possible combinations of transfection combinations of expression vectors (**70**) with the Co-smad and R-smad each containing half of the Rluc 8 gene at either the amine terminus (NTR) or carboxylic acid terminus (CTR) of the expressed protein

The assay always required the presence of the Co-smad4 and the R-smad (1, 5 or 8) to be co-transfected allows the two Rluc halves (8.1 and 8.2) to unite providing a signal. **Table 2** outlines the combinations that were attempted to provide the best readout with altering the position of the Rluc halves on the smad protein. With the generation of DNA plasmids

with the outlined combinations, the first cells to be transfected were HEK293T cells, a human embryonic kidney cell line along with a control plasmid, LacZ for transfection control, (**Figure 8**).

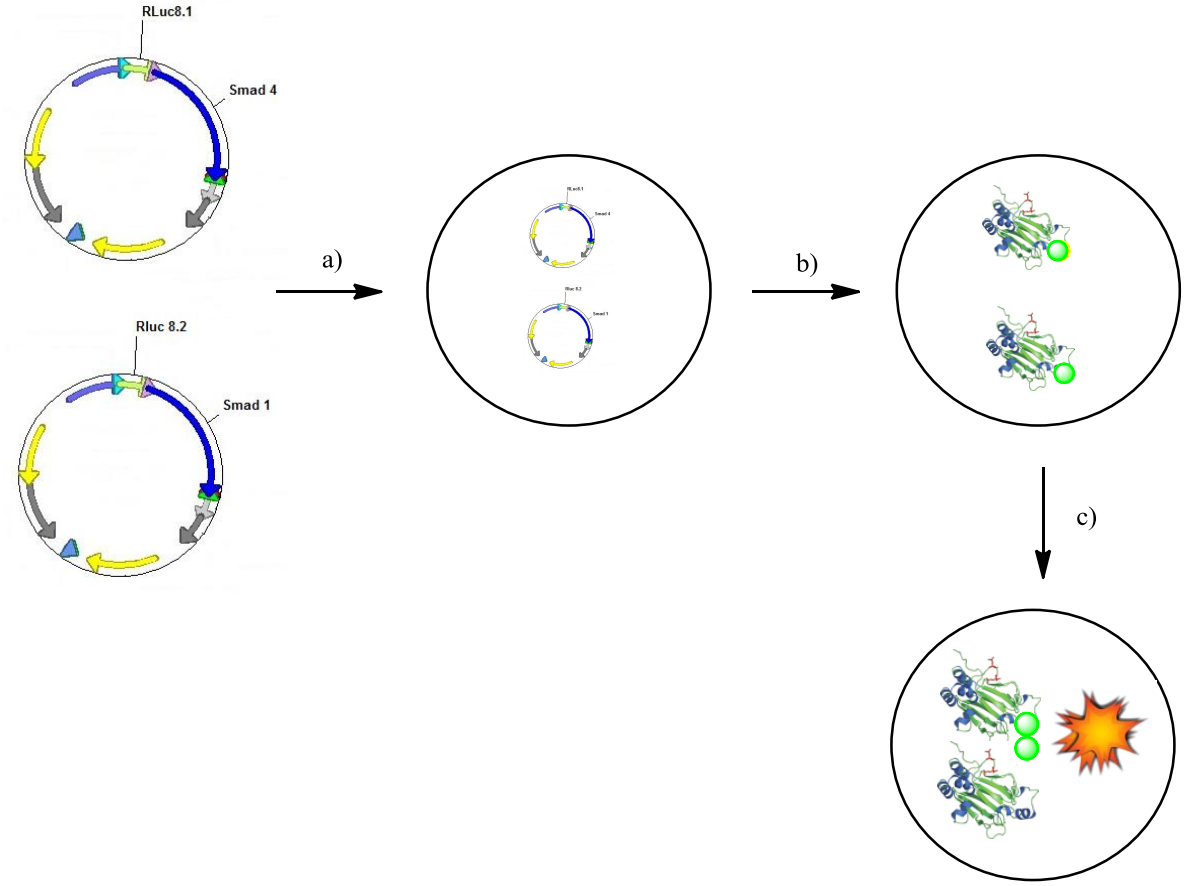

Figure 8 Outline of PCA protocol, a) transfection of plasmids into HEK293T cells b) overnight incubation allowed protein expression driven by the CMV promoter c) BMP pathway activation by stimulation with BMP-4 leads to smad dimerisation and reconstitution of the Rluc 8 halves. The intact Rluc 8 oxidises the substrate (coelenterazine) to generate luminescence

The assay, would allow the quantification of protein-protein interaction between R-smad and Co-smad4 by BMP pathway activation. Recombinant BMP-4 and BMP-2 protein were used as the positive controls to identify whether there was a significant difference in activity between the two isoforms. Preliminary results would anticipate ligand activated BMPR to produce a clear signal to noise ratio in the assay.

Unfortunately the results provided no significant difference in the luminescence reading

between the unstimulated cells and the BMP activated ones (**Figure 9**). A possible reason for the high levels of luminescence in the unstimulated cell could be the over-expression of the smad proteins as a result of high activity of the CMV promoter. The promoter is responsible for driving the expression of the particular gene, and if its activity is too pronounced, high concentrations of the proteins are present, providing a possible explanation for the high level of background luminescence. A possible solution would be to replace the CMV promoter with a less potent constitutive promoter or use a regulated promoter, which is only activated with a stimulus, to reduce the quantity of protein produced and reduce base activation levels.

Interestingly it can be noted that one combination; the smad4 protein with Rluc 8.2 and smad1 protein with the Rluc 8.1 both expressed at the amine terminus, provide a higher relative luminescence unit (RLU) reading of 900’000 (graph **C** in **Figure 9**) compared to the other three combinations (250,000-350,000). This combination displays a luminescence nearly 3 fold greater indicating toward a possible preference of Rluc position. However, even in this example the unstimulated cells still displayed equal levels of coelenterazine oxidation to the ligand treated cells. This indicates the possibility that even when the BMP pathway is not activated, smad proteins come into close enough proximity to reconstitute Rluc 8 activity. Alternatively, the affinity of the split luciferase halves is too strong and displays activity with no stimulation. Efforts to reduce the baseline luminescence produced had to be undertaken to make this assay work.

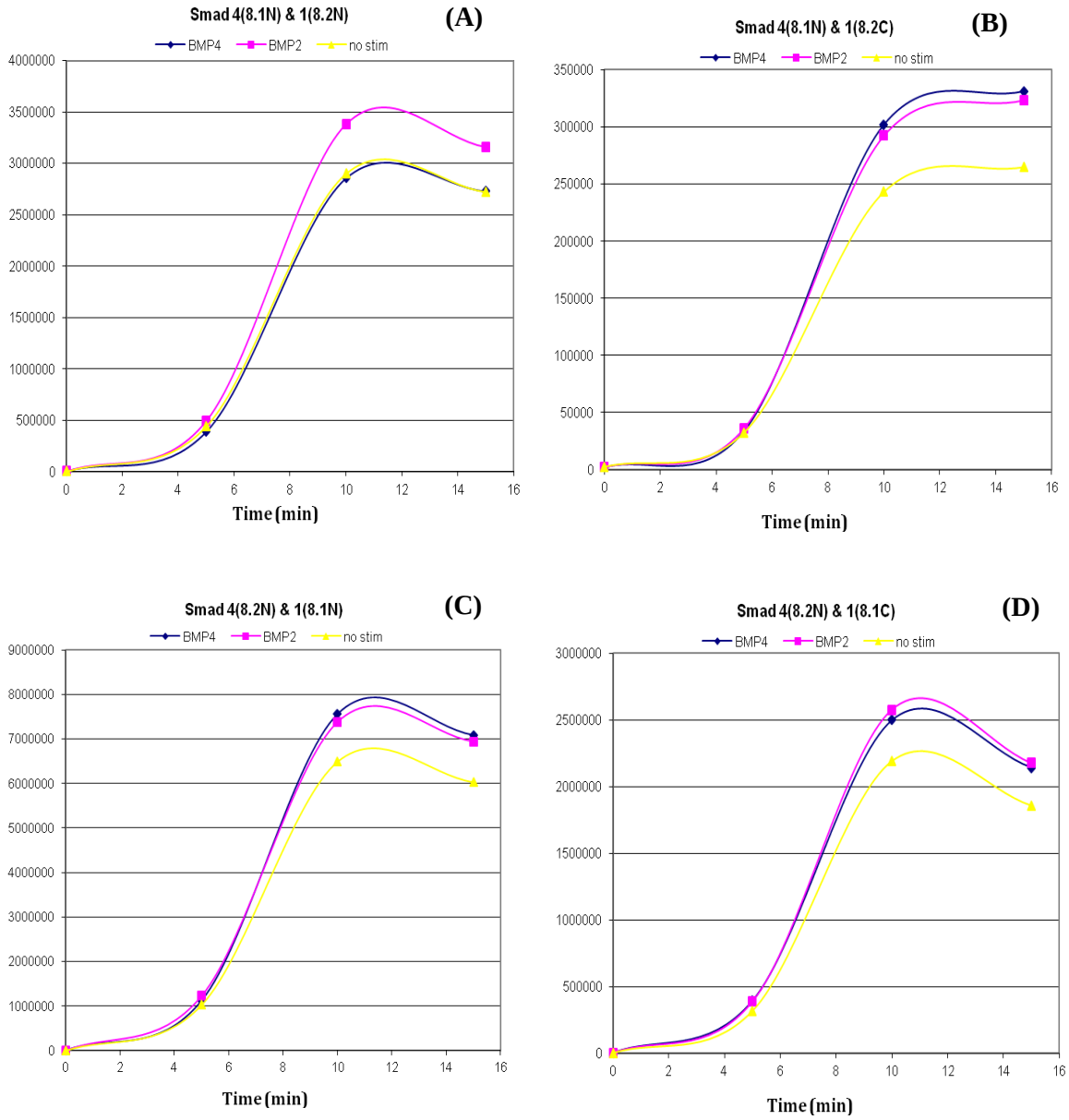

Figure 9 Relative luminescence units (RLU) of the four R-smad1 and Co-smad4 possibilities (**A-D**) transfected at 40 ng of each plasmid and stimulated with 10 ng/mL BMP protein

The first variation attempted to reduce the baseline expression of the Rluc tagged smads was to reduce the concentration of the transfected plasmids from 80 ng, to 40 ng and ultimately, as little as 20 ng final plasmid was transfected. 4 fold reduction of plasmid concentration still resulted in high background luminescence. Maintaining low levels of transfected plasmid, the stimulation of the cells using the BMPs were investigated across a range of BMP-4 and BMP-2 concentrations (1-150 ng/mL), also with no apparent effect. The cell line used was also varied from the HEK293T, to a mouse myoblast cell line

(C2C12) and a monkey kidney fibroblast line (COS7). A concern was the possibility of receptor concentration on the cell surface. Altering to another cell line could provide changes in BMPR on the cell surface and therefore a more sensitive assay for low concentrations of BMP ligand. However this also did not reduce the luminescence of the unstimulated cells. Finally, different incubation time (1-16 h) were tested and evaluated also to no effect. Following, the unsuccessful attempts to reduce background luminescence by variation of a range of parameters, the final attempt involved the use of different R-smads. Finally, measuring protein expression levels could provide insight into levels of the smad proteins, however this proved too time consuming to be undertaken at this early point in the project.

All the combinations of R-smads (1, 5 and 8) with Co-smad4 were attempted but as previously observed, protein expression in the unstimulated cells was too high to observe a good enough signal to noise ratio for further use. Even with the use of a BMP antagonist, dorsomorphin (**30**), luminescence was not reduced, supporting the hypothesis of high levels of protein expression. An alternative assay had to be developed to establish activity of small molecules on the BMP pathway.

3.4.2 Firefly Luciferase assay

The levels of protein expression and high luminescence in the Rluc bound luciferase assay forced an alternative method to be developed for screening of the small library of compounds. An alternative method involved a transiently transfected HEK293T cell line with a BMP-responsive element (BRE) attached to a firefly luciferase gene (Fluc) and cotransfected with renilla luciferase (Rluc8) for transfection efficiency control. The BREluc plasmid was kindly provided by Peter Ten Dijke and consisted of a PGL3 basics vector (Promega) and two BRE's driving expression of the Fluc gene (**Figure 10**).[131] The translocated smad dimer binds to the BRE in the nucleus which consequently initiates a

cascade of events starting with the transcription of the luciferase mRNA and leading to the expression of luciferase. This assay allows for quantitative assessment of BMP pathway dependent gene activation by the expression of luciferase, which in the assay converts luciferin (**71**) to oxyluciferin (**72**) releasing light, with the consumption of adenosine triphosphate (ATP) (**Figure 10**).

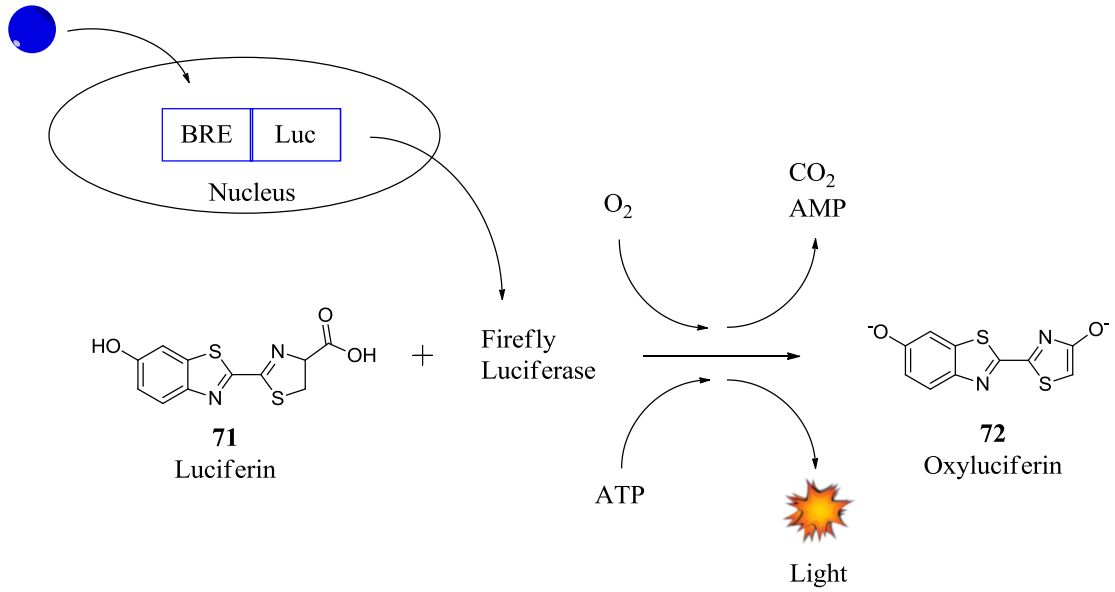

Figure 10 Outline of the process in which firefly luciferase oxidises luciferin (**71**) to produce light in the presence of ATP

After screening of a number of possible cell lines (HEK293T, COS7, C2C12), the most appropriate, C2C12 mouse myoblast cell line was transfected with a BREluc containing plasmid and validated with recombinant BMP-4 protein. The C2C12 cell line provided the best signal to noise ration with BMP-4 stimulation (**Figure 11**). BMP-4 was used as the positive control over other binding proteins and small molecules due to its high levels of BMP upregulation (UpR) of up to 20 fold from the baseline at concentrations of 10 ng/mL. The cells were incubated at 37 °C for 24 h, washed and lysed ($TrisPO_4$, CDTA, Glycerol, Triton-X 100 and water). The levels of luciferase were measured by addition of assay mixture (luciferin, ATP, DTT and water) and normalised to the protein concentration obtained from the absorbance reading using the Bradford assay. Dorsomorphin (**30**) was

used to confirm that BMP-4 activity can be attenuated and at high concentrations was shown to completely suppress the agonist signal of BMP-4 (**Figure 12**). **30** was discovered to block phosphorylation of the receptor but mode of interaction was not established.[107] Subsequent studies since conducting the virtual screen have shown the co-crystal structure analysis that **30** can bind to the intracellular ATP-binding pocket of the BMPR.

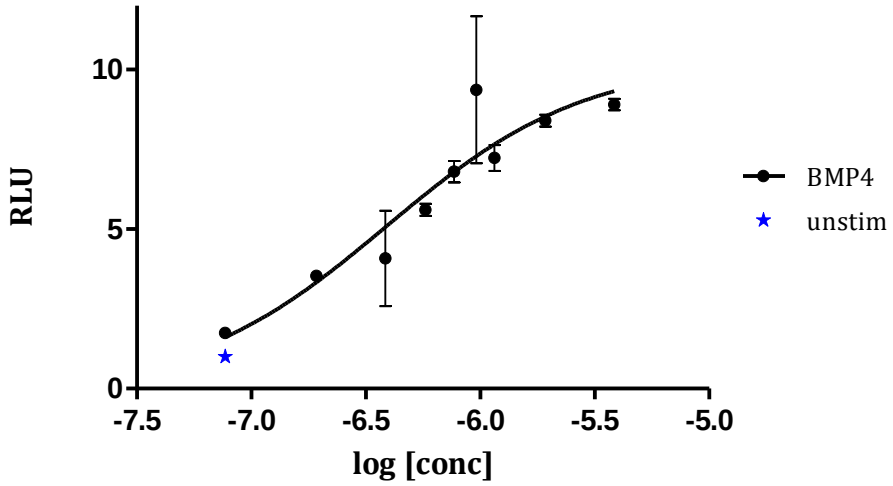

Figure 11 Dose response curve using BMPR agonist BMP-4 at concentrations of 1 ng/mL – 25 ng/mL in transiently transfected C2C12 mouse myoblast cells with the BREluc plasmid. Unstimulated (unstim) cells display Relative luminescence units (RLU) of 1.

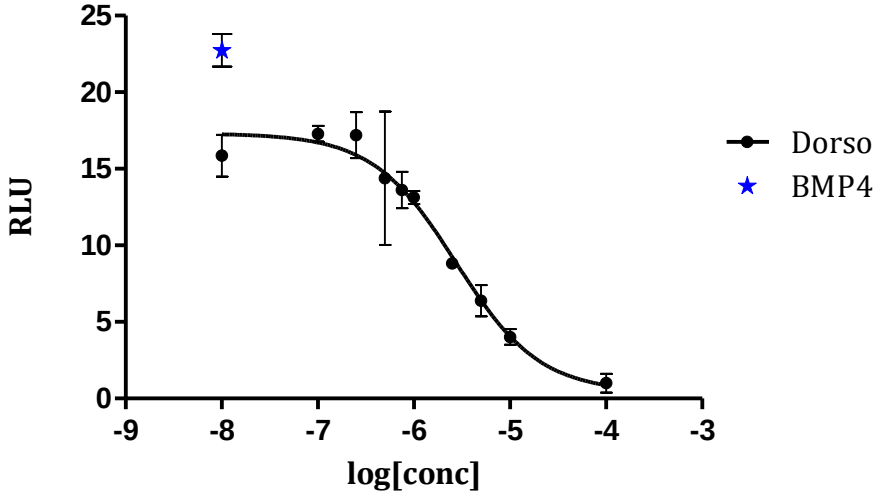

Figure 12 Dose response curve in relative luminescence units (RLU) of transiently transfected C2C12 cells lines with the BREluc plasmid, with BMPRI antagonist, Dorsomorphin (Dorso, **30**), at concentrations of 10 µM – 10 nM and addition of BMP-4 at 10 ng/mL to generate a base signal. Unstimulated cells display RLU of 1, and 10 ng/mL BMP-4 stimulated cells only, provide RLU of 20

Compounds identified through this method suffer the risk of displaying activity through modulation of the activity of the luciferase enzyme. Future control procedures to remove false positives could include competitive binding assays at the BMPR binding site with a known ligand, allowing the detection of leads that bind directly to the BMPR, as opposed to interfere downstream to the receptor. Additionally, a test with the enzyme and substrate could be established to detect the of target activity on the luciferase enzyme.

3.4.2.1 Compound Testing in Transiently Transfected Cells

Having established a luciferase assay with good signal to noise ratio, activity off the BMP pathway could be quantified. The small library of synthetic analogues of (±)**38**, which was identified to promote expression of gene markers *in vivo*, was evaluated in this assay. Unfortunately the compounds did not provide increased luminescence to the unstimulated cells, whereas the positive (BMP-4) and negative (Dorsomorphin, **30**) controls provided the expected signal activation and suppression of signal respectively (**Figure 13**).

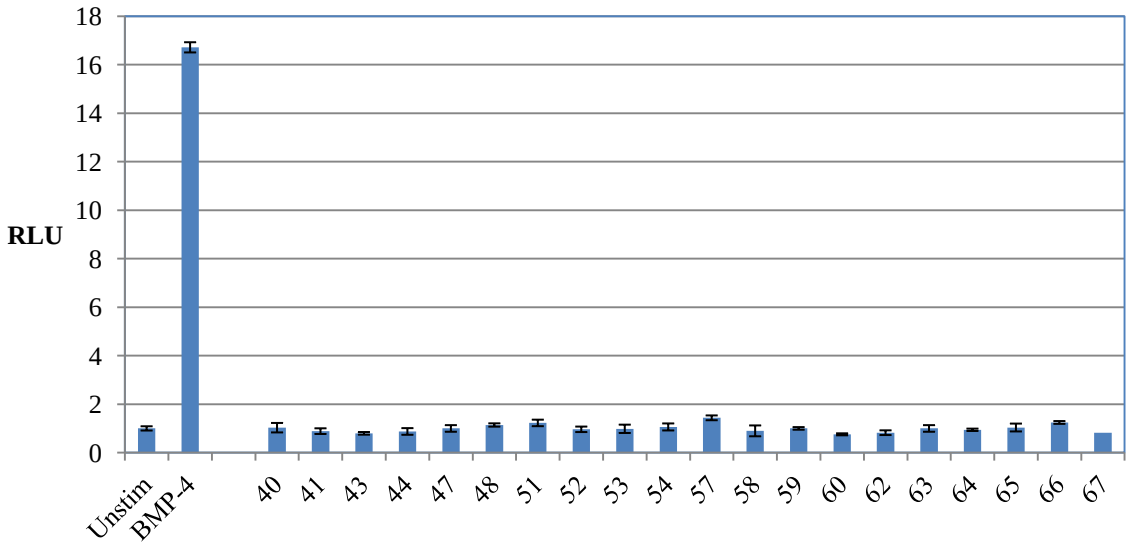

Figure 13 Screen displaying relative luminescence units (RLU) of **41** and its structural analogues using transiently transfected C2C12 cells. Final compound concentration was 10 µM, and BMP-4 was 10 ng/mL. Unstim = unstimulated cells

This was not completely unexpected, as dorsoventral axis development and the visualisation of the gene transcripts in the zebrafish assay are not entirely caused by

activation of BMP signalling. FGF and TGF-β signalling are also known to be involved in the formation of the dorsoventral axis and expression of the genes in early stages of embryo development in zebrafish.[132,133] In addition, the lack of activity in the cell based assay could be attributed to lack of translation across the two species. The cells used in this assay were C2C12 mouse myoblast derived cells, activity in the zebrafish will not necessarily be recapitulated in the mouse cells. Unfortunately it had to be concluded that the series of compounds did not increase levels of luminescence in comparison to the unstimulated cells and was therefore not of interest in this study. However, a new assay was successfully developed for screening of small libraries of compounds for the identification of BMP agonist and antagonist molecules.

3.4.2.2 Stable Transfected Cell Line

After validation of the transiently transfected cell line, a C2C12 cell line stably transfected with the BREluc reporter was obtained (a kind gift from Christian Siebold) in order to test subsequent generated libraries in higher throughput screens. The current method of transfecting cells individually with the BREluc plasmid has several limitations. It is extremely labour intensive, to manually transfect hundreds of wells with the transfection mix of the BREluc plasmid and transfection reagents. Additionally each well is subsequently treated with a small molecule which requires the cells to be removed from their incubation conditions and disturbed for a substantial amount of time. Moreover, the efficiency of the transfection can vary greatly between treated cells leading to variations and inconsistencies of the measured signal. By producing a stable transfected cell line, the number of cells per well possessing the BREluc plasmid would be more consistent and thus eliminate previous inconsistencies to produce more reliable readouts. Combining the luminescence provided by cells treated at 10 ng/mL, a total of 60 measurements were assessed to generate a z-score. The z-score is a statistical measure of the signal to noise

ratio indicating the robustness, sensitivity and reliability of the biological assay.[134] The closer the number of the z-factor is to 1, the more reliable the assay is. The value is obtained from the difference between the dynamic range (difference in mean of positive and negative control) and the separation band (difference in standard deviation) (**Figure 14**). The smaller the difference between the dynamic range and separation band, the closer the value to 1.

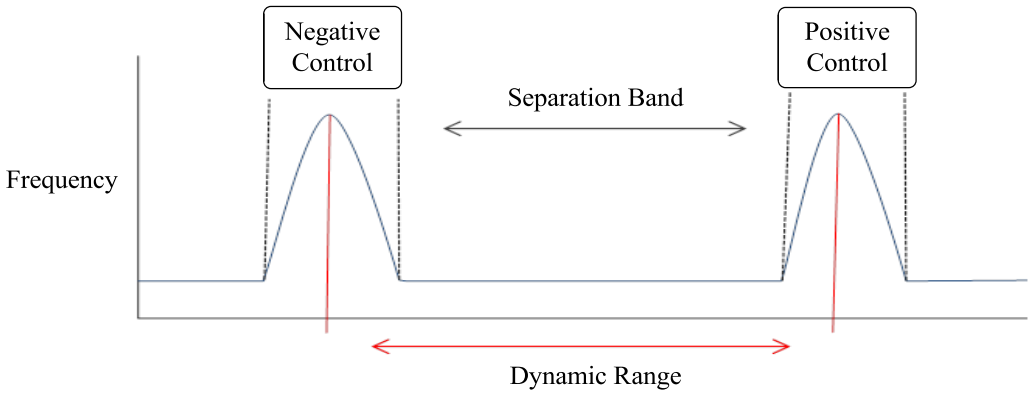

Figure 14 Graph displaying Frequency of value, dynamic range and separation band of positive and negative controls

The hypothesis is that all the control values provide the same readout. Using this, the score will provide information on how close the values are to the mean. The obtained value from the test is 0.9845, which concludes that the controls have the same mean and the assay is very robust.

As the original set of compounds around the structure of (±)**38** failed to provide a BMP pathway activating hit, a new set of compounds had to be identified to test on the newly established assay for identification of a novel hit compound.

3.5 Ligand Based Virtual Screen

3.5.1 Library Mining

As discussed in the introduction (section 1.2.2.1.1), the method of ligand based virtual screening has been successfully applied in identifying new hit molecules. Using a known small molecule regulating the BMP pathway, a screen can be carried out against a virtual

library to identify new BMP pathway regulating molecules. Dorsomorphin (**30**) had been identified as a BMP antagonist binding to the BMP type I receptor and disrupts smad phosphorylation. A slight structural modification of an antagonist can sometimes lead to an inversion of the role of the ligand, to an agonist. A study investigated very minor structural variations around olmesartan (**73**). It was discovered that the inverse agonist activity at the Angiotensin II type 1 receptor (AT_1), a member of the GPCR superfamily, changed to a neutral agonist by the replacement of an acid (**73**) to an amide functionality (**74**) (**Figure 15**).[135] By a further addition of a *p*-hydroxyl group (**75**) to a different part of the molecule changed the observed effect on the AT_1 to that of a full agonist. A further example in which minor chemical changes on a structure can influence activity at the cannabinoid 2 receptor (CB_2R) was investigated by Tabrizi *et al*.[136] By altering the isoxazopyridine core to a thienopyridine, the activity altered from being a full agonist (**76**), to an inverse agonist (**77**) (**Figure 15**). Therefore, small structural modifications can often result in modified effect at the receptor.

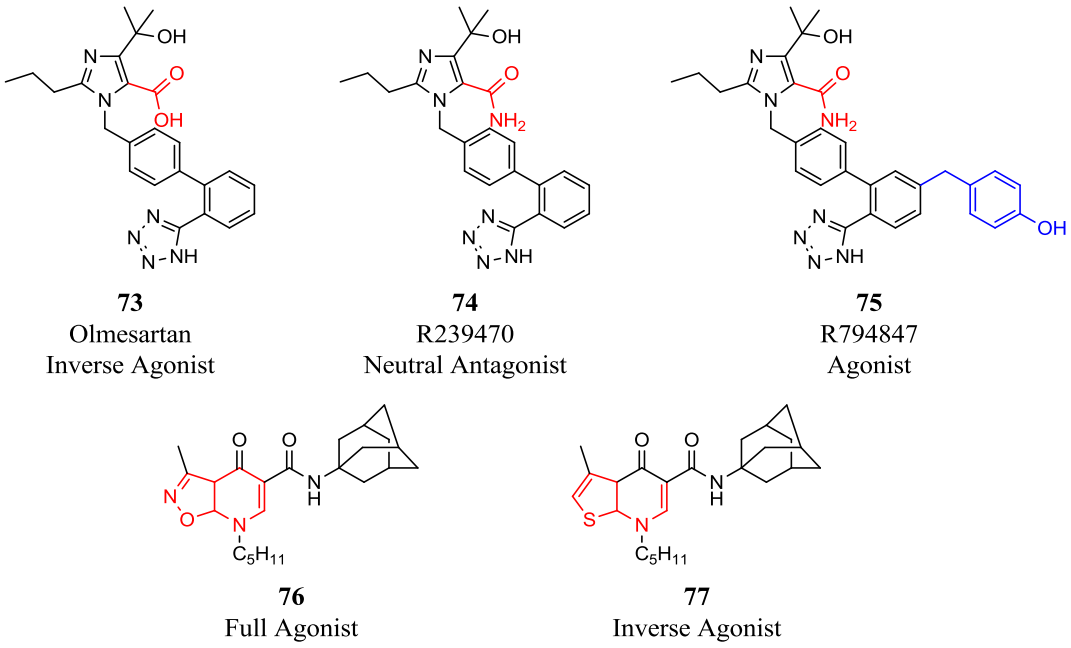

Figure 15 Structures of Angiotensin type II receptor inverse agonist Olmesartan (**73**), neutral agonist R239470 (**74**) and full agonist R794847 (**75**). Structures of cannabinoid 2 receptor full agonist (**76**) and inverse agonist (**77**)

Dorsomorphin (**30**) was used as a template in the ligand based virtual screen to identify small molecules with similar structures that would possibly possess agonist or antagonist activity at the BMPR (**Figure 16**). **30** was selected due to its commercial availability and previously reported to interfere and bind to the BMPR and leading to inhibition of downstream BMP signalling.

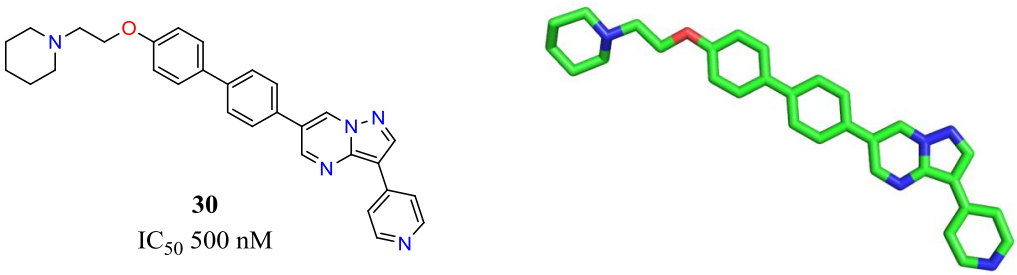

Figure 16 Template molecules, known BMP antagonist dorsomorphin (**30**) and its 3D structure

Using ROCS, the 25,000-member in house virtual database was mined for compounds with good overlay to dorsomorphin **30**. The combo score, calculated by combining the shape Tanimoto score and the colour score, was used as a ranking system and the resulting top 54 compounds, which comprised of 5 different compound classes, were tested in the BREluc assay (**Figure 17**). The 3D structure of dorsomorphin **30** demonstrates how flat and rigid the majority of the molecule is (**Figure 16**). Only the ethoxy linking the piperidine was predicted to display considerable flexibility. The resulting hits from the virtual screen using **30** as a template also display for the most part a flat core with aryl substituent's, and in cases **78** and **82** a hydrazone linker extends out from the core to outer cyclic substituents.

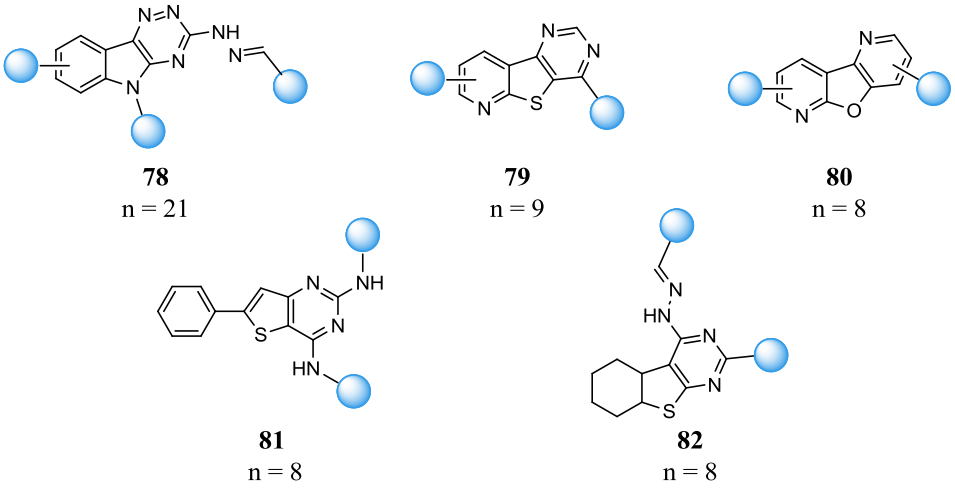

Figure 17 Number of compounds with the relative core structure in the 54 compounds discovered from the ligand based virtual screen using dorsomorphin (**30**), which were subsequently tested in the first BREluc assay
n = number of compound with the core structure in the top 54 compounds identified

3.5.2 Screening of Dorsomorphin-Mimetics

Using the C2C12 cell line stably transfected with the BREluc reporter the compounds were tested in agonist and antagonist mode (**Figure 18**). The agonist mode tests the compound in the absence of any other stimulus, while in antagonist mode, the cells are treated with BMP-4 to provide a base signal and possible antagonist effect to suppress the stimulus. Compounds were added at a final concentration of 10 µM and incubated for 24 h at 37 °C, the cells were then analysed following the luciferase assay protocol (See appendix 1).

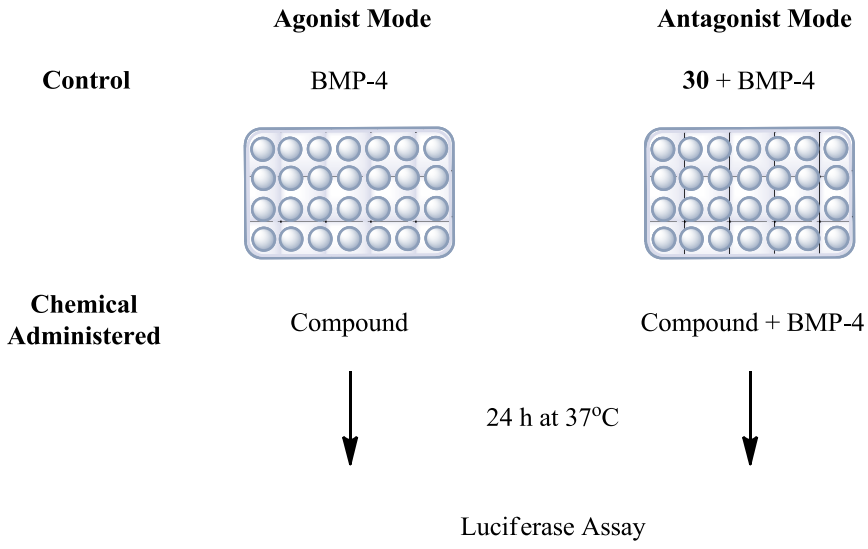

Figure 18 Outline of controls in agonist (BMP-4) and antagonist Dorsomorphin (**30**) assay mode and compound administration in each well. The antagonist mode treats the cells with BMP-4 to generate a base signal in addition to a compound for possible pathway antagonism

From the first antagonist screen, three core structures emerged, the 6-phenyl thienopyrimidine core with variations at the C(2) and C(4) (**83** and **84**), the 1,2,4-triazino indole scaffold with variations of the thioester substituent (**87 - 89**), and finally the tetrahydrothienopyrimidine (**85 and 86**) (**Figure 19** and **20**). It was decided to explore further SAR using the thienopyrimidine scaffold due to its promising inhibition of the BMP pathway. The core provided a suitable starting point for possible future structural diversification to explore preliminary SAR's through variation at the C(2) and C(4) of the bicycle.

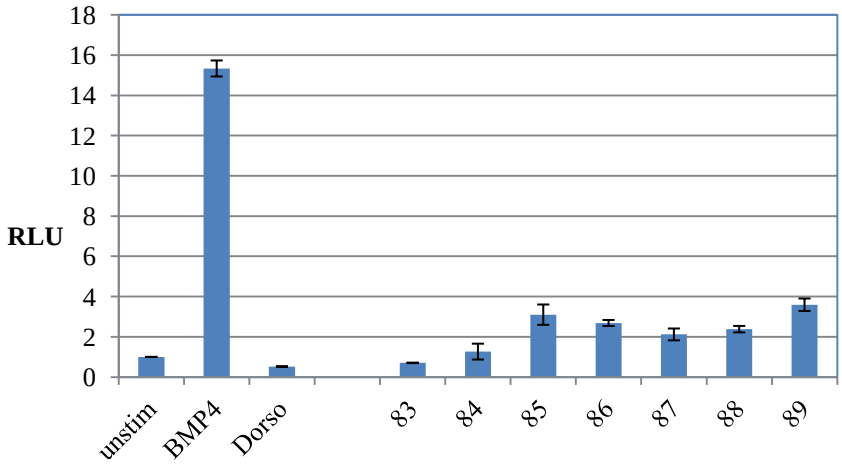

Figure 19 Graph illustrating the relative luminscence units (RLU) of the most potent antagonists discovered (**83-89**) in the screen of the 54 compounds, tested at 10 uM. 3 common structures emerged and activity was compared to the unstimulated (unstim) cells, normalised to 1. Dorso = dorsomorphin treated cells, and BMP-4 were dosed at 10 µM and 10 ng/mL respectively.

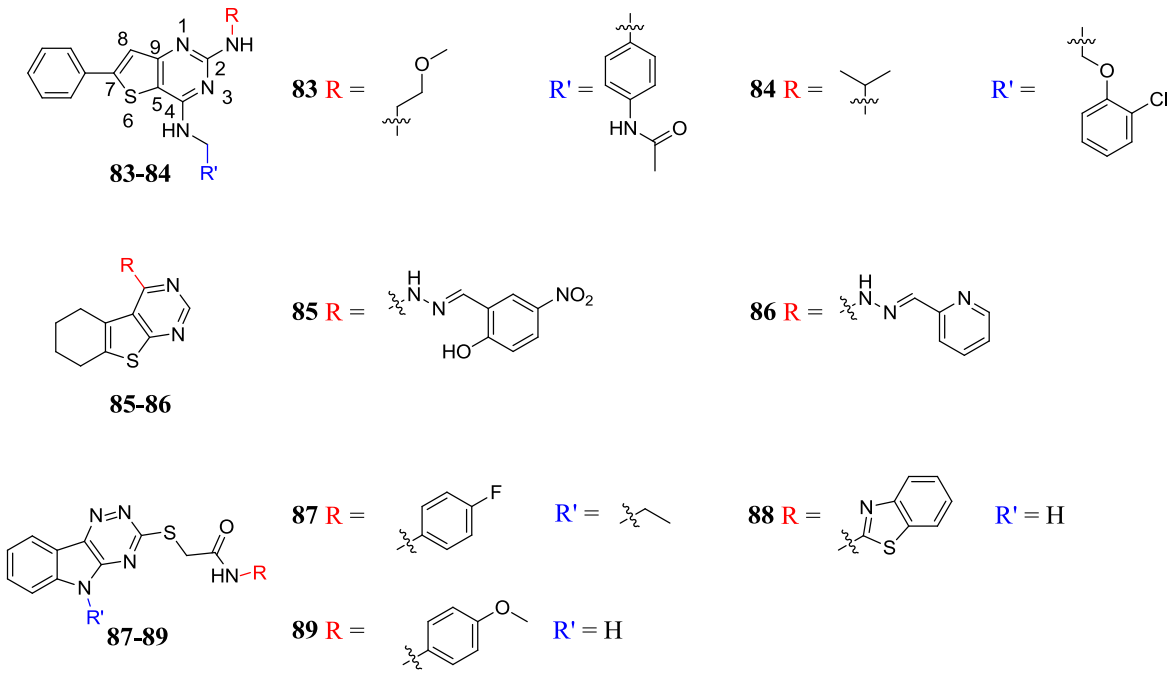

Figure 20 Structure of potent BMP pathway antagonist discovered in the 54 compound screens

A substructure search was carried out using the thienopyrimidine core of compounds **83-84** against the in-house database, identifying a further 17 substructures. These were also tested in the BREluc assay measuring luminescence. **Figure 21** illustrates the antagonist activity of all the compounds with the 2-phenyl thienopyrimidine core, where XX and XXa indicate the compounds tested from 2 independent samples derived from the compound

library. The values are recorded as a percentage of the total signal produced upon stimulation with only 10 ng/mL of BMP-4 protein. From the set of compounds, minor preliminary SAR can be derived at C(2) and C(4) positions of the thienopyrimidine core. The C(2)-amino functionality was conserved throughout the set of compounds and modifications to this substituent did not appear to influence activity greatly. Variations at C(4) position seemed to have a more pronounced impact of the activity of the molecules. An imidazolidinone group was not well tolerated with a reduction of activity for compounds **93** and **94**. This functional group also displays high degrees of variability between screens possibly due to toxicity or poor solubility of the compounds. The assay was consequently performed using transparent bottom plates to allow the visualisation using a microscope of the viability of the compounds. Previously opaque white plates were used, however with interest in compound toxicity, these were replaced with transparent bottoms to visualise the well-being of the cells. No serious toxicity was observed however, with the compounds indicating the variability was likely due to their low solubility.

Replacing the amine funtionality at the C(4) position with a larger more electronegative oxygen without H-bond donor ability led to an interesting observation; antagonist activity is completely removed with all three compounds **97**, **100** and **101**. In fact, **97** (RLU 137) and **101** (RLU 150) resulted in the generation of a greater signal than BMP-4 alone indicating at a possible additive or cooperative effect with BMP-4 (highlighted in blue). The mechanism of action of these compounds is however yet to be determined, however they could be acting as agonists of the pathway.

The most active antagonist **99** discovered from this screen completely inhibited the BMP-4 stimulus at a final concentration of 10 μM (RLU -0.8, highlighted in purple). **99** was the only compound with a dimethylamino group at C(2) position possibly contributing to the observed activity.

An extensive library of compounds would be required to gain a deeper understanding in the functionality directly involved in improving antagonist activity. Dose response curves were generated of the most active antagonist molecules to gain an understanding of their IC_{50} values and compare this to literature values of Dorsomorphin (**30**) (IC_{50} 500 nM).

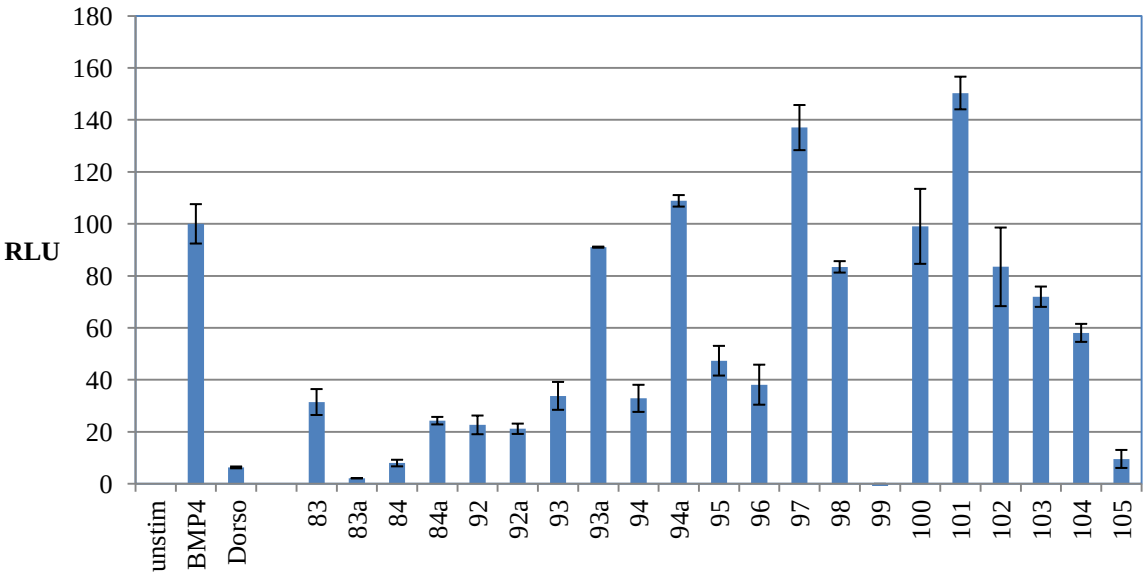

Figure 21 Antagonist screen of the 21 compounds with the 2-phenyl thienopyrimidine core in the C2C12 cell line stably transfected with the BREluc reporter, each well is treated with 10 ng/mL BMP-4 to provide a stimulus repeated in triplicates. Relative luminescence units (RLU) were normalised to the unstimulated (unstim) cells with BMP-4 (100, 10 ng/mL) and dorsomorphin (Dorso, **30**, 10 µM) used as the controls. XX and XXa indicate the compound tested from 2 independent samples derived from the compound library.

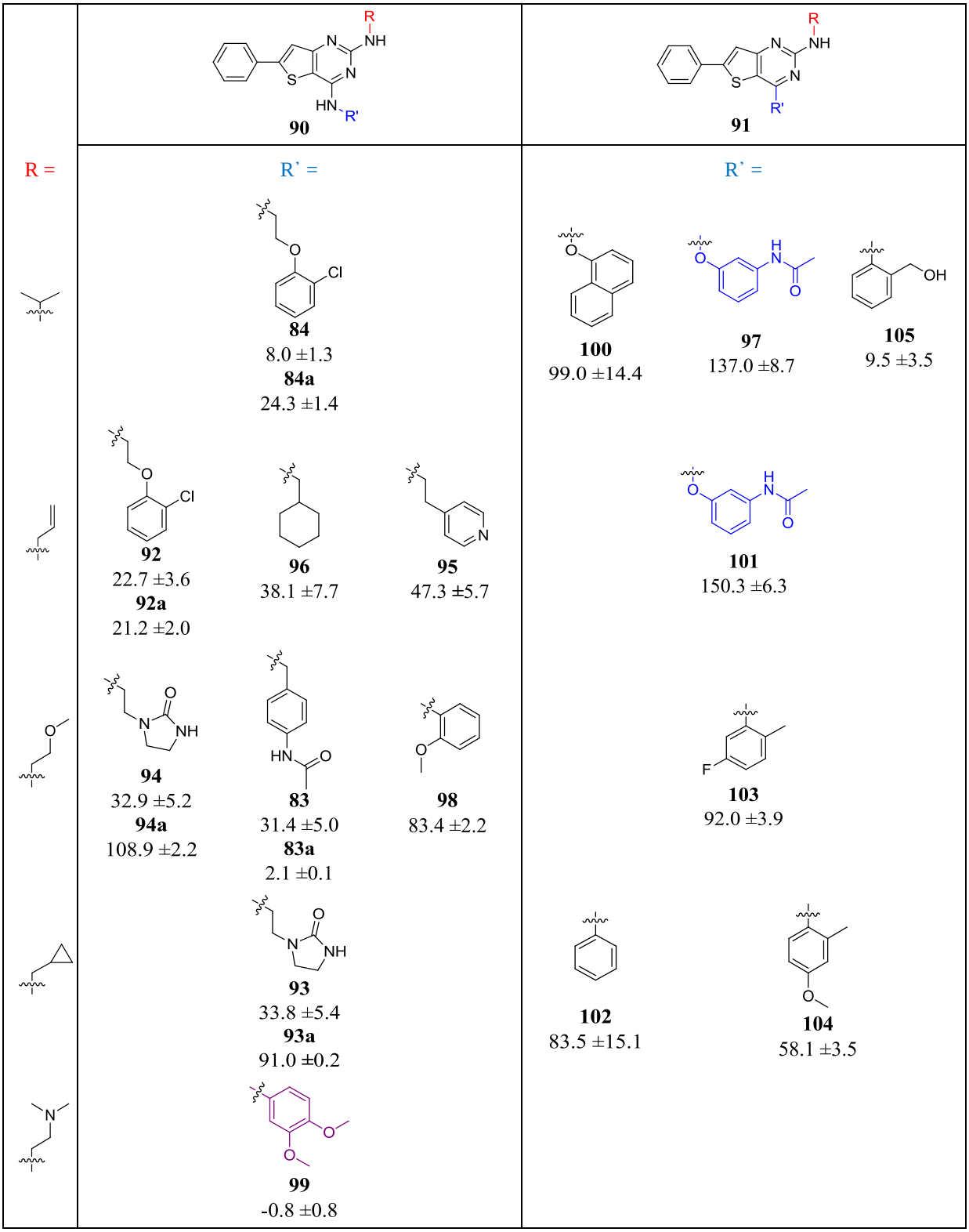

Table 3 Structures of the 21 thienopyrimidines tested with measured values of relative light units (RLU) in respect to the full BMP-4 signal (100). XX and XXa indicate the compound tested from 2 independent samples derived from the compound library.

Dose response curves were made of the five most promosing antagonists displaying clear dose dependent responses with full inhibition of luminescence at maximum concentration (10 μM) (**Figure 22** and **23**).

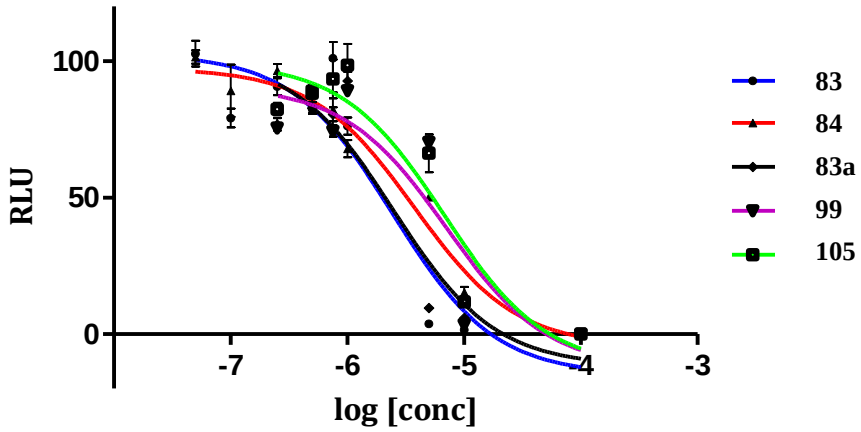

Figure 22 Dose response curves of antagonists **83**, **84**, **83a**, **99** and **105** each concentration is tested with addition of BMP-4 (10 ng/mL) displayed in relative luminescence units (RLU). Controls are BMP-4 (10 ng/mL, RLU = 100) treated and unstimulated (unstim, RLU = 6.7) cells

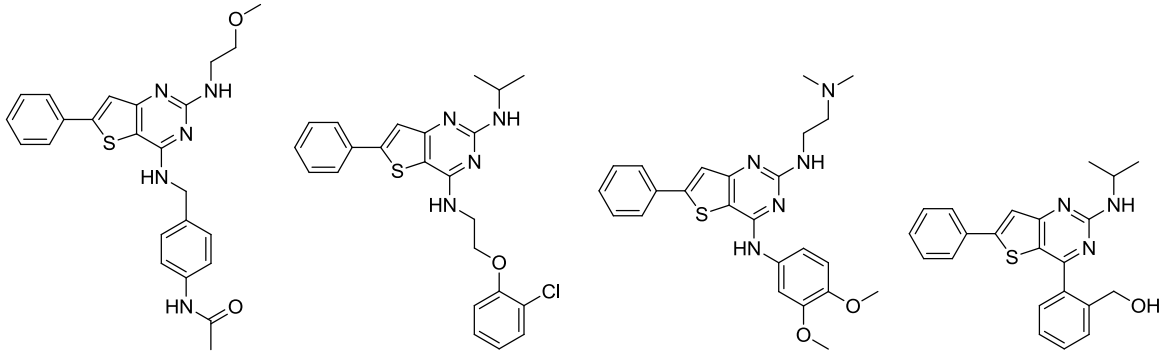

83 IC_{50} 2470 μM
83a IC_{50} 3600 μM
84 IC_{50} 3760 μM
99 IC_{50} 8000 μM
105 IC_{50} 7890 μM

Figure 23 Structures of most active antagonist molecules identified from the thienopyrimidine series with relative IC_{50} values

This work led to the identification of a new class of putative BMP antagonist molecules with some preliminary SAR indicating substitutions at C(2) and C(4) positions of the 6-phenyl thienopyrimidine core which contribute to suppressed luminescence in the BREluc reporter assay.

3.5.3 Agonist Identification

To identify agonist molecules the C2C12 BREluc cell line was treated with molecules in the absence of recombinant BMP-4 protein. The first aim was to identify agonist molecules displaying increased expression of BMP target genes in the absence of BMP-4, and finally BMP-4 was added to observe whether there is a possible additive or synergistic effect of the compound together with the BMP-4 stimulus.

The cells were treated with a final compound concentration of 10 µM and incubated for 24 h at 37 °C. BMP-4 treatment was only used as a positive control for BREluc activation. The original 54 compounds were tested and several weakly activating molecules were initially identified (**Figure 24**).

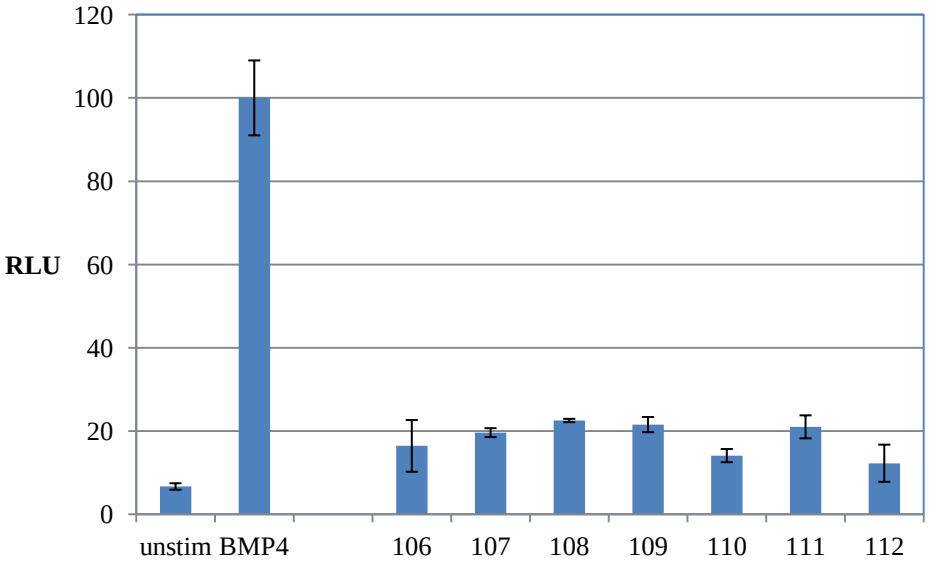

Figure 24 Most promising agonist molecules identified from screening of the 54 compounds, identified in the ligand based virtual screen overlaying dorsomorphin (**30**), displaying the relative luminescence units (RLU) in comparison to the BMP-4 signal (100, 10 ng/mL) and unstimulated cells (unstim)

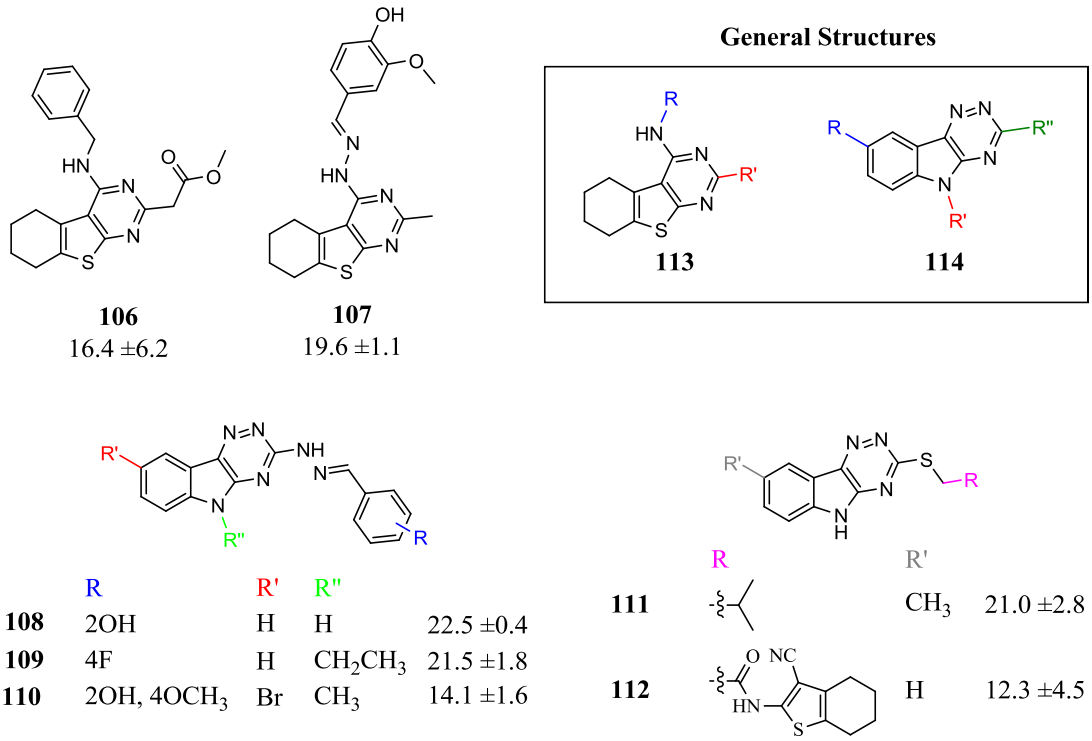

Figure 25 Cores **113** and **114** identified in the agonist screen to upregulate BMP target genes and individual structures of molecules discovered in the first screen of 54 Dorsomorphin (**30**) mimetics. Activity is displayed in relative luminescence units (RLU) produced in comparison to the control BMP-4 activated cells (100, 10 ng/mL)

The most active compounds all belonged to two classes of compounds, the cyclohexyl thienopyrimidines **113** with substituent's at C(2) and an amino group at C(4), and the 1,2,4-triazino indole **114** with C(3), *N*(5) and C(8) substitutions (**Figure 25**). The highest activity of this preliminary screen was displayed by **108** (RLU ~22). Interestingly, the core structure of the 1,2,4-triazino indole resembles that of previously discovered antagonists **87-89**. Having identified a core structure with functionality which provided agonist activity in the reporter assay, the in-house database was mined for substructures of **115** to establish preliminary SAR on this series, this identified a further 19 compounds which were tested for BMP agonism (**Figure 26** and **Figure 27**).

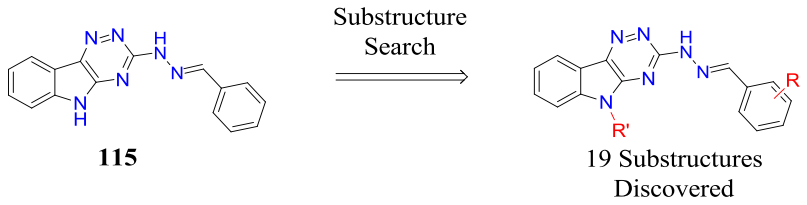

Figure 26 Substructure search with the triazino indole core resulting in the discovery of 19 substructures of **115**

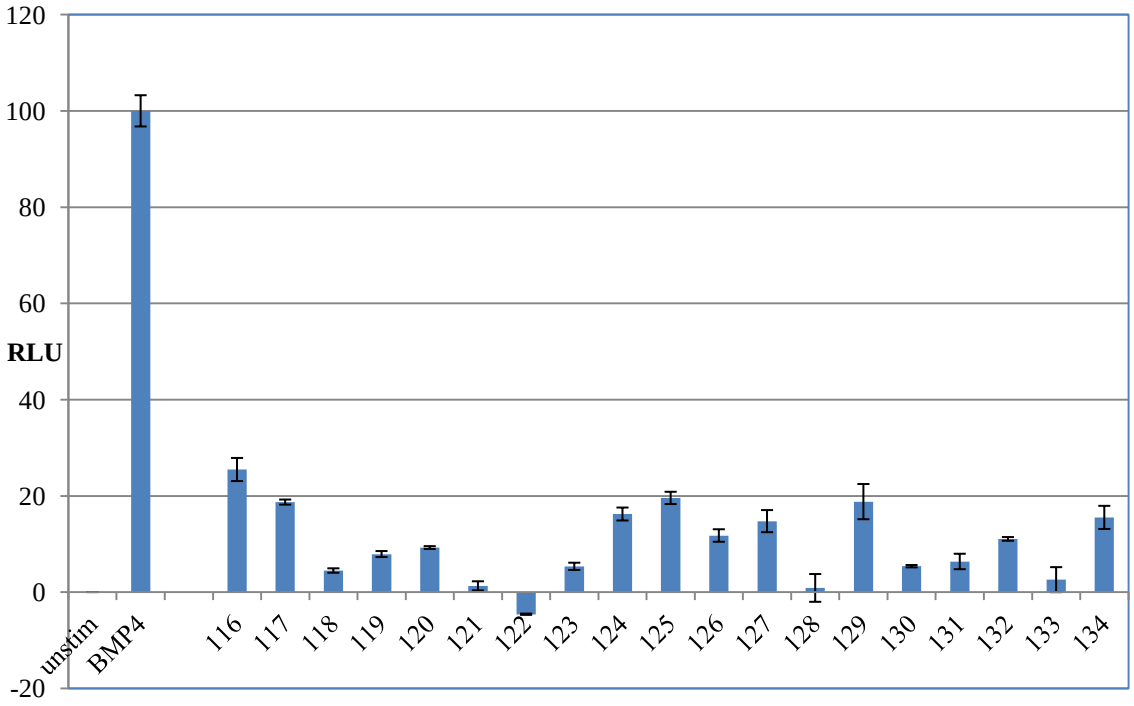

Figure 27 relative luminescence units (RLU) of the 19 available substructures of **115** using BMP-4 as the control signal (100, 10 ng/mL)

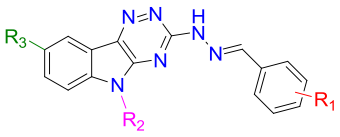

	R_1	R_2	R_3	RLU
125	3-Br	H	H	19.7 ±1.3
126	3,5-Di Br, 4-OH	H	H	11.8 ±1.3
131	2-O^{n}Pr	H	H	6.4 ±1.6
130	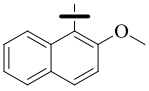	H	H	5.4 ±0.3
118	2-OH, 3-Cl	CH_2CH_3	H	4.5 ±0.5
128	3-F	CH_2CH_3	H	0.9 ±2.9
133	4-F	CH_2CH_3	H	2.6 ±2.6
134	4-Br	CH_2CH_3	H	15.5 ±2.4
116	2-OH	$CH_2C_6H_5$	H	25.5 ±2.4
117	3-NO_2	$CH_2C_6H_5$	H	18.7 ±0.5
119	2-OH, 3-Cl	$CH_2C_6H_5$	H	4.5 ±0.6
120	4-NO_2	$CH_2C_6H_5$	H	9.3 ±0.3
121	2-OH, 3-NO_2	$CH_2C_6H_5$	H	1.3 ±0.9
127	4-Cl	H	CH_3	14.4 ±2.3
132	3-I	H	CH_3	6.4 0.4
124	4-OCH_3	CH_3	Br	16.2 ±1.4

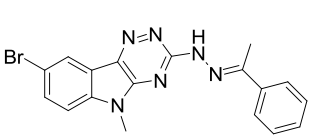

129 18.8 ±3.7

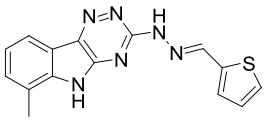

123 5.3 ±0.8

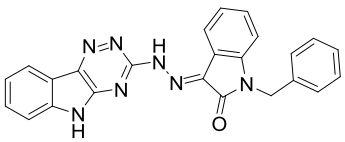

122 -4.6 ±0.1

Table 4 Structures of the 19 substructures identified of **115** with their relative luminescence units (RLU)

Of the 19 compounds that were tested some displayed promising levels of increased luminescence. With some preliminary SAR derived from the compound set, it can be noted that structural variations at various positions have an effect on the luminescence readout (**Table 4**). The replacement of the phenyl hydrazone gives the most notable change in activity. Examples include thiophene **123** (RLU 5.3) and indolinone **122** (RLU -4.6) linked hydrazones which led to a major loss in activity. This indicates the importance of the phenyl group in retaining activity. Substitutions around the phenyl ring also influenced

luminescence, however additional compounds would need to be synthesised to allow full SAR investigation into electronic, steric and positional effects variations around this group. Similarly, introducing changes at *N*(5), C(6) and C(8) displayed different levels of activity, but the limited number of compounds does not allow conclusions to be drawn.

In conclusion, the screening of a small library of triazino indoles identified **116**, containing a 2-hydroxy benzyl hydrazone at C(3), benzylic group at *N*(5) and unsubstituted C(6) to C(9) positions, providing the highest levels of activity (RLU 25.5). Having discovered a suitable compound to carry out further investigations with, a solid sample was synthesised and tested to validate activity in the assay.

3.5.3.1 Synthesis of 116

To confirm the verity of the putative hit compound from the in-house library, an authentic sample of **116** was synthesised. The first route examined, began with the benzylation of isatin (**135**) to yield **136** (**Scheme 7**).[137] This was followed by condensation with thiosemicarbazide at reflux in water. Analysis of the isolated product by mass spectrometry and ^{13}C NMR spectrum revealed that the cyclised product **137** had formed. Attempts to dehydrate **137** to form **138** were performed using various acidic conditions (**Table 5**). On a small (100 mg, 0.32 mmol) scale dehydrated product **138** was obtained in 20% yield by the treatment with AcOH, in a sealed tube at 150 °C over 24 h. However attempts to scale up, this procedure returned no product.

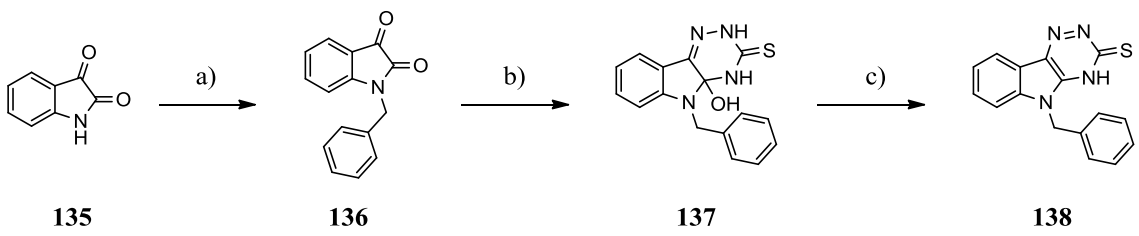

Scheme 7 First synthetic route to **116** a) BnBr, K_2CO_3, DMF, 150 °C 15 min, 65% b) thiosemicarbazide, K_2CO_3, H_2O, reflux 3 h, 96% c) Conditions outlined in table 4, only successful with AcOH, 150 °C 24 h, 20%

Reaction	Solvent	Reagent	T (°C)	Yield
1	AcOH	-	Reflux*	sm
2	PPA	-	150*	cm
3	PPA	-	150	cm
4	EtOH	NaOMe	150	sm
5	AcOH	Et_3N	150	sm
6	AcOH	-	150	20%
7	AcOH	$(Ac_2O)_2O$	150	cm
8	TFA	-	150	cm

Table 5 Dehydrating conditions generating the aromatic product **138** from **137**, in either a sealed vial or alternative
*Open vial
sm = starting material isolated
cm = complex mixture of product from which **138** could not be isolated

Another synthetic route to **116** was therefore devised which would circumvent the difficulty of the final dehydration step. In this synthesis the first step was the cyclisation of isatin (**135**) with thiosemicarbazide to successfully yield the tricyclic compound **139** (**Scheme 8**). Treatment of **139** with an excess of benzyl bromide provided the dibenzylated product **140**, while 1eq of BnBr reacted to furnish the *S*-benzylated derivative **141** as the side product. Initial attempts to replace the *S*-benzyl sulphide with hydrazine did not yield the desired product **143**. Therefore, **140** was first oxidised with *m*CPBA, to form the more electron withdrawing sulfone **142** which was subsequently treated with a small excess of hydrazine monohydrate in EtOH. This yielded the hydrazine intermediate **143**. It was later identified that reflux of **140** in neat hydrazine monohydrate yielded **143** in good yield on a large scale (10 g, 26.2 mmol). Finally **143** was treated with 2-hydroxy benzaldehyde to provide the desired product **116** in good yield.

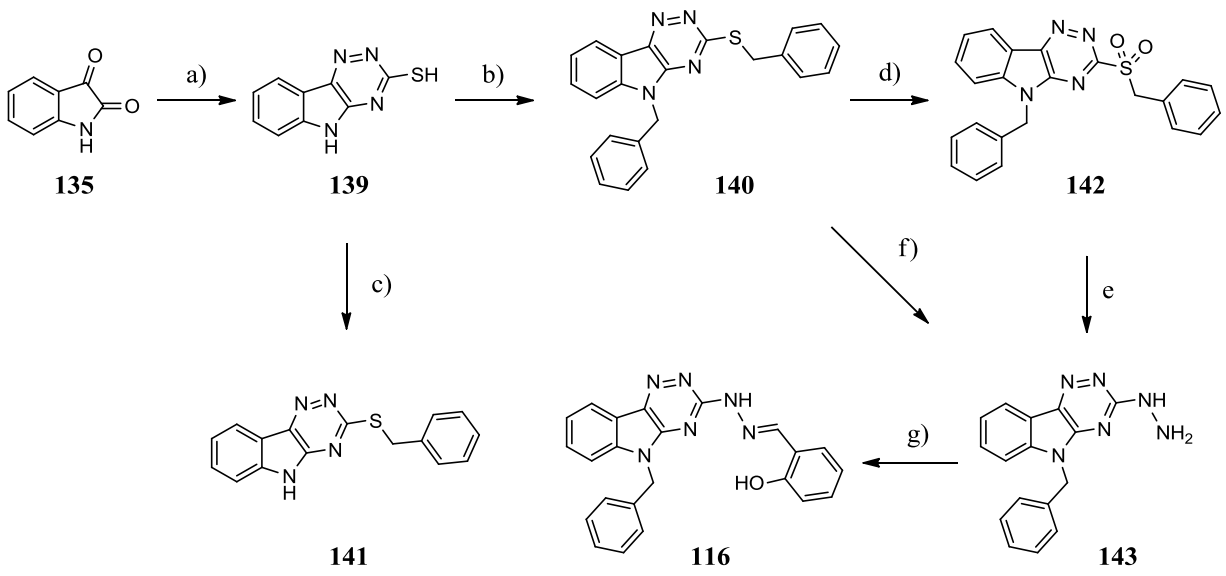

Scheme 8 a) thiosemicarbazide, K_2CO_3, H_2O, reflux 3 h, 91% b) BnBr, K_2CO_3, DMF, rt 16 h, 63% c) BnBr (1eq), K_2CO_3, rt 16 h, 90% d) *m*CPBA (72%), CH_2Cl_2, rt 16 h, 41% e) Hydrazine monohydrate, EtOH (1:1), 80 °C 3 h, 53% f) Hydrazine monohydrate, 3h reflux, 84% g) 2-Salicylaldehyde, MeOH, rt 16 h, 99%

With a synthetic route to make **116** devised, a small library of compounds was prepared to investigate some preliminary SAR around the *N*(5) position (**Scheme 9**). The first step involved the methylation of the secondary amine on isatin (**135**) with methyl iodide to yield **144**. This was followed by the cyclisation to **145** using thiosemicarbazide, which proceeded in very good yield. Previously, the thiol was benzylated and oxidised to the corresponding sulfone to allow nucleophilic displacement, however under more forceful conditions it was found that, refluxing **145** and **139** in neat hydrazine monohydrate overnight, produced **146** and **148**. Converting the sulphide directly into the hydrazine allowed for a more efficient synthesis to the final product in higher yields.[138] Finally the hydrazine was reacted with salicylaldehyde to yield **147** in good yield. Similarly, the unsubstituted *N*(5) compound **150** was generated with no initial methylation of isatin but direct cyclisation to the tricycle **139**, followed by generation of the hydrazone **148** which was finally reacted with the aldehyde to generate **149**.

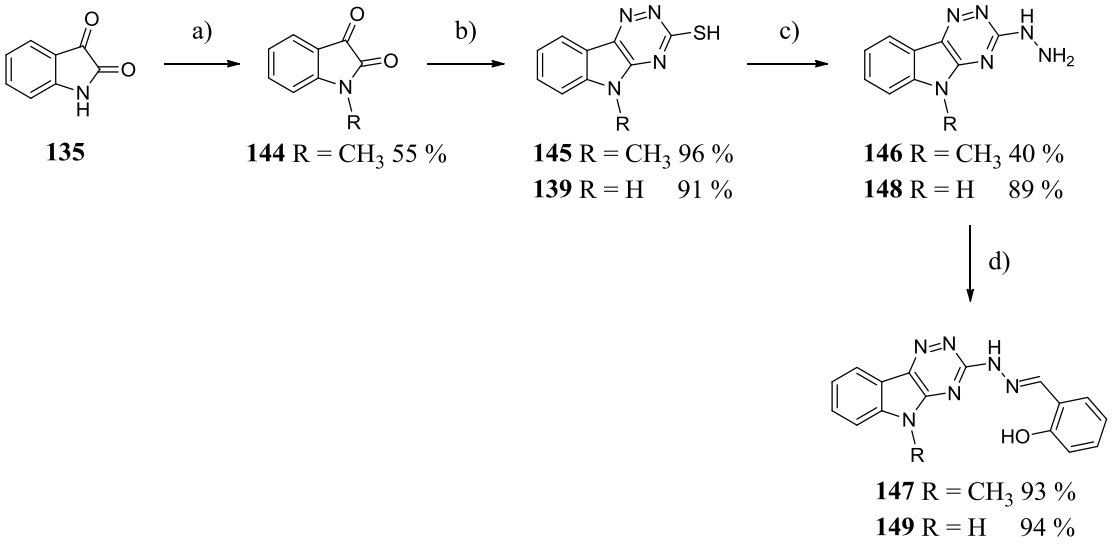

Scheme 9 a) MeI, K_2CO_3, DMF, 150 °C 20 min, 55% b) thiosemicarbazide, K_2CO_3, H_2O, reflux 3 h c) hydrazine monohydrate, reflux 3 h d) 2-Salicylaldehyde, MeOH, rt 16 h

The synthesis of **116** provided an authentic solid sample of the compound to confirm that the actual structure in the library corresponds to that of the assigned structure. **116** and its analogues were tested in an agonist screen but unfortunately the activity of the synthesised compound was observed to be significantly lower (RLU 3.6) than previously recorded with the sample of **116** obtained from the compound library (RLU 25.5) (**Figure 28**). The library sample, **116** still possessed agonist activity in the repeat BREluc reporter assay however, even this displayed much lower levels of activity than previously measured (RLU -47%). The conclusion to be drawn from this is that the compound from the library could have been victim of degradation to a possible precursor, for example the hydrazine **143**. The degradation process could have been assisted by the continuous freeze-thaw process the compound stock solutions undergo when removed from storage. To identify whether intermediates were responsible for the observed activity, all the synthetic intermediates were also tested in a BMP agonist mode, but unfortunately this also provided no activity. This leads to the possible conclusion that the limited solubility was responsible for the variability in activity.

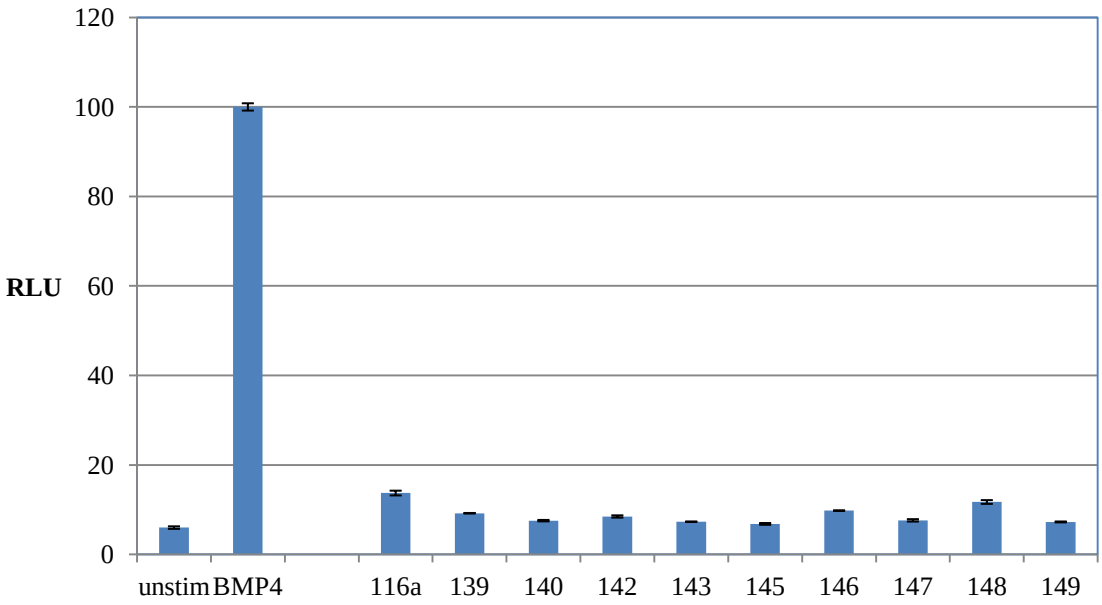

Figure 28 Agonist assay of the synthesised compound **116** along with the reactive intermediates, activity displayed in relative luminescence units (RLU). Unstimulated (unstim) and BMP-4 (100, 10 ng/mL) treated cells provided the controls

The resynthesis of **116** was successful, however, **116** did not provide promising activity in the BREluc reporter assay previously observed (RLU 8). This series was also abandoned and as the results obtained from the compound library could not be replicated. A possible explanation for the difficulties in replicating activity of the library sample could be due to contamination, degradation or mislabel. To verify the integrity of the library sample in future, HPLC and LCMS could be run on the sample to determine the purity and match the molecular weight to the expected structure. The activity displayed by the solid samples in this study was deemed to small an effect to pursue in further optimisation studies, therefore an alternative method was suggested.

3.6 Final Approach

A final screen was performed using a range of compounds from the in-house database, based on previous hits, and possible BMP modulators from the literature.

3.6.1 BMP Modulators in Stem Cells

This screen tested a total of 320 compounds using the C2C12 BREluc stable transfected cell line, therefore the compound selection criteria had to be relatively stringent. The criteria implemented for the generation of this library was established using knowledge in the public domain or previously obtained data from this piece of work. Compounds from the literature included known cardiomyogenesis enhancers, epigenetic modulators and molecules known to upregulate expression of BMP dependent transcriptional genes. These, alongside a selection of compounds from the in-house library based around previous structures discovered to influence luminescence were selected to make up the compound library. Using the stable transfected cell line and the use of a liquid handling robot, larger numbers of compounds were able to be tested in a short period of time.

In summary, a range of compounds have been discovered to have an effect on enhancing cardiomyogenesis *in vitro* at some point in the differentiation process and 39 representative compounds were screened in the BREluc reporter assay (**Table 6**). Their mode of action in cardiomyogenesis is often not known and the aim of the screen was to discover whether it was BMP pathway dependent.

Amongst the selection of literature compounds, some had been shown to bind to the BMP type I receptor such as Dorsomorphin **30** and the optimised BMPRI antagonist LDN-193189 (**33**) (**Table 6**). Further, the list comprises several antioxidants including ascorbic acid (**24**), serotonin (**150**) and apigenin (**151**). The BMPR is a protein kinase, therefore it appears logical to include other kinase inhibitors that have already been proven to have an effect on cardiomyogenesis. Mitogen activating protein (MAP) kinase activation has also

been shown to have an effect on smad signalling, of particular interest in the phosphorylation of smad1.[139] Additionally another kinase inhibitor was of interest, namely Genistein (**152**) which was identified to interfere with cardiomyogenesis. It was found to display activity as a tyrosine kinase inhibitor which, has also been shown to be involved in smad dependent reporter gene activation which is the reason for the inclusion of a small set of these compounds.[140] Several antioxidants have been shown to be involved in the regulation of differentiation to cardiomyocytes, however a study has shown that not all antioxidants promote cardiomyogenesis.[72] Interestingly, a different study investigates the effect of low levels of reactive oxygen species, in particular hydrogen peroxide and observe promoted cardiomyogenesis of ES cells.[141] In addition reactive oxygen species have a prominent effect on the differentiation to heart muscle cells.[142] As molecules identified to possess antioxidant and oxidising activity have an effect on cardiomyogenesis it would be interesting to see if the effect on stem cell differentiation is possibly BMP pathway mediated.

Several other compounds are included which have known activity on ion channels (Cl^- and Ca^{2+}) and histamine receptors.

Finally, a selection of known epigenetic modulators was prepared for the screen. Histone deacetylase (HDAC) inhibitor valproic acid (VPA, **155**) amongst others were found to promote cardiomyogenesis, intracellular smad activity and influence the expression of cardiac genes (Nkx2.5, Gata4 and MEF2).[143]

Cmpd	Name	Structure	Putative MOA	Effect
30	Dorsomorphin	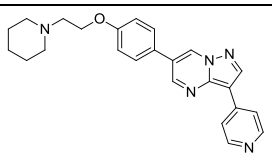	BMPRI kinase domain[62]	Activator
33	LDN-193189	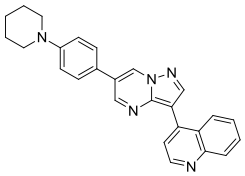	BMPRI kinase domain[110]	Activator
152	Genistein	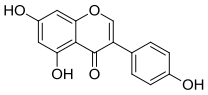	Tyrosine kinase[144]	inhibitor
153	Tyrophostin	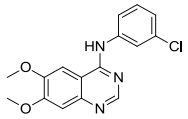	Tyrosine kinase[145]	No effect
25	Retinoic Acid	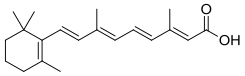	MAP kinase inhibitor[73]	Activator
154	SB203580	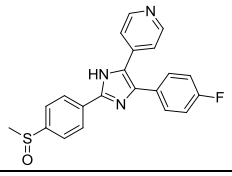	MAP kinase inhibitor[146]	Inhibitor
22	5-azacytidine	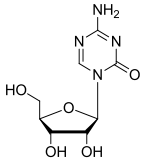	DNA methyl Transferase[147]	Activator
155	Valproic acid	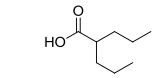	HDAC inhibitor[148]	Activator
156	Sulfonylhydrazone	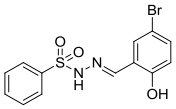	Nkx2.5, Gata4, MEF2 increase[149]	Activator
157	Cardiogenol C	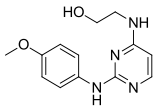	Nkx2.5, Gata4, MEF2 increase[150]	Activator
158	Reversine	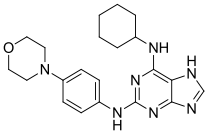	Nkx2.5 increase[151]	Activator
159	NPPB	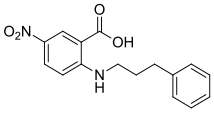	Cl^- channel blocker[152]	Activator
160	Verapramil	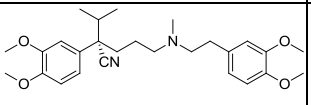	Ca^{2+} channel blocker[153]	Activator

161	Dexamethasone	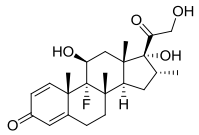	Glucocorticoid Receptor[154]	Inhibitor
162	Histamine	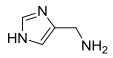	Histamine Receptors[155]	Inhibitor
150	Serotonin	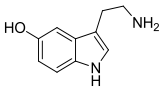	Antioxidant[156]	Activator
24	L-Ascorbic Acid	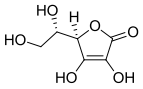	Antioxidant[72]	Activator
151	Apigenin	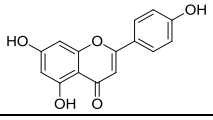	Antioxidant[157]	Inhibitor
163	Forskolin	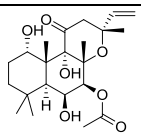	cAMP metabolism[158]	Activator
176	SAHA	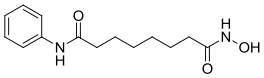	HDAC inhibitor	-
394	Histone deacetelase inhibitor VII	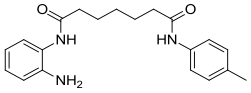	HDAC inhibitor	-
178	Histone deacetelase inhibitor VI	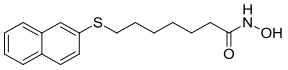	HDAC inhibitor	-
395	Phenamil	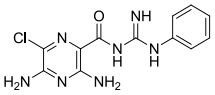	Smad stabilisation[69]	-
396	AICAR	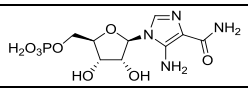	AMPK[159]	-
181	EGCG	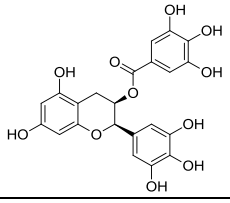	Antioxidant[153]	Inhibitor
396	chelerythrine hydrochloride	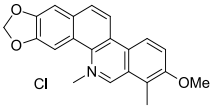	Protein kinase C inhibitor[160]	-
397	Blebbistatin	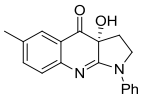	Myosin class II inhibitor[161]	-
398	5′-Deoxy-5′-(methylthio)adenosine	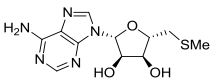	Methyl transferase inhibitor[162]	-
399	S-(5′-Adenosyl)-L-methionine	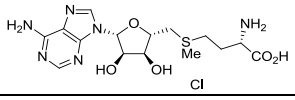	ATP regulator[163]	-

400	Mitoxantrone hydrochloride	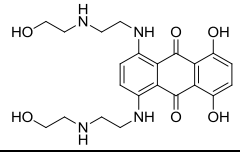	PIM kinase inhibitor[164]	-
177	PAOA	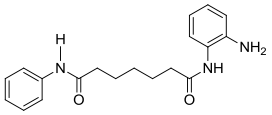	HDAC inhibitor[165]	-
401	Doxorubicin	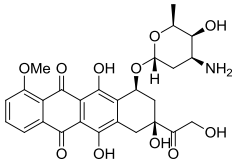	PIM kinase inhibitor[166]	-
402	IBMX	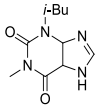	PDE inhibitor[167]	-
179	Histone deacetylase inhibitor III	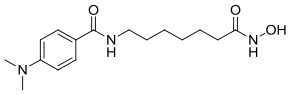	HDAC inhibitor	-
403	Purmorphamine	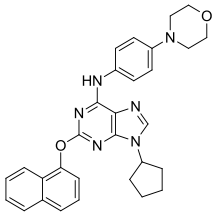	Hedgehog signalling[168]	-
404	indolactam V	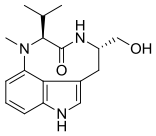	Protein kinase C activator[169]	-
180	5175092	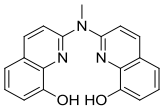	Fe Chelator[170]	-
405	simvastatin	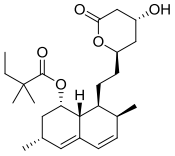	GATA4, Nkx2.5, and DTEF[171]	-
406	mevastatin	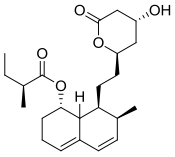	HMG CoA reductase[172]	-

Table 6 List of representative cardiomyogenesis mediating molecules
Cmpd = compound
Putative mode of action (MOA) = Putative molecular mechanism of action contributing to cardiomyogenesis
Effect = effect on cardiomyogenesis

3.6.2 In-House Compound Selection

3.6.2.1 Epigenetic and Cannabinoid Receptor (CBR) Modulators

Once having selected 39 molecules known to influence cardiomyogenesis from the literature, a selection of compounds was also made from the in-house library. Epigenetic modulators have been identified to promote cardiomyogenesis (*vide supra*) which led to the inclusion of compounds with known activity on methyl transferase and histone modification. DNA methyl transferases (DNMT) are responsible for controlling gene expression by methylating, primarily adenine and cytosine, DNA bases. Histone methyl transferases (HMT) regulate methylation of histones leading to a control of gene expression. Previous work within the group had led to the identification of a number of scaffolds as inhibitors of protein arginine methyl transferases (PRMTs) and a representative selection of these were incorporated (**164**-**166**).[173] A diverse group of 24 PRMT modulating compounds were selected (**Figure 29**).

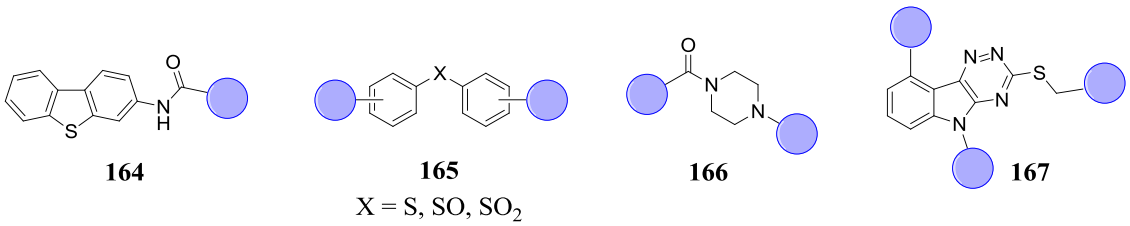

164 **165** **166** **167**

X = S, SO, SO_2

Figure 29 general compounds structure of known PRMT inhibitors **164**, **165** and **166** and CBR modulators **167**

Analogues of **167** were also included. These were coincidentally prepared in a separate project aimed at developing cannabinoid 2 receptor (CB_2R) agonists (See chapter 5). CBR agonism has been shown to promote osteogenesis, this study would demonstrate whether the observed effect is BMP pathway related.

A selection of 21 compounds varying at the C(3), *N*(5) and C(9) positions with activity at the CBR, were selected. Firstly, to observe if these compounds have receptor promiscuity and secondly to study whether CBR modulation displays activity in the luciferase assay.

The final set of compounds was derived from the top ranked compounds identified through the ligand based virtual screening exercise performed using **30**. Structurally similar molecules were identified in the literature to have gene transcriptional upregulatory effect (**169-172**) (**Figure 30**). For example SMT C1100 (**168**) also possessing a similar bicyclic core was observed to upregulate utrophin gene transcription for the potential treatment in duchenne muscular dystrophy.[174] In the literature it was also observed in a study that a series of benzofuran derivatives upregulate the expression of BMP-2 and leading to reducing bone loss.[175] However, the mode of action does not appear to be determined.

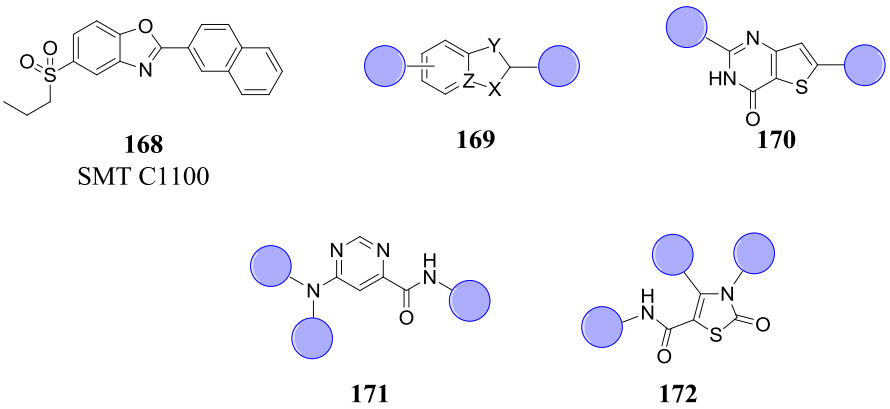

168
SMT C1100

169

170

171

172

Figure 30 Structure of utrophin transcriptional upregulator **168**. General structure of core scaffold **169** compounds selected from in-house library to test in the BREluc reporter assay. Structure of thienopyrimidine **170** previously identified to possess antagonist activity and further two core structures pyrimidine **171** and dihydrothioazole **172**

Having established a medium sized library of 320 compounds, testing these in the C2C12 stable transfected BREluc reporter cell line was the next action.

3.7 Medium throughput screening

An automated system was used to combine the 320 compounds at a stock concentration of 10 mM in DMSO on a 384 well plate. The C2C12 stable transfected cells with the BREluc reporter were treated with compound at 10 µM and 2 µM. The treated cells were tested in the same manner as was previously described for the luciferase assay. The assay procedure involved the incubation at 37 °C overnight, washing, lysis followed by addition of the

assay mixture to measure the readout of luminescence produced by the oxidation of luciferin by the luciferase enzyme generated in each well (*vide supra*).

To improve the quality of the readout obtained, it was decided that low concentrations of BMP-4 (2.5 ng/mL) would be added in addition to the test compound. The selected BMP-4 concentration allowed for simultaneous discovery of agonists as well as antagonists of BREluc expression. The concentration of recombinant BMP-4 protein was on the lower end of the slope of the dose response curve, thus rendering the assay sensitive to increase (agonist) and decrease (antagonist) effect on the BMP signalling (**Figure 31**).

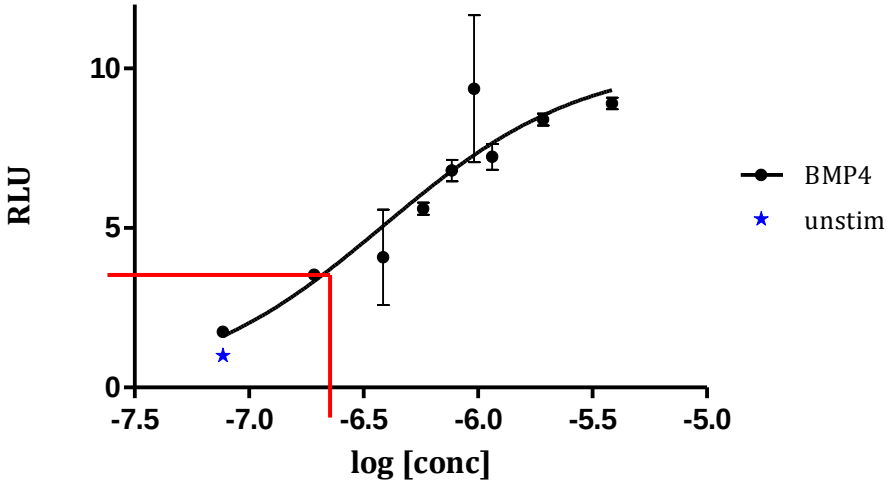

Figure 31 BMP4 dose response curve in relative luminescence units (RLU) displaying 2.5 ng/mL concentration and ability of assay to measure for agonists as well as antagonists

A summary of the compound selected for the screen are outlined in **Table 7**. The screen was carried out using single point concentrations (10 µM) and all experiments were done only in singletons. The results displayed some extremely promising results.

Class	Different Cores	# of Compounds
PRMT	3	24
HDAC	2	5
CBR	1	21
Cardiomyogenesis	27	39
In-house library	10	236
TOTAL		**320**

Table 7 Summary of the compounds selected with the number of different cores and number of compounds in each class
PRMT = protein receptor methyl transferase inhibitors
HDAC = histone deacetylase inhibitors
CBR = cannabinoid receptor binding molecules
Cardiomygenesis = literature compounds found to influence cardiomyogenesis
In-house = selected compounds from virtual based screen and gene transcription activators

Several compound classes from the in-house compound selection displayed increased luminescence. These included some bicycles, tricycles and some of the cardiomyogenesis modulators from the literature.

3.7.1 Results

3.7.1.1 Bicyclic and Tricyclic Series

The first series of compounds identified to increase expression of luciferase was the benzoxazole (**173**) (**Figure 32** and **33**). Of the 26 compounds that were tested with this core, all produced a higher signal than the cells treated with BMP-4 alone. The highest levels of activation in this series provided nearly 5 fold greater luminescence over the only BMP-4 stimulated cells. Similarly, the series of benzofurans **174** provided a similar trend (**Figure 34** and **35**). All the tested 29 benzofuran compounds increased the luminescence recorded by the plate reader in comparison to BMP-4 only stimulated cells.

Finally, the last class of compounds that also behaved in a similar way to the two bicyclics was the triazinoindole series **175** which were tested based on the similarity in the core of **116**. Also in this screen of 21 compounds, the majority displayed greater activity peaking at 5 fold that of BMP-4 only signal (**Figure 36** and **37**).

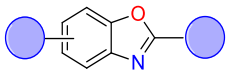

173

Figure 32 General Structure of benzoxazole derivatives

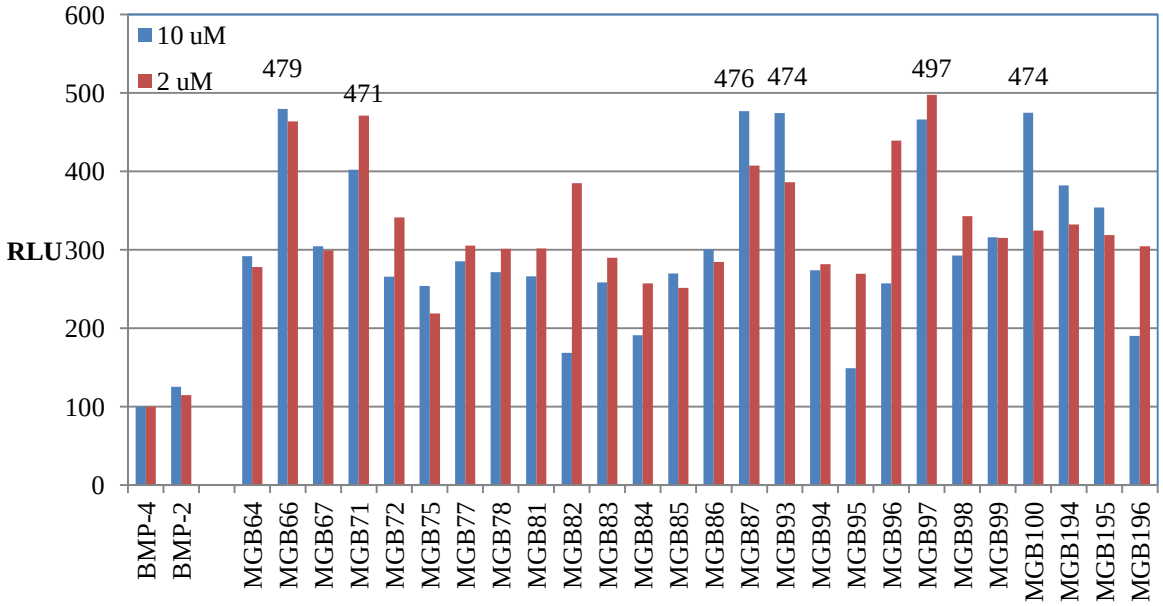

Figure 33 Relative luminescence units (RLU) of benzoxazole (**173**) series, treated with 2.5 ng/mL BMP-4

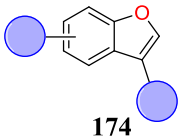

174

Figure 34 General structures of benzofuran derivatives

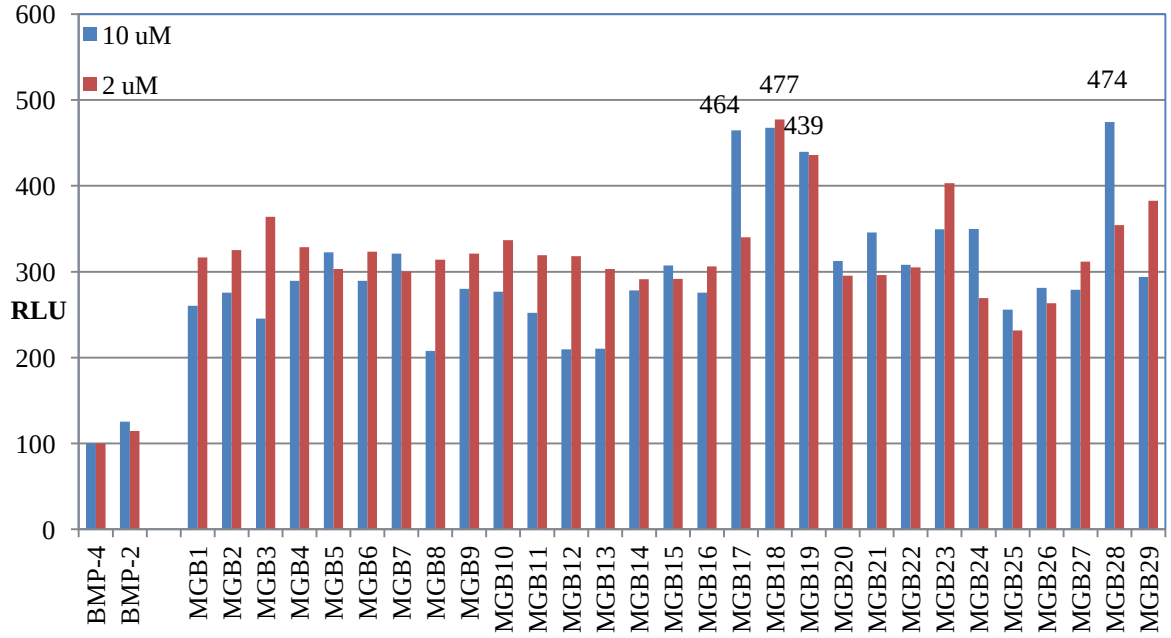

Figure 35 Relative luminescence units (RLU) of benzofuran (**174**) series, all treated with 2.5 ng/mL BMP-4

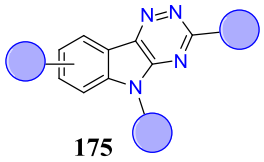

175

Figure 36 General structure of triazinoindole series

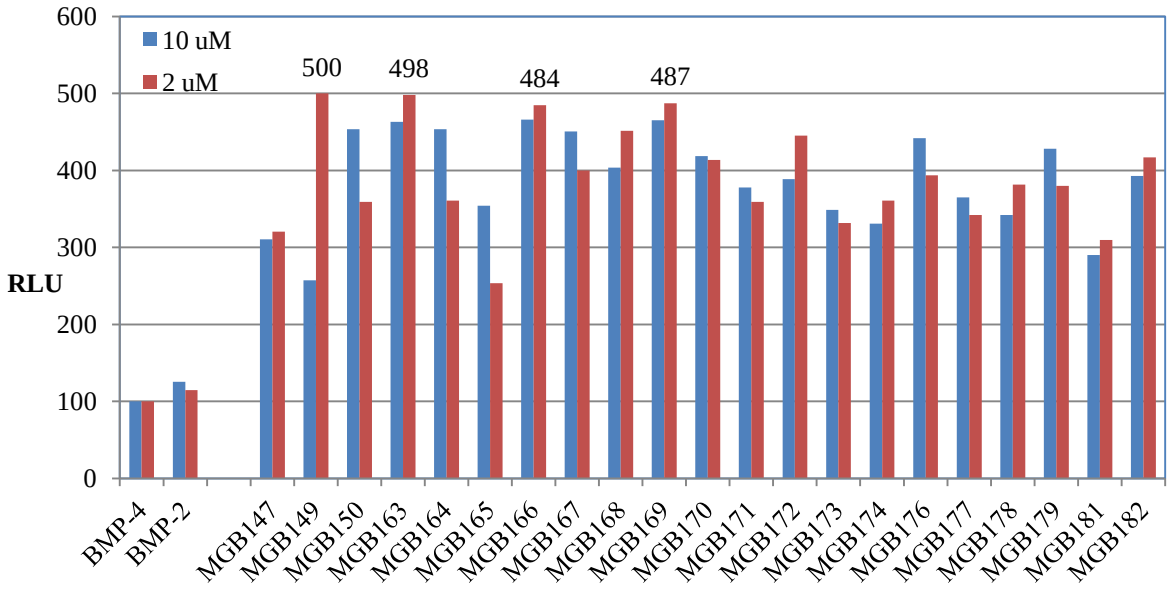

Figure 37 Relative luminescence units (RLU) of triazinoindole (**175**) series, all treated with 2.5 ng/mL BMP-4

3.7.1.2 Literature Compounds

The final set of compounds which arguably provided the most interesting results were those derived from the literature. High levels of activity were observed by the addition of several compounds in the presence of low levels of BMP-4 (**Figure 38**).

The most notable set of compounds are SAHA (**176**, MGB127), **177** (MGB128), **178** (MGB129) and **179** (MGB159) which are all connected by the common action of HDAC inhibition. The weakest of HDAC inhibitors tested in this screen displayed over 15 fold activity compared to the BMP-4 only treated cells (**Figure 37**). The highest levels of luminescence displayed by the HDAC's displayed RLU of over 26 fold of BMP-4 only treated cells and 2608% greater signal than BMP untreated cells.

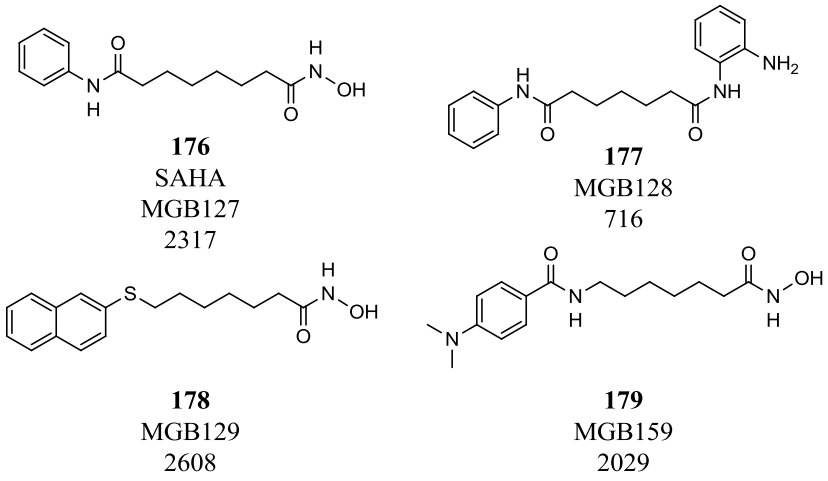

Figure 38 Structure some active HDAC inhibitors tested at 10 μM and their relative luminescence units (RLU), BMP-4 positive control is normalised to 100

Further to the HDAC inhibitors, a molecule of significant interest discovered in the MTS was **156** (MGB152**)** which is a member of the sulfonyl-hydrazones and was shown to induce cardiomyocyte differentiation and expression of cardiac markers (**Figure 39**).[149,176] **156** displayed over 10 fold larger signal in comparison to the BMP-4 only treated cells. It was hypothesised in the literature that **156** acts through HDAC inhibition however, subsequent experiments excluded action *via* HDACs.[149] Additionally the study investigated other common pathways associated with cardiomyogenesis including the BMP, Wnt and TGF-β pathways and reported no activation through these components. Finally, it was proposed that the compound could possibly act *via* MAPK signalling. Amongst the tested molecules, there were another two molecules that acted as MAPK inhibitors amongst other targets, retinoic acid (**25**, MGB125) and SB203580 (**154**, MGB112), which displayed activity of 2.4 and 2.6 fold greater that BMP4 only treated cells (**Table 6**).

Amongst the highly activating molecules derived from the literature was **180** (MGB118) which provided nearly 16 fold increased activity compared to the BMP-4 only signal (**Figure 39**). This compound was identified to have iron chelation ability in the literature.[170] The BMP pathway has been linked to expression of hepcidin, which a key player in iron homeostasis (**Figure 40**) With the use of Dorsomorphin (**30**), a BMP

antagonist, iron levels increased, however, the direct influence of iron levels on BMP signalling is not fully understood.[107]

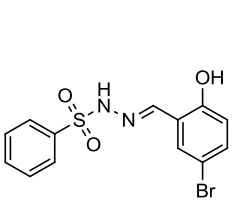

156
MGB152
Shz-1
1070

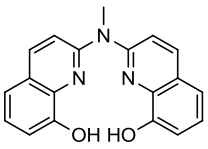

180
MGB118
1552

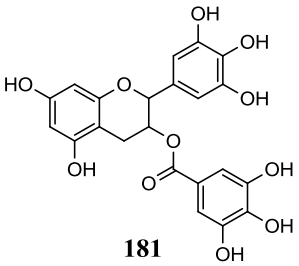

181
MGB101
EGCG
172

Figure 39 Cardiac enhancing molecules **156** and two compounds identified to have Fe^{2+} chelating properties, **180** and **181**, and their respective relative light units (RLU) at 10 μM with BMP4 normalised at 100

Several of the HDAC inhibitors that increase BMP activity have also been shown to chelate to iron, however in the BREluc assay display high levels of activity.[177] **175** (SAHA) was shown to chelate to iron and still exhibits very high levels of BMP activity at 23 fold upregulation. Contrary to the previous 2 examples, another iron chelating molecule, Epigallocatechin gallate (EGCG or **181**, MGB101) only displays relatively low levels of activity, of 1.8 fold at 10 μM (**Figure 39**). **181** was also found to have antioxidant properties and have affinity to the CB_1R. However, not all compounds with iron chelating ability tested in the assay displayed increased levels of luminescence. Therefore, the proposed mechanism of action would be through an alternative method and not displaying activity *via* sequestration of iron.

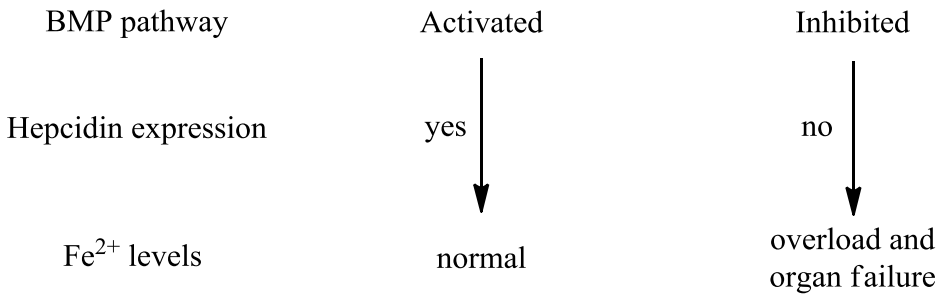

Figure 40 Involvement of BMP pathway, hepcidin expression and Fe^{2+} levels

3.7.1.3 Discussion of Compound Classes

The observed trend with all three of the bicyclic and tricyclic series could be due to two possible reasons; a synergistic or additive effect in which the compounds promote the activity of the added BMP-4 protein. Or alternatively the series could genuinely be BMP pathway enhancing molecules, by either binding to the BMPR or an alternative kinase that phosphorylates the intracellular R-smads and the combined effect of the BMP-4 protein and the test compound provides a greater combined signal. However, mechanistic studies would have to be undertaken to fully understand the mode in which the benzoxazoles, benzofurans and triazinoindoles are acting to provide the observed enhanced transcriptional upregulation of the BMP response genes.

The high levels of activity observed with the HDAC inhibitors could be explained by the involvement of HDACs in regulating gene expression. Deoxy ribonucleic acid (DNA) in the nucleus is compact and coiled around proteins called histones. Histones are the main components of chromatin alongside DNA. Chromatin can reside in two forms, one in which the histones are deacetylated, allowing for a strong interaction between the positive charged amino groups on the lysine residues and the negatively charged phosphates on the DNA. The second, the acetylated form, in which the positive charge on the histones is removed and the chromatin structure is resting in a more relaxed conformation and more accessible to gene transcription. HDAC's and histone acetyl transferases (HAT) are responsible for the process involving the addition and removal of the acetyl groups on the lysine amino acids of the DNA wrapped around the histones. Lysine, containing a terminal amine offers a suitable position for acetylation. Activity of HDAC's is believed to have an effect on transcriptional regulation of genes.[178] By HDAC inhibition, more acetylated histones are present which leads to an increase in gene transcription. Using this knowledge of HDACs it can be translated to this piece of work. With the addition of the four HDAC

inhibitors, alongside low concentrations of BMP-4, it can be hypothesised that the HDACs are promoting transcription of the BRE*luc* unit in the genome. The fact that this observation is consistent across these four known HDAC mediating molecules indicates to a possible trend between HDAC inhibition and transcriptional upregulation ultimately leading to the production of luciferase.

The MTS screen carried out of the 320 compounds yielded some very interesting results where novel groups of compounds containing bicyclic and tricyclic cores provided good BMP activity (**Figure 41**). In addition literature cardiomyogenesis activators also proved to activate BMP signalling especially known HDAC inhibitors. This led to the testing of further HDAC inhibitors and subsequent synthesis of the most promising hits and structural analogues thereof.

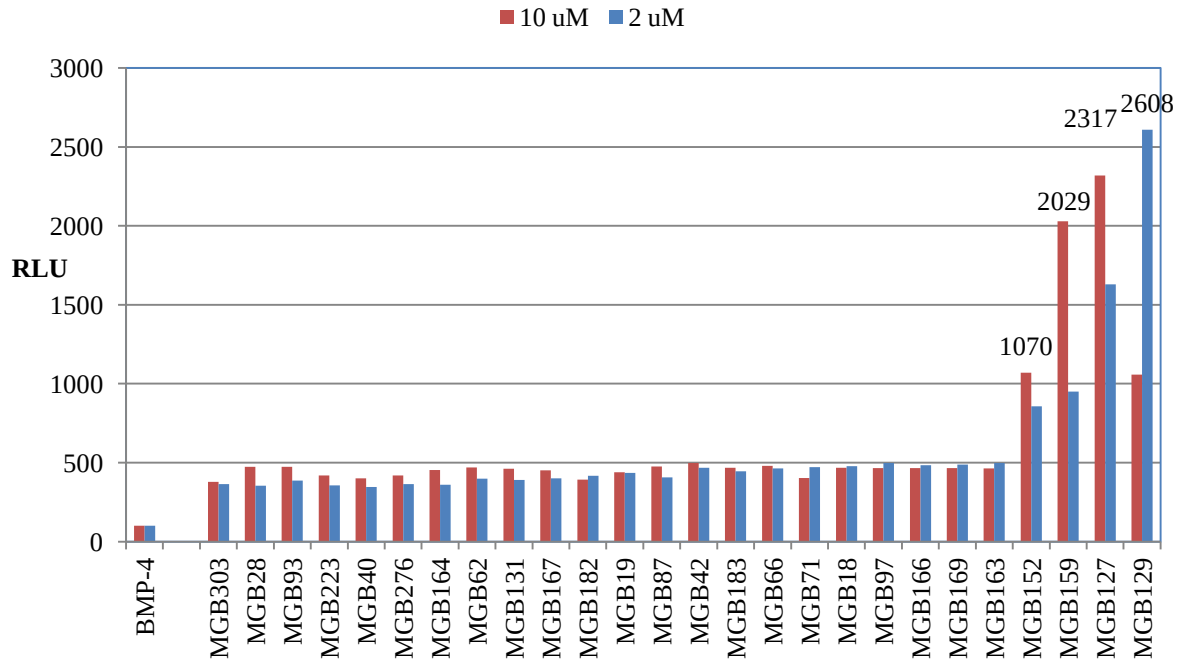

Figure 41 Most active compounds displayed by their relative luminescence units (RLU), from the 320 compound screen tested in singletons (10 μM) and normalised against positive control (BMP4) at 2.5 ng/mL

3.8 Derivatives of HDAC Inhibitors

Having identified HDAC inhibitors to provide increased activity in the luciferase reporter assay, further known HDAC inhibitors were acquired and tested in the reporter assay (**Figure 42** and **43**). The aim of investigating the activity of further HDAC inhibitors was to observe discrimination between the HDAC inhibitor profiles and correlate this to their observed activity in the reporter and RT-PCR assay. This led to the further discovery of another 8 compounds of interest **182-189**.

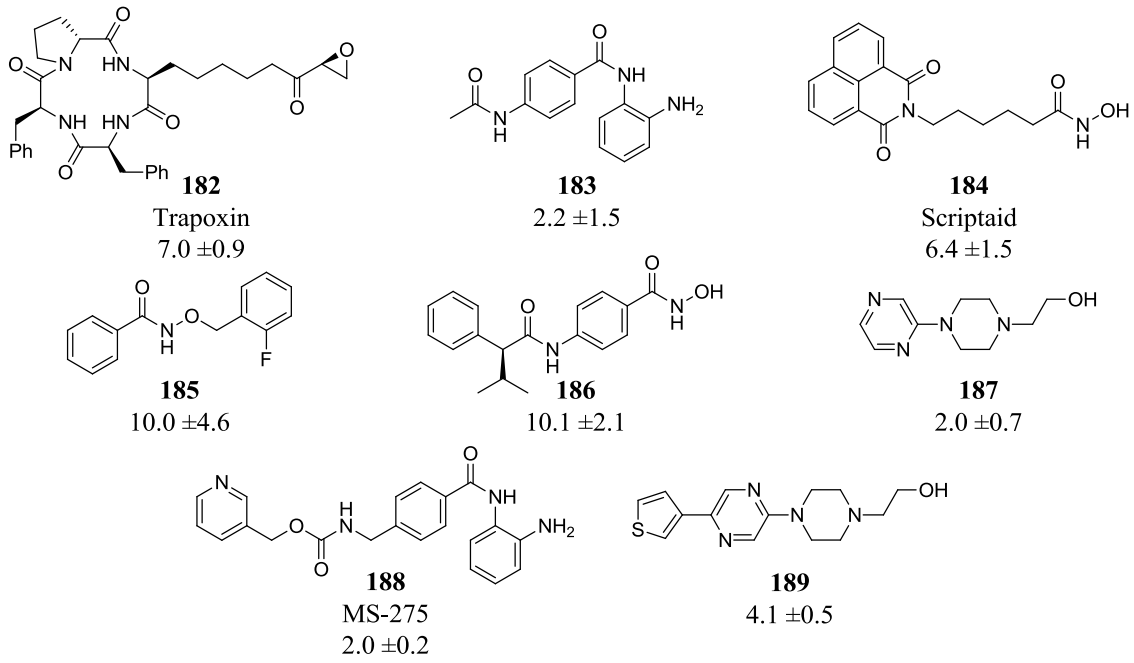

Figure 42 Structure and relative luminescence units (RLU) of the 8 most interesting activators discovered from screening of the HDAC inhibitors using the BRELuc reporter assay

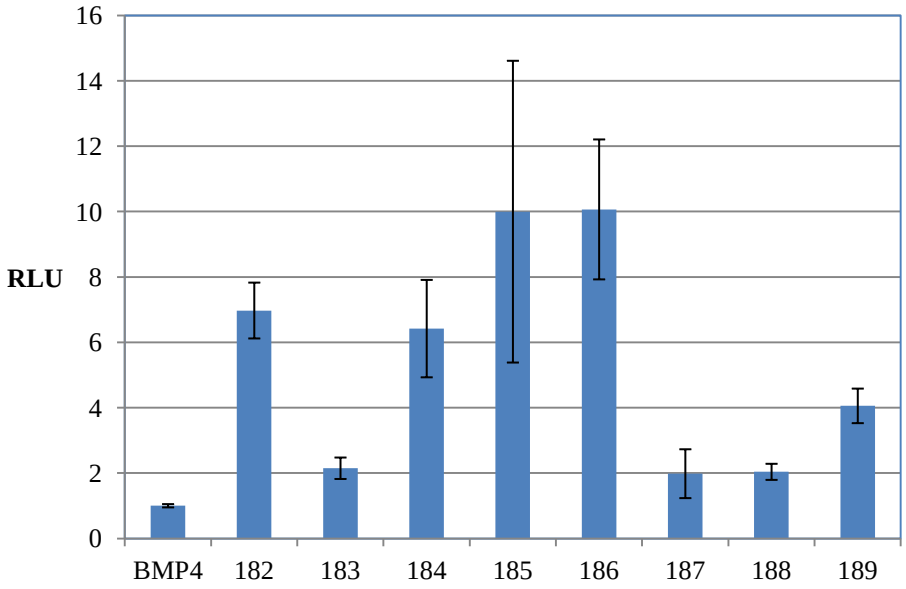

Figure 43 Activity measured in relative luminescence units (RLU) of the HDAC's **182-189** in the BREluc assay, with addition of 2.5 ng/mL BMP4 (RLU 1)

Following the identification of 8 interesting HDAC inhibitors (**182-189**), they had to be screened in an alternative assay to build evidence that their activity is truly *via* regulation of the BMP pathway. Firstly, the compounds were tested using a stably transfected CAGAluc COS7 cells line. The CAGA acts as the downstream response element of TGF-β pathway activation and promotes the transcription of the luciferase gene. In this reporter assay, luciferase is expressed during activation of the TGF-β pathway and lack of activity in this assay would provide evidence of possible specificity for the BMP pathway.[179] The compounds all displayed no activity in the stably transfected CAGAluc cell line.

Additionally, an independent assay was established measuring gene expression of BMP pathway activated genes.[180] The method applied was a real-time reverse transcription polymerase chain reaction (RT-PCR), which converts mRNA strands with the use of specific primers into DNA and amplifies it.[181] Through the use of this technique, expression levels of two BMP specific genes were measured, these were hepcidin and Id1, using a human hepatoma cell line (HuH7.5).[182,183] By administration of compounds and

measuring levels of the target mRNA transcripts at a specific time point, expression levels of the genes can be quantified.

The above identified compounds were tested in the RT-PCR assay in singlicants and some promising data was obtained (**Figure 44**). **188** provided the highest levels of hepcidin gene expression (RmRNA 27.7) with another two compounds displaying good levels of hepcidin expression, **183** (RmRNA 14.0) and **189** (RmRNA 8.2), compared to the control. The high levels of activity displayed by **188** provided an interesting starting point for further investigations into activity of compounds with this core structure.

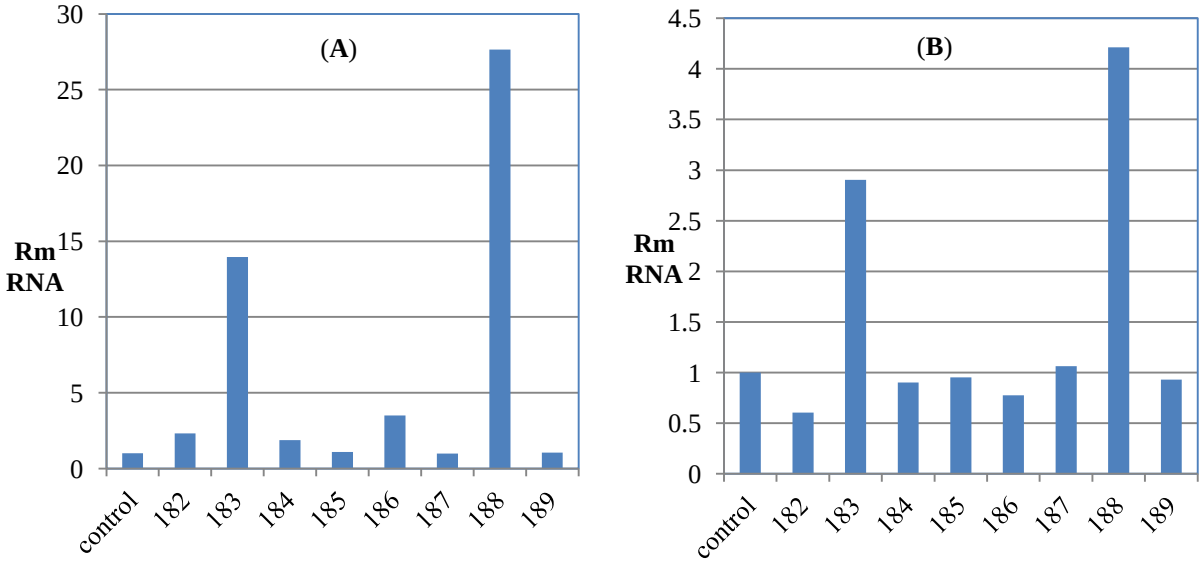

Figure 44 Hepcidin (**A**) and Id1 (**B**) expression levels with the compounds measured at 10 µM (n = 1) using real-time RT-PCR to quantify mRNA transcript levels. BMP-6 positive control showed levels of relative mRNA (RmRNA) of 80 and untreated cells of 1

188 was discovered to be a potent activator of hepcidin and Id1 gene expression (RmRNA 27.7 and 4.21 respectively). The HDAC selectivity profile provides evidence that the compounds exhibit different activity across the 11 known HDACs (**Table 8**). This could contribute to the difference in the activity observed in the BREluc assay as well as expression levels in the RT-PCR. **188** demonstrated a different selectivity profile to **182** and **184** with weak activity at HDACs 2 and 3, and no activity at 4, 6-8. However interestingly does provide strong inhibition of HDAC 9. Further EC50's are required to make conclusive remarks on the correlation between HDAC selectivity profile and BREluc and BMP related gene expression.

Compound	HDAC										
	1	2	3	4	5	6	7	8	9	10	11
182		nd	nd		nd		nd	nd	nd	nd	nd
184				nd	nd		nd	nd	nd	nd	nd
188					nd					nd	nd

Table 8 Example of three literature HDAC inhibitors and their HDAC selectivity profile

	strong inhibition (EC_{50} <5 fold x EC_{50} relative to most sensitive HDAC isoform)
	weak inhibition (EC_{50} >5 fold x EC_{50} relative to most sensitive HDAC isoform)
	no inhibition (EC_{50} >10 fold x EC_{50} relative to most sensitive HDAC isoform)
nd	no data published

Additionally HDAC's are known to exhibit activity by chelation to catalytic zinc in the active site of the enzyme, it was hypothesised that derivatives with alternative chelating motifs would prove to be active. **188** was synthesised to confirm activity using an authentic solid sample, additional derivatives with zinc chelating functionality on the benzamide motif (**190**) were generated and tested in the gene expression assay to generate some preliminary SAR (**Figure 45**).[184]

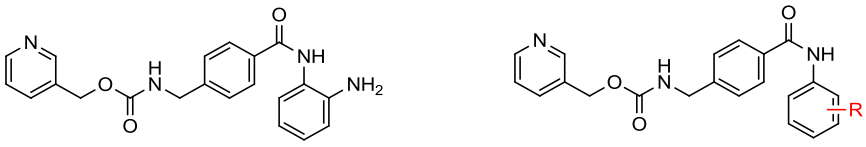

188 **190**

Figure 45 Structure of **188** and general structure of analogues synthesised **190**

3.8.1 Synthesis of 188

The synthesis of **188** was carried out *via* two step synthesis from 3-pyridinemethanol (**191**) and carbonyldiimidazole (CDI) and subsequent treatment of intermediate **192** with 4-(aminoethyl) benzoic acid and 1,8-diazabicyclo[5.4.0]undec-7-ene (DBU) to generate the

acid **193** (**Scheme 10**).[185] The acid **193** was then converted to the acid chloride **194** using oxalyl chloride on large scale (10.0 g, 35.1 mmol). To form the amide bond, the acid chloride **194** was dissolved in pyridine and 2-aminoanaline was added *in situ* to generate **188**. **195** and **196** were synthesised by treating the acid chloride with pyridine and treatment with 2-aminophenol and 2-aminopyridine respectively.

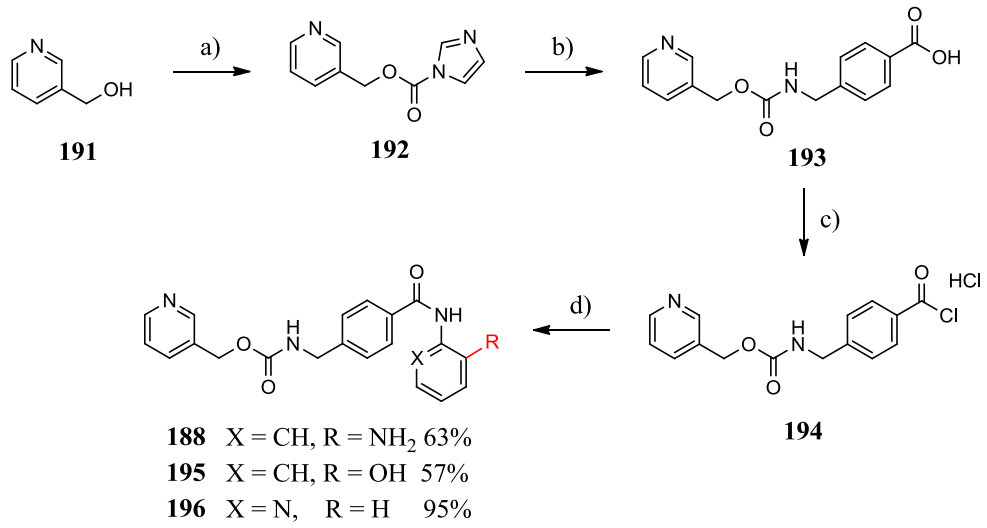

Scheme 10 Synthesis of **188** and simple derivatives thereof **195** and **196** a) CDI, THF, 10 °C – rt 1 h b) 4-(aminoethyl)benzoic acid, DBU, Et_3N, THF, rt 5 h over 2 steps 90% c) oxalyl chloride, toluene, DMF, rt 4 h, 83% d) Corresponding analine, pyridine, rt 2 h

188 was tested in the RT-PCR assay to verify the results obtained from the commercial sample alongside other substituted amides. The results confirm that **188** increased mRNA expression levels of hepcidin and Id1.

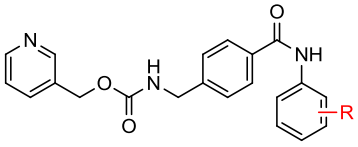

		HP	Id1
188	R = $2NH_2$	27.5	3.6
195	R = 2OH	8.2	2.0
197	R = 2F	0.8	0.9
198	R = 2H	0.8	0.8
199	R = 2SH	0.7	0.9
200	R = $3NH_2$	0.7	0.8

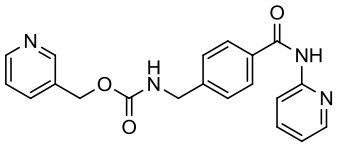

196		0.7	0.9

Figure 46 188 and its synthesised structural mimetics tested for hepcidin and Id1 gene expression in RmRNA concentrations (fold increase), HP = Hepcidin gene expression levels, Id1 = Id1 gene expression levels

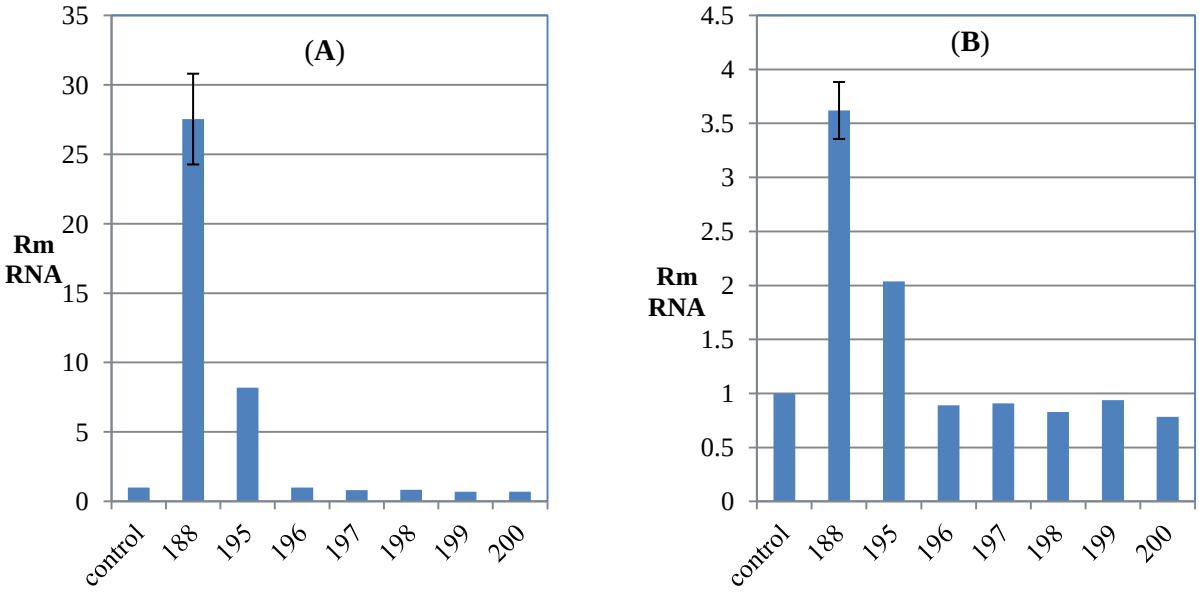

Figure 47 RmRNA levels of hepcidin (**A**) and Id1 (**B**) (fold increase) after treatment with the compounds at 10µM. BMP6 and DMSO were used as controls in both assays
Control = DMSO only

Both, hepcidin and Id1 expression levels have been shown to be regulated *via* BMP smad signalling. This assay demonstrated that with the administration of BMP ligand BMP6 (hepcidin RmRNA 80), levels hepcidin and Id1 of gene transcripts increase. Upon treatment with **188** concentration of both hepcidin and Id1 gene transcripts increase in respect to the control (hepcidin RmRNA 27.5 ± 3.3, Id1 RmRNA 3.62 ±0.26). This provides some evidence that the action of **188** is BMP pathway dependent, resulting in the

upregulation of gene expression dependent of BMP pathway activity and not due to non-specific luciferase activation (**Figure 46** and **47**).

3.9 Conclusion and Future Work

The process of identification of a novel BMP agonist molecule was proved difficult. Using the *in situ* hybridisation method with zebrafish embryos, compounds were identified to increase temporal and spatial gene expression patterns of BMP regulated mRNA. Synthesis and subsequent screening using the BREluc transiently transfected cell line, activity of the compounds could not be recapitulated. This indicated that their activity on gene expression in the zebrafish assay is possibly mediated *via* another mechanism, not through the BMP pathway. Alternatively the effect could be species specific, namely to the zebrafish. Further work to comprehend the mode of action and elaborate the activity profile needs to be undertaken.

Throughout this project a range of screening methods were established and investigated. Conceptually, the protein complimentary assay (PCA) using the luciferase bound smad proteins would allow the quantification of smad dimerisation, post receptor activation. Unfortunately, high levels of protein expression, possibly due to the excessive activity of the promoter, led to high background levels of luminescence which could not be increased further by BMP activating ligands. The very low signal-noise ratio made the assay unsuitable for library screening. As a range of conditions have already been investigated, the final suggestion would be to replace the current CMV promoter, with alternative weaker promoters such as Ubiquitin C promoter (UBC) or phosphoglycerate kinase 1 promoter (PGK).[186]

As a result of the high levels of expression, an alternative reporter assay was developed by transfecting a BREluc plasmid into C2C12 mouse myoblast cells. This was initially verified in transiently transfected cells to screen low numbers of compounds manually but

was further developed into a high throughput assay using a stably transfected cells line using an automated system. The reliability of the assay was confirmed by the z-score of 0.9845. The assay allowed the screening of hundreds of compounds from the in-house library. The use of ligand based virtual screening, using a known BMP antagonist dorsomorphin (**30**), has been implemented several times throughout the project to provide a targeted screening library.

Screening of a larger and more varied set of compounds including epigenetic modulators, kinase inhibitors and in-house molecules, led to the discovery of a number of active compounds displaying promising levels of luminescence in the BREluc assay. Focusing on the HDAC inhibitors, a larger set of known HDAC inhibitors was tested, which showed that activity in the BREluc assay is exhibited by a number of HDAC inhibitors, but not all. The interesting hits were subsequently screened in a RT-PCR assay, measuring gene expression levels of Id1 and hepcidin. The mRNA expression levels of BMP regulated genes, were both greater than the DMSO control. Of particular interest is **188** which displayed the highest levels of hepcidin expression (RmRNA 27.5 ± 3.3) and Id1 (RmRNA 3.62 ± 0.26).

Of the tested HDAC inhibitors not all provided activity in the BREluc assay. The selectivity profile of the HDAC inhibitors towards the 11 isoforms differs between compounds. Additional investigations into the relation of the activity at the relative HDACs and activity in the reporter assay could be investigated to gain a further understanding in the role of HDAC inhibition and BMP pathway activity. It has been shown in the literature that HDACs act as negative regulators of downstream smad activity of the BMP pathway.[187,188,189,190] Further literature compounds with known HDAC selectivity profiles could be tested to shed light on the correlation of the inhibition of the HDAC isoforms and BMP pathway activation.

To investigate the relationship between HDAC isoform activity and BMP pathway dependent gene expression, experiments using small interfering RNA's (siRNA) could be carried out. The administration of siRNA of a particular HDAC and stimulation of the BMP pathway with the use of BMP-4, could show dependence of BMP pathway activity on the relative HDAC. Combinations of siRNA of different HDACs could subsequently be measured to investigate the possible involvement of several HDACs on the BMP pathway.

Additionally to using literature compounds, further SAR could be developed around **188**. A study published by Finnin *et al* demonstrates TSA bound to the active site of the HDAC enzyme (**Figure 48**).[191] This X-ray crystal structure could prove useful in developing the next generation of compounds to be tested assays measuring activity of the BMP pathway and gene expression. The hydroxamic acid binds to the zinc ion in the groove of the active site, while the hydrophobic core is sandwiched between two phenylalanine residues (Phe141 and Phe198). Finally the tail of the molecule is solvent exposed outside the binding site. Docking studies suggest that **188** binds in a similar manner inside the pocket but the tail interacts with different amino acid residues providing a different selectivity profile.[192,185] SAR around the carbamate and pyridyl could therefore modify interactions and selectivity at the different HDACs. Further work is required to identify the mode of action of **188** and whether the observed activity is due to its HDAC isoform selectivity or an alternative target. With the used of DNA microarray, a method of measuring expression levels of a large number of genes, the mode of action of compounds could be identified.

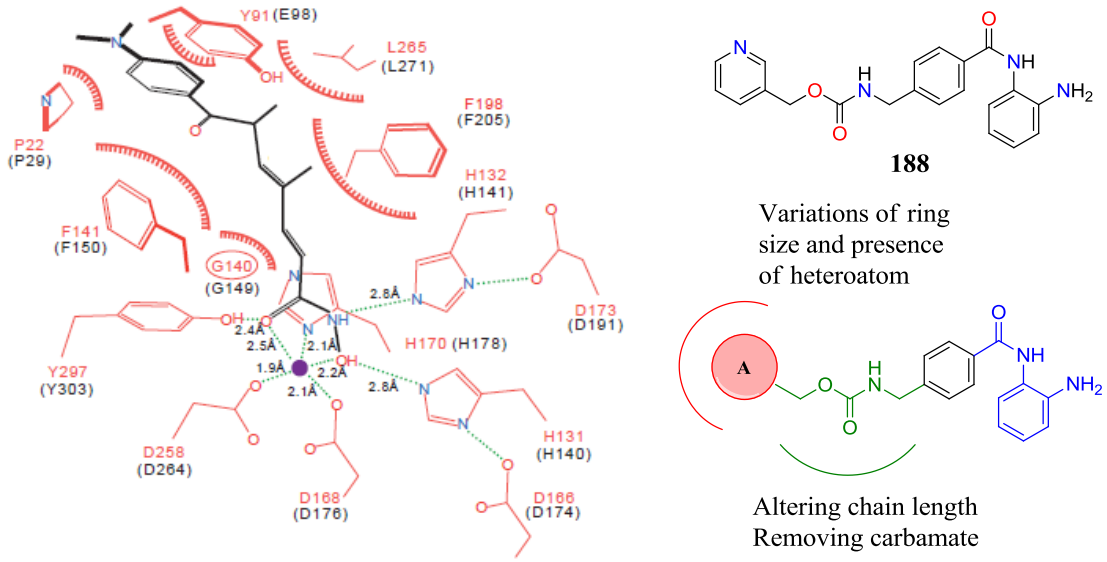

Figure 48 Schematic representation of the HDAC homologue (red) (representative of the sequence homology of the HDAC family), HDAC1 (Black) and TSA (**23**) bound in the active site of the enzyme with the zinc (purple) and H-bonding interactions (green lines). Structure of **188** discovered to increase luminescence in the BRELuc assay and mRNA levels in the RT-PCR assay. Possible structural modifications around the core of **188**

With the discovery of a compound displaying activity in the BRELuc reporter and RT-PCR assay further experiments could be carried out. The subsequent step would involve translating the observed activity of cardiomyogenesis in stem cells. Activation of the BMP pathway has been shown to increase the number of beating cardiomyocytes from a population of undifferentiated stem cells. The activity in promoting cardiac differentiation could be measured by quantifying expression of cardiac gene markers such as GATA-4, Nkx2.5 and MEF-2, or alternatively observe a change in phenotype to beating cardiomyocytes.

Finally, optimisation of the physicochemical properties of **188**, would allow for *in vivo* animal models investigating recovery of heart function after inducing myocardial infarction. Previous studies provide evidence that **188** suffers from low microsomal stability ($t_{1/2}$ = ~1h), future optimisation would require improved resistance to microsomes.[193]

This piece of work has successfully developed a high throughput assay for the screening of large number of compounds. Additionally, it identified a number of compound classes that display antagonist and agonist activity on the BMP pathway. Finally, a group of compounds that were identified to provide activity in the BREluc reporter assay were tested for BMP related gene expression and found to increase gene expression. The mode of action is yet to be determined, whether to be regulating activity of the BMP pathway by inhibition of HDACs, or whether **188** displays activity *via* an alternative method.

Part II: Discovery of a Novel Cannabinoid 2 Receptor Agonist

Chapter 4: The Discovery of Novel Agonist Molecules at the Cannabinoid 2 Receptor

4.1 The importance of Cannabinoid Research

Cannabinoid receptor (CBR) activity is involved in the regulation of many biological processes including: metabolism, craving, pain, anxiety, bone growth and immune function.[194] It is an essential regulatory pathway in homeostasis of functions in the body including weight and also in controlling adaptive responses such as the immune system and pain. Historically, pain relief has been the main focus of CBR regulation and has been exploited for medicinal and recreational purposes for millennia by the consumption of extracts from the plant *Cannabis sativa*. It is however only in the last 25 years that there have been remarkable advances in identifying the components involved and understanding the importance of this pathway. During this period, two cannabinoid receptors have been identified along with numerous selective, non-selective, activating and deactivating receptor binding molecules, both synthetic and from natural sources.

The activation of CBR in the suppression of inflammation is an area that has gained much attention recently.[195] Current therapies for treatment of acute and chronic inflammation are by suppression of pro-inflammatory cytokines preventing the development of a full inflammatory response (**Figure 1**). Cytokines are small proteins released by cells involved in intracellular communication. An alternative approach is to increase the anti-inflammatory cytokines reducing recruitment of cells to the site of the insult. As the chronic condition is plagued by a continuous inflammatory response, this strategy would provide for effective control of cytokine release and macrophage recruitment.

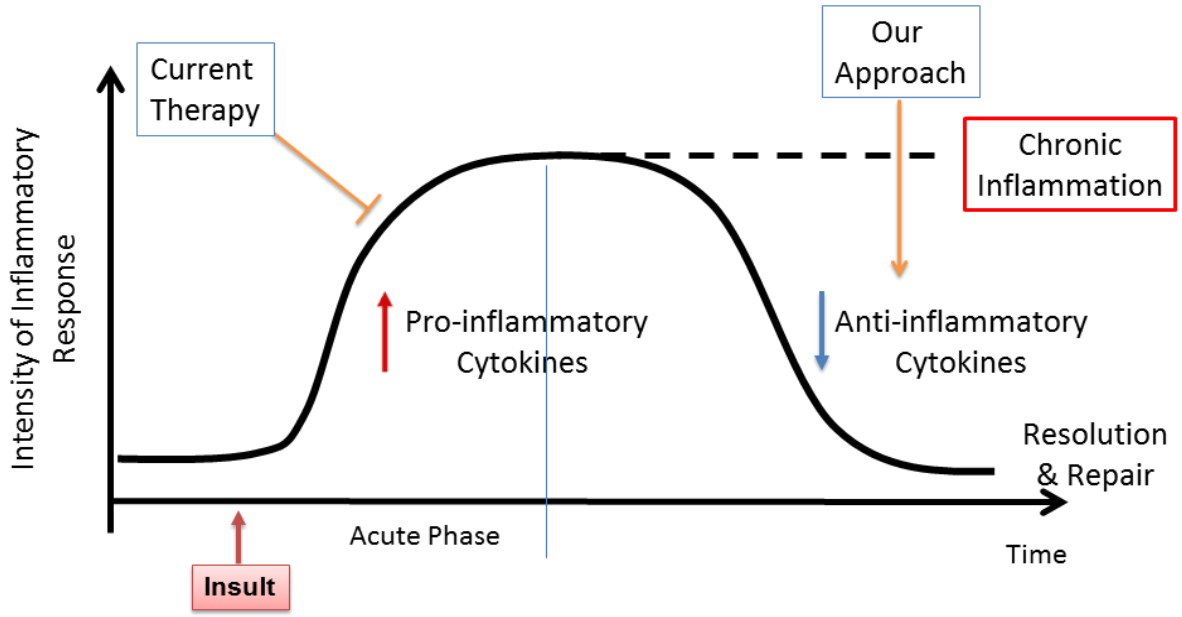

Figure 1 Inflammatory response curve initiated by release of pro-inflammatory cytokines to suppress an initial insult followed by release of anti-inflammatory cytokines to resolve the inflammation. Current therapies target the suppression of pro-inflammatory cytokine release, while our approach focuses on increasing release of anti-inflammatory cytokines

4.2 The Inflammation Process

Inflammation is the defensive response of the immune system towards harmful stimuli, for example the detection of pathogens, damaged cells or irritants. There are two different manifestations of inflammation namely acute, which is short lived, lasting up to several days, and chronic, which is sustained inflammation over a period of weeks to months. An acute inflammatory response is necessary in the body to repair an injured tissue, if the acute inflammation is not resolved and persists from months to years, the condition becomes chronic. The principle difference between the two classes is the difference in process the body undergoes to clear itself of the affected condition.

4.2.1 Acute Inflammation

When an acute inflammation occurs, there is immediate vasodilatation, resulting in an influx of blood to the site of inflammation. Neutrophils, a specific type of white blood cells, are short lived and the most plentiful types of white blood cells in the body. They are the first cells to be recruited by chemokines, which are small proteins released by cells

responsible for recruitment of cells to the site of injury.[196] The chemotactic response of neutrophils and increased blood flow to the site of infection or injury allows for the rapid reduction of inflammation by processes such as phagocytosis.

4.2.2 Chronic Inflammation

If the inflammation does not recede quickly, the disease progresses to a more severe (chronic) stage. The advanced stage of the disease is marked by continued inflammation due to injury or infection leading on from the acute stage.[197,198] Acute inflammation begins with the recruitment of neutrophils to the site of infection or injury (**Table 1**). By contrast, the chronic inflammation stage is marked by the migration of a different type of leukocyte, termed monocytes. Monocytes normally resident in the spleen but are recruited to the site of infection by chemokines and terminally differentiate to macrophages and dendritic cells upon arrival at the inflamed tissue.[199,200]

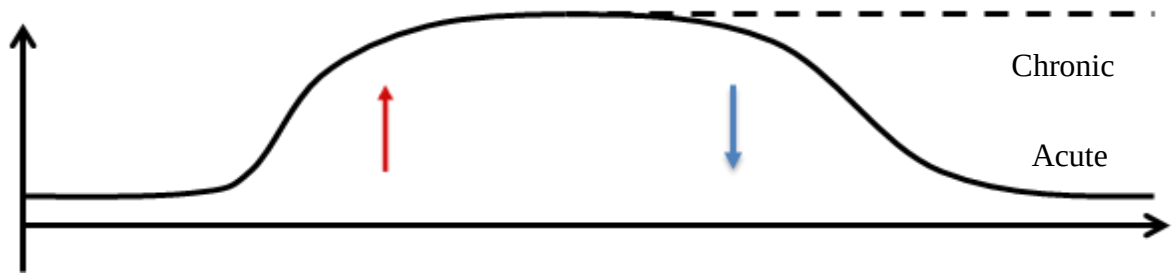

Action	Acute	Chronic
Duration	Short lived	Long term
Onset time	Onset is well defined	Vague onset
Effect on tissue	Pronounced vasodilatation and tissue permeability	Mild effects on tissue
Cells recruited	Neutrophils	Monocytes

Table 1 Simple comparison of symptoms between acute and chronic inflammations

Several diseases are the result of chronic inflammation for example atherosclerosis, where injury to the arterial wall ultimately leads to plaque formation and risk of myocardial

infarction.[201] Autoimmune diseases also originate from chronic inflammation for example multiple sclerosis, which involves plaque development on the damaged myelin of axons.

4.2.2.1 Atherosclerosis

Atherosclerosis begins with damage to the healthy endothelium (**A**) causing an initial inflammatory response (**Figure 2**). Over time, the damage to the wall leads to deposition of cholesterol, platelets and other particles thickening the inner layer of the endothelium (**B**). This leads to hardening of arterial walls prompted by the accumulation of white blood cells and low density lipoproteins (LDL) at the site of injury.[202] The result is an atherosclerotic plaque, consisting of macrophages on the outside of the plaque, a solid layer of cholesterol crystals and extracellular calcium deposits (**C**), which can rupture and lead to the formation of a thrombus (**D**).[203]

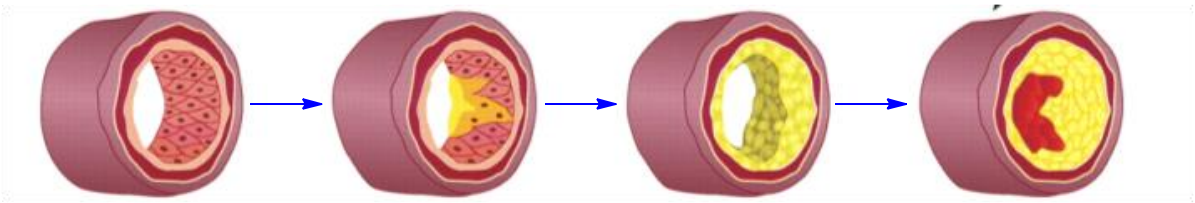

Figure 2 Progression of atherosclerosis: healthy artery (**A**), cholesterol build-up (**B**), development of atherosclerotic plaque (**C**), plaque ruptures followed by thrombus formation (**D**)

It has been observed that leukocytes, particularly monocytes, are important in the development of atherosclerosis.[204] As monocytes are highly plastic cells, they can differentiate to a variety of different cell types in response to local cytokines. They are recruited to the site of inflammation by different inducing factors and differentiate to macrophages and dendritic cells.[205] Furthermore it has been shown that reduction of monocyte count in rabbits, with the use of small molecules targeting the CB_2R, leads to a reduction in plaque size compared to untreated subjects.[206]

Diseases associated with atherosclerosis account for the largest death rate in the developed world with up to 50% of deaths in which coronary heart disease (CHD) is the principal cause.[207] In the USA in 2009, 1 in 4 deaths in adults are caused by CHD.[208] Fatalities originate from the hardening of the blood vessels and development of a plaque leading to reduced or complete lack of blood flow to vital organs. Current treatments for regression of atherosclerotic plaques involve the use of statins however, with considerable side effects such as headache and diarrhoea to varying degrees.[201] Alternatively, surgical intervention can remove plaques hindering blood supply to the heart to reduce the risk of CHD. Developing new therapies, to control the formation, development and promote regression of atherosclerotic plaques, would to reduce the number of deaths associated with this disease.

4.2.3 CB_2R Involvement in Inflammation

Cannabinoid 2 Receptors (CB_2R) are known to be primarily expressed on cells associated with immune function. It was hypothesised that their activity has an involvement in immunoregulation. CB_2R agonism has previously been shown to have an osteogenic effect in addition to analgesic modulation, but most interestingly it was discovered that modulation of CB_2R has an effect on monocyte recruitment to sites of inflammation.[209] As monocyte chemotaxis is an essential stage in the progression of atherosclerosis, it has been suggested that CB_2R modulation could have a pronounced effect on controlling the process.[207] It was previously demonstrated that control of immune function can be modulated by the administration of a weak CB_2R agonist. By feeding mice a low oral dose of Δ^9-tetrahydrocannabinol (Δ^9-THC, **201**) formation of atherosclerotic plaques was reduced.[210,211] More importantly, elevated levels of CB_2R were detected in atherosclerotic plaques of humans and mice, leading to the hypothesis that CB_2R expression has potential involvement in the regulation of atherosclerosis via mediation of monocyte recruitment.[212]

The effect of a CB_2R antagonist on atherosclerotic progression has also been investigated. With administration of the first potent and highly selective CB_2R antagonist, SR144528 (**202**) (CB_2R over CB_1R > 700 fold, K_i CB_2R 0.6 nM), the activation of the CB_2R by the partial agonist GW405833 (**203**) (K_i CB_2R 3.9 nM) was suppressed resulting in a renewed progression of the disease (**Figure 3**).[213,214] Additionally, Steffens *et al* observed that monocyte recruitment was prominently reduced with the use CB_2R agonist **203** (K_i CB_2R 3.9 nM). When co-administering the antagonist **202**, progression of the disease was again observed, supporting the possible involvement of this pathway in regulating atherosclerosis *in vivo*.[212,215] With this fundamental discovery an established i*n vivo* model was set up using Apolipoprotein E knockout mice ($ApoE^{-/-}$), which are healthy upon birth but lack an essential transport system in metabolism of lipids.[216] In $ApoE^{-/-}$ mice, development of aortic atherosclerotic was observed.[217] Using this and elevated cholesterol levels by feeding mice high cholesterol diets, atherosclerotic progression was assessed in the presence and absence of **201**, a low affinity agonist of the CB_2R. The conclusion supports the view that modulation of the CB_2R is involved in the control and recession of atherosclerosis, as disease regression was observed in mice receiving the Δ^9-THC (**201**) treatment.

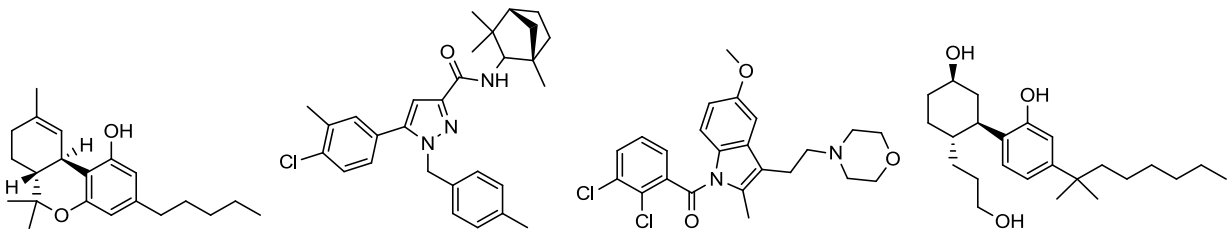

201
Δ^9-THC
Partial Agonist
CB_1R 35.3 nM
CB_2R 3.9 nM

202
SR144528
Antagonist
CB_1R 437 nM
CB_2R 0.6 nM

203
GW405833
Partial Agonist
CB_1R 4772 nM
CB_2R 3.9 nM

204
CP55940
Full Agonist
CB_1R 0.58 nM
CB_2R 0.68 nM

Figure 3 Structures and affinity values at the CB_1R and CB_2R of Δ^9-THC **(201)**, SR144528 (**202**), GW405833 (**203**) and CP55940 (**204**)

4.3 Cannabinoid Receptors

The roles of the cannabinoid system in the body, *vide supra*, have sparked interest in research into these receptors. Interestingly, studies of cannabinoid receptor binding molecules had commenced long before the receptors had been identified. There was prior knowledge that the ingredients of marijuana had medicinal effect, for example in treatment of migranes, asthma and insomnia, but the target was still unknown. The discovery of the first of the two identified CBRs was only possible with the development of higher affinity ligands, which will be discussed in the next section. With the discovery of more potent binding ligands, the use of isotopic labelling was employed to identify cannabinoid receptors in plasma membranes. Subsequent screening of orphan G protein coupled receptors (GPCR's) from a rat cDNA library resulted in the cloning of the first cannabinoid receptor, CB_1R.[218,219] Several years later another GPCR was discovered which due to its homology and ligand binding profile was classified as part of the CBR family, named CB_2R.[219, 220,221]

The two CBRs display 47% sequence homology, but their expression and function was discovered to be very different. The CB_1R are mainly expressed in the central nervous system (CNS) on axons and nerve terminals. They are largely responsible for motor control, cognition, motor response, emotional behaviour and regulation of immune response.[222,223] The CB_2R on the other hand are predominantly found on immune cells and in low concentrations in the brain. It was first established that CB_2R were present in lymphoid tissues by the use of a radiolabelled CB_2R agonist binding ligand ^{3}H-CP55940 (**204**) (**Figure 3**).[215] In addition RNA transcripts of the CB_2R were found by analysis of the cell contents.[224] Binding of agonists molecules leads to the activated receptor promoting coupling of G_i and G_0 heteromeric proteins (**Figure 4**).[225] Control of CBR's activity leads to downstream effects on adenylate cyclase, important in the conversion of adenosine

triphosphate to cyclic adenosine monophosphate, leading to the control of many biological processes and mitogen activated protein kinases (MAPK) which controls phosphorylation of intracellular proteins. Regulation of CB_1R activity can also regulate voltage sensitive Ca^{2+} channels (VSCC) and levels of intracellular Ca^{2+}.[222,226,227]

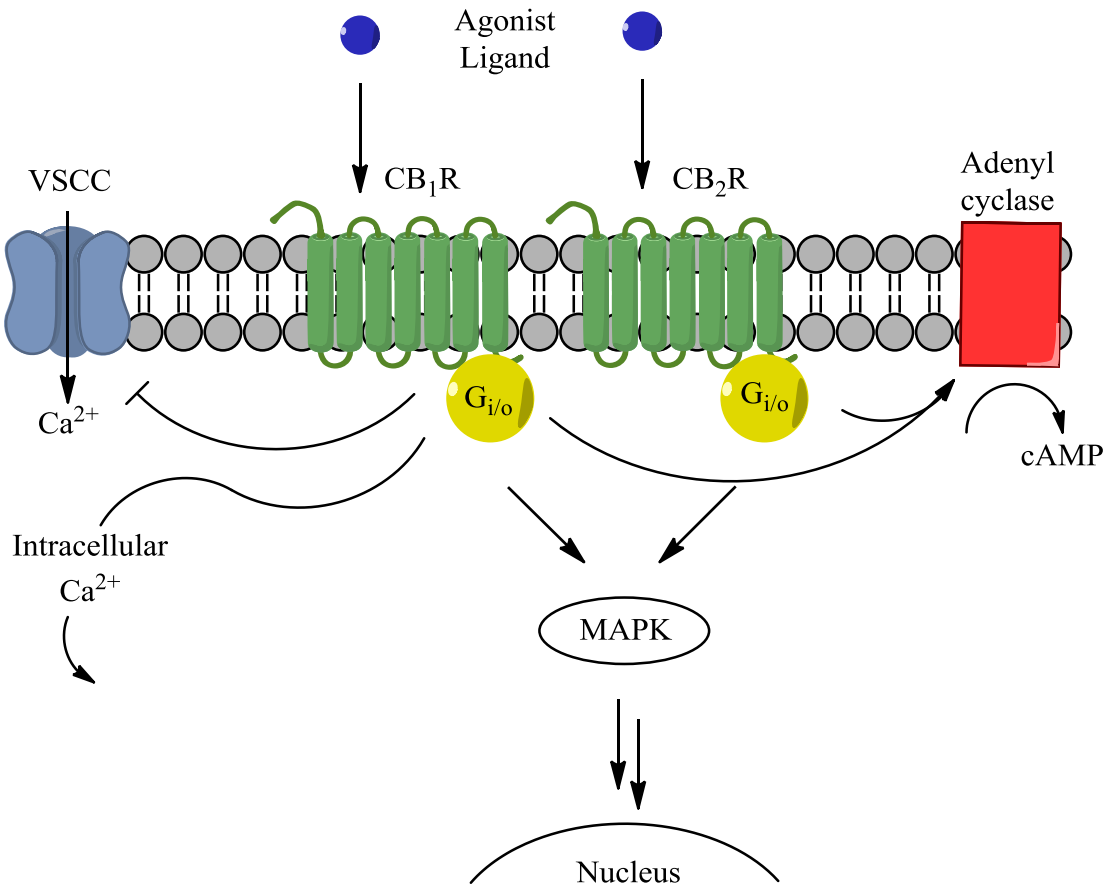

Figure 4 Summary of cannabinoid receptor major signalling pathways, activation of CB_1R and CB_2R leads to $G_{i/o}$ coupling and inhibition of adenylyl cyclase and voltage sensitive calcium channels (VSCC). CBR activation also regulates MAPK signalling pathways and intracellular calcium release

4.3.1 Cannabinoid Receptor Ligands

4.3.1.1 Endocannabinoids

As the receptors are widespread throughout the body and CBR activation is very rapid, it was suspected that endogenous ligands are produced and released locally. Further investigations identified two main ligands which unlike classical neurotransmitters, are stored in secretory vesicles; anandamide (AEA or **205**) and 2-arachidonyl glycerol **(**2-AG

or **206**) (**Figure 5**).[228,229,230] **205** was the first endocannabinoid to be discovered, and the fatty acid derivative was found to have a weak binding affinity to both CB_1R and CB_2R. **206** was discovered later and was recognized to act as a full agonist of CB_1R inducing a rapid increase in free intracellular Ca^{2+} in neuroblastoma X glioma cells. In addition it was found to also activate the CB_2R.[231]

Both ligands are metabolites of arachidonic acid and have been shown to be important in lipid signalling and metabolic pathways.[225] The endogenous ligands act locally and their activity can be terminated by cellular uptake and hydrolysis by hydrolase enzymes.[232] Both endocannabinoid families can be mobilised by the local transport system to reduce their activity, however they vary in their method of degradation in that **205** is hydrolysed by fatty acid amino hydrolase (FAAH), while **206** is hydrolysed by monoacylglycerol lipase (MAGL) both resulting in the recycling of arachidonic acid.[233]

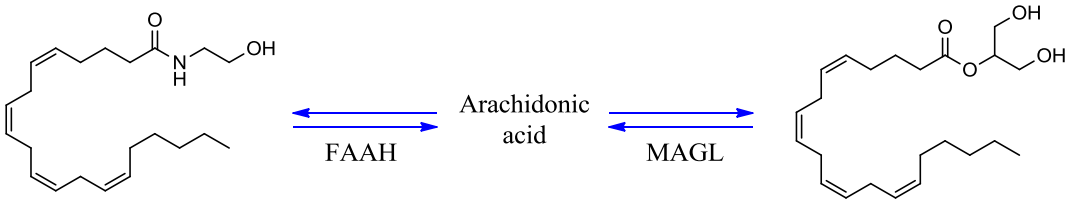

205
Anandamide

206
2-Arachindonoylglycerol

Figure 5 Metabolites of Arachindonic acid include endocannabinoids Anandamide (**205**) and 2-Arachidonoylglycerol (**206**) and hydrolysis converting them back to arachidonic acid

4.3.1.2 Phytocannabinnoids

The *C. sativa* plant, also known as marijuana, is the most abundant source of phytocannabinoids. With knowledge that the plant had a number of biologically active components that could be used in a range of diseases, further research was dedicated to isolating and identifying these. This led in 1964, to the isolation and characterisation of numerous active components, of which **201**, cannabidiol (CBD or **207**) and cannabinol (CBN or **208**) were the most abundant (**Figure 3** and **6**).[234] These phytocannabinoids show

non-selective binding profiles at the two CBR's and their action leads to analgesic, appetite enhancing, and anti-rheumatic effects. The marketed drug Sativex consists of a combination of phytocannabinoids including equal portions of **201** and **207**, with small quantities of other cannabinoids administered as a sublingual spray. It was developed for the treatment of neuropathic pain in multiple sclerosis (MS) patients, and as an analgesic, pain modulator, in cancer patients.[235,236,237] However, use of these natural cannabimimetics was limited due to their psychotropic side effects.

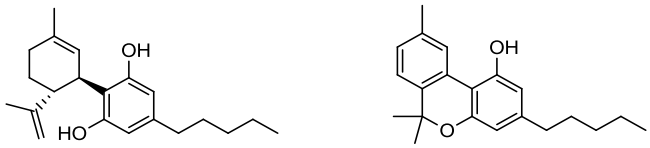

207
Cannabidiol

208
Cannabinol

Figure 6 Main components of the *cannabis sativa* extracts

The application of phytocannabinoids in therapeutics, but limited utility due to their side effects and unfavourable chemical properties, inspired research to develop alternative synthetic ligands.

4.3.1.3 Synthetic Cannabinoids

In the 1980's research began to discover alternative ligands for the cannabinoid receptors. SAR around the structure of Δ^9-THC (**201**) led to the discovery of a series of more potent receptor binding molecules. Of this series **204** (K_i CB_1R 0.58 nM, CB_2R 0.68 nM), was the most studied compound and was discovered through the optimisation of a previous compound, CP47497 (**209**) (**Figure 7**).[238,239] **204** differs from the starting molecule, **201**, at several sites. Replacement of the 2,2-dimethyl pyran with an alkyl chain introducing four additional rotatable bonds which provides more flexibility at this position. The supplementary alcohol at the end of the alkyl chain and on ring A, provides possible hydrogen bonding options to the binding pocket leading to increased binding affinity. A

further modification observed throughout the series of Δ^9-THC (**201**) derivatives introduces a gem dimethyl group on the alkyl chain of ring C, this is observed to increase affinity at the receptors. Another possible reason is to improve the stability of the compounds due to the metabolic liability of benzylic positions. The methylene neighbouring the aryl group is susceptible to metabolic oxidation, and by a replacement with a gem dimethyl group removes the possibility for oxidation at this position. Finally, by the opening of the pyran ring, the rigid tricyclic core of **201** is lost and another rotatable bond in introduced between ring A and ring C.

Another important classical cannabinoid derivative, JWH-133 (**210**) (K_i CB_2R 3.4 nM, CB_1R 677 nM) displays improved selectivity over precursors **212** and **204**, possibly due to loss of the hydroxyl group and possibly also the shortening of the alkyl chain.

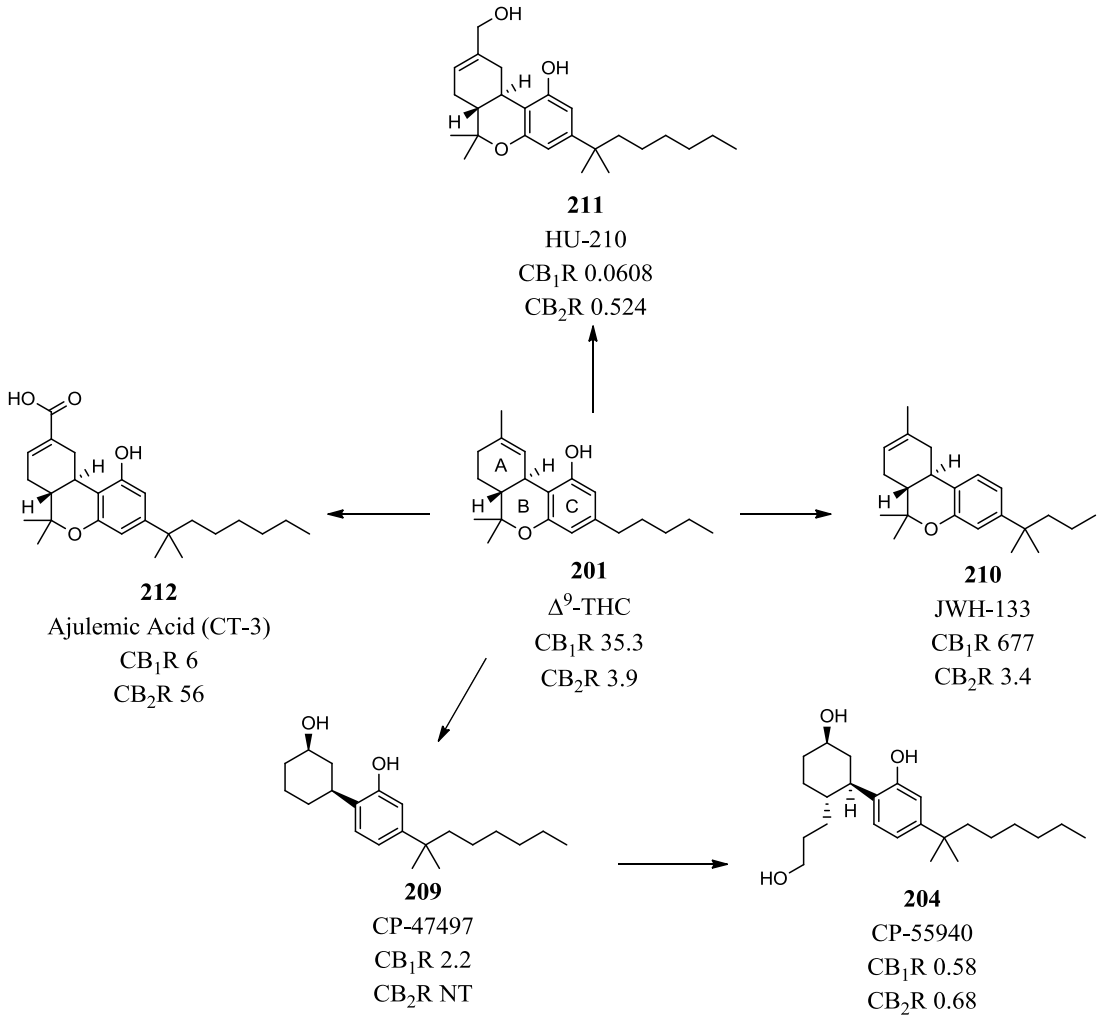

Figure 7 Derivatives of the series of "classical cannabinoid" receptor binding molecules **204**, **209**, **210** **211** and **212** derived from SAR around the known structure of Δ^9-THC (**201**) and their binding affinity at the CB_1R and CB_2R (K_i in nM) NT = not tested

Further variation around the tricyclic dibenzopyran motif in Δ^9-THC (**201**) in the category of "classical cannabinoids" led to the discovery of compounds including HU-210 (**211**) (K_i CB_1R 0.061 nM, CB_2R 0.524 nM) (dexanabinol, Pharmos Corporation) and ajulemic acid (CT-3 or **212**) (K_i CB_1R 6 nM, CB_2R 56 nM) (**Figure 7**).[240,241] Both of these molecules were suspected to have an alternative mode of action through modulation of the arachidonic acid pathway of the peroxisome proliferator-activated receptor (PPAR).[242,243] PPARs are nuclear receptor proteins that have been shown to be involved in regulating gene expression linked to metabolism.

A group of synthetic cannabimimetic ligands were discovered and developed by researchers at Sanofi, with the intention of finding a new drug through CB_1R inhibition with anti obesity and weight control activity. CB_1R was identified as a viable target based on the observation that consumption of marijuana enhances appetite, therefore by suppressing the stimulus, the opposite effect could be achieved.[244] This was arguably the most successful group of CBR ligands developed to date and the series for which most SAR data has been generated.

This family of compounds was based on a substituted pyrazole scaffold and led to the discovery of a selective CB_2R inverse agonist **202**, and a successfully marketed selective antagonist/inverse agonist of the CB_1R, SR141716A (rimonabant or Acomplia®, **213**).[213,245]

Derivatives of the pyrazole series have provided insight into what parts of the molecule have an effect on affinity and selectivity at the CB_1R.[246] Highest binding affinity and antagonistic effect at the CB_1R was observed with the introduction of halogens or alkyl groups at the *para* position on the phenyl group at the pyrazole C(5) position (**Figure 8**).[247] A methyl group at the pyrazole C(4) position, demonstrated best CB_1R selectivity over the demethylated or longer alkyl chain counterpart. Lengthening the alkyl chain increased metabolic resistance to oxidation and decreased selectivity between the two receptors. Finally, substitution at the C(3) carboxamide group proved essential for CB_1R antagonist activity possibly by hydrogen bonding through the carboxamide in addition to hydrophobic interactions with a lipophilic group in the binding pocket *via* the pipperidyl. Any substituent including alkyl amides, ethers and alcohols showed a lower affinity in comparison to the C(3) amido piperidyl group. Changes in ring size to a 5 and 7 membered ring gave agonist activity indicating a possible spatial restriction and a likely lipophilic groove at this site of the pocket. Finally, Surinabant (**214**) was discovered with a 2,4-

dichloro phenyl substitution pattern at the pyrazole *N*(1) position was most tolerated with observed loss in affinity at the CB_2R .[248,249]

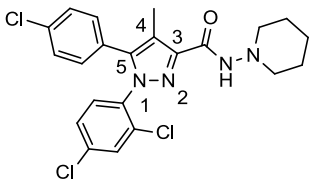

213
SR141716A
Rimonabant
CB_1R antagonist
CB_1R 5.6
CB_2R >1000

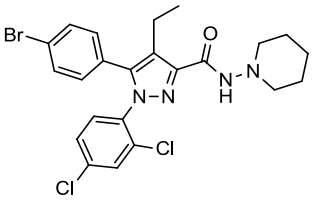

214
SR147778
Surinabant
CB_1R antagonist
CB_1R 3.5
CB_2R 442

Figure 8 Structures of CB_1R antagonist **213** and **214** and CB_2R with relative binding affinities (K_i in nM)

Another class of CBR binding ligands that deserve mention are the aminoalkylindoles (AAA) (Figure 9). These were originally developed by researchers at Sterling in the early nineties as potent and selective CB_1R acting compounds and include WIN 48098 (pravadoline or **215**) (K_i CB_1R 1.9 nM) which was identified to have anti-inflammatory and analgesic properties. Development was discontinued due to its kidney toxicity, leading to the investigation of alternative functional groups around the alkylindole core.[250] By the addition of another ring, WIN 55212-2 (**216**) was discovered also introducing a stereogenic center and demonstrated full agonist effect at the CB_1R. Interestingly, the *R*-enantiomer **216** displays agonist activity at CB_1R, while the *S*-enantiomer WIN 51212-3 (**217**) demonstrates inverse agonist activity at CB_2R.[251] **215** has the morpholino group linked to the indole *via* an ethyl linker allowing flexibility and mobility around the two rotatable bonds. With the introduction of a fused 6, 6-dihydro morpholine and fixed stereochemistry, the morpholine group is conformationally restricted, favouring activity at the CB_1R.

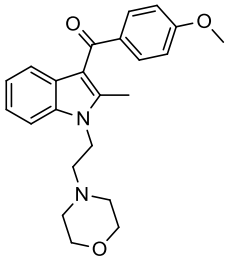

215
WIN 48098
Agonist
CB_1R 1.9
CB_2R NT

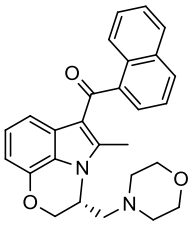

216
WIN 55212-2 (*R*)
Agonist
CB_1R 9.94
CB_2R 16.2

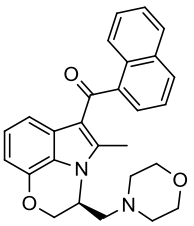

217
WIN 55212-3 (*S*)
Inverse agonist

Figure 9 Aminoalkylindole (AAA) compounds **215**, *R* enantiomer **216** and S enantiomer **217** (K_i in nM)
NT = not tested

Only a small number of these CB_1R modulating ligands have been marketed after successfully demonstrating efficacy and low toxicity in clinical trials. Rimonabant (**213**), was first discovered in 1994, marketed in 2006 and removed from the market in 2008 due to its potential CNS side effects including depression, anxiety and sleep disturbance.[252] A small number of other compounds were advanced to clinical phase including surinabant (**214**) (Sanofi-Aventis), taranabant (**218**) (Merck) and otenabant (**219**) (Pfizer) but these have all been discontinued (**Figure 8** and **10**). Poor physicochemical properties and off target effects have limited the progression of many CB_1R modulators and with knowledge in the field progressing, interest in the discovery of molecules acting on the CB_2R, particularly after the discovery of the first selective CB_2R molecule **202** by Sanofi, has increased.

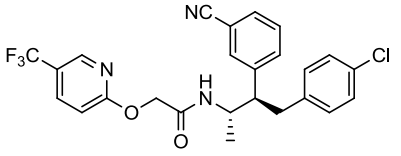

218
Taranabant

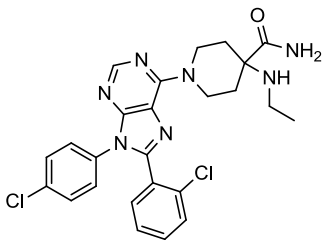

219
Otenabant

Figure 10 Cannabinoid receptor ligands **218** and **219** to have been discontinued during clinical trials

4.4 Cannabinoid 2 Receptor Binding Molecules

As previously mentioned, cannabinoid receptor ligands are thought to have significant potential for treatment of a range of conditions, however problems associated with their use are caused by the penetration of the blood brain barrier (BBB) and activity at the CB_1R leading to psychotropic effects. To avoid these damaging side effects a drug needs to display good selectivity towards the CB_2R or show reduced CNS penetration.

After the original work by Sanofi identifying the first selective CB_1R and CB_2R substituted pyrazole based ligands, work by other groups led to the discovery of group of ligands showing improved selectivity towards the CB_2R. Mussinu *et al* used **213** as the lead structure for modification.[253] Retention at the *N*(1) and C(3) substituent's from **213** in addition to generating a fused tricycle led to the discovery of **222** (CB_1R K_i 363 nM, CB_2R 0.037 nM, selectivity 9810 fold) (**Figure 11**). The replacement of the biaryl system with a joined tricycle reduced flexibility of the phenyl group at the C(5) position and led to a significant improvement in selectivity towards the CB_2R. This indicates a considerable difference between the binding pockets of the two receptors, where the CB_1R requires more flexibility around the C(5) position possibly requiring the phenyl group to be twisted perpendicular to the pyrazole.

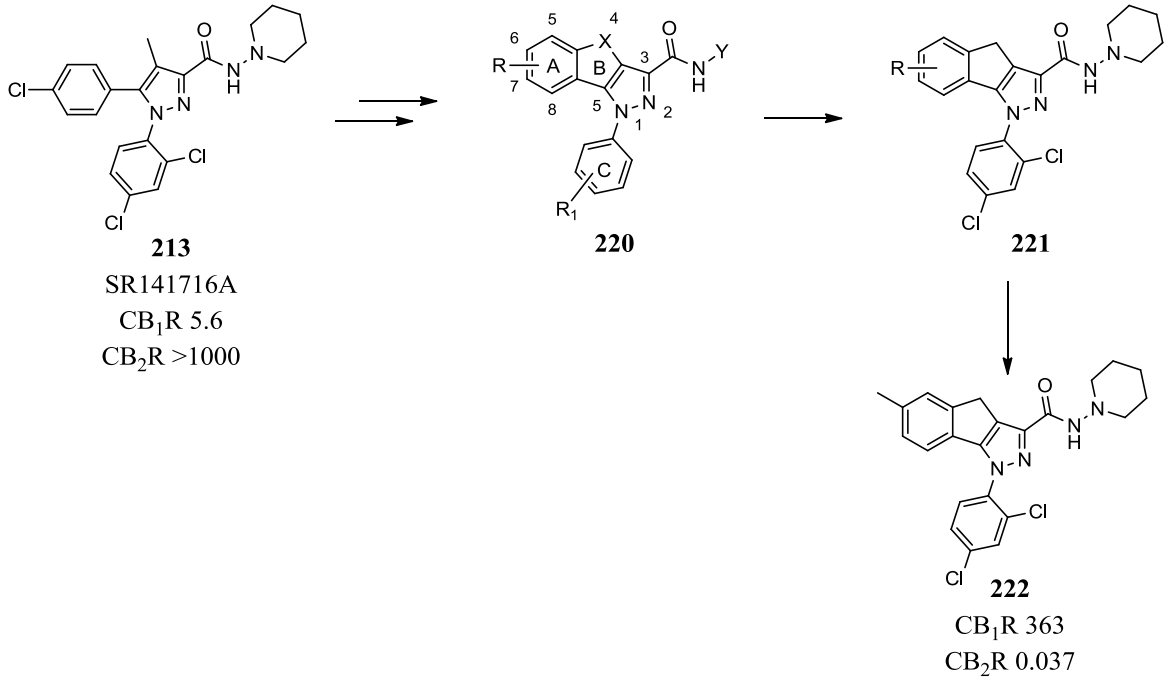

Figure 11 Structural variations undertaken by Mussinu *et al* on **213** leading to synthesis of **222,** a potent and selective binder to the CB_2R (K_i in nM)

CB_2R selective molecules were also discovered in SAR studies around the natural phytocannabinoids. Structural derivatives of Δ^8-THC (**223**), which are also active components of marijuana, including L759633 (**224**) and L759656 (**225**), which were also discovered to have significant affinities for the CB_2R by Merck Frosst (**Figure 12**).[254,255] The methylation of the phenolic group led to the development of a series of selective CB_2R binding molecules, indicating at the importance for selectivity of this substituent. **224** and **225** were shown to have 163 fold and 414 fold selectivity for the CB_2R over the CB_1R respectively. It was also shown by synthesis of JWH-051 (**227**) (K_i CB_1R 1.2 nM, CB_2R 0.032 nM) that totally removing the phenolic group results in an unexpected increase in binding affinity to the CB_2R but not a loss in affinity at the CB_1R.[256] A possible reason could be the involvement of the allylic alcohol in providing the hydrogen bonding interaction lost by the removal of the phenolic/methoxy group. This is also observed in the final example of a selective CB_2R agonist, HU-308 (**226**) (K_i CB_2R 22.7 nM, CB_1R >10 μM) (**Figure 12**).[257] Makriyannis and Khanolkar kept the allylic alcohol and the methoxy

groups to retain activity. Removal of the dihydro pyran provided additional rotation of the molecule ultimately leading to the discovery of the most promising selectivity profile for a CB_2R agonist to date, with selectivity of over 5000 fold for the CB_2R over CB_1R.[258]

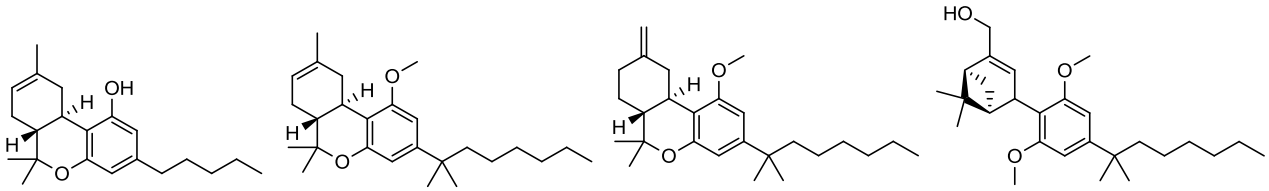

223
Δ^8-THC
CB_1R 44
CB_2R 44
0 x

224
L759633
CB_1R 6.4
CB_2R 1043
163 x

225
L759656
CB_1R 4888
CB_2R 11.8
414 x

226
HU-308
CB_1R >10000
CB_2R 22.7
> 5000 x

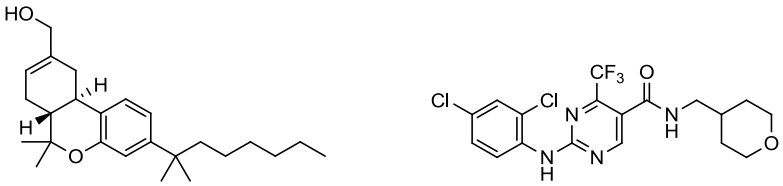

227
JWH-051
CB_1R 1.2
CB_2R 0.032

228
GW842166
EC_{50} CB_1R >30000
EC_{50} CB_2R 63

Figure 12 Structural derivatives of **223**, including **224**, **226**, **227** and **228** and their relative agonist activity (K_i in nM) and selectivity (CB_2R fold over CB_1R). Structure and activity (EC_{50} in nM) of pre-clinical candidate **228**

CB_2R selective agonists have been shown to have high efficacy in pre-clinical *in vivo* models for immune function, however only one molecule has progressed to phase one clinical trials, GW842166 **(228)** (GlaxoSmithKline).[259] An extensive amount of effort has been invested into the research for cannabinoid receptor modulators however with little reward. Reasons for this are the fact that CBR ligands are notoriously lipophilic with unfavourable physicochemical property leading to BBB penetration and low exposure due to poor solubility in aqueous media.[260] Antihistamines present a suitable example of modification of physicochemical properties allowing control of BBB penetration. First generation antihistamines were highly lipophilic and displayed CNS side effects including sedation. Future generation of antihistamines, including loratadine, are very polar,

sometimes even zwitterionic, and have increased selectivity for the peripheral H_1 histamine receptor thus preventing CNS penetration and undesired off target side effects. Additionally, compounds can be actively effluxed across the BBB by P-glygoproteins (P-gp). To avoid this, general guidelines include, low molecular weight (Mw < 400) and pka > 8.[261] Similarly this applies to research in the CBR field, a compound with a high degrees of selectivity towards the CB_2R, and favourable physicochemical properties, increases exposure *in vivo* and reduces CNS side effects.

4.5 Project Aim

Previous studies have identified CB_2R agonism, by the administration of a weak agonist Δ^9-THC (**201**), to be involved in the regression of atherosclerosis *in vivo*. Based on this discovery, the objective of this project is to discover a new CB_2R agonist displaying high functional efficacy, selectivity between the two receptors and be BBB impenetrant. Selectivity is crucial as activity to the CB_1R could lead to undesired side effect within the CNS. In addition to selectivity, the compound needs to exhibit favourable physicochemical properties including solubility and metabolic stability. Previous CB_2R agonists have been published however, they exhibited high ClogP values and low aqueous solubility due to their lipophilicity. Finally, the CB_2R agonist would be expected to demonstrate a positive effect in an *in vivo* inflammation assay. A selective CB_2R agonist with improved physicochemical properties and *in vivo* anti inflammatory effect would be of significant clinical importance with potential in the treatment of patients with atherosclerosis.

Chapter 5: Virtual Screening Identifies a Family of Selective Cannabinoid Receptor Agonists

5.1 Identification of CB_2R Agonists

The first challenge was to identify a small molecule which exhibited agonist activity at the CB_2R to provide a starting point for initial SAR development. In other areas homology models have been employed with great efficiency for unresolved three-dimensional structures of targets in order to identify a suitable molecule. The first published study uses bovine rhodopsin as a starting point to establish a CB_1R homology model, although an important caveat is that bovine rhodopsin only has a 23% sequence homology to the human CB_1R.[262] Through a similar computational exercise, the first CB_2R homology model was developed by Xie *et al* for use in virtual based screening.[263] In a study carried out by Markt *et al* a library of nearly 1 million compounds were evaluated in a virtual screen using the CB_2R homology model to discover new molecular scaffolds which may be able to bind to the CB_2R.[264] After data mining and physicochemical property filtering, binding studies confirmed 3 novel pharmacophores to be CB_2R binding molecules with low micromolar (μM) affinities. However, this is an exception, since bovine rhodopsin displays low levels of sequence homology to the CB_1R (23%) and low levels of homology between the CB_1R and CB_2R (44%) and this approach is often unreliable in identifying new hits. High degrees of similarity are required to establish a robust and reliable homology model, therefore a different approach was required. As the opportunity of using a homology model, and the facilities to perform a HTS were not available, an alternative approach was evaluated using a ligand based virtual screen. Foloppe *et al* have validated

this method by using previously discovered potent and selective CBR ligands and applying these in a virtual screens to identify new scaffolds, including benzofuran derivatives, with confirmed nanomolar affinity at the CB_1R .[265,266]

5.2 Hit Discovery

5.2.1 Ligand Based Virtual Screen

A set of CB_2R agonists from the literature were investigated and their respective affinities for the CB_1R and CB_2R were assessed when making the final selection for a template molecule (**Table 1**). GW-405833 (**203**) was identified to be a selective partial agonist at the CB_2R with proven in vivo antihyperalgesic and anti-inflammatory effect.[267] HU-308 was characterised as a full agonist of the CB2R with analgesic and anti inflammatory effects in vivo.[268] Ultimately, HU-308 (**226**) was the preferred template for the virtual screen due to its high degree of selectivity for CB_2R over the CB_1R (>400 fold), lowest affinity to the CB_1R (>10 μM) and its full agonist response at the CB_2R. The aim of the project was not to establish further SAR around already well documented CB_2R binding molecules with poor physiochemical properties, but to identify a novel class of CB_2R binding molecules with improved properties and develop SAR around this.

CB_2R agonists	Structure	Affinity at CB_1R (nM)	Affinity at CB_2R (nM)	Selectivity CB_2R/CB_1R
226 HU-308	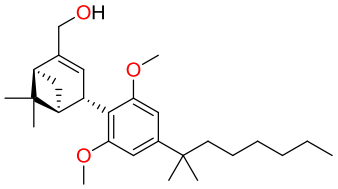	>10000	22.7	>440
229 AM-1241	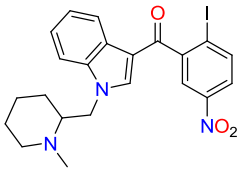	280	3.4	82
203 GW-405833	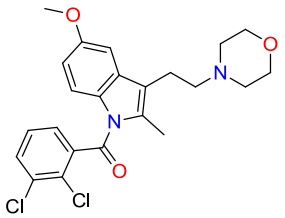	4772	3.9	1200
210 JWH-133	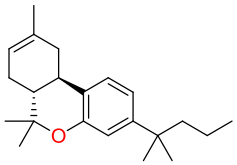	677	3.4	200

Table 1 Name, structure and affinities (K_i in nM) towards the CB_1R and CB_2R and the calculated selectivity from the affinity values (fold selectivity CB_2R vs CB_1R)

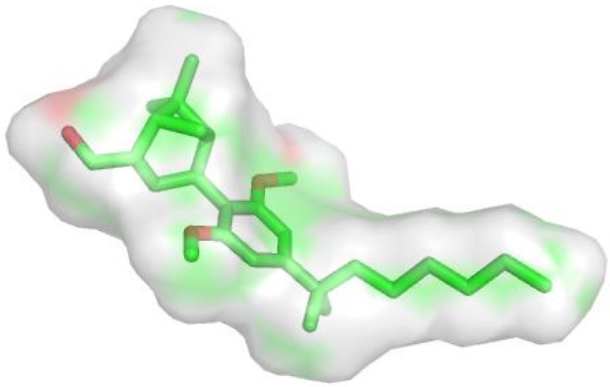

Figure 1 3D representation one of the lowest energy conformation of **226**, a CB_2R agonist with >440 fold selectivity over the CB_1R. Conformations were generated by Omega by rotations of the single bonds

Using the program Omega, 40 possible low energy conformers of **226** were established based on the minimised energy conformations of the molecule (kcal/mol) (example in **Figure 1**).[269] Up to 100 conformers were also generated of every molecule in our in-house library of 25,000 molecules. Conformers were generated by the altering the rotating

flexible bonds around its axis. Finally the 40 conformers of **226** were screened against the virtual library using the programme rapid overlay of chemical structures (ROCS).[124] The screen was performed under default parameters using full optimisation mode. The compounds were ranked in order according to their shape similarity compared to any of the 40 conformers of **226**. The top 100 compounds that presented most similarity in their overlay with HU-308 (**226**) were of interest. The overall score was based on a combination of two calculated parameters, the colour score and shape Tanimoto score (see Chapter 3 section 3.2.1).

An example of the results obtained by the programme from the screen of **226**, are shown in **Table 2**, these were the molecules with the highest calculated combo score from the virtual screen. To establish real hits from the virtual screen, 120 compounds, the 60 with the highest combo score and 30 from each the colour score and shape Tanimoto score, were tested in an *in vitro* biological assay. Ultimately, 94 compounds were selected and screened in a biological cell based assay to provide a suitable compound for further work.

Rank	Structure	Colour Score	Shape Tanimoto	Combo Score	Activity CB_2R	
					1 μM	3 μM
1	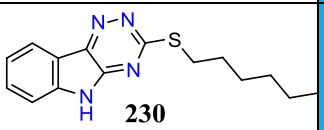 **230**	0.504	0.713	1.217	102.46	75.97
2	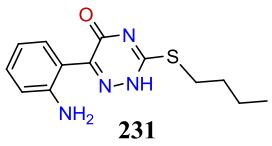 **231**	0.493	0.697	1.19	93.52	61.62
3	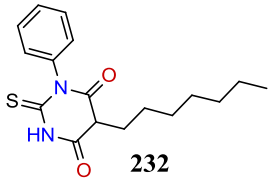 **232**	0.491	0.68	1.17	111.42	98.06
4	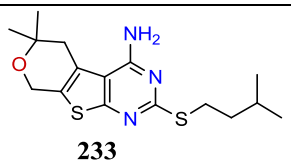 **233**	0.447	0.715	1.162	76.71	85.30
5	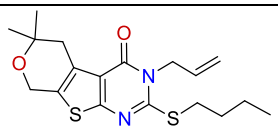 **234**	0.467	0.689	1.155	76.32	36.72
13	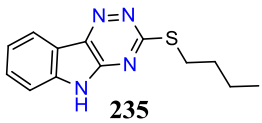 **235**	0.459	0.674	1.133	52.10	57.18

Table 2 Examples of results displayed by ROCS with the top 5 ranked compounds by their combo scores calculated by combining the shape tanimoto with the colour score. Molecule ranked at 13 was selected to continue research on. Activities are shown as a percentage inhibition of cAMP production (% of original 100%) *via* CB_2R activation

5.3 Hit Verification

5.3.1 Biological Assay and Library Screening

The 94 compounds were screened using a commercially available competitive immunoassay measuring levels β-galactosidase (β-gal) labelled cAMP (**Figure 2**).[270,271] The assay was performed using CB_2R over-expressing chinese hamster ovary (CHO) cells stimulated with forskolin. In the absence of an agonist binding to the CB_2R, cellular cAMP competes with the existing labelled cAMP for binding to the anti cAMP antibody increasing levels of free β-gal labelled cAMP in the cell. This is complemented by the

enzyme acceptor to produce a signal. By the addition of a CB_2R agonist, activity of the adenylate cyclase is inhibited by the $G_{\alpha i}$ complex formed by receptor activation, leading to low levels of competitive cAMP allowing the labelled cAMP to bind to the antibody ultimately resulting in a small signal.

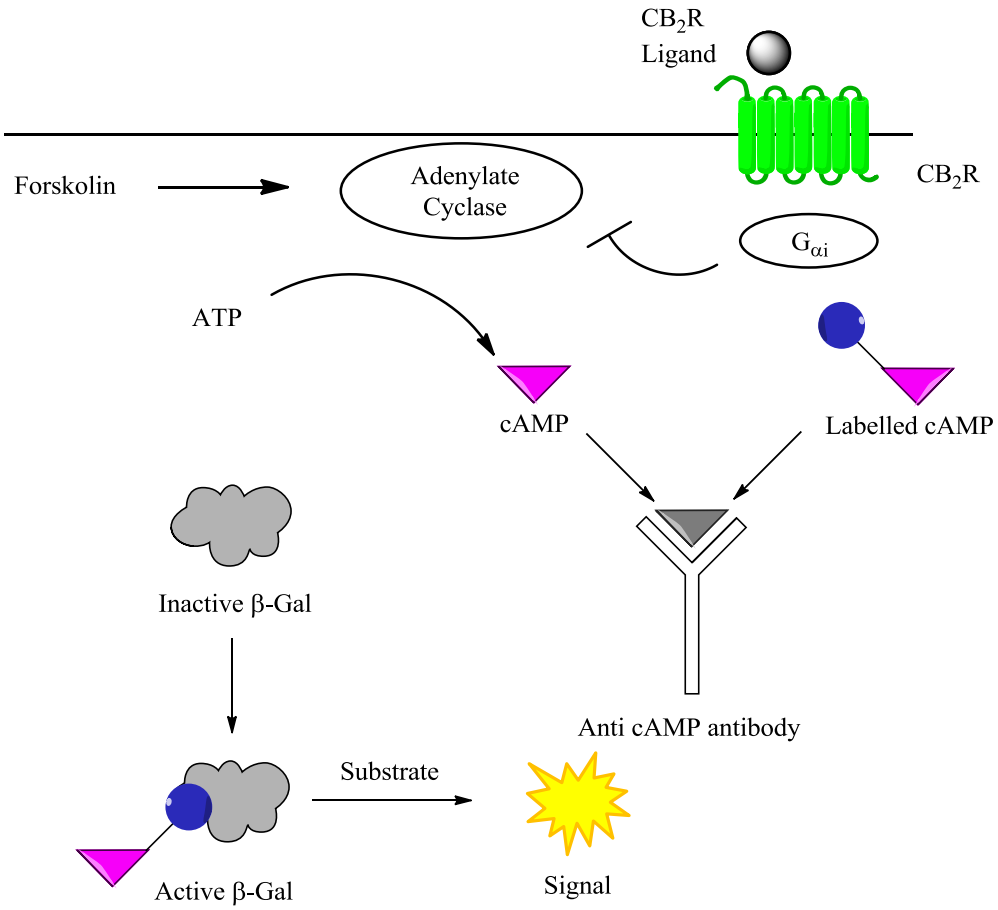

Figure 2 Activation of CB_2R promotes formation of $G_{\alpha i}$ complex which inhibits activity of adenylate cyclase. Competitive anti cAMP antibody binding regulates concentrations of β-gal cAMP and signal levels. No activity of the CB_2R leads to high levels of unlabelled cAMP and a strong signal due to high binding competition to the antibody resulting in a strong signal.

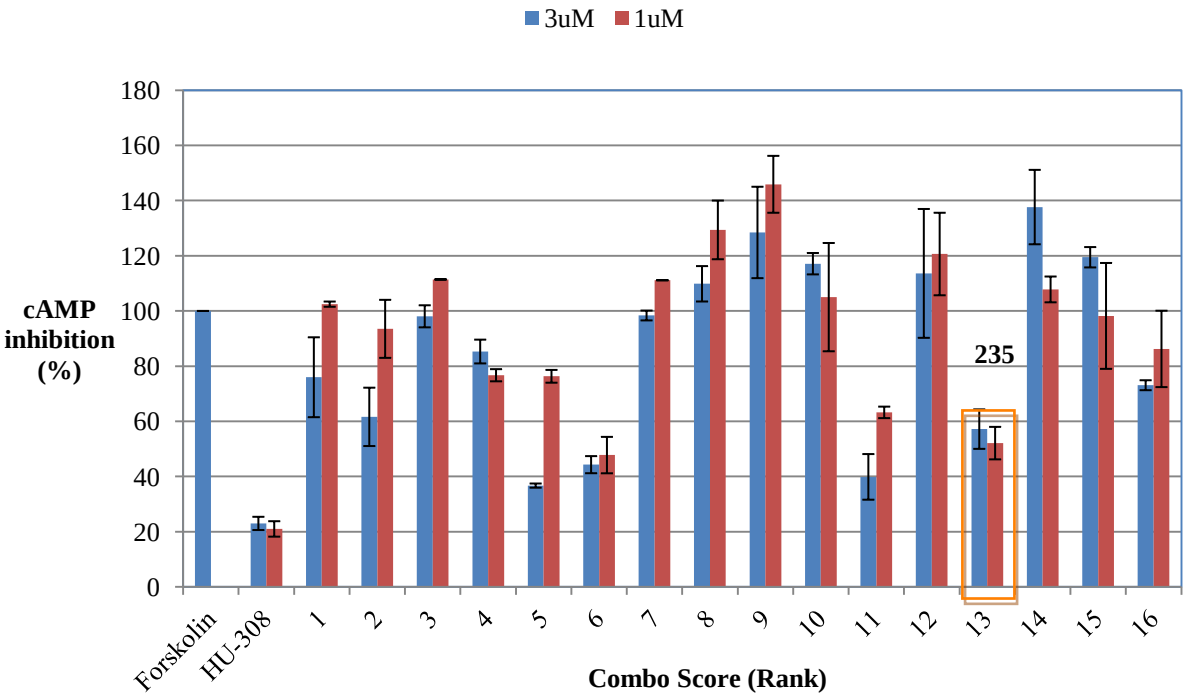

Figure 3 Activity of top 16 compounds tested at 1 µM and 3 µM concentrations, bars indicating relative inhibition of cAMP (%) tested in the protein complementation assay, with HU-308 (**226**) only as positive control. Highlighted in orange box is compound **235**

From the 94 compounds tested several CB_2R activators were identified as having modest activity. **235** was selected to pursue further studies on (highlighted by orange box **Figure 3**). This compound exhibited good activity and in a dose dependent manner at the CB_2R, 3 µM (57.2%) and 1 µM (52.1%). The selected compound ranked 13th (**235**) in the virtual screen based on its combo score (**Table 2**) and contains a triazino indole core with C(3) substituted *S*-butyl group (**Figure 4**). An individual overlay, with **226** using ROCS software, illustrates the hydrophobic alkyl chain and the lipophilic core in both molecules aligning well, suggesting that the molecules could be binding to the pocket in a similar manner.

The virtual screen provided a list of possible active molecules and the *in vitro* assay confirmed **235** to be a potent agonist (see appendix 2 for top 16). Interestingly the compound that ranked highest, **230**, in the virtual screen did not demonstrate the highest activity in the *in vitro* assay (**Table 2**). 6 different cores were present in the top 16 hits, illustrating the variability of the structures from the virtual screen. The compound ranked

13, **235**, in the virtual screen provided the most promising *in vitro* result. This underlines the importance of selecting a set of compounds rather than individual compounds, due to solubility challenges and possibly false positives or inadequate computational methods.

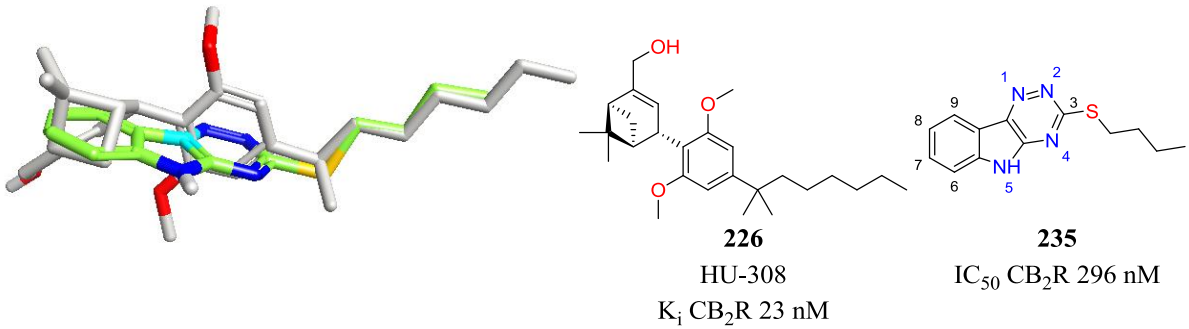

226
HU-308
K_i CB_2R 23 nM

235
IC_{50} CB_2R 296 nM

Figure 4 Overlay of **226** and **235** and their structures and activities

Following the identification of **235** as an active hit, the in-house library was further mined using the 3-thiol triazino indole core of **235** to identify available molecules with the same substructure to allow screening of close analogues. This, provided an important and cost effective exercise to develop preliminary SAR. This search identified a further 30 compounds with variations at the C(3), *N*(5), and C(6-9) position on the phenyl ring (**Figure 5**). The compounds were screened in the cAMP assay and **236** exhibited improved activity (EC_{50} 120 nM), in comparison to **235** (EC_{50} 296 nM). **236** was not amongst the top 16 ranked compounds in the virtual screen, in fact, it did not appear in the top 400 compounds based on their combo score. It retains the triazinoindole core with variations only at the C(3) position by replacing the *S*-alkyl chain with a C(2) cyano benzyl group.

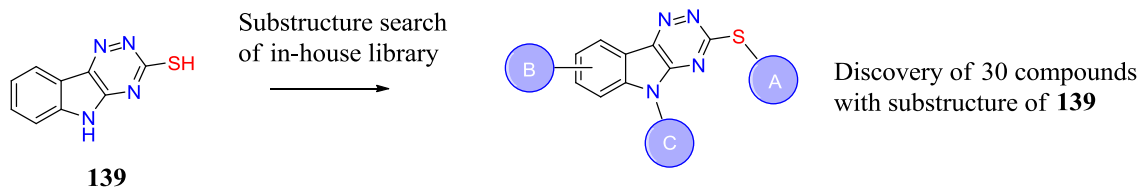

139

Figure 5 Substructure search using **139**, resulting in the discovery of 30 compounds

5.4 Validating Activity of 236

Hit validation was necessary, as the compounds were selected from a 25,000 compound library and samples were stored in solution allowing for possible contamination and degradation. Verification of the activity of **235** and **236** was carried out *via* the re-synthesis of an authentic sample (**Scheme 1**). **236** was synthesised *via* a cyclisation of isatin **135** with thiosemicarbazide to yield the tricycle **139**, followed by benzylation or alkylation of the thiol in aq NaOH to yield **235** and **236** in overall yield of 70% and 73% respectively.[137,272]

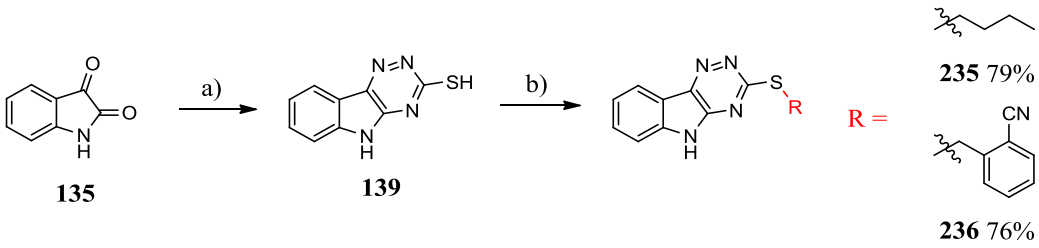

Scheme 1 Synthesis of **235** and **236** a) thiosemicarbazide, K_2CO_3, H_2O, reflux 16 h, 92% b) iodobutane/2-cyano benzyl bromide, aq NaOH (4%), rt 16 h

The resynthesised sample of **236** was tested in the cAMP assay and an EC_{50} of 110 nM was obtained. This confirmed the activity of the original sample from the library, providing a good reliable starting point for further SAR investigations around this molecule.

5.5 SAR Investigation of 236

With no reliable structural data available to guide compound optimisation, SAR relationships were established through analogue synthesis. Possible points of diversification were identified on the lead compound **236** including variations around the sulphide, functionalisation off the indole nitrogen and finally a positional scan and subsequent substitution on ring A (**Figure 6**). Synthetic routes to access these analogues were developed to allow more efficient library establishment.

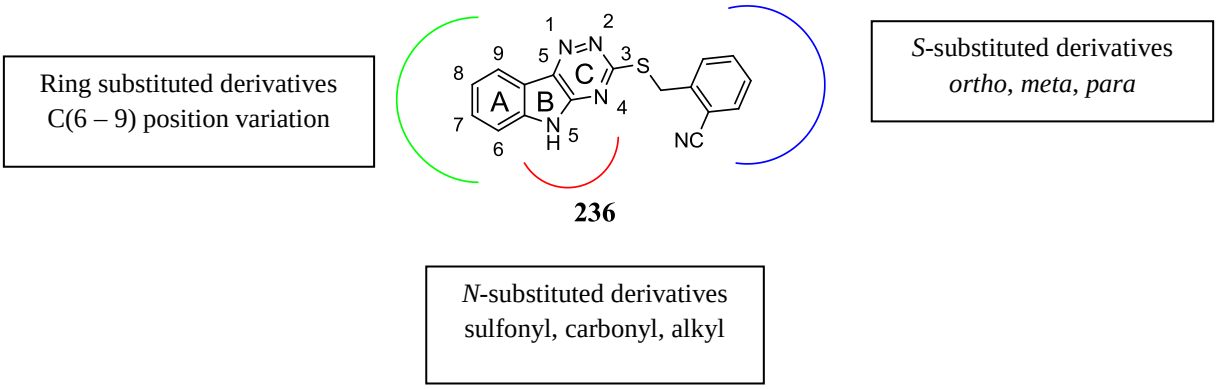

Figure 6 Possible points of diversification around the core structure of **236**

5.5.1 Sulfide Substituents

The first area investigated were substitutions of the C(3) benzyl thiol moiety. **235** was the first active molecule identified by the screen and possess an *n*-butyl chain. A small investigation into exploring the importance of the alkyl chain, *via* cyclisation of isatin **135** with thiosemicarbazide and subsequent alkylation in the presence of base to yield **230**, **235** and **237** (**Scheme 2**) led to a quick discovery that activity is very sensitive to the alkyl chain length. The free sulfide **139** gives no activity (>3 μM), nor does the methyl substituted compound **237** (>3 μM). A butyl group **235** improves the activity extensively (296 nM), however increasing the hydrocarbon chain length to 6 (**230**) led again to a loss of activity (>3 μM). This indicates that there are steric constraints on that side of the molecule leading to a control in activity at the CB_2R. Finally, functionality involving a benzyl group, present in **236**, was decided to be pursued over the alkyl chain.

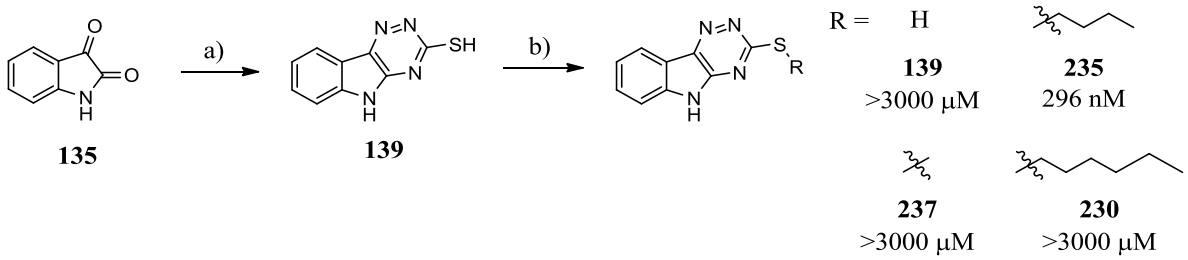

Scheme 2 Synthesis of alkyl derivatives a) thiosemicarbazide, K_2CO_3, H_2O, reflux 16 h, 92% b) alkyl halide, K_2CO_3 or Cs_2CO_3, MeOH, 16 h rt, 80 - 95% and activity at the CB_2R

5.5.1.1 *S*-Benzyl Derivatives

235 led us to the discovery of **236** by mining the compound collection, which instead of an alkyl chain contains a benzylic group with an electron withdrawing nitrile group at the C(2) position. Hunter *et al* established method to quantify the H-bonding ability of substituents.[273] The nitrile functionality provides a good H-bonding acceptor ability (HBA 4.7) for possibly important interaction to the binding site of the protein (**Table 3**).

A synthetic route enabling a library to be efficiently established was optimised from the previous synthesis of **236**. The optimised route led first to the intermediate **139** being prepared by two consecutive condensations of the thiosemicarbazide on the isatin **135** under basic conditions, followed by acidification with AcOH to yield **139** as a precipitate.[274] This intermediate allowed efficient substitution, *via* a nucleophilic addition of the thiol to a range of electrophiles in the presence of Et_3N to yield the final compounds **141, 236** and **238-245**, which were isolated by filtration and purified by subsequent MeOH and aq. Et_3N (10%) washes (**Scheme 3**).

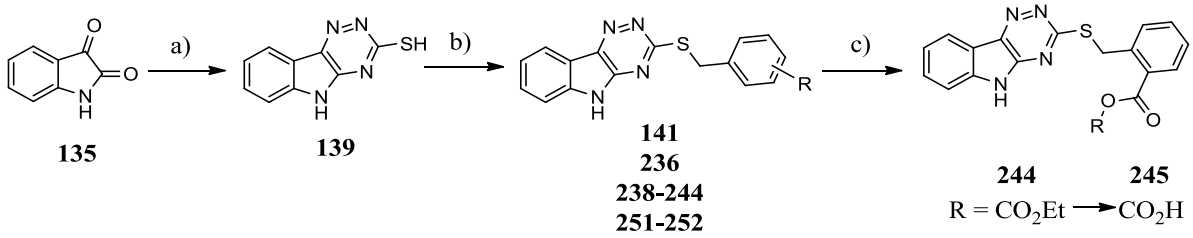

Scheme 3 Optimised synthetic route to **236** leading to the development of a small library of *S*-benzyl substituted compounds: a) thiosemicarbazide, K_2CO_3, H_2O, reflux 16 h, 92% b) R-substituted benzyl bromide, Et_3N, MeOH, rt 16 h, 50-98% c) aq NaOH (1M) rt 16 h, 99%

A library of compounds with different electronic properties was prepared *via* this route, where *ortho* substituted benzylic groups were the first to be investigated. It appears, similar to the parent compound **236**, that other electron withdrawing groups (EWG's) are tolerated including the nitro **239** (EC_{50} 33 nM) and the carboxylic acid **246** (EC_{50} 2.19 µM) (**Table 3**). On Hunter's scale of HBA ability the carboxylic acid (**246**) ranks highest (5.3) with the

nitrile **236** (4.7) and nitro **239** (3.7) holding similar values, indicating at the possible importance of a strong HBA to be present at the C(2) position of the benzyl group (**Table 3**). Altering this position to a weaker EWG and lower HBA scoring substituent, such as a chloro **241** or hydrogen **141**, results in a loss of activity. Interestingly, the ester group **245** displays no activity at the CB_2R (EC_{50} >3 μM) which is unexpected if using HBA strength as a guideline. It has high HBA value (5.3) yet does not show activity at the receptor. This possibly indicates for a further parameter to be important for activity. This hypothesis is supported by the surprise activity of the methyl compound **243** (EC_{50} 215 nM). This could be possibly due to a hydrophobic pocket being present on the alternative side of the benzyl group. EWG interact for example on the C(2) position *via* H-bonding, while the methyl would act at the C(6) position allowing for opposite properties to be tolerated. The inactivity of **242**, with a CF_3 donor group could be due to a possible dipole being present as a result of the fluorines. The difference in activity between the chloro (**241**) and methyl (**243**) is unusual as methyl groups and chlorine can sometimes be considered isosteric, and similar activity would be expected.

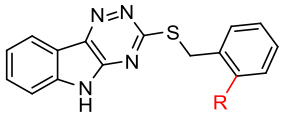

141, 236, 238-246

Compound	R =	Yield (%)	EC_{50} CB_2R (nM)	HBA
141	H	75	1000-3000	2.2
238	F	57	>3000	1.6
239	NO_2	98	33	3.7
240	CF_3	74	>3000	NR
236	CN	99	112	4.7
241	Cl	79	>3000	1.6
242	OCF_3	50	>3000	NR
243	CH_3	77	215	0
244	5-tetrazoyl	75	11	NR
245	CO_2Et	83	>3000	5.3
246	CO_2H	NA	2185	5.3

Table 3 *Ortho S*-benzyl substituted compounds with yield, activity at the CB_2R and Hydrogen bond acceptor strength (HBA)
NM = not recorded

The *meta* and *para* positions were also studied with the same functional groups at the *ortho* position to allow a direct comparison (**Table 4** and **5**). The results provide clear SAR around the *S*-benzylated system. Functional groups on the phenyl ring need to be present to provide activity. Additionally, the *meta* and *para* positions do not seem to be tolerated at all, giving us a dramatic loss in activity in comparison to the *ortho* substituents. This site of the molecule therefore appears to provide an essential interaction to the binding site of the protein. The presence of EWG with hydrogen acceptor ability could likely provide H-bond interactions to the active site of the pocket in addition sterics also appear to play a critical role in providing activity.

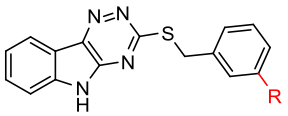

247-248

Compound	R =	Yield (%)	EC_{50} CB_2R (nM)
236	-	99	112
247	Cl	73	>3000
248	CN	58	6500

Table 4 *Meta* substituted compounds with yield and activity

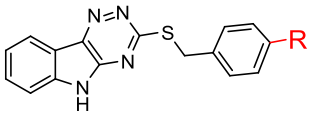

249-250

Compound	R =	Yield (%)	EC_{50} CB_2R (nM)
236	-	99	112
249	F	82	>3000
250	Cl	59	>3000

Table 5 *Para* substituted compounds with yield and activity

With a better understanding of the type of *ortho* substituent required, a few select compounds were synthesised to observe whether activity is retained or lost when multiple substitutions were present on the aryl ring (**Figure 7**). Initial attempts were made into the synthesis of the 2-cyano, 6-methyl derivative, however this proved synthetically challenging. A 2,4-dinitro benzyl group **251** replaced the 2-nitro benzyl group on **239** *via* the same synthetic route are previously used (**Scheme 3**). Previously *para* substitutions led to loss in activity (EC_{50} >3 μM), however the 2,4-dinitro compound **251** gave reduced activity (EC_{50} 576 nM) but not complete loss. A replacement of the benzyl substituent with a 2-nitro, 6-fluoro benzyl group **252** similarly led to reduced activity (EC_{50} 539 nM). Additional functionalisation at other positions around the *o*-NO_2 benzyl group does not lead to improved activity with >10 fold loss in potency at the CB_2R.

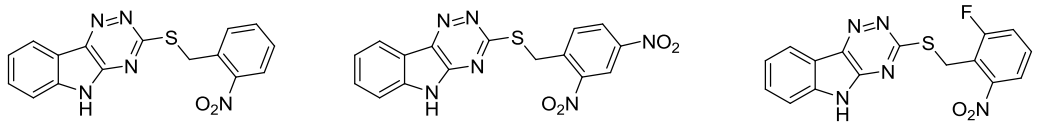

239
33 nM

251
576 nM

252
539 nM

Figure 7 *o*-NO_2 derivatives **239** and **251-252** with additional substituents at the *meta* and *para* positions

With this knowledge, two further compounds were synthesised to provide insight into the linkage between the tricycle and C(2) substituted phenyl ring. The first, involved the removal of the methylene which was prepared *via* a nucleophilic aromatic reaction (S_NAr) between the thiol **139** and 2-fluoro-nitrophenyl to yield **253** in moderate yield (41%). With the exclusion of this CH_2 unit, loss in activity was also observed (EC_{50} >3 μM), possibly due to the lack of flexibility around the methylene connection between the thiol and the phenyl group. As thiols are prone to oxidation, the sulfoxide **254** was made chemoselectively, using a solution of trifluoroacetic acid (CF_3CO_2H) and peroxytrifluoroacetic acid (**Scheme 4**). This however, also led to a reduction of activity in our *in vitro* assay of 3.55 μM which gives us vital insight for the future, if the compound with the thiol is metabolically susceptible to oxidation, then loss in activity would be observed. Further attempts were made to alter the thiol to an ether or amine linked benzylic group, however this was not accomplished due to synthetic challenges.

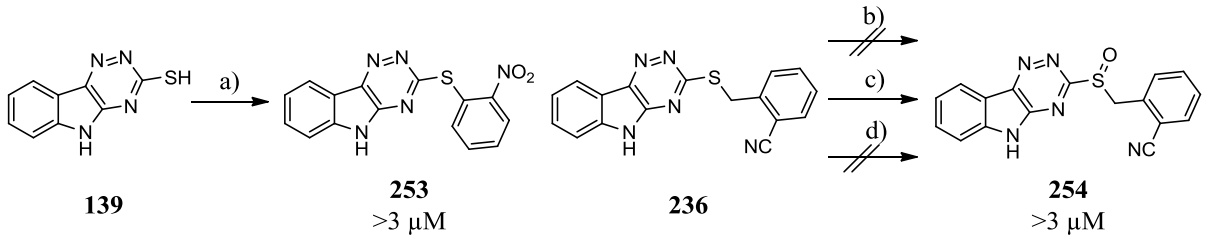

139

253
>3 μM

236

254
>3 μM

Scheme 4 S_NAr reaction a) 2-fluoro nitrobenzene, K_2CO_3, 100 °C 24 h, 41%, conditions to make the sulfoxide b) H_5O_6I, $FeCl_3$, MeCN, rt, 16 h c) CF_3CO_2H, peroxytrifluoroacetic acid (4 M), rt 16 h, 95% d) mCPBA (70%) 1-10 eq, CH_2Cl_2, rt 16 h

5.5.1.2 Binding Studies of 236 and 239

Following successful SAR investigations around the thiol moiety, compounds were evaluated for their affinity to the binding site of the CB_2R and their observed activity is not due to interaction with another target. Two representative compounds were submitted for affinity studies to Cerep SA. The most promising hits so far were the 2-nitro **239** and 2-cyano **236** *S*-benzyl derivatives (**Figure 8**). Affinity studies were carried out using known cannabinoid receptor binding molecules mentioned previously, namely CP 55940 (**204**) for the CB_1R and WIN 55212-2 (**216**) for the CB_2R. The procedure carried out was a radioligand displacement assay using tritiated isotopes of the above mentioned receptor binding ligands (**204** and **216**). The affinity of our compounds on the CB_1R is measured by the displacement of [^{3}H]CP 55940 by the test compounds in human CBR transfected into CHO cells.[275] To measure the affinity at the CB_2R, displacement of radioligand [^{3}H]WIN 55212-2 was measured after incubation with our compound for 120 minutes and is represented by the K_i.[276]

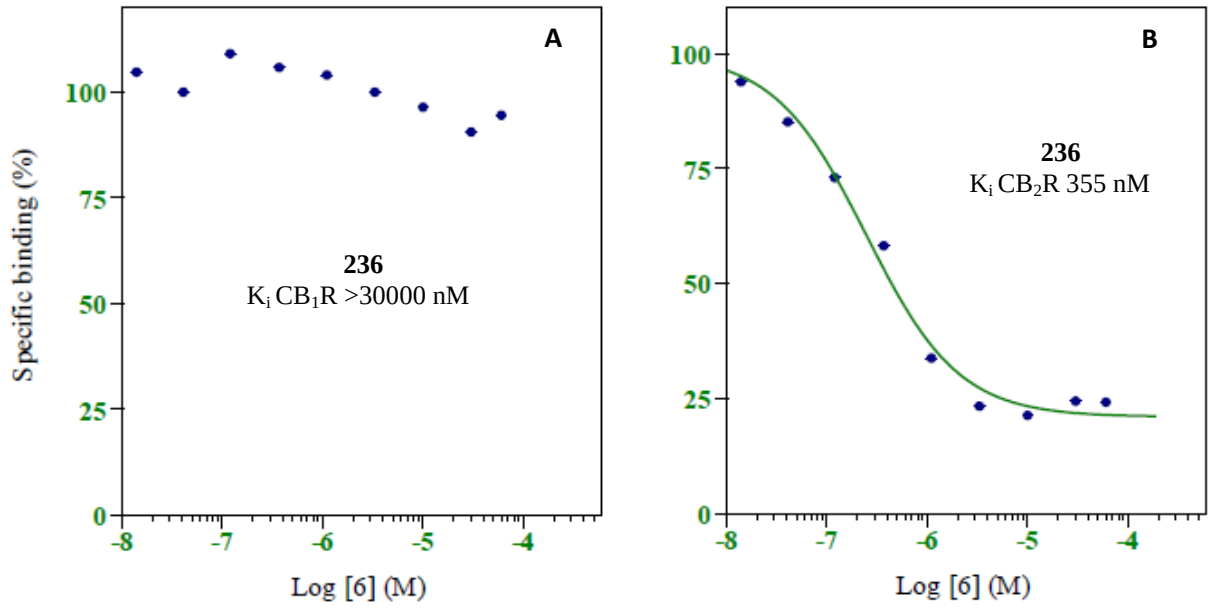

Figure 8 Affinity graphs for **236** at the CB_1R (**A**) and the CB_2R (**B**)

The affinity studies confirm the binding of **239** (K_i CB_2R 155 nM) and **236** (K_i CB_2R 355 nM) to the active site of the CB_2R *via* the displacement of the tritiated ligand. Complete lack of binding at the CB_1R (K_i CB_1R > 30 μM) provides evidence for this series of compounds to have a promising future as selective CB_2R ligands. This prompted further SAR investigations in an effort to improve activity and gain an understanding of what is tolerated by this unresolved protein active site. The compound chosen for further SAR studies was **236**. The nitrile (**236**) was favoured over the nitro (**239**) due to the possible toxicophores presented by the nitro group upon metabolic degradation.[7]

5.5.2 Ring Substituted Derivatives

After successful SAR development on the thiol, further optimisation on **236** was carried out by substitutions on ring A of the core. Initially a large lipophilic bromine was introduced at different sites on ring A to establish which position could accommodate further substitution. The optimised synthetic route of **236** was employed using brominated isatins (**Scheme 5**). The respective C(6 – 9) bromoisatins (**255-258**) were cyclised with thiosemicarbazide to yield the tricyclic intermediate **259-262**, which was treated with 2-cyanobenzyl bromide to yield the desired bromo derivatives **263-266**. After *in vitro* testing the results displayed loss in activity at the CB_2R (EC_{50} >3 μM) in substitutions at all positions except the C(9) position (**263**) which displayed very good activity (EC_{50} 39 nM) (**Table 6**).

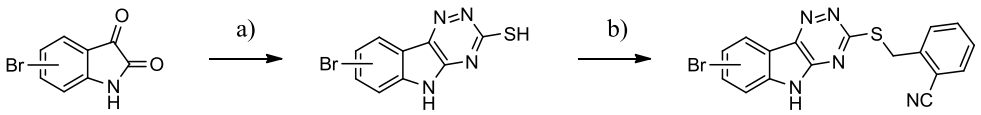

255	**259** 6-Br 34%	**263** 6-Br 87%
256	**260** 7-Br 90%	**264** 7-Br 92%
257	**261** 8-Br 97%	**265** 8-Br 78%
258	**262** 9-Br 95%	**266** 9-Br 64%

Scheme 5 Synthesis of C(6) – C(9) bromo substituted compounds **263-266**, a) thiosemicarbazide, K_2CO_3, H_2O, reflux 16 h 34-97% b) 2-cyano benzyl bromide, Et_3N, MeOH, rt 16 h 64-87%

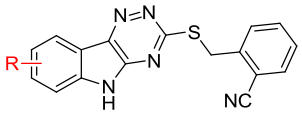

Compound	R =	EC_{50} CB_2R (nM)
236	H	112
263	6-Br	>3000
264	7-Br	>3000
265	8-Br	>3000
266	9-Br	39

Table 6 Yield and activity of the C(6-9) bromo substituted compounds **263-266**

Having established what positions are tolerated around Ring A of the core, the aim was to introduce a range of groups *via* Suzuki cross coupling reactions at the C(9) position.[277] Little chemistry had been reported using unprotected 4-bromo isatin (**255**) in cross coupling reactions, although a literature precedent using a similar substrate 4-bromo-1-methyl-1,3-dihydro-indol-2-one (**267**) to make the cyclopropyl product **268** *via* a Suzuki coupling with $Pd(dppf)_2Cl_2$ and potassium cyclopropyltrifluoroborate has been reported (**Scheme 6**).[278] Preliminary SAR identified the *N*-methyl to result in loss of activity (EC_{50} >3 μM) (*vide infra*), therefore different protecting groups were attempted. The four protecting groups (**269-273**) used did not endure the harsh conditions of the Suzuki cross coupling and 9-bromoisatin (**262**) was mostly isolated and a low yield of debrominated isatin (<10%). Therefore, the synthesis of the C(4) substituted derivatives had to be carried out using the unprotected **258** as the starting material.

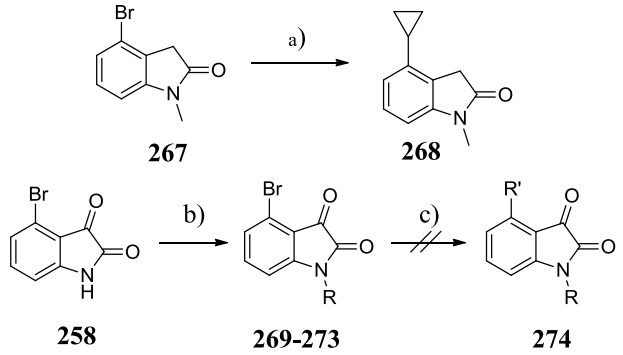

Scheme 6 Literature reaction a) potassium cyclopropyltrifluoroborate, $Pd(dppf)_2Cl_2$, K_3PO_4, CH_2Cl_2, THF, water, 130 °C 4 h. Attempted 4-bromoisating functionalisation using different protecting groups (R) b) Protecting group (BnBr, *p*-tol sulfonyl chloride, boc anhydride and BzCl), NaH (60%), DMF or THF, 0 °C – rt

5.5.2.1 Cross Coupling Condition Investigations

Initial attempts using 4-bromoisatin (**258**) in cross coupling reactions with phenyl boronic acids proved unsuccessful (**Scheme 8**). Using tributylphenylstannane, also did not yield product (**Table 7**, entry 1). Following this, boronic acids were used in conjunction with a small range of bases and solvents in the presence of tetrakis(triphenyl phosphine)palladium catalyst with also no product isolation (entries 2-5).

To circumvent possible problems with aryl boronic acids (**275**), which can undergo protodeboronation (**276**) and homocoupling (**277**) (**Scheme 7**), aryl trifluoroborates (**278**) were used. Trifluoroborates have been shown to provide a good alternative to boronic acids in Suzuki-Miyaura coupling under aqueous conditions.[279,280]

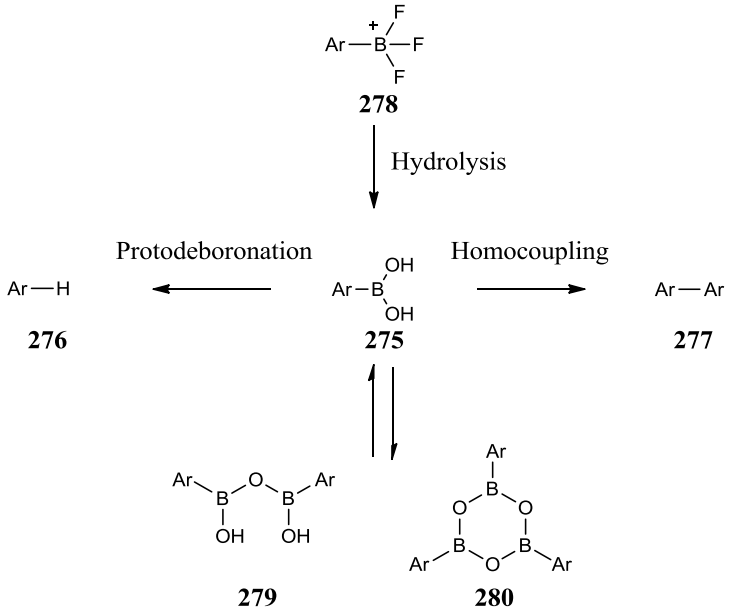

Scheme 7 Possible reactions aryl boronic acids **275** can undergo to decrease yields and activation of trifluoroborate salts **278**

It has been shown in a study by Lloyd-Jones *et al* that the use of trifluoroborate salt increase the yield of the reaction and but still undergo the cross coupling through *in situ* base hydrolysis of the trifluoroborate **278** to the boronic acid **275**, which then reacts with the metal catalyst. With the knowledge that the boronic acid is in equilibrium with its dimer **279** and cyclotrimer **280** which are both unreactive, slow hydrolysis of the trifluoroborate to the acid decreases the concentration of the boronic acid present and consequently the levels of unreactive boron species in solution. Therefore, the hydrolysis of the trifluoroborate affects the catalytic rate of the reaction. Supporting the observation that the boronic acid undergoes oxidative addition to the metal is shown by the energy transition states of the palladium complexes. The trifluoroborate (**281**, X = F) goes *via* the highest energy transition state (-11.3 – 9.8 kj/mol), whereas the corresponding boronic acid (**283**, X = OH) intermediate is considerably lower in energy (-32.6 – 16.4 kj/mol), and thus the preferred reagent in the coupling (**Figure 9**).

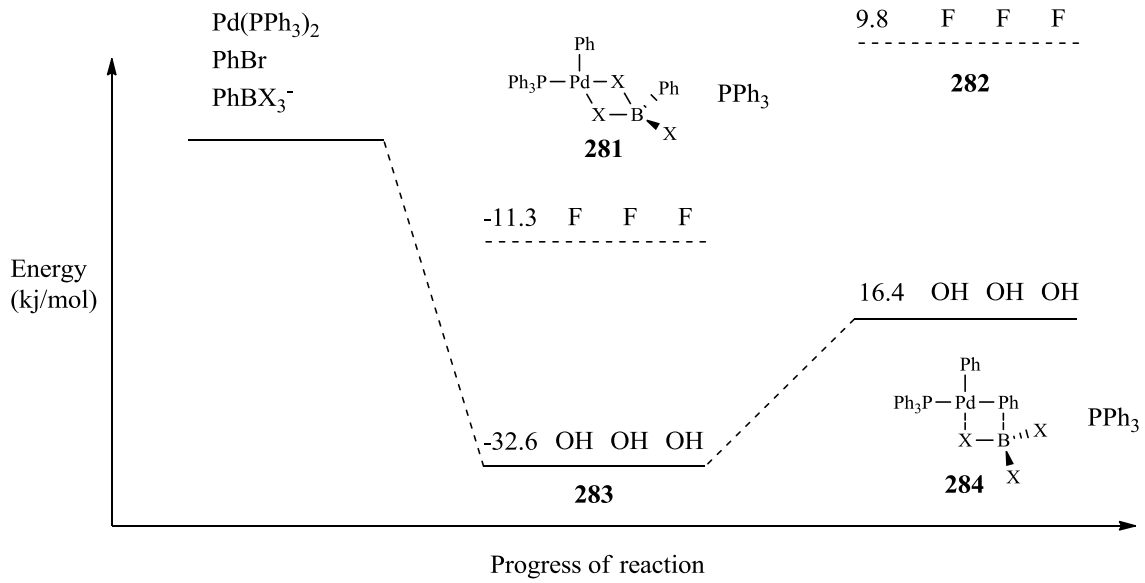

Figure 9 Transition state (in kj/mol) of the oxidative addition step of the phenyl trifluoro borate and phenyl boronic acid reagent to the palladium catalyst [279]

Reactions with the use of trifluoroborates provided product in the reaction where previously no product was isolated when boronic acids were trialled as the coupling partner (**Table 7**, entries 6-16).

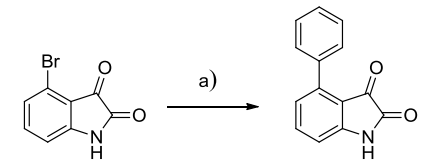

258 **285**

Scheme 8 Cross coupling conditions a) investigated in **Table 14**

Entries	Base	Catalyst	Solvent	Reagent	Yield (%)
1	K_2CO_3	$Pd(PPh_3)_4$	Toluene	Bu_3SnPh	-
2	Na_2CO_3	$Pd(PPh_3)_4$	H_2O/dio 1:1	$B(OH)_3Ph$	-
3	Na_2CO_3	$Pd(PPh_3)_4$	DME/EtOH 1:1	$B(OH)_3Ph$	-
4	Cs_2CO_3	$Pd(PPh_3)_4$	DME/EtOH 1:1	$B(OH)_3Ph$	-
5	**K_3PO_4**	**$Pd(PPh_3)_2Cl_2$**	**THF/H_2O 3:1**	$B(OH)_3Ph$	-
6	K_2CO_3	**$Pd(PPh_3)_2Cl_2$**	Dioxane	**BF_3KPh**	8
7	K_2CO_3	**$Pd(PPh_3)_2Cl_2$**	Dioxane	$B(OH)_3Ph$	16
8	**K_3PO_4**	**$Pd(PPh_3)_2Cl_2$**	Dioxane	**BF_3KPh**	43
9	K_2CO_3	**$Pd(PPh_3)_2Cl_2$**	EtOH	**BF_3KPh**	29
10	**K_3PO_4**	**$Pd(PPh_3)_2Cl_2$**	EtOH	**BF_3KPh**	36
11	**K_3PO_4**	$Pd(acac)_2/PPh_3$	EtOH	**BF_3KPh**	17
12	**K_3PO_4**	$Pd(PPh_3)_4$	EtOH	**BF_3KPh**	47
13	**K_3PO_4**	**$Pd(PPh_3)_2Cl_2$**	Toluene	**BF_3KPh**	17
14	**K_3PO_4**	**$Pd(PPh_3)_2Cl_2$**	DMF	**BF_3KPh**	58
15	**K_3PO_4**	**$Pd(PPh_3)_2Cl_2$**	THF	**BF_3KPh**	62
16	**K_3PO_4**	**$Pd(PPh_3)_2Cl_2$**	**THF/H_2O 3:1**	**BF_3KPh**	**85**

Table 7 Conditions under which the cross couplings to **285** were attempted with the best condition highlighted in bold

It was discovered that using potassium phosphate as a base yielded the most positive results in conjunction with the potassium aryl trifluoroborate salt. The solvent system employed affected the yield as well. By using a combination of THF and H_2O (3:1), the yield was observed to be the highest. The mixture of two co-solvents presumably aided solubility of the reagents, the hydrolysis of the trifluoroborates to the boronic acids *in situ* and subsequent activation of the boronic acids for the transmetallation step.

Investigations into the most effective catalyst in the cross coupling was also carried out. With the use of palladium tetrakis (triphenyl phosphine) ($Pd(PPh_3)_4$) no additional spot was observed by thin layer chromatography (tlc). The oxidative addition did not appear to take place. Slow kinetics of phosphine ligand dissociation on the palladium catalyst leading to the active $Pd(PPh_3)_2$ species could be responsible for this. Replacing the catalyst with palladium acetylacetonate ($Pd(acac)_2$), possessing a bidentate ligand, some product was isolated (**Table 7**, entry 11, 17%). With a final replacement of catalyst to palladium triphenyl phosphate dichloro ($Pd(PPh_3)_2Cl_2$) lead to consumption of starting bromoisatin (**Table 7**, entries 5-10 and 13-16). Further observations by tlc and NMR spectroscopy analysis using this catalyst showed the varying proportions of debrominated product **135** (10-80%) and product (0-85%). The highest yield was obtained with optimised conditions using the trifluoroborate, phosphate base in aqueous solvent and Pd^{2+} catalyst (**Table 7**, entry 16, 85%), the product was unambiguously identified by NMR and lack of the characteristic bromine peak in mass spectrometry also confirmed product formation.

Having optimised conditions for the cross coupling, a library of compounds with various groups at the C(9) position were synthesised. To improve synthetic efficiency, coupling to yield **266** with the trifluoroborate salt under the optimised conditions was attempted to allow late stage diversification of a common intermediate (**Scheme 9**). Efforts to substitute the C(9) position of **266** did not yield the cross coupled product **286**, nor in the case of the free thiol **262**. The principal reasons could be due to the increased steric bulk of the tricyclic core and low solubility of the starting materials. In the case of **262** solubility could be the cause of the problem, in addition to the free thiol, since some literature indicates that thiols can poison the active palladium complex.[281] Therefore, the cross coupling had to be carried out on 4-bromoisatin **258** to avoid issues with solubility and catalyst deactivation.

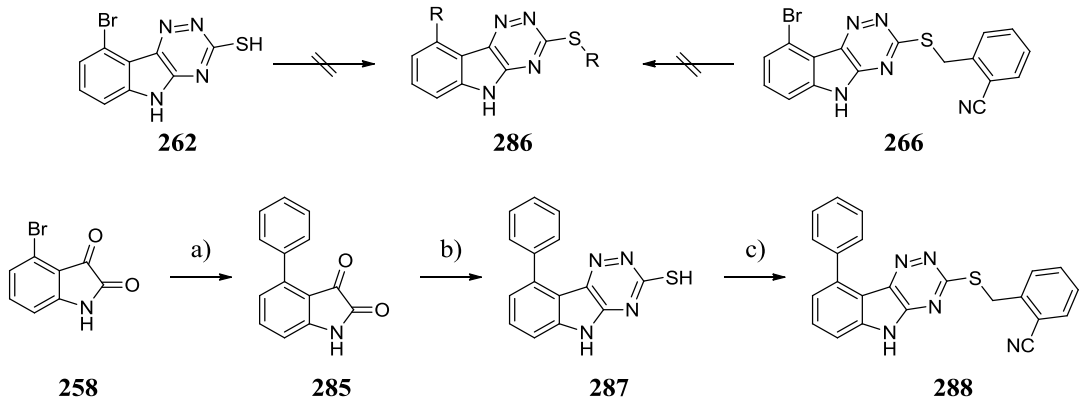

Scheme 9 Attempted cross coupling on more advanced intermediates in the synthesis, a) Potassium trifluoroborate salt, K_3PO_4, $Pd(PPh_3)_2Cl_2$, THF/H_2O (3:1),130 °C 4 h. Synthesis of **288** a) $PhBF_3K$, K_3PO_4, $Pd(PPh_3)_2Cl_2$, THF/H_2O (3:1),130 °C 4 h, MW, 85% b) thiosemicarbazide, K_2CO_3, H_2O, reflux 16 h, 65% c) 2-cyano benzyl bromide, Et_3N, MeOH, rt 16 h, 63%

A small library of C(9) phenyl substituted compounds was synthesised starting with the cross coupling reaction on 4-bromoisatin (**258**) with phenyl potassium trifluoroborate, K_3PO_4 and palladium catalyst in collaboration with Rebecca Cross (**Scheme 9**).[277] The cross coupled product **285** was then cyclised to the triazine **287** and finally benzylated to yield the C(9) phenyl substituted product **288**. To investigate steric effects, the phenyl group was replaced by 2, 3 and 4-tolyl groups at the C(9) position following the same procedure to yield **295-297** (**Scheme 10**).

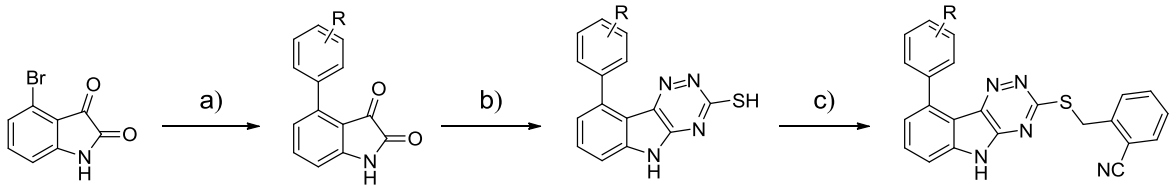

Scheme 10 Synthesis of small library of 9-substituted compounds **286-288**, a) Potassium trifluoroborate salt, K_3PO_4, $Pd(PPh_3)_2Cl_2$, THF/H_2O (3:1),130 °C 4 h, MW, 30-91% b) thiosemicarbazide, K_2CO_3, H_2O, reflux 16 h, 23-93% c) 2-cyano benzyl bromide, Et_3N, MeOH, rt 16 h, 40-61%[277]

Ortho substitution also introduces rotational restriction around the C-C bond between the C(9) of the core and 2-substituted phenyl by changing the size of the dihedral angle of the most energetically favourable predicted structure (41 °) as opposed to the unsubstituted

phenyl compound **288** (31°) (**Figure 10**). Lowest yield amongst the methyl substituted trifluoroborates was in the generation of **295**. The presence of *ortho* substituents has been reported to reduce the efficiency and the rate of the catalytic turnover.[282] This is known to affect the transmetallation step, where the steric hindrance reduces the rate of addition.

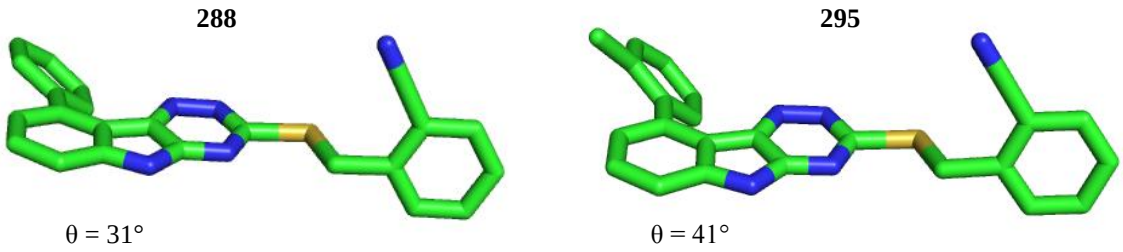

Figure 10 3D representation of one of the lowest energy conformations of **288** and **295**, calculated using ChemBio 3D[283]

Compounds **298** and **299** containing different substituents at the *para* position, were also made through Suzuki cross coupling of the respective 4-phenyl substituted trifluoroborate salts and 4-bromoisatin (**258**) using the previously optimised conditions (**Table 8**).

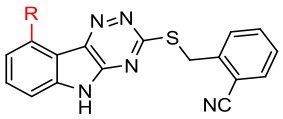

Compound	R =	Yield Coupling (%)	EC_{50} CB_2R (nM)	K_i CB_2R (nM)
236	H	NA	112	355
266	Br	NA	39	225
288	Ph	85	2370	-
295	*o*-Me-Ph	59[1]	2440	-
296	*m*-Me-Ph	91[1]	3280	-
297	*p*-Me-Ph	68[1]	>3000	-
298	*p*-OMe-Ph	63[1]	2340	-
299	*p*-Cl-Ph	30[1]	>3000	-
300	Thiophene	59[1]	1760	-
301	Cyclopropyl	43[2]	231	-

Table 8 Yields of the Palladium cross coupling reaction, activity and binding affinity for the tested compound
NA = not applicable
[1] catalyst used was $Pd(PPh_3)_2Cl_2$
[2] catalyst used was $Pd(dppf)_2Cl_2$

Addition of functional groups at the C(9) position generally led to significant reduction of activity at CB_2R with the exception of the bromo substituted compound **266** (EC_{50} 39 nM) (**Table 8**). With the addition of a phenyl group **288** the activities are all observed to be >2 µM, which is a loss in activity more than 10 fold to the original hit **236** (EC_{50} 112 nM). Changing the phenyl group to one of its bioisosteres, a thiophene **300**, led to an improvement in activity (EC_{50} 1.76 µM). The lowest predicted energy conformation of the thiophene (43.1 kcal mol^{-1}) displays a dihedral angle of just 5° which is significantly smaller than the phenyl derivatives (**Figure 11**). The introduction of a small saturated carbacyclic group at the C(9) position, such as a cyclopropyl **301**, shows lowest energy conformation (27.2 Kcal mol^{-1}) with the substituent orientated out the plane on one face of the molecule. One would predict the most stable conformation to have the cyclopropyl perpendicular to the plane of the phenyl to maximise conjugation (29.0 kcal mol^{-1}).

Possible improved activity (EC_{50} 231 nM) could be observed as a result of the cyclopropyl substituent lying above or below the plane of the tricycle and feeding into a hydrophobic pocket.

Figure 11 lowest energy conformation of C(9) substituted compounds containing a thiophene (**300**) or cyclopropyl (**301**) group

The 9-bromo substituted compound **266** was selected for affinity testing at the receptors due to its high activity at the CB_2R. It resulted in high binding affinity at the CB_2R (K_i 225 nM) and moderate affinity to the CB_1R (K_i 3.2 µM) (**Table 9**). Variations of the C(9) position could provide future investigations into functional groups influencing selectivity between the two CBRs.

Having identified that this position also appears to influence the selectivity, the small library of compounds **288** and **295-301** synthesised was tested for activity on the CB_1R (**Table 9**). The assay used to test for activity at the CB_1R was also a complementary cAMP assay providing a signal dependent on the amount of labelled cAMP bound to the enzyme. Δ^9-THC (**201**), a CB_1R agonist, led to the inhibition of adenylase cyclase and antibody binding of labelled cAMP which ultimately leads in a low signal.

The small library of C(9) substituted compounds were tested in this assay and did not appear to give any detectable activity within the assay range (<3 µM). Therefore, we can conclude that modulation at the C(9)-position has an effect on potency of the CB_2R activation but also appears to have an effect at higher concentrations on the activity on the

CB_1R. Unfortunately solubility constraints prevented the use of the compounds in the assay at concentrations higher than 3 µM.

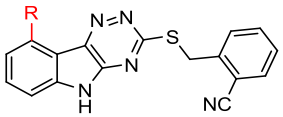

Compound	R =	EC_{50} CB_2R (nM)	EC_{50} CB_1R (µM)
236	H	112	>3
266	Br	248	>3
288	Ph	85	>3
295	*o*-Me-Ph	2440	>3
296	*m*-Me-Ph	3280	>3
297	*p*-Me-Ph	>3000	>3
298	*p*-OMe-Ph	2340	>3
299	*p*-Cl-Ph	>3000	>3
300	Thiophene	1760	>3
301	Cyclopropyl	231	>3

Table 9 C(9) position derivatives and their relative activities in the cAMP assay at the CB_1R and CB_2R

5.5.3 *N*(5) Substituted Derivatives

Work so far indicated *ortho* EWG on the *S*-benzyl group to be essential for activity, in addition to unsubstituted or a small carbacyclic functional group at the C(9) position. A further point of diversification around the original *S*-benzylated triazino indole core to be investigated was the *N*(5) position.

5.5.3.1 First Generation - Steric Investigations

A range of differently sized functional groups were added to the nitrogen and their effect on the activity at the CB_2R observed. Initial attempts of functionalising the *N*(5) position on **236**, which was accessed *via* a two step synthesis involving the cyclisation to the tricycle and subsequent thiol benzylation, using mild bases did not yield any product due to the lack of reactivity of the amine. Limited solubility in organic solvents of the starting material and products also proved troublesome in the purification and their separation

could not be carried out *via* recrystallisation or flash column chromatography. Initial attempts yielded product with the use of Et_3N, DMAP in CH_2Cl_2, however, this was very limited and had to be replaced by alternative conditions (**Table 10**). Therefore, a range of organic and inorganic bases were investigated, leading to the use of NaH (60% in mineral oil), which deprotenated the *N*(5) position of **236** allowing for subsequent nucleophilic attack on the electrophile. The optimal solvent was identified to be the polar, water miscible dimethylformamide (DMF) (**Scheme 11**). Addition of **135** to the solvent generated a pale yellow suspension, however upon addition of NaH, the deprotenated species dissolved in the DMF. The challenges with solubility of this series of compounds originates from their lipophilic nature, by introduction of a charge, it would be predicted that the compound would dissolve in a polar aprotic solvent, DMF. After the reaction was completed, the product could be precipitated with dropwise addition of water, to quench the excess unreacted NaH, which was miscible with the DMF. The polarity of the water caused the product to precipitate out due to its lipophilic nature. Initial attempts at methylating the *N*(5) position led to the synthesis of **302** which also added a methyl group on the benzylic group.

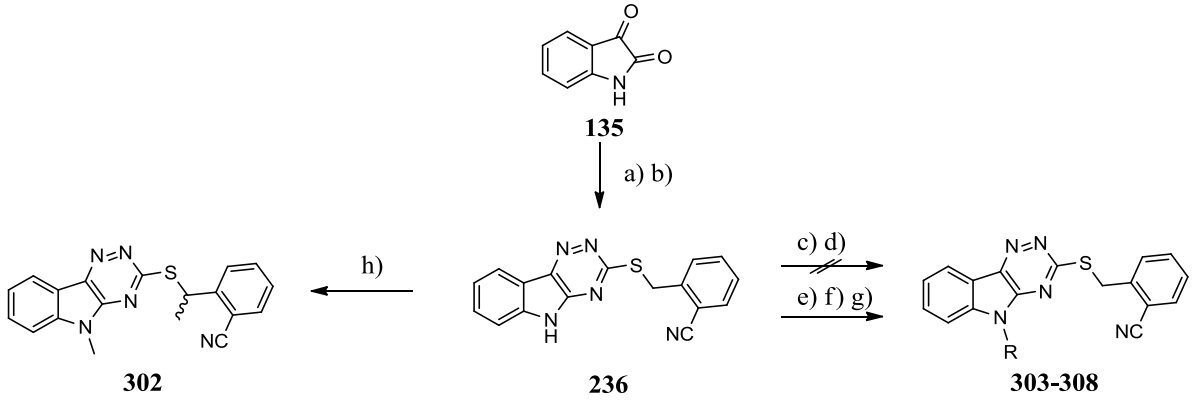

Scheme 11 Some conditions attempted in the synthesis of *N*-derivatives of **236**, a) thiosemicarbazide, K_2CO_3, H_2O, reflux 16 h, 92% b) 2-cyano benzyl bromide, Et_3N, MeOH, rt 16 h,99% c) 2-cyano benzyl bromide, base, solvent (see table 16), h) MeI, base, solvent (see table 17)

Reaction	Base	Solvent	Conditions	Yield (%)
c	aq NaOH (4%)	H_2O	rt 16 h	NP
d	K_2CO_3	$(CH_3)_2CO$	reflux 16 h	NP
e	Et_3N, DMAP	CH_2Cl_2	rt 16 h	69-80
f	NaH,	THF	0 °C rt 16 h	NP
g	NaH	DMF	0 °C-rt 16 h	19-78
h	K_2CO_3	DMF	rt 16 h	89

Table 10 Outline of some of the conditions attempted in functionalisation of the *N*(5) position
Np = no product isolation

After establishing suitable conditions, a small library of compounds with alkyl groups **303-308** of varying steric bulk was synthesised (**Table 11**), and screened in the cAMP assay. The activities of the compounds provide interesting information about the steric constraints of the enzyme binding pocket assuming the compounds utilise a consistent binding mode.

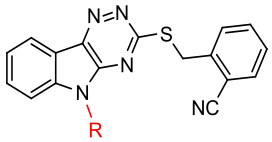

Compound	R =	Yield (%)	EC_{50} CB_2R (nM)
236	H	NA	112
303		69[A]	>3000
304		78[B]	314
305	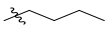	68[B]	200
306		52[B]	141
307	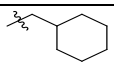	19[B]	270
308	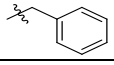	80[A]	214

Table 11 Different *N*-substituted compounds probing the steric constraints at the *N*(5) position and their relative yields and activities
[A] = Et_3N, DMAP, CH_2Cl_2
[B] = NaH, DMF

Generally, the introduction of substituents at the *N*(5) position is well tolerated and retains activity at the CB_2R. Surprisingly by the addition of the smallest possible hydrocarbon substituent **294**, activity is lost (EC_{50} >3 µM). This could be the result of poor solubility in the assay conditions or cytotoxicity displayed by the compound. Alternatively, larger

groups provide additional interactions to the binding site of the receptor. Binding studies of **303** could provide further insight into the cause in loss of activity with the *N*-methylated compound..

Any of the larger substituents from alkyl chains to saturated and unsaturated carbacycles provided good activity (EC_{50} 214 – 314 nM). Further investigations were initially carried out by replacing the benzyl moiety with functionalised benzyl groups.

A small group of benzyl derivatives were made which demonstrated good activities (EC_{50} 45 - 201 nM) however, solubility of the compounds was poor, making it difficult to handle. From the *N*-benzyl series, compound **308** was submitted for affinity studies at Cerep, displaying very good binding affinity to the CB_2R (K_i 11 nM), however also at the CB_1R (K_i 61 nM) (**Figure 12**). Alterations at this site were shown to influence selectivity between the two CBR making further investigations of functional groups at this site of great interest for current CB_2R agonist research and possibly for future studies of CB_1R agonists.

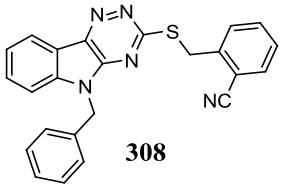

308

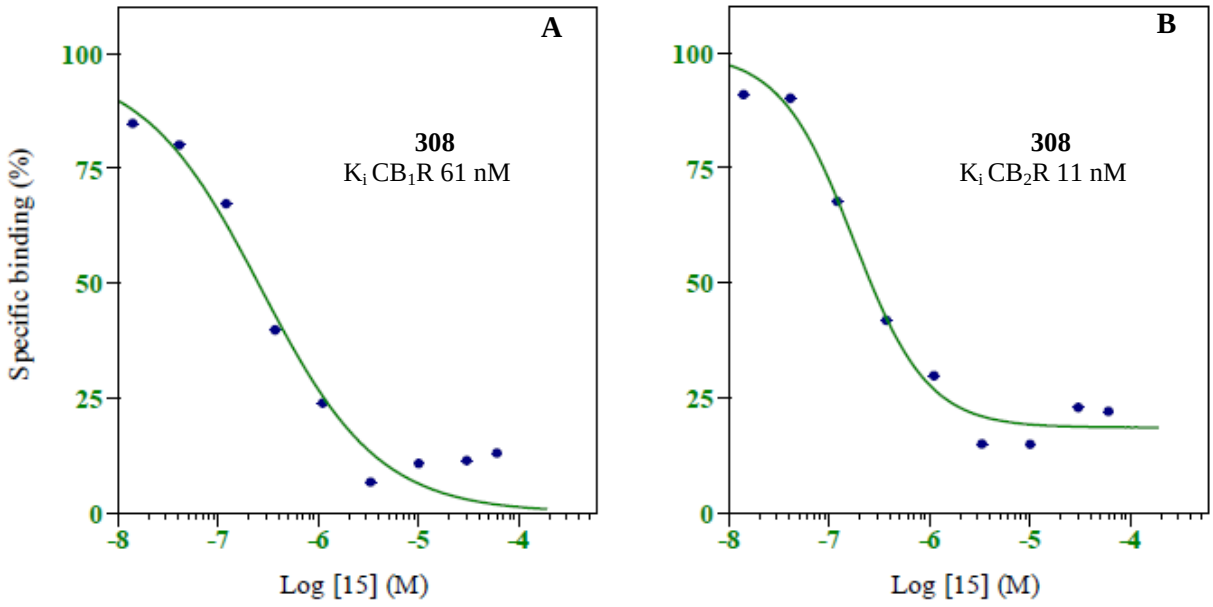

Figure 12 Affinity graphs for **308** at the CB_1R (**A**) and the CB_2R (**B**)

Following the synthesis of benzylic derivatives, alternative functional groups containing heteroatoms were considered in hope of regaining the selectivity previously observed with **236**.

5.5.3.2 Second Generation – Retention of CB_2R:CB_1R Selectivity

The broad tolerance of substituents at the *N*(5) position prompted further investigations at this site allowing investigation into optimising chemical properties such as solubility. Synthesis of the next generation of structures included *N*-carbonyl, *N*-sulfonyl and *N*-methyl carbonyl containing compounds (**Scheme 12**, **Table 12**). Introducing heteroatoms at the *N*(5) position, could potentially provide novel H-bonding interactions to the active site of the receptor and demonstrate discrimination between receptors in addition to improving physicochemical properties.

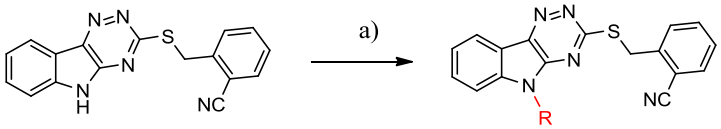

236 **309-316**

Scheme 12 Synthesis of series of *N*-derivatives **309-316** a) carbonyl chloride, sulfonyl chloride or chloroformate, NaH (60%), DMF 0 °C-rt 16 h 39-96%

Compound	R =	Yield (%)	EC_{50} CB_2R (nM)
236	H	NA	112
309	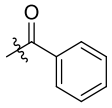	72	113
310	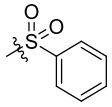	84	76
311	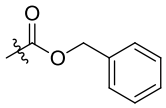	96	>3000
312	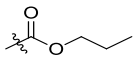	44	375
313	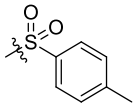	92	>3000
314	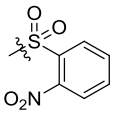	83	>3000
315	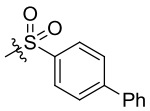	83	>3000
316	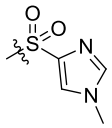	39	>3000

Table 12 various *N*(5) derivatives synthesised **309-316** and their relative activities at the CB_2R

The generation of a set of *N*(5) substituted compounds provided some valuable SAR (**Table 12**). With the introduction of a phenyl sulfone **310** good activity was obtained (EC_{50} 76 nM). However, adding functionality around the phenyl ring **313** and **315** or replacing the phenyl group with a methyl imidazole **316** led to loss of activity (EC_{50} >3 µM). The addition of a benzoyl group at the *N*(5) position **300** resulted in an activity (EC_{50} 113 nM) comparable to the hit compound **236** and an improvement on the benzyl

compound (**299**). Screening of the carbamates displayed a loss in activity (EC_{50} >3 μM) in the presence of the benzyl group, however nanomolar activity was observed with an *n*-propyl chain **312** (EC_{50} 375 nM). The cause could possibly be the difference in solubility as **312** was observed to have low solubility and proved challenging in dissolving.

Having identified tolerance by the receptors towards the carbonyl **309** and sulfone **310** linked phenyl groups, it was decided to evaluate the effect of this functionality on selectivity of the receptors. Interestingly the introduction of a sulfone or carbonyl group gave much less rotational flexibility around the amide bond in comparison to the methylene due to the additional functionality (**Figure 14**). **309** was submitted for affinity studies and was found to have very good binding to the CB_2R (K_i 113 nM), and even more pleasing was the lack of binding affinity at the CB_1R (K_i >30 μM) (**Figure 13**).

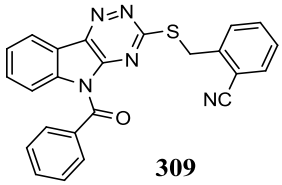

309

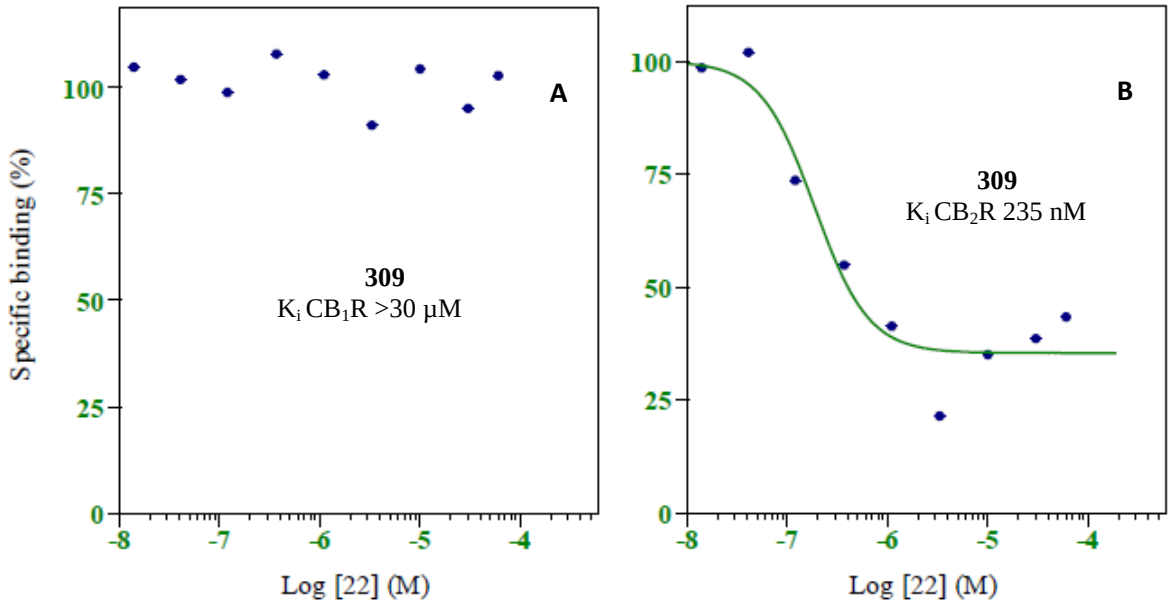

Figure 13 Affinity graphs for **309** at the CB_1R (**A**) and the CB_2R (**B**)

The results obtained from the affinity studies submitted indicated that the presence of a benzoyl group is preferred over benzyl, possibly because the carbonyl can either interact directly with the active site through H-bonding, or introduce conformational restraints which are not tolerated at the CB_1R, but without structural information, it is impossible to say for sure. It demonstrates that the replacement of a benzyl to a benzoyl group at the *N*(5) position leads to dramatic improvements in selectivity between the two cannabinoid receptors.

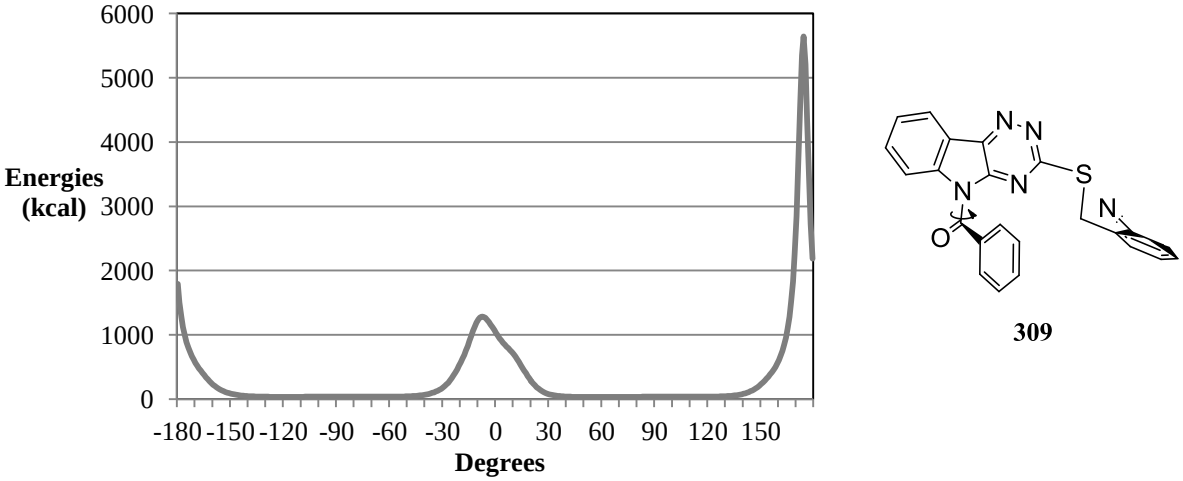

Figure 14 Graph with conformational energies around rotation of the amide bond of **309,** lowest energy conformation at 33.6 kcal/mol, generated using ChemBio 3D[283]

5.5.3.3 Carbonyl Derivatives

Having shown that the incorporation of an *N*-carbonyl substituent **309** was tolerated and showed equipotent activity and selectivity for the CB_2R as **236**, the logical progression was towards the generation of a library of different carbonyl derivatives. The new series of compounds were to probe the tolerance of the binding site towards a range of *N*-carbonyl substituents and with this knowledge, synthesise compounds with polar groups to improve solubility of the series.

A library of compounds was synthesised by using the previously optimised conditions *via* cyclisation of isatin (**135**) with thiosemicarbazide and subsequent benzylation of the sulphide. The final step involved the preparation of a suspension of **236** in DMF, followed by the addition of NaH to yield a yellow solution. This was followed by the addition of the relevant acid chloride and stirred overnight. *N*(5) carbonyl containing derivatives included substituted phenyl's, saturated carbacycles and open chain substituents. The isolation of the product in most cases could be performed by a careful dropwise addition of water and cooling to produce a precipitate which was filtered, washed with methanol and dried to yield the product without requiring further purification (**Scheme 13**).

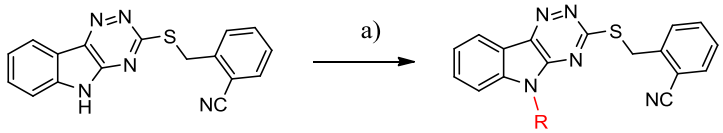

236 **317-330**

Scheme 13 Synthesis of series of *N*-derivatives **317-330** a) thiosemicarbazide, K_2CO_3, H_2O, reflux 16 h, 92% b) 2-cyano benzyl bromide, Et_3N, MeOH, rt 16 h, 99% c) Acid chloride, NaH (60%), DMF 0 °C-rt 16h 42-81%

Loss of activity at the CB_2R was only observed for **317** (EC_{50} >3 µM), which supports the hypothesis that functional groups at this position need to be of certain size (Table 19). An ethyl **318** (EC_{50} 48 nM) or propyl **319** (EC_{50} 42 nM) linked methyl esters were produced in high yields and with good activities. A small series of compounds were made with functional groups around a phenyl ring. *Para* and *meta* substituents **320-324** on the compounds retained very good activity (EC_{50} 27 – 73 nM), however both compounds, **325** and **326**, with functional groups on the *ortho* position lead to a loss in activity (EC_{50} >3 µM). The intolerance towards *ortho* substitutions could indicate that the free rotation of the phenyl group is important for binding within the pocket. Replacing the flat lipophilic phenyl ring, a furfuryl compound **327** was made and found to have excellent activity (EC_{50} 46 nM) in addition to three saturated carbacycles, namely the cyclohexyl **328** (EC_{50} 32 nM), cyclopentyl **329** (EC_{50} 49 nM) and cyclopropyl **330** (EC_{50} 181 nM). The results suggest that the active site of the binding pocket appears to tolerate a range of aryl and alkyl derivatives off the amide linkage.

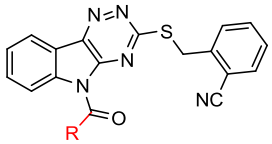

317-330

Figure 15 General structure for table 13

Compound	R =	Yield (%)	EC_{50} CB_2R (nM)
236	NA	NA	112
317		77	>3000
318	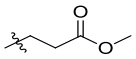	81	48
319	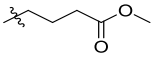	81	42
309		72	113
320	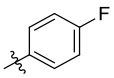	67	57
321	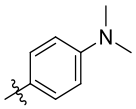	55	136
322	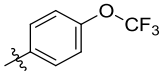	67	73
323	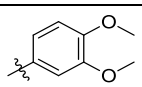	56	160
324	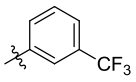	58	27
325	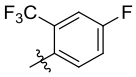	42	>3000
326	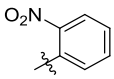	81	>3000
327		78	46
328		71	32
329		42	49
330		76	181

Table 13 First generation of *N*-substituted carbonyl derivatives with yield of the final coupling and their relative activity at the CB_2R

The tolerance to a range of diverse ring system led to further investigations into ligand efficiency (LE) for the compound series.

5.5.4 Ligand Efficiency (LE) and Lipophilic Ligand Efficiency (LLE)

Ligand efficiency (LE) has been introduced to provide a correlation between activity and various properties of compounds, generally molecular weight (Mw).[284] Lipophilicity has been identified to be crucial and arguably the most important chemical property in the development of a drug candidate. Lipinski established the rule of five, which states that a compounds should have a ClogP lower than 5, resulting in higher levels of drug absorption and cell permeability.[10] Correlating potency (pEC_{50}) and lipophilicity (ClogP) results in a calculated parameter called the lipophilic ligand efficiency (LLE) (**A**). Favourable LLE values (>5) have been correlated to aqueous solubility, potency and *in vivo* efficacy.[285,13,12] Generally, optimisation of compounds increases activity, but often adds mass and increases lipophilicity, therefore it is important to consider the impact of these properties during compound development. Just a few example of LLE values of available drugs are morphine (8.25), propranolol (5.17) and cetitizine (4.34).

Lipophilic Ligand Efficiency = pEC_{50} – ClogP **(A)**

The general tolerance of substituents on the *N*-carbonyl allowed some initial investigations into LLE. The LLE improved significantly from initial *N*(5) substituted **308** (LLE 1.32) to the *N*-carbonyl furfuryl derivative **327** (LLE 3.58) (**Figure 16**).

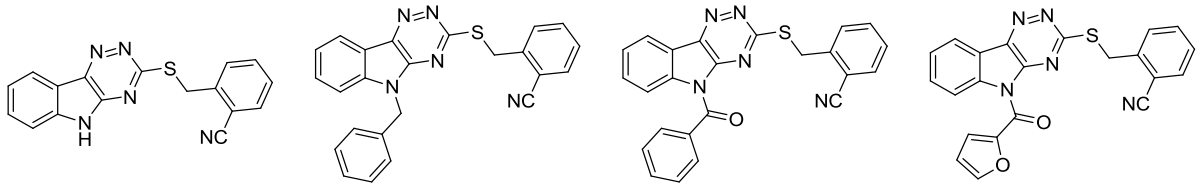

236 3.19 **308** 1.32 **309** 2.37 **327** 3.58

Figure 16 Initial investigations into *N*(5) substiuents and their LLE values

Having identified that polar groups on the *N*-carbonyl retains potency and improves the overall LLE, further derivatives were made investigating solubility.

5.6 Solubility Studies

Previously reported cannabinoid receptor binding molecules have been known to be very lipophilic and poorly soluble in aqueous medium (**Figure 17**). Improving potency and reducing calculated partition coefficient (ClogP) values, to increase solubility in aqueous media, results in higher LLE providing favourable drug-like properties and improved oral bioavailability for future *in vivo* studies.

Our template molecule used in the structure based virtual screen, **226** (HU-308), has a ClogP of 8.0 which was calculated using ChemDraw software. Studies have identified the median ClogP of marketed drugs to be 2.5.[12,13,283] Other examples of cannabinoid receptor modulators also display similarly high ClogP values, indicating that the receptors have a preference for hydrophobic ligands. Reduced lipophilicity in CB_2R agonist research is especially of importance due to the blood brain barrier penetration leading to increased concentrations of drug in the CNS and possible psychoactive side effects. However, if the BBB permeability is removed the psychotropic side effects are removed, rendering the compound a more likely drug candidate. Antihistamines are a suitable example, where improved physicochemical properties, reduced lipophilicity, prevented CNS penetration and reduced associated side effects. **Figure 17** displays some ClogP values of known CB_2R agonists which all display values greater than Lipinski's criteria (ClogP < 5) and Teague's lead-like guide (ClogP $3 < X < 4.5$).[10,18] **236** in comparison has a ClogP value of 3.8 which is within the expectations of the guides and a positive starting point for further improvement.

As observed, a range of cyclic and acyclic groups were tolerated on the *N*-carbonyl position retaining activity and selectivity at the CB_2R. Solubility and ClogP values had proved very problematic, however preliminary investigations showed that improvements could be made. Two additional examples were made, via the same synthetic route as

previously outlined, bearing a isoxazole group **331** (EC_{50} 92 nM) and a morpholine group, **332** (EC_{50} 19 nM) at the *N*-carbonyl position with ClogP values of 3.1 and 2.6 and LLE values of 3.9 and 5.4 respectively (**Scheme 14**, **Table 14**). These compounds displayed favourable ClogP values and **331** and **332** display very promising LLE for this series.

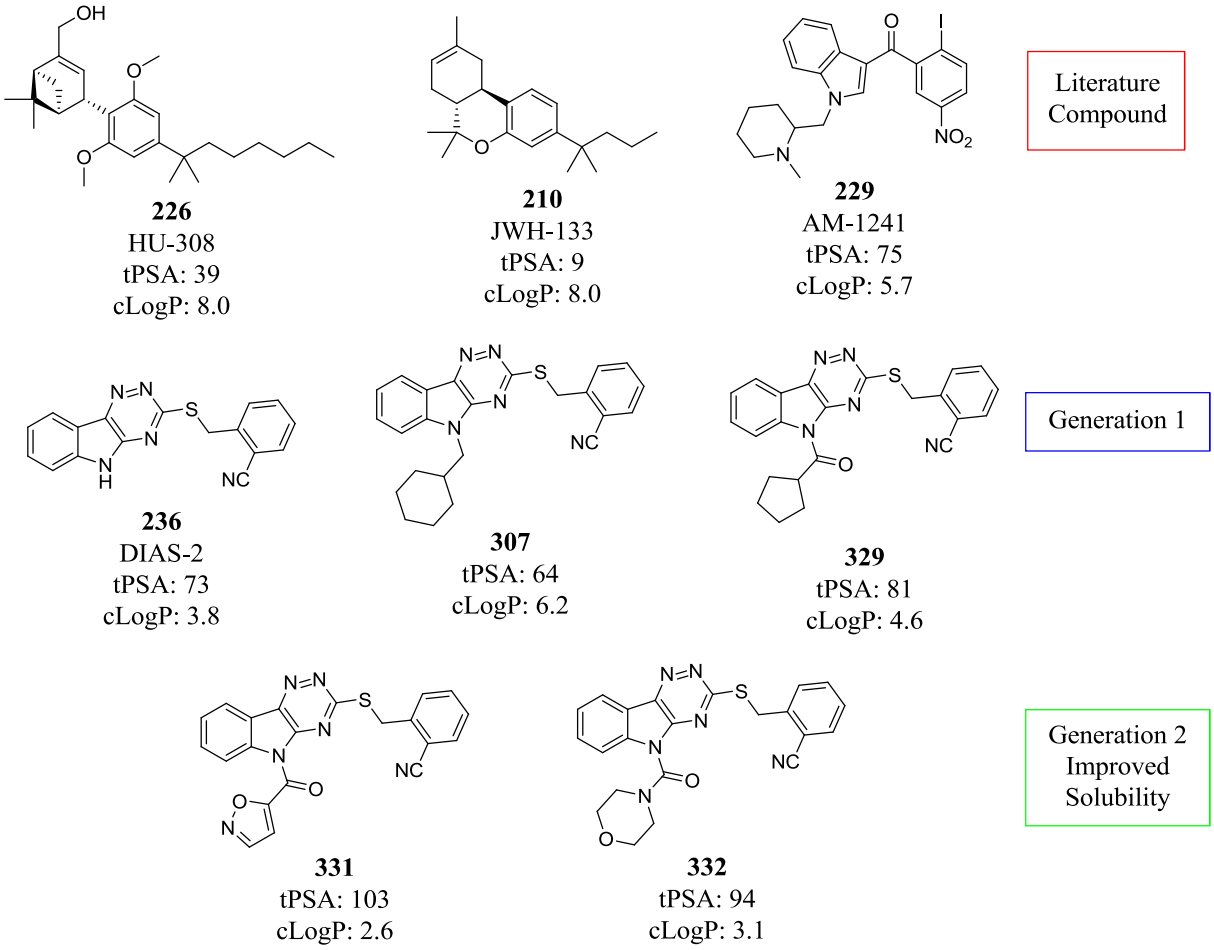

Figure 17 Examples of CB_2R in the literature and progression of our project related compounds with their respective total polar surface area (tPSA in Å) and ClogP values

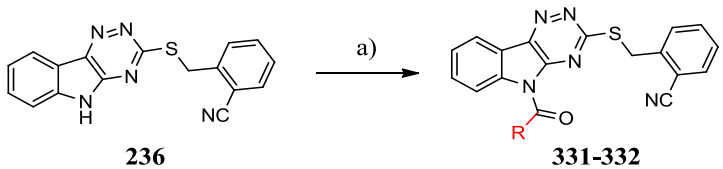

Scheme 14 Synthesis of series of *N*-derivatives **331-332** a) thiosemicarbazide, K_2CO_3, H_2O, reflux 16 h, 92% b) 2-cyano benzyl bromide, Et_3N, MeOH, rt 16 h, 99% c) Acid chloride, NaH (60%), DMF 0 °C-rt 16 h 72-85%

Compound	R =	Yield (%)	EC_{50} CB_2R (nM)	ClogP	LLE
236	NA	NA	112	3.8	3.19
331		85	19	2.6	5.16
332		72	92	3.1	3.90

Table 14 Addition of solubilising polar groups on the carbonyl group with the yield, activity and calculated ClogP values

5.6.1 ClogP and LLE Progression

The first set of synthesised compounds of the triazino indole series (**Figure 18**, orange circle) varied only with functional groups around the mercaptobenzyl unit, leading to no dramatic variations in lipophilicity (ClogP 5 – 6). Subsequent functionalisation of the C(9) position and *N*-substitutions increased lipophilicity by introducing a hydrophobic substituent (**Figure 18** Red Circle). Finally more potent *N*-carbonyl substituents were replaced to demonstrate an example of compounds with high levels of selectivity between the two receptors, excellent potency, with ClogP and LLE value in the desired range (**Figure 18**, green circle).

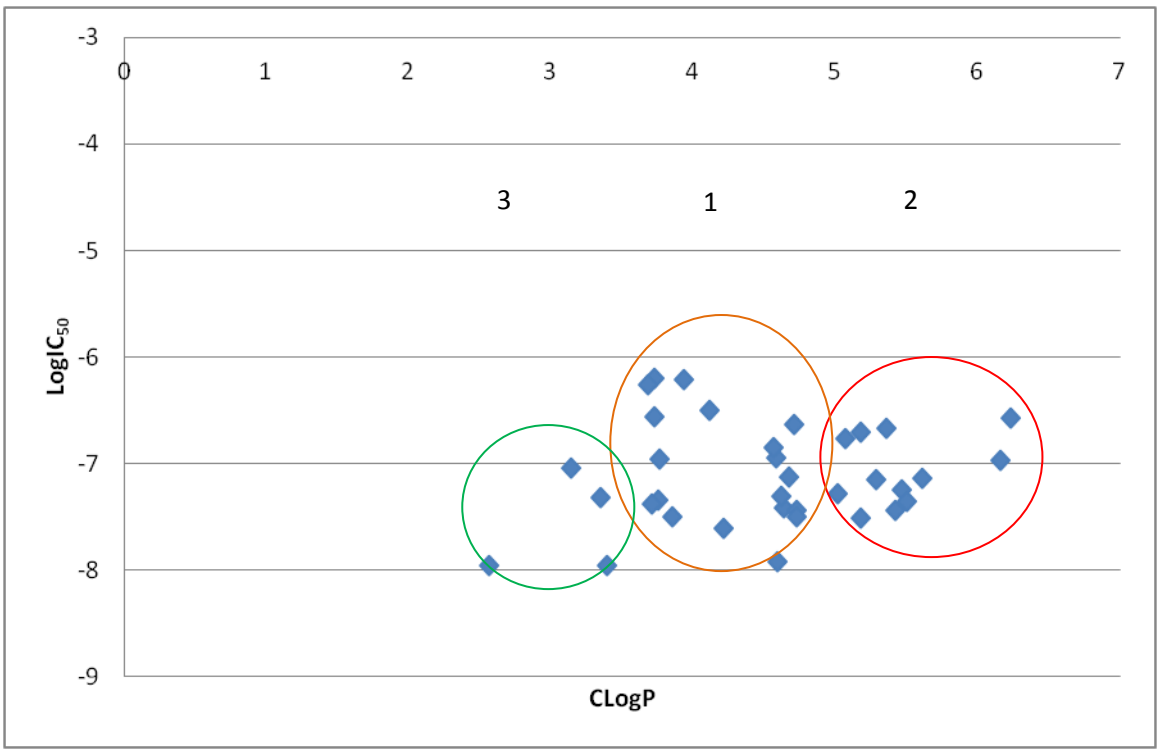

Orange Circle (1)	• 1st generation • S-benzyl
Red Circle (2)	• 2nd generation • Sulfones, carbamates, carbonyl and alkyl
Green Circle (3)	• 3rd generation • Optimised solublising group containing

Figure 18 Progression of project and variations in activities and ClogP of synthesised compounds

A plot correlating the potency (pEC_{50}) and ClogP values for each active compound produces an important result (**Figure 19**). This project has successfully reduced undesired lipophilicity and maintained activity at the CB_2R. The plot displays activity increases and ClogP decreases. Pleasingly both graphs illustrate an inverse correlation of what would usually be predicted to happen as activity increases. Generally an increase of ClogP would be observed.

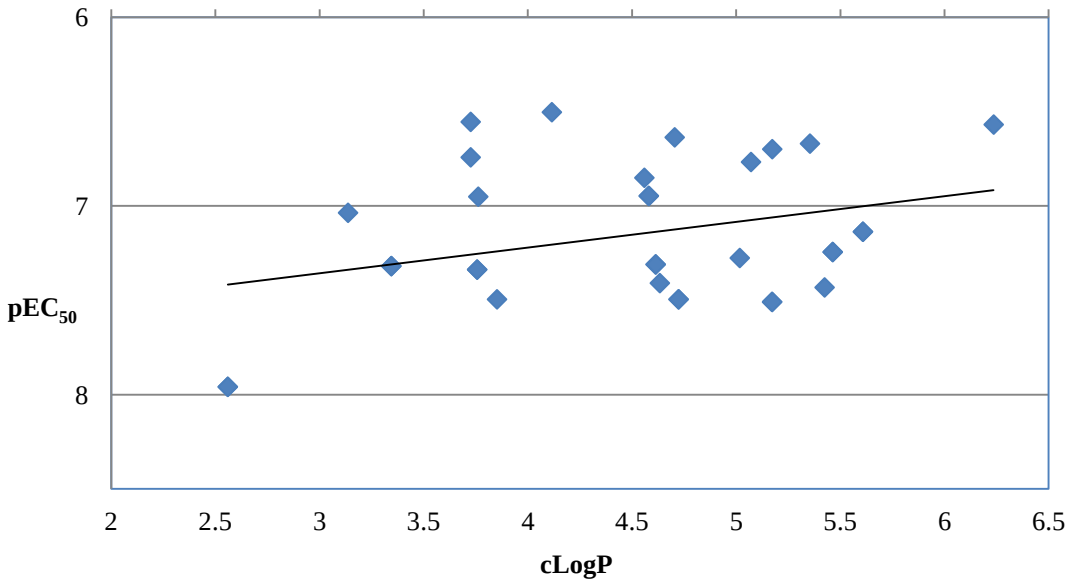

Figure 19 pEC_{50} and ClogP correlation of triazinoindole series

The introduction of polar groups into the compound series decreased the value of ClogP to the lowest observed so far. In order to quantitatively assess the effect of these changes on physicochemical properties, a selection of compounds was evaluated for their turbidimetric aqueous kinetic solubility. The estimated precipitation range is calculated by measuring the absorbance at 620 nm after incubation of a DMSO stock solution with a buffer at 37 °C for 2 hours, any difference in absorbance is as a result of turbidity.[286] The value generated is the mid-point between the upper and lower boundary. The first compounds to be tested for solubility were **235** (2.0 µM) and **236** (3.75 µM), and these were chosen as reference, since they were initially identified through the virtual based screening method (**Figure 20**). Representative examples were identified from the library of amide linked derivatives and an additional 5 compounds were submitted for solubility studies (**Table 15**). The most notable compounds with increased solubility were **331** containing the carbonyl isoxazole group (6.50 µM) and where a solubilising group namely a morpholine (**332**) (10.5 µM), leading to nearly doubling of value for the solubility from the next best (**332**, 6.50 µM). For reference, the positive control in the assay is nicardipine (20 µM). Generally

compounds with solubility values <1 µM are considered as insoluble, between 1 – 100 µM to be partially soluble and >100 µM to be soluble.

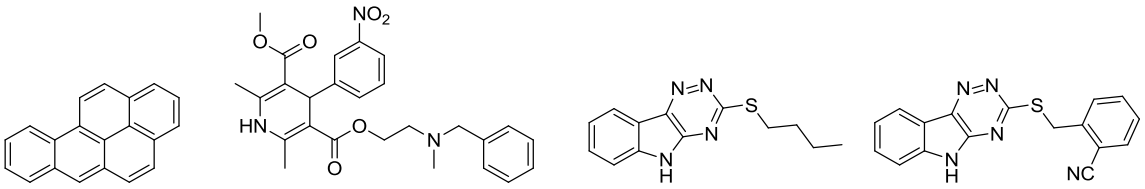

Pyrene
6.5 µM

Nicardine
20 µM

235
2.00 µM

236
3.75 µM

Figure 20 Turbidimetric aqueous kinetic solubility of the two controls, pyrene and nicardine, and **235** and **236**

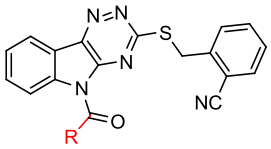

Compound	**R =**	**EC_{50} CB_2R (nM)**	**ClogP**	**Solubility (µM)**
Nicardipine	-	-	-	20
309		113	4.6	2.00
318	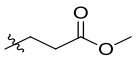	48	3.3	3.75
319	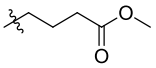	42	3.7	3.75
332		19	2.6	6.50
332		92	3.1	10.5

Table 15 Table of positive control nicardipine and carbonyl derivatives with activity, ClogP and solubility (mid point)

Addition of polar groups on the *N*-carbonyl retains activity at the CB_2R and improves solubility. Attempts to improve solubility were investigated further through truncating the triazinoindole core to avoid the presence of the flat lipophilic framework.

5.6.1.1 Synthesis of Truncated Derivatives

To reduce lipophilicity, the flat heteroatom rich triazino indole core **334** could be dissected simply to the 1,2,4-triazino ring **333** or to the bicyclic pyrrolo-1,2,4-triazinio ring **335** to introduce more rotatable bonds and remove possible unnecessary bulk (**Figure 21**). Removing the left hand side of the molecule could influence potency as identified by the functionalisation of the C(9) and N(5) positions.

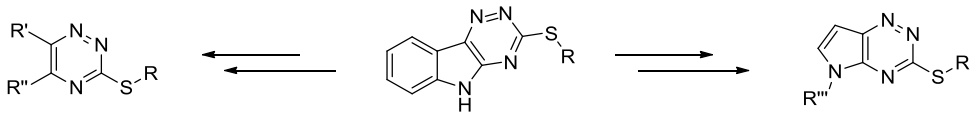

333 Traget 1 **334** Tricyclic Core **335** Target 2

Figure 21 Synthetic targets **333** and **335** with a truncated tricyclic core of **334** to reduce lipophilicity

A similar synthetic strategy for making 1,2,4-triazines could be implemented by using 1,2-diketones and reacting these *via* a condensation reaction with a thiosemicarbazide. There are several literature conditions that explore similar structures involving a ring closure under acidic and basic conditions to make the triazines. However, two alternative routes were investigated outlined in **Scheme 15**. The first utilises the condensation reaction between the 1,2-diketone **336** and thiosemicarbazide to yield the triazine-3-thiol **337**, which was then benzylated under conditions previously developed for the 2-cyanobenzylbromide with Et_3N to yield **338**. An alternative route proceeds *via* the functionalisation of the sulphide on thiosemicarbazide **339** with the combination of 2-cyanobenzylbromide and thiosemicarbazide in EtOH to yield the HBr salt **340**.[287] **340** is then cyclised by reaction with the 1,2-diketone **336** to yield the product **338**.

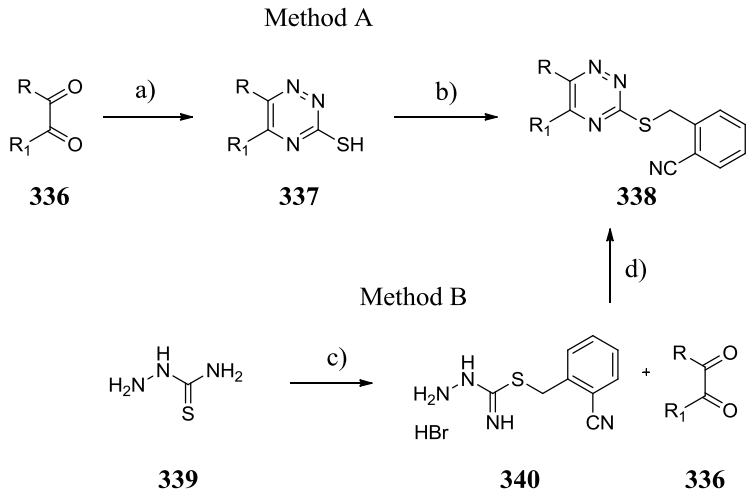

Scheme 15 2 routes to the synthesis of truncated derivatives, a) thiosemicarbazide, AcOH 120 °C 16 h b) 2-cyano benzyl bromide, Et_3N, MeOH rt 16 h c) EtOH 60 °C 30 min d) NaOAc 120 °C 30 min-16 h

With these two possible routes, 2'-(((1,2,4-triazin-yl)thio)methyl)benzonitrile **341**, was synthesised by the addition of the **340** *S*-benzylated thiosemicarbazide following method B to yield **341** which was unfortunately found to be inactive (EC_{50} >3 μM) (**Table 16**). Initial attempts led to an effort to mimic the secondary amine in **236** to investigate whether the presence of H-bonding acceptor or donor properties influences activity. Synthesis of two 5-hydroxy triazines **342** and **343** both displayed lack of activity in the cAMP assay.

This led to the synthesis of compounds with larger functional groups at R and R_1 *via* the more straight forward method B to investigate whether introduction of the lipophilic core contributed to observed activity. **344** and **345** with a phenyl group at the C(5) or C(6) position both demonstrated lack of activity in the cell assay. However, substitution at the C(5) and C(6) position with large lipophilic phenyl group **346** gave an activity of 343 nM.

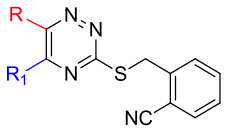

Compound	R =	R_1 =	Yield (b or d) (%)	EC_{50} CB_2R (nM)	ClogP
236	-	-	-	112	3.76
341	H	H	79[A]	>3000	-0.99
342	H	OH	29[A]	>3000	1.04
343	CH_3	OH	92[A]	>3000	2.63
344	H	Ph	71[B]	>3000	3.39
345	Ph	OH	81[B]	>3000	3.98
346	Ph	Ph	79[B]	343	4.90

Table 16 truncated derivatives **341-346** maintaining the triazino ring with a 2-cyanobenzyl substituted thiol
A = synthesis *via* method A
B = synthesis *via* method B

From the table above the only promising compounds was **346**, which contained a biphenyl 5, 6 substituted triazino ring. This compound however, has a ClogP value (4.90) greater than the original tricyclic hit (3.76).

Attempts to prepare the pyrrolo-1,2,4-triazino bicycle **347** proved unsuccessful (**Scheme 16**). Initial Sonogashira coupling on ethyl-2-chloro oxoacetate **348** yielded the ester **349**. Subsequent cyclisation attempts with thiosemicarbazide or the *S*-benzylated equivalent led to product **350** formation, however only in low yields and small scale (max 135 mg). The final steps of the synthesis including chlorination to **351** with phosphoryl chloride or thionyl chloride followed by the cyclisation with ammonia were attempted, but only a complex mixture was obtained.

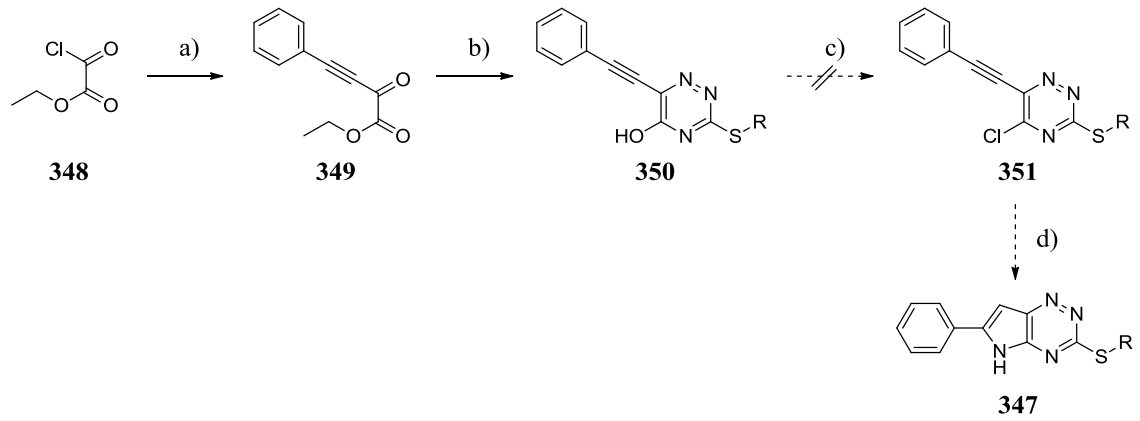

348 **349** **350** **351** **347**

Scheme 16 Attempted synthesis of pyrrolo-1,2,4-triazino **347** a) Copper iodide, Et_3N, PhCCH, THF, 16 h rt, 80% b) thiosemicarbazide, $NaHCO_3$, EtOH, 3 h 120 °C, 43% c) $POCl_3$ or $SOCl_2$ d) NH_3, MeOH, Δ

The series of truncated triazinoindole derivatives provided a small library to explore whether or not compounds with smaller core sizes and lower ClogP values were tolerated. The conclusion was that only two relatively bulky groups retained activity at the CB_2R, which could be useful for future investigations, although it would need to be explored further.

5.7 Stability

Modifications at the *N*(5) position led to the development of a group of CB_2R agonist molecules with improved solubility and potency from the parent compound **236**. Another ADME property, namely metabolic stability is a good indicator of the drug like properties of a compound. Metabolic stability is an essential property of a compound as it defines the duration of which the molecule will remain in its original administered form and its susceptibility to chemical transformation. Metabolic stability is an *in vitro* assay which aims to generate an estimate of drug metabolism *in vivo* and is measured by its half life ($t_{1/2}$), which represents the amount of time taken to reach half the initial compound concentration in the presence of the microsomes (**Figure 22**). This property is very important to assess the pharmacological and toxicological profile of test compounds and suitability to be tested *in vivo*.

Metabolic instability can be an advantage when the parent compound is more toxic or less active than the metabolite produced. Short lived capecitabine ($t_{1/2}$ 38-45 min) is a chemotherapeutic agent which is administered as a substituted tetrahydrofuran pyrimidine and is metabolised to 5-fluorouracil which inhibits DNA synthesis.[288] An example of a less active prodrug which is modified in the desired cell type is the antiviral acyclovir ($t_{1/2}$ 2.2-20 h). The guanosine analogue is phosphorylated by viral kinases to form the monophosphate and ultimately the active triphosphate compound which provides 100 times greater affinity towards viral polymerase over cellular polymerase.[289]

To assess the stability of active CB_2R compounds, they were incubated with mouse liver microsomes and the concentration of the parent compound was measured over time (t = 0, 5, 15, 30, 45 min) by liquid chromatography mass spectrometry (LCMS).[290] Diazepam ($t_{1/2}$ 5-10 min) and diphenhydramine ($t_{1/2}$ 30-40 min) were used as controls.

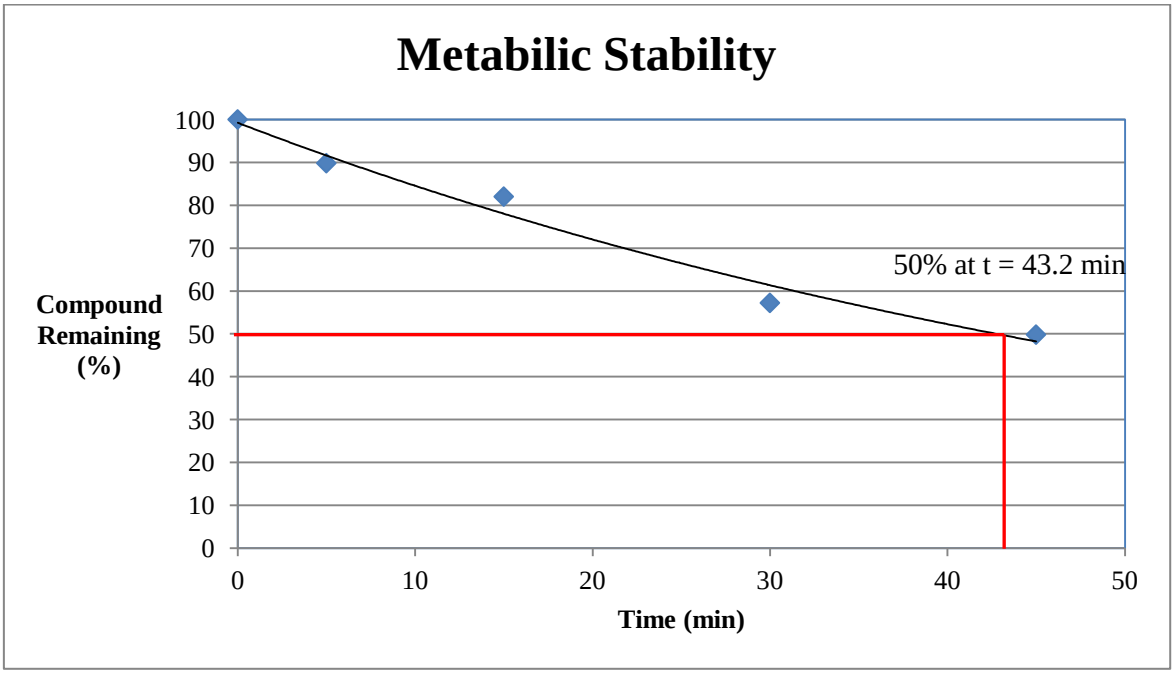

Figure 22 Example of metabolic stability graph of **236**, half life ($t_{1/2}$ in min) is measured where the concentration of the compound is at 50%

From the literature, there are a number of functional groups and core structures that have been shown to be very metabolically labile. Metabolic instability can equally be associated

with the generation of toxicophores such as nitroso groups formed by the reduction of nitroaromatics.[7] The sulphide group is another possible group that could be unstable in this compounds series, since the sulfide can be readily oxidised by enzymes forming sulfoxides and sulfones. A first group of compounds with a cross section of functionalities was submitted to gain an overview of the metabolic stability in the presence of microsomes. This included *S*-benzyl derivatives **236** and **239**, the C(9)-bromo derivative **266** and finally *N*(5) substituted compound **307**-**310** (**Table 17**).

Compound	Structure	ClogP	Stability ($T_{1/2}$)	EC_{50} CB_2R (nM)
236	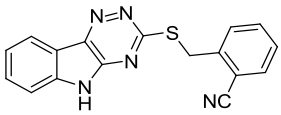	3.8	45.7	112
239	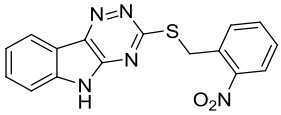	3.9	43.2	32
266	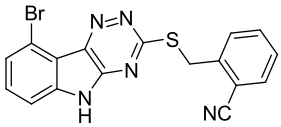	4.6	5.4	39
307	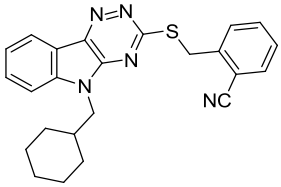	6.2	2.9	270
308	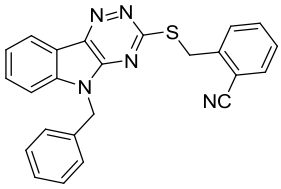	5.4	2.9	214
309	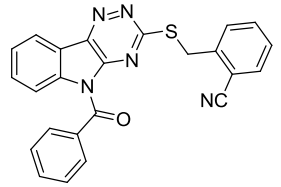	5.0	ND*	113
310	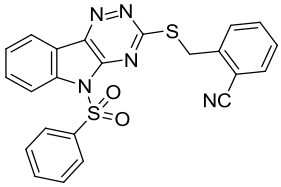	5.1	4.2	76

Table 17 A range of derivatives with the tricyclic core submitted for metabolic stability (*ND = not detectable in the assay)

Parent compound **236** provided a good starting point for improvement of metabolic stability ($t_{1/2}$ 45.7 min). Replacing the 2-cyanobenzyl on **236** with a 2-nitrobenzyl group on **239** did not influence the stability of the compound greatly ($t_{1/2}$ 43.2 min).

The next compound of interest was the C(9) bromo substituted compound **266**, which displayed stability ($t_{1/2}$ 5.4 min) 10 fold lower than the lead compound **236**. More lipophilic compounds have been shown to be better substrates for microsomes resulting in decreased half-life by being metabolised more rapidly.[291] Compounds with substitutions on

the *N*(5) position, a similar loss in stability is observed. For example, by the addition of a methyl cyclohexyl **307** ($t_{1/2}$ 2.88 min) or benzyl **308** ($t_{1/2}$ 2.92 min) groups, the compounds are turned over within minutes. Similarly, with a carbonyl **309** ($t_{1/2}$ not detectable) and sulfone **301** ($t_{1/2}$ 4.15 min) group, the metabolic stability is very low. In all of the studies carried out on *N*(5) substituted compounds, the mass 317 corresponding to compound **236** was observed during the LCMS analysis, indicating that cleavage of the N-C bond is a major contribution the metabolic fate. A control in the study tests for stability in the absence of the cofactor (Nicotinamide adenine dinucleotide phosphate, NADPH) at 45 min only. For all compounds concentrations of >90% of the compound were detected at this time point, making compound metabolism cofactor dependent and not simply due to chemical instability. A possible mechanism leading to the cleavage of the C-N bond is by the hydrolysis on the electron poor atom neighbouring the nitrogen, in the example of the carbonyl **309** and sulfone **310** (**Figure 23**). From the 3D model generated it can be seen that in the predicted ground state conformation the carbonyl would be susceptible to nucleophilic attack. Amide bonds are usually quite robust towards hydrolysis due to the resonance hybridisation with donation into the π to the π^* orbitals. However, for the compounds in this study the preferred conformation is predicted to have no such hybridisation. More likely, is an enzymatic instability observed by the incubation with microsomes. The increased lipophilicity renders compounds better substrates for microsomes, for example cytochromes leading to shorter half-lives (*vide supra*).

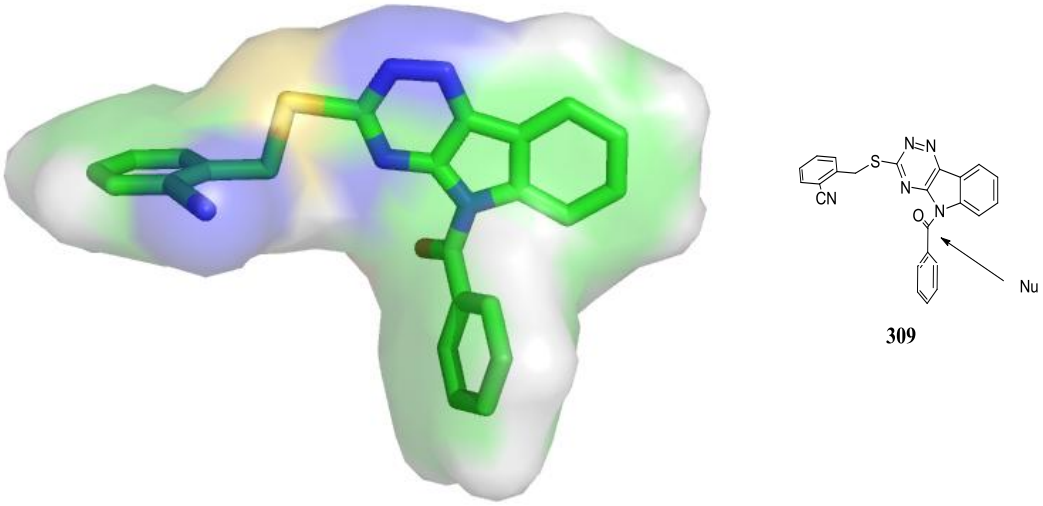

Figure 23 3D representation of a local minima energy conformation of **309**, the arrow shows the direction of attack of a nucleophile from a much unhindered bottom side of the molecule

To investigate whether the reactivity of the hydrolysis is the cause for the instability and if so, can be slowed, two possibilities were investigated; by increasing steric bulk around the carbonyl in an attempt to hinder the nucleophilic attack or adding electron density onto the carbonyl to decrease its reactivity and decrease ClogP. To increase the steric bulk, the aryl group was retained and methyl groups were added at the 2, 4 and 6 position, to give compound **352**, however with no increase in stability in the presence of the microsomes ($t_{1/2}$ 1.97 min). This was successfully applied to lidocaine **353**, where 2,6-dimethyl groups were introduced to improve the stability and resistance to hydrolysis of the amide (**Scheme 17**). However, the introduction of the tolyl groups increased the oxidation of the *meta* position of the phenyl ring.

To increase the electron density at the carbonyl carbon, electron donating groups were added around the aryl substituent. 3,4,5-Trimethoxy substituted phenyl group **354** and a dioxolane **355** substituent were separately introduced. However, it was noted that *O*-methoxy groups are in themselves metabolic labile groups, through the demethylation to the hydroxyl functionality. All of these compounds were made in a similar way (*vide supra*). These three compounds were evaluated in order to examine the effect on stability

of differing electron density around the C-N bond. Although the trimethoxy compound appeared to be the only analogue with increased microsomal stability, the results in this area were complicated by the insolubility of the compounds tested (**Table 18**). However, the parent compound **236** was again the principal peak in MS analysis indicating the instability of the C-N bond.

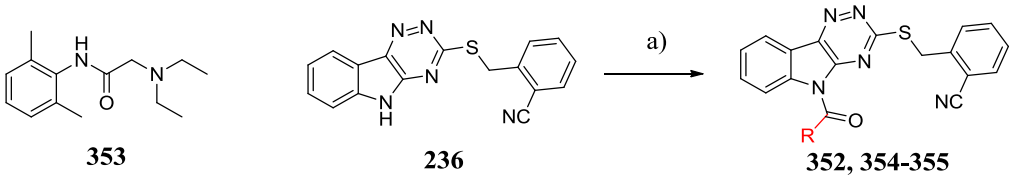

353 **236** **352, 354-355**

Scheme 17 Lidocaine (**353**), synthesis of series of *N*-derivatives a) Acid chloride, NaH (60%), DMF 0 °C-rt 16 h 22-71%

Compound	R =	Yield (%)	Activity (%)	ClogP	Stability ($t_{1/2}$)
352	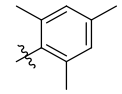	22	70	6.8	1.97
354	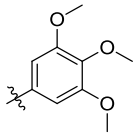	47	65	4.7	50.0*
355	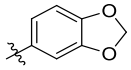	71	70	5.3	ND

Table 18 Compounds made in attempt to increase the stability with retention of the carbonyl phenyl group with steric and electronic variants
Activity = % Activity compared to the forskolin only treated cells (0%) at 10 μM concentrations. Positive control HU-308 (**226**) displayed activity of 70 %.
(ND = not detectable)
*not fully dissolved at start of study

Consequently, other functional groups were investigated at the *N*(5) position in an effort to increase the short half-life currently experienced with *N*-substituted compounds. Carbonyl cyclopropyl **330** displayed very low stability ($t_{1/2}$ 1.28 min) (**Table 19**). Introduction of a methylene group, between the carbonyl and *N*(5) position in **358**, was carried out by a bromination of the methyl ketone **356** and subsequent addition on the *N*(5) position of **236** to produce **358** (**Scheme 18**). Introducing a methylene group would hopefully introduce more stability into the C-N bond and also provide additional SAR on the importance of

position of the carbonyl. Unfortunately, this did not lead to any significant improvement of stability ($t_{1/2}$ 2.53 min) nor activity.

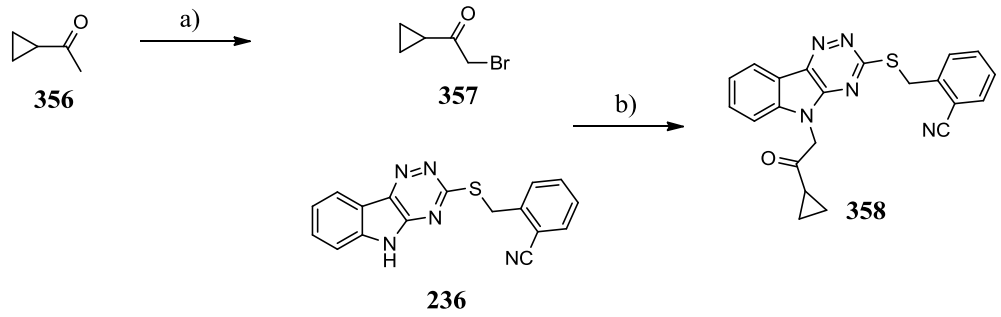

Scheme 18 Synthesis of **358** a) cyclopropylmethyl ketone, Br_2, MeOH, H_2O, 0 °C-rt 16 h, quant b) cyclopropyl carbonyl methyl bromide, NaH (60%), DMF 0 °C-rt 16 h 54%

It would be predicted that the metabolic stability would improve upon removal of the carbonyl from the neighbouring amine due to decreased electron density on the carbonyl, however the alkyl linked *N*(5) derivatives synthesised did not display significant improvement in stability (**Table 19**). Investigations into removing the carbonyl group in **305** and **306**, interestingly also provided short half-lives with the dealkylation being observed by MS analysis in the stability assay providing the parent compound (**236**). Replacement of the carbonyl with the less reactive carbamate **312** also had no influence on stability ($t_{1/2}$ <1 min) as did further methylene carbonyl derivatives **359-361** ($t_{1/2}$ 2.53 - 4.70 min). These were all accessed *via* similar synthetic protocols to those previously described (**Scheme 19**).

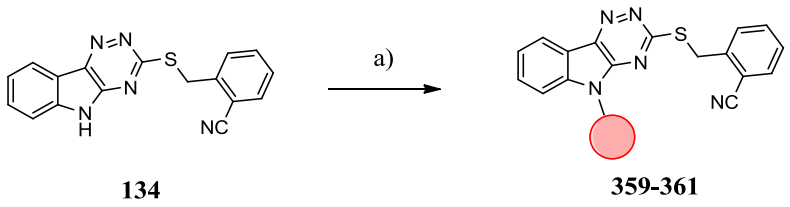

Scheme 19 Synthesis of series of *N*(5) derivatives a) carbonyl methyl ketone, propyl chloroformate, alkyl halide or acid chloride, NaH (60%), DMF 0 °C-rt 16 h 44-97%

Compound	Structure	Yield (%)	$T_{1/2}$ (min)	EC_{50} CB_2R (nM)
305	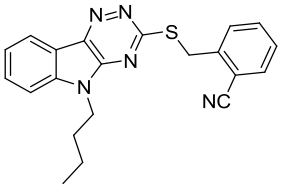	68	0.916	200
306	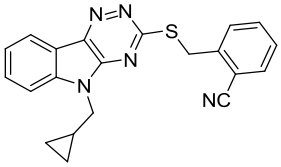	52	2.57	141
312	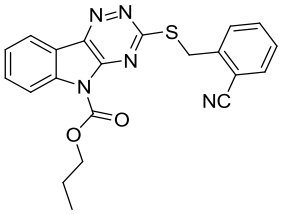	44	ND	376
330	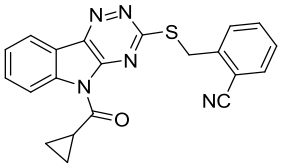	76	1.28	181
359	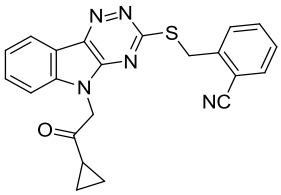	52*	2.53	549
360	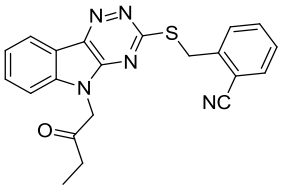	97	4.70	116
361	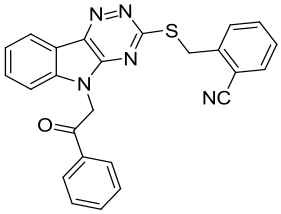	47	3.16	>3000

Table 19 Compounds with yield for the final N-functionalisation step, microsomal stability and activity
*Yield over two steps
ND not detectable

In conclusion, substitution at either the C(9) or the *N*(5) position of the tricycle do not appear to improve metabolic stability. In the presence of microsomes, the molecules are metabolised within minutes mostly to the parent compound **236** with molecular weight of 317. Attempts to increase the metabolic stability on *N*-substituted compounds by variation

of the electronic and steric demands were unsuccessful, with all the substituted analogues demonstrating half-lives in the presence of microsomes shorter than that of the parent compound **236**.

The use of ligand based virtual screening method followed by a subsequent substructure search provided the initial hit **236,** successful development of SAR around this provided a general overview of the type of functional groups which are tolerated on the sulphide and around the tricycle (**Figure 24**). We have identified that the incorporation of any groups on the *meta* and *para* positions of the *S*-benzyl group leads to loss in activity and it appears only *ortho* EWG are tolerated. Additionally, the active site only tolerates substitutions at the C(9) position. Smaller groups are preferred if any at all. Finally, directed SAR was developed around the *N*(5) position leading to the conclusion that addition of the carbonyl group to the *N*(5) position leads to significant increase in selectivity towards the CB_2R.

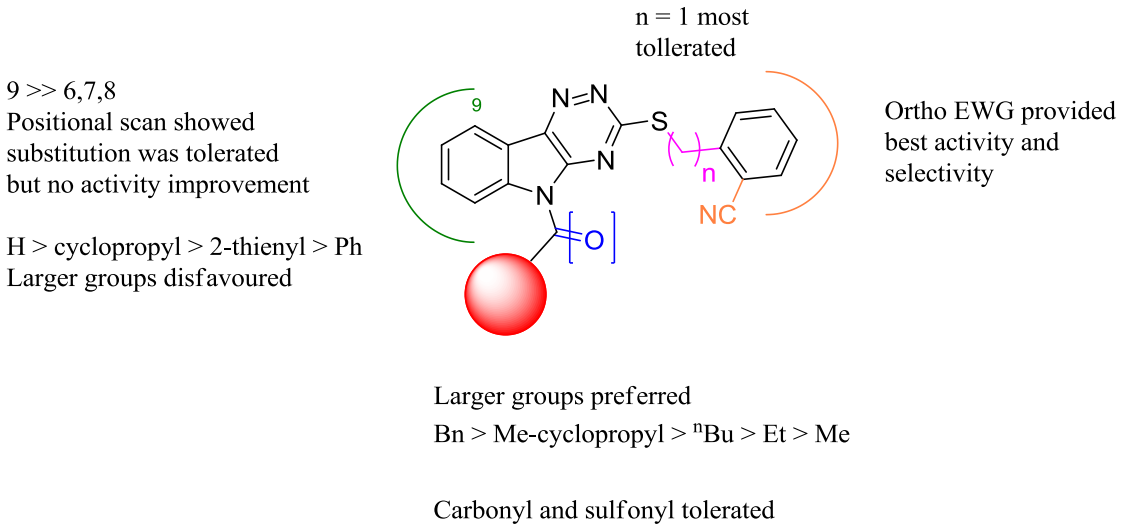

Figure 24 Summary of the established SAR around the tricyclic core

Concerning pharmacochemical properties, it was successfully discovered that modifications to carbonyl linked polar groups at the *N*(5) position retains activity and importantly increase solubility of the compounds. LLE investigations provide evidence of improved LLE as the series progressed with reduction of ClogP values and increased activity at the CB_2R. Unfortunately, the short metabolic half life of *N*(5) substituted

compounds could not be improved with the use of bulky or electron donating groups. With these observations, **236** was selected to be taken through to carry out additional experiments studying the *in vivo* and *in vitro* property of this compound as it had the best balance of properties.

5.8 Further Investigations using 236

236 was identified as a most promising candidate for subsequent evaluation using *in vitro* and *in vivo* experiments. A range of physicochemical properties were gathered for this compound (**Table 20**), showing its good activity and selectivity for the CB_2R (EC_{50} CB_1R >30 µM, EC_{50} CB_2R 120 nM). A molecular weight of 317 and ClogP value of 3.76 are both figures within the predicted Lipinski's and Teague's guides for drug-like compounds. A further property previously mentioned, is the metabolic stability of 45 minutes, whilst not ideal, this was acceptable for the planned experiments. Additionally, screens were carried out against a number of other targets to observe the selectivity across a range of 24 related targets. As CB_2R is a GPCR, it was useful to see whether activity towards this particular receptor was unique, or whether the compound showed promiscuity amongst a range of representative GPCRs. From the screen, the highest percentage activation of the total signal provided by the reference agonists molecules at concentrations of 1 µM was 21%, at the ML1A melatonin receptor (MT_1 ML_{1A}) (See appendix 3, GPCR CEREP screen).

Further to the GPCR selectivity screen, a kinase screen was carried out. The reason was that there was the possibility that **236** was acting through the binding to a kinase which was phosphorylating the $G_{i/o}$ complex leading to an intracellular response. The screen included a panel of 97 different kinases where the binding interaction to the receptor is reported in % residual activity of the target. The unaffected receptor gives a 100% reading, lower numbers indicate a stronger binding hit. The compound was incubated at 10 µM and the

highest binding discovered was less than 30% to that of the control on the CB_2R (See appendix 4 Kinase CEREP screen).

The final physicochemical property that was investigated was the permeability of the compound into and out of cells. Madin-Darby canine kidney (MDCK) cells are transfected with multidrug resistance protein 1 (MDR-1) to generate the cell line MDCK-MDR1 which overexpressed the P-glycoprotein transporters. The results provide an idea of the net flux ratio of the compound, which has an influx of 3.21 x 10^{-6} cms^{-1} which shows the compound is well absorbed (**Table 26**). The flux ratio B → A /A → B being <1 indicates our compound is not a P-glycoprotein substrate. This data also indicates that the compound would be on the boundary of predicted CNS penetration according to data published by Cyprotex plc.[292],[293] HU-308 (**226**) did not provide a comparison due to its unfavourable physicochemical properties, including low solubility, the MDCK test provided unreliable results. This indicates again, that **236** has significantly better properties to previously discovered CB_2R agonist.

Activity: EC_{50} on (CB_2R) 120 nM	EC_{50} (CB_1R) >30'000 nM
Affinity: K_i (CB_2R) 355 nM	K_i (CB_1R) >30 µM
Mw: 317 Da	**ClogP**: 3.76
Solubility: 3.75 µM	**Stability** MLM $T_{1/2}$: 45 min
Clean profile in GPCR counterscreen	Clean profile in 97 kinase receptor screen
Cell permeability MDR1-MDCK:	
A → B 3.21 x 10^{-6} cms^{-1}	B→ A 0.312 x 10^{-6} cms^{-1}

Table 20 Summary of the physicochemical properties of **236**

5.9 *In vivo* Studies

5.9.1 Anti-inflammatory Assay

Having found that compound **236** has a balanced set of physicochemical properties, the compound was advanced to evaluation to *in vivo* pharmacokinetic studies.[294] As outlined in the introduction, other studies have observed that the CB_2R is involved in the regulation of progression of atherosclerotic plaques. CB_2R modulation was observed to have an effect on the recruitment of leukocytes to the site of inflammation. The aim was to establish an *in vivo* anti-inflammatory model in collaboration with the Greaves lab, in which the effect of compound **236** administration had on the recruitment of monocytes could be evaluated.

An anti-inflammatory response was stimulated by the intraperitoneal (IP) administration of zymosan to the mouse. Zymosan is found on the cell wall of fungi and generates a proinflammatory response by promoting the release of cytokines from neighbouring cells. The cytokines are responsible for attracting leukocytes to the site, which will attempt to fight the pathogens. As cannabinoid receptor binding molecules are notoriously lipophilic, previous studies have reported problems with the administration of the compounds. An additive can be included in the solution to help solubilise the drug, usually either a detergent called Tween 80, or alternatively β-cyclodextrin.[295,296,297]

The IP administration method was chosen due to the lipophilic nature of the compounds which had to be dissolved in an aqueous solution with cyclodextrin to aid the solubility. The modest half-life also supported the decision to use IP to allow for rapid absorption into the blood stream. Solubility of compound **236** was not the deciding factor in using IP administration method and using β-cyclodextrin, but the insoluble nature of the control compound, JWH-133 **(210**), forced us to alter the assay conditions. With these suitable conditions the assay was established by causing a stimulating pro-inflammatory response

at t = 0, after 4 hours, the compound solution was added IP, and after 6 hours the experiment was terminated (**Figure 25**).

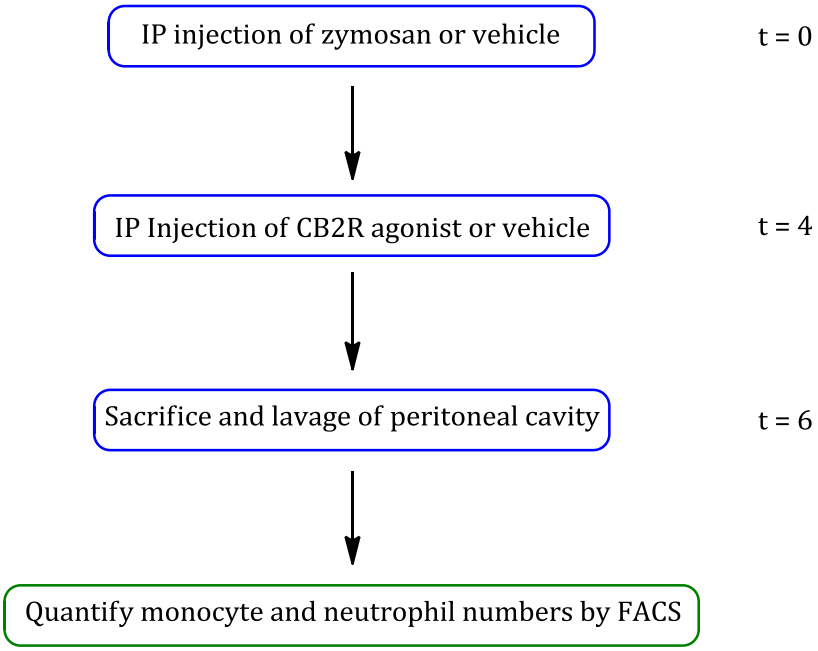

Figure 25 Procedure for the *in vivo* anti-inflammatory assay

The numbers of neutrophils and monocytes recruited to the sites were counted by Fluorescence-activated cell sorting (FACS) analysis. The first test experiment consisted of IP administration of compound **236** and analysis of the effect the CB_2R agonist had on the recruitment of neutrophils and monocytes. It was observed that administration of compound **236** reduced the number of monocytes to the site of inflammation (**Figure 26**).

The results indicate that by injection of **236** the number of monocytes recruited to the peritoneal cavity is affected. The positive control gives us a cell count of 1.5 $x10^6$, upon addition of as little of **236** as 0.01 mg/kg, a reduction of monocytes is already visible, yet a statistically non significant amount. When the dose was further increased to 1 mg/kg, the maximum suppression of monocyte recruitment is reached, with a count of 0.65 $x10^6$ cells. This indicates that the addition of the CB_2R agonist decreases the number of monocytes counted in the peritoneal cavity by over 50%. This result supports the hypothesis that the

discovered CB_2R agonist **236** can regulate the migration of monocytes to the site of inflammation.

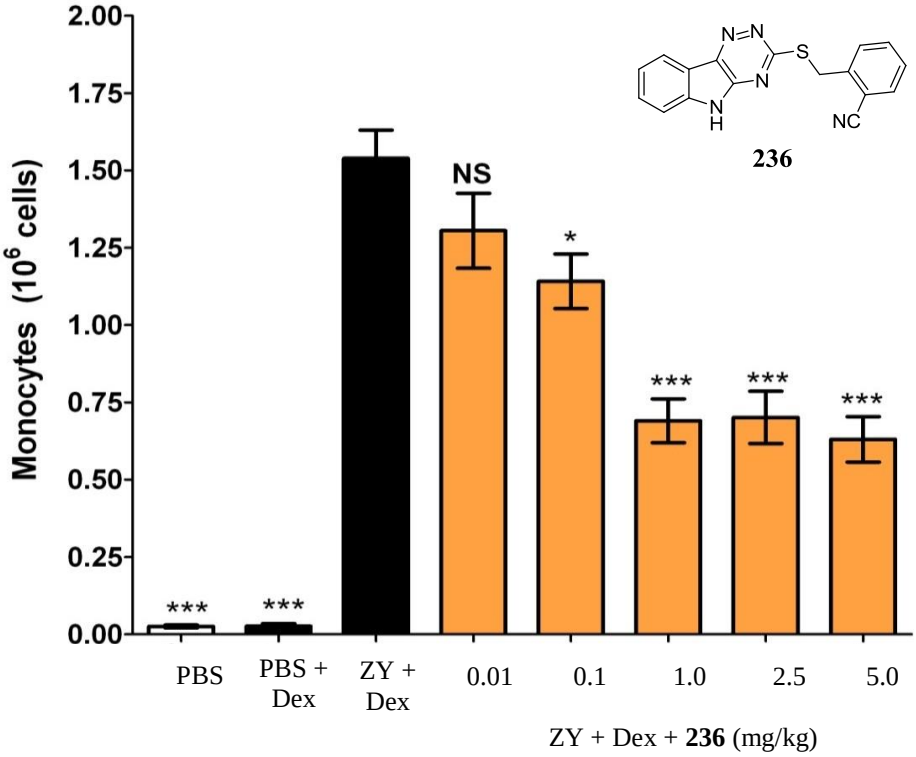

Figure 26 *In vivo* dose response curve of varying concentrations of **236** in reducing the number of monocytes recruited to site of inflammation
PBS = Phosphate Buffered Saline
Dex = cyclodextrin
ZY = zymosan
* $P \leq 0.05$
*** $P \leq 0.001$ (statistically significant difference)

In addition to confirming that CB_2R activation has an effect on the recruitment of monocytes, the next study involves the use of a compound with a subtle structural change that was inactive at the CB_2R. This would allow to directly link the reduction of monocytes counted to the activity at the CB_2R. For this experiment, compound **141** was selected which was shown to have no activity at the CB_1R or the CB_2R up to 30 µM concentrations. An additional compound was selected, namely a known CB_2R agonist molecule **210** with a K_i of 3.4 nM. Predicted outcomes for this study would show no effect on monocyte

recruitment by administration of **141**, but a significant reduction with **210** and **236**. **Figure 27** demonstrates the actual results obtained from this study.

The results displayed present some interesting and slightly unexpected results. It is surprising to see no reduction in monocyte count with the administration of a known CB_2R binding molecule, **210**. **210** is shown to bind to the CB_2R with strong affinity, the explanation for the observed lack of reduced monocyte count could be due to a previously outlined phenomena, namely functional selectivity. Even though the ligand binds to the CB_2R, the downstream effect is different from that of **236**, leading to activation of possibly an alternative pathway and ultimately transcriptional regulation. The observed activity of **236** was initially thought to be due to *in vivo* activity through another receptor, however the selectivity screens carried out on a range of GPCRs and kinases prove that no significant off target effect is involved. As previously outlined, the compound provided a very clean GPCR profile as well as a very good kinase profile, with no significant activation of any unwanted receptors. This confirms that activation of the CB_2R is responsible for the observed reduction of monocyte count in the *in vivo* anti-inflammatory assay, where receptor activation with **236** causing to an intracellular response leading ultimately to a reduced recruitment of monocytes.

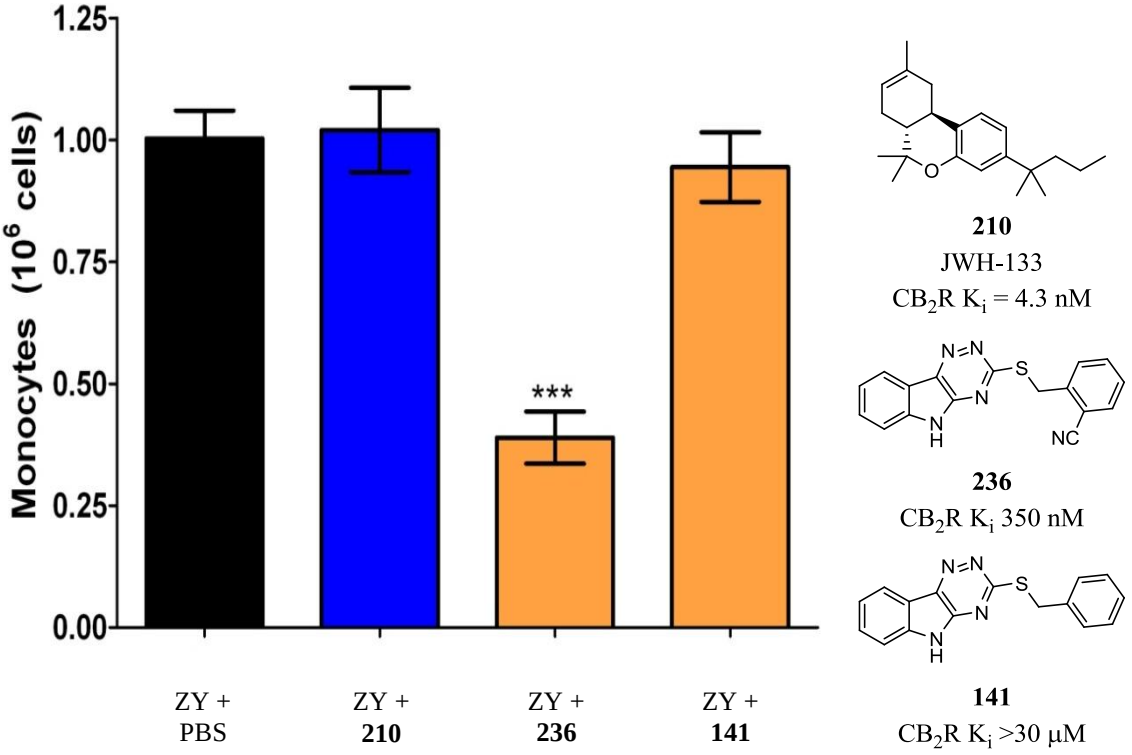

Figure 27 IP administration of a known CB_2R agonist, JWH-133 (**210**), CB_2R agonist (**236**) and **141** which was shown to be inactive to 30 μM at the CB_2R administered at 1 mg/kg
PBS = Phosphate Buffered Saline
Dex = cyclodextrin
ZY = zymosan

5.10 Conclusion and Future Work

This research has outlined the identification, optimisation and *in vivo* efficacy of a novel CB_2R agonist as an inflammatory agent. A novel CB_2R activating molecule has been discovered with the use of ligand based computational approach using a known CB_2R agonist HU-308 (**226**) as a template. SAR was developed around the tricyclic core identifying EWG at the *ortho* position of the mercaptobenzyl group gave the best activity at the CB_2R. Additionally, by functionalisation of the C(9) position it was observed that smaller groups are better tolerated than the larger flat phenyl group. However substitution of the C(9) position also introduced a small degree of activity at the CB_1R. Most interestingly, varying the substituents at the *N*(5) position allowed modification of selectivity between the two CBRs. Potency varied from equipotent nanomolar activity at the CB_1R and CB_2R with benzylic substituent **308**, to loss of up to 30 μM of potency at the

CB_1R with retention of high degrees of activity at the CB_2R by the introduction of a carbonyl group.

An issue with known cannabinoid receptor binding molecules is the lipophilicity, HU-308 (**226**) displayed a high value for the calculated LogP and of very insoluble nature. After SAR development, more polar groups were introduced at the carbonyl on the *N*(5) position reducing ClogP values and increasing solubility of compounds. With successful modification of one physicochemical property, attempts to improve stability were made, but did not yield fruitful results. Any functionalisation at the *N*(5) position was metabolised, to a compound of Mw 317 correlating to the parent compound **236**, within minutes. Altering the steric and electronic parameters did not improve the half life of the compounds.

Possible modifications could include addition of small electron withdrawing fluorines around the C(6) – C(9) position in an attempt to influence electronic density and stability of the C-N bond. From the literature, CB_2R agonist WIN-55212 (**216**) could provide inspiration to the next generation of compounds. **216** contains a fused morpholine ring attached at the *N*(1) and C(7) positions of the indole. Zhang *et al.* used tandem HPLC-mass spectrometry to study the metabolites of **216** by fragmentation patterns and compound isolation after incubating with rat liver microsomes.[298] In the study, no *N*-dealkylation was observed nor ring opening of removal of the morpholinyl side chain, indicating that the tricycle possesses a favourable degree of stability. By incorporating an additional ring system off the *N*(5) position joined to the C(6) position in ring A, possible metabolic liabilities of the compound could be circumvented.

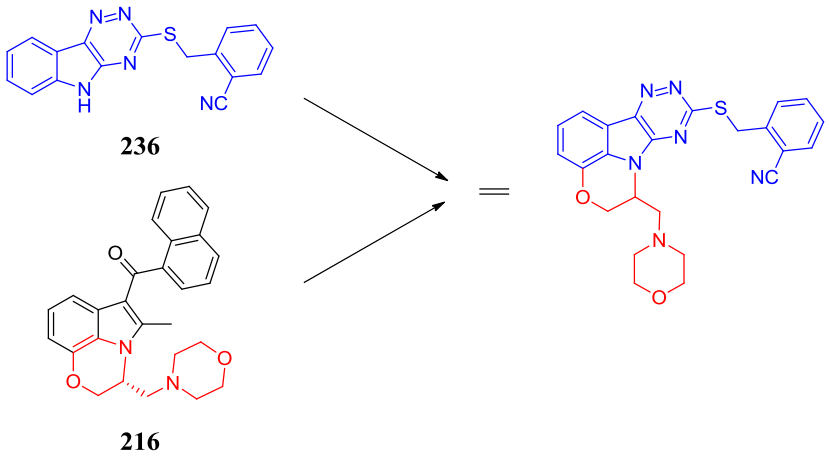

Figure 28 Fusing elements of **236** and **216** would provide potential metabolically stable compound.

Attempts in truncating the tricycle in reducing lipophilicity did not yield active compound, only with a bi-phenyl substituted compound did we retain any activity, however with introduction of a high degree of ClogP. More efforts could be committed to synthesising truncated derivatives with the removal of the flat lipophilic tricyclic core. Additionally, replacing the existing heteroatoms in the 1,2,4-triazino ring would provide further information on their importance in binding to the target and possibility of reducing lipophilicity, by the removal of the flat heteroatom containing tricycle. Similarly, replacement of the sulphide, with an amine or ether for example, would reduce ClogP values, possibly improve metabolic stability and shed further light on SAR around **236**.

Finally, an *in vivo* anti-inflammatory model was established to examine the effect of our newly discovered CB_2R agonist **236** on monocyte recruitment. Administration of our compound (**236**) with the most favourable physicochemical profile provided a promising result. Monocyte recruitment was observed to be reduced in mice where **236** was administered to in contrast to the control and mice that were treated with a CB_2R inactive molecule **141**. The observation of lack of efficacy by **210**, could potentially be explained by the functional selectivity of the compounds caused by a different downstream effect after binding to the receptor. This hypothesis is supported by the fact that both **141** and **236**

display agonist activity at the CB_2R of 136 nM and 112 nM respectively. In addition the GPCR and kinase screen demonstrated lack of activity at all receptors excluding the CB_2R. Further studies to confirm **236** truly exhibits anti-inflammatory activity *via* the CB_2R *in vivo* could be carried out by co-administering **236** with a known CB_2R antagonist, for example SR144528, to suppress the anti-inflammatory signal or alternatively by breeding $CB_2R^{-/-}$ mice and administering **236** post inflammatory response stimulation. If monocyte recruitment is not reduced, it can be concluded that **236** selectively acts *via* the CB_2R to reduce inflammation and provides a positive proof of principle that in a mouse model, selective CB_2R activation, reduces the monocyte recruitment and possible atherosclerotic development. Follow up *in vivo* studies could investigate the direct effect of the CB_2R agonist on the development of the atherosclerotic plaque directly in an appropriate *in vivo* model.

Having successfully discovered a novel CB_2R binding molecule, with favourable physicochemical properties and desirable *in vivo* efficacy, the method of ligand based drug discovery could be re-utilised using **236** to develop a new library of compounds, which could be tested in the cAMP assay at 2 concentrations, and subsequently for CB_2R affinity, selectivity and physicochemical properties. Alternatively a library could be generated using developed homology models and for their selectivity for the CB_2R over the CB_1R.

Establishing a greater library of CB_2R agonists would allow further investigations into the aspect of functional selectivity. JWH-133 (**210**) did not provide anti-inflammatory response *in vivo* whereas **236** did. This indicated a possible discrepancy of pathway activation downstream from the receptor. Both have been proven to bind to the CB_2R, but display different efficacy. Generating a more diverse library of selective CB_2R agonists, studies could be carried out to investigate whether only **236** provides the desired *in vivo*

effect, or whether other compounds behave similarly. Alternatively, **210** could be submitted for selectivity profiling against a range of GPCRs and kinases.

Supporting the observed anti-inflammatory activity of **236** in the murine system to be *via* CB_2R activation is the selectivity profile against a library of GPCRs and kinases. It was believed that other GPCRs or kinases could possibly be involved in the reduction of monocyte recruitment, but these do not appear to be activated by our molecule.

Part III: Experimental Section

Chapter 6: Experimental Section

6.1 General Experimental

All reactions involving organometallic or moisture-sensitive reagents were carried out under an argon atmosphere using standard vacuum line techniques and glassware that was flame dried and cooled under argon before use. Solvents were dried according to the procedure outlined by Grubbs and co-workers. H_2O was purified by an Elix® UV-10 system. All other solvents and reagents were used as supplied (analytical or HPLC grade) without prior purification. Organic layers were dried over anhydrous Mg_2SO_4. Pet ether refers to the fraction of petroleum spirit boiling between 30 and 40 °C. Microwave reactions were performed on a Biotage Initiator Microwave Synthesizer. Melting points, in °C, were recorded either on a Gallenkamp Hot Stage apparatus or an EZ-Melt Automated Melting Point Apparatus (denoted as §) and are uncorrected. IR spectra were recorded on a Bruker Tensor 27 FT−IR spectrometer with a diamond ATR module. Selected characteristic peaks are reported in cm^{-1}. Low-resolution mass spectra were recorded on either a VG MassLab 20-250 or a Micromass Platform 1 spectrometer. Accurate mass measurements were run on either a Bruker MicroTOF internally calibrated with polyalanine, or a Micromass GCT instrument fitted with a Scientific Glass Instruments BPX5 column (15 m × 0.25 mm) using amyl acetate as a lock mass, by the mass spectrometry service of the Chemistry Research Laboratory, University of Oxford, UK. HPLC analysis was carried out on a WatersXterra reverse phase C_{18} with gradients of H_2O (0.1 % TFA) and acetonitrile (0.1 % TFA) (See table **1** and **2**)

6.1.1 Chromatography

Flash column chromatography was carried out using Kieselgel 60 silica on a glass column, alternatively using the Biotage SP4 flash column chromatography platform. Thin layer chromatography was performed on aluminium plates coated with 60 F254 silica. Plates were visualised using UV light (254 nm) or 1% aq $KMnO_4$.

6.1.2 Spectroscopy

1H and 13C NMR spectra were recorded using a Bruker 500, 400, 300 or 250 MHz spectrometer running ACD Labs™ software and are quoted in ppm for measurement against a tetramethylsilane (TMS) or residual solvent peaks as internal standards. The field was locked by external referencing to the relevant deuteron resonance. Chemical shifts (δ) are reported in parts per million (ppm) and coupling constants (*J*) are reported in Hertz (Hz) and are unaveraged. The ^{1}H NMR spectra are reported as follows: δ / ppm (number of protons, multiplicity, coupling constant *J* / Hz (where appropriate), assignment). Multiplicity is abbreviated as follows: s = singlet, br = broad, d = doublet, dd = doublet of doublets, t = triplet, dt = doublet of triplet, q = quartet, dq = doublet of quartet, quint. = quintet, sept. = septet, m = multiplet, v = very. Compound names are those generated by ChemBioDraw™ (CambridgeSoft) following IUPAC nomenclature. However, the NMR assignment numbering used is arbitrary and does not follow any particular convention. The ^{13}C NMR spectra are reported as follows: δ / ppm (number of carbons, multiplicity, coupling constant *J* / Hz (where appropriate), assignment). Two-dimensional (COSY, HSQC, HMBC) NMR spectroscopy was used to assist the assignment of signals in the ^{1}H and ^{13}C NMR spectra.

Synthetic Procedures

6.1.3 Numbering system for Compounds in Chapter 3

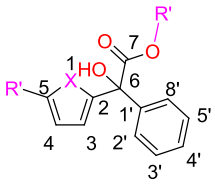

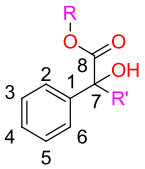

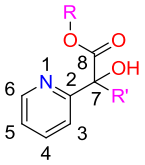

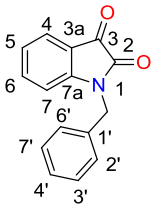

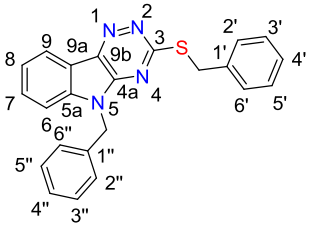

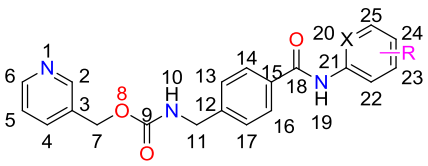

6.1.4 Numbering system for Compounds in Chapter 5

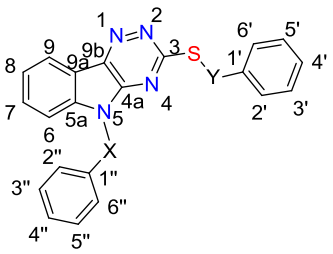

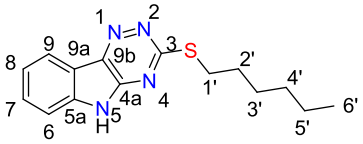

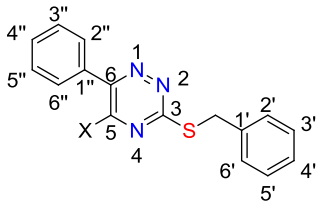

6.1.5 General Procedures

General Procedure 1

Base Hydrolysis

1M aq NaOH (1 equiv) was added to a solution of the corresponding ethyl ester (1 equiv) in MeOH (5 mL) and stirred at rt for 16 h. The resulting solution was then concentrated *in vacuo* and the resulting solid was azeotropically dried with MePh (2 x 2 mL) to yield the sodium carboxylate salt which did not require further purification.

General Procedure 2

Grignard Reaction

The corresponding ethyl ester (1 equiv) was dissolved in Et_2O (5 mL) and cooled to -78 °C. To the cooled solution was added a solution of Grignard reagent (1 equiv) in Et_2O (10 mL). The reaction mixture was allowed to warm to rt over 30 min and stirred for 1 h. The resulting solution was quenched with sat aq NH_4Cl (40 mL) and extracted with Et_2O (2 x 30 mL). The organic fractions were combined and washed with brine (40 mL), dried over $MgSO_4$, filtered and concentrated *in vacuo* to yield the crude product as a clear liquid. Purification *via* flash column chromatography on silica gel afforded the title compound.

General Procedure 3

Thiol Benzylation

To a suspension of 5*H*-[1,2,4]triazino[5,6-*b*]indole-3-thiol (1 equiv) in MeOH (5 mL) was added Et_3N (1.5 equiv). To the resulting suspension was added the requisite electrophile (1 equiv) and the reaction mixture stirred at rt for 16 h. The resulting precipitate was filtered and washed with a solution of Et_3N in H_2O (1:25, 5% Et_3N), which was dried *in vacuo* to yield the *S*-substituted product which, if purified further is specified in each example below.

General Procedure 4

Amine Functionalisation

A flask was flame dried and cooled under an atmosphere of argon. To the flask was added the *S*-substituted-5*H*-[1,2,4]triazino[5,6-*b*]indole-3-thiol (1 equiv) and anhydrous DMF or THF (5 mL) under argon. The resulting suspension was cooled to 0 °C using an ice bath. NaH (60 % in mineral oil, 1.1 - 1.5 equiv) was added, resulting in a clear yellow solution, which was stirred for 15 mins at 0 °C. The corresponding electrophile (1.5 equiv) was added gradually (dropwise or portionwise) at 0 °C. After addition was complete, the reaction mixture was allowed to warm to rt and stirred for 16 h under argon. The reaction was quenched with H_2O and the product extracted as specified below.

6.1.6 HPLC Methods

Method 1

Time	Device	Command
0.00	H_2O (0.1% TFA) / MeCN	1 (mL/min): 95% H_2O (0.1% TFA), 5% MeCN
0.02	Detector	Balance Detector
0.04	partial loop fill for 215 as FC	<start> inject volume (30 uL)
0.06	System Controller	SyNCHronize
0.10	Data Channels	Start DAD Channels
1.20	System Controller	SyNCHronize
10.00	H_2O (0.1% TFA) / MeCN	1 (mL/min): 5% H_2O (0.1% TFA), 95% MeCN
15.00	H_2O (0.1% TFA) / MeCN	1 (mL/min): 5% H_2O (0.1% TFA), 95% MeCN
18.00	H_2O (0.1% TFA) / MeCN	1 (ml/min): 95% H_2O (0.1% TFA), 5% MeCN
20.00	Data Channels	Stop DAD Channels
20.05	Data Channels	Stop Chromatogram Channels
23.10	H_2O (0.1% TFA) / MeCN	1 (mL/min): 95% H_2O (0.1% TFA), 5% MeCN

Table 1 High performance liquid chromatography (HPLC) method 1

Method 2

Time	Device	Command
0.00	H_2O (0.1% TFA) / MeCN	1 (mL/min): 95% H_2O (0.1% TFA), 5% MeCN
0.02	Detector	Balance Detector
0.04	partial loop fill for 215 as FC	<start> inject volume (30 µL)
0.06	System Controller	SyNCHronize
0.10	Data Channels	Start DAD Channels
1.20	System Controller	SyNCHronize
10.00	H_2O (0.1% TFA) / MeCN	1 (mL/min): 5% H_2O (0.1% TFA), 95% MeCN
15.00	H_2O (0.1% TFA) / MeCN	1 (mL/min): 5% H_2O (0.1% TFA), 95% MeCN
23.00	H_2O (0.1% TFA) / MeCN	1 (mL/min): 95% H_2O (0.1% TFA), 5% MeCN
25.00	Data Channels	Stop DAD Channels
25.05	Data Channels	Stop Chromatogram Channels
28.10	H_2O (0.1% TFA) / MeCN	1 (mL/min): 95% H_2O (0.1% TFA), 5% MeCN

Table 2 High performance liquid chromatography (HPLC) method 2

6.2 Compound Characterisation

Ethyl 3,3,3-trifluoro-2-hydroxy-2-(methylfuran-2-yl)propanoate 40[128]

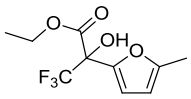

Ethyl 3,3,3-trifluoro pyruvate (1.27 mL, 1.02 mmol) was added dropwise to neat ice-cold 2-methyl furan **39** (1.00 mL, 1.02 mmol) and the resulting solution was stirred at rt for 1 h. The crude liquid was purified *via* flash column chromatography on silica gel (eluent petrol:EtOAc 10%) to yield **40** as a faint yellow liquid (1.82 g, 68 %); δ_H (400 MHz, $CDCl_3$, 363 K) 1.32 (3 H, t, *J* = 7.0 Hz, $CH_2C\underline{H}_3$), 2.39 (3 H, s, CH_3), 4.32 (1 H, s, OH), 4.42 (2 H, q, *J* = 7.0 Hz, CH_2), 5.98 (1 H, d, *J* = 3.5 Hz, C(3)H), 6.59 (1 H, d, *J* = 3.5 Hz, C(4)H); δ_C (100 MHz, $CDCl_3$) 13.5 (CH_2-$\underline{C}H_3$), 13.8 (CH_3), 64.5 ($\underline{C}H_2CH_3$), 75.3 (q, *J* = 40 Hz, C6), 106.7 (C4), 111.4 (C3), 122.5 (q, *J* = 286 Hz, CF_3), 143.9 (C2), 153.9 (C5), 167.4 (C7); δ_F (376 MHz, $CDCl_3$) -76.23 (CF_3); *m/z* (ESI^+) 275 ($[M+Na]^+$, 100%)

Sodium 3,3,3-trifluoro-2-hydroxy-2-(5-methyl furan-2-yl) propanoate 41

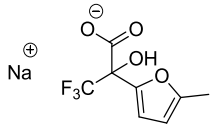

Following **General Procedure 1:** 1M aq NaOH (650 µL, 0.65 mmol) was added to a solution of ethyl 3,3,3-trifluoro-2-hydroxy-2-(methylfuran-2-yl)propanoate **40** (164 mg, 0.65 mmol) in MeOH (5 mL) and stirred at rt for 16 h. The solution was concentrated *in vacuo* to yield **41** as a white solid (143 mg, 98 %); δ_H (400 MHz, DMSO-d_6, 363 K) 2.22 (3 H, s, CH_3), 5.96 - 5.99 (1 H, m, C(4)H), 6.13 (1 H, br s, OH), 6.24 - 6.26 (1 H, m, C(3)H); δ_C (100 MHz, DMSO-d_6) 13.3 (CH_3), 73.3 (q, *J* = 27.7 Hz, C6), 106 (C4), 108.9 (C3), 124.5 (q, *J* = 284.2 Hz, CF_3), 149.5 (C2), 150.8 (C5), 165.1 (C7); δ_F (376 MHz, $CDCl_3$) -73.9 (CF_3); mp hydroscopic solid; *m/z* (ESI^+) 247 ($[M-H]^-$, 100%); HRMS (ESI^+)

$C_9H_7F_3O_4^-$ ([M-H]$^-$) requires 223.0224; found 223.0222; ν_{max} (solid) 3387 (OH), 2639 (OH acid), 1638 (C(O)), 1178 (CF_3)

Diethyl 2-(5-methyl furan-2-yl)-2-(trifluoro methyl) malonate 44[299]

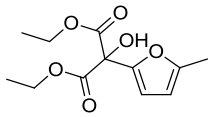

Diethyl-2-oxomalonate (1.04 mL, 0.55 mmol) was added to neat 2-methyl furan **39** (500 µL, 0.55 mmol) at 0 °C. The reaction mixture was allowed to warm to rt and stirred for 1.5 h. The crude reaction mixture was purified *via* flash column chromatography on silica gel (eluent petrol:EtOAc 20%) to yield **44** as a clear liquid (1.02 g, 71 %); δ_H (400 MHz, $CDCl_3$, 363 K) 1.31 (6 H, t, *J* = 7.2 Hz, $CH_2C\underline{H}_3$), 2.29 (3 H, s, CH_3), 4.34 (4 H, q, *J* = 7.2 Hz, CH_2), 5.29 (1 H, s, OH), 5.95 - 5.98 (1 H, m, C(3)H), 6.46 - 6.49 (1 H, m, C(4)H); δ_C (100 MHz, $CDCl_3$) 13.6 (CH_3), 13.9 (CH_2-$\underline{C}H_3$), 53.4 (CH_2), 76.5 (C6), 106.4 (C3), 110,8 (C4), 146.8 (C5), 153.2 (C2), 168.1 (2C, 2xC7); *m/z* (ESI$^+$) 279 ([M-H]$^-$, 100%)

Ethyl 2-hydroxy-2-(5-methyl furan-2-yl) propanoate 45

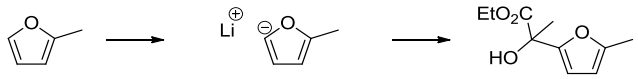

^{n}BuLi (2.5 M in hexanes, 887 µL, 0.26 mmol) was added dropwise to the cooled solution at -78 °C of 2-methyl furan **39** (200 µL, 0.23 mmol) dissolved in THF (10 mL). The reaction mixture was allowed to warm to rt and ethyl-2-oxopropanoate (251 uL, 0.23 mmol) was added and the mixture was stirred for 1 h at rt. The solution was concentrated *in vacuo* to give a complex mixture of products.

Ethyl 3,3,3-trifluoro-2-hydroxy-2-(methyl thiophene-2-yl) propanoate 47[128]

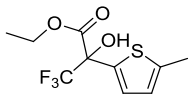

$SnCl_4$ (100 mg, 0.52 mmol) was added to an ice-cold solution of 2-ethyl thiophene **46** (1.00 mL, 1.02 mmol) in CH_2Cl_2 (5 mL) followed by drop wise addition of ethyl 3,3,3-trifluoro pyruvate (1.20 mL, 1.02 mmol). The resulting mixture was stirred at rt for 1 h, diluted with CH_2Cl_2 (40 mL) and washed with water (40 mL). The organic layer was separated and washed with brine (40 mL), dried over $MgSO_4$, filtered and concentrated *in vacuo*. The crude oil was purified *via* flash column chromatography on silica gel (eluent petrol:EtOAc 10%) to afford **47** as a pale yellow liquid (2.10 g, 78 %); δ_H (400 MHz, $CDCl_3$, 363 K) 1.40 (3 H, t, *J* = 7.1 Hz, $CH_2C\underline{H}_3$), 2.48 (3 H, s, CH_3), 4.40 - 4.46 (2 H, q, *J* = 7.1 Hz, $C\underline{H}_2CH_3$), 4.52 (1 H, s, OH), 6.68 (1 H, d, *J* = 3.4 Hz, C(3)H), 7.18 (1H, d, *J* = 3.4 Hz, C(4)H); δ_C (100 MHz, $CDCl_3$) 13.8 (CH_2-$\underline{C}H_3$), 15.1 (CH_3), 64.6 (CH_2), 76.6 (d, *J* = 40 Hz, C6), 122.4 (q, *J* = 285 Hz, CF_3), 125.5 (C3), 127.5 (C4), 132.9 (C5), 141.9 (C2), 168.2 (C7); δ_F (376 MHz, $CDCl_3$) -78.0 (CF_3); *m/z* (ESI^+) 291 ($[M+Na]^+$, 100%)

Sodium 3,3,3-trifluoro-2-hydroxy-2-(5-methyl thiophene-2-yl) propanoate 48

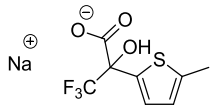

Following **General Procedure 1:** 1M aq NaOH (610 µL, 0.61 mmol) was added to a solution of ethyl 3,3,3-trifluoro-2-hydroxy-2-(methyl thiophene-2-yl) propanoate **47** (163 mg, 0.16 mmol) in MeOH (5 mL) and stirred at rt for 16 h. The solution was concentrated *in vacuo* to produce **48** as a white solid (131 mg, 96 %); δ_H (400 MHz, DMSO-d_6, 363 K) 2.37 (3 H, s, CH_3), 6.36 (1 H, br s, OH), 6.60 - 6.64 (1H, m, C(4)H), 7.02 (1H, d, *J* = 3.5 Hz, C(3)H); δ_C (100 MHz, DMSO-d_6) 14.8 (CH_3), 75.1 (q, *J* = 27.8 Hz, C6), 124.5 (C4),

125.6 (q, J = 285 Hz, CF_3), 124.7 (C3), 138.4 (C2), 138.9 (C5), 166.3 (C7); δ_F (376 MHz, $CDCl_3$) -75.73 (CF_3); mp hydroscopic solid; *m/z* (ESI^+) 239 ($[M-H]^-$, 100%); HRMS (ESI^-) $C_9H_7F_3O_3S^-$ ($[M-H]^-$) requires 238.9995; found 239.0004; ν_{max} (solid) 3392 (OH), 2925 (acid OH), 1633 (C=O), 1150 (CF_3)

Ethyl 3,3,3-trifluoro-2-hydroxy-2-(1*H*-pyrrol-2-yl) propanoate 51[129]

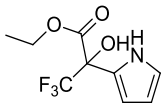

Ethyl 3,3,3-trifluoro pyruvate (0.76 mL, 5.77 mmol) was added to neat pyrrole **49** (400 µL, 5.77 mmol) at rt and stirred for 2 h. The crude reaction mixture was purified *via* flash column chromatography on silica gel (eluent petrol:EtOAc 10%) to yield **51** as a clear liquid (1.2 g, 89 %); δ_H (400 MHz, $CDCl_3$, 363 K) 1.41 (3 H, t, J = 7.1 Hz, CH_3), 4.35 - 4.50 (2 H, m, CH_2), 6.23 - 6.27 (1 H, m, C(3)H), 6.47 - 6.49 (1 H, m, C(4)H), 6.83 - 6.86 (1 H, m, C(5)H), 8.50 (1 H, br s, NH); δ_C (100 MHz, $CDCl_3$) 13.9 (CH_3), 64.6 (CH_2), 75.0 (q, J = 32 Hz, C6), 108.9 (C3), 109.4 (C4), 118.8 (C5), 122.8 (q, J = 227 Hz, CF_3), 123.9 (C2), 168.4 (C7); δ_F (376 MHz, $CDCl_3$) -78.4 (CF_3); *m/z* (ESI^+) 260 ($[M-H]^-$, 100%)

Ethyl 3,3,3-trifluoro-2-hydroxy-2-(*N*-methy pyrrol-2-yl) propanoate 52[129]

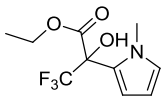

Ethyl 3,3,3-trifluoro pyruvate (0.76 mL, 5.77 mmol) was added to neat *N*-methylpyrrole **50** (400 µL, 5.77 mmol) at rt and stirred for 2 h. The crude reaction mixture was purified *via* flash column chromatography on silica gel (eluent petrol:EtOAc 10%) to yield **52** as a clear liquid (1.03 g, 92 %); δ_H (400 MHz, $CDCl_3$, 363 K) 1.37 (3 H, t, J = 7.2 Hz, $CH_2C\underline{H}_3$), 3.67 (3 H, s, NCH_3), 4.35 (1H, br s, OH), 4.36 - 4.52 (2 H, m, CH_2), 6.08 - 6.11

(1 H, m, C(3)H), 6.40 - 6.43 (1 H, m, C(4)H), 6.63 - 6.65 (1 H, m, C(5)H); δ_C (100 MHz, $CDCl_3$) 13.9 (CH_3), 35.8 (NCH_3), 64.6 (OCH_2), 76.3 (q, *J* = 33.2 Hz, C6), 106.9 (C3), 111.3 (C4), 122.2 (C5), 122.8 (q, *J* = 287.4 Hz, CF_3), 126.1 (C2), 168.9 (C7); δ_F (376 MHz, $CDCl_3$) -75.5 (CF_3); *m/*z (ESI^+) 250 ($[M-H]^-$, 100%)

Sodium 3,3,3-trifluoro-2-hydroxy-2-(1*H* pyrrole-2-yl) propanoate 53

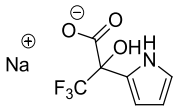

Following **General Procedure 1:** 1M aq NaOH (510 µL, 0.51 mmol) was added to a solution of ethyl 3,3,3-trifluoro-2-hydroxy-2-(1*H*-pyrrol-2-yl) propanoate **51** (120 mg, 0.51 mmol) in MeOH (5 mL). The solution was concentrated in vacuo isolated **53** as a white solid (103 mg, 97 %); δ_H (400 MHz, DMSO-*d*$_6$, 363 K) 5.89 - 5.93 (1 H, m, C(4)H), 5.95 (1H, br s, OH), 6.09 - 6.12 (1 H, m, C(3)H), 6.59 - 6.63 (1 H, m, C(5)H), 10.37 (1H, br s, NH); δ_C (100 MHz, (DMSO-*d*$_6$) 73.5 (q, *J* = 27.7 Hz, C6), 106.4 (C3), 106.8 (C4), 117.1 (C5), 124.7 (q, *J* = 285 Hz, CF_3), 137.1 (C2), 175.4 (C7); δ_F (376 MHz, $CDCl_3$) -75.8 (CF_3); mp hydroscopic solid; *m/z* (ESI^+) 208 ($[M-H]^-$, 100%); HRMS (ESI^+) $C_9H_8F_3NO_3^-$ ($[M-H]^-$) requires 208.0227; found 208.0229; ν_{max} (solid) 3407 (NH), 1632 (C=O), 1161 (CF_3)

Sodium 3,3,3-trifluoro-2-hydroxy-2-(*N*-methyl pyrrole-2-yl) propanoate 54

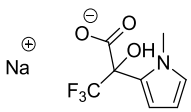

Following **General Procedure 1:** 1M aq NaOH (610 µL, 0.61 mmol) was added to a solution of ethyl 3,3,3-trifluoro-2-hydroxy-2-(*N*-methylpyrrol-2-yl) propanoate **52** (154 mg, 0.61 mmol) in MeOH (5 mL). The solution was concentrated *in vacuo* to yield **54** as a

white solid (120 mg, 88 %); δ_H (400 MHz, DMSO-d_6, 363 K) 3.36 (3 H, s, NCH_3), 5.81 - 5.84 (1 H, m, C(4)H), 6.13 - 6.16 (1H, m, C(3)H), 6.29 (1H, br s, OH), 6.57 - 6.60 (1H, m, C(5)H); δ_C (100 MHz, DMSO-d_6) 34.9 (CH_3), 74.6 (q, J = 26.7 Hz, C6), 105.3 (C4), 109.2 (C3), 123.5 (C5), 125.2 (q, J = 285 Hz, CF_3) 127.8 (C2), 166.8 (C7); δ_F (376 MHz, DMSO-d_6) -75.9 (CF_3); mp hydroscopic solid; *m/z* (ESI^+) 222 ($[M-H]^-$, 100 %); HRMS (ESI^+) $C_{10}H_{10}F_3NO_3^-$ ($[M-H]^-$) requires 222.0384; found 222.0393; ν_{max} (solid) 3419 (OH), 1642 (C=O), 1303 (N-C), 1159 (CF_3)

Ethyl 3,3,3-trifluoro-2-hydroxy-2-phenyl propanoate 57[300]

6.3 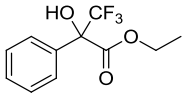

Following **General Procedure 2: A** solution of PhMgBr (3 M in Et_2O, 1.50 mL, 4.53 mmol) in Et_2O (10 mL) was added to a solution of ethyl 3,3,3-trifluoropyruvate (600 µL, 4.53 mmol) in Et_2O (5 mL) -78 °C. After aqueous work up and purification of the crude product *via* flash column chromatography on silica gel (eluent petrol:EtOAc 20%) **57** was isolated as a colourless liquid (820 mg, 73 %); δ_H (400 MHz, $CDCl_3$, 363 K) 1.38 (3 H, t, J = 7.1 Hz, $CH_2C\underline{H}_3$), 4.32 (1 H, s, OH), 4.43 (2 H, q, J = 4.7 Hz, CH_2), 7.36 - 7.47 (3 H, m, C(2)H, C(4)H and C(6)H), 7.78 - 7.83 (2 H, m, C(3)H and C(5)H); δ_C (100 MHz, $CDCl_3$) 13.9 (CH_3), 54.5 (q, J = 33.0 Hz, C7), 64.4 (CH_2), 121.6 (C4), 123.6 (q, J = 280 Hz, CF_3) 126.7 (2C, C2 and C6), 128.4 (2C, C3 and C5), 129.5 (C1), 166.1 (C8); δ_F (376 MHz, $CDCl_3$) -76.3 (CF_3); *m/z* (ESI^+) 271 ($[M+Na]^+$, 100%)

Ethyl 2-hydroxy-2-phenyl propanoate 58[301]

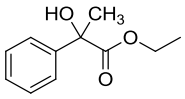

Following **General Procedure 2:** A solution of PhMgBr (3 M in Et_2O, 630 µL, 1.89 mmol) in Et_2O (10 mL) was added to a solution of ethyl pyruvate (209 µL, 1.89 mmol) in Et_2O (5 mL) at -78 °C. After aqueous work up, the crude product was purified *via* flash column chromatography on silica gel (eluent petrol:EtOAc 0 to 10%), **58** was isolated as a colourless liquid (290 mg, 83 %); δ_H (400 MHz, $CDCl_3$, 363 K) 1.25 (3 H, t, *J* = 7.0 Hz, $CH_2C\underline{H}_3$), 2.21 (3 H, s, CH_3), 4.12 (1 H, br s, OH), 4.32 (2 H, m, CH_2), 7.32 - 7.37 (3 H, m, C(2)H, C(6)H and C(4)H), 7.52 - 7.62 (2H, m, C(3)H and C(5)H); δ_C (100 MHz, $CDCl_3$) 14.0 ($CH_2C\underline{H}_3$), 20.6 (CH_3), 63.0 (CH_2), 80.9 (C7), 125.1 (C4), 127.4 (2C, C3 and C5), 128.4 (2C, C2 and C6), 141.4 (C1), 174.4 (C8); *m/z* (ESI^+) 217 ($[M+Na]^+$, 100%)

Ethyl 2-hydroxy-2-phenyl-2-(thiophene-2-yl) acetate 59[302]

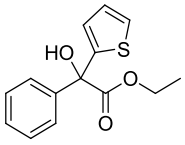

Following **General Procedure 2**, A solution of PhMgBr (3 M in Et_2O, 630 µL, 1.89 mmol) in Et_2O (10 mL) was added to a solution of ethyl thiophene-2-glyoxylate (278 µL, 1.89 mmol) in Et_2O (5 mL) at -78 °C. After aqueous work up and purification *via* flash column chromatography on silica gel (eluent petrol:EtOAc 0 to 10%) **59** was obtained as a colourless liquid (148 mg, 30 %); δ_H (400 MHz, $CDCl_3$, 363 K) 1.29 (3 H, t, *J* = 7.1 Hz, CH_3), 4.36 (2 H, q, *J* = 7.1 Hz, CH_2), 4.59 (1H, br s, OH), 7.00 - 7.03 (1 H, m, C(3)H), 7.10 - 7.13 (1 H, m, C(4)H), 7.30 - 7.39 (4 H, m, C(5)H, C(2')H, C(4')H and C(6')H), 7.50 - 7.55 (2 H, m, C(3')H and C(5')H); δ_C (100 MHz, $CDCl_3$) 14.0 ($CH_2\underline{C}H_3$), 63.3 (CH_2), 78.7 (C6), 125.8 (C3), 126.3 (C4), 126.6 (2C, C2' and C6'), 126.7 (C5), 128.2 (2C, C3'

and C5'), 128.3 (C4'), 141.6 (C2), 146.0 (C1'), 173.3 (C8); *m/z* (ESI^+) 285 ($[M+Na]^+$, 100%); HRMS (ESI^+) $C_{14}H_{14}O_3S$ ($[M+Na]^+$) requires 285.0556; found 285.0551; ν_{max} (liquid) 3484 (OH), 3064 (CH), 1722 (C(O)), 1228, 1143

Ethyl 2-hydroxy-2,2-diphenyl acetate 60[303]

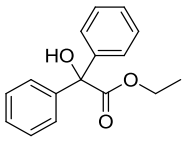

Following **General Procedure 2:** A solution of PhMgBr (3 M in Et_2O, 630 µL, 1.89 mmol) in Et_2O (10 mL) was added to a solution of ethylbenzoylformate (300 µL, 1.89 mmol) in Et_2O (5 mL) at -78 °C. After aqueous work up and purification *via* flash column chromatography on silica gel (eluent petrol:EtOAc 0% to 10%) **60** was isolated as a clear liquid (201 mg, 41 %); δ_H (400 MHz, $CDCl_3$, 363 K) 1.31 (3H, t, *J* = 7.0 Hz, $CH_2C\underline{H}_3$), 4.29 (1 H, s, OH), 4.34 (2 H, q, *J* = 7.0 Hz, CH_2), 7.30 - 7.41 (6 H, m, 6xAr-H), 7.41 - 7.49 (4 H, m, 4xAr-H); δ_C (100 MHz, $CDCl_3$) 14.0 (CH_3), 62.4 (CH_2), 80.8 (q, *J* = 29.9 Hz, C7), 127.3 (C4), 127.7 (2C, C2 and C6), 128.3 (2C, C3 and C5), 142.8 (C1), 205.9 (C8); *m/z* (ESI^+) 256.0 ($[M+Na]^+$, 100%)

Ethyl-3,3,3-trifluoror-2-hydroxy-2-(pyridin-2-yl)propanoate 62[304]

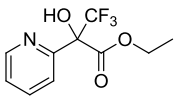

^{n}BuLi (2.5 M, 7.41 mL, 18.5 mmol) was added to a stirring solution of 2-bromopyridine (1.50 mL, 15.4 mmol) at -78 °C and further stirred at rt for 1 h. Ethyl 3,3,3-trifluoropyruvate (2.25 mL, 16.9 mmol) was dissolved in Et_2O (10 mL) and cooled to -78 °C and transferred *via* cannula to the solution of PyMgBr **61**. The resulting brown suspension was stirred at rt for 16 h. The reaction mixture was quenched with sat aq NH_4Cl

(40 mL) and extracted with EtOAc (3 x 30 mL). The combined organic extracts were dried over $MgSO_4$, filtered and concentrated *in vacuo*. The crude product was purified *via* flash column chromatography (eluent petrol:EtOAc 12%) to yield **62** as a brown oil (1.30 g, 32 %); δ_H (400 MHz, $CDCl_3$, 363 K) 1.22 (3H, t, *J* = 7.1 Hz, CH_3), 4.20 - 4.28 (2H, m, CH_2), 6.77 (1H, br s, OH), 7.36 - 7.39 (1H, m, C(5)H), 7.76 - 7.80 (2H, m, C(3)H and C(4)H), 8.53 - 8.56 (1H, m, C(6)H); δ_C (100 Hz, $CDCl_3$) 14.1 (CH_3), 60.3 (CH_2), 122.4 (C3), 123.0 (q, *J* = 286 Hz, CF_3), 125.0 (C5), 137.8 (C4), 147.6 (C6), 149.3 (C7), 167.0 (C2), 171.1 (C8); δ_F (376 MHz, $CDCl_3$) -76.4 (CF_3); *m/z* (ESI^+) 250 ($[M+H]^+$, 100%); HRMS (ESI^+) $C_{10}H_{10}F_3NNaO_3$ ($[M+Na]^+$) requires 272.0505; found 272.0494; ν_{max} (liquid) 3262 (OH), 2987 (aromatic CH), 1748 (C(O)), 1249, 1181 (CF_3)

Sodium 3,3,3-trifluoro-2-hydroxy-2-phenyl propanoate 63

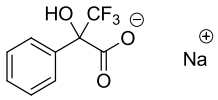

Following **General Procedure 1**, 2M aq NaOH (605 µL, 1.21 mmol) was added to a solution of ethyl 3.3.3-trifloro-2-hydroxy-2-phenyl propanoate **57** (300 mg, 1.21 mmol) in MeOH (5 mL) to yield **63** as a white hygroscopic solid, which required no further purification (250 mg, 94 %); δ_H (400 MHz, CD_3OD, 363 K) 7.30 - 7.34 (3H, m, C(1)H, C(3)H and C(5)H), 7.88 - 7.92 (2H, m, C(2)H and C(4)H); δ_C (100 MHz, CD_3OD) 78.3 (q, *J* = 32.0 Hz, C7), 123.2 (q, *J* = 289 Hz, CF_3), 126.4 (C3), 127.2 (2C, C1 and C5), 127.6 (2C, C2 and C4), 128.1 (C6), 137.1 (C7), 171.6 (C8); ^{19}F NMR (376 MHz, CD_3OD): δ_F (376 MHz, $CDCl_3$) 77.0 (CF_3); *m/z* (ESI^+) 242 ($[M+Na]^+$, 100%)

Sodium 2-hydroxy-2-phenyl propanoate 64

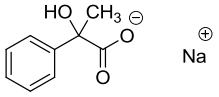

Following **General Procedure 1**, 3M aq NaOH (260 µL, 0.77 mmol) was added to a solution of ethyl 2-hydroxy-2-phenyl propanoate **58** (150 mg, 0.77 mmol) in MeOH (3 mL) to yield **64** as a white hygroscopic solid (124 mg, 97 %); δ_H (400 MHz, CD_3OD, 363 K) 1.71 (3H, s, CH_3), 7.18 - 7.21 (1H, m, C(3)H), 7.28 (2H, app t, *J* = 7.4 Hz, C(2)H and C(4)H), 7.62 (2H, app d, *J* = 7.4 Hz, C(1)H and C(5)H); δ_C (100 MHz, CD_3OD) 26.3 (CH_3), 76.7 (C7), 125.7 (2C, C1 and C5), 126.5 (C3), 127.7 (2C, C2 and C4), 146.5 (C6), 180.8 (C8); *m/z* (ESI^+) 188 ($[M+Na]^+$, 100%)

Sodium 2-hydroxy-2-phenyl-2-(thiophen-2-yl)acetate 65

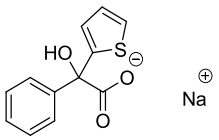

Following **General Procedure 1**, 1M aq NaOH (588 uL, 0.59 mmol) was added to a solution of ethyl 2-hydroxy-2-phenyl-2-(thiophene-2-yl) acetate **59** (154 mg, 0.59 mmol) in MeOH (5 mL) to yield **65** as a white hygroscopic solid (128 mg, 93 %); δ_H (400 MHz, DMSO-d_6, 363 K) 6.48 (1H, s, OH), 6.87 (1H, dd, *J* = 3.5, 5.0 Hz, C(4)H), 7.12 (1H, dd, *J* =1.3, 3.5 Hz, C(3)H), 7.13 (1H, app tt, *J* = 1.3, 7.6 Hz, C(4')H), 7.20 (2H, app t, *J* = 7.6 Hz, C(3')H and C(5')H), 7.22 (1H, dd, *J* = 1.3, 5.0 Hz, C(5)H), 7.60 – 7.64 (2H, m, C(2')H and C(4')H; δ_C (100 MHz, (DMSO-d_6) 77.7 (C6), 123.4 (C1'), 123.9 (C3), 125.8 (C4), 125.9 (C5), 126.2 (2C, C2' and C6'), 126.9 (2C, C3' and C5'), 146.7 (C1'), 152.2 (C2), 173.2 (C7); *m/z* (ESI^+) 233 ($[M-H]^-$, 100%); HRMS (ESI^-) $C_{12}H_9O_3S^-$ ($[M-H]^-$)

requires 233.0278; found 233.0286; ν_{max} (liquid) 3529 (OH), 3060 (aromatic CH), 1611 (CO) salt), 1378, 1278, 1156

Sodium 2-hydroxy-2,2-diphenyl acetate 66

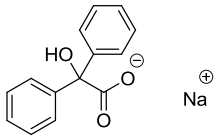

Following **General Procedure 1**, 1M aq NaOH (3 M, 197 µL, 0.77 mmol) was added to a solution of ethyl 2-hydroxy-2,2-diphenyl acetate **60** (150 mg, 0.77 mmol) in MeOH (3 mL) to yield **66** as a white hydroscopic solid (133 mg, 91 %); δ_H (400 MHz, CD_3OD, 363 K) 7.21 - 7.30 (6H, m, C(1)H, C(3)H, C(5)H, C(1')H, C(3')H and C(5')H), 7.51 (4H, app d, *J* = 7.3 Hz, C(2)H, C(4)H, C(2')H and C(4')H); δ_C (100 MHz, CD_3OD) 65.0 (C7), 126.8 (C3), 127.4 (C1 and C5), 128.0 (C2 and C4), 140.9 (C6), 178.4 (C8); *m/z* (ESI^+) 248 ($[M+Na]^+$, 100%)

Sodium 3,3,3-trifluoro-2-hydroxy-2-(pyridin-2-yl)propanoate 67

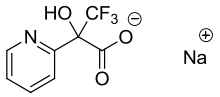

Following **General Procedure 1**, 2M aq NaOH (800 µL, 0.80 mmol) was added to a solution of ethyl-3,3,3-trifluoror-2-hydroxy-2-(pyridin-2-yl)propanoate **62** (200 mg, 0.80 mmol) in MeOH (5 mL) to yield **67** as a light brown hygroscopic solid, which required no further purification (192 mg, 98 %); δ_H (400 MHz, DMSO, 363 K) 7.39 (1H, td, *J* = 7.8, 1.5 Hz, C(5)H), 7.79 (1H, d, *J* = 7.8 Hz, C(3)H), 7.86 (1H, td, *J* = 7.8, 1.5 Hz, C(4)H), 8.59 (1H, d, *J* = 7.8 Hz, C(6)H); δ_C (100 Hz, DMSO) 122.0 (C3), 123.1 (C5), 124.2 (q, *J* = 286 Hz, CF_3) 136.9 (C4), 148.5, 157.9 (C7), 167.1 (C2), 175.3 (C8); δ_F (376 MHz, $CDCl_3$) -72.2 (CF_3); *m/z* (ESI^-) 220 ($[M-H]^-$, 40%); HRMS (ESI^+) $C_8H_6F_3NNaO_3$ ($[M+Na]^+$)

requires 244.0197; found 244.0186; ν_{max} (liquid) 3381 (OH), 1641 (Carboxylate), 1382, 1166, 1137

2-((2-(5-Benzyl-5*H*-[1,2,4]triazino[5,6-*b*]indol-3-yl)hydrazono)methyl)phenol 116

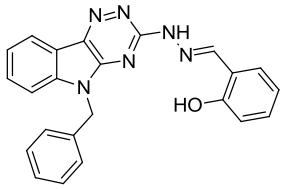

Salicylaldehyde (22.0 µL, 0.21 mmol) was added to a solution of 5-benzyl-3-hydrazinyl-5*H*-[1,2,4]triazino[5,6-*b*]indole **143** (60 mg, 0.21 mmol) in MeOH (7 mL) and stirred at rt for 16 h. The precipitate was filtered, washed with MeOH (2 x 10 mL) and dried *in vacuo* to yield **116** as a bright yellow solid (81 mg, 99 %); δ_H (400 MHz, DMSO-d_6, 363 K) 5.57 (2H, s, NCH_2), 6.92 (1H, app t, *J* = 7.8 Hz, C(5')H), 6.94 (1H, d, *J* = 7.8 Hz, C(3')H), 7.25 - 7.34 (4H, m, C(7)H, C(8)H, C(3'')H and C(5'')H), 7.42 - 7.44 (3H, m, C(2'')H, C(4'')H and C(6'')H), 7.46 (1H, d, *J* = 7.8 Hz, C(6)H), 7.60 (1H, app t, *J* = 7.8 Hz, C(4')H), 7.67 (1H, d, *J* = 7.8 Hz, C(6')H), 8.25 (1H, d, *J* = 7.3 Hz, C(9)H), 8.42 (1H, s, CH), 11.76 (1H, br s, NH), 12.19 (1H, br s, OH); δ_C (125 MHz, DMSO-d_6) 43.9 (CH_2), 111.2 (C6), 116.4 (C3'), 118.6 (C9b), 119.0 C(4a), 119.3 (C8), 120.4 (C7), 122.7 (C9a), 127.4 (Ar-C), 127.6 (2C, C3'' and C5''), 127.8 (Ar-C), 128.7 (Ar-C), 128.8 (2C, C2'' and C6''), 129.2 (Ar-C), 129.6 (Ar-C), 130.4 (C4'), 136.1 (C1'), 140.2 (C5a), 144.2 (CH), 147.8 (C2'), 157.2 (C3); Mp >300 °C; *m/z* (ESI^-) 393 ($[M-H]^-$, 100%); HRMS (ESI^+) $C_{21}H_{18}N_6NaSO$ ($[M+Na]^+$) requires 417.1434; found 417.1426; ν_{max} (solid) 3094, 1621, 1578, 1360

1-Benzylindoline-2,3-dione 136[305]

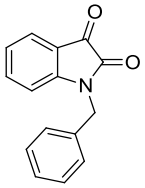

K_2CO_3 (1.13 g, 8.16 mmol) was added to a solution of isatin **135** (1.00 g, 6.80 mmol) in DMF (15 mL), and stirred at rt for 10 min. After observing a colour change of orange to dark red, benzyl bromide (1.39 g, 8.16 mmol) was added dropwise over 5 min. The solution was further stirred at 150 °C for 15 min. The reaction mixture was cooled, concentrated *in vacuo* and the resulting residue was diluted with EtOAc (50 mL) and washed with water (3 x 100 mL), brine (100 mL), dried over $MgSO_4$, filtered and concentrated *in vacuo*. The solid was recrystallised from EtOH to yield **136** as an orange crystalline solid (1.05 g, 65 %); δ_H (400 MHz, $CDCl_3$, 363 K) 4.91 (2 H, s, NCH_2), 6.97 (1 H, app d, *J* = 8.3 Hz, C(7)H), 7.11 (1 H, app t, *J* = 7.5 Hz, C(5)H), 7.26 - 7.30 (1 H, m, C(4')H), 7.33 - 7.36 (2 H, m, C(3')H and C(5')H), 7.41 - 7.45 (2 H, m, C(2')H and C(6')H), 7.56-7.59 (2 H, m, C(4)H and C(6)H); δ_C (100 MHz, $CDCl_3$) 43.8 (CH_2) 111.9 (C7), 118.6 (C3a), 124.2 (C5), 125.4 (C2' and C6'), 128.2, 128.4 (C4 and C6), 129.5 (C3' and C5'), 136.4 (C4'), 138.8 (C1'), 151.2 (C7a), 159.2 (C2), 184.0 (C3); *m/z* (ESI^+) 237.0 ($[M+H]^+$, 100%)

5-Benzyl-4a-hydroxy-4a,5-hydydro-2*H*-[1,2,4]triazino[5,6-b]indole-1(4*H*)-thione 137

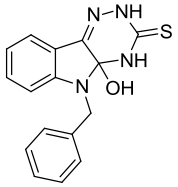

K_2CO_3 (2.5 g, 18.2 mmol) was added in one portion to a solution of 1-benzylindoline-2,3-dione **136** (3.11 g, 12.1 mmol) in water (100 mL). The resulting solution was stirred at rt for 10 min before addition of thiosemicarbizide (1.10 g, 12.1 mmol). The resulting suspension was then heated to reflux for 16 h. The orange solution was then acidified with AcOH (10 mL) producing a yellow precipitate, which was filtered and washed with water (2 x 15 mL). The filtered solid was dried azeotropically with MePh (3 x 10 mL) and concentrated *in vacuo* to yield **137** as a yellow powder (3.60 g, 96 %); δ_H (400 MHz, DMSO-d_6, 363 K) 4.99 (2 H, s, CH_2), 7.04 (1 H, d, *J* = 7.9 Hz, C(6)H), 7.15 (1 H, app t, *J* = 7.6 Hz, C(8)H), 7.29 (1 H, tt, C(4')H), 7.35 (2 H, app t, *J* = 7.9 Hz, C(3')H and C(5'(H), 7.37-7.41 (3 H, m, C(7)H, C(2')H and C(6')H), 7.73 (1H, d, *J* = 7.6 Hz, C(9)H), 8.77 (1 H, s, NH), 9.11 (1 H, s, NH), 12.42 (1 H, s, OH); δ_C (100 MHz, DMSO-d_6) 42.9 (CH_2), 110.3 (C6), 119.5 (C9a), 120.8 (C9), 123.0 (C8), 127.3 (C7), 127.4 (2C, C3' and C5'), 127.6 (C4'), 128.7 (2C, C2' and C6'), 130.9 (C1'), 131.0 (C4a), 135.7 (C5a), 142.6 (C9b), 178.7 (C3); mp 246-248 °C; *m/z* (ESI^-) 309.0 ($[M-H]^-$, 100%); HRMS (ESI^+) $C_{16}H_{13}N_4NaOS$ ($[M+Na]^+$) requires 333.0781; found 333.0774; ν_{max} (solid) 3457 (OH), 3337 (NH), 3259 (aromatic CH), 2841 (OH), 1683, 1587, 1465

5-Benzyl-4,5-dihydro-3*H*-[1,2,4]-triazino[5,6-*b*]indole-3-thione 138

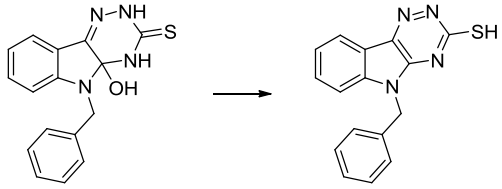

Reaction	Solvent	Reagent	T (°C)	Time	Yield
1	-	AcOH	rt	48 h	s.m.
2	-	PPA	MW 150	5 min	-
3	-	PPA	150	24 h	20%
4	EtOH	NaOMe	100	24	s.m.
5	AcOH	Et_3N	100	24	s.m.
6	-	AcOH	150	24	s.m.
7	AcOH	$(AcO)_2$	100	24	Acetylated
8	-	TFA	100	48	-

Table 1 Range of conditions attempted in the dehydration to the aromatised triazino ring

5-benzyl-4a-hydroxy-4a,5-hydydro-2*H*-[1,2,4]triazino[5,6-b]indole-1(4*H*)-thione **137** (100 mg, 0.32 mmol) was dissolved in polyphosphoric acid (3 mL) and stirred at 150 °C for 24 h. The reaction was carefully quenched with sat aq K_2CO_3 (100 mL) and extracted with EtOAc (50 mL). The organic layer was washed with brine (100 mL), dried over $MgSO_4$, filtered and concentrated *in vacuo* to yield **138** as a light orange/yellow solid (18.3 mg, 20 %); δ_H (400 MHz, $CDCl_3$, 363 K) 4.96 (2H, s, CH_2), 6.79 (1H, d, *J* = 8.2 Hz, C(6)H), 7.11 (1H, t, *J* = 7.5 Hz, C(8)H, 7.28-7.36 (6H, m, C(7)H and 5xAr-H), 7.63 (1H, d, *J* = 7.5 Hz, C(9)H); δ_C (100 MHz, ($CDCl_3$) 44.0 (CH_2), 112.0 (C6), 117.6 (C9b), 121.9 (C9), 123.6 (C8), 127.3 (C7), 127.6 (2C, C3' and C5'), 127.7 (C4'), 131.0 (2C, C2' and C6'), 131.7 (C4a), 135.4 (C5a), 143.3 (C9a), 148.4 (C1'), 179.2 (C3); mp 265-266 °C, lit. mp 269-271 °C[306]; *m/z* (ESI^-): 292 ($[M-H]^-$, 100%); HRMS (ESI^+) $C_{16}H_{12}N_4NaS$ ($[M+Na]^+$) requires 315.0680; found 315.0692; ν_{max} (solid) 3456 (NH), 2841, 1548, 1465, 1164

4,5-Dihydro-3*H*-[1,2,4]triazino[5,6-*b*]indole-3-thione 139

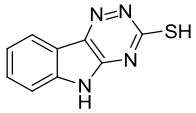

K_2CO_3 (7.05 g, 51 mmol) was added in one portion to a suspension of isatin **135** (5.00 g, 33.2 mmol) in water (100 mL). The resulting solution was stirred at rt for 10 min before addition of thiosemicarbizide (3.09 g, 33.2 mmol). The reaction was then heated to reflux for 16 h. The resulting mixture was acidified with acetic acid (15 mL) producing a precipitate, which was filtered and washed with water (2 x 15 mL). The filtered solid was dried azeotropically with MePh (3 x 15 mL) and concentrated *in vacuo.* The crude solid was recrystallised from DMF to yield **139** as a yellow powder (6.25 g, 91 %); δ_H (400 MHz, DMSO-d_6, 363 K) 7.34 (1 H, app t, J = 7.6 Hz, C(8)H) 7.44 (1 H, d, J = 8.1 Hz, C(6)H) 7.62 (1 H, app t, J = 7.6Hz, C(7)H) 8.00 (1 H, d, J = 7.6 Hz, C(9)H); δ_C (100 Hz, DMSO-d_6) 113.9 (C6), 118.6 (C9b), 122.7 (C9), 123.9 (C8), 132.7 (C7), 136.5 (C9a), 144.0 (C4a), 150.0 (C5a), 179.9 (C3); mp >300 °C, lit mp 300 °C [307]; *m/z* (ESI$^-$) 201 ([M-H]$^-$, 100%); HRMS (ESI$^+$) $C_9H_6N_4NaS$ ([M+Na]$^+$) requires 225.0205; found 225.0205; ν_{max} (solid) 2785 (NH), 1585 (NN), 1426, 1379, 1144 (CS),

5-Benzyl-3-(benzylthio)-5*H*-[1,2,4]triazino[5,6-b]indole 140

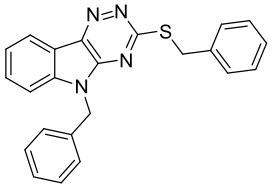

K_2CO_3 (3.42 g, 24.8 mmol) was added to a solution of 4,5-dihydro-3*H*-[1,2,4]triazino[5,6-b]indole-3-thione **139** (1.00 g, 4.95 mmol) in DMF (30 mL) and the resulting mixture was stirred at rt for 15 min before dropwise addition of benzyl bromide (1.76 mL, 14.9 mmol) and subsequently stirred further for 16 h. The reaction mixture was concentrated *in vacuo*

and the residue extracted in EtOAc (2 x 50 mL). The combined organic phases were washed with water (3 x 100 mL), brine (100 mL), dried over $MgSO_4$, filtered and concentrated *in vacuo* to yield the crude product. The resulting solid was recrystallised from 40-60 °C petrol and EtOAc (10:1) to yield **140** as a gold solid (1.2 g, 63 %); δ_H (400 MHz, DMSO-d_6, 363 K) 4.59 (2H, s, SCH_2), 5.66 (2H, s, NCH_2), 7.19 - 7.35 (8H, m, 8xAr-H), 7.43 - 7.52 (3H, m, 3xAr-H), 7.66 - 7.77 (2H, m, 2xAr-H), 8.36 (1H, d, *J* = 7.8 Hz, (C9)H); δ_C (100 MHz, DMSO-d_6) 34.0 (SCH_2), 44.2 (NCH_2), 111.6 (C6), 117.6 (C9b), 121.6 (C8), 123.1 (C7), 127.1 (C9), 127.3 (2C, C2'' and C6''), 127.8 (C4''), 128.4, 128.8, 129.0 (6C, C2', C6', C3', C5', C3'' and C5''), 130.9 (C4'), 135.9 (C9a), 137.8 (C4a), 140.7, 140.9 (C1' and C1''), 146.1 (C5a), 167.1 (C3); mp 146–148 °C, lit 149-150 °C[137]; HRMS (ESI^+) ($[M+Na]^+$) requires 405.1144; found 405.1142; *m/z* (ESI^-) 417 ($[M+Cl]^-$, 100%); ν_{max} (solid) 3027 (aromatic CH), 1565, 1452, 1171 (CS)

azino[5,6-*b*]indole 141[274]

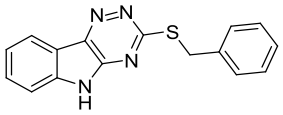

To an aqueous solution of NaOH (4 %, 5.00 mL) was added 5*H*-[1,2,4]triazino[5,6-*b*]indole-3-thiol **139** (100 mg, 0.49 mmol) followed by benzyl bromide (58.5 µL, 0.49 mmol). The reaction was stirred overnight at rt and resulting precipitate was filtered, washed with MeOH and dried to yield **141** as a light yellow solid (68 mg, 75 %). δ_H (400 MHz, DMSO-d_6) 4.57 (2H, s, CH_2), 7.27 (1H, t, *J* = 7.9 Hz, C(4')H), 7.34 (2H, app *t*, *J* = 7.6 Hz, C(3')H and C(5')H), 7.44 (1H, app t, *J* = 7.7 Hz, C(8)H), 7.52 (2H, d, *J* = 7.6 Hz, C(2')H and C(6')H), 7.59 (1H, d, *J* = 7.7 Hz, C(6)H), 7.70 (1H, app t, *J* = 7.7 Hz, C(7)H), 8.31 (1H, d, *J* = 7.7 Hz, C(9)H), 12.66 (1H, br s, NH); δ_C (126 Hz, DMSO-d_6) 34.0 (CH_2), 112.7 (C6), 117.6 (C9a), 121.5 (C9), 122.5 (C8), 127.2 (C4'), 128.5 (2C, C3' and C5'),

129.1 (2C, C2' and C6'), 130.9 (C7), 137.6 (C9b), 140.3 (C1'), 141.1 (C4a), 146.6 (C5a), 166.7 (C3); *m/z* (ESI⁻) 291 ([M - H]⁻, 100%); HRMS (ESI⁺) $C_{16}H_{12}NaN_4S$ ([M+Na]⁺) requires 315.0675; found 315.0663; mp 290-292 °C, lit 280 °C[274]; ν_{max} (solid) 3059 (N-H), 2799 (aromatic C-H), 1600, 1579, 1461 (N-H), 1321; HPLC (Method 1) >99%, rt = 11.06 min

5-Benzyl-3-(benzylsulfonyl)-5*H*-[1,2,4]triazino[5,6-*b*]indole 142

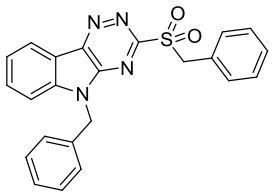

*m*CPBA (452 mg, 2.62 mmol) was added to a solution of 5-benzyl-3-(benzylthio)-5*H*-[1,2,4]triazino[5,6-*b*]indole **140** (500 mg, 1.31 mmol) in CH_2Cl_2 (10 mL) at 0 °C and stirred at rt for 16 h. The resulting suspension was filtered and the precipitate was washed with CH_2Cl_2 (2 x 10 mL). The resulting filtrate was dissolved in EtOAc (50 mL), washed with sat aq $NaHCO_3$ (2 x 40 mL), sat aq Na_2SO_3 (2 x 40 mL), dried over $MgSO_4$, filtered and concentrated *in vacuo*. The solid was recrystallised from 40-60 °C petrol and EtOAc (10:1) to yield **142** as a fine yellow powder (220 mg, 41 %); δ_H (400 MHz, DMSO-d_6, 363 K) 5.14 (2H, s, SCH_2), 5.76 (2H, s, NCH_2), 7.28 - 7.36 (10H, m, 10xAr-H), 7.62 (1H, t, *J* = 7.9 Hz, C(8)H), 7.83 (1H, d, *J* =7.9 Hz, C(6)H), 7.88 (1H, app t, *J* = 7.9 Hz, C(7)H), 8.58 (1H, d, *J* = 7.9 Hz, C(9)H); δ_C (125 MHz, DMSO-d_6) 44.7 (NCH_2), 57.6 (SCH_2), 112.2 (C6) 116.9 (C9b) 123.1 (C8) 123.9 (C7) 127.4 (2C, C3'' and C5'') 127.5 (C9a) 127.9 (C9) 128.4 (2C, C3' and C5') 128.5 (C4'') 128.8 (2C, C2'' and C6''), 131.5 (2C, C2' and C6') 133.1 (C4'), 135.3 (C4a) 142.7 (C1'') 144.8 (C1') 145.9 (C5a) 160.7 (C3); mp 244-245 °C; *m/z* (ESI⁺) 437.0 ([M+Na]⁺, 100%); HRMS (ESI⁺) $C_{23}H_{18}N_4NaO_2S$ ([M+Na]⁺)

requires 437.1043; found 437.1032; ν_{max} (solid) 3455, 3337, 2838, 1584, 1466, 1309 (SO), 1137 (SO)

5-Benzyl-3-hydrazinyl-5*H*-[1,2,4]triazino[5,6-*b*]indole 143

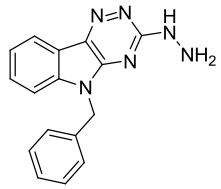

Method A: Hydrazine monohydrate (87.9 µL, 1.81 mmol) was added to a solution of 5-Benzyl-3-(benzylsulfonyl)-5*H*-[1,2,4]triazino[5,6-*b*]indole **142** (150 mg, 0.362 mmol) in EtOH (20 mL) and heated to 85 °C for 3 h. The clear yellow solution was cooled to form a precipitate, which was filtered and washed with MeOH (2 x 10 mL) to yield **143** as a faint green powder (55 mg, 53 %);

Method B: 5-Benzyl-4,5-dihydro-3*H*-[1,2,4]-triazino[5,6-*b*]indole-3-thione **140** (150 mg, 0.51 mmol) was added to hydrazine monohydrate (5 mL) and stirred at reflux for 16 h. Ths solution was cooled to form a precipitate which was filtered, washed with water, MeOH and dried *in vacuo* to yield **143** as a pale green solid (126 mg, 84 %); δ_H (400 MHz, DMSO-d_6, 363 K) 4.43 (2H, s, NH_2), 5.50 (2H, s, NCH_2), 7.24 - 7.35 (6H, m, 6xAr-H), 7.50 (1H, t, *J* = 8.0 Hz, C(7)H), 7.55 (1H, d, *J* = 8.0 Hz, C(6)H), 8.16 (1H, d, *J* = 7.6 Hz, C(9)H), 8.76 (1H, br s, NH); δ_C (125 MHz, DMSO-d_6) 43.5 (NCH_2), 110.9 (C6), 119.0 (C9b), 119.8 (C8), 122.2 (C7), 127.4 (2C, C3' and C5'), 127.6 (C4'), 128.3 (C9), 128.7 (2C, C2' and C6'), 136.3 (C4a), 139.6 (C5a), 148.0 (C1'), 162.5 (C3); mp 224-226 °C; *m/z* (ESI^+) 291 ($[M+H]^+$, 70%), 313 ($[M+Na]^+$, 80%); HRMS (ESI^+) $C_{16}H_{14}N_6Na$ ($[M+Na]^+$) requires 313.1172; found 313.1167; ν_{max} (solid) 3306 (NH), 1632, 1517, 1391, 1355

1-Methylindoline-2,3-dione 144

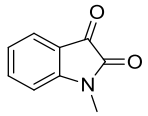

K_2CO_3 (1.13 g, 8.16 mmol) was added to a solution of isatin **135** (1.00 g, 6.80 mmol) in DMF (15 mL) and stirred at rt for 10 min. After observing a colour change from orange to dark red, methyl iodide (508 μL, 8.16 mmol) was added dropwise over 5 min. The solution was stirred at 150 °C for 20 min before being cooled and concentrated *in vacuo*. The resulting residue was dissolved in EtOAc (50 mL). The organic phase was washed with water (3 x 100 mL), brine (100 mL), dried over $MgSO_4$, filtered and concentrated *in vacuo* to yield an orange solid. The crude solid was recrystallised from EtOH to yield **144** as an orange crystalline solid (590 mg, 55 %); δ_H (400 MHz, DMSO-d_6, 363 K) 3.27 (3 H, s, NCH_3), 7.11 (1H, d, J = 7.8 Hz, C(4)H), 7.11 (1H, app td, J = 7.8, 1.0 Hz, C(5)H), 7.51 (1H, dd, J = 7.8, 1.3 Hz), 7.66 (1H, app td, J = 7.8, 1.3 Hz, C(6)H); δ_C (100 MHz, DMSO-d_6) 26.8 (NCH_3), 111.4 (C7), 118.2 (C3a), 124.0 (C4), 125.1 (C5), 139.0 (C6), 152.2 (C7a), 159.0 (C2), 184.3 (C3)[308]; mp 129-131 °C, lit 130-132 °C [309]; *m/z* (ESI^+) 184 ($[M+Na]^+$, 90%); ν_{max} (solid) 1717 (CO 1,2-diketone), 1601 (CO amide), 1467, 1324; HRMS (ESI^+) $C_9H_7NO_2$ ($[M+Na]^+$) requires 184.0369; found 184.0367

5-Methyl-4,5-dihydro-3*H*-[1,2,4]triazino[5,6-*b*]indole-3-thione 145[310]

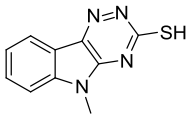

K_2CO_3 (758 mg, 5.49 mmol) was added in one portion to a solution of 1-methylindoline-2,3-dione **144** (590 mg, 3.66 mmol) in water (50 mL). The resulting solution was stirred at rt for 10 min before addition of thiosemicarbizide (333 mg, 3.66 mmol). The reaction was then heated to reflux for 16 h. The resulting mixture was acidified with AcOH (7 mL)

producing a precipitate, which was filtered and washed with water (2 x 10 mL). The filtered solid was azeotropically dried using MePh (3 x 10 mL) and concentrated *in vacuo* to yield **145** as a yellow powder (759 mg, 96 %); δ_H (400 MHz, DMSO-d_6, 363 K) 3.65 (3H, s, CH_3), 7.40 (1H, app t, *J* = 8,1 Hz, C(8)H), 7.65 (1H, d, *J* = 8.1 Hz, C(6)H), 7.71 (1H, app t, J = 8.1 Hz, C(7)H), 8.02 (1H, d, *J* = 8.1 Hz, C(9)H), 14.56 (1H, s, SH); δ_C (100 MHz, DMSO-d_6) 28.3 (NCH_3), 112.4 (C6), 118.2 (C9b), 122.5 (C9), 124.3 (C8), 132.6 (C7), 136.1 (C9a), 145.2 (C4a), 149.1 (C5a), 179.9 (C3); mp 250-252 °C; *m/z* (ESI^+): 217.0 ($[M+H]^+$, 100%); ν_{max} (solid) 3424 (SH), 2844 (NCH_3), 1572, 1467, 1365; HRMS (ESI^+) $C_{10}H_8N_4S$ ($[M+Na]^+$) requires 239.0362; found 239.0360

3-Hydrazono-5-methyl-4.5-dihydro-3*H*-[1,2,4]triazino[5,6-*b*]indole 146[138]

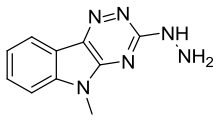

Hydrazine monohydrate (338 μL, 6.94 mmol) was added slowly to a solution of 5-methyl-4,5-dihydro-3*H*-[1,2,4]triazino[5,6-*b*]indole-3-thione **145** (500 mg, 2.32 mmol) in EtOH (10 mL) and the resulting solution was heated to 85 °C for 3 h. The clear yellow solution was then cooled to form a precipitate, which was filtered and washed with MeOH (2 x 10 mL) to yield **146** as a pale green powder (190 mg, 40 %); δ_H (400 MHz, DMSO-d_6, 363 K) 3.71 (3 H, s, NCH_3), 4.40 (2H, br s, NH_2), 7.35 (1 H, app td, *J* = 7.6, 1.3 Hz, C(8)H), 7.57 (1 H, app td, *J* = 7.6, 1.3 Hz, C(7)H), 7.61 (1 H, d, *J* = 7.6 Hz, C(6)H), 8.13 (1 H, d, *J* = 7.6 Hz, C(9)H), 8.67 (1 H, br s, NH); δ_C (100 MHz, DMSO-d_6) 26.8 (NCH_3), 110.4 (C6), 118.7 (C9b), 119.6 (C8), 122.0 (C7), 128.3 (C9), 136.6 (C9a), 140.6 (C4a), 148.0 (C5a), 162.4 (C3); mp 229-231 °C; *m/z* (ESI^+): 237.0 ($[M+Na]^+$, 100%); HRMS (ESI^+) $C_{10}H_{10}N_6Na$ ($[M+Na]^+$) requires 237.0859; found 237.0858; ν_{max} (solid) 3198 (NH), 2832 (R_2NC), 1588 (NH), 1527, 1398

2-((2-(5-methyl-[1,2,4]triazino[5,6-b]indol-3-yl)hydrazono)methyl)phenol 147[311]

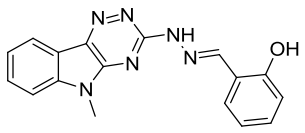

Salicylaldehyde (29 µL mg, 0.28 mmol) was added to a suspension of 3-hydrazinyl-5*H*-methyl-[1,2,4]triazino[5,6-*b*]indole **146** (60 mg, 0.28 mmol) in MeOH (10 mL) and stirred at rt for 16 h. The precipitate was filtered, washed with MeOH (2 x 10 mL) and dried *in vacuo* to yield **147** as a bright yellow solid (83 mg, 93 %); δ_H (400 MHz, DMSO-d_6, 363 K) 3.80 (3H, s, NCH_3), 6.93 (1H, app t, *J* = 8.2 Hz, C(5')H), 6.96 (1H, d, *J* = 8.2 Hz, C(3')H), 7.28 (1H, app t, *J* = 7.7 Hz, C(7)H), 7.43 (1H, app t, *J* = 7.9 Hz, C(8)H), 7.47 (1H, d, *J* = 7.9 Hz, C(6)H), 7.67 (1H, app t, *J* = 8.2 Hz, C(4')H), 7.71 (1H, d, *J* = 8.2 Hz, C(6')H), 8.24 (1H, d, *J* = 7.9 Hz, C(9)H), 8.42 (1H, s, CH), 11.79 (1H, br s, NH), 12.12 (1H, br s, OH); δ_C (100 MHz, DMSO-d_6) 27.0 (NCH_3), 110.7 (C6'), 116.4 (C3'), 118.4 (C9b), 119.1 (C5'), 119.2 (C4a), 120.2 (C9), 122.4 (C8), 129.2 (C(4'), 129.4 (C6), 130.3 (C7), 141.2 (C1'), 143.8 (CH), 147.9 (C5a), 157.2 (C2'), 159.1 (C3); mp >300 °C; *m/z* (ESI^-): 317.0 ($[M-H]^-$, 100%); HRMS (ESI^+) $C_{17}H_{12}N_6NaO$ ($[M+Na]^+$) requires 341.1121; found 341.1132; ν_{max} (solid) 3109 (NH), 2833 (OH), 1632, 1588, 1401

3-Hydrazono-4,5-dihydro-3*H*-[1,2,4]triazino[5,6-*b*]indole 148[138]

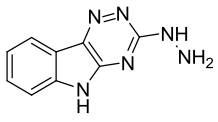

4,5-Dihydro-3*H*-[1,2,4]triazino[5,6-*b*]indole-3-thione **139** (400 mg, 4.95 mmol) was dissolved in hydrazine monohydrate (19 mL) and heated to reflux for 3 h. The clear yellow solution was cooled to rt to form a precipitate. The precipitate was filtered, washed with water (1 x 10 mL) and MeOH (2 x 10 mL) to afford **148** as a faint yellow powder (350 mg,

89 %); δ_H (500 MHz, DMSO-d_6, 363 K) 4.33 (2H, s, NH_2) 7.30 (1H, app t, J = 7.9 Hz, C(8)H), 7.42 (1H, d, J = 7.9 Hz, C(6)H), 7.50 (1H, app t, J = 7.9 Hz, C(7)H), 8.11 (1H, d, J = 7.9 Hz, C(9)H), 8.57 (1H, br s, NH); δ_C (125 Hz, DMSO-d_6) 112.0 (C6), 119.0 (C9b), 119.7 (C8), 121.7 (C7), 128.4 (C9), 136.8 (C9a), 139.3 (C4a), 148.5 (C5a), 162.6 (C3); mp 271-273 °C, lit 278 °C[312]; *m/z* (ESI^+): 200.0 ($[M+H]^+$, 100%); HRMS (ESI^+) ($[M+Na]^+$) requires 223.0703; found 223.0701; ν_{max} (solid) 3269 (NH), 3057 (aromatic CH), 2764, 1618 (NH_2), 1423

2-((2-(5*H*-[1,2,4]triazino[5,6-*b*]indol-3-yl)hydraxono)methyl)phenol 149

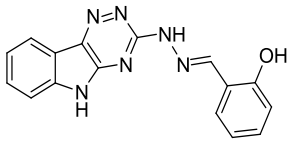

Salicylaldehyde (31.6 µL, 0.30 mmol) was added to a solution of 3-hydrazinyl-5*H*-[1,2,4]triazino[5,6-*b*]indole **148** (60 mg, 0.30 mmol) in MeOH (10 mL) and stirred at rt for 16 h. The precipitate was filtered, washed with MeOH (2 x 10 mL) and dried *in vacuo* to yield **149** as a bright yellow solid (86 mg, 94 %); δ_H (400 MHz, DMSO-d_6, 363 K) 3.17 (1 H, s, N*H*), 6.90 - 6.95 (2 H, m, C(3')H and C(6')H), 7.26 (1H, app t, J = 7.6 Hz, C(4')H), 7.36 (1 H, app t, J =7.6 Hz, C(5')H), 7.47 (1 H, app t, J = 7.8 Hz, (C(8)H), 7.49 (1H, d, 7.8 Hz, C(6)H), 7.57 (1H, app t, J = 7.8 Hz, C(7)H), 8.20 (1 H, d, J = 7.8 Hz, C(9)H), 8.41 (1 H, s, C*H*), 11.55 (1 H, s, N*H*), 11.76 - 12.20 (1 H, br s, O*H*); δ_C (100 MHz, DMSO-d_6); 113.1 (*C6*), 117.2 (*C3'*), 119.5 (C9b), 120.0 (C9a), 120.1 (*C5'*), 121.2 (*C9*), 122.9 (*C8*), 130.0 (*C6'*), 130.1 (*C7*), 131.1 (*C4'*), 139.5 (C1'), 140.8 (C4a), 144.5 (CH), 149.2 (C5a), 157.9 (C2'), 158.6 (C3); mp 244-246 °C; ν_{max} (solid) 3306 (NH), 1632, 1589, 1517, 1491, 1355; *m/z* (ESI^-): 303.0 ($[M-H]^-$, 100%); HRMS (ESI^+) $C_{16}H_{12}N_6O$ ($[M+Na]^+$) requires 327.0970; found 327.0968

Pyridin-3-ylmethyl-4-((2-aminophenyl)carbonyl)benzylcarbamate 188

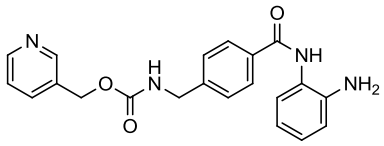

Pyridin-3-ylmethyl-4-(chlorocarbonyl)benzylcarbamate hydrochloride **194** (300 mg, 0.85 mmol) was dissolved in pyridine (8 mL) to generate a yellow coloured solution. 2-amino analine (105 mg, 0.97 mmol) was added to the solution and stirred at rt for 2 h in which the solution turned bright orange. The solvent was removed under reduced pressure to yield **188** as a white solid (210 mg, 63%); δ_H (400 MHz, DMSO-d_6, 363 K) 4.29 (2H, d, J = 6.1 Hz, NCH_2), 4.90 (2H, s, NH_2), 5.11 (2H, s, OCH_2), 6.61 (1H, td, J = 7.6, 1.2 Hz, C(23), 6.79 (1H, dd, J = 7.6, 1.2 Hz, C(25)H), 6.98 (1H, td, J = 7.6, 1.2 Hz, C(24)H), 7.18 (1H, d, J = 7.6 Hz, C(22)H), 7.38 (2H, d, J = 8.1 Hz, C(13)H and C(17)H), 7.43 (1H, m, C(5)H), 7.80 (1H, m, C(4)H), 7.94 (2H, d, J = 8.1 Hz, C(14)H and C(16)H), 8.54 (1H, dd, J = 7.6, 1.5 Hz, C(6)H), 8.61 (1H, d, J = 1.5 Hz, C(2)H), 9.64 (1H, s, NH amide); δ_C (100 MHz, DMSO-d_6) 44.1 (OCH_2), 63.7 (NCH_2), 116.6 (C23), 116.7 (C25), 123.8 (C21), 124.0 (C5), 126.9 (C24), 127.1 (2C, C13 and C17), 128.3 (2C, C14 and C16), 133.2 (C15), 133.7 (C3), 136.2 (C4), 143.6 (C12), 149.6 (2C, C2 and C6), 156.7 (C20); mp 155-156 °C; *m/z* (ESI^-): 375 ($[M-H]^-$, 100%); HRMS (ESI^+) $C_{21}H_{20}N_4NaO_3$ ($[M+Na]^+$) requires 399.1428; found 399.1415; ν_{max} (solid) 3342, 2160, 1692, 1632, 1523

4-((pyridine-3-ylmethoxycarbonyl)aminomethyl)menzoic acid 193[185]

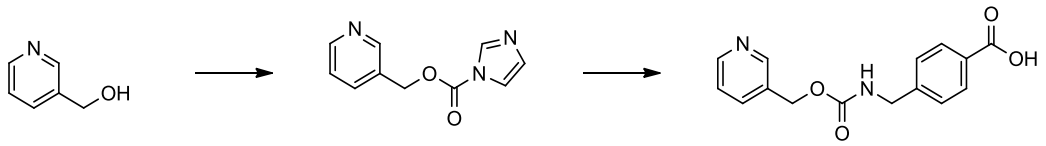

3-pyridinemethanol (6.00 g, 55.0 mmol) was added to a suspension of carbonyldiimidazole (8.92 g, 55.0 mmol) in THF (40 mL) at 10 °C and stirred at rt for 1h to produce **192** *in situ*. A solution of 4-(aminoethyl) benzoic acid (8.30 g, 55.0 mmol), DBU (8.22 mL, 55.0 mmol) and Et_3N (7.66 mL, 55.0 mmol) in THF (30 mL) was added to the solution and further stirred at rt for 5 h. The mixture was concentrated *in vacuo* and dissolved in water (100 mL). The aqueous solution was acidified using 1M aq HCl to pH 5 to form a precipitate. The resulting precipitate was collected by filtration, washed with water, MeOH and dried *in vacuo* to yield **193** as a white solid (14.2 g, 90.4 %); δ_H (400 MHz, DMSO-d_6, 363 K) 4.27 (2H, d, J = 6.3 Hz, NCH_2), 5.09 (2H, s, OCH_2), 7.36 (2H, d, J = 8.1 Hz, C(13)H and C(17)H), 7.41 (1H, dd, J = 7.8, 4.6 Hz, C(5)H), 7.78 (1H, dd, J = 7.8, 4.6 Hz, C(4)H), 7.89 (2H, d, J = 8.1 Hz, C(14)H and C16)H), 7.97 (1H, t, J = 6.3 Hz, NH), 8.52 – 8.54 (1H, m, C(6)H), 8.59 (1H, d, J = 1.8 Hz, C(2)H), 12.40 (1H, br s, OH); δ_C (100 MHz, DMSO-d_6) 49.5 (NCH_2), 64.1 (OCH_2), 124.4 (C5), 127.9 (2C, C14 and C16), 130.2 (C15), 130.3 (2C, C13 and C17), 133.5 (C3), 136.7 (C4), 145.6 (C12), 150.0 (C2), 150.0 (C6), 157.1 (C(O) carbamate), 168.0 (C(O) carboxylic acid); mp 201-204 °C; *m/z* (ESI^-): 285 ($[M-H]^-$, 100%); HRMS (ESI^+) $C_{15}H_{14}N_2NaO_4$ ($[M+Na]^+$) requires 309.0846; found 309.0860; ν_{max} (solid) 3297 (OH), 2161, 1735 (CO carbamate), 1526 (R_2NH), 1286, 1245

Pyridin-3-ylmethyl-4-(chlorocarbonyl)benzylcarbamate hydrochloride 194

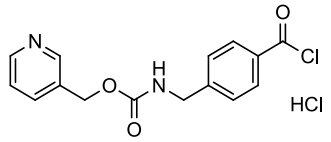

DMF (20 µL) and oxalyl chloride (6.03 mL, 70.2 mmol) were added to a suspension of 4-((pyridine-3-ylmethoxycarbonyl)aminomethyl)menzoic acid **193** (20.0 g, 35.1 mmol) in MePh (50 mL), and stirred at rt for 4 h. The resulting white solid formed was collected by filtration and washed with MePh (10 mL), diisopropyl ether (10 mL) and dried *in vacuo* to yield **194** as a white solid (9.90 g, 83 %); δ_H (400 MHz, DMSO-d_6, 363 K) 4.28 (2H, d, J = 6.1 Hz, NCH_2), 5.27 (2H, s, OCH_2), 7.37 (2H, d, J = 8.3 Hz, C(13)H and C(17)H), 7.89 (2H, d, J = 8.3 Hz, C(14)H and C(16)H), 8.09 – 8.13 (1H, m, C(5)H), 8.19 (1H, t, J = 6.1 Hz, NH), 8.58 (1H, d, J = 8.1 Hz, C(4)H), 8.91 (1H, d, J = 5.6 Hz, C(6)H), 8.94 (1H, s, C(2)H); δ_C (100 MHz, DMSO-d_6) 44.5 (NCH_2), 62.8 (OCH_2), 126.2 (2C, C14 and C16), 129.1 (C3), 129.8 (2C, C13 and C17), 130.3 (C15), 138.2 (C4), 141.1 (C2), 141.9 (C6), 145.4 (C12), 156.7 (C(O) carbamate), 168.0 (C(O) acid chloride); mp 120-122 °C; *m/z* (ESI^+): 301 ([methyl ester observed in MeOH]$^+$, 70%); ν_{max} (solid) 3243, 2497, 1733 (CO carbamate), 1532 (R_2NH), 1241

Pyridin-3-ylmethyl-4-((2-hydroxyphenyl)carbonyl)benzylcarbamate 195

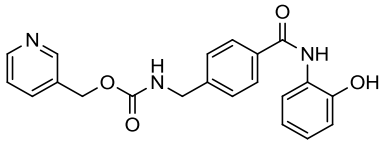

Pyridin-3-ylmethyl-4-(chlorocarbonyl)benzylcarbamate hydrochloride **194** (300 mg, 0.85 mmol) was dissolved in pyridine (8 mL) generating a yellow coloured solution. 2-amino phenol (106 mg, 0.97 mmol) was added and stirred at rt for 2 h in which the solution turned bright orange. The solvent was removed under reduced pressure to yield **195** as a

white solid (190 mg, 57%); δ_H (400 MHz, DMSO-d_6, 363 K) 4.22 (2H, d, J = 6.1 Hz, NCH_2), 5.04 (2H, s, OCH_2), 6.77 (1H, td, J = 7.6, 1.2 Hz, C(23), 6.85 (1H, dd, J = 7.6, 1.2 Hz, C(25)H), 6.94 – 6.99 (1H, m, C(24)H), 7.32 (2H, d, J = 8.1 Hz, C(13)H and C(17)H), 7.33 – 7.36 (1H, m, C(5)H), 7.61 (1H, dd, J = 7.6, 1.2 Hz, C(22)H), 7.71 – 7.73 (1H, m, C(4)H), 7.85 (2H, d, J = 8.1 Hz, C(14)H and C(16)H), 7.91 (1H, t, J = 6.1 Hz, NH carbamate), 8.47 (1H, dd, J = 7.6, 1.2 Hz, C(6)H), 8.53 (1H, d, J = 1.5 Hz, C(2)H), 9.41 (1H, s, OH), 9.64 (1H, s, NH amide); δ_C (100 MHz, DMSO-d_6) 44.1 (NCH_2), 63.7 (OCH_2), 116.5 (C25), 119.5 (C23), 124.0 (C5), 124.5 (C22), 126.1 (C24), 126.3 (C21), 127.4 (2C, C13 and C17), 128.1 (2C, C14 and C16), 133.1 (C15), 133.4 (C3), 136.2 (C4), 144.0 (C12), 149.6 (2C, C2 and C6), 149.7 (C20), 156.7 (C(O) amide), 165.5 (C(O) carbamate); mp 182-183 °C; *m/z* (ESI^-): 376 ($[M-H]^-$, 100%); HRMS (ESI^+) $C_{21}H_{19}N_3NaO_4$ ($[M+Na]^+$) requires 400.1268; found 400.1270; ν_{max} (solid) 3425, 3290, 1716, 1663, 1512

Pyridin-3-ylmethyl-4-(pyridine-2-ylcarbamoyl)benzylcarbamate 196

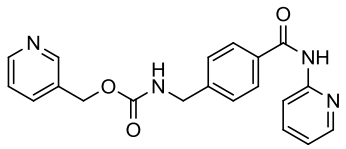

Pyridin-3-ylmethyl-4-(chlorocarbonyl)benzylcarbamate hydrochloride **194** (300 mg, 0.85 mmol) was dissolved in pyridine (8 mL) generating a yellow coloured solution. The solvent was removed under reduced pressure to yield **196** as a white crystalline solid (303 mg, 95%); δ_H (400 MHz, DMSO-d_6, 363 K) 4.28 (2H, d, J = 6.1 Hz, NCH_2), 5.10 (2H, s, OCH_2), 7.15 - 7.18 (1H, m, C(24)H), 7.37 (2H, d, J = 8.3 Hz, C(13)H and C(17)H), 7.40 – 7.43 (1H, m, C(5)H), 7.77 – 7.81 (1H, m, C(4)H), 7.82 – 7.86 (1H, m, C(22)H), 7.97 – 7.99 (1H, m, NH carbamate), 7.98 (2H, d, J = 8.3 Hz, C(14)H and C(16)H), 8.17 – 8.21 (1H, m, C(23)H), 8.38 – 8.40 (1H, m, C(25)H), 8.54 (1H, dd, J = 4.8, 1.8 Hz, C(6)H), 8.59 (1H, d, J = 1.8 Hz, C(2)H), 10.74 (1H, s, NH amide); δ_C (100 MHz, DMSO-d_6) 44.0

(NCH_2), 63.8 (OCH_2), 115.1 (C23), 120.3 (C24), 124.0 (C5), 127.3 (2C, C13 and C17), 128.6 (2C, C14 and C16), 133.1 (2C, C3 and C15), 136.3 (C4), 138.6 (C22), 144.3 (C12), 148.4 (C25), 149.6 (2C, C2 and C6), 152.7 (C21), 156.7 (C(O) carbamate), 166.2 (C(O) amide); mp 129-130 °C; *m/z* (ESI^+): 363 ($[M+H]^+$, 80%), 385 ($[M+Na]^+$, 100%); HRMS (ESI^+) $C_{20}H_{18}N_4NaO_3$ ($[M+Na]^+$) requires 385.1217; found 385.1270; ν_{max} (solid) 3362, 3257, 2161, 1717, 1660, 1520

6.3.1 Triazinoindole Library

3-(Hexylthio)-5*H*-[1,2,4]triazino[5,6-*b*]indole 230

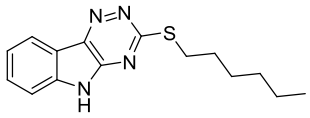

Following **General Procedure 3:** 1-bromohexane (139 µL, 0.99 mmol) was added to 5*H*-[1,2,4]triazino[5,6-*b*]indole-3-thiol **139** (200 mg, 0.99 mmol), and Et_3N (207 µL, 1.49 mmol) in MeOH (10 mL). The resulting precipitate was filtered and washed to give **230** as a pale yellow solid (108 mg, 38 %); δ_H (400 MHz, DMSO-d_6, 363K) 0.87 (3H, m, CH_3), 1.30 (4H, m, C(4')H_2 and C(5')H_2), 1.44 (2H, m, C(3')H_2), 1.74 (2H, m, C(2')H), 3.26 (2H, t, *J* = 7.3 Hz, C(1')H), 7.43 (1H, app t, *J* = 7.6 Hz, C(8)H), 7.57 (1H, d, *J* = 7.6 Hz, C(6)H), 7.68 (1H, app t, *J* = 7.6 Hz, C(7)H), 8.29 (1H, d, *J* =7.6 Hz, C(9)H); δ_C (100 MHz, DMSO-d_6) 14.4 (C6'), 22.5 (C5'), 28.5 (C4'), 29.3 (C3'), 30.4 (C2'), 31.3 (C1'), 113.1 (C6), 118.1 (C9a), 121.9 (C9), 123.9 (C8), 131.2 (C7), 140.7 (C9b), 141.3 (C5a), 147.1 (C4a), 167.8 (C3); mp 245-246 °C; *m/z* (ESI^+) 287 ($[M + H]^+$, 70%); (ESI^-) 285 ($[M - H]^-$, 100%); HRMS (ESI^+) $C_{15}H_{18}N_4NaS$ ($[M+Na]^+$) requires 309.1144; found 309.1156; ν_{max} (solid) 3060 (N-H), 2926 and 2857 (aromatic C-H), 1608, 1461, 1425, 1337;

HPLC (Method 2) >99%, rt = 11.14

3-(Butylthio)-5*H*-[1,2,4]triazino[5,6-*b*]indole 235

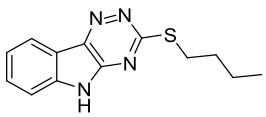

iodobutane (45 µL, 0.4 mmol) was added to a suspension of 5*H*-[1,2,4]triazino[5,6-*b*]indole-3-thiol **139** (80 mg, 0.40 mmol) and Cs_2CO_3 (194 mg, 0.94 mmol) in MeOH (10 mL) and the resulting mixture stirred for 16 h at 80 °C to afford a yellow solution. Upon

cooling, the solvents were removed *in vacuo* and resulting solid was filtered and washed mixture to yield **235** a yellow solid (82 mg, 80 %); δ_H (400 MHz, DMSO-d_6, 363K) 0.94 (3H, t, *J* = 7.3 Hz, C(4')H), 1.42 - 1.53 (2H, m, C(3')H), 1.71 - 1.77 (2H, m, C(2')H), 3.28 (2H, t, *J* = 7.7 Hz, C(1')H), 7.44 (1H, app t, *J* = 7.9 Hz, C(8)H) 7.57 (1H, d, *J* = 8.2 Hz, C(6)H) 7.66 - 7.72 (1H, m, C(7)H), 8.30 (1H, d, *J* = 7.9 Hz, C(9)H); δ_C (100 MHz, DMSO-d_6) 13.5 (C4'), 21.5 (C3'), 29.6 (C2'), 30.9 (*S*-C1'), 112.7 (C6), 117.7 (C9a), 121.4 (C8) 122.4 (C7), 130.7 (C9), 140.3 (C9b), 140.9 (C5a), 146.7 (C4a), 167.3 (C3); mp 249-252 °C; *m/z* (ESI^+) 281 ($[M + Na]^+$, 100%); HRMS (ESI^+) $C_{13}H_{14}N_4NaS$ ($[M+Na]^+$) requires 281.0831; found 281.0821; ν_{max} (solid) 3058 (N-H), 2957 and 2802 (aromatic C-H), 1607, 1461, 1186; $C_{13}H_{14}N_4NaS \cdot 0.3\ H_2O$ requires C, 59.20; H, 5.58; N, 2.24%; found C, 59.27; H, 5.34; N, 21.40%; HPLC (Method 2) >99%, rt = 10.73 min

3-((2'-Cyanobenzyl)thio)-5*H*-[1,2,4]triazino[5,6-*b*]indole 236

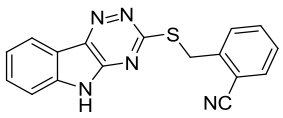

Following **General Procedure 3:** 2-cyano benzyl bromide (2.19 g, 11.2 mmol) was added to 5*H*-[1,2,4]triazino[5,6-*b*]indole-3-thiol **139** (2.26 g, 11.2 mmol) and Et_3N (2.33 mL, 16.8 mmol) in MeOH (40 mL) and the resulting mixture stirred at rt for 16h. The precipitate was filtered and washed to give **236** as a pale yellow solid (3.60 g, quant). δ_H (400 MHz, DMSO-d_6, 363 K) 4.73 (2 H, s, CH_2), 7.41 - 7.49 (2 H, m, C(8)H and C(4')H), 7.58 (1 H, d, *J*=7.8 Hz, C(6')H), 7.64 – 7.71 (2 H, m, C(3')H and C(7)H), 7.82 (1 H, m, C(5')H), 7.85 (1H, d, *J* = 7.6 Hz, C(6)H), 8.30 (1 H, d, *J* = 7.8 Hz, C(9)H), 12.66 (1 H, br s, NH); δ_C (100 MHz, DMSO-d_6) 32.4 (CH_2), 111.9 (C2'), 112.6 (C6), 117.3 (CN), 117.4 (C9a), 121.4 (C9), 122.4 (C8), 128.1 (C5'), 130.2 (C3'), 130.9 (C7), 133.0 (C6'), 133.2 (C4'), 140.2 (C5a), 141.1 (C9b), 141.2 (C1'), 146.4 (C4a), 165.6 (C3); mp 276-278 °C;

m/z (ESI$^-$) 316 ([M - H]$^-$, 100%); HRMS (ESI$^+$) $C_{17}H_{10}N_5S^-$ ([M - H]$^-$) requires 316.0662; found 316.0673; ν_{max} (solid) 3061 (N-H), 2971 (aromatic C-H), 2804, 2226 (CN), 1598, 1580 (N-H), 1342; HPLC (Method 1) >99%, rt = 10.85 min

3-(methylthio)-5*H*-[1,2,4]triazino[5,6-*b*]indole 237

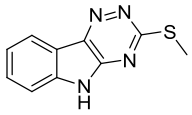

Methyl iodide (308 uL, 4.95 mmol) was added to a stirring solution on 5*H*-[1,2,4]triazino[5,6-*b*]indole-3-thiol **139** (1g, 4.95 mmol) and K_2CO_3 (683 mg, 4.95 mmol) and stirred at rt for 16 h in which the yellow solution turned green. The solvent was removed under reduced pressure to yield **237** as a light green solid (1.01 g, 95 %); δ_H (400 MHz, DMSO-d_6, 363K) 2.66 (3H, s, CH_3), 7.43 (1H, app td, *J* = 8.2, 1.0 Hz, C(8)H), 7.58 (1H, app dt, *J* = 8.2, 1.0 Hz, C(6)H), 7.67 – 7.71 (1H, m, C(7)H), 8.31 (1H, app dt, *J* = 8.2, 1.0 Hz, C(9)H), 12.60 (`1H, br s, NH); δ_C (100 MHz, DMSO-d_6) 13.4 (CH3), 112.7 (C6), 117.7 (C9a), 121.4 (C8), 122.4 (C7), 130.8 (C9), 140.3 (C9b), 140.8 (C5a), 146.7 (C4a), 167.6 (C3); mp (EZ Melt) >300 °C; *m/z* (ESI$^-$) 215 ([M - H]$^-$, 100%); HRMS (ESI$^+$) $C_{10}H_8N_4NaS$ ([M+Na]$^+$) requires 239.0362; found 239.0360; ν_{max} (solid) 3056, 2799, 1600, 1576, 1460, 1415, 1232; HPLC (Method 2) >99%, rt = 11.31

3-((2'-Fluorobenzyl)thio)-5*H*-[1,2,4]triazino[5,6-*b*]indole 238

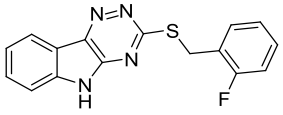

To an aqueous solution of NaOH (4 %, 5 mL) was added 5*H*-[1,2,4]triazino[5,6-*b*]indole-3-thiol **139** (150 mg, 0.74 mmol) and 2-fluoro benzyl bromide (89.6 µL, 0.74 mmol) and the reaction was stirred overnight at rt. The resulting precipitate was filtered, washed with

MeOH and dried to yield **238** as a light yellow solid (131 mg, 57 %). δ_H (400 MHz, DMSO-d_6) 4.59 (2H, s, CH_2), 7.16 (1H, app t, J = 7.6 Hz, C(5')H), 7.21 - 7.24 (1H, m, C(6')H), 7.32 - 7.35 (1H, m, C(3')H), 7.43 (1H, app t, J = 7.6 Hz, C(8)H), 7.58 (1H, d, J = 7.6 Hz, C(6)H), 7.65 (1H, app t, J = 7.6 Hz, C(4')H), 7.69 (1H, app t, J = 7.6 Hz, C(7)H), 8.30 (1H, d, J = 7.6 Hz, C(9)H), 12.67 (1H, br s, NH); δ_C (126 Hz, DMSO-d_6) 27.6 (CH_2), 112.7 (C6), 115.4 (d, J = 21 Hz, C3'), 117.6 (C9a), 121.5 (C8), 122.5 (C7) ,124.3 (d, J = 14 Hz, C1'), 124.5 (C9), 129.5 (d, J = 8 Hz, C4') 130.9 (C8), 131.4 (d, J = 4 Hz, C6'), 140.3 (C9b), 141.2 (C4a), 146.6 (C5a), 160.6 (d, J = 246 Hz, C2'-F), 166.3 (C3); δ_F (470 MHz, DMSO-d_6) -116.6 (C2'-F); *m/z* (ESI^-) 309 ($[M - H]^-$, 100%); HRMS (ESI^+) $C_{16}H_{11}FNaN_4S$ ($[M+Na]^+$) requires 333.0581; found 333.0572; mp 285-286 °C; ν_{max} (solid) 3054 (NH), 2800 (aromatic C-H), 1492 (N-H), 1461, 1323, 1176 (CF); HPLC (Method 1) 97.0%, rt = 11.13 min

3-((2'-Nitrobenzyl)thio)-5*H*-[1,2,4]triazino[5,6-*b*]indole 239

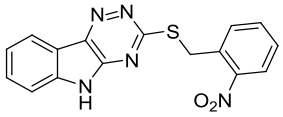

Following **General Procedure 3:** 2-nitrobenzyl bromide (160 mg, 0.74 mmol) was added to 5*H*-[1,2,4]triazino[5,6-*b*]indole-3-thiol **139** (150 mg, 0.74 mmol), Et_3N (155 μL, 1.11 mmol) in MeOH (5 mL). The resulting precipitate was filtered and washed to give **239** as a pale yellow solid (246 mg, 98 %). δ_H (400 MHz, DMSO-d_6, 363 K) 4.87 (2 H, s, CH_2), 7.40 - 7.43 (1 H, m, C(8)H), 7.55 (1H, app t, J = 7.3 Hz, C(4')H), 7.58 (1 H, d, J = 7.3 Hz, C(6)H), 7.66 - 7.72 (2H, m, C(7)H and C(5')H), 7.91 (1H, dd, J = 7.3, 1.3 Hz, C(6')H), 8.05 (1H, d, J = 7.3 Hz, C(3')H), 8.98 (1H, d, J = 7.3 Hz, C(9)H), 12.62 (1 H, bs, NH); δ_C (100 Hz, DMSO-d_6) 31.1 (CH_2), 112.4 (C6), 117.5 (C9a), 121.5 (C9), 122.5 (C8), 124.9 (C4'), 128.9 (C6'), 131.0 (C7), 132.5 (C5'), 133.1 (C9b), 133.7 (C3'), 140.4 (C5a), 141.3

(C1'), 146.5 (C4a), 148.4 (C2'), 166.0 (C3); mp 264-265 °C; *m/z* (ESI⁻) 336 ([M - H]⁻, 100%); HRMS (ESI⁺) $C_{16}H_{11}NaN_5O_2S$ ($[M+Na]^+$) requires 360.0526; found 360.0516; ν_{max} (solid) 3066 (NH), 2965 (aromatic C-H), 2793, 1602, 1524 and 1336 (NO_2); $C_{16}H_{11}N_5O_2S$ requires C, 56.96; H, 3.29; N, 20.76%; found C, 56.75; H, 3.16; N, 20.55%

3-((2'-(Trifluoromethyl)benzyl)thio)-5*H*-[1,2,4]triazino[5,6-*b*]indole 240

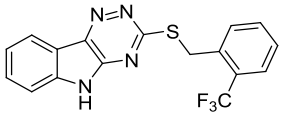

Following **General Procedure 3:** 2-trifluoromethyl benzyl bromide (176 mg, 0.74 mmol) was added to 5*H*-[1,2,4]triazino[5,6-*b*]indole-3-thiol **139** (150 mg, 0.74 mmol) and Et_3N (155 µL, 1.11 mmol) in MeOH (5 mL) and the resulting mixture was reacted at rt for 16 h. The precipitate was filtered and washed to give **240** as a faint yellow solid (196 mg, 74 %). δ_H (400 MHz, DMSO-d_6, 363 K) 4.76 (2 H, s, CH_2), 7.41 - 7.47 (1 H, m, C(8)H)), 7.49 - 7.55 (1 H, m, C(7)H), 7.59 (1 H, d, *J* = 8.2 Hz, C(6')H), 7.63 - 7.72 (2 H, m, C(5') and C(4')H), 7.78 (1 H, d, *J* = 7.9 Hz, C(3')H), 7.87 (1 H, d, *J* = 7.9 Hz, C(6)H), 8.32 (1 H, d, *J* = 7.9 Hz, C(9)H), 12.68 (1 H, br s, NH); δ_C (100 Hz, DMSO-d_6) 30.8 (CH_2), 112.7 (C6), 117.6 (C9a), 121.5 (C9), 122.5 (C8), 124.4 (q, *J* = 275 Hz, C2'), 126.2 (q, *J* = 5.7 Hz, C1')), 127.2 (q, J = 29 Hz, C3'), 128.1 (C9b), 131.0 (C7), 131.8 (C5'), 132.9 (C6'), 135.5 (C4'), 140.4 (C5a), 141.3 (C1'), 146.6 (C4a), 166.1 (C3); δ_F (470 MHz, DMSO-d_6) -58.1 (CF_3); mp 269-270 °C; *m/z* (ESI⁻) 359 ([M - H]⁻, 100%); HRMS (ESI⁻) $C_{17}H_{10}F_3N_4S^-$ ($[M-H]^-$) requires 359.0584; found 359.0595; ν_{max} (solid) 3061 (NH), 2970 (aromatic C-H), 2804, 1739, 1600, 1581 (N-H), 1299; HPLC (Method 1) >99%, rt = 11.71 min

3-((2'-Chlorobenzyl)thio)-5*H*-[1,2,4]triazino[5,6-*b*]indole 241

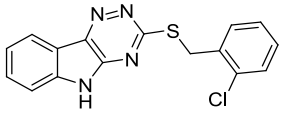

Following **General Procedure 3:** 2-chloro benzyl bromide (97 µL, 0.74 mmol) was added to 5*H*-[1,2,4]triazino[5,6-*b*]indole-3-thiol **139** (150 mg, 0.74 mmol) and Et_3N (155 µL, 1.11 mmol) in MeOH (5 mL) and the resulting mixture stirred at rt for 16 h. The precipitate was filtered and washed to give **241** as a faint yellow solid (190 mg, 79 %). δ_H (400 MHz, DMSO-d_6, 363 K) 4.67 (2 H, s, CH_2), 7.32 - 7.36 (2 H, m, C(8)H and C(6')H), 7.43 – 7.46 (1 H, m, C(7)H), 7.49 - 7.53 (1 H, m, C(4')H), 7.59 (1 H, d, *J* = 8.2 Hz, C(6)H), 7.70 (1 H, d, J = 7.6 Hz, C(3')H), 7.72 - 7.74 (1H, m, C(5')H), 8.32 (1 H, d, *J* = 7.6 Hz, C(9)H), 12.69 (1 H, br s, NH); δ_C (100 MHz, DMSO-d_6) 32.1 (CH_2), 112.7 (C6), 117.6 (C9a), 121.5 (C9), 122.5 (C8), 127.4 (C4'), 129.3 (C6'), 129.5 (C7), 131.0 (C5'), 131.5 (C3'), 133.4 (C1'), 134.9 (C2'), 140.4 (C5a), 141.3 (C9b), 146.6 (C4a), 166.3 (C3); mp 266-267 °C; *m/z* (ESI$^-$) 325 ([M - H]$^-$, 100%); HRMS (ESI$^+$) $C_{16}H_{10}ClNaN_4S$ ([^{35}ClM+Na]$^+$) requires 349.0285; found 349.0286, $C_{16}H_{10}ClNaN_4S$ ([^{37}Cl M+-Na]$^+$) requires 351.0256; found 351.0262; ν_{max} (solid) 3026 (N-H), 2973 (aromatic C-H), 2804, 1599, 1580 (N-H), 1342, 1177; HPLC (Method 1) >99%, rt = 11.44 min

3-((2'-(Trifluoromethoxy)benzyl)thio)-5*H*-[1,2,4]triazino[5,6-*b*]indole 242

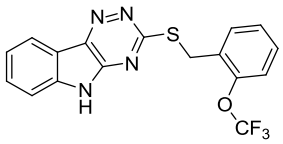

Following **General Procedure 3:** 2-(trifluoromethoxy)benzyl bromide (119 µL, 0.74 mmol) was added to 5*H*-[1,2,4]triazino[5,6-*b*]indole-3-thiol **139** (150 mg, 0.74 mmol) and Et_3N (155 µL, 1.11 mmol) in MeOH (5 mL) and the resulting mixture stirred was stirred at rt for 16 h. The precipitate was washed to give **242** as a pale yellow solid (139 mg, 50 %).

δ_H (400 MHz, DMSO-*d*$_6$, 363 K) 4.64 (2 H, s, CH_2), 7.36 – 7.39 (1H, m, C(4')H), 7.39 - 7.47 (3 H, m, C(8)H, C(5')H and C(6')H), 7.60 (1 H, d, *J* = 7.9 Hz, C(6)H), 7.71 (1 H, app t, *J* = 7.9 Hz, C(7)H), 7.76 (1 H, dd, *J* = 7.6, 1.6 Hz, C(3')H), 8.32 (1 H, d, *J* = 7.9 Hz, C(9)H), 12.67 (1 H, br s, NH); δ_C (100 MHz, DMSO-*d*$_6$) 28.4 (CH_2), 112.7 (C6), 117.6 (C9a), 120.2 (q, *J* = 257 Hz, CF_3), 120.4 (C9), 121.5 (C8), 122.5 (C3'), 127.5 (C5'), 129.5 (C7), 129.9 (C1'), 131.0 (C6'), 131.7 (C4'), 140.4 (C5a), 141.3 (C9b), 146.6 (C4a), 146.9 (C2'), 166.1 (C3); δ_F (470 MHz, DMSO-*d*$_6$) -55.9 (OCF_3); mp 285-288 °C; *m/z* (ESI^-) 375 ($[M - H]^-$, 100%); HRMS (ESI^+) $C_{17}H_{11}F_3N_4NaOS$ ($[M+Na]^+$) requires 399.0498; found 399.0499; ν_{max} (solid) 3062 (N-H), 2969 (aromatic C-H), 2805, 1607, 1461 (N-H), 1423; HPLC (Method 1) >99%, rt = 11.70 min

3-((2'-Methylbenzyl)thio)-5*H*-[1,2,4]triazino[5,6-*b*]indole 243

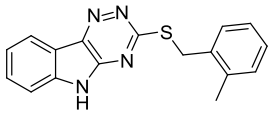

Following **General Procedure 3:** 2-methylbenzyl bromide (132 µL, 0.99 mmol) was added to 5*H*-[1,2,4]triazino[5,6-*b*]indole-3-thiol **139** (200 mg, 0.99 mmol), and Et_3N (206 µL, 1.49 mmol) in MeOH (5 mL). The resulting precipitate was filtered and washed to give **243** as a faint yellow solid (235 mg, 77 %). δ_H (400 MHz, DMSO-*d*$_6$, 363K) 2.42 (3 H, s, CH_3), 4.56 (2 H, s, SCH_2), 7.11 - 7.24 (3 H, m, C(4')H, C(5')H and C(6')H), 7.42 (1 H, t, *J* = 7.8 Hz, C(8)H), 7.49 (1 H, d, *J* = 7.8 Hz, C(3')H), 7.57 (1 H, d, *J* = 7.8 Hz, C(6)H), 7.65 - 7.72 (1 H, app t, *J* = 7.8 Hz, C(7)H), 8.30 (1 H, d, *J* = 7.8 Hz, C(9)H), 12.65 (1 H, br s, NH); δ_C (100 MHz, DMSO-*d*$_6$) 19.8 (CH_3), 33.3 (CH_2), 113.6 (C6), 118.5 (C9b), 122.3 (C9a), 123.3 (C8), 126.9 (C7), 128.4, 130.8, 131.2, 131.7 (C9, C4', C5' and C6'), 135.6 (C3'), 137.6 (C2'), 141.2 (C1'), 142.0 (C5a), 147.5 (C4a), 167.7(C3); mp 202-203 °C; *m/z* (ESI^-) 305 ($[M - H]^-$, 100%); HRMS (ESI^-) $C_{17}H_{13}N_4S^-$ ($[M-H]^-$) requires 305.0866; found

305.0870; ν_{max} (solid) 3060 (N-H), 2969 and 2801 (aromatic C-H), 1579, 1461, 1341, 1175; $C_{17}H_{14}N_4S$ requires C, 66.64; H, 4.61; N, 18.29%; found C, 66.40; H, 4.53; N, 18.24%

3-((2'(2H-tetrazol-5-yl)benzyl)thio)-5*H*-[1,2,4]triazino[5,6-*b*]indole 244

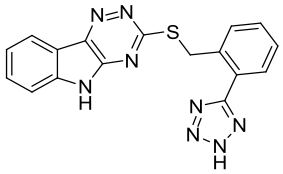

3-((2'-Cyanobenzyl)thio)-5*H*-[1,2,4]triazino[5,6-*b*]indole **236** (100 mg, 0.32 mmol) was added to a solution of NaN_3 (26 mg, 0.40 mmol), NH_4Cl (21 mg, 0.40 mmol) in DMF (5 mL) and heated at 120 °C for 16 h. The resulting solution was acidified using HCl (1M, 10 mL) and extracted with EtOAc (50 mL). The organic layer was washed with H_2O (50 mL), brine (50 mL), dried over Mg_2SO_4, then filtered and left to crystallise for 16 h. The resulting precipitate was filtered and dried to yield **244** as a yellow solid (86 mg, 75%); δ_H (500 MHz, DMSO-*d6*, 363K) 4.68 (2 H, s, SCH_2), 7.37 (1 H, app t, *J* = 7.6 Hz, C(8)H), 7.41 (1 H, app t, *J* = 7.6 Hz, C(5')H), 7.52 (1 H, d, *J* = 7.6 Hz, C(6')H), 7.58 - 7.66 (2 H, m, C(7)H and C(4')H), 7.77 (1 H, d, *J* = 7.7 Hz, C(6)H), 7.80 (1H, d, *J* = 7.6 Hz, C(3')H), 8.25 (1 H, d, *J* = 7.6 Hz, C(9)H); δ_C (125 MHz, DMSO-*d6*) 32.9 (SCH_2), 113.1 (C6), 117.9 (C9a), 121.9 (C9), 122.9 (C8), 128.6 (C5'), 130.8 (C3'), 131.4 (C7), 133.5 (C6'), 133.7 (C4'), 137.2 (C2'), 140.8 (C5a), 141.6 (C9b), 141.8 (C1'), 146.9 (C4a), 163.7 (C2'(C)N_2), 166.1 (C3); mp 272-273°C (decomp); *m/z* (ESI^-) 359 ($[M - H]^-$, 100%); HRMS (ESI^+) $C_{17}H_{11}N_8S^-$ ($[M-H]^-$) requires 359.0833; found 359.0832; ν_{max} (solid) 3256 (N-H), 3054, 1735, 1280; HPLC (Method 2) >97%, rt = 10.77 min

Ethyl 2'-(((5*H*-[1,2,4]triazino[5,6-*b*]indol-3-yl)thio)methyl)benzoate 245

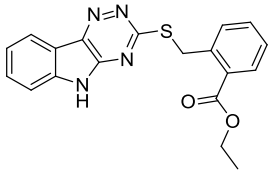

Following **General Procedure 3:** ethyl 2-(bromomethyl)benzoate (361 mg, 1.53 mmol) was added to 5*H*-[1,2,4]triazino[5,6-*b*]indole-3-thiol **139** (200 mg, 0.99 mmol) and Et_3N (303 µL, 2.18 mmol) in MeOH (10 mL) and stirred at rt for 16 h. The resulting precipitate was washed to give **245** as a faint yellow solid (436 mg, 83 %); δ_H (400 MHz, DMSO-d_6, 363K) 1.31 (3 H, t, *J* = 7.0 Hz, CH_3), 4.34 (2 H, q, *J* = 7.0 Hz, OCH_2-CH_3), 4.88 (2 H, s, SCH_2), 7.37 - 7.45 (2 H, m, C(8)H and C(5')H), 7.53 (1 H, app t, *J* = 7.7 Hz, C(7)H), 7.57 (1 H, d, *J* = 7.7 Hz, C(6)H) 7.63 - 7.70 (1 H, m, C(4')H), 7.75 (1 H, d, *J* = 7.7 Hz, C(6')H), 7.88 (1 H, dd, *J* = 7.8, 1.3 Hz, C(3')H), 8.29 (1 H, d, *J* = 7.8 Hz, C(9)H), 12.62 (1 H, s, NH); δ_C (100 MHz, DMSO-d_6) 14.9 (CH_3), 33.4 (SCH_2), 61.8 (OCH_2), 113.6 (C6), 118.5 (C9a), 122.3 (C9), 123.3 (C8), 128.5 (C5'), 130.3 (C9b), 131.4 (C3'), 131.7 (C4'), 132.4 (C6'), 133.1 (C7), 140.0 (C2'), 141.2 (C5a), 142.0 (C4a), 147.4 (C1'), 167.5 (C(O)), 167.7 (C3); mp 205-206 °C; *m/z* (ESI^-) 363 ($[M - H]^-$, 100%); ν_{max} (solid) 3151 (N-H), 2989 (aromatic C-H), 1707 (ester), 1597, 1250, 1079; HRMS (ESI^-) $C_{19}H_{15}N_4O_2S^-$ ($[M-H]^-$) requires 363.0921; found 363.0927; HPLC (Method 2) >95%, rt = 11.36 min

2'(((5*H*-[1,2,4]triazino[5,6-*b*]indol-3-yl)thio)methyl)benzoic acid 246

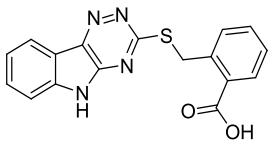

Ethyl 2'-(((5*H*-[1,2,4]triazino[5,6-*b*]indol-3-yl)thio)methyl)benzoate **245** (100 mg, 0.27 mmol), was added to a solution of aq. NaOH (1M, 270 µL, 0.27 mmol) in H_2O (5 mL) and

stirred at rt for 16 h. The solution was acidified with aq. HCl (1M) until a precipitate was formed, which was filtered and dried *in vacuo* to yield **246** as the final product (92 mg, 99%); δ_H (500 MHz, DMSO-*d6*, 363K) 4.99 (2 H, s, SCH_2), 7.12 - 7.22 (3 H, m, C(7)H, C(8)H and C(4')H), 7.47 - 7.52 (3 H, m, C(6)H, C(5')H and C(6')H), 7.68 - 7.72 (1 H, m, C(3')H), 8.15 (1 H, d, *J* = 7.6 Hz, C(9)H); δ_C (125 MHz, DMSO-*d6*) 32.1 (SCH_2), 114.9 (C6), 119.1 (C9a), 119.7 (C9), 120.7 (C8), 126.0 (C5'), 127.4 (C3'), 129.2 (C7), 129.5 (C6'), 129.6 (C4'), 130.0 (C2'), 137.2 (C9b), 141.1 (C5a), 142.5 (C4a), 150.4 (C1'), 166.4 (C3), 171.6 (COOH); mp >300 °C; *m/z* (ESI^-) 335 ($[M - H]^+$, 100%), *m/z* (ESI^+) 337 ($[M + H]^+$, 30%); HRMS (ESI^-) $C_{17}H_{11}N_4O_2S^-$ ($[M-H]^-$) requires 335.0608; found 335.0612; ν_{max} (solid) 3241 (v br), 1712 (COOH), 1553, 1378, 1166, 1090; HPLC (Method 2) >99%, rt = 10.11 min

3-((3'-Chlorobenzyl)thio)-5*H*-[1,2,4]triazino[5,6-*b*]indole 247

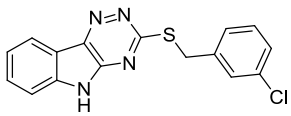

Following **General Procedure 3:** 3-chloro benzyl bromide (97 µL, 0.74 mmol) was added to 5*H*-[1,2,4]triazino[5,6-*b*]indole-3-thiol **139** (150 mg, 0.74 mmol) and Et_3N (155 µL, 1.11 mmol) in MeOH (5 mL) and the resulting mixture stirred at rt for 16 h. The precipitate was filtered and washed to give **247** as a very pale yellow solid (175 mg, 73 %). δ_H (400 MHz, DMSO-d_6, 363 K) 4.58 (2H, s, CH_2), 7.31 – 7.34 (1H, m, C(6')H), 7.36 (1H, t, *J* = 7.6 Hz, C(5')H), 7.44 (1H, app t, *J* = 7.6 Hz, C(8)H), 7.51 (1H, app d, *J* = 7.6 Hz, C(4')H), 7.57 - 7.62 (2H, m, C(6)H and C(1')H), 7.70 (1H, app t, *J* = 7.6 Hz, C(7)H), 8.31 (1H, d, *J* = 7.6, Hz C(9)H), 12.67 (1H, br s, NH); δ_C (100 MHz, DMSO-d_6) 33.3 (CH_2), 112.7 (C6), 117.6 (C9a), 121.5 (C9), 122.5 (C8), 127.1 (C5'), 127.8 (C6'), 128.8 (C2'), 130.3 (C4'), 131.0 (C7), 132.9 (C3'), 140.3 (C1'), 140.5 (C5a), 141.2 (C9b), 146.6 (C4a),

166.3 (C3); mp 266-267 °C; *m/z* (ESI⁻) 325 ([M - H]⁻, 100%); HRMS (ESI⁺) $C_{16}H_{10}{}^{35}ClN_4S$ ([M-H]⁻) requires 325.0320; found 325.0330, $C_{16}H_{10}{}^{37}ClN_4S$ ([M-H]⁻) requires 327.0291; found 327.0306; ν_{max} (solid) 3059 (N-H), 2799 (aromatic C-H), 1597, 1574, 1461 (N-H), 1336; HPLC (Method 2) >99%, rt = 11.54 min

3-((3'-Cyanobenzyl)thio)-5*H*-[1,2,4]triazino[5,6-*b*]indole 248

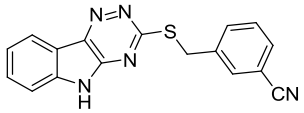

Following **General Procedure 3:** 3-cyano benzyl bromide (146 mg, 0.74 mmol) was added to 5*H*-[1,2,4]triazino[5,6-*b*]indole-3-thiol **139** (150 mg, 0.74 mmol) and Et_3N (155 µL, 1.11 mmol) in MeOH (5 mL) and the resulting mixture was stirred overnight. The precipitate was filtered and washed to give **248** as a faint yellow solid (137 mg, 58 %). δ_H (400 MHz, DMSO-d_6, 363 K) 4.62 (2H, s, CH_2), 7.44 (1H, app t, *J* = 7.6 Hz, C(8)H), 7.55 (1H, app t, *J* = 7.6 Hz, C(5')H), 7.59 (1H, app t, *J* = 7.6 Hz, C(6)H), 7.70 (1H, app t, *J* = 7.6 Hz, C(7)H), 7.72 – 7.75 (1H, m, C(6')H), 7.90 (1H, d, *J* = 8.2 Hz, C(4')H), 7.99 (1H, s, C(2')H), 8.32 (1H, d, *J* = 7.6 Hz, C(9)H), 12.67 (1H, br s, NH); δ_C (100 MHz, DMSO-d_6) 33.1 (CH_2), 111.3 (C3'), 112.7 (C6), 117.6 (CN), 118.7 (C9a), 121.5 (C9), 122.5 (C8), 129.7 (C6'), 131.0 (2C, C7 and C4'), 132.5 (C2'), 134.0 (C5'), 139.9 (C1'), 140.3 (C5a), 141.3 (C9b), 146.6 (C4a), 166.1 (C3); mp 279-281 °C; *m/z* (ESI⁻) 316 ([M - H]⁻, 100%); HRMS (ESI⁺) $C_{17}H_{11}N_5NaS$ ([M+Na]⁺) requires 340.0627; found 340.0619; ν_{max} (solid) 3120 (N-H), 2228 (CN), 1596, 1579 (N-H), 1338, 1173; $C_{17}H_{11}N_5S$ requires C, 64.34; H, 3.49; N, 22.07%; found C, 64.07; H, 3.33; N, 22.02%

3-((4'-Fluorobenzyl)thio)-5*H*-[1,2,4]triazino[5,6-*b*]indole 249

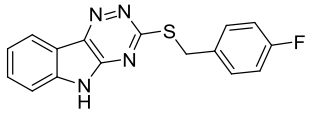

2-fluoro benzyl bromide (92.5 µL, 0.74 mmol) was added to aq NaOH (4 %, 5 mL) and 5*H*-[1,2,4]triazino[5,6-*b*]indole-3-thiol **139** (150 mg, 0.74 mmol) and. The reaction was stirred overnight at rt and resulting precipitate was filtered. Recrystallisation from MeOH yielded **249** as a light yellow solid (187 mg, 82 %). δ_H (400 MHz, DMSO-d_6, 363 K) 4.56 (2H, s, CH_2), 7.15 (2 H, app t, *J* = 8.8 Hz, C(3')H and C(5')H), 7.42 (1H, app t, *J* = 7.9 Hz, C(8)H), 7.56 (1H, d, *J* = 7.9 Hz, C(6)H), 7.57 (2 H, d, *J* = 7.9 Hz, C)2')H and C(6')H), 7.68 (1H, app t, *J* = 7.9 Hz, C(7)H), 8.29 (1H, d, *J* = 7.9 Hz, C(9)H), 12.64 (1H, br s, NH); δ_C (100 Hz, DMSO-d_6) 33.2 (CH_2), 112.7 (C6), 115.2 (2C, d, J = 21 Hz, C3' and C5'), 117.6 (C9a), 121.5 (C8), 122.4 (C7), 130.9 (C9), 131.0 (2C, d, *J* = 8 Hz, C2' and C6'), 133.9 (d, *J* = 3 Hz, C1'), 140.3 (C9b), 141.1 (C4a), 146.6 (C5a), 161.3 (d, *J* = 243 Hz, C4'), 166.5 (C3); δ_F (470 MHz, DMSO-d_6) 115.3 (C4'-F); mp 261-264 °C; *m/z* (ESI^-) 309 ($[M - H]^-$, 100%); HRMS (ESI^+) $C_{16}H_{11}FN_4NaS$ ($[M+Na]^+$) requires 333.0581; found 333.0576; ν_{max} (solid) 3054 (NH), 2798 (aromatic C-H), 1600, 1539, 1461 (N-H), 1417; HPLC (Method 1) >97%, rt = 11.11 min

3-((4'-Chlorobenzyl)thio)-5*H*-[1,2,4]triazino[5,6-*b*]indole 250

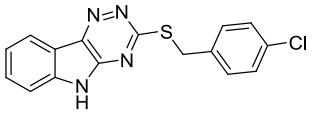

Following **General Procedure 3:** 3-chloro benzyl bromide (152 mg, 0.74 mmol) was added to 5*H*-[1,2,4]triazino[5,6-*b*]indole-3-thiol **139** (150 mg, 0.74 mmol) and Et_3N (155 µL, 1.11 mmol) in MeOH (5 mL) and the resulting mixture stirred at rt for 16 h. The precipitate was filtered and washed to give **250** as a pale yellow solid (142 mg, 59 %). δ_H

(400 MHz, DMSO-d_6, 363 K) 4.56 (2H, s, CH_2), 7.38, (2H, d, J = 8.8 Hz, C(2')H and C(6')H), 7.44 (1H, app t, J = 7.6 Hz, C(8)H), 7.55 (2H, d, J = 8.8 Hz, C(3')H and C(5')H), 7.58 (1H, d, J = 7.6 Hz, C(6)H), 7.70 (1H, app t, J = 7.6 Hz, C(7)H), 8.31 (1H, d, J = 7.6 Hz, C(9)H), 12.66 (1H, br s, NH); δ_C (100 MHz, DMSO-d_6) 33.2 (CH_2), 112.7 (C6), 117.6 (C9a), 121.5 (C9), 122.5 (C8), 128.4 (2C, C2' and C6'), 128.6 (C7), 130.9 (2C, C3' and C5'), 131.8 (C4'), 137.0 (C1'), 140.3 (C5a), 141.2 (C9b), 146.6 (C4a), 166.4 (C3); mp 248-250 °C; *m/z* (ESI$^-$) 325 ([^{35}ClM - H]$^-$, 100%), 327 ([^{37}Cl M – H]$^-$, 45%); HRMS (ESI$^+$) $C_{16}H_{10}{}^{35}ClNaN_4S$ ([M+H]$^+$) requires 349.0285; found 349.0284, $C_{16}H_{10}{}^{37}ClNaN_4S$ ([M+H]$^+$) requires 351.0256; found 351.0258; ν_{max} (solid) 3054 (N-H), 2797 (aromatic C-H), 1600, 1578, 1489 (N-H), 1461, 1338; HPLC (Method 1) >98%, rt = 11.51 min

3-((2',4'-Dinitrobenzyl)thio)-5*H*-[1,2,4]triazino[5,6-*b*]indole 251

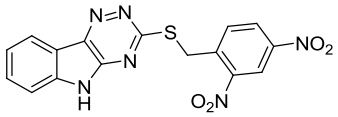

Following **General Procedure 3:** 2,4-dinitrobenzyl bromide (129 mg, 0.50 mmol) was added to 5*H*-[1,2,4]triazino[5,6-*b*]indole-3-thiol **139** (100 mg, 0.50 mmol) and Et_3N (103 µL, 0.74 mmol) in MeOH (5 mL) and stirred at rt for 16 h. The resulting precipitate was filtered washed to give **251** as a faint yellow solid (132 mg, 70 %); δ_H (500 MHz, DMSO-d_6, 363K) 4.95 (2H, s CH_2), 7.43 (1H, t, J = 8.0 Hz, C(8)H), 7.59 (1H, d, J = 8.0 Hz, C(6)H), 7.70 (1H, app t, J = 8.0 Hz, C(7)H), 8.19 (1H, d, J = 8.6 Hz, C(6')H), 8.29 (1H, d, J = 8.0 Hz, C(9)H), 8.49 (1H, dd, J = 8.6, 2.5 Hz, C(5')H), 8.74 (1H, d, J = 2.5 Hz, C(3')H), 12.63 (1H, br s, NH); δ_C (125 MHz, DMSO-d_6) 30.8 (CH_2), 112.8 (C6), 117.5 (C9a), 120.2 (C3'), 121.6 (C9), 122.6 (C8), 127.5 (C5'), 131.1 (C7), 134.0 (C6'), 140.3 (C5a), 140.5 (C9b), 141.5 (C1'), 146.5 (C4a), 146.6 (C4'), 148.4 (C2'), 165.3 (C3); mp 255-259 °C; *m/z* (ESI$^-$) 381 ([M - H]$^-$, 100%); HRMS (ESI$^+$) $C_{16}H_{10}N_6NaO_4S$ ([M+Na]$^+$)

requires 405.0376; found 405.0372; ν_{max} (solid) 3054 (N-H), 2803 (aromatic C-H), 1604, 1529 and 1338 (NO_2), 1217; $C_{16}H_{10}N_6O_4S$ requires C, 50.08; H, 2.64; N, 21.98%; found C, 50.08; H, 2.52; N, 21.83%

3-((2'-Fluoro-6'-nitrobenzyl)thio)-5*H*-[1,2,4]triazino[5,6-*b*]indole 252

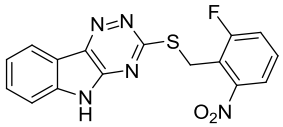

Following **General Procedure 3:** 2-fluoro-6-nitrobenzyl bromide (116 mg, 0.50 mmol) was added to 5*H*-[1,2,4]triazino[5,6-*b*]indole-3-thiol **139** (100 mg, 0.50 mmol) and Et_3N (103 μL, 0.74 mmol) in MeOH (5 mL). The resulting precipitate was filtered and washed to give **252** as a faint yellow solid (135 mg, 75 %); δ_H (500 MHz, DMSO-d_6, 363K) 4.86 (2 H, s, CH_2), 7.40 (1 H, app t, *J* = 7.8 Hz, C(8)H), 7.53 - 7.72 (4 H, m, C(3')H, C(4')H, C(6)H and C(7)H), 7.87 (1 H, d, *J* = 8.1 Hz, C(5')H), 8.28 (1 H, d, *J* = 7.8 Hz, C(9)H), 12.57 (1 H, br s, NH); δ_C (125 MHz, DMSO-d_6) 24.8 (d, *J* = 3.2 Hz, CH_2), 113.6 (C6), 118.4 (C9a), 121.7 (d, *J* = 22 Hz, C3'), 121.8 (d, *J* = 3.2 Hz, C4'), 121.9 (d, *J* = 17 Hz, C5'), 122.4 (C8), 123.4 (C7), 130.9 (d, *J* = 9.6 Hz, C1'), 131.8 (C9), 141.3 (C5b), 142.3 (C9b), 147.3 (C4a), 150.5 (d, *J* = 7.4 Hz, C6'), 160.2 (C3), 164.6 (d, *J* = 250 Hz, C2'); δ_F (470 MHz, DMSO-d_6) -110.5 (C1'-F); mp 271-172 °C; *m/z* (ESI^-) 354 ($[M - H]^-$, 100%), *m/z* (ESI^+) 378 ($[M + Na]^+$, 100%); HRMS (ESI^+) $C_{16}H_{10}FN_5NaO_2S$ ($[M+Na]^+$) requires 378.0431; found 378.0425; ν_{max} (solid) 3233 (N-H), 1597, 1581, 1531 (NO_2), 1178; $C_{16}H_{10}FN_5O_2S$ requires C, 54.08; H, 2.84; N, 19.72%; found C, 53.97; H, 2.82; N, 19.57%

3-((2'-Nitrophenyl)thio)-5*H*-[1,2,4]triazino[5,6-*b*]indole 253

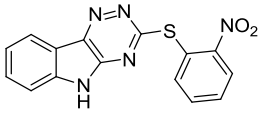

2-fluoronitrobenzene (87 µL, 0.82 mmol) was added to a stirring suspension of 5*H*-[1,2,4]triazino[5,6-*b*]indole-3-thiol **139** (150 mg, 0.74 mmol) in DMF (5 mL), K_2CO_3 (205 mg, 1.49 mmol) at rt. The resulting suspension was heated to 100 °C for 24 h. Upon cooling, the reaction mixture was diluted with H_2O (50 mL) and extracted with ethyl acetate (3 x 30 mL). The combined organic extracts were washed with brine (50 mL), dried over $MgSO_4$, filtered and concentrated *in vacuo* to yield **253** as an orange solid (97 mg, 41 %). δ_H (400 MHz, DMSO-d_6, 363 K) 7.43 (1 H, app t, *J* = 7.6 Hz, C(8)H), 7.54 (1 H, d, *J* = 8.1 Hz, C(6)H), 7.69 - 7.81 (3 H, m, C(7)H, C(4')H and C(5')H), 7.92 (1 H, d, *J* = 7.6, Hz, C(6')H), 8.19 (1 H, dd, *J* = 7.3 Hz, C(3')H), 8.31 (1 H, d, *J* = 7.6 Hz, C(9)H), 12.81 (1 H, br s, NH); δ_C (100 MHz, DMSO-d_6) 113.7 (C6), 118.2 (C9a), 122.6 (C9), 123.6 (C8), 126.1 (C6'), 126.4 (C4'), 131.0 (C5'), 132.3 (C7), 134.5 (C3'), 137.1 (C9b), 141.6 (C5a), 142.9 (C1'), 147.6 (C4a), 151.3 (C2'), 165.9 (C3); mp 262-264 °C; *m/z* (ESI^-) 322 ($[M-H]^-$, 100%); HRMS (ESI^+) $C_{15}H_9N_5NaO_2S$ ($[M+Na]^+$) requires 346.0369; found 346.0366; ν_{max} (solid) 3064 (N-H), 2799, 1605, 1580, 1525 (NO_2), 1459; HPLC (Method 1) >99%, rt = 11.33 min

2-(((5*H*-[1,2,4]Triazino[5,6-*b*]indol-3-yl)sulfinyl)methyl)benzonitrile 254

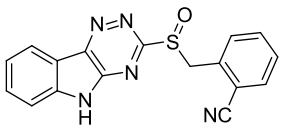

2'(((5*H*-[1,2,4]triazino[5,6-*b*]indol-3-yl)thio)methyl)benzonitrile **236** (50 mg, 0.16 mmol) was added to a solution of trifluoroacetic acid (5 mL) and peroxytrifluoroacetic acid (4 M, 40 µL, 0.16 mmol) and stirred for 16 h at rt. The resulting solution was concentrated *in*

vacuo to yield the crude product which was washed with MeOH to yield the sulfoxide **254** as a yellow solid (50 mg, 95 %); δ_H (500 MHz, DMSO-d_6, 363K) 4.64 (1H, d, J = 13.2, SCH_2), 4.81 (1H, d, J = 13.2 Hz, SCH_2), 7.43 (1H, d, J = 7.6 Hz, C(6)H), 7.52 (1H, app td, J = 7.6, 1.3 Hz, C(8)H), 7.55 (1H, app t, J = 7.6 Hz, C(5')H), 7.65 (1H, app td, J = 7.6, 1.3 Hz, C(7)H), 7.72 (1H, d, J = 7.6 Hz, C(3')H), 7.80 (1H, dd, J = 7.6, 1.0 Hz, C(6')H), 7.84 (1H, app t, J = 7.6, 1.3 Hz, C(4')H), 8.48 (1H, d, J = 7.6 Hz, C(9)H), 13.19 (1H, br s, NH); δ_C (125 MHz, DMSO-d_6) 57.7 (CH_2), 112.9 (C2'), 113.2 (C6), 117.0 (C9a), 117.2 (CN), 122.6 (C9), 123.1 (C5'), 129.0 (C8), 132.1 (C3'), 132.5 (C7), 133.1, 133.1 (C6' and C4'), 133.2 (C9b), 141.7 (C5a), 144.5 (C1'), 147.1 (C4a), 166.5 (C3); mp 237-239 °C (EZ Melt); *m/z* (ESI⁻) 332 ([M - H]$^-$, 100%); HRMS (ESI$^+$) $C_{17}H_{11}N_5NaOS$ ([M+Na]$^+$) requires 356.0577; found 356.0571; ν_{max} (solid) 3244 (N-H), 2228 (CN), 1621, 1591, 1570, 1416, 1183; HPLC (Method 2) >95%, rt = 9.22 min

6-Bromo-5*H*-[1,2,4]triazino[5,6-*b*]indole-3-thiol 259

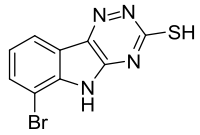

7-Bromoisatin **255** (1.00 g, 4.45 mmol), thiosemicarbizide (405 mg, 4.45 mmol) and K_2CO_3 (920 mg, 6.67 mmol) were suspended in H_2O (50 mL). The reaction mixture was stirred at reflux for 16 h over which time the dark brown suspension became a clear light brown solution. The solution was carefully acidified by dropwise addition of glacial acetic acid and resulting precipitate was filtered. The precipitate was triturated with hot DMF to yield **259** as a red solid (416 mg, 34 %). δ_H (500 MHz, DMSO-d_6, 363K) 7.28 (1H, app t, J = 7.6 Hz, C(8)H), 7.84 (1H, d J = 7.6 Hz, C(7)H), 8.01 (1H, d, J = 7.6 Hz, C(9)H); δ_C (125 MHz, DMSO-d_6) 116.1 (C9), 117.5 (C9a), 123.8 (C8), 124.9 (C6), 126.3 (C7), 135.5 (C9b), 144.6 (C5a), 149.9 (C4a), 176.6 (C3); mp >300 °C; *m/z* (ESI⁻) 279 ([^{79}BrM - H]$^-$,

100%), 281 ([^{81}BrM - H]$^-$, 100%); HRMS (ESI$^+$) $C_9H_5BrN_4NaS$ ([^{79}BrM+Na]$^+$) requires 278.9346; found 278.9355, ([^{81}BrM+Na]$^+$) requires 280.9325; found 280.9334; ν_{max} (solid) 2849 (br, S-H), 1629, 1603, 1581 (N-H), 1386, 1151

7-Bromo-5*H*-[1,2,4]triazino[5,6-*b*]indole-3-thiol 260

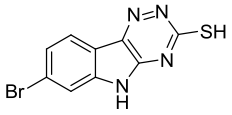

6-Bromoisatin **256** (1.00 g, 4.45 mmol), thiosemicarbizide (405 mg, 4.45 mmol) and K_2CO_3 (920 mg, 6.67 mmol) were suspended in H_2O (50 mL). The reaction mixture was stirred at reflux for 16 h over which time the dark brown suspension became a clear light brown solution. The solution was carefully acidified by dropwise addition of glacial acetic acid and resulting precipitate was filtered. The precipitate was triturated with hot DMF to yield **260** as a red solid (1.12 g, 90 %). δ_H (500 MHz, DMSO-d_6, 363K) 7.50 (1H, d, J = 7.5 Hz, C(8)H), 7.60 (1H, s, C(6)H), 7.94 (1H, 1H, d, J = 7.5 Hz, C(9)H); δ_C (125 MHz, DMSO-d_6) 105.5 (C7), 120.3 (C6), 121.3 (C9), 124.8 (C8), 134.6 (C9a), 136.1 (C9b), 142.4 (C5a), 150.2 (C4a), 179.8 (C3); mp >300 °C; *m/z* (ESI$^-$) 279 ([^{79}BrM - H]$^-$, 100%), 281 ([^{81}BrM - H]$^-$, 100%); HRMS (ESI$^+$) $C_9H_5BrN_4NaS$ ([^{79}BrM+Na]$^+$) requires 278.9346; found 278.9351, ([^{81}BrM+Na]$^+$) requires 280.9325; found 280.9330; ν_{max} (solid) 2919 (br, S-H), 1589 (N-H), 1422, 1359, 1161

8-Bromo-5*H*-[1,2,4]triazino[5,6-*b*]indole-3-thiol 261

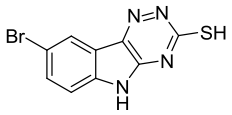

5-Bromoisatin **257** (1.00 g, 4.45 mmol), thiosemicarbizide (405 mg, 4.45 mmol) and K_2CO_3 (920 mg, 6.67 mmol) were suspended in H_2O (50 mL). The reaction mixture was

stirred at reflux for 16 h over which time the dark brown suspension became a clear light brown solution. The solution was carefully acidified by dropwise addition of glacial acetic acid and resulting precipitate was filtered. The precipitate was triturated with hot DMF to yield **261** as a red solid (1.23 g, 97 %). δ_H (500 MHz, DMSO-d_6, 363K) 1.90 (1H, br s, NH), 7.38 (1H, d, J = 8.6 Hz, C(6)H), 7.74 (1H, dd, J = 8.6, 1.8 Hz, C(7)H), 8.15, (1H, d, J = 1.8 Hz, C(9)H); δ_C (125 MHz, DMSO-d_6) 115.6 (C8), 115.9 (C6), 120.8 (C9), 125.0 (C7), 134.9 (C9a), 135.8 (C9b), 143.5 (C5a), 150.4 (C4a), 180.1 (C3); mp >300 °C; *m/z* (ESI$^-$) 279 ([^{79}BrM - H]$^-$, 100%), 281 ([^{81}BrM - H]$^-$, 100%); HRMS (ESI$^+$) $C_9H_5BrN_4NaS$ ([^{79}BrM+Na]$^+$) requires 278.9346; found 278.9354, ([^{81}BrM+Na]$^+$) requires 280.9325; found 280.9333; ν_{max} (solid) 3097 (N-H), 2858 (S-H), 1603, 1589 (N-H), 1446, 1311

9-Bromo-5*H*-[1,2,4]triazino[5,6-*b*]indole-3-thiol 262

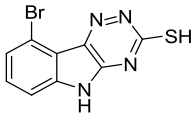

4-Bromoisatin **258** (1.00 g, 4.45 mmol), thiosemicarbizide (405 mg, 4.45 mmol) and K_2CO_3 (920 mg, 6.67 mmol) were suspended in H_2O (50 mL). The reaction mixture was stirred at reflux for 16 h over which time the dark brown suspension became a clear light brown solution. The solution was carefully acidified by dropwise addition of glacial acetic acid and resulting precipitate was filtered. The precipitate was triturated with hot DMF to yield **262** as a red solid (1.18 g, 95 %). δ_H (500 MHz, DMSO-d_6, 363K) 7.43- 7.52 (3H, m, C(6)H, C(7)H) and C(8)H), 14.68 (1H, br s, NH); δ_C (125 MHz, DMSO-d_6) 113.0 (C6), 117.0 (C9), 118.3 (C8), 127.4 (C7), 133.5 (C9a), 136.1 (C9b), 145.3 (C4a), 149.9 (C5a), 180.0 (C3); mp >300 °C; *m/z* (ESI$^-$) 279 ([^{79}BrM - H]$^-$, 100%), 281 ([^{81}BrM - H]$^-$, 100%); HRMS (ESI$^+$) $C_9H_5BrN_4S$ ([^{79}BrM+Na]$^+$) requires 278.9346; found 278.9350,

($[^{81}BrM+Na]^+$) requires 280.9325; found 280.9331; ν_{max} (solid) 3389 (br, N-H), 3297 (S-H), 1604, 1573 (N-H), 1140

6.3.1.1 Phenyl Substituted Derivatives

2'-(((6-Bromo-5*H*-[1,2,4]triazino[5,6-*b*]indol-3-yl)thio)methyl)benzonitrile 263

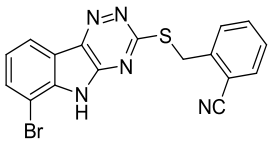

Following **General Procedure 3:** 2-cyanobenzyl bromide (70 mg, 0.36 mmol) was added to 6-bromo-5*H*-[1,2,4]triazino[5,6-*b*]indol-3-thiol **259** (100 mg, 0.36 mmol) and Et_3N (75 µL, 0.54 mmol) in MeOH (5 mL) and stirred at rt for 16 h. The resulting precipitate was filtered and washed to give **263** as a light yellow solid (128 mg, 87 %). δ_H (500 MHz, DMSO-d_6, 363K) 4.74 (2H, s, CH_2), 7.34 (1H, app t, J = 7.8 Hz, C(8)H), 7.47 (1H, app t, J = 8.1 Hz, C(4')H), 7.66 (1H, app t, J = 7.8 Hz, C(5')H), 7.84 - 7.89 (3H, m, C(7)H, C(3')H and C(6')H), 8.29 (1H, d, J = 7.6 Hz, C(9)H), 12.94 (1H, br s, NH); δ_C (125 MHz, DMSO-d_6) 33.45 (CH_2), 106.0 (C6), 112.8 (C2'), 118.31 (CN), 120.6 (C9a), 121.5 (C9), 124.7 (C8), 129.1 (C5'), 131.4, 134.0, 134.2, 134.2 (4xAr-C) 139.9 (C9b), 141.9 (C1'), 142.2 (C5a), 148.0 (C4a), 167.4 (C3); mp 226-228 °C; *m/z* (ESI^+) 418 ($[^{79}BrM + Na]^+$, 50%), 420 ($[^{81}BrM + Na]^-$, 50%), *m/z* (ESI^-) 394 ($[^{79}BrM - H]^-$, 100%), 396 ($[^{81}BrM - H]^-$, 100%); HRMS (ESI^+) $C_{17}H_{10}BrN_5NaS$ ($[^{79}BrM+Na]^+$) requires 417.9732; found 417.9733, ($[^{81}BrM+Na]^+$) requires 419.9712; found 419.9717; ν_{max} (solid) 3065 (N-H), 2780, 2228 (CN), 1600 ,1401, 1436; HPLC (Method 2) >97%, rt = 11.47 min

2-(((7-Bromo-5*H*-[1,2,4]triazino[5,6-*b*]indol-3-yl)thio)methyl)benzonitrile 264

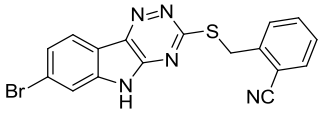

Following **General Procedure 3:** 2-cyano benzyo bromide (70 mg, 0.36 mmol) was added to 8-bromo-5*H*-[1,2,4]triazino[5,6-*b*]indole-3-thiol **260** (100 mg, 0.36 mmol) and Et_3N (75 µL, 0.54 mmol) in MeOH (5 mL) and stirred at rt for 16 h. The resulting precipitate was

filtered and washed to give **264** as a light yellow solid (130 mg, 92 %). δ_H (400 MHz, DMSO-d_6) 4.75 (2 H, s, CH_2), 7.48 (1 H, app t, J = 7.9 Hz, C(5')H), 7.60 (1 H, dd, *J* = 8.2, 1.6 Hz, C(8)H), 7.68 (1 H, app t, *J* = 7.9 Hz, C(4')H), 7.77 (1 H, d, *J* = 1.6 Hz, C(6)H), 7.84 (1 H, d, *J* = 7.9 Hz, C(3')H), 7.88 (1H, dd, *J* = 7.9, 1.3 Hz, C(6')H), 8.26 (1 H, d, *J* = 8.2 Hz, C(9)H) 12.81 (1 H, br s, NH); δ_C (100 MHz, DMSO-d_6) 32.5 (CH_2) 112.0 (C2'), 115.5 (C7), 116.9 (C6), 117.5 (CN), 123.2, 123.7, 125.6 (3xAr-C), 128.3 (C5'), 130.4 (C3'), 133.1, 133.3 (2xAr-C), 140.9 (C9b), 141.1 (C1'), 141.3 (C5a), 146.9 (C4a), 166.2 (C3); mp 289-291 °C; *m/z* (ESI^+) 418 ($[^{79}BrM + Na]^-$, 20%), 420 ($[^{81}BrM + Na]^+$, 20%), *m/z* (ESI^-) 394 ($[^{79}BrM - H]^-$, 100%), 396 ($[^{81}BrM - H]^-$, 100%); HRMS (ESI^+) $C_{17}H_{10}BrN_5NaS$ ($[^{79}BrM+Na]^+$) requires 417.9732; found 417.9737, ($[^{81}BrM+Na]^+$) requires 419.9712; found 419.9719; ν_{max} (solid) 3076 (N-H), 3012 (aromatic C-H), 2701, 2228 (CN), 1608, 1420; $C_{17}H_{10}BrN_5S \cdot 0.35H_2O$ requires C, 51.62; H, 2.41; N, 17.37%; found C, 50.72; H, 2.68; N, 17.40%

2-(((8-Bromo-5*H*-[1,2,4]triazino[5,6-*b*]indol-3-yl)thio)methyl)benzonitrile 265

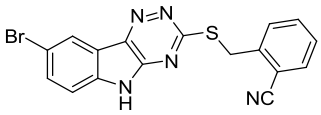

Following **General Procedure 3:** 2-cyanobenzyl bromide (70 mg, 0.36 mmol) was added to 8-bromo-5H-[1,2,4]triazino[5,6-b]indole-3-thiol **261** (100 mg, 0.36 mmol), Et_3N (75 µL, 0.54 mmol) in MeOH (5 mL) and stirred at rt for 16 h. The resulting precipitate was washed to give **265** as a light yellow solid (110 mg, 78 %). δ_H (400 MHz, DMSO-d_6) 4.73 (2H, s, CH_2), 7.47 (1H, t, *J* = 7.6 Hz, C(4')H), 7.53 (1H, d, *J* = 8.6 Hz, C(6)H), 7.66 (1H, t, *J* = 7.6 Hz, C(5')H), 7.78 - 7.88 (3H, m, C(7)H, C(3')H and C(6')H), 8.43 (1H, s, C(9)H), 12.80 (1H, br s, NH); δ_C (100 MHz, DMSO-d_6) 33.4 (CH_2), 112.9 (C2'), 115.4 (C6), 115.7 (C8), 118.3 (CN), 120.4 (C9a), 124.7, 129.11, 131.3, 134.0, 134.2, 140.0 (6xAr-C), 142.0

(C9b) 147.5 (C1') 153.7 (C5a), 155.0 (C4a), 167.4 (C3); mp 286-288 °C; *m/z* (ESI^+) 418 ($[^{79}BrM + Na]^-$, 20%), 420 ($[^{81}BrM + Na]^+$, 20%), *m/z* (ESI^-) 394 ($[^{79}BrM - H]^-$, 100%), 396 ($[^{81}BrM - H]^-$, 100%); HRMS (ESI^+) $C_{17}H_{10}BrN_5NaS$ ($[^{79}BrM+Na]^+$) requires 417.9732; found 417.9732, ($[^{81}BrM+Na]^+$) requires 419.9712; found 419.9718; ν_{max} (solid) 3091 (N-H), 2967 (aromatic C-H), 2796, 2225 (CN), 1591; HPLC (Method 2) >95%, rt = 11.72 min

2'-(((9-Bromo-5*H*-[1,2,4]triazino[5,6-*b*]indol-3-yl)thio)methyl)benzonitrile 266

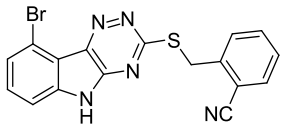

Following **General Procedure 3:** 2-cyanobenzyl bromide (70 mg, 0.36 mmol) was added to 9-bromo-5*H*-[1,2,4]triazino[5,6-*b*]indol-3-thiol **262** (100 mg, 0.36 mmol) and Et_3N (75 µL, 0.54 mmol) in MeOH (5 mL) and stirred at rt for 16 h. The resulting precipitate was filtered and washed to give **266** as a light yellow solid (91 mg, 64 %). δ_H (400 MHz, DMSO-d_6, 363K) 4.76 (2 H, s, CH_2), 7.48 (1 H, app t, *J* = 7.8 Hz, C(5')H), 7.55 - 7.64 (3 H, m, C(6)H, C(7)H, C(9)H), 7.67 (1 H, app t, *J* = 7.8 Hz, C(4')H), 7.83 (1 H, d, *J* = 7.8 Hz, C(3')H), 7.88 (1 H, dd, *J* = 7.8, 1.0 Hz, C(6')H), 12.89 (1 H, br s, NH); δ_C (100 MHz, DMSO-d_6) 33.4 (CH_2), 112.8 (C6), 112.9 (C9), 116.9 (C2'), 117.9 (CN), 118.3 (C9a), 127.0, 129.1, 131.2, 132.5 (4xAr-C), 134.0 (C6'), 134.2 (C4'), 141.9 (C9b), 142.5 (C5a), 147.3 (C1'), 149.1 (4a), 167.0 (C3); mp 283-284 °C; *m/z* (ESI^+) 418 ($[^{79}BrM + Na]^+$, 50%), 420 ($[^{81}BrM + Na]^-$, 50%), *m/z* (ESI^-) 394 ($[^{79}BrM - H]^-$, 100%), 396 ($[^{81}BrM - H]^-$, 100%); HRMS (ESI^+) $C_{17}H_{10}BrN_5NaS$ ($[^{79}BrM+Na]^+$) requires 417.9732; found 417.9730, ($[^{81}BrM+Na]^+$) requires 419.9712; found 419.9718; ν_{max} (solid) 3269 (br, N-H), 3076 and 3039 (aromatic C-H), 2232 (CN), 1583, 1304, 1168; HPLC (Method 2) >99%, rt = 11.42 min

4-Phenyl indoline-2,3-dione 285

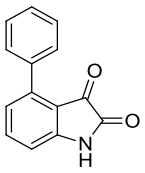

$Pd(PPh_3)_2Cl_2$ (31 mg, 0.04 mmol) was added to a degassed suspension of 4-bromoisatin **258** (100 mg, 0.44 mmol), potassium phenyltrifluoroborate (114 mg, 0.62 mmol), K_3PO_4 (338 mg, 1.59 mmol) in a THF/ H_2O (2.5 mL, 3:1) mixture and reacted at 120 °C for 16 h to yield gave the crude reaction mixture. The mixture was extracted with EtOAc (40 mL), washed with H_2O (40 mL), brine (40 mL), dried over $MgSO_4$, filtered and concentrated in vacuo. The crude oil was purified *via* flash column chromatography (eluent 40-60 °C, petrol/EtOAc, 4:1) to afford **285** as an orange solid (40 mg, 42%); δ_H (500 MHz, DMSO-d_6, 363K) 6.89 (1H, d, *J* = 7.7 Hz, C(7)H), 7.01 (1H, d, *J* = 7.7 Hz, C(5)H), 7.40 - 7.48 (3 H, m, C(3')H C(4')H and C(5')H), 7.51 - 7.57 (2H, m, C(2')H and C(6')H), 7.60 (1H, app t, *J* = 7.7Hz, C(6)H), 11.13 (1H, br s, NH); δ_C (125 MHz, DMSO-d_6) 112.0 (C7), 115.1 (C3a), 125.2 (C5), 128.2 (C4), 128.9 (C5'), 129.5 (C6'), 129.7 (C3'), 134.9 (C2'), 137.2 (C1'), 138.7 (C6), 142.4 (C4), 152.3 (7a), 159.9 (C2), 183.8 (C3); mp 205-206 °C; *m/z* (ESI^-) 222 ($[M - H]^-$, 100%); HRMS (ESI^+) $C_{14}H_9NNaO_2$ ($[M + Na]^+$) requires 246.0525; found 246.0526; ν_{max} (solid) 3114 (aromatic C-H), 2928 (C-H), 1722 (C=O carbonyl), 1589 (C=O amide)

9-Phenyl-5*H*-[1,2,4]triazino[5,6-*b*]indole-3-thiol 287

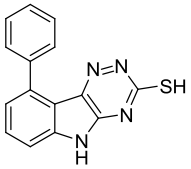

Method A: 9-bromo-5H-[1,2,4]triazino[5,6-b]indole-3-thiol **262** (170 mg, 0.61 mmol), potassium phenyltrifluoroborate (156 mg, 0.85 mmol), K_3PO_4 (463 mg, 2.19 mmol) and

$Pd(PPh_3)_2Cl_2$ (42.6 mg, 0.06 mmol) in THF/water (3:1, 3 mL) under nitrogen at 120 °C for 16 h, produced a complex mixture. No conversion to product was observed.

Method B: Following **General Procedure 2**: 4-Phenyl indoline-2,3-dione **285** (70 mg, 0.31 mmol), thiosemicarbizide (29 mg, 0.31 mmol) and K_2CO_3 (65 mg, 0.47 mmol) in water (7 mL) produced **287** as a yellow solid (59 mg, 67%); mp >300 °C; νmax 3425 (N-H), 3251 (C-H aromatic), 2491 (S-H), 1513 (C=C aromatic); δ_H (500 MHz, DMSO-d_6) 7.28 (1H, d, *J* = 7.6, C(6)H), 7.42 – 7.46 (2H, m, C(8)H and C(2')H or C(6')H), 7.46 - 7.50 (2H, m, C(4')H and C(2')H or C(6')H), 7.67 - 7.71 (3H, m, C(7)H, C(3')H and C(5')H), 12.54 (1H, br s, NH), 14.33 (1H, s, SH)**;** δ_C (125 MHz, DMSO-d_6) 111.8 (C8), 114.9 (C9a), 124.3 (C6), 128.28 (C4'), 128.3 (2C, C2' and C6'), 128.8 (2C, C3' and C5'), 131.8 (C7), 135.8 (C9b), 138.0 (C1'), 138.7 (C9), 143.7 (C5a), 149.0 (C4a), 178.6 (C3); *m/z* (LRMS, ESI^-) 277 ($[M-H]^-$, 100%); HRMS (ESI^-) $C_{15}H_9N_4S^-$ ($[M-H]^-$) requires 277.0553; found 277.0556.

2''-(((9-Phenyl-5*H*-[1,2,4]triazino[5,6-*b*]indol-3-yl)thio)methyl)benzonitrile 288

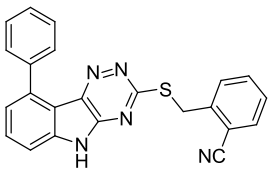

Method A: 2-(((9-bromo-5H-[1,2,4]triazino[5,6-b]indol-3-yl)thio)methyl)benzonitrile **266** (150 mg, 0.38 mmol), potassium phenyltrifluoroborate (98 mg, 0.53 mmo), K_3PO_4 (290 mg, 1.37 mmol) and $Pd(PPh_3)_2Cl_2$ (31 mg, 0.04 mmol) in THF/ H_2O (3.0 mL, 3:1), under nitrogen at 120 °C for 16 h, gave mostly starting material back

Method B: Following **General Procedure 3:** 2-(bromomethyl)benzonitrile (28 mg, 0.14 mmol) was added to a suspension of 9-Phenyl-5*H*-[1,2,4]triazino[5,6-*b*]indole-3-thiol **287** (40 mg, 0.14 mmol) and Et_3N (30 μL, 0.22 mmol) in MeOH (2.5 mL) to give **288** as a pale

yellow solid (36 mg, 63%); mp 144-146 °C; νmax 3074 (N-H), 3060 (C-H aromatic), 2970 (C-H alkane), 2226 (CN), 1738 (C=C aromatic); δ_H (400 MHz, DMSO-d_6) 4.72 (2H, s, SCH_2), 7.37 (1H, d, *J* = 7.8, C(6)H), 7.42 - 7.55 (4H, m, C(2')H, C(4')H, C(6')H and C(4")H), 7.58 (1H, d, *J* = 7.8, C(8)H), 7.66 (1H, app td, *J* = 7.7, 1.1, C(5")H), 7.74 (1H, app t, *J* = 7.8, C(7)H), 7.77 - 7.83 (3H, m, C(3')H, C(5')H and C(6'')H), 7.86 (1H, d, *J* = 7.9, C(3")H), 12.80 (1H, br s, NH)**;** δ_C (100 MHz, DMSO-d_6) 33.3 (SCH_2'), 112.4 (C8), 112.8 (C2''), 115.5 (C9a), 118.3 (CN), 118.4 (C4'), 124.7 (C6), 129.0 (2C, C2' and C6'), 129.2 (C4''), 129.7 (C6"), 130.1 (2C, C3' and C5'), 131.2 (C7), 131.8 (C9), 134.1 (C3''), 134.3 (C5''), 139.4 (C1'), 139.6 (C5a), 141.9 (C4a), 141.9 (C1"), 147.2 (C9b), 166.3 (C3); *m/z* (ESI^-) 392 ($[M-H]^-$, 100%); HRMS (ESI^-) $C_{23}H_{14}N_5S^-$ ($[M-H]^-$) requires 392.0968; found 392.0964.

5-Methyl-3-((1-(2'-nitrophenyl)ethyl)thio)-5*H*-[1,2,4]triazino[5,6-*b*]indole 302

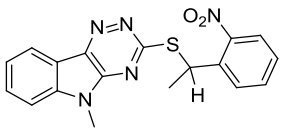

methyl iodide (37 µL, 0.59 mmol) was added to 3-((2'-nitrobenzyl)thio)-5*H*-[1,2,4]triazino[5,6-*b*]indole **239** (100 mg, 0.32 mmol) and K_2CO_3 (82 mg, 0.59 mmol) in DMF (10 mL) at rt. The resulting solution was heated to 100 °C in a sealed vial under microwave irradiation for 30 minutes. The precipitate was filtered and washed with MeOH to yield **302** a light brown solid (96 mg, 89 %). δ_H (500 MHz, pyr-d_5) 1.87 (3H, d, *J* = 7.3 Hz, CH_3), 3.53 (3H, s, NCH_3), 5.98 (1H, q, *J* = 7.3 Hz, SCH), 7.27 - 7.38 (3H, m, C(8)H, C(4')H and C(6)H), 7.53 (1H, app t, *J* = 7.9 Hz, C(7)H), 7.58 (1H, app t, *J* = 7.9 Hz, C(5')H), 7.94 (1H, d, *J* = 7.9 Hz, C(6')H), 8.07 (1H, d, *J* = 7.9 Hz, C(3')H), 8.32 (1H, d, *J* = 7.9 Hz, C(9)H); δ_C (125 MHz, pyr-d_5) 23.6 (CH_3), 28.5 (NCH_3), 41.0 (SCH_2), 112.2 (C6), 120.0 (C9a), 123.5, 124.6 (2xAr-CH), 125.5 (C9b), 125.9, 129.9, 131.7, 132.5, 135.2

(5xAr-CH), 141.6 (C5a), 143.2 (C1'), 143.3 (C4a), 148.1 (C2'), 168.5 (C3); mp 214-217 °C; *m/z* (ESI^+) 366 ($[M + H]^+$, 100%), 753 ($[2M+Na]^+$, 80%); HRMS (ESI^+) $C_{18}H_{15}N_5NaO_2S$ ($[M+Na]^+$) requires 388.0844; found 388.0840; ν_{max} (solid) 3061 (aromatic C-H), 1929, 1570, 1516 (NO_2), 1470, 1353 (NO_2), 1322; HPLC (Method 2) >95%, rt = 11.62 min

2-(((5-Methyl-5*H*-[1,2,4]triazino[5,6-*b*]indol-3-yl)thio)methyl)benzonitrile 303

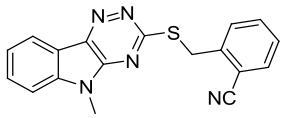

Following **General Procedure 4**, methyl iodide (29 µL, 0.47 mmol) was added to 5*H*-[1,2,4]triazino[5,6-*b*]indole-3-thiol **236** (100 mg, 0.32 mmol) and NaH (60%, 13.8 mg, 0.35 mmol) in THF (5 mL) at 0 °C and the resulting mixture stirred at rt for 16 h. The reaction mixture was quenched with H_2O (30 mL) and CH_2Cl_2 (30 mL) added. The organic layer was separated and washed with brine (30 mL), dried over $MgSO_4$, filtered and concentrated *in vacuo*. The resulting solid was washed with MeOH to yield **303** as a yellow solid (72 mg, 69 %). δ_H (400 MHz, pyr-d_5, 363K) 3.68 (2H, s, SCH_2), 4.99 (3H, s, NCH_3), 7.30 (1H, t, *J* = 7.8 Hz, C(5')H), 7.42 (1H, t, *J* = 7.8 Hz, C(8)H), 7.46 (1H, d, *J* = 7.8 Hz, C(6)H), 7.52 (1H, t, *J* = 7.8 Hz, C(4')H), 7.66 (1H, t, *J* = 7.8 Hz, C(7)H), 7.74 (1H, d, *J* = 7.8 Hz, C(3')H), 7.95 (1H, d, *J* = 7.8 Hz, C(6')H), 8.43 (1H, d, *J* = 7.8 Hz, C(9)H); δ_C (100 MHz, pyr-d_5) 28.7 (NCH_3), 35.1 (SCH_2), 112.4 (C2'), 118.2 (C6), 118.6 (CN), 120.2 (C9a), 123.6 (C9), 124.8 (C8), 129.0 (C5'), 129.9 (C9b), 132.4 (C3'), 132.7 (C7), 134.6 (C6'), 134.9 (C4'), 143.6 (C4a), 144.1 (C5a), 144.9 (C1'), 167.2 (C3); mp 219-221 °C; *m/z* (ESI^+) 354 ($[M + Na]^+$, 100%); HRMS (ESI^+) $C_{18}H_{13}N_5NaS$ ($[M+Na]^+$) requires 354.0784; found 354.0786; ν_{max} (solid) 3392 (aromatic C-H), 2221 (CN), 1573, 1467, 1358, 1325; HPLC (Method 1) >99%, rt = 10.93 min

2'-(((5-Ethyl-5*H*-[1,2,4]triazino[5,6-*b*]indol-3-yl)thio)methyl)benzonitrile 304

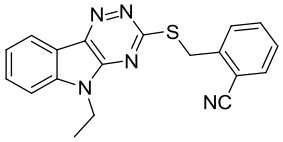

Following **General Procedure 4**, 2'(((5*H*-[1,2,4]triazino[5,6-*b*]indol-3-yl)thio)methyl)benzonitrile **236** (100 mg, 0.32 mmol) was added to DMF (5 mL) and cooled to 0 °C. NaH (60%, 13.8 mg, 0.34 mmol) was added to the cooled solution and stirred at 0 °C for 10 min. Ethyl iodide (38 μL, 0.47 mmol) was added and reaction mixture was allowed to warm to rt and stirred for 16 h. The reaction mixture was quenched by dropwise addition of H_2O until a precipitate was formed, this was collected by filtration and dried to yield **304** as a white powder (85 mg, 78 %); δ_H (500 MHz, DMSO-d_6, 363K) 1.34 (3H, t, J = 7.3 Hz, CH_3), 4.45 (2H, q, J = 7.3 Hz, NCH_2), 4.77 (2H, s, SCH_2), 7.45 – 7.48 (1H, m, C(8)H), 7.49 (1H, app t, J = 7.6 Hz, C(5')H), 7.67 (1H, app td, J = 7.6, 1.3 Hz, C(4')H), 7.78 (1H, app t, J = 7.6 Hz, C(7)H), 7.82 - 7.88 (3H, m, C(6)H, C(3')H and C(6')H), 8.34 (1H, d, J = 7.6 Hz, C(9)H); δ_C (125 MHz, DMSO-d_6) 13.4 (CH_3), 32.4 (SCH_2), 36.0 (NCH_2), 111.2 (C6), 112.0 (C2'), 117.4 (CN), 117.6 (C9a), 121.7 (C9), 122.9 (C8), 128.1 (C5'), 130.2 (C3'), 131.1 (C7), 133.0 (C6'), 133.3 (C4'), 140.5 (C5a), 141.1 (C9b), 141.6 (C1'), 145.5 (C4a), 165.9 (C3); mp 187-189 °C (EZ Melt); *m/z* (ESI^+) 368 ($[M + Na]^+$, 100%); HRMS (ESI^+) $C_{19}H_{15}N_5NaS$ ($[M+Na]^+$) requires 368.0940; found 368.0936; ν_{max} (solid) 2923 and 2853 (aromatic C-H), 2225 (CN), 1570, 1335, 1169; HPLC (Method 2) >96%, rt = 11.31 min

2-(((5-Butyl-5*H*-[1,2,4]triazino[5,6-*b*]indol-3-yl)thio)methyl)benzonitrile 305

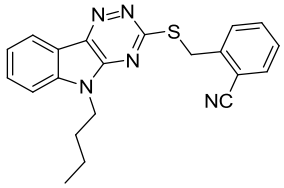

Following **General Procedure 4**, 2'(((5*H*-[1,2,4]triazino[5,6-*b*]indol-3-yl)thio)methyl)benzonitrile **236** (100 mg, 0.32 mmol), was added to DMF (5 mL) and cooled to 0 °C. To the cooled solution was added NaH (60 %, 13.8 mg, 0.35 mmol) and stirred at 0 °C for 10 mins. Iodobutane (54 μL, 0.47 mmol) was added and reaction mixture was stirred for 16 h at rt, quenched and the resulting precipitate was filtered and dried to yield **305** as a white powder (79 mg, 68 %); δ_H (500 MHz, DMSO-d_6, 363 K) 0.86 (3H, t, *J* = 7.6 Hz, CH_3), 1.22 – 1.30 (2H, m, C(3'')H_2), 1.70 – 1.76 (2H, m, C(2'')H_2), 4.38 (2H, t, *J* = 7.6 Hz, NCH_2), 4.76 (2H, s, SCH_2), 7.47 (1H, app t, *J* = 7.9 Hz, C(8)H), 7.48 (1H, app t, *J* = 7.6 Hz, C(5')H), 7.66 (1H, app t, *J* = 7.6 Hz, C(4')H), 7.75 (1H, app t, *J* = 7.9 Hz, C(7)H), 7.81 (1H, d, *J* = 7.9 Hz, C(6)H), 7.84 (1H, d, *J* = 7.6 Hz, C(3')H), 7.87 (1H, dd, *J* = 7.6, 1.3 Hz, C(6'), 8.33 (1H, d, *J* = 7.9 Hz, C(9)H); δ_C (125 MHz, DMSO-d_6) 13.6 (C4''), 19.5 (C3''), 29.9 (C2''), 32.4 (SCH_2), 40.8 (NCH_2), 111.4 (C6), 111.9 (C2'), 117.3 (CN), 117.6 (C9a), 121.6 (C9), 122.9 (C8), 128.1 (C5'), 130.0 (C3'), 131.0 (C7), 133.0 C6'), 133.3 (C4'), 140.8 (C5a), 140.9 (C9b), 141.5 (C1'), 145.9 (C4a), 165.9 (C3); mp 159-161 °C (EZ Melt); *m/z* (ESI^+) 396 ($[M + Na]^+$, 100%); HRMS (ESI^+) $C_{21}H_{19}N_5NaS$ ($[M+Na]^+$) requires 396.1253; found 396.1247; ν_{max} (solid) 2954 and 2925 (aromatic C-H), 2221 (CN), 1561, 1466, 1171; HPLC (Method 2) >95%, rt = 11.97 min

2'-((5-(Cyclopropylmethyl)-5*H*–[1,2,4,]triazino[5,6-*b*]indol-3-ylthio)methyl)benzonitrile 306

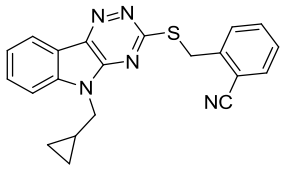

Following **General Procedure 4**, 2'(((5*H*-[1,2,4]triazino[5,6-*b*]indol-3-yl)thio)methyl)benzonitrile **236** (100 mg, 0.32 mmol) was added to DMF (5 mL), cooled to 0 °C followed by the addition of NaH (60%, 13.8 mg, 0.35 mmol) and stirred at 0 °C for 10 mins. Bromomethylcyclopropane (31 µL, 0.32 mmol) was added and stirred at rt for 16 h. The reaction mixture was quenched with H_2O and resulting precipitate was filtered and washed with MeOH to yield **306** as a pale yellow solid (62 mg, 52 %); δ_H (500 MHz, DMSO-d_6, 363K) 0.37 - 0.50 (4H, m, C(2")H_2 and C(3")H_2), 1.19 - 1.33 (1H, m, C(1")H), 4.32 (1H, d, *J* = 6.9 Hz, NCH_2), 4.73 (2H, s, SCH_2), 7.48 (2H, m, C(8)H and C(4')H), 7.67 (1H, app t, *J* = 7.8 Hz, C(7)H), 7.77 (1H, app t, *J* = 7.6 Hz, C(5')H), 7.8 (1H, d, *J* = 7.8 Hz, C(6)H), 7.81 - 7.99 (2H, m, C(3')H and C(6')H), 8.34 (1H, d, *J* = 7.8 Hz, C(9)H); δ_C (125 MHz, DMSO-d_6) 3.8 (2C, C2'' and C3"), 10.2 (C1"), 32.4 (SCH_2), 45.2 (NCH_2), 111.6 (C2'), 111.9 (C6), 117.3 (CN), 117.6 (C9a), 121.6 (C9), 122.9 (C8), 128.1 (C4'), 130.0 (C3'), 131.0 (C7), 133.0 (C6'), 133.4 (C5'), 140.9 (C5a), 141.0 (C4a), 141.5 (C1'), 145.8 (C9b), 166.0 (C3); mp 149 - 150 °C; *m/z* (ESI^+) ($[M + Na]^+$, 100%) 394 ($[M + Na]^+$, 64%); HRMS (ESI^+) $C_{20}H_{20}N_5NaS$ ($[M+Na]^+$) requires 394.1094; found 394.1095; ν_{max} (solid) 3030, 2923, 2251 (CN), 1740; HPLC (Method 2) >99%, rt = 1.66 min

2'-(((5-(Cyclohexylmethyl)-5*H*-[1,2,4]triazino[5,6-*b*]indol-3-yl)thio)methyl)benzonitrile 307

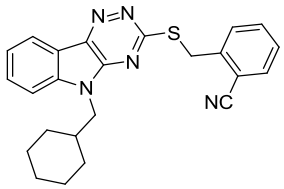

Following **General Procedure 4**, 2'(((5*H*-[1,2,4]triazino[5,6-*b*]indol-3-yl)thio)methyl)benzonitrile **236** (100 mg, 0.32 mmol) was added to DMF (5 5 mL), cooled to 0 °C followed by the addition of NaH (60%, 13.8 mg, 0.34 mmol) and stirred at 0 °C for 10 mins. Bromomethyl cyclohexane (44 μL, 0.32 mmol) was added, stirred for 16 h and quenched with H_2O. The resulting precipitate was filtered and dried to yield **307** as a white solid (25 mg, 19 %); δ_H (500 MHz, DMSO-d_6, 363K) 0.97 - 1.12 (6H, m, 6xCH), 1.45 - 1.50 (2H, m, 2xCH), 1.56 - 1.63 (4H, m, 4xCH), 1.85 - 1.92 (1H, m, C(1'')H), 4.21 (1H, d, J = 7.3 Hz, NCH_2), 4.77 (2H, s, SCH_2), 7.46 - 7.52 (2H, m, C(5')H and C(8)H), 7.68 (1H app td, J = 7.6, 1.3 Hz, C(4')H), 7.76 (1H, app t, J = 7.6 Hz, C(7)H), 7.81 - 7.87 (2H, m, C(3')H and C(6)H), 7.90 (1H, dd, J = 7.6, 1.0 Hz, C(6')H), 8.35 (1H, d, J = 7.6 Hz, C(9)H); δ_C (125 MHz, DMSO-d_6) 25.1 (2C, C3'' and C5''), 25.6 (C4''), 30.0 (2C, C2'' and C6''), 32.4 (C1'), 36.6 (SCH_2), 46.9 (NCH_2), 111.8 (C6), 111.9 (C2'), 117.3 (CN), 117.7 (C9a), 121.5 (C9), 122.9 (C8), 128.1 (C5'), 129.8 (C3'), 131.0 (C7), 133.0 (C6'), 133.4 (C4'), 140.8 (C5a), 141.2 (C9b), 141.6 (C1'), 146.2 (C4a), 166.1 (C3); mp 201-203 °C (EZ Melt); *m/z* (ESI^+) 414 ($[M + H]^+$, 100%); HRMS (ESI^+) $C_{24}H_{23}N_5NaS$ ($[M+Na]^+$) requires 436.1566; found 436.1555; ν_{max} (solid) 2926 and 2850 (aromatic C-H), 2219 (CN), 1571, 1170; HPLC (Method 2) >99%, rt = 12.40 min

2'-(((5-Benzyl-5*H*-[1,2,4]triazino[5,6-*b*]indol-3-yl)thio)methyl)benzonitrile 308

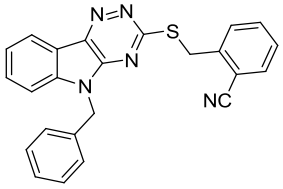

Following **General Procedure 4**, benzyl bromide (25 μL, 0.24 mmol) was added to 3-((2'-cyanobenzyl)thio)-5*H*-[1,2,4]triazino[5,6-*b*]indole **236** (50 mg, 0.15 mmol) and NaH (10 mg, 0.24 mmol) in THF (5 mL) at 0 °C, the resulting mixture stirred at rt for 16 h. The reaction mixture was quenched with H_2O (30 mL) and diluted in CH_2Cl_2 (30 mL). The organic layer was separated and washed with brine (30 mL), dried over $MgSO_4$, filtered and concentrated *in vacuo* to yield **308** as a light yellow solid (49 mg, 80 %). δ_H (500 MHz, DMSO-d_6, 363 K) 4.77 (2 H, s, SCH_2), 5.68 (2 H, s, NCH_2), 7.23 - 7.33 (5 H, m, C(2'')H, C(3'')H, C(4''), C(5'')H and C(6'')H), 7.42 - 7.45 (1 H, m, C(8)H), 7.47 - 7.51 (1 H, m, C(4')H), 7.53-7.56 (1 H, m, C(7)H), 7.69 - 7.74 (2 H, m, C(3')H and C(6')H), 7.75 - 7.81 (2 H, m, C(6)H and C(5')H), 8.37 (1 H, d, J = 7.9 Hz, C(9)H); δ_C (125 MHz, DMSO-d_6) 32.4 (SCH_2), 44.2 (NCH_2), 111.7 (C2'), 111.9 (C6), 117.5 (CN), 117.6 (C9a), 119.3 (C9), 121.7 (C7), 123.2 (C8), 127.3 (C3'' and C5''), 127.7 (C4''), 128.1 (C5'), 128.8 (C2'' and C6''), 130.2 (C3'), 133.1 (C6'), 133.2 (C4'), 135.8 (C9b), 140.7 (C1''), 141.2 (C5a), 141.5 (C1'), 146.2 (C4a), 166.2 (C3); mp 197-200 °C; *m/z* (ESI^+) 430 ($[M + Na]^+$, 100%); HRMS (ESI^+) $C_{24}H_{17}N_5NaS$ ($[M+H]^+$) requires 430.1097; found 430.1081; ν_{max} (solid) 2215 (CN), 1571, 1520, 1468, 1328; HPLC (Method 2) >97%, rt = 11.96 min

2'-(((5-(Benzoyl-5*H*-[1,2,4]triazino[5,6-*b*]indol-3-yl)thio)methyl)benzonitrile 309

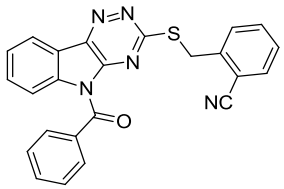

Following **General Procedure 4**, benzoyl chloride (55 μL, 0.47 mmol) was added to 2'(((5*H*-[1,2,4]triazino[5,6-*b*]indol-3- yl)thio)methyl)benzonitrile **236** (100 mg, 0.32 mmol) and NaH (13.8 mg, 0.52 mmol) in DMF (5 mL) at 0 °C and the resulting mixture stirred for 16 h, was quenched with H_2O until a precipitate formed. The precipitate was filtered and dried to give **309** as a faint yellow solid (97 mg, 72 %); δ_H (500 MHz, DMSO-d_6, 363K) 4.06 (2 H, s, SCH_2), 7.34 (1 H, d, *J* = 7.9 Hz, C(6')H), 7.47 (1 H, app t, *J* = 7.6 Hz, C(8)H), 7.52 (2 H, app t, *J* = 7.3 Hz, C(3'')H and C(5'')H), 7.60 (1H, app t, *J* = 7.9 Hz, C(5')H), 7.63 (1H, app t, *J* = 7.9 Hz, C(4')H), 7.66 (1H, app t, *J* = 7.6 Hz, C(7)H), 7.82 - 7.86 (2H, m, C(3')H and C(4'')H), 7.94 (2 H, d, *J* = 7.3 Hz, C(2'')H and C(6'')H), 8.30 (1 H, d, *J* = 7.6 Hz, C(6)H), 8.44 (1 H, d, *J* = 7.6 Hz, C(9)H); δ_C (125 MHz, DMSO-d_6) 31.8 (CH_2), 111.7 (C2'), 116.2 (C6), 117.2 (CN), 119.7 (C9a), 121.3 (C9), 125.6 (C8), 128.3 (2C, C3'' and C5''), 128.4 (C5'), 130.0 (2C, C2'' and C6''), 130.3 (C3'), 131.6 (C7), 133.2 (C6'), 133.2 (C4''), 133.3 (C4'), 133.9 (C1''), 139.4 (C9b), 140.2 (C5a), 142.1 (C1'), 147.2 (C4a), 166.4 (C3), 167.8 (C(O)); mp 201-202 °C; *m/z* (ESI^+) 444 ($[M + Na]^+$, 100%); HRMS (ESI^+) $C_{24}H_{15}N_5NaOS$ ($[M+Na]^+$) requires 444.0890; found 444.0885; ν_{max} (solid) 3056 (aromatic C-H), 2228 (CN), 1699 (CO), 1600, 1290; $C_{24}H_{15}N_5OS$ requires C, 68.39; H, 3.59; N, 16.62%; found C, 68.19; H, 3.45; N, 16.62%

2'-(((5-(Phenylsulfonyl)-5*H*-[1,2,4]triazino[5,6-*b*]indol-3-yl)thio)methyl)benzonitrile 310

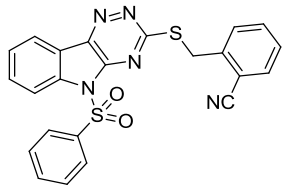

Following **General Procedure 4**, 2'(((5*H*-[1,2,4]triazino[5,6-*b*]indol-3-yl)thio)methyl)benzonitrile **236** (100 mg, 0.32 mmol) was added to DMF (5 mL), cooled to 0 °C followed by the addition of NaH (60%, 13.8 mg, 0.35 mmol) and stirred at 0 °C for 10 mins. Phenyl sulfonyl chloride (40 μL, 0.32 mmol) was added, stirred for 16 h and quenched with H_2O. The resulting precipitate was filtered and dried to yield **310** as a white solid (121 mg, 84 %); δ_H (500 MHz, DMSO-d_6, 363K) 4.81 (2H, s, SCH_2), 7.52 (1H, app t, *J* = 7.9 Hz, C(5')H), 7.63 (1H, app t, *J* = 7.6 Hz, C(8)H), 7.63 (2H, app td, *J* = 8.8, 1.0 Hz, C(3'')H and C(5'')H), 7.69 (1H, app td, *J* = 7.9, 1.6 Hz, C(4')H), 7.78 (1H, tt, *J* = 8.8, 1.0 Hz, C(4'')H), 7.85 (1H, td, *J* = 7.6, 1.3 Hz, C(7)H), 7.89 (1H, d, *J* = 7.9, C(3')H), 7.91 (1H, dd, *J* = 7.9, 1.0 Hz, C(6')H), 8.10 (2H, dd, *J* = 8.8, 1.0, C(2'')H and C(6'')H), 8.33 (1H, d, *J* = 7.6 Hz, C(6)H), 8.37 (1H, d, *J* = 7.6 Hz, C(9)H); δ_C (125 MHz, DMSO-d_6) 32.8 (CH_2), 112.0 (C2'), 114.5 (C6), 117.5 (CN), 119.3 (C9a), 121.8 (C9), 125.8 (C8), 127.4 (2C, C2'' and C6''), 128.4 (C5'), 130.0 (2C, C3'' and C5''), 130.2 (C3'), 132.2(C7), 133.3 (C6'), 133.4 (C4'), 135.6 (C4''), 136.8 (C1''), 137.9 (C5a), 140.7 (C9b), 141.9 (C1'), 147.1 (C4a), 167.2 (C3); mp 176-177 °C (EZ Melt); *m/z* (ESI^+) 480 ($[M + Na]^+$, 100%); HRMS (ESI^+) $C_{23}H_{15}N_5NaO_2S_2$ ($[M+Na]^+$) requires 480.0559; found 480.0549; ν_{max} (solid) 2220 (CN), 1568, 1448, 1354 and 1174 (R_2NSO_2); $C_{23}H_{15}N_5NaO_2S_2$ requires C, 60.38; H, 3.30; N, 15.31%; found C, 60.26; H, 3.21; N, 15.16%

Benzyl-3-((2'-cynaobenzyl)thio)- 5*H*-[1,2,4]triazino[5,6-*b*]indole-5-carboxylate 311

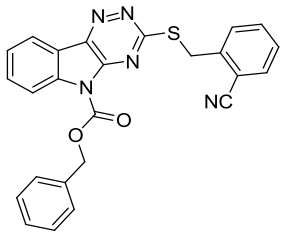

Following **General Procedure 4**, benzyl chloroformate (23.4 µL mg, 0.21 mmol) was added to 2'(((5*H*-[1,2,4]triazino[5,6-*b*]indol-3-yl)thio)methyl)benzonitrile **236** (60 mg, 0.19 mmol) and NaH (11.0 mg, 0.28 mmol) in THF (5 mL) at 0 °C and the resulting mixture stirred for 16 h at rt, quenched with H_2O and the resulting precipitate was filtered and washed with MeOH to yield **311** as an off white solid (82 mg, 96%); δ_H (500 MHz, DMSO-d_6, 363K) 4.54 (2H, s, SCH_2), 5.61 (2H, s, OCH_2), 7.26 (1H, t, *J* = 7.6 Hz, C(4'')H), 7.35 (2 H, app t, *J* = 7.6 Hz, C(3'')H and C(5'')H), 7.49 (1 H, app t, *J* = 7.6 Hz, C(4')H), 7.60 - 7.64 (4H, m, C(2'')H and C(6'')H, C(8)H and C(5')H), 7.73 (1H, d, *J* = 7.6 Hz, C(6')H), 7.82 (1H, app t, *J* = 7.6 Hz, C(7)H), 7.89 (1H, d, *J* = 7.6 Hz, C(3')H), 8.37 (1H, d, *J* = 7.6 Hz, C(6)H), 8.39 (1H, d, *J* = 8.2 Hz, C(9)H); δ_C (125 MHz, DMSO-d_6) 32.4 (SCH_2), 69.3 (OCH_2), 111.9 (C2'), 116.09 (C6), 117.4 (CN), 119.32 (C9a), 121.3 (C8), 125.4 (C7), 128.4 (C1''), 128.4 (3C, C2'' and C6'' and 1xAr-C) , 128.5 (2C, C3'' and C5''), 130.6, 131.9, 133.1, 133.4 (4xAr-CH), 134.7 (C1''), 138.7 (C9b), 140.8 (C1'), 142.2 (C5a), 147.0 (C4a), 149.9 (CO), 167.3 (C3); mp 97-99 °C; *m/z* (ESI^+) 474 ($[M + Na]^+$, 20%), *m/z* (ESI-) 316 ($[M - (PhCH_2CO_2)H]^-$, 100%); ν_{max} (solid) 3426, 3063 (aromatic C-H), 2232 (CN), 1739 (urethaneNC(O)OR), 1582, 1392, 1195; HRMS (ESI^+) $C_{25}H_{17}N_5NaO_2S$ ($[M+Na]^+$) requires 474.0995; found 474.0993; $C_{25}H_{17}N_5O_2S \cdot 0.89\ H_2O$ requires C, 64.22; H, 4.05; N, 14.98%; found C, 64.51; H, 3.77; N, 14.69%

Propyl-3-((2'-cyanobenzyl)thio)-5*H*-[1,2,4]triazino[5,6-*b*]indole-5-carboxylate 312

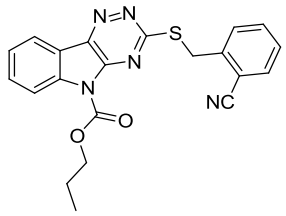

Following **General Procedure 4**, NaH (60%, 13.8 mg, 0.35 mmol) was added to 2'(((5*H*-[1,2,4]triazino[5,6-*b*]indol-3-yl)thio)methyl)benzonitrile **236** (100 mg, 0.32 mmol) in DMF (5 mL), at 0 °C and stirred for 10 mins. Propyl chloroformate (34 µL, 0.32 mmol) was added, stirred for 16 h at rt and quenched with H_2O. The resulting precipitate was filtered and washed with MeOH to yield **312** as a white solid (56 mg, 44 %); δ_H (500 MHz, DMSO-d_6, 363K) 1.05 (3H, t, J = 7.6 Hz, C(5'')H_3), 1.78 – 1.87 (2H, m, C(4'')H_2), 4.48 (2H, t, J = 6.4 Hz, OC(3'')H_2), 4.79 (2H, s, SCH_2), 7.49 (1H, app t, J = 7.6 Hz, C(5')H), 7.60 (1H, app t, J = 7.6 Hz, C(8)H), 7.66 (1H, app t, J = 7.6 Hz, C(4')H), 7.79 – 7.83 (1H, m, C(7)H), 7.86 (1H, d, J = 7.6 Hz, C(3'')H), 7.89 (1H, d, J = 7.6 Hz, C(6')H), 8.33 – 8.38 (2H, m, C(9)H and C(6)H); δ_C (125 MHz, DMSO-d_6) 10.3 (C5''), 21.5 (C4''), 32.5 (SCH_2), 69.5 (C3''), 111.9 (C2'), 116.1 (C6), 117.4 (CN), 119.2 (C9a), 121.3 (C9), 125.4 (C8), 128.4 (C5'), 130.4 (C3'), 131.9 (C7), 133.2 (C6'), 133.4 (C4'), 138.7 (C5a), 141.0 (C9b), 142.2 (C1'), 147.0 (C4a), 150.0 (CO), 167.2 (C3); mp 148-149 °C; *m/z* (ESI^+) 426 ($[M + Na]^+$, 100%); HRMS (ESI^+) $C_{21}H_{17}N_5NaO_2S$ ($[M+Na]^+$) requires 426.0948; found 426.0991; ν_{max} (solid) 3062 and 2969 (aromatic C-H), 2226 (CN), 1738 (NC=O), 1578

2'-(((5-tosyl-5*H*-[1,2,4]triazino[5,6-*b*]indol-3-yl)thio)methyl)benzonitrile 313

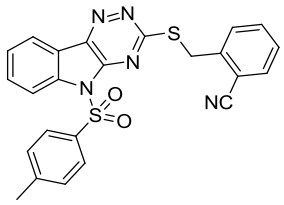

Following **General Procedure 4**, 2'(((5*H*-[1,2,4]triazino[5,6-*b*]indol-3-yl)thio)methyl)benzonitrile **236** (60 mg, 0.19 mmol) was added to THF (5 mL), cooled to 0 °C followed by the addition of NaH (60%, 11.0 mg, 0.28 mmol) and stirred at 0 °C for 10 mins. *p*-toluene sulfonyl chloride (40 mg, 0.21 mmol) was added, stirred for 16 h and quenched with H_2O (50 mL) and extracted with EtOAc (50 mL). The organic layer was separated, washed with brine (30 mL), dried over $MgSO_4$, filtered and concentrated *in vacuo*. The resulting solid was washed with MeOH to yield **313** as a white crystalline solid (82 mg, 92%). δ_H (500 MHz, DMSO-d_6, 363K) 2.28 (3 H, s, C(4')CH_3), 4.83 (2 H, s, SCH_2), 7.37 (2 H, d, *J* = 8.3 Hz, C(3'')H and C(5'')H), 7.49 (1 H, app t, *J* = 7.8 Hz, C(4')H), 7.59 (1 H, t, *J* = 7.8 Hz, C(8)H), 7.66 (1 H, app t, *J* = 7.8 Hz, C(5')H), 7.82 (1 H, app t, *J* = 7.8 Hz, C(7)H), 7.87 - 7.92 (2 H, m, C(3')H and C(6')H), 8.01 (2 H, d, *J* = 8.3 Hz, C(2'')H and C(6'')H), 8.31 - 8.37 (2 H, m, C(6)H and C(9)H); δ_C (125 MHz, DMSO-d_6) 21.2 (CH_3), 32.7 (CH_2), 112.0 (C2'), 114.5 (C6), 117.5 (CN), 119.2 (C9a), 121.8, 125.8 (2xAr-C)), 127.4 (2C, C2'' and C6''), 128.4, 130.2 (2xAr-C), 130.4 (2C, C3'' and C5''), 132.2, 133.3, 133.4 (3xAr-C)), 133.8 (C1''), 137.9 (C9b), 140.7 (C1'), 141.8 (C5a), 146.7 (C4a), 147.0 (C4''), 167.2 (C3); mp 220-222 °C;*m/z* (ESI^+) 494 ($[M + Na]^+$, 45%), *m/z* (ESI^-) 316 ($[M – (2CN-Bn)]^-$, 100%); HRMS (ESI^+) $C_{24}H_{17}N_5NaO_2S_2$ ($[M+Na]^+$) requires 494.0716; found 494.0738; ν_{max} (solid) 2230 (CN), 1595, 1449, 1370 and 1177 (SO_2N); HPLC (Method 2) >99%, rt = 12.37 min

2'-(((2''-Nitro-5*H*-[1,2,4]triazino[5,6-*b*]indol-3-yl)thio)methyl)benzonitrile 314

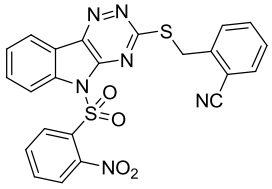

Following **General Procedure 4**, 2-Nitro sulfonyl chloride (47 mg, 0.21 mmol) was added to 2'(((5*H*-[1,2,4]triazino[5,6-b]indol-3-yl)thio)methyl)benzonitrile **236** (60 mg, 0.19 mmol) and NaH (60%, 11.0 mg, 0.28 mmol) in THF (5 mL) at 0 °C and stirred for 16 h. The reaction mixture was quenched dropwise with H_2O. The resulting precipitate was filtered and washed with MeOH to yield **314** as an off white solid (79 mg, 83%); δ_H (500 MHz, DMSO-d_6, 363K) 4.70 (2H, s, SCH_2), 7.50 (1H, app t, *J* = 7.6 Hz, C(4')H), 7.63 (1H, app t, *J* = 7.6 Hz, C(5')H), 7.67 (1H, app t, *J* = 7.6 Hz, C(4'')H), 7.76 (1H, d, *J* = 7.6 Hz, C(6')H), 7.84 - 7.91 (2H, m, C(3')H and C(5'')H), 7.97 (1H, app t, *J* = 7.6 Hz, C(8)H), 8.06 (1H, app t, *J* = 7.6 Hz, C(7)H), 8.09 (1H, d, *J* = 8.5 Hz, C(6'')H), 8.18 (1H, dd, *J* = 7.6, 1.3 Hz, C(6)H), 8.42 (1H, d, *J* = 7.6 Hz, C(3'')H), 8.49 (1H, dd, *J* = 7.6, 1.3 Hz, C(9)H); δ_C (125 MHz, DMSO-d_6) 32.77 (SCH_2), 112.0 (C2'), 115.0 (C6), 117.4 (CN), 119.0 (C9a), 121.8, 125.9, 126.0, 128.5, 129.4, 130.4 (6xAr-C) 132.3 (C1''), 132.6, 133.2, 133.4, 133.5 (4xAr-C) 137.4 (C9b), 138.6 (C3''), 140.4 (C1'), 141.9 (C5a), 147.0 (C4a), 147.10 (C2''), 167.0 (C3); mp 217-218 °C; *m/z* (ESI^-) 501 ($[M - H]^-$, 20%), 316 ($[M – (2''-NO_2PhSO_2)H]^-$, 100%); ν_{max} (solid) 2921 and 2853 (aromatic C-H), 2228 (CN), 1546 (NO_2), 1373 and 1184 (secondary NSO_2); HRMS (ESI^+) $C_{23}H_{14}N_6NaO_4S_2$ ($[M+Na]^+$) requires 525.0410; found 525.0425; HPLC (Method 2) >97%, rt = 12.07 min

2'-(((5-([1',1''-biphenyl]-4-ylsulfonyl)-5*H*-[1,2,4]triazino[5,6-*b*]indol-3-yl)thio)methyl)benzonitrile 315

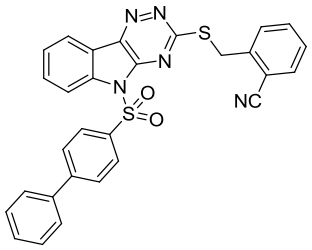

Following **General Procedure 4**, 4-biphenyl sulfonyl chloride (53 mg, 0.21 mmol) was added to 2'(((5*H*-[1,2,4]triazino[5,6-*b*]indol-3-yl)thio)methyl)benzonitrile **236** (60 mg, 0.19 mmol) and NaH (60%, 11.0 mg, 0.28 mmol) in THF (5 mL) at 0 °C and the resulting mixture stirred at rt for 16 h, quenched with H_2O and the resulting precipitate was filtered and washed with MeOH to yield **315** as an off white solid (79 mg, 83%); δ_H (400 MHz, DMSO-d_6, 363K) 4.82 (2H, s, SCH_2), 7.43 - 7.52 (4H, m, 4xAr-H), 7.62 (1H, t, *J* = 7.6 Hz, Ar-H), 7.64 - 7.70 (3 H, m, 3xAr-H), 7.83 - 7.91 (5H, m, 5xAr-H), 8.17 (2H, d, *J* = 8.3 Hz, C(2'')H and C(6'')H), 8.34 - 8.38 (2H, m, C(9)H and C(6)H); δ_C (125 MHz, DMSO-d_6) 32.8 (SCH_2), 112.0 (C2'), 114.5 (C6), 117.5 (CN), 119.3 (C9a), 121.9, 125.8 (2xAr-C), 127.2 (2C, C3'' and C5''), 128.1, 128.2, 128.4, 129.1 (4xAr-C), 129.2 (2C, C2'' and C6''), 130.3, 132.3, 133.3, 133.5 (4xAr-C), 135.3 (C1''), 137.7 (C1'''), 138.0 (C9b), 140.7 (C1'), 141.9 (C5a), 146.9 (C4a), 147.1 (C4'') 167.2 (C3); mp 210-211 °C; *m/z* (ESI^+) 556 ($[M + Na]^+$, 10%), *m/z* (ESI^-), 316 ($[M - (4''\text{-}PhPhSO_2)H]^-$, 100%); ν_{max} (solid) 3074 (aromatic C-H), 2222 (CN), 1391 and 1173 (secondary NSO_2); HRMS (ESI^+) $C_{29}H_{19}N_5NaO_2S_2$ ($[M+Na]^+$) requires 556.0872; found 556.0880; HPLC (Method 2) >99%, rt = 12.95 min

2'-(((5-(4''-Methyl-1*H*-imidazol-4-yl)sulfonyl)-5*H*-[1,2,4]triazino[5,6-*b*]indol-3-yl)thio)methyl)benzonitrile 316

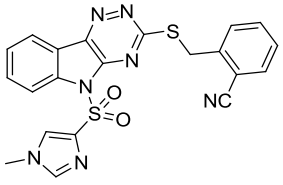

Following **General Procedure 4**, 2'(((5*H*-[1,2,4]triazino[5,6-*b*]indol-3-yl)thio)methyl)benzonitrile **236** (100 mg, 0.32 mmol) was added to DMF (5 mL), cooled to 0 °C followed by the addition of NaH (60%, 13.8 mg, 0.34 mmol) and stirred at 0 °C for 10 mins. 1-Methyl-1*H*-imidazole-4-sulphonyl chloride (57 µL, 0.32 mmol) was added, stirred for 16 h and subsequently quenched with H_2O. The resulting precipitate was filtered to yield **316** as a white solid (57 mg, 39 %); δ_H (500 MHz, DMSO-d_6, 363K) 3.68 (3H, s, NCH_3), 4.78 (2H, s, SCH_2), 7.50 (1H, app td, *J* = 7.6, 1.3 Hz, C(4')H), 7.62 (1H, app t, *J* = 7.6 Hz, C(8)H), 7.67 (1H, td, *J* = 7.6, 1.3 Hz, C(5')H), 7.80 (1H, d, *J* = 1.0 Hz, C(5'')H), 7.84 (1H, app t, *J* = 7.6, 1.0 Hz, C(7)H), 7.90 (1H, dd, *J* = 7.6, 1.0 Hz, C(3')H), 7.96 (1H, d, *J* = 7.6 Hz, C(6')H), 8.28 (1H, d, *J* = 7.6 Hz, C(6)H), 8.36 (1H, *J* = 7.6 Hz, C(9)H), 8.42 (1H, d, *J* = 1.0 Hz, C(3'')H); δ_C (125 MHz, DMSO-d_6) 32.6 (SCH_2), 33.9 (NCH_3), 112.0 (C2'), 114.9 (C6), 117.5 (CN), 119.0 (C9a), 121.6 (C9), 125.7 (C8), 128.4 (C4'), 128.4 (C3''), 130.6 (C6'), 132.0 (C7), 133.2 (C3'), 133.4 (C5'), 135.3 (C5a), 138.4 (C9b), 141.1 (C1'), 141.2 (C5''), 141.6 (C1''), 147.0 (C4a), 167.2 (C3); mp 223-225 °C (EZ Melt); *m/z* (ESI^+) 484 ($[M + Na]^+$, 100%); HRMS (ESI^+) $C_{21}H_{15}N_7NaO_2S_2$ ($[M+Na]^+$) requires 484.0621; found 484.0604; ν_{max} (solid) 2924, 2225 (CN), 1573, 1449, 1378 and 1174 (R_2NSO_2); HPLC (Method 2) >98%, rt = 11.19 min

2'(((5-Acetyl-5*H*-[1,2,4]triazino[5,6-*b*]indol-3-yl)thio)methyl)benzonitrile 317

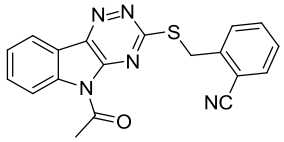

Following **General Procedure 4**, acetyl chloride (33.8 μL, 0.47 mmol) was added to 2'(((5*H*-[1,2,4]triazino[5,6-*b*]indol-3- yl)thio)methyl)benzonitrile **236** (100 mg, 0.32 mmol) and NaH (60%, 13.8 mg, 0.35 mmol) in DMF (5 mL) at 0 °C and the resulting mixture stirred for 16 h, quenched with H_2O until a precipitate formed. The precipitate was filtered and dried to give **317** as a faint yellow solid (89 mg, 77 %); δ_H (500 MHz, DMSO-d_6, 363K) 2.94 (3 H, s, CH_3), 4.82 (2 H, s, SCH_2), 7.51 (1 H, app t, *J* = 7.6 Hz, C(5')H), 7.63 (1 H, app t, *J* = 7.8 Hz, C(8)H), 7.70 (1 H, app t, *J* = 7.6, Hz, C(4')H), 7.81 (1H, app t, *J* = 7.8 Hz, C(7)H), 7,83 (1H, d, *J* = 7.6 Hz, C(3')H), 7.90 (1 H, d, *J* = 7.6 Hz, C(6')H), 8.38 (1 H, d, *J* = 7.8 Hz, C(6)H), 8.58 (1 H, d, *J* = 7.8 Hz, C(9)H); δ_C (125 MHz, DMSO-d_6) 27.4 (CH_3), 32.8 (CH_2), 112.0 (C2'), 117.2 (C6), 117.4 (CN), 119.3 (C9a), 121.2 (C9), 125.7 (C8), 128.4 (C5'), 130.2 (C3'), 132.1 (C7), 133.2 (C6'), 133.5 (C4'), 139.3 (C9b), 140.5 (C1'), 142.5 (C5a), 147.3 (C4a), 166.6 (C3), 170.3 (C(O)); mp 207-209 °C; *m/z* (ESI^+) 382 ($[M + Na]^+$, 100%); HRMS (ESI^+) $C_{19}H_{13}N_5NaOS$ ($[M+Na]^+$) requires 382.0733; found 382.0724; ν_{max} (solid) 2227 (CN), 1721 (NC=O), 1377, 1177; HPLC (Method 2) >99%, rt = 11.53 min

Methyl 4''-(3-((2'-cyanobenzyl)thio)-5*H*-[1,2,4]triazino[5,6-*b*]indol-5-yl)-4''-oxobutanoate 318

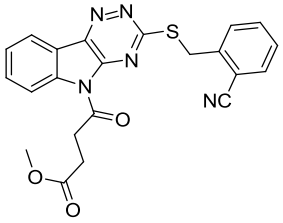

Following **General Procedure 4**, methyl-5-chloro-5-oxopentoate (87 μL, 0.71 mmol) was added to 2'(((5*H*-[1,2,4]triazino[5,6-*b*]indol-3-yl)thio)methyl)benzonitrile **236** (150 mg, 0.47 mmol) and NaH (20.8 mg, 0.52 mmol) in DMF (5 mL) at 0 °C and stirred at rt for 16 h. The reaction mixture was quenched with H_2O until a precipitate formed. The precipitate was filtered and dried to give **318** as a faint yellow solid (165 mg, 81 %); δ_H (500 MHz, DMSO-d_6, 363K) 2.80 (2 H, t, J = 6.3 Hz, N-C(O)-CH_2), 3.62 (3 H, s, CH_3), 3.69 (2 H, t, J = 6.3 Hz, CH_2-C(O)-O), 4.82 (2 H, s, SCH_2), 7.51 (1 H, app t, J = 7.6 Hz, C(8)H), 7.62 (1 H, app t, J = 7.6 Hz, C(5')H), 7.70 (1 H, t, J = 7.6 Hz, C(4')H), 7.80 (H, app t, J = 7.6 Hz, C(7)H), 7.83 (1H, d, J = 7.6 Hz, C(3')H), 7.90 (1 H, d, J = 7.6 Hz, C(6')H), 8.38 (1 H, d, J = 7.6 Hz, C(6)H), 8.56 (1 H, d, J = 7.6 Hz, C(9)H); δ_C (125 MHz, DMSO-d_6) 27.9, (C3''H_2-C(O)-O), 32.9 (N-C(O)-C2''H_2), 34.2 (SCH_2), 51.5 (OCH_3), 111.9 (C2'), 117.2 (C6), 117.4 (CN), 119.4 (C9a), 121.2 (C9), 125.8 (C8), 128.4 (C5'), 130.2 (C3'), 132.1 (C7), 133.2 (C6'), 133.5 (C4'), 139.2 (C9b), 140.5 (C5a), 142.5 (C1'), 147.3 (C4a), 166.5 (C3), 172.3 (N-C1''(O)), 172.4 (C5''(O)-OCH_3); mp 144-145 °C; *m/z* (ESI^+) 454 ([M + $Na]^+$, 100%); HRMS (ESI^+) $C_{22}H_{17}N_5NaO_3S$ ([M+$Na]^+$) requires 454.0944; found 454.0924; ν_{max} (solid) 2953 (aromatic C-H), 2228 (CN), 1739 (CO ester), 1713 (NC=O), 1379, 1188; HPLC (Method 2) >98%, rt = 11.76 min

Methyl 5''-(3-((2'-cyanobenzyl)thio)-5*H*-[1,2,4]triazino[5,6-*b*]indol-5-yl)-5''-oxopentanoate 319

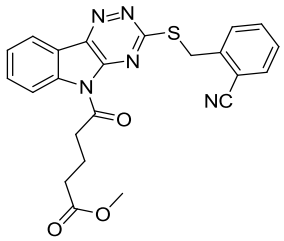

Following **General Procedure 4**, methyl-5-chloro-5-oxopentoate (98 μL, 0.71 mmol) was added to 2'(((5*H*-[1,2,4]triazino[5,6-*b*]indol-3-yl)thio)methyl)benzonitrile **236** (150 mg, 0.47 mmol) and NaH (20.8 mg, 0.52 mmol)in DMF (5 mL) at 0 °C and stirred at rt for 16 h. The reaction mixture was quenched with H_2O until a precipitate formed. The precipitate was filtered and dried to give **319** as a faint yellow solid (170 mg, 81 %); δ_H (500 MHz, DMSO-d_6, 363K) 1.96 - 2.04 (2H, m, -CH_2-) 2.45 (2H, t, *J* = 7.4 Hz, CH_2-C(O)-O), 3.48 (2H, t, *J* = 7.4 Hz, CH_2-C(O)-N), 3.55 (3H, s, OCH_3), 4.80 (2H, s, SCH_2), 7.52 (1H, app t, *J* = 7.7 Hz, C(8)H), 7.61 (1H, t, *J* =7.6 Hz, C(5')H), 7.70 (1H, app td, *J* = 7.7, 1.3 Hz, C(4')H), 7.79 (1H, app td, *J* = 7.6, 1.3 Hz, C(7)H), 7.81 (1H, d, J = 7.6 Hz, C(3')H), 7.91 (1H, d, *J* = 7.6 Hz, C(6')H), 8.36 (1H, d, *J* = 7.6 Hz, C(6)H), 8.58 (1H, d, *J* = 7.8 Hz, C(9)H); δ_C (125 MHz, DMSO-d_6) 19.0 (-C3''H_2-), 32.3 (-C2''H_2-C(O)-N), 32.8 (-C4''H_2-C(O)-O), 37.9 (SCH_2) 51.2 (OCH_3), 112.0 (C2'), 117.3 (C6), 117.4 (CN), 119.3 (C9a), 121.1 (C9), 125.7 (C8), 128.5 (C5'), 130.3 (C3'), 132.1 (C7), 133.2 (C6'), 133.6 (C4'), 139.3 (C9b), 140.4 (C5a), 142.4 (C1'), 147.1 (C4a), 166.6 (C3), 172.9, 173.0 (C5''(O)-O and C2''(O)-N); mp 166-167 °C; *m/z* (ESI^+) 468 ($[M + Na]^+$, 100%); HRMS (ESI^+) $C_{22}H_{17}N_5NaO_3S$ ($[M+Na]^+$) requires 468.1101; found 468.1107; ν_{max} (solid) 2954 (aromatic C-H), 2231 (CN), 1730 (CO ester), 1716 (NC=O), 1381; HPLC (Method 2) >99%, rt = 11.53 min

2'-(((5-(4''-Fluorobenzoyl)-5*H*-[1,2,4]triazino[5,6-*b*]indol-3-yl)thio)methyl)benzonitrile 320

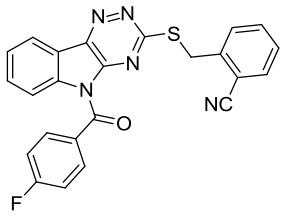

Following **General Procedure 4**, 4-fluoro benzoyl bromide (56 μL, 0.47 mmol) was added to 2'(((5*H*-[1,2,4]triazino[5,6-*b*]indol-3- yl)thio)methyl)benzonitrile **236** (100 mg, 0.32 mmol) and NaH (13.8 mg, 0.35 mmol) in DMF (5 mL) at 0 °C and stirred for 16 h. The reaction mixture was quenched with H_2O until a precipitate formed. The precipitate was filtered and dried to give **320** as a faint yellow solid (95 mg, 67 %); δ_H (500 MHz, DMSO-d_6, 363K) 4.16 (2 H, s, CH_2), 7.34 (2H, app t, J = 8.8 Hz, C(3'')H and C(5'')H), 7.41 (1H, d, J = 7.6 Hz, C(3')H), 7.48 (1H, app td, J = 7.6, 1.3 Hz, C(5')H), 7.62 (1H, td, J = 7.6, 1.3 Hz, C(8)H), 7.66 (1H, app t, J = 7.6 Hz, C(4')H), 7.82 - 7.86 (2H, m, C(6')H and C(7)H), 7.98 - 8.06 (2 H, m, C(2'')H and C(6'')H), 8.28 (1 H, d, J = 7.8 Hz, C(6)H), 8.43 (1 H, d, J = 7.6 Hz, C(9)H); δ_C (125 MHz, DMSO-d_6) 31.9 (CH_2), 111.7 (C2'), 115.5 (2C, d, J = 23 Hz, C3'' and C5''), 116.3 (C6), 117.2 (CN), 119.7 (C9a), 121.4 (C9), 125.6 (C8), 128.4 (C5'), 130.2 (C3'), 130.3 (d, J = 2.9 Hz, C1''), 131.7 (C7), 133.2 (C6'), 133.2 (2C, d, J = 9.5 Hz, C2'' and C6''), 133.4 (C4'), 139.5 (C5a), 140.1 (C9b), 142.2 (C1'), 147.3 (C4a), 165.1 (d, J = 253 Hz, C4''), 166.4 (C3), 166.7 (C(O)); δ_F (470 MHz, DMSO-d_6) -110.4 (C4''-F); mp 202-204 °C; *m/z* (ESI^+) 462 ($[M + Na]^+$, 70%); HRMS (ESI^+) $C_{24}H_{14}FN_5NaOS$ ($[M+Na]^+$) requires 462.0795; found 462.0794; ν_{max} (solid) 2940, 2227 (CN), 1702 (NC=O), 1599, 1573, 1318; $C_{24}H_{14}FN_5OS$ requires C, 65.59; H, 3.21; N, 15.94%; found C, 65.31; H, 3.18; N, 15.98%

2'-(((5-(4''-Dimethylamino)benzoyl)-5*H*-[1,2,4]triazino[5,6-*b*]indol-3-yl)thio)methyl)benzonitrile 321

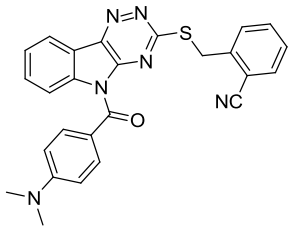

4-dimethylaminobenzoyl chloride (83 mg, 0.48 mmol) was added to a stirred suspension of 2'(((5*H*- [1,2,4] triazino [5,6-*b*] indol-3-yl) thio)methyl)benzonitrile **236** (100 mg, 0.32 mmol), DMAP (0.8 mg, 0.06 mmol) and Et_3N (86 μL, 0.63 mmol) in CH_2Cl_2 (5 mL) at rt for 16 h. CH_2Cl_2 (30 mL) was added to the suspension and washed with H_2O (30 mL). The organic layer was washed with brine (30 mL), dried over $MgSO_4$, filtered and concentrated *in vacuo*. The resulting solid was washed with MeOH and driend to yield **321** as a white solid (81 mg, 55 %); δ_H (400 MHz, pyr-d_5, 363K) 2.84 (6H, s, NCH_3), 5.04 (2H, s, SCH_2), 6.74 (2H, d, *J* = 9.1 Hz, C(3'')H and C(5'')H), 7.28 (1 H, app t, *J* = 7.6 Hz, C(8)H), 7.45 (1H, app t, *J* = 7.6 Hz, C(7)H), 7.56 (1H, app t, *J* = 7.6 Hz, C(4')H), 7.59 (1H, d, *J* = 7.6 Hz, C(3')H), 7.62 - 7.71 (2 H, m, C(5')H and C(6')H), 8.08 (2 H, d, *J* = 9.1 Hz, C(2'')H and C(6'')H), 8.19 (1 H, d, *J* = 7.6 Hz, C(6)H), 8.48 (1 H, d, *J* = 7.6 Hz, C(9)H); δ_C (125 MHz, pyr-d_5) 33.5 (CH_2), 39.7 (CH_3), 111.2 (2C, C3'' and C5''), 113.2 (C2'), 116.2 (C6), 118.1 (CN), 119.4 (C9a), 120.2 (C9b), 121.9 (C9), 125.1 (C8), 128.4 (C5'), 131.1 (C7), 131.5 (C3'), 133.2 (C6'), 133.5 (C4'), 134.0 (2C, C2'' and C6''), 140.9 (C1''), 141.7 (C5a), 142.4 (C1'), 147.6 (C4a), 154.9 (C4''), 166.8 (C(O)), 168.0 (C3); mp 196-197 °C; *m/z* (ESI⁻) 463 ($[M - H]^-$, 50%); HRMS (ESI^+) $C_{26}H_{20}N_6NaOS$ ($[M+Na]^+$) requires 487.1312; found 487.1310; ν_{max} (solid) 2917, 2229 (CN), 1679 (NC=O), 1603, 1184; $C_{26}H_{21}N_6OS \cdot 0.3\ H_2O$ requires C, 66.45; H, 4.42; N, 17.88%; found C, 66.24; H, 4.37; N, 17.92%; HPLC (Method 2) >95 %, rt = 12.15 min

2'-(((5-(4''-(Trifluoromethoxy)benzoyl)-5*H*-[1,2,4]triazino[5,6-*b*]indol-3-yl)thio)methyl)benzonitrile 322

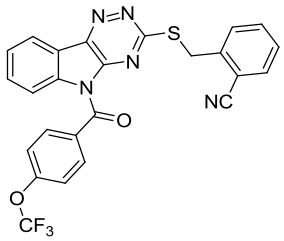

Following **General Procedure 4**, 4-(trifluoromethoxy)benzoyl chloride (74 μL, 0.47 mmol) was added to 2'(((5*H*-[1,2,4]triazino[5,6-*b*]indol-3-yl)thio)methyl)benzonitrile **236** (100 mg, 0.32 mmol) and NaH (60%, 13.8 mg, 0.35 mmol) in DMF (5 mL) at 0 °C and stirred for 16 h at rt. The reaction mixture was quenched with H_2O until a precipitate formed. The precipitate was filtered and dried to give **322** as a white solid (109 mg, 67 %); δ_H (500 MHz, DMSO-d_6, 363K) 4.08 (2 H, s, SCH_2), 7.39 (1 H, d, *J* = 7.6 Hz, C(6')H), 7.45 - 7.53 (3 H, m, C(3'')H, C(5'')H and C(8)H), 7.61 (1 H, app td, *J* = 7.7, 1.2 Hz, C(7)H), 7.68 (1 H, app t, *J* = 7.4 Hz, C(4')H), 7.81 - 7.88 (2 H, m, C(3')H and C(5')H), 8.08 - 8.14 (2 H, m, C(2'')H and C(6'')H), 8.37 (1 H, d, *J* = 7.7 Hz, C(6)H), 8.43 (1 H, d, *J* = 7.3 Hz, C(9)H); δ_C (125 MHz, DMSO-d_6) 32.5 (CH_2), 111.7 (C2'), 116.5 (C6), 117.1 (CN), 119.7 (C9a), 120.4 (2C, C3'' and C5''), 120.7 (C9), 121.3 (C8), 125.8 (C1''), 128.5 (C5'), 129.5 (q, *J* = 258 Hz, C4''-CF_3), 130.3 (C3'), 131.7 (C7), 132.4 (2C, C2'' and C6''), 133.1 (C6'), 133.4 (C4'), 139.4 (C9b), 140.0 (C1'), 142.2 (C5a), 147.3 (C4a), 151.4 (C4''), 166.6 (C3), 170.3 (C(O)); δ_F (470 MHz, DMSO-d_6) -56.8 (CF_3); mp 169-170 °C; *m/z* (ESI^+) 528 ($[M + Na]^+$, 50%); HRMS (ESI^+) $C_{25}H_{14}F_3N_5NaO_2S$ ($[M+Na]^+$) requires 528.0718; found 528.0713; ν_{max} (solid) 2926 (aromatic C-H), 2224 (CN), 1701 (NC=O), 1458; HPLC (Method 2) >97%, rt = 12.07 min

2'-(((5-(3'', 4''-Dimethoxybenzoyl)-5*H*-[1,2,4]triazino[5,6-*b*]indol-3-yl)thio)methyl)benzonitrile 323

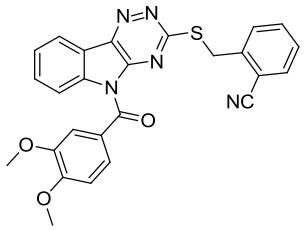

3,4-Dimethoxybenzoyl chloride (95 mg, 0.48 mmol) was added to a stirred suspension of 2'(((5*H*-[1,2,4]triazino[5,6-*b*]indol-3-yl) thio) methyl)benzonitrile **236** (100 mg, 0.32 mmol), DMAP (0.8 mg, 0.06 mmol) and Et_3N (86 μL, 0.63 mmol) in CH_2Cl_2 (5 mL) at rt for 16 h. CH_2Cl_2 (30 mL) was added to the suspension and washed with H_2O (30 mL). The organic layer was washed with brine (30 mL), dried over $MgSO_4$, filtered and concentrated *in vacuo*. The resulting solid was washed with MeOH and dried to yield **323** as a white solid (87 mg, 56 %); δ_H (500 MHz, DMSO-d_6, 363 K) 3.73 (3H, s, C3''-OCH_3), 3.80 (3H, s, C4''-OCH_3), 4.25 (2H, s, SCH_2), 7.09 (1H, d, J = 8.5 Hz, C(5'')H), 7.35 (1H, d, J = 7.9 Hz, C(3')H), 7.46 (1H, app td, J = 7.6, 1.3 Hz, C(5')H), 7.55 (1H, d, J = 1.9 Hz, C(2'')H), 7.59 (1H, td, J = 7.6, 1.3 Hz, C(4')H), 7.63 - 7.67 (2H, m, C(8)H and C(6'')H), 7.80 - 7.85 (2H, m, C(7)H and C(6)'), 8.14 (1H, d, J = 8.5 Hz, C(6)H), 8.43 (1H, d, J = 7.9 Hz, C(9)H); δ_C (125 MHz, DMSO-d_6) 32.1 (CH_2), 55.8 (C4''-OCH_3), 55.9 (C3''-OCH_3), 110.8 (C6) 111.7 (C2'), 113.4 (C5''), 115.9 (C2''), 117.2 (CN), 119.5 (C9a), 121.4 (C9), 125.1 (C1''), 125.3 (C8), 125.5 (C6''), 128.3 (C5'), 130.2 (C3'), 131.5 (C7), 133.2 (C6'), 133.2 (C4'), 139.7 (C1'), 140.5 (C5a), 142.2 (C9b), 147.3 (C4a), 148.4 (C4''), 153.8 (C3''), 166.3 (C3), 166.8 (C(O)); mp 234-235 °C; *m/z* (ESI^+) ($[M + Na]^+$, 100%); HRMS (ESI^+) $C_{26}H_{19}N_5NaO_3S$ ($[M+Na]^+$) requires 504.1110; found 504.1107; ν_{max} (solid) 3115 and 2932 (aromatic C-H), 2229 (CN), 1697 (NC=O), 1514, 1378; HPLC (Method 2) >99%, rt = 11.81 min

2'-(((5-(3''-Trifluoromethyl)benzoyl)-5*H*-[1,2,4]triazino[5,6-*b*]indol-3-yl)thio)methyl)benzonitrile 324

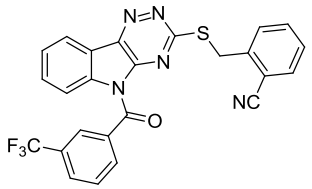

Following **General Procedure 4**, 3-(trifluoromethyl)benzoyl chloride (71 μL, 0.47 mmol) was added to 2'(((5*H*-[1,2,4]triazino[5,6-*b*]indol-3-yl)thio)methyl)benzonitrile **236** (100 mg, 0.32 mmol) and NaH (13.8 mg, 0.35 mmol) in THF (5 mL) followed by at 0 °C and the resulting mixture stirred for 16 h. The reaction mixture was quenched with H_2O until a precipitate formed. The precipitate was filtered, washed with MeOH and dried to give **324** as a faint yellow solid (89 mg, 58 %); δ_H (500 MHz, DMSO-d_6, 363K) 4.74 (2 H, s, $_{SCH2}$), 7.36 (1 H, d, *J* = 8.0 Hz, C(6')H), 7.46 -7.68 (4 H, m, C(7)H, C(8)H, C(4') and C(5'')H) 7.73 – 7.78 (2 H, m, C(3')H and C(5')H), 7.95 (1 H, s, C(2'')H), 8.18 – 8.23 (2 H, m, C(4'')H and C(6'')H), 8.40 (1 H, d, *J* = 8.4 Hz, C(6)H), 8.43 (1H, d, *J* = 7.3 Hz, C(9)H); δ_C (125 MHz, DMSO-d_6) 31.8 (CH_2), 111.7 (C2'), 116.6 (C6), 117.1 (CN), 119.8 (C9a) 121.4 (C9), 123.7 (q, *J* = 273 Hz, CF_3), 125.9 (C8), 126.6 (q, *J* = 3.8 Hz, C2''), 128.4 (C5'), 129.1 (q, *J* = 3.8, C4''), 129.1 (q, *J* = 32 Hz, C3''), 129.5 (C7), 130.2 (C3'), 131.8 (C5''), 133.2 (C6'), 133.4 (C4'), 133.6 (C6''), 135.3 (C9b), 139.4 (C1'), 140.0 (C5a), 142.5 (C1''), 147.4 (C4a), 166.2 (C3), 166.6 (C(O)); δ_F (470 MHz, DMSO-d_6) 61.2 (CF_3); mp 155-156 °C; *m/z* (ESI$^+$) 512 ([M + Na]$^+$, 100%); HRMS (ESI$^+$) $C_{25}H_{14}F_3N_5NaOS$ ([M+Na]$^+$) requires 512.0769; found 512.0759; ν_{max} (solid) 2228 (CN), 1701 (NC=O), 1592, 1580, 1377, 1339; HPLC (Method 2) >95%, rt = 12.19 min

2'-(((5-(2''-Trifluoromethyl-4''-fluorobenzoyl)-5*H*-[1,2,4]triazino[5,6-*b*]indol-3-yl)thio)methyl)benzonitrile 325

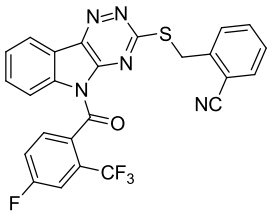

Following **General Procedure 4**, 2-trifluoromethyl-4-fluoro benzoyl bromide (72 µL, 0.47 mmol) was added to 2'(((5*H*-[1,2,4]triazino[5,6-*b*]indol-3-yl)thio)methyl)benzonitrile **236** (100 mg, 0.32 mmol) and NaH (13.8 mg, 0.35 mmol)in DMF (5 mL) at 0 °C and stirred at rt for 16 h. The reaction mixture was quenched with H_2O until a precipitate formed. The precipitate was filtered, washed with MeOH and dried to give **325** as a faint yellow solid (67 mg, 42 %); δ_H (500 MHz, DMSO-d_6, 363K) 4.01 (2H, s, SCH_2), 7.50 - 7.54 (2H, m, C(8)H and C(3')H), 7.65 (1H, app td, *J* = 7.6, 1.3 Hz, C(5')H), 7.67 - 7.71 (1H, m, C(5'')H), 7.73 (1H, app t, *J* = 7.6 Hz, C(4')H), 7.83 (1H, dd, *J* = 7.6, 1.3 Hz, C(3'')H), 7.88 (1H, dd, *J* = 7.6, 1.6 Hz, C(6')H), 7.92 (1H, app td, *J* = 7.6, 1.3 Hz, C(7)H), 8.01 - 8.03 (1H, m, C(6'')H), 8.46 (1H, d, *J* = 7.6 Hz, C(6)H), 8.62 (1H, d, *J* = 7.6 Hz, C(9)H); δ_C (125 MHz, DMSO-d_6) 31.8 (CH_2), 111.8 (C2'), 114.5 (dq, *J* = 26, 4.8 Hz, C3''), 117.0 (CN), 117.0 (C6), 120.0 (d, *J* = 21 Hz, C5''), 120.2 (q, *J* = 276 Hz, CF_3), 121.5 (C9), 123.7 (C9a), 126.6 (C8), 128.4 (qd, *J* = 32, 7.6 Hz, C3''), 128.6 (C5'), 130.2 (m, C1''), 130.2 (C3') 132.0 (d, *J* = 8.6, C6''), 132.4 (C7), 133.2 (C6'), 133.5 (C4'), 138.9 (C9b), 139.3 (C1'), 142.5 (C5a), 147.1 (C4a), 161.7 (C(O)), 163.7 (C3), 165.7 (d, *J* = 238 Hz, C4''); δ_F (470 MHz, DMSO-d_6) -102.4 (q, J = 8.7 Hz, 4''F), 53.8 (CF_3); mp 193-194 °C (EZ Melt); *m/z* (ESI$^+$) 542 ($[M + Cl]^+$, 40%); HRMS (ESI$^+$) $C_{25}H_{13}F_4N_5NaOS$ ($[M + Na]^+$) requires 530.0669; found 530.0678; ν_{max} (solid) 2230 (CN), 1716 (NC=O), 1384, 1292; HPLC (Method 2) >99%, rt = 12.18 min

2'-(((5-(2''-Nitrobenzoyl)-5*H*-[1,2,4]triazino[5,6-*b*]indol-3-yl)thio)methyl)benzonitrile 326

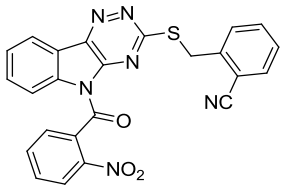

Following **General Procedure 4**, NaH (60%, 13.8 mg, 0.35 mmol) was added to 2'(((5*H*-[1,2,4]triazino[5,6-*b*]indol-3-yl)thio)methyl)benzonitrile **236** (100 mg, 0.32 mmol) in DMF (5 mL) at 0 °C and stirred for 10 mins. 2-nitrobenzoyl bromide (41.6 µL, 0.32mmol) was added, stirred for 16 h and quenched with H_2O. The resulting precipitate was filtered to yield **326** as a white solid (119 mg, 81 %); δ_H (500 MHz, DMSO-d_6, 363K) 3.97 (2H, s, SCH_2), 7.48 - 7.53 (2H, m, C(3')H and C(5')H), 7.63 (1H, app td, *J* = 7.6, 1.3 Hz, C(4')H), 7.75 (1H, app t, *J* = 7.6 Hz, C(7)H), 7.80 (1H, app td, *J* = 7.6, 1.3 Hz, C(4'')H), 7.87 (1H, d, *J* = 7.6 Hz, C(6')H), 7.93 (1H, d, *J* = 7.6, C(6'')H, 7.94 (1H, app td, *J* = 7.6, 1.3 Hz, C(8)H), 7.97 (1H, app td, *J* = 7.6, 1.3 Hz, C(5'')H), 8.27 (1H, d, *J* = 7.6 Hz, C(3'')H), 8.47 (1H, d, *J* = 7.6 Hz, C(6)H), 8.73 (1H, d, *J* = 7.6 Hz, C(9)H); δ_C (125 MHz, DMSO-d_6) 31.9 (SCH_2), 111.8 (C2'), 117.2 (C6''), 119.8 (CN), 121.6 (C9), 124.4 (C6), 126.6 (C7), 128.6 (C5'), 129.0 (C8), 130.3 (C3'), 131.6 (C4''), 131.7 (C9a), 132.5 (C3''), 133.2 (C6'), 133.5 (C4'), 135.6 (C5'), 138.8 (C5a), 139.4 (C1'), 142.3 (C9b), 144.7 (C1''), 146.7 (C4a), 146.8 (C2'') 164.7 (CO), 166.8 (C3); mp 210-213 °C (EZ Melt); *m/z* (ESI^+) 489 ($[M + Na]^+$, 100%); HRMS (ESI^+) $C_{24}H_{14}N_6NaO_3S$ ($[M+Na]^+$) requires 489.0740; found 489.0733; ν_{max} (solid) 2261 (CN), 1711 (NC=O), 1524 (NO_2), 1453, 1383, 1346 (NO_2), 1292; $C_{24}H_{14}N_6O_3S \cdot 0.2\ H_2O$ requires C, 61.32; H, 3.09; N, 17.88%; found C, 61.22; H, 2.86; N, 17.83%

2'-(((5-(Furan-2''-carbonyl)-5*H*-[1,2,4]triazino[5,6-*b*]indol-3-yl)thio)methyl)benzonitrile 327

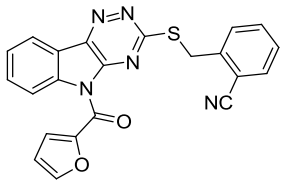

Following **General Procedure 4**, 2-furfuryl chloride (46 μL, 0.47 mmol) was added to 2'(((5*H*-[1,2,4]triazino[5,6-*b*]indol-3-yl)thio)methyl)benzonitrile **236** (100 mg, 0.32 mmol) and NaH (13.8 mg, 0.35 mmol) in DMF (5 mL) at 0 °C and stirred for 16 h. The reaction mixture was quenched with H_2O until a precipitate formed. The precipitate was filtered and dried to give **327** as a faint yellow solid (103 mg, 78 %); δ_H (500 MHz, DMSO-d_6, 363K) 4.49 (2 H, s SCH_2), 6.83 (1 H, dd, *J* = 3.8, 1.8 Hz, C(4'')H), 7.46 (1 H, app td, *J* = 7.6, 1.3 Hz, C(5')H), 7.53 (1H, d, *J* = 7.6 Hz, C(6')H), 7.59 (1H, app t, *J* = 7.8 Hz, C(8)H), 7.60 – 7.64 (1H, m, C(4')H), 7.73 - 7.80 (2 H, m, C(7)H and C(5'')H), 7.84 (1 H, dd, *J* = 7.6, 1.0 Hz, C(3')H), 8.02 (1 H, d, *J* = 8.3 Hz, C(6)H), 8.20 (1H, dd, *J* = 3.8, 0.8 Hz, C(3'')H), 8.38 (1 H, d, *J* = 7.8 Hz, C(9)H); δ_C (125 MHz, DMSO-d_6) 33.3 (CH_2), 112.7 (C2'), 114.0 (C4''), 116.1 (C6), 118.2 (CN), 120.0 (C9a), 122.3 (C9), 125.1 (C8), 126.2 (C5''), 129.2 (C5'), 131.1 (C3'), 132.4 (C7), 134.1 (C6'), 134.2 (C4'), 139.9 (C5a), 141.3 (C1'), 142.7 (C9b), 146.5 (C1''), 147.8 (C4a), 150.8 (C3''), 156.4 (C(O)), 167.3 (C3); mp 177-178 °C; *m/z* (ESI^+) 434 ($[M + Na]^+$, 100%); HRMS (ESI^+) $C_{22}H_{13}N_5NaO_2S$ ($[M-H]^-$) requires 434.0682; found 434.0680; ν_{max} (solid) 2924 (aromatic C-H), 2227 (CN), 1692 (NC=O), 1382, 1309; HPLC (Method 2) >97%, rt = 11.63 min

2'-(((5-(Cyclohexanecarbonyl)-5*H*-[1,2,4]triazino[5,6-*b*]indol-3-yl)thio)methyl)benzonitrile 328

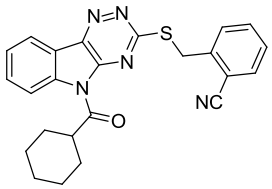

Following **General Procedure 4**, cyclohexane carbonyl chloride (63 μL, 0.47 mmol) was added to 2'(((5*H*-[1,2,4]triazino[5,6-*b*]indol-3-yl)thio)methyl)benzonitrile **236** (100 mg, 0.32 mmol and NaH (13.8 mg, 0.35 mmol)) in DMF (5 mL) at 0 °C and the resulting mixture stirred for 16 h at rt, quenched with H_2O until a precipitate formed. The precipitate was filtered and dried to give **328** as a faint yellow solid (98 mg, 71 %); δ_H (500 MHz, DMSO-d_6, 363K) 1.18 - 1.38 (4 H, m, 2xC(3'')H and 2xC(5'')H), 1.45 – 1.55 (2 H, m, C(4'')H), 1.75 - 1.83 (2 H, m, C(2'')H or C(6'')H) 2.02 – 2.07 (2 H, m, C(2'')H or C(6'')H), 4.04 - 4.12 (1H, m, C(1'')H), 4.84 (2 H, s, SCH_2), 7.53 (1 H, app td, *J* = 7.6, 1.1 Hz, C(8)H), 7.60 - 7.65 (1 H, m, C(4')H or C(6')H), 7.71 (1 H, app td, *J* = 7.6, 1.1 Hz, C(7)H) 7.77 - 7.85 (2 H, m, C(3')H and C(4')H or C(6')H), 7.89 - 7.93 (1 H, m, C(5')H), 8.38 (1 H, d, *J* = 6.9 Hz, C(6)H), 8.59 (1 H, d, *J* = 8.5 Hz, C(9)H); δ_C (125 MHz, DMSO-d_6) 25.1, 25.3 (2xC, C3'' and C5''), 28.5 (C4''), 32.8 (SCH_2), 44.7 (C1''), 112.0 (C6), 112.8 (C2'), 117.4 (C9a), 117.5 (CN), 119.6 (C8), 121.1 (C9), 125.7 (C5'), 128.5 (C5'), 130.4 (C3'), 132.1 (C7), 133.6 (C6'), 139.6 (C9b), 140.3 (C5a), 142.6 (C1'), 147.0 (C4a), 166.5 (C3), 176.2 (C(O)); mp 194-197 °C; *m/z* (ESI^+) 450 ($[M + Na]^+$, 100%); HRMS (ESI^+) $C_{24}H_{21}N_5NaOS$ ($[M+Na]^+$) requires 450.1364; found 450.1362; ν_{max} (solid) 2932, 2854, 2226 (CN), 1720 (NC=O), 1453, 1379; HPLC (Method 2) >95%, rt = 12.67 min

2'-(((5-(Cyclopentanecarbonyl)-5*H*-[1,2,4]triazino[5,6-*b*]indol-3-yl)thio)methyl)benzonitrile 329

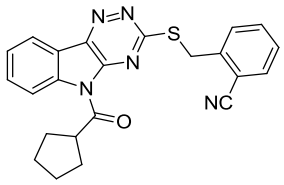

Following **General Procedure 4**, cyclopentane carbonyl chloride (58 μL, 0.47 mmol) was added to 2'(((5*H*-[1,2,4]triazino[5,6-*b*]indol-3-yl)thio)methyl)benzonitrile **236** (100 mg, 0.32 mmol) and NaH (60%, 13.8 mg, 0.35 mmol) in DMF (5 mL) at 0 °C and stirred for 16 h at rt. The reaction mixture was quenched with H_2O until a precipitate formed. The precipitate was filtered and dried to give **329** as a faint yellow solid (56 mg, 42 %); δ_H (500 MHz, DMSO-d_6, 363K) 1.56 - 1.64 (2 H, m, C(3'')H and C(4'')H), 1.66 - 1.74 (2 H, m, C(3'')H and C4'')H), 1.87 - 2.03 (4 H, m, C(2'')H and C(5'')H), 4.35 - 4.42 (1 H, m, C(1'')H), 4.81 (2 H, s, SCH_2), 7.52 (1 H, app t, *J* = 7.6 Hz, C(8)H), 7.62 (1 H, app t, *J*=7.6 Hz, C(5')H), 7.71 (1 H, app td, *J* = 7.6, 1.1 Hz, C(4')H), 7.79 (1H, app t, J = 7.6 Hz, C(7)H), 7.80 (1H, d, *J* = 7.6 Hz, C(3')H), 7.92 (1 H, d, *J* = 7.6 Hz, C(6')H), 8.38 (1 H, d, *J* = 7.6 Hz, C(6)H), 8.58 (1 H, d, *J* = 7.6 Hz, C(9)H); δ_C (125 MHz, DMSO-d_6) 25.6 (2C, C3'' and C4''), 29.5 (2C, C2'' and C5''), 32.7 (CH_2), 45.9 (C1''), 111.9 (C2'), 117.4 (CN), 117.5 (C6), 119.5 (C9a), 121.1 (C9), 125.7 (C8), 128.4 (C5'), 130.4 (C3'), 132.0 (C7), 133.2 (C6'), 133.6 (C4'), 139.6 (C9b), 140.2 (C1'), 142.5 (C5a), 147.0 (C4a), 166.6 (C3), 176.3 (C(O)); mp 173-174 °C; *m/z* (ESI^+) 436 ($[M + Na]^+$, 100%); HRMS (ESI^+) $C_{23}H_{19}N_5NaOS$ ($[M+Na]^+$) requires 436.1203; found 436.1198; ν_{max} (solid) 2871 (aromatic C-H), 2229 (CN), 1720 (NC=O), 1577, 1380; HPLC (Method 2) >98%, rt = 12.32 min

2'-(((5-(Cyclopropanecarbonyl)-5*H*-[1,2,4]triazino[5,6-*b*]indole-3-yl)thio)methyl)benzonitrile 330

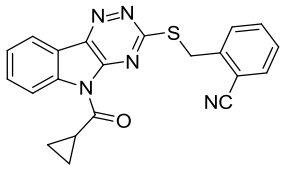

Following **General Procedure 4**, Cyclopropane carbonyl chloride (29 µL, 0.32 mmol) was added to 2'(((5*H*-[1,2,4]triazino[5,6-*b*]indol-3-yl)thio)methyl)benzonitrile **236** (100 mg, 0.32 mmol) and NaH (60%, 13.8 mg, 0.35 mmol) in DMF (5 mL) at 0 °C and stirred at rt for 16 h. Reaction mixture was quenched with H_2O and the resulting precipitate was filtered and washed with MeOH to yield **330** as a white solid (83 mg, 76 %); δ_H (500 MHz, DMSO-d_6, 363K) 1.16 - 1.28 (4H, m, C(2")H_2 and C(3")H_2), 3.50 - 3.56 (1H, m, C(1")H), 4.78 (2H, s, SCH_2), 7.5 (1H, t, *J* = 7.9 Hz, C(8)H), 7.58 (1H, app t, *J* = 7.7 Hz, C(5')H), 7.69 (1H, app td, *J* = 7.7, 1.2 Hz, C(4')H), 7.74 (1H, app t, *J* = 7.9 Hz, C(7)H), 7.80 (1H, d, *J* = 7.9 Hz, C(6)H), 7.89 (1H, dd, *J* = 7.7, 1.2 Hz, C(3')H), 8.33 (1H, d, *J* = 7.7 Hz, C(6')H), 8.46 (1H, d, *J* = 7.9 Hz, C(9)H); δ_C (125 MHz, DMSO-d_6) 11.6 (2C, C2" and C3"), 16.1 (C1"), 32.8 (SCH_2), 111.8 (C2'), 117.1 (C6), 117.4 (CN), 119.1 (C9a), 121.1 (C9), 125.6 (C8), 128.4 (C4'), 130.0 (C7), 130.5 (C3'), 131.9 (C6'), 133.2 (C5'), 133.5 (C9b), 139.3 (C1'), 142.5 (C5a), 147.4 (C4a), 166.4 (C3), 174.0 (CO); mp 183 - 184 °C; *m/z* (ESI^+) 386 ($[M + H]^+$, 100%); HRMS (ESI^+) $C_{21}H_{16}N_5OS$ ($[M+H]^+$) requires 386.1073; found 386.1073; ν_{max} (solid) 3045 and 2924 (aromatic C-H), 2224 (CN), 1702 (NC=O); HPLC (Method 2) >99%, rt = 11.89 min

2'-(((5-(Isoxazole-5''-carbonyl)-5*H*-[1,2,4]triazino[5,6-*b*]indol-3-yl)thio)methyl)benzonitrile 331

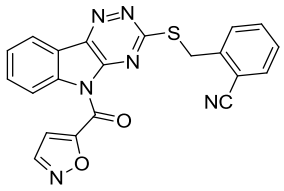

Following **General Procedure 4**, isoxazole-5-carbonyl chloride (62 μL, 0.47 mmol) was added to 2'(((5*H*-[1,2,4]triazino[5,6-*b*]indol-3-yl) thio) methyl)benzonitrile **236** (100 mg, 0.32 mmol) and NaH (60%, 13.8 mg, 0.35 mmol) in DMF (5 mL) at 0 °C and stirred for 16 h. The reaction mixture was quenched with H_2O until a precipitate formed. The precipitate was filtered and dried to give **331** as a faint yellow solid (112 mg, 85 %); δ_H (500 MHz, DMSO-d_6, 363K) 4.44 (2 H, s, CH_2), 7.48 (1H, d, *J* = 1.9 Hz, C(5'')H), 7.49 (1H, app td, *J* = 7.6, 1.3 Hz, C(5')H), 7.60 – 7.67 (2H, m, C(8)H and C(7)H), 7.69 (1H, app t, *J* = 7.6 Hz, C(4')H), 7.83 - 7.87 (2 H, m, C(3')H and C(6')H), 8.32 (1 H, d, *J* = 7.6 Hz, C(6)H), 8.42 (1 H, d, *J* = 7.6 Hz, C(9)H), 8.91 (1 H, d, *J* = 1.9 Hz, C(4'')H); δ_C (125 MHz, DMSO-d_6) 32.4 (CH_2), 110.7 (C5''), 111.9 (C2'), 116.3 (C6), 117.5 (CN), 122.5 (C9), 126.4 (C7), 128.5 (C5'), 130.3 (C3'), 132.0 (C7), 133.1 (C6'), 133.4 (C4'), 138.6 (C9a), 140.1 (C5a), 141.2 (C9b), 142.3 (C1'), 147.2 (C4a), 151.9 (C4''), 155.5 (C1''), 160.5 (C(O)), 166.5 (C3); mp 195-196 °C; *m/z* (ESI^+) 413 ($[M + Na]^+$, 100%); HRMS (ESI^+) $C_{21}H_{12}N_6NaO_2S$ ($[M+Na]^+$) requires 413.0815; found 340.0610 (corresponds to parent compound); ν_{max} (solid) 2923, 2227 (CN), 1709 (NC=O), 1299; HPLC (Method 2) >95%, rt = 11.47 min

2'-(((5-(Morpholine-4''-carbonyl)-5*H*-[1,2,4]triazino[5,6-*b*]indol-3-yl)thio)methyl)benzonitrile 332

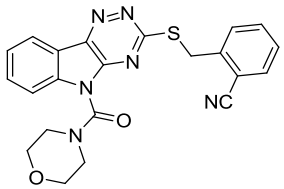

Following **General Procedure 4**, NaH (60%, 13.8 mg, 0.34 mmol) was added to a suspension of 2'(((5*H*-[1,2,4]triazino[5,6-*b*]indol-3- yl)thio)methyl)benzonitrile **236** (100 mg, 0.32 mmol) in DMF (5 mL) at 0 °C followed for 10 mins. Morpholine carbonyl chloride (47 μL, 0.32 mmol) was added, stirred for 16 h, cooled in an ice bath and quenched slowly with dropwise addition of H_2O. The resulting precipitate was filtered and dried to yield **332** as a white solid (98 mg, 72 %); δ_H (500 MHz, DMSO-d_6, 363K) 3.40 - 3.79 (8H, m, 8xCH), 4.78 (2H, s, SCH_2), 7.50 (1H, app td, *J* = 7.8, 1.3 Hz, C(5')H), 7.57 (1H, app t, *J* = 7.6 Hz, C(8)H), 7.68 (1H, app td, *J* = 7.8, 1.3 Hz, C(4')H), 7.76 (1H, d, *J* = 7.8 Hz, C(3')H), 7.79 (1H, app t, *J* = 7.6 Hz, C(7)H), 7.83 (1H, d, *J* = 7.6 Hz, C(6)H), 7.89 (1H, dd, *J* = 7.8, 1.3 Hz, C(6')H), 8.37 (1H, d, *J* = 7.6 Hz, C(9)H); δ_C (125 MHz, DMSO-d_6) 32.7 (SCH_2), 44.7 (2C, C2'' and C6''), 66.1 (2C, C3'' and C5''), 112.0 (C6), 113.9 (C9), 117.5 (CN), 118.5 (C9a), 121.6 (C9), 124.3 (C8), 128.3 (C5'), 130.4 (C3'), 131.5 (C7), 133.2 (C6'), 133.3 (C4'), 139.4 (C9b), 140.9 (C5a), 141.8 (C1'), 145.7 (C4a), 148.4 (CO), 166.3 (C3); mp 191-193 °C (EZ Melt); *m/z* (ESI^+) 453 ($[M + Na]^+$, 100%); HRMS (ESI^+) $C_{22}H_{18}N_6NaO_2S$ ($[M+Na]^+$) requires 453.1104; found 453.1087; ν_{max} (solid) 2928 and 2867 (aromatic C-H), 2223 (CN), 1688 (urea NC=ON), 1570, 1389; HPLC (Method 2) >99%, rt = 10.86 min

2-(2-Amino-2-hydrazinylethyl)benzonitrile hydrobromide 340[287]

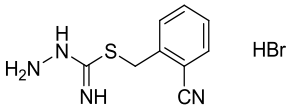

Thiosemicarbizide (1 g, 11.0 mmol), and 2-cyano benzyl bromide (2.15 g, 11.0 mmol) were added to EtOH (30 mL) and heated to 60 °C for 30 mins. The suspension was filtered and resulting solid was washed with EtOH and dried *in vacuo* to yield **340** as a fine white crystalline solid (2.20 g, 96 %); δ_H (500 MHz DMSO-d_6 363 K) 4.58 (1H, s, CH_2), 5.35 (1H, br s, NH), 7.53 (1H, app t, *J* = 7.6 Hz, C(4)H), 7.65 (1H, d, *J* = 7.6 Hz, C(6)H), 7.71 (1H, app t, *J* = 7.6 Hz, C(5)H), 7.88 (1H, d, *J* = 7.6 Hz, C(3)H), 9.19 (2H, br s, NH_2), 10.74 (1H, br s, NH); δ_C (100 Hz, DMSO-d_6) 33.6 (CH_2), 112.6 (C2), 118.0 (CN), 129.7 (C4), 131.2 (SCH_2), 134.4 (C3), 134.4 (C5), 155.1 (C1), 155.5 (NC(N)); mp 166-167 °C; *m/z* (ESI^-) 205 ($[M - H]^-$, 100%); HRMS (ESI^+) $C_9H_{11}N_4S^+$ ($[M+H]^+$) requires 207.0699; found 207.0700; ν_{max} (solid) 3295, 3170, 2954, 2235 (CN), 1646, 1607, 1311

2'-(((1,2,4-triazin-yl)thio)methyl)benzonitrile 341

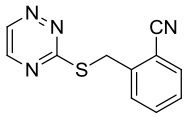

2-(2-amino-2-hydrazinylethyl)benzonitrile hydrobromide **340** (200 mg, 0.70 mmol), glyoxal (304 µL, 2.10 mmol) and NaOAc (57 mg, 0.70 mmol) were dissolved in H_2O (5 mL) and heated in a sealed vial at 120 °C for 16 rt. The solution was allowed to cool to rt and resulting precipitate was filtered and dried to yield **341** as a white solid (126 mg, 79 %); δ_H (400 MHz $CDCl_3$ 363 K) 4.69 (2H, s, CH_2), 7.37 (1H, app t, *J* = 7.6 Hz,), 7.54 (1H, t, *J* = 7.6 Hz,), 7.67 (1H, d, *J* = 7.6 Hz, C(6')H), 7.72 (1H, d, *J* = 7.6 Hz, C(3')H), 8.41 (1H, d, *J* = 2.2 Hz, C(5)H), 8.97 (1H, d, *J* = 2.2 Hz, C(6)H); δ_C (100 Hz, $CDCl_3$) 33.0 (CH_2), 113.1 (C2'), 117.5 (CN), 128.1 (C4'), 130.4 (C6'), 133.0 (C5'), 133.2 (C3'), 140.7

(C1'), 145.9 (C5), 148.4 (C6), 173.1 (C3); mp 78-79 °C; *m/z* (ESI$^-$) 227 ([M - H]$^-$, 100%); HRMS (ESI$^+$) $C_{11}H_8N_4NaS$ ([M+Na]$^+$) requires 251.0362; found 251.0363; ν_{max} (solid) 2224 (CN), 1596, 1511, 1381, 1199; HPLC (Method 2) >95%, rt = 9.52 min

2-(((5-hydroxy-1,2,4-triazin-3-yl)thio)methyl)menzonitrile 342

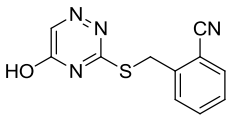

Ethyl glyoxylate (69 uL, 0.70 mmol) was added to a solution of 2-cyanobenzyl hydrazinecarbimidothioate hydrobromide **340** (200 mg, 0.70 mmol) and NaOAc (86 mg, 1.05 mmol) in H_2O (5 mL) and stirred in a sealed vial at 120 °C. A precipitate immediately formed, after 1 hr, the reaction mixture was cooled, filtered and resulting residue was washed with EtOAc to yield **342** as a faint yellow solid (49 mg, 29 %); δ_H (400 MHz, DMSO-*d*$_6$, 363K) 4.57 (2H, s, CH_2), 7.50 (1H, app td, *J* = 7.2, 1.3 Hz, C(5')H), 7.65 (1H, s, C(6)H), 7.68 (1H, app td, *J* = 7.2, 1.3 Hz, C(4')H), 7.71 (1H, d, J = 7.2 Hz, C(3')H), 7.87 (1H, d, *J* = 7.2 Hz, C(6')H), 14.08 (1H, br s, OH); δ_C (100 MHz, DMSO-*d*$_6$) 32.1 (CH_2), 112.8 (C2'), 118.1 (CN), 129.4 (C5'), 131.4 (C3'), 134.1 (C6'), 134.3 (C4'), 141.1 (C1'), 143.1 (C6), 166.1 (C3), 169.2 (C5); mp 200-201 °C (EZ Melt); *m/z* (ESI$^-$) 243 ([M - H]$^-$, 100%); HRMS (ESI$^+$) $C_{11}H_8N_4NaOS$ ([M+Na]$^+$) requires 267.0311; found 267.0311; ν_{max} (solid) 2510 (br, O-H), 2222 (CN), 1583, 1533, 1432, 1368; HPLC (Method 2) >99%, rt = 8.07 min

2'-(((5-Hydroxy-6-methyl-1,2,3-triazin-3-yl)thio)methyl)benzonitrile 343

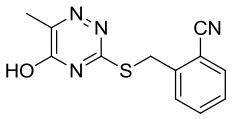

2-(2-amino-2-hydrazinylethyl)benzonitrile **389** (200 mg, 0.07 mmol) was added to a solution of NaOAc (57 mg, 0.07 mmol) and pyruvic acid (49 uL, 0.70 mmol) in H_2O (5 mL) and stirred in a sealed vial at rt for 16 h. The precipitate was filtered and washed with EtOAc to yield **343** as a light brown solid (165 mg, 92 %); δ_H (500 MHz DMSO-d_6 363 K) 2.11 (3H, s, CH_3), 4.56 (2H, s, CH_2), 7.49 (1H, app t, J = 7.8 Hz, C(4')H), 7.67 (1H, app td, J = 7.8, 1.3 Hz, C(5')H), 7.70 (1H, d, J = 7.8 Hz, C(6')H), 7.86 (1H, d, J = 7.8 Hz, C(3')H), 13.81 (1H, br s, OH); δ_C (100 Hz, DMSO-d_6) 17.6 (CH_3), 32.2 (SCH_2), 112.7 (C2'), 118.1 (CN), 129.4 (C4'), 131.4 (C6'), 134.1, 134.3 (C3' and C5'), 141.2 (C3), C5 and C6 were not visible; mp 206-207 °C; *m/z* (ESI$^-$) 257 ([M - H]$^-$, 100%); HRMS (ESI$^+$) $C_{12}H_{10}N_4NaOS$ ([M+Na]$^+$) requires 281.0468; found 281.0465; ν_{max} (solid) 3147, 2938 (O-H), 2228 (CN), 1613, 1356, 1263; HPLC (Method 2) >99%, rt = 8.47 min

2-(((5-phenyl-1,2,4-triazin-3-yl)thio)methyl)benzonitrile 344

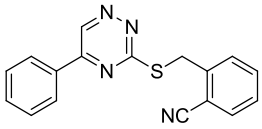

Phenyl glyoxylate monohydrate (300 mg, 1.97 mmol) was added to a solution of 2-cyanobenzyl hydrazinecarbimidothioate hydrobromide **340** (734 mg, 1.97 mmol) and NaOAc (162 mg, 1.97 mmol) in EtOH (5 mL) and stirred in a sealed vial at 120 °C for 16 h. The yellow suspension turned to a yellow solution overnight forming a precipitate when cooled back to rt. The precipitate was filtered and resulting residue was washed with EtOH to yield **344** as a faint yellow solid (423 mg, 71 %); δ_H (400 MHz, DMSO-d_6, 363K) 4.78 (2H, s, CH_2), 7.48 (1H, app t, J = 8.0 Hz, C(4')H), 7.58 – 7.62 (2H, m, C(3'')H and C(5'')H), 7.64 – 7.69 (2H, m, C(4'')H and C(5')H), 7.79 (1H, d, J = 8.0 Hz, C(6')H), 7.88 (1H, d, J = 8.0 Hz, C(3')H), 8.29 – 8.31 (2H, m, C(2'')H and C(6'')H, 9.85 (1H, s, C(6)H); δ_C (100 MHz, DMSO-d_6) 32.8 (CH_2), 112.4 (C2'), 117.9 (CN), 128.5 (2C, C2'' and C6''), 128.8 (C4'), 129.8 (2C, C3'' and C5''), 130.7 (C6'), 133.0 (C1''), 133.5 (C4'' or C5'), 133.7 (C3'), 133.9 (C4'' or C5'), 141.3 (C1'), 144.0 (C6), 155.0 (C5), 171.4 (C3); mp (EZ Melt) 120-121 °C; *m/z* (ESI^+) 327 ($[M + Na]^+$, 100%); HRMS (ESI^+) $C_{17}H_{12}N_4NaS$ ($[M+Na]^+$) requires 327.0675; found 327.0678; ν_{max} (solid) 2926, 2222, 1527, 1500; HPLC (Method 2) >99%, rt = 11.29

2-(((5-hydroxy-6-phenyl-1,2,4-triazin-3-yl)thio)methyl)benzonitrile 345

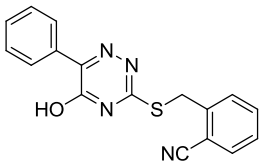

2-cyanobenzyl hydrazinecarbimidothioate hydrobromide **340** (572 mg, 1.99 mmol) was added to a suspension of NaOAc (109.3 mg, 1.33 mmol) in EtOH (5 mL). The suspension

was heated until dissolution and 2-oxo-2-phenylacetic acid (200 mg, 1.33 mmol) was added. The sealed vial was heated to 120C and stirred for 16 h in which the solution changed from a yellow to a light brown solution. Upon cooling to rt, a precipitate formed, which was filtered and washed with EtOH to yield **345** as a yellow solid (346 mg, 81%); δ_H (400 MHz, DMSO-d_6, 363K) 4.64(2H, s, CH_2), 7.45 – 7.49 (3H, C(3'')H, C(5'')H and C(4'')H), 7.51 (1H, td, *J* = 7.6, 1.3 Hz, C(5')H), 7.70 (1H, td, *J* = 7.6, 1.3 Hz, C(3')H), 7.89 (1H, dd, *J* = 7.6, 1.3 Hz, C(6')H), 8.02 (2H, dd, *J* = 8.2, 1.3 Hz, C(2'')H and C(6'')H), 14.28 (1H, br s, OH); δ_C (100 MHz, DMSO-d_6) 31.6 (CH2), 111.9 (C2'), 117.3 (CN), 128.1 (2C, C2'' and C6''), 128.5 (2C, C3'' and C5''), 128.6 (C5'), 130.0 (C3'), 130.6; mp (EZ Melt); 247-248 °C; *m/z* (ESI^-) 319 ($[M - H]^-$, 100%); HRMS (ESI^+) $C_{17}H_{12}N_4NaOS$ ($[M+Na]^+$) requires 343.0630; found 343.0621; ν_{max} (solid) 2985 (OH), 2222 (CN), 1603, 1526, 1444, 1281; HPLC (Method 2) >99%, rt = 11.31

2-(((5,6-diphenyl-1,2,4-triazin-3-yl)thio)methyl)benzonitrile 346

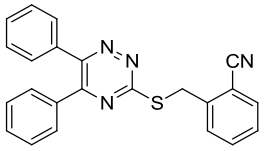

Following **General Procedure 3:** 2-cyano benzyl bromide (111 mg, 0.57 mmol) was added to 5,6-diphenyl-1,2,4-triazine-3-thiol **390** (100 mg, 0.38 mmol) and Et_3N (79 uL, 0.57 mmol) in MeOH (15 mL) and stirred for 16 h at rt. The resulting solid was filtered and washed with a solution of aq Et_3N to yield **346** as a yellow solid (110 mg, 77%); δ_H (400 MHz DMSO-d_6 363 K) 4.79 (2H, s, CH_2), 7.34-7.50 (11H, m, 11xAr-H), 7.66 (1H, app td, *J* = 7.8, 1.3 Hz, C(5')H), 7.81 (1H, d, *J* = 7.8 Hz, C(6')H), 7,87 (1H, d, *J* = 7.6 Hz, C(3')H); δ_C (100 Hz, DMSO-d_6) 33.4 (CH_2), 112.9 (C2'), 118.3 (CN), 129.2 (2C, C3'' and C5''), 129.3 (4C, C3''' and C5''', C4'' and C4'''), 130.2 (2C, C2'' and C6''), 130.6 (2C, C2''' and C6'''), 131.3 (C6'), 131.7 (C4'), 134.0 (C1''), 134.2 (C1'''), 135.7 (C5'), 136.0

(C3'), 141.7 (C1'), 155.4 (C5), 156.8 (C6), 169.6 (C3); mp 128-129 °C; *m/z* (ESI^+) 403 ($[M + Na]^-$, 100%); HRMS (ESI^+) $C_{23}H_{16}N_4NaS$ ($[M-H]^-$) requires 403.0988; found 403.0974; ν_{max} (solid) 2221 (CN), 1475, 1342, 1185; $C_{23}H_{16}N_4NaS$ requires C, 72.60; H, 4.24; N, 14.73%; found C, 72.30; H, 4.25; N, 14.62%

Methyl-2-oxo-4-phenylbut-3-ynoate 349[313]

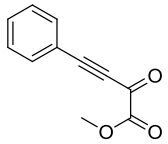

Copper Iodide (177 mg, 0.9 mmol) was added to a solution of Et_3N (3.8 mL, 27.4 mmol) in THF (30 mL) and stirred until a colourless solution formed. Phenylacetylene (1.5 mg, 13.7 mmol) and methyl chlorooxoacetate (3.07 mg, 27.4 mmol) were added to the solution and stirred at rt for 16 h. The mixture was diluted with Et_2O (100 mL) and washed with bicarb (100 mL). Aqueous layer was washed with Et_2O (50 mL). Combined organic extracts were washed with brine (100 mL), dried over $MgSO_4$, filtered and concentrated *in vacuo* to yield the crude product as a brown oil which was purified by flash column chromatography (eluent EtOAc: Pet Ether, 3:1) to afford **349** as a yellow liquid (2.25 g, 80%); δ_H (400 MHz $CDCl_3$ 363 K) 3.97 (3H, s, OCH_3), 7.43 (2H, app t, *J* = 7.6 Hz, C(3)H and C(5)H), 7.51 - 7.55 (1H, m, C(4)H), 7.68 (2H, d, *J* = 7.6 Hz, C(2)H and C(6)H); δ_C (100 Hz, $CDCl_3$) 53.7 (CH_3), 87.1 ($CH_3CO_2C(O)\underline{C}{\equiv}C$), 98.2 ($CH_3CO_2C(O)C{\equiv}\underline{C}$), 119.0 (C1), 128.8 (2C, C3 and C5), 131.9 (C4), 133.8 (2C, C2 and C6), 159.6 ($CH_3O\underline{C}(O)$), 169.1 (C4); *m/z* (ESI^+) 211 ($[M + Na]^+$, 100%), *m/z* (ESI^-) 174 ($[M - (CH_3)H]^-$, 50%); HRMS (ESI^+) $C_{11}H_8NaO_3$ ($[M+Na]^+$) requires 211.0366; found 211.0363; ν_{max} (liquid) 2180 (alkyne), 1729 (1,2-diketone), 1660, 1249, 1077

3-mercapto-6-(phenylethynyl)-1,2,4-triazin-5-ol 350

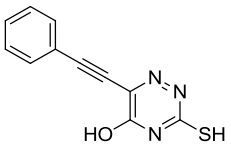

Thiosemicarbizide (135 mg, 1.49 mmol) was added to a suspension of $NaHCO_3$ (137 mg, 1.63 mmol) in EtOH (6 ml) and heated until a homogeneous solution was formed. Methyl-2-oxo-4-phenylbut-3-ynoate **349** (300 mg, 1.49 mmol) was added and heated for 3 hr in a sealed vial at 120 °C. The solution was cooled to rt, the resulting precipitate was filtered and washed with Et_2O to yield **350** as a yellow solid (145 mg, 43 %); δ_H (400 MHz DMSO-d_6 363 K) 6.20 (1H, s, OH), 7.31 (1H, tt, J = 7.6, 1.3 Hz, C(4')H), 7.38 (2H, app t, J = 7.6 Hz, C(3')H and C(5')H), 7.73 (2H, d, J = 7.6 Hz, C(2')H and C(6')H), 11.91 (1H, br s, SH); δ_C (100 Hz, DMSO-d_6) 101.8 (2C, 2x alkyne C), 125.6 (2C, C3' and C5'), 127.6 (C4'), 128.2 (2C, C2' and C6'), 138.4 (C1') 148.3 (C5), 164.8 (C5), 166.5 (C3); mp >300 °C; *m/z* (ESI$^-$) 228 ([M - H]$^-$, 100%); HRMS (ESI$^-$) $C_{11}H_6N_3OS$ ([M-H]$^-$) requires 228.0237; found 228.0232; ν_{max} (solid) 2050 (alkyne), 1639, 1561, 1520, 1497, 1319

2'-(((5-(2,4,6-Trimethylbenzoyl)-5*H*-[1,2,4]triazino[5,6-*b*]indol-3-yl)thio)methyl)benzonitrile 352

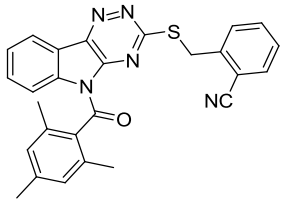

Following **General Procedure 4**, 2,4,6-Trimethylbenzoyl chloride (52 µL, 0.32 mmol) was added to 2'(((5*H*-[1,2,4]triazino[5,6-*b*]indol-3-yl)thio)methyl)benzonitrile **236** (100 mg, 0.32 mmol) and NaH (60%, 13.8 mg, 0.35 mmol) in DMF (5 mL) at 0 °C and subsequently stirred at rt for 16 h at rt. Quenched with H_2O and the resulting precipitate

was filtered and washed with MeOH to yield **352** as a white solid (32 mg, 22 %); δ_H (500 MHz, DMSO-d_6, 363K) 1.97 (3H, s, C(4'')CH_3), 2.09 (6H, s, C(2'')CH_3 and C(6'')CH_3), 3.76 (2H, s, SCH_2), 6.84 (2H, s, C(3'')H and C(5'')H), 7.45 (1H, d, *J* = 7.6 Hz, C(3')H), 7.53 (1H, app t, *J* = 7.6 Hz, C(5')H), 7.66 (1H, app t, *J* = 7.6 Hz, C(4')H), 7.71 (1H, app t, *J* = 7.6 Hz, C(7)H), 7.86 – 7.92 (2H, m, C(8)H and C(6')H), 8.46 (1H, d, *J* = 7.6 Hz, C(6)H), 8.72 (1H, d, *J* = 8.3 Hz, C(9)H); δ_C (125 MHz, DMSO-d_6) 18.8 (C4''$\underline{C}H_3$), 20.5 (2C, C2''$\underline{C}H_3$ and C6''$\underline{C}H_3$), 31.3 (SCH_2), 111.7 (C2'), 117.1 (C6), 117.2 (CN), 120.1 (C9a), 121.4 (C9), 126.3 (C8), 128.2 (2C, C3'' and C5''), 128.6 (C5'), 130.6 (C3'), 132.1 (C7), 133.2 (C6'), 133.5 (C4'), 134.0 (3C, C1'', C2'' and C6''), 138.5 (C4''), 139.1 (C9b), 139.9 (C1'), 142.1 (C5a), 146.7 (C4a), 167.7 (C3), 169.1 (CO); mp 218-219 °C (EZ Melt); *m/z* (ESI^+) 486 ($[M + Na]^+$, 100%); HRMS (ESI^+) $C_{27}H_{21}N_5NaOS$ ($[M+Na]^+$) requires 486.1359; found 486.1358; ν_{max} (solid) 2225 (CN), 1706 (NC=O), 1580, 1451, 1386, 1287

2'-(((5-(3'',4'',5''-trimethoxybenzoyl)-5*H*-[1,2,4]triazino[5,6-*b*]indol-3-yl)thio)methyl)benzonitrile 354

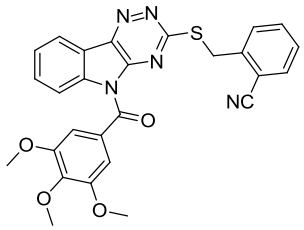

Following **General Procedure 4**, 3,4,5-Trimethoxybenzoyl chloride (73 mg, 0.32 mmol) was added to 2'(((5*H*-[1,2,4]triazino[5,6-*b*]indol-3-yl)thio)methyl)benzonitrile **236** (100 mg, 0.32 mmol) and NaH (60%, 13.8 mg, 0.35 mmol) in DMF (5 mL) at 0 °C for 16 h and quenched with H_2O. The resulting precipitate was filtered and washed with MeOH to yield **354** as a white solid (76 mg, 47 %); δ_H (500 MHz, DMSO-d_6, 363K) 3.60 (3H, s, C4''OCH_3), 3.75 (6H, C3''OCH_3 and C5''OCH_3), 4.20 (2H, s, SCH_2), 7.35 (2H, s, C(2'')H and C(6'')H), 7.45 (1H, app t, *J* = 7.6 Hz, C(5')H), 7.60 (1H, app t, *J* = 7.6 Hz,

C(4')H), 7.65 (1H, app t, *J* = 7.3 Hz, C(8)H), 7.81 – 7.87 (2H, m, C(7)H and C(6')H), 8.25 (1H, d, *J* = 7.3 Hz, C(6)H), 8.44 (1H, d, *J* = 7.3 Hz, C(9)H); δ_C (125 MHz, DMSO-d_6) 31.9 (SCH_2), 56.4 (2C, C3''OCH3 and C5''OCH3), 60.0 (4''OCH_3), 108.3 (2C, C2'' and C6''), 111.7 (C2'), 116.2 (C6), 117.2 (CN), 119.8 (C9a), 121.3 (C9), 125.5 (C8), 128.5 (C5'), 128.6 (C1''), 130.4 (C3'), 131.6 (C7), 133.2 (C6'), 133.3 (C4'), 139.6 (C1'), 140.5 (C5a), 142.0 (C4''), 142.4 (C9b), 147.4 (C4a), 152.7 (2C, C3'' and C5''), 166.2 (C3), 167.1 (CO); mp 209-212 °C; *m/z* (ESI^+) 534 ($[M + Na]^+$, 100%); HRMS (ESI^+) $C_{27}H_{21}N_5NaO_4S$ ($[M+Na]^+$) requires 534.1159; found 534.1156; ν_{max} (solid) 2941, 2227 (CN), 1692 (NC=O), 1589, 1292, 1124

2'-(((5-(benzo[*d*][1,3]dioxole-5-carbonyl)-5*H*-[1,2,4]triazino[5,6-*b*]indol-3-yl)thio)methyl)benzonitrile 355

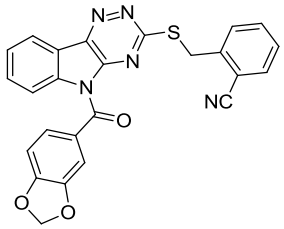

Following **General Procedure 4**, Piperonyloyl chloride (55 mg, 0.32 mmol) was added to 2'(((5*H*-[1,2,4]triazino[5,6-*b*]indol-3-yl)thio)methyl)benzonitrile **236** (100 mg, 0.32 mmol) and NaH (60%, 13.8 mg, 0.35 mmol) in DMF (5 mL) at 0 °C for 16 h at rt and quenched with H_2O. The resulting precipitate was filtered, washed with MeOH to yield **355** as white solid (104 mg, 71 %); δ_H (500 MHz, DMSO-d_6, 363K) 4.30 (2H, s, SCH_2), 6.10 (2H, s, OCH_2O), 7.01 (1H, d, *J* = 8.3 Hz, C(3')H), 7.39 (1H, d, *J* = 7.6 Hz, C(5'')H), 7.46 (1H, app t, *J* = 7.6 Hz, C(5')H), 7.54 (1H, d, *J* = 7.6 Hz, C(2'')H), 7.58 – 7.62 (2H, m, C(4')H and C(6'')H), 7.63 (1H, app t, *J* = 7.6 Hz, C(8)H), 7.79 – 7.86 (2H, m, C(7)H and C(6')H), 8.13 (1H, d, *J* = 7.9 Hz, C(6)H), 8.43 (1H, d, *J* = 7.6 Hz, C(9)H); δ_C (125 MHz, DMSO-d_6) 32.1 (SCH_2), 102.3 (OCH_2), 108.1 (C3'), 110.2 (C2''), 111.7 (C2'), 115.9 (C6), 117.3

(CN), 119.5 (C9a), 121.4 (C9), 125.3 (C8), 127.0 (C1''), 127.1 (C6''), 128.3 (C5'), 130.2 (C5''), 131.5 (C7), 133.2 (C6'), 133.3 (C4'), 139.6 (C1'), 140.5 (C5a), 142.1 (C9b), 147.3 (C3''), 147.4 (C4a), 152.1 (C4''), 166.5 (C3), 167.6 (CO); mp 246-248 °C; *m/z* (ESI^+) 488 ($[M + Na]^+$, 100%); HRMS (ESI^+) $C_{25}H_{15}N_5NaO_3S$ ($[M+Na]^+$) requires 488.0793; found 488.0776; ν_{max} (solid) 2916, 2228 (CN), 1693, 1268, 1191

2'-(((5-(2-cyclopropyl-2-oxoethyl)-5*H*-[1,2,4]triazino[5,6-*b*]indol-3-yl)thio)methyl)benzonitrile 359

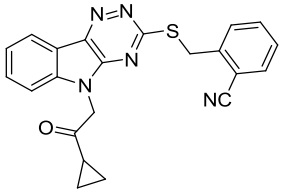

Following **General Procedure 4**, 2'(((5*H*-[1,2,4]triazino[5,6-*b*]indol-3-yl)thio)methyl)benzonitrile **236** (100 mg, 0.32 mmol) was added to DMF (5 mL), cooled to 0 °C followed by the addition of NaH (60%, 13.8 mg, 0.35mmol) and stirred at 0 °C for 10 mins. 2-bromo-1-cyclopropylethanone **359** (77 mg, 0.47mmol) was added, stirred overnight and quenched with H_2O. The resulting precipitate was filtered to yield a white solid (66 mg, 52 %); δ_H (500 MHz, DMSO-d_6, 363K) 1.14 - 1.26 (4H, m, C(2")H2 and C(3")H_2), 3.25 - 3.31 (1H, m, C(1")H), 4.72 (2H, s, SCH_2), 5.31 (2H, s, NCH_2), 7.52 - 7.56 (2H, m, C(5')H and C(7)H), 7.71 - 7.76 (2H, m, C(4')H and C(8)H), 7.81 (1H, d, *J* = 7.6, C(3')H), 7.86 (1H, d, *J* = 7.6, C(6')H), 8.33 (1H, d, *J* = 7.6, C(6)H), 8.43 (1H, d, *J* = 8.1, C(9)H); δ_C (125 MHz, DMSO-d_6) 10.7 (2C, C2" and C3"), 17.5 (C1"), 34.3 (SCH_2), 69.1 (NCH_2) 111.8 (C2'), 116.6 (C9), 117.9 (CN), 120.6 (C9a), 124.3 (C6), 126.3 (C7), 129.0 (C5'), 130.8 (C3'), 133.6 (C8), 133.9 (C6'), 135.1 (C4'), 141.0 (C5a), 144.5 (C4a), 147.9 (C9b), 167.2 (C3), 208.1 (C(O)); mp 183 - 184 °C; *m/z* (ESI^-) 398 ($[M - H]^+$, 60%); ν_{max}

(solid) 3044 and 2929 (C-H aromatic), 2268 (CN), 1679 (C=O carbonyl), 1516; HRMS (ESI^+) $C_{22}H_{17}N_5NaOS$ ($[M+Na]^+$) requires 422.1046; found 422.1044

2'-(((5-(2''-oxobutyl)-5*H*-[1,2,4]triazino[5,6-*b*]indol-3-yl)thio)methyl)benzonitrile 360

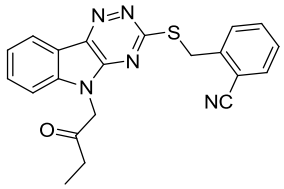

Following **General Procedure 4**, 2'(((5*H*-[1,2,4]triazino[5,6-*b*]indol-3-yl)thio)methyl)benzonitrile **236** (100 mg, mmol) was added to DMF (5 mL), cooled to 0 °C followed by the addition of NaH (60%, 13.8 mg, 0.35 mmol) and stirred at 0 °C for 10 mins. 1-Bromo-2-butanone (32 µL, 0.32 mmol) was added, stirred at rt for 16 h and quenched with H_2O. The resulting precipitate was filtered and washed with MeOH to yield **360** as a white solid (118 mg, 97 %); δ_H (500 MHz, DMSO-d_6, 363K) 1.01 (3H, t, J = 7.3 Hz, CH_3), 2.76 (2H, q, J = 7.3 Hz, $\underline{C}H_2CH_3$), 4.73 (2H, s, NCH_2), 5.47 (2H, s, SCH_2), 7.42 – 7.51 (2H, m, C(8)H and C(5')H), 7.62 (1H, app td, J = 7.6, 1.3 Hz, C(4')H), 7.69 – 7.76 (2H, m, C(7)H and C(6)H), 7.79 (1H, d, J = 7.6 Hz, C(3')H), 7.84 (1H, dd, J = 7.6, 1.0 Hz, C(6')H), 8.36 (1H, d, J = 7.6 Hz, C(9)H); δ_C (125 MHz, DMSO-d_6) 7.1 ($CH_2\underline{C}H_3$), 32.3 ($\underline{C}H_2CH_3$), 32.4 (SCH_2), 49.6 (NCH_2), 111.4 (C6), 111.9 (C2'), 117.2 (CN), 117.7 (C9a), 121.5 (C9), 123.2 (C8), 128.2 (C5'), 130.3 (C3'), 131.1 (C7), 133.0 (C6'), 133.3 (C4'), 141.1 (C9b), 141.3 (C5a), 141.6 (C1'), 146.2 (C4a), 166.0 (C3), 204.0 (CO); mp 219-220 °C; *m/z* (ESI^+) 410 ($[M + Na]^+$, 100%); HRMS (ESI^+) $C_{21}H_{17}N_5NaOS$ ($[M+Na]^+$) requires 410.1046; found 410.1033; ν_{max} (solid) 3039 and 2969 (aromatic C-H), 2233 (CN), 1724 (C=O), 1574

2'-(((5-(2-Oxo-2-phenylethyl)-5*H*-[1,2,4]triazino[5,6-*b*]indol-3-yl)thio)methyl)benzonitrile 361

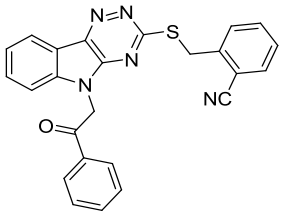

Following **General Procedure 4**, 2'(((5H-[1,2,4]triazino[5,6-b]indol-3-yl)thio)methyl)benzonitrile **236** (100 mg, 0.32 mmol) was added to DMF (5 mL), cooled to 0 °C followed by the addition of NaH (60%, 13.9 mg, 0.35 mmol) and stirred at 0 °C for 10 mins. 2-Bromoacetophenone **361** (62.8 mg, 0.32 mmol) was added, stirred overnight and bright red solution was quenched with H_2O. The resulting precipitate was filtered to yield **361** as a white solid (64 mg, 47 %); δ_H (500 MHz, DMSO-d_6, 363K) 4.69 (2H, s, SCH_2), 6.23 (2H, s, NCH_2), 7.36 (1H, app td, *J* = 7.6, 1.3 Hz, C(5')H), 7.43 (1H, app td, *J* = 7.6, 1.3 Hz, C(4')H), 7.52 (1H, app t, *J* = 7.9 Hz, C(8)H), 7.64 (1H, dd, *J* = 7.6, 1.3 Hz, C(3')H), 7.66 - 7.70 (2H, m, C(3'')H and C(5'')H), 7.70 - 7.75 (2H, m, C(6)H and C(6')H), 7.79 - 7.83 (2H, m, C(4'')H and C(7)H), 8.18 (2H, d, *J* = 8.5, C(2'')H and C(6'')H), 8.41 (1H, d, *J* = 7.9 Hz, C(9)H); δ_C (125 MHz, DMSO-d_6) 32.3 (SCH_2), 48.0 (NCH_2), 111.6 (C6), 111.8 (C2'), 117.3 (CN), 117.6 (C9a), 121.6 (C9), 123.2 (C8), 128.0 (C5'), 128.5 (2C, C2'' and C6''), 129.0 (2C, C3'' and C5''), 130.2 (C7), 131.2 (C6'), 132.9 (C3'), 133.0 (C4'), 134.1 (C1''), 134.4 (C4''), 141.2 (C5a), 141.6 (C4a), 141.6 (C9b), 164.5 (C1'), 166.1 (C3), 192.3 (CO); mp 234-235 °C (EZ Melt); *m/z* (ESI^+) 436 ($[M + Na]^+$, 100%); HRMS (ESI^+) $C_{25}H_{17}N_5NaOS$ ($[M+Na]^+$) requires 458.1046; found 458.1038; ν_{max} (solid) 2975, 2932, 2226 (CN), 1739, 1684 (C=O), 1577, 1170; $C_{25}H_{17}N_5NaOS \cdot 0.15\ H_2O$ requires C, 68.52; H, 3.98; N, 15.98%; found C, 68.48; H, 3.83; N, 15.92%

Ethyl 2-(furan-2-yl)-2-hydroxy propanoate 362

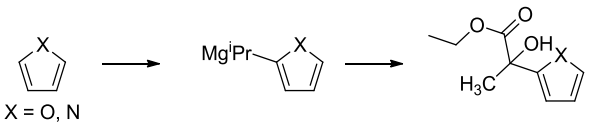

Furan (300 µL, 4.41 mmol) was dissolved in a mixture of Et_2O/ THF (1:2, 3.0 mL: 6.0 mL) and cooled to 0 °C. ^{i}PrMgBr (2 M in Et_2O, 2.64 mL, 5.29 mmol) was added to the solution and stirred for 1 h at rt. The *in situ* formed Grignard reagent was added to a solution of ethyl pyruvate (450 µL, 4.41 mmol) in Et_2O (5 mL) dropwise over a period of 5 min at rt. The reaction mixture was further stirred for 1 h after which the excess Grignard reagent was quenched with sat aq NH_4Cl (40 mL) and extracted with Et_2O (40 mL). The organic layer was washed with brine (40 mL), dried over $MgSO_4$, filtered and concentrated *in vacuo*. Flash column chromatography purification was attempted for product isolation, no product was isolated.

Ethyl-2-(bromomethyl)benzoate 363

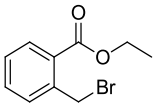

2-(bromomethyl)benzoic acid (1.00 g, 4.65 mmol) was added to thionyl chloride (5 mL) and heated to reflux for 1 hr. The resulting solution was concentrated *in vacuo* and washed with hexane (2x5 mL). EtOH (15 mL) was added to the crude oil and stirred at rt for 16 h, in which the solution turned yellow. The solution was diluted in Et_2O (50 mL), washed with bicarb (40 mL), brine (40 mL). The resulting organic extract was dried over $MgSO_4$, filtered and concentrated *in vacuo* to yield **363** as a light yellow oil (1.06 g, 95%); δ_H (400 MHz $CDCl_3$ 363 K) 1.43 (3H, t, *J* = 7.1 Hz, CH_3), 4.41 (2H, q, *J* = 7.1 Hz, $C\underline{H}_2CH_3$), 5.34 (2H, s, $C\underline{H}_2Br$), 7.51 (1H, d, *J* = 7.6 Hz, C(3)H), 7.55 (1H, app t, *J* = 7.6 Hz, C(5)H), 7.70 (1H, app t, *J* = 7.6 Hz, C(4)H), 7.94 (1H, d, *J* = 7.6 Hz, C(6)H); δ_C (100 Hz, $CDCl_3$) 11.5

(CH_3), 31.6 (CH_2-Br), 69.7 (OCH_2), 122.1 (C3), 125.8 (C5), 129.1 (C4), 134.0 (C6), 146.5 (C1), 154.5 (C2), 171.1 (C(O)); *m/z* (ESI^+) 265 ($[^{79}BrM + Na]^+$, 100%), 267 ($[^{81}BrM + Na]^+$, 100%); HRMS (ESI^+) $C_{10}H_{11}BrNaO_2$ ($[^{79}BrM+Na]^+$) requires 264.9835; found 264.8846; ν_{max} (solid) 2970, 2361, 2341, 1739, 1366

3-((2',6'-Difluorobenzyl)thio)-5*H*-[1,2,4]triazino[5,6-*b*]indole 364

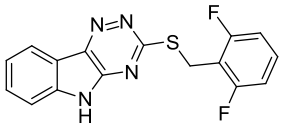

Following **General Procedure 3:** 2,6-difluoro benzyl bromide (154 mg, 0.74 mmol) was added to 5*H*-[1,2,4]triazino[5,6-*b*]indole-3-thiol **139** (150 mg, 0.74 mmol) and Et_3N (155 µL, 1.11 mmol) in MeOH (5 mL) and the resulting mixture was reacted at rt for 16 h. The precipitate was filtered and washed to give **364** as a faint yellow solid (132 mg, 54 %). δ_H (400 MHz, DMSO-d_6, 363 K) 4.66 (2H, s, CH_2), 7.14 - 7.18 (2H, m, C(3')H and C(5')H), 7.42 - 7.46 (2H, m, C(8)H and C(4')H), 7.59 (1H, d, *J* = 7.9Hz, C(6)H), 7.71 (1H, app t, *J* = 7.9 Hz, C(7)H), 8.33 (1H, d, *J* = 7.9 Hz, C(9)H), 12.69 (1H, br s, NH); δ_C (100 Hz, DMSO-d_6) 21.7 (CH_2), 111.8 (2C, dd, *J* = 20, 5 Hz, C3' and C5'), 112.7 (C6), 112.8 (C9a), 117.6 (C9b), 121.6 (C8), 122.5 (C7), 130.2 (t, *J* = 11 Hz, C1'), 131.0 (C9), 140.4 (C4'), 141.3 (C5a), 146.6 (C4a), 160.9 (2C, dd, *J* = 248, 7.6 Hz, C2' and C6'), 166.0 (C3); δ_F (470 MHz, DMSO-d_6) -113.1 (2F, C2'-F and C6'-F); mp 292-294 °C; *m/z* (ESI^-) 327 ($[M - H]^-$, 100%); HRMS (ESI^-) $C_{16}H_9F_2N_4S^-$ ($[M-H]^-$) requires 327.0521; found 327.0536; ν_{max} (solid) 3065 (NH), 2968 (aromatic C-H), 2802, 1626, 1594, 1578, 1470 (N-H), 1343 (CF); HPLC (Method 1) >96%, rt = 11.28 min

3-((4'-Nitrobenzyl)thio)-5*H*-[1,2,4]triazino[5,6-*b*]indole 365

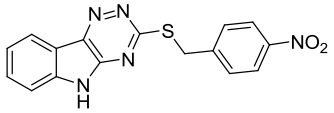

Following **General Procedure 3:** 4-nitrobenzyl bromide (160 mg, 0.74 mmol) was added to 5*H*-[1,2,4]triazino[5,6-*b*]indole-3-thiol **139** (150 mg, 0.74 mmol), Et_3N (155 μL, 1.11 mmol) in MeOH (15 mL) and were reacted at rt for 16 h. The resulting precipitate was filtered and washed to give **365** as a light yellow solid (97 mg, 62 %)δ_H (500 MHz, DMSO-d_6, 363K) 4.69 (2H, s, CH_2), 7.43 (1H, app t, *J* = 7.6 Hz, C(8)H), 7.58 (1H, d, *J* = 7.6 Hz, C(6)H), 7.70 (1H, app td, *J* = 7.6, 1.3 Hz, C(7)H), 7.81 (2H, d, *J* = 8.8 Hz, C(2')H and C(6')H), 8.18 (2H, d, *J* = 8.8 Hz, C(3')H and C(5')H), 8.30 (1H, d, *J* = 7.6 Hz, C(9)H), 12.66 (1H, s, NH); δ_C (125 MHz, DMSO-d_6) 33.6 (CH_2), 113.1 (C6), 117.9 (C9a), 121.9 (C9), 122.9 (C8), 123.8 (2C, C3' and C5'), 130.6 (2C, C2' and C6'), 131.4 (C7), 140.7 (C9b), 141.7 (C5a), 146.7 (C1'), 146.9 (C4a), 146.9 (C4'), 166.3 (C3); mp 235-237 °C (EZ Melt); *m/z* (ESI^-) 336 ($[M - H]^-$, 100%); HRMS (ESI^+) $C_{16}H_{11}NaN_5O_2S$ ($[M+Na]^+$) requires 360.0526; found 360.0516; ν_{max} (solid) 3455 (N-H), 3336, 1680, 1584 (NO_2), 1466, 1438; HPLC (Method 2) >99%, rt = 11.09 min

3-((cyclohexylmethyl)thio)-5*H*-[1,2,4]triazino[5,6-*b*]indole 366

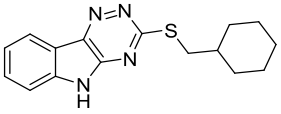

Following **General Procedure 3:** bromomethyl cyclohexane (104 μL, 0.74 mmol) was added to 5*H*-[1,2,4]triazino[5,6-*b*]indole-3-thiol **139** (150 mg, 0.74 mmol) and Et_3N (155 μL, 1.11 mmol) in MeOH (5 mL), the resulting suspension was stirred at rt for 16 h. The precipitate was filtered and washed to give **366** as a faint yellow solid (149 mg, 67 %). δ_H (400 MHz, DMSO-d_6, 363 K) 1.04 - 1.25 (5H, m, 5 x CH), 1.63 - 1.73 (4H, m, 4 x CH),

1.87 - 1.91 (2H, m, 2 x CH), 3.20 (2H, d, *J* = 6.7 Hz, SCH_2), 7.43 (1H, app t, *J* = 7.6 Hz, C(7)H), 7.57 (1H, d, *J* = 7.6 Hz, C(6)H), 7.69 (1H, app t, *J* = 7.6 Hz, C(8)H), 8.30 (1H, d, *J* = 7.6 Hz, C(9)H), 12.60 (1H, br s, NH); δ_C (100 MHz, DMSO-*d*$_6$) 25.5 (2C, C3' and C5'), 25.8 (C4'), 32.1 (2C, C2' and C6'), 36.7 (C1'), 37.1 (C4'), 112.6 (C6), 117.7 (C9a), 121.4 (C9), 122.4 (C8), 130.8 (C7), 140.2 (C9b), 140.9 (C5a), 146.6 (C4a), 167.5 (C3); mp 298-300 °C; *m/z* (ESI^-) 297 ($[M-H]^-$, 100%); HRMS (ESI^+) $C_{16}H_{18}N_4NaS$ ($[M+Na]^+$) requires 321.1144; found 321.1143; ν_{max} (solid) 3059 (N-H), 2918 (aromatic C-H), 1603, 1582, 1460 (N-H), 1420, 1336; HPLC (Method 1) >95%, rt = 11.62 min

6-Bromo-3-((2'-nitrobenzyl)thio)-5*H*-[1,2,4]triazino[5,6-*b*]indole 368

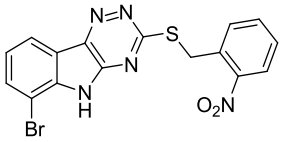

Following **General Procedure 3:** 2-nitrobenzyl bromide (70 mg, 0.36 mmol) was added to 6-bromo-5*H*-[1,2,4]triazino[5,6-*b*]indol-3-thiol **367** (100 mg, 0.36 mmol) and Et_3N (75 µL, 0.54 mmol) in MeOH (5 mL) and stirred at rt for 16 h. The resulting precipitate was filtered and washed to give **368** as a light yellow solid (133 mg, 90 %); δ_H (500 MHz, DMSO-*d*$_6$, 363K) 4.87 (2H, s, CH_2), 7.33 (1H, app t, *J* = 7.7 Hz, C(8)H), 7.54 (1H, app t, *J* = 7.7 Hz, C(4')H), 7.70 (1H, app t, *J* = 7.7 Hz, C(5')H), 7.86 (1H, d, *J* = 7.7 Hz, C(7)H), 7.96 (1H, d, *J* = 7.7 Hz, C(6')H), 8.06 (1H, d, *J* = 7.7 Hz, C(3')H), 8.27 (1H, d, *J* = 7.7 Hz, C(9)H), 12.91 (1H, br s, NH); δ_C (125 MHz, DMSO-*d*$_6$) 32.2 (CH_2), 106.0 (C6), 120.6 (C9a), 121.5 (C8), 124.7 (C7), 125.9 (C6'), 129.8 (C4'), 133.6 (C9), 134.0 (C9b), 134.1, 134.7 (C3' and C5'), 139.9 (C1'), 142.2 (C5a), 147.9 (C4a), 149.1 (C2'), 167.7 (C3); mp 224-227 °C; *m/z* (ESI^+) 438 ($[^{79}BrM + Na]^+$, 40%), 440 ($[^{81}BrM + Na]^+$, 40%), *m/z* (ESI^-) 414 ($[^{79}BrM - H]^-$, 100%), 416 ($[^{81}BrM - H]^-$, 100%); HRMS (ESI^+) $C_{16}H_{10}BrN_5NaO_2S$ ($[^{79}BrM+Na]^+$) requires 413.9666; found 413.9680, ($[^{81}BrM+Na]^+$) requires 415.9646;

found 415.9658; ν_{max} (solid) 2960 (N-H), 1597 (NO_2), 1494, 1340 (NO_2); HPLC (Method 2) >98%, rt = 11.72 min

7-Bromo-3-((2'-nitrobenzyl)thio)-5*H*-[1,2,4]triazino[5,6-*b*]indole 369

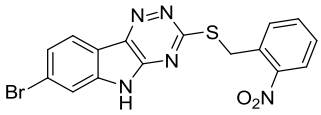

Following **General Procedure 3:** 2-nitrobenzyl bromide (77 mg, 0.36 mmol) was added to 8-bromo-5*H*-[1,2,4]triazino[5,6-*b*]indol-3-thiol **367** (100 mg, 0.36 mmol), and Et_3N (75 µL, 0.54 mmol) in MeOH (5 mL) and stirred at rt for 16 h. The resulting precipitate was filtered and washed to give **369** as a light yellow solid (29 mg, 87 %). δ_H (400 MHz, DMSO-d_6) 4.88 (2H, s, CH_2), 7.56 (1H, app t, *J* = 7.9 Hz, C(4')H), 7.60 (1H, dd, *J* = 8.2, 1.6 Hz, C(8)H), 7.71 (1H, app t, *J* = 7.9 Hz, C(5')H), 7.78 (1H, d, *J* = 1.6 Hz, C(6)H), 7.91 (1H, dd, *J* = 7.9, 1.3 Hz, C(6')H), 8.07 (1H, dd, *J* = 7.9, 1.3 Hz, C(3')H), 8.26 (1H, d, *J* = 8.2 Hz, C(9)H), 12.76 (1H, br s, NH); δ_C (100 MHz, DMSO-d_6) 31.1 (CH_2), 115.6 (C6), 116.9 (C7), 123.2 (C5'), 123.7 (C9a), 124.9, 125.5, 128.9, 132.5, 133.0, 133.8 (6xAr-C), 140.9 (C1'), 141.4 (C5a), 146.9 (C4a), 148.4 (C2'), 166.5 (C3); mp 297-298 °C; *m/z* (ESI^-) 415 ($[^{79}BrM - H]^-$, 100%), 417 ($[^{81}BrM - H]^-$, 100%); HRMS (ESI^+) $C_{16}H_{10}BrN_5NaO_2S$ ($[^{79}BrM+Na]^+$) requires 413.9666; found 413.9680, ($[^{81}BrM+Na]^+$) requires 415.9646; found 415.9658; ν_{max} (solid) 3221 (N-H), 3115 (aromatic C-H), 1592, 1517 and 1338 (NO_2); HPLC (Method 2) >99%, rt = 11.86 min

8-Bromo-3-((2'-nitrobenzyl)thio)-5*H*-[1,2,4]triazino[5,6-*b*]indole 370

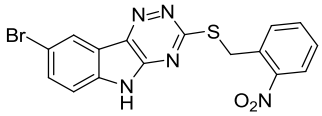

Following **General Procedure 3:** 2-nitrobenzyl bromide (77 mg, 0.36 mmol) was added to 8-bromo-5*H*-[1,2,4]triazino[5,6-*b*]indol-3-thiol **367** (100 mg, 0.36 mmol) and Et_3N (75 µL, 0.54 mmol) in MeOH (5 mL) and stirred at rt for 16 h. The resulting precipitate was washed to give **370** as a light yellow solid (98 mg, 66 %). δ_H (500 MHz, DMSO-d_6, 363K) 4.87 (2 H, s, CH_2), 7.40 - 7.61 (2 H, m, C(6)H and C(7)H), 7.63 - 7.74 (1 H, m, C(4')H), 7.79 (1 H, d, J = 7.3 Hz, C(6')H), 7.86 - 7.98 (1 H, m, C(5')H), 8.06 (1 H, d, J = 7.0 Hz, C(3')H), 8.41 (1 H, s, C(9)H), 12.76 (1 H, br s, NH); δ_C (125 MHz, DMSO-d_6) 31.2 (CH_2), 114.5 (C6), 114.8 (C8), 119.5 (C9a), 123.7 (C9), 125.0 (C4'), 128.9 (C6'), 132.5 (C7), 133.0 (C5'), 133.3 (C9b), 133.8 (C3'), 139.1 (C1'), 140.4 (C5a), 146.6 (C4a), 148.4 (C2'), 166.8 (C3); mp 288-289 °C; *m/z* (ESI^-) 415 ($[^{79}BrM - H]^-$, 100%), 417 ($[^{81}BrM - H]^-$, 100%); HRMS (ESI^+) $C_{16}H_{10}BrN_5NaO_2S$ ($[^{79}BrM+Na]^+$) requires 413.9666; found 413.9680, ($[^{81}BrM+Na]^+$) requires 415.9646; found 415.9658; ν_{max} (solid) 3091 (NH), 2969 (aromatic C-H), 2795, 1524 and 1332 (NO_2); HPLC (Method 2) >96%, rt = 11.81 min

9-Bromo-3-((2'-nitrobenzyl)thio)-5*H*-[1,2,4]triazino[5,6-*b*]indole 371

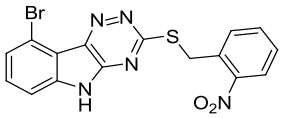

Following **General Procedure 3:** 2-nitrobenzyl bromide (70 mg, 0.36 mmol) was added to 9-bromo-5*H*-[1,2,4]triazino[5,6-*b*]indol-3-thiol **367** (100 mg, 0.36 mmol) and Et_3N (75 µL, 0.54 mmol) in MeOH (5 mL) and stirred at rt for 16 h. The resulting precipitate was filtered and washed to give **371** as a light yellow solid (98 mg, 66 %). δ_H (400 MHz, DMSO-d_6, 363K) 4.90 (2 H, s, CH_2), 7.42 - 7.62 (4 H, m, C(6)H, C(7)H, C(8)H and

C(4')H), 7.69 (1 H, app t, *J* = 7.8, 1.3 Hz, C(5')H), 7.93 (1 H, dd, *J* = 7.8, 1.3 Hz, C(6')H), 8.06 (1 H, dd, *J* = 7.8, 1.3 Hz, C(3')H); δ_C (100 MHz, DMSO-d_6) 32.0 (CH_2), 112.6 (C6), 116.9 (C9a), 118.1 (C9), 125.8 (C4'), 126.7 (C8), 128.5 (C6'), 129.7 (C7), 132.3 (C5'), 133.3 (C3'), 134.6 (C9b), 141.2 (C1'), 142.4 (C5a), 147.2 (C4a), 149.2 (C2'), 167.1 (C3); mp 285-286 °C; *m/z* (ESI^+) 438 ($[^{79}BrM + Na]^+$, 40%), 440 ($[^{81}BrM + Na]^+$, 40%), *m/z* (ESI^-) 414 ($[^{79}BrM - H]^-$, 100%), 416 ($[^{81}BrM - H]^-$, 100%); HRMS (ESI^+) $C_{16}H_{10}BrN_5NaO_2S$ ($[^{79}BrM+Na]^+$) requires 413.9666; found 413.9680, ($[^{81}BrM+Na]^+$) requires 415.9646; found 415.9658; ν_{max} (solid) 3111 (br, N-H), 2877 and 2832 (aromatic C-H), 1606, 1521 and 1338 (NO_2); $C_{16}H_{10}BrN_5O_2S$ requires C, 46.17; H, 2.42; N, 16.82%; found C, 46.12; H, 2.29; N, 16.63%

5-Methyl-3-((2'-nitrobenzyl)thio)-5*H*-[1,2,4]triazino[5,6-*b*]indole 371

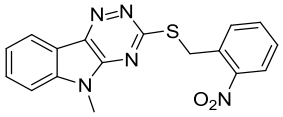

Following **General Procedure 4**, methyl iodide (28 µL, 0.45 mmol) was added to 3-((2'-nitrobenzyl)thio)-5*H*-[1,2,4]triazino[5,6-*b*]indole **239** (100 mg, 0.30 mmol) in THF (5 mL) NaH (60%, 18 mg, 0.45 mmol) at 0 °C and the resulting mixture stirred at rt for 16 h. The reaction mixture was quenched with H_2O (30 mL) and extracted with CH_2Cl_2 (30 mL). The organic layer was separated and washed with brine (30 mL), dried over $MgSO_4$, filtered and concentrated *in vacuo*. The resulting solid was washed with MeOH to yield **371** a yellow solid (68 mg, 64 %). δ_H (400 MHz, pyr-d_5, 363K) 3.64 (3 H, s, NCH_3), 5.14 (2 H, s, SCH_2), 7.36 (1 H, app t, J = 7.6 Hz, C(8)H), 7.39 - 7.48 (2 H, m , C(6)H and C(4')H), 7.56 (1 H, app t, J = 7.6 Hz, C(7)H), 7.67 (1 H, app t, J = 7.3 Hz, C(5')H), 8.04 - 8.11 (2 H, m, C(3')H and C(6')H), 8.42 (1 H, d, J = 7.6 Hz, C(9)H); δ_C (100 MHz, pyr-d_5) 28.7 (NCH_3), 33.9 (SCH_2), 112.4 (C6), 120.2 (C9a), 123.6 (C9), 124.8 (C4'), 127.1 (C7),129.3 (C6'), 130.5 (C9b), 132.7 (C5'), 134.8 (C3'), 135.3 (C8), 143.6 (C5a), 148.4 (C4a), 150.9 (C1'), 154.1 (C2'), 168.8 (C3); mp 175-176 °C; *m/z* (ESI^+) 374 ($[M + Na]^+$, 100%), *m/z* (ESI^-) 336 ($[M - CH_3]^-$, 100%); HRMS (ESI^+) $C_{17}H_{13}N_5NaO_2S$ ($[M+Na]^+$) requires 374.0682; found 374.0677; ν_{max} (solid) 1585, 1512 (NO_2), 1469, 1333, 1311 (NO_2), 1190; HPLC (Method 1) >98%, rt = 11.46 min

5-Benzyl-3-((2'-nitrobenzyl)thio)-5*H*-[1,2,4]triazino[5,6-*b*]indole 372

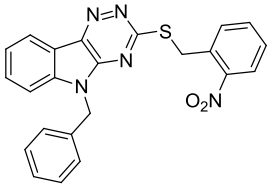

Following **General Procedure 4**, benzyl bromide (21 μL, 0.18 mmol) was added to 3-((2'-nitrobenzyl)thio)-5*H*-[1,2,4]triazino[5,6-*b*]indole **239** (60 mg, 0.18 mmol) and NaH (60%, 11 mg, 0.27 mmol) in THF (5 mL) at 0 °C and the resulting mixture stirred for 16 h. The reaction mixture was quenched with H_2O until a precipitate formed. The precipitate was filtered and dried to give **372** as a faint yellow solid (63 mg, 82 %); δ_H (500 MHz, DMSO-d_6, 363K) 4.89 (2 H, s, SCH_2), 5.66 (2 H, s, NCH_2), 7.25 - 7.34 (5 H, m, 5xAr-H), 7.47 (1H, tt, *J* = 7.9, 2.2 Hz, C(4'')H), 7.49-7.53 (2 H, m, C(2'')H and C(6'')H), 7.67 - 7.74 (2 H, m, C(5')H and C(6')H), 7.81 (1 H, dd, *J* = 5.7, 3.5 Hz, C(6)H), 8.03 (1 H, dd, *J* = 6.0, 3.8 Hz, C(3')H), 8.35 (1 H, d, *J* = 7.6 Hz, C(9)H); δ_C (125 MHz, DMSO-d_6) 31.2 (SCH_2), 44.2 (NCH_2), 111.6 (C6) 117.5 (C9a) 121.7, 123.1, 125.0 (3xAr-C), 127.2 (2C, C3'' and C5''), 127.7 (1xAr-C), 128.8 (2C, C2'' and C6''), 128.9, 131.0, 132.4, 133.3, 133.6 (5xAr-C), 135.8 (C1''), 140.8 (C1'), 141.1 (C5a), 146.1 (C4a), 148.3 (C2'), 166.4 (C3); mp 160-162 °C; *m/z* (ESI$^-$) 426 ([M - H]$^-$, 40%), 336 ([M – ($2NO_2$Bn)H]$^-$, 100%); HRMS (ESI$^+$) $C_{23}H_{17}N_5NaO_2S$ ([M+Na]$^+$) requires 450.0995; found 450.0993; ν_{max} (solid) 3061, 3005 and 2859 (aromatic C-H), 1578, 1518 (NO_2), 1167; HPLC (Method 2) >97%, rt = 11.88 min

5-Benzyl-3-(2'-fluorobenzylthio)-5*H*-[1,2,4]triazino[5,6-*b*]indole 373

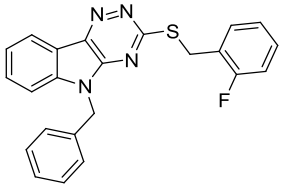

Following **General Procedure 4**, benzyl bromide (25 µL, 0.24 mmol) was added to 3-((2-fluorobenzyl)thio)-5*H*-[1,2,4]triazino[5,6-b]indole **238** (50 mg, 0.16 mmol) and NaH (10 mg, 0.24 mmol) in THF at 0 °C, the resulting mixture stirred at rt for 16 h. The reaction mixture was quenched with H_2O (30 mL) and CH_2Cl_2 (30 mL) added. The organic layer was separated and washed with brine (30 mL), dried over $MgSO_4$, filtered and concentrated *in vacuo* to yield **373** as a light yellow solid (26 mg, 40 %); δ_H (500 MHz, DMSO-d_6, 363 K) 4.62 (2 H, s, SCH_2), 5.67 (2 H, s, NCH_2), 7.02 – 7.05 (1 H, m, C(5')H), 7.18 (1 H, app t, *J* = 7.6 Hz, C(4')H), 7.25 - 7.35 (6 H, m, C(8)H, C(2'')H, C(3'')H, C(5'')H, C(6'')H and C(6')H), 7.49 (1 H, app t, *J* = 6.9 Hz, C(7)H), 7.56 – 7.59 (1 H, m, C(4')H), 7.68 - 7.76 (2 H, m, C(6)H and C(3')H), 8.37 (1 H, d, *J* = 7.9 Hz, C(9)H); δ_C (125 MHz, DMSO-d_6) 27.5 (SCH_2), 44.2 (NCH_2), 111.6 (C6), 115.3 (d, *J* = 21 Hz, C3'), 117.6 (C9a), 121.7 (C8), 123.1 (C7), 124.4 (d, *J* = 2.9 Hz, C5'), 124.7 (C9), 127.3 (2C, C2'' and C6''), 127.8 (C4''), 128.8 (2C, C3'' and C5''), 129.4 (d, *J* = 8.6 Hz, C6'), 131.0 (C9b), 131.3 (d, *J* = 3.8 Hz, C4'), 135.9 (C1''), 140.7 (d, *J* = 31 Hz, C1'), 141.0 (C5a), 146.2 (C4a), 160.5 (d, *J* = 246 Hz, C2'-F), 166.7 (C3); δ_F (470 MHz, DMSO-d_6) -116.9 (C2'-F); mp 139-141 °C; *m/z* (ESI^+) 423 ($[M + Na]^+$, 100%); HRMS (ESI^+) $C_{23}H_{17}FN_4NaS$ ($[M+Na]^+$) requires 423.1050; found 423.1042; ν_{max} (solid) 3064 (aromatic C-H), 1572, 1491, 1467, 1351, 1333, 1175; HPLC (Method 2) >97%, rt = 12.17 min

5-(2''-Fluorobenzyl)-3-((2'-nitrobenzyl)thio)-5H-[1,2,4]triazino[5,6-b]indole 374

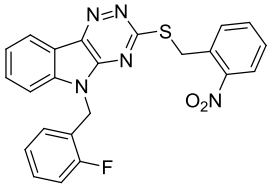

Following **General Procedure 4**, 2-fluoro benzyl bromide (22 μL, 0.18 mmol) was added to 3-((2'-nitrobenzyl)thio)-5*H*-[1,2,4]triazino[5,6-*b*]indole **239** (60 mg, 0.18 mmol) and NaH (10.7 mg, 0.27 mmol) in THF (5 mL) at 0 °C and stirred for 16 h at rt. The reaction mixture was quenched with H_2O until a precipitate formed. The precipitate was filtered and dried to give **374** as a faint yellow solid (50 mg, 63 %); δ_H (500 MHz, DMSO-d_6, 363K) 4.87 (2 H, s, SCH_2), 5.70 (2 H, s, NCH_2), 7.09 (1 H, app td, *J* = 7.6, 1.0 Hz, C(5'')H), 7.15 (1H, app td, *J* = 7.9, 1.6 Hz, C(4')H), 7.26 (1H, app t, *J* = 7.6 Hz, C(8)H), 7.35 - 7.39 (1H, m, C(4'')H), 7.47 - 7.53 (3H, m, C(6)H, C(7)H and C(6'')H), 7.70 (1H, d, *J* = 7.9 Hz, C(6')H), 7.73 (1H, app td, *J* = 7.9, 1.3 Hz, C(5')H), 7.78 - 7.80 (1H, m, C(5'')H), 8.02 - 8.04 (1H, m, C(3')H), 8.37 (1H, d, *J* = 7.6 Hz, C(9)H), 12.62 (1 H, br s, NH); δ_C (125 MHz, DMSO-d_6) 31.1 (SCH_3), 45.3 (NCH_2), 111.4 (C6), 115.6 (d, *J* = 21 Hz, C3''), 117.6 (C9a), 121.7 (1xAr-C), 122.4 (d, *J* = 14 Hz, C4''), 123.2 (1xAr-C), 124.8 (d, *J* = 2.9 Hz, C6''), 129.4 (d, *J* = 2.9 Hz, C5''), 129.5 (1xAr-C), 130.0 (d, *J* = 8.6 Hz, C1''), 130.1, 131.1, 132.3, 133.3, 133.6 (5xAr-C), 140.7 (C1'), 141.1 (C5a), 146.2 (C4a), 148.3 (C2'), 160.1 (q, *J* = 245 Hz, C2''), 166.4 (C3); δ_F (470 MHz, DMSO-d_6) -117.2 (C2''-F); mp 106-108 °C; *m/z* (ESI^+) 445 ($[M + H]^+$, 30%), *m/z* (ESI^+) 468 ($[M + Na]^+$, 100%); HRMS (ESI^+) $C_{23}H_{16}FN_5NaO_2S$ ($[M+Na]^+$) requires 468.0901; found 468.0906; ν_{max} (solid) 2925 and 2854 (aromatic C-H), 1522 and 1355 (NO_2), 1152; HPLC (Method 2) >96%, rt = 12.17 min

2'-(((5-(2-Cyanobenzyl)-5*H*-[1,2,4]triazino[5,6-*b*]indol-3-yl)thio)methyl)benzonitrile 375

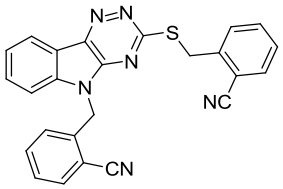

Following **General Procedure 4**, 2-cyano benzyl bromide (40.1 mg, 0.21 mmol) was added to 2'(((5*H*-[1,2,4]triazino[5,6-*b*]indol-3-yl)thio)methyl)benzonitrile **236** (60 mg, 0.19 mmol) amd NaH (60%, 11.0 mg, 0.28 mmol) in THF (5 mL) at 0 °C. The resulting solution was stirred for 16 h at rt. The reaction mixture was quenched with H_2O and resulting precipitate was filtered and washed with MeOH to yield **375** as an off white solid (79 mg, 96 %); δ_H (400 MHz, DMSO-d_6, 363K) 4.71 (2H, s, SCH_2), 5.88 (2H, s, NCH_2), 7.08 (1H, d, J = 8.0 Hz, C(6'')H), 7.39 (1 H, d, *J* = 7.3 Hz, Ar-H), 7.46 - 7.55 (4H, m, 4xAr-H), 7.62 (1H, d, *J* = 8.3 Hz, Ar-H), 7.67 - 7.75 (3H, m, 3xAr-H), 7.94 (1H, d, *J* = 7.6 Hz, C(6)H), 8.40 (1H, d, J = 8.0 Hz, C(9)H); δ_C (100 Hz, DMSO-d_6) 32.3 (SCH_2), 43.0 (NCH_2), 110.3 (C2''), 111.4 (C6), 111.9 (C2'), 117.1 (CN), 117.5 (C9a), 117.7 (CN), 121.8 (1xAr-C) 123.4 (C8) 127.5 (C7) 128.1, 128.6, 130.2, 131.2, 132.9, 133.1, 133.6, 133.8 (8xAr-CH) 139.1 (C9b), 140.7 (C1''), 141.2 (C1'), 141.5 (C5a), 146.6 (C4a), 166.2 (C3); mp 179-180 °C; *m/z* (ESI^-) 431 ($[M - H]^-$, 100%), 316 ($[M – (2''-CNBn)H]^-$, 95%); HRMS (ESI^+) $C_{25}H_{15}N_6S$ ($[M-H]^-$) requires 431.1084; found 431.1071; ν_{max} (solid) 2923 and 2854 (aromatic C-H), 2225 (CN), 1573, 1519, 1465; HPLC (Method 2) >95%, rt = 11.54 min

2'-(((5-(2''-Nitrobenzyl)-5*H*-[1,2,4]triazino[5,6-*b*]indol-3-yl)thio)methyl)benzonitrile 376

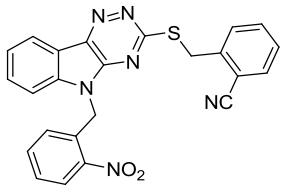

Following **General Procedure 4**, 2-nitro benzyl bromide (40 mg, 0.0.21 mmol) was added to 2'(((5*H*-[1,2,4]triazino[5,6-*b*]indol-3-yl)thio)methyl)benzonitrile **236** (60 mg, 0.19 mmol) and NaH (60%, 11 mg, 0.28 mmol) in THF (5 mL) at 0 °C, the resulting mixture stirred for 16 h at rt, quenched with H_2O and resulting precipitate was filtered and washed with MeOH to give **376** as an off white solid (79 mg, 96 %);δ_H (500 MHz, pyr-d_5, 363K) 4.65 (2 H, s, SCH_2), 6.02 (2 H, s, NCH_2), 6.71 (1 H, d, *J* = 7.1 Hz, C(6'')H), 7.42 - 7.72 (7 H, m, 7xAr-H), 7.81 – 7.89 (2 H, m, C(3'' and C(6)H), 8.31 (1 H, d, *J* = 7.8 Hz, C(3')H), 8.40 (1 H, d, *J* = 7.6 Hz, C(9)H); δ_C (125 MHz, pyr-d_5) 35.0 (SCH_2), 45.2 (NCH_2), 112.9 (C6), 115.0 (C2'), 119.3 (C9a), 119.9 (CN), 120.7 (C8), 124.0 (C9a), 126.7, 129.3, 129.8, 130.4, 132.2, 133.0, 134.8, 134.8, 135.4 (9xAr-C), 141.1 (C3''), 142.7 (C1'), 143.7 (C5a), 143.9 (C1''), 148.9 (C4a), 155.1 (C2''), 169.2 (C3); mp 225-226 °C (dec); *m/z* (ESI^+) 452 ($[M + H]^+$, 10%), *m/z* (ESI^-) 316 ($[M - (2''\text{-}NO_2Bn)H]^-$, 100%); HRMS ($ESI^+$) $C_{24}H_{16}N_6NaO_2S$ ($[M\text{-}H]^-$) requires 475.0948; found 475.954; ν_{max} (solid) 3061 and 2804 (aromatic C-H), 2226 (CN), 1580 and 1340 (NO_2), 1175; HPLC (Method 2) >96%, rt = 11.72 min

2'-(((5-(4''-fluorobenzyl)-5*H*-[1,2,4]triazino[5,6-*b*]indol-3-yl)thio)methyl)benzonitrile 377

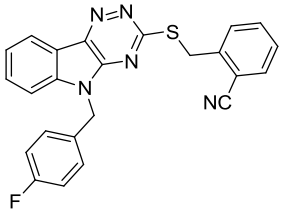

Following **General Procedure 4**, 2'(((5*H*-[1,2,4]triazino[5,6-*b*]indol-3-yl)thio)methyl)benzonitrile **236** (100 mg, 0.32 mmol) was added to DMF (5 mL), cooled to 0 °C followed by the addition of NaH (60%, 13.8 mg, 0.34 mmol) and stirred at 0 °C for 10 mins. 4-Fluorobenzyl bromide (39.3 μL, 0.32 mmol) was added, stirred for 16 h and quenched with H_2O and resulting precipitate was filtered and washed to yield **377** as a white solid (107 mg, 80 %); δ_H (500 MHz, DMSO-d_6, 363K) 4.77 (2H, s, SCH_2), 5.66 (2H, s, NCH_2), 7.12 (2H, app t, *J* = 8.8 Hz, C(3'')H and C(5'')H), 7.34 (2H, m, C(2'')H and C(6'')H), 7.45 (1H, app td, *J* = 7.6, 1.3 Hz, C(5')H), 7.48 (1H, m, C(8)H), 7.57 (1H, app td, *J* = 7.6, 1.3 Hz, C(4')H), 7.71 - 7.74 (2H, m, C(7)H and C(3')H), 7.76 - 7.88 (2H, m, C(6)H and C(6')H), 8,37 (1H, d, *J* = 7.6 Hz, C(9)H); δ_C (125 MHz, DMSO-d_6) 32.4 (SCH_2), 43.5 (NCH_2), 111.6 (C6), 111.9 (C2'), 115.5 (2C, d, *J* = 22 Hz, C3'' and C5''), 115.6 (CN), 117.6 (C9a), 121.7 (C9), 123.2 (C8), 128.1 (C5'), 129.5 (2C, d, *J* = 8.6 Hz, C2'' and C6''), 130.2 (C3'), 131.1 (C7), 132.0 (d, *J* = 3.8 Hz, C1''), 133.1 (C6'), 133.3 (C4'), 140.6 (C1'), 141.2 (C9b), 141.5 (C5a), 146.1 (C4a), 166.2 (C3), 161.6 (d, *J* = 244 Hz, C4''); mp 185-187 °C (EZ Melt); *m/z* (ESI^-) 424 ($[M - H]^-$, 100%); HRMS (ESI^+) $C_{24}H_{16}FN_5NaS$ ($[M+Na]^+$) requires 448.1003; found 448.0991; ν_{max} (solid) 2229 (CN), 1580, 1509, 1222, 1183; HPLC (Method 2) >99%, rt = 11.91 min

2'(((5-(4''-Chlorobenzyl)-5*H*-[1,2,4]triazino[5,6-*b*]indol-3-yl)thio)methyl)benzonitrile 378

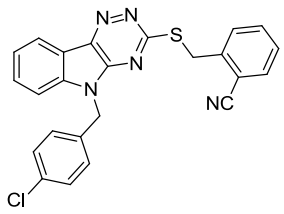

Following **General Procedure 4**, 4-chloro benzyl bromide (97 mg, 0.47 mmol) was added to 3-((2'-cyanobenzyl)thio)-5*H*-[1,2,4]triazino[5,6-*b*]indole **236** (100 mg, 0.32 mmol) and NaH (19 mg, 0.47 mmol) in THF (5 mL at 0 °C and the resulting mixture stirred for 16 h, quenched with H_2O (30 mL) and extracted with CH_2Cl_2 (30 mL). The organic layer was separated and washed with brine (30 mL), dried over $MgSO_4$, filtered and concentrated *in vacuo* to yield **378** as a yellow solid (82 mg, 58 %). δ_H (500 MHz, DMSO-d_6, 363 K) 4.75 (2 H, s, SCH_2), 5.66 (2 H, s, NCH_2), 7.28 (2 H, d, J = 8.5 Hz, C(2'')H and C(6'')H), 7.34 (2H, d, J = 8.5 Hz, C(3'')H and C(5'')H, 7.42 (1H, t, J = 7.6 Hz, C(8)H), 7.47 (1 H, app t, J = 7.6 Hz, C(5')H), 7.55 (1 H, app t, J = 7.6, C(4')H), 7.65 - 7.80 (4 H, m, C(6)H, C(7)H, C(3')H and C(6')H), 8.35 (1 H, d, J = 7.6 Hz, C(9)H); δ_C (125 MHz, DMSO-d_6) 33.2 (SCH_2), 44.4 (NCH_2), 112.4 (C6), 112.8 (C2'), 118.5 (CN), 122.6 (C9a), 124.1 (C8), 129.0 (C5'), 129.6 (2C, C2'' and C6''), 130.1 (2C, C3'' and C5''), 131.0 (C1''), 131.9, 133.2, 133.9, 133.9, 134.1, 135.7 (6 x CH), 141.4 (C5a), 142.0 (C1'), 142.4 (C1''), 147.0 (C4a), 167.1 (C3); mp 178-179 °C; *m/z* (ESI^+) 464 ($[M + Na]^+$, 100%); HRMS (ESI^+) $C_{24}H_{16}ClN_5NaS$ ($[^{35}ClM+Na]^+$) requires 464.0707; found 464.0705, ($[^{37}ClM+Na]^+$) requires 466.0679; found 466.0673; ν_{max} (solid) 3049 (aromatic C-H), 2225 (CN), 1585, 1562, 1465 (N-H), 1171; HPLC (Method 2) >97%, rt = 12.23 min

5-(4''-Chlorobenzyl)-3-((2'-nitrobenzyl)thio)-5*H*-[1,2,4]triazino[5,6-*b*]indole 379

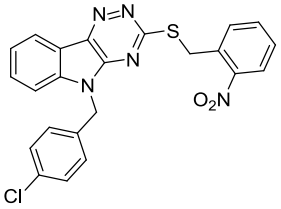

Following **General Procedure 4**, 4-chloro benzyl bromide (97 mg, 0.45 mmol) was added to 3-((2'-nitrobenzyl)thio)-5*H*-[1,2,4]triazino[5,6-*b*]indole **239** (100 mg, 0.30 mmol) and NaH (18 mg, 0.45 mmol) in THF (5 mL) at 0 °C and the resulting mixture stirred at rt for 16 h. The reaction mixture was quenched with H_2O (30 mL) and extracted with CH_2Cl_2 (30 mL) added. The organic layer was separated and washed with brine (30 mL), dried over $MgSO_4$, filtered and concentrated *in vacuo* to yield **379** as a yellow solid (76 mg, 55 %). δ_H (500 MHz, pyr-d_5, 363K) 5.08 (2 H, s, SCH_2), 5.57 (2 H, s, NCH_2), 7.17 - 7.39 (6 H, m, C(7)H, C(8)H, C(3'')H, C(4'')H, C(5'')H and C(6'')H), 7.49 - 7.55 (3 H, m, C(4')H, C(5')H and C(6')H), 7.92 (1 H, dd, *J* = 7.6, 1.1 Hz, C(6)H), 7.99 - 8.03 (1 H, dd, *J* = 7.9, 1.0 Hz, C(3')H), 8.43 (1 H, dd, *J* = 7.8, 0.8 Hz, C(9)H); δ_C (125 MHz, pyr-d_5) 32.5 (SCH_2), 45.1 (NCH_2), 111.6 (C6), 122.3 (C9), 123.5 (C8), 125.6 (C4'), 127.8 (2C, C2'' and C6''), 128.5 (C6'), 129.0 (C9a)), 129.5 (2C, C3'' and C5''), 131.3 (C7), 133.2 (C5'), 133.8 (C9b), 134.5 (C3'), 136.4 (C4''), 141.4 (C5a), 142.1 (C1'), 142.4 (C1''), 147.0 (C4a), 153.9 (C2'), 166.9 (C3); mp 100-102 °C; *m/z* (ESI^+) 462 ($[^{35}ClM + H]^+$, 80%), 464 ($[^{37}ClM+H]^+$, 30%); HRMS (ESI^+) $C_{23}H_{17}ClN_5O_2S^+$ ($[^{35}ClM+H]^+$) requires 461.0713; found 462.0716, ($[^{37}ClM+H]^+$) requires 463.0684; found 463.0680; ν_{max} (solid) 3063 (aromatic C-H), 2925, 1575, 1519 (NO_2), 1334 (NO_2); HPLC (Method 2) >95%, rt = 12.11 min

1-(3-((2'-Nitrobenzyl)thio)-5*H*-[1,2,4]triazino[5,6-*b*]indol-5-yl)ethanone 380

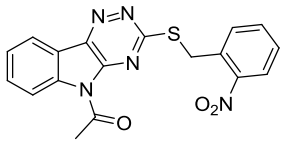

acetyl chloride (19 µL, 0.27 mmol) was added to a stirring solution of 3-((2'-nitrobenzyl)thio)-5*H*-[1,2,4]triazino[5,6-*b*]indole **239** (60 mg, 0.18 mmol), DMAP (0.45 mg, 0.04 mmol) and Et_3N (50 µL, 0.36 mmol) in CH_2Cl_2 (5 mL), and stirred at rt for 16 h. The resulting solution was diluted with CH_2Cl_2 (30 mL) washed with H_2O (30 mL). The organic layer was separated and washed with brine (30 mL), dried over $MgSO_4$, filtered and concentrated *in vacuo*. The solid was washed with MeOH to yield **380** as a white solid (68 mg, 99 %). δ_H (500 MHz, DMSO-d_6, 363K) 2.91 (3 H, s CH_3), 4.93 (2 H, s, SCH_2), 7.58 (1 H, app t, J = 7.9 Hz, C(5')H), 7.61 (1 H, app t, J = 7.9 Hz, C(4')H), 7.73 (1 H, app t, J = 7.6 Hz, C(7)H), 7.78 (1 H, app t, J = 7.8 Hz, C(8)H), 8.09 (1H, dd, J = 7.9, 1.3 Hz, C(6')H), 7.88 (1 H, dd, J = 7.8, 1.3 Hz, C(6)H), 8.34 (1 H, d, J = 7.9 Hz, C(3')H), 8.54 (1 H, d, J = 7.8 Hz, C(9)H); δ_C (125 MHz, DMSO-d_6) 27.4 (CH_3), 32.8 (CH_2), 111.9 (C6), 117.2 (C9a), 119.3 (C9), 121.2 (C8), 125.7 (C4'), 128.4 (C6'), 130.2 (C7), 132.2 (C5'), 133.2 (C9b), 133.5 (C3'), 139.3 (C5a), 140.5 (C1'), 142.5 (C4a), 147.3 (C2'), 166.6 (C3), 170.3 (C(O)); mp 204-205 °C; *m/z* (ESI^+) 402 ($[M + Na]^+$, 40%), *m/z* (ESI^-) 337 ($[M - Ac]^-$, 70%); HRMS (ESI^+) $C_{18}H_{13}N_5NaO_3S$ ($[M+Na]^+$) requires 402.0631; found 402.0626; ν_{max} (solid) 1714 (CO), 1576, 1517, 1287, 1183; $C_{18}H_{13}N_5O_3S \cdot 0.3H_2O$ requires C, 56.98; H, 3.45; N, 18.46%; found C, 57.16; H, 3.56; N, 18.20%

(3-((2'-Nitrobenzyl)thio)-5*H*-[1,2,4]triazino[5,6-*b*]indol-5-yl)(phenyl)methanone 381

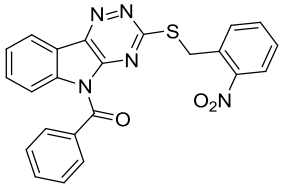

benzoyl bromide (51 µL, 0.45 mmol) was added to 3-((2'-nitrobenzyl)thio)-5*H*-[1,2,4]triazino[5,6-*b*]indole **239** (100 mg, 0.30 mmol), DMAP (0.7 mg, 0.05 mmol) and Et_3N (82 µL, 0.59 mmol) in CH_2Cl_2 (5 mL) and the resulting mixture was stirred at rt for 16 h. The reaction was quenched with H_2O (30 mL) and extracted with CH_2Cl_2 (30 mL). The organic layer was washed with brine (30 mL), dried over $MgSO_4$, filtered and concentrated *in vacuo*. The resulting solid was washed with MeOH to yield **381** as a white solid (96 mg, 73 %). δ_H (500 MHz, pyr-d_5, 363K) 4.53 (2 H, s, SCH_2), 7.37 (1H, app t, J = 7.6 Hz, C(4'')H), 7.42 (1 H, d, J = 7.6 Hz, C(6')H), 7.47 - 7.63 (5 H, m, C(8)H, C(3'')H, C(5'')H, C(4')H and C(5')H), 7.71 (1 H, app t, J = 7.6, C(7)H), 8.04 - 8.11 (3 H, m, C(2'')H, C(6'')H and C(3')H), 8.41 - 8.49 (2 H, m, C(6)H and C(9)H); δ_C (125 MHz, pyr-d_5) 33.6 (SCH_2), 111.7 (C6), 116.3 (C9a), 119.7 (C9), 122.2 (C8), 125.6 (C4'), 127.5 (2C, C3'' and C5''), 128.3 (C6'), 129.9 (C4''), 130.1 (C7), 130.9 (2C, C2'' and C6''), 133.4 (C5'), 134.6 (C9b), 135.2 (C3'), 135.5 (C1'), 136.3 (C1''), 141.7 (C4a), 143.6 (C5a) 149.2 (C2'), 167.1 (C3), 170.0 (C(O)); mp 209-210 °C; *m/z* (ESI^+) 464 ($[M + Na]^+$,20%), m/z (ESI^-) 336 ($[M - NBz]^-$,100%); HRMS (ESI^+) $C_{23}H_{15}N_5NaO_3S$ ($[M+Na]^+$) requires 464.0788; found 464.0782; ν_{max} (solid) 3059 (aromatic C-H), 1694 (tertiary amide), 1577 (NO_2), 1488, 1388 (NO_2); HPLC (Method 2) >97%, rt = 12.03 min

(3-((4'-Fluorobenzyl)thio)-5*H*-[1,2,4]triazino[5,6-*b*]indol-5-yl)(phenyl)methanone 382

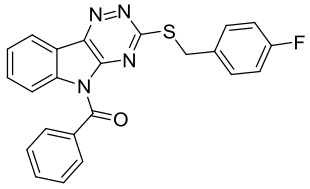

Following **General Procedure 4**, Benzoyl chloride (56 uL, 0.48 mmol) was added to 3-((4-fluorobenzyl)thio)-5*H*-[1,2,4]triazino[5,6-*b*]indole **249** (100 mg, 0.32 mmol) and NaH (60 %, 14 mg, 0.36 mmol) in DMF (5 mL) at 0 °C and stirred for 16 h at rt, quenched and resulting precipitate was filtered to yield **382** as a white solid (98 mg, 73 %); δ_H (500 MHz, DMSO-d_6, 363K) 3.85 (2H, s, SCH_2), 7.09 (2H, app t, *J* = 7.9 Hz, C(3')H and C(5')H), 7.16 - 7.21 (2H, m, C(4'')H and C(8)H), 7.54 (2H, d, *J* = 7.9 Hz, C(2')H and C(6')H), 7.66 (2H, app t, *J* = 7.9 Hz, C(3'')H and C(5'')H), 7.84 (1H, app td, *J* = 7.9, 1.3 Hz, C(7)H), 7.96 (2H, d, *J* = 7.9 Hz, C(2'')H and C(6'')H), 8.31 (1H, d, *J* = 8.5 Hz, C(9)H), 8.42 (1H, d, *J* = 7.9 Hz, C(6)H); δ_C (125 MHz, DMSO-d_6) 32.5 (2H, CH_2), 115.1 (2C, d, *J* = 22 Hz, C3' and C5'), 116.2 (C6), 119.8 (C9a), 121.3 (C9), 125.6 (C8), 238.4 (2C, C3'' and C5''), 130.1 (2C, C2'' and C6''), 130.8 (2C, d, *J* = 8.6 Hz, C2' and C6'), 131.5 (C4''), 133.2 (2C, C1' and C7), 134.0 (C9b), 139.4 (C1''), 141.9 (C5a), 147.3 (C4a), 161.3 (d, *J* = 243 Hz, C4'), 167.2 (C3), 167.9 (C(O)); mp 200-201 °C (EZ Melt); *m/z* (ESI^+) 437 ($[M + Na]^+$, 100%); HRMS (ESI^+) $C_{23}H_{15}FN_4NaOS$ ($[M+Na]^+$) requires 437.0843; found 437.0832; ν_{max} (solid) 2971 (aromatic C-H), 1739, 1699 (NC=O), 1375, 1293; HPLC (Method 2) >98%, rt = 12.17 min

Cyclopentyl(3-((4'-fluorobenzyl)thio)-5*H*-[1,2,4]triazino[5,6-*b*]indol-5-yl)methanone 383

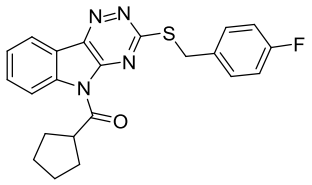

Following **General Procedure 4**, Cyclopentane carbonyl chloride (89 µL, 0.48 mmol) was added to 3-((4-fluorobenzyl)thio)-5*H*-[1,2,4]triazino[5,6-*b*]indole **249** (100 mg, 0.32 mmol) and NaH (60 %, 14 mg, 0.36 mmol) in DMF (5 mL) at 0 °C. The reaction mixture was stirred for 16 h at rt, quenched and resulting precipitate was filtered to yield **383** as a white solid (103 mg, 79 %); δ_H (500 MHz, DMSO-d_6, 363K) 1.55 - 1.71 (4H, m, 4xCH), 1.89 - 2.01 (4H, m, 4xCH), 4.42 (1H, app q, J = 8.0 Hz, C(1'')H), 4.60 (2H, s, SCH_2), 7.17 (2H, app t, J = 8.0 Hz, C(3')H and C(5')H), 7.55 (2H, dd, J = 8.0, 5.7 Hz, C(2')H and C(6')H), 7.62 (1H, t, J = 7.6 Hz, C(8)H), 7.79 (1H, t, J = 7.6 Hz, C(7)H), 8.37 (1H, d, J = 7.6 Hz, C(6)H), 8.59 (1H, d, J = 7.6 Hz, C(9)H); δ_C (125 MHz, DMSO-d_6) 25.5 (2C, C3'' and C4''), 29.6 (2C, C2'' and C5''). 33.3 (SCH_2), 46.0 (C1''), 115.2 (2C, d, J = 21 Hz, C3' and C5'), 117.5 (C6), 119.5 (C9a), 121.0 (C9), 125.7 (C8), 130.8 (2C, d, J = 8.6 Hz, C2' and C6'), 131.9 (C7), 133.1 (C9b), 139.5 (C1''), 142.2 (C5a), 147.0 (C4a), 161.2 (d, J = 244 Hz, C4'), 167.5 (C3), 176.3 (CO); mp 271-272 °C (EZ Melt); *m/z* (ESI^+) 429 ([M + $Na]^+$, 100%); HRMS (ESI^+) $C_{22}H_{19}FN_4NaOS$ ([M-H]$^-$) requires 429.1156; found 429.1161; ν_{max} (solid) 3052 and 2922 (aromatic C-H), 1599 (NC=O), 1507, 1184; HPLC (Method 2) >99%, rt = 10.99 min

Methyl-4''-(3-((4'-fluorobenzyl)thio)-5*H*-[1,2,4]triazino[5,6-*b*]indol-5-yl)oxobutanoate 384

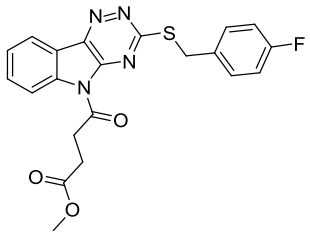

Following **General Procedure 4**, NaH (60%, 14 mg, 0.36 mmol) was added to 3-((4-fluorobenzyl)thio)-5*H*-[1,2,4]triazino[5,6-*b*]indole **249** (100 mg, 0.32 mmol) in DMF (5 mL) at 0 °C and stirred for 10 mins. Methyl-4-chloro oxobutyrate (59.5 µL, 0.48 mmol) was added, stirred for 16 h at rt and quenched with H_2O. The resulting precipitate was filtered to yield **384** as a white solid (83 mg, 61 %); δ_H (500 MHz, DMSO-d_6, 363K) 2.79 (2H, t, J = 6.4 Hz, NC(O)CH_2), 3.60 (3H, s, OCH_3), 3.69 (2H, t, J = 6.4 Hz, OC(O)CH_2), 7.16 (2H, app t, J = 8.0 Hz, C(3')H and C(5')H), 7.59 (2H, dd, J = 8.0, 5.6 Hz, C(2')H and C(6')H), 7.59 (1H, t, J = 7.6 Hz, C(8)H), 7.75 (1H, t, J = 7.6 Hz, C(7)H), 8.32 (1H, d, J = 7.6 Hz, C(6)H). 8.52 (1H, d, J = 7.6 Hz, C(9)H); δ_C (125 MHz, DMSO-d_6) 27.9 (C3''), 33.0 (C2''), 34.2 (SCH_2), 51.5 (OCH_3), 115.1 (2C, d, J = 22Hz, C3' and C5'), 117.2 (C6), 119.4 (C9a), 121.0 (C9), 125.8 (C8), 130.7 (2C, d, J = 8.9 Hz, C2' and C6'), 131.2 (C7), 132.5 (C9b), 139.0 (C1'), 142.1 (C5a), 147.2 (C4a), 161.3 (d, J = 244 Hz, C4'), 167.6 (C3), 172.5 (CO), 172.3 (CO); mp 122-124 °C (EZ Melt); *m/z* (ESI^+) 447 ($[M + Na]^+$, 100%); HRMS (ESI^+) $C_{21}H_{17}FN_4NaO_3S$ ($[M+Na]^+$) requires 447.0898; found 447.0903; ν_{max} (solid) 3404, 1713 (ester C=O), 1657 (NC=O), 1378, 1187; HPLC (Method 2) >95%, rt = 11.91 min

Ethyl-2'-(((benzoyl-5*H*-[1,2,4]triazino[5,6-*b*]indol-3-yl)thio)methyl)benzoate 385

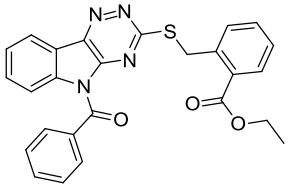

Following **General Procedure 4**, Benzoyl bromide (48.0 µL, 0.41 mmol) was added to ethyl 2'-(((5*H*-[1,2,4]triazino[5,6-*b*]indol-3-yl)thio)methyl)benzoate **245** (100 mg, 0.28 mmol) and NaH (60%, 12.1 mg, 0.30 mmol) in DMF (5 mL) at 0 °C and stirred for 16 h, and quenched with H_2O. The resulting precipitate was filtered to yield **385** as a faint yellow solid (125 mg, 97 %);δ_H (500 MHz, DMSO-d_6, 363K) 1.31 (3H, t, *J* = 7.3 Hz, CH_3), 4.19 (2H, s, SCH_2), 4.30 (2H, q, *J* = 7.3 Hz, OCH_2), 7.00 (1H, d, *J* = 7.6 Hz, C(6')H), 7.37 (1H, app td, *J* = 7.3, 1.3 Hz, C(8)H), 7.43 (1H, app td, *J* = 7.6, 1.3 Hz, C(4')H), 7.56 (2H, app t, *J* = 7.6 Hz, C(3'')H and C(5'')H), 7.64 (1H, app t, *J* = 7.6 Hz, C(5')H), 7.66 (1H, tt, *J* = 7.6, 1.3 Hz, C(4'')H), 7.82 (1H, app t, *J* = 7.3 Hz, C(7)H), 7.84 (1H, d, *J* = 7.6 Hz, C(3')H), 8.00 (2H, d, *J* = 7.6 Hz, C(2'')H and C(6'')H), 8.28 (1H, d, *J* = 7.3 Hz, C(6)H), 8.40 (1H, d, *J* = 7.3 Hz, C(9)H);δ_C (125 MHz, DMSO-d_6) 14.0 (CH_3), 32.0 (SCH_2), 61.0 (OCH_2), 116.2 (C6), 119.7 (C9a), 121.2 (C9), 125.6 (C8), 127.8 (C4'), 128.4 (2C, C3'' and C5''), 129.0 (C2'), 130.1 (2C, C2'' and C6''), 130.5 (C6'), 131.4 (C4'), 131.5 (C5'), 132.3 (C3'), 133.5 (C7), 133.8 (C1''), 138.5 (C1'), 139.3 (C9b), 141.7 (C5a), 147.2 (C4a), 166.4 (C3), 167.7 (CO), 167.9 (CO); mp 125-126 °C (EZ Melt); *m/z* (ESI^+) 491 ($[M + Na]^+$, 100%); HRMS (ESI^+) $C_{26}H_{20}N_4O_3S$ ($[M-H]^-$) requires 491.1148; found 491.1136; ν_{max} (solid) 3390 (br), 1695 (ester C=O), 1658 (NC=O) 1374, 1292, 1267; HPLC (Method 2) >95 %, rt = 12.33 min

Ethyl-2'-(((5-(cyclopentanecarbonyl)-5*H*-[1,2,4]triazino[5,6-*b*]indol-3-yl)thio)methyl)benzoate 386

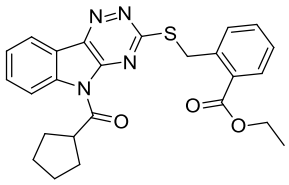

Following **General Procedure 4**, Cyclopentane carbonyl chloride (50.0 µL, 0.41 mmol) was added to ethyl 2'-(((5*H*-[1,2,4]triazino[5,6-*b*]indol-3-yl)thio)methyl)benzoate **245** (100 mg, 0.28 mmol) and NaH (60%, 12.1 mg, 0.30 mmol) in DMF (5 mL) at 0 °C and stirred for 16 h at rt, quenched with H_2O. The resulting precipitate was filtered to yield **386** as a white solid (96 mg, 76 %); δ_H (500 MHz, DMSO-d_6, 363K) 1.35 (3H, t, *J* = 7.3 Hz, CH_3), 1.57 - 1.71 (4H, m, 4xCH), 1.88 - 2.01 (4H, m, 4xCH). 4.35 (2H, q, *J* = 7.3 Hz, *OCH*$_2$), 4.42 (1H, app quint, *J* = 7.6 Hz, C(1'')H), 4.95 (2H, s, SCH_2), 7.45 (1H, t, *J* = 7.6 Hz, C(8)H), 7.57 (1H, t, *J* = 7.6 Hz, C(4')H), 7.60 (1H, t, *J* = 7.6 Hz, C(5)H), 7.72 (1H, d, *J* = 7.6 Hz, C(6')H), 7.77 (1H, t, *J* = 7.6 Hz, C(7)H), 7.93 (1H, d, *J* = 7.6 Hz, C(3')H), 8.35 (1H, d, *J* = 7.6 Hz, C(6)H), 8.57 (1H, d, *J* = 7.6 Hz, C(9)H); δ_C (125 MHz, DMSO-d_6) 14.1 ($CH_2\underline{C}H_3$), 25.6 (2C, C3'' and C4''), 29.5 (2C, C2'' and C5''), 32.8 (SCH_2), 46.0 (1C''), 61.0 (OCH_2), 117.4 (C6), 119.6 (C9a), 121.0 (C9), 125.6 (C8), 127.9 (C4'), 129.4 (C2'), 130.6 (C6'), 131.1 (C5'), 131.9 (C3'), 132.5 (C7), 138.2 (C1'), 139.5 (C9b), 142.2 (C5a), 147.0 (C4a), 166.5 (C3), 167.6 (CO), 176.3 (CO); mp 154-155 °C (EZ Melt); *m/z* (ESI^+) 483 ($[M + Na]^+$, 100%); HRMS (ESI^+) $C_{25}H_{24}N_4NaO_3S$ ($[M+Na]^+$) requires 483.1461; found 483.1460; ν_{max} (solid) 2966 and 2873 (aromatic C-H), 1711 (ester C=O)1709 (NC=O), 1573, 1374, 1187; HPLC (Method 2) >98%, rt = 12.90 min

Ethyl-2'-(((5-(4''-methoxy-4''-oxobutanoyl)-5*H*-[1,2,4]triazino[5,6-*b*]indol-3-yl)thio)methyl)benzoate 387

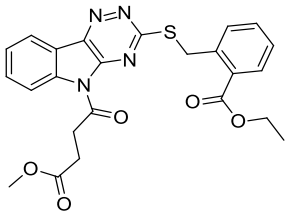

Following **General Procedure 4**, Methyl-4-chloro-oxobutyrate (50.5 µL, 0.41 mmol) was added to ethyl 2'-(((5*H*-[1,2,4]triazino[5,6-*b*]indol-3-yl)thio)methyl)benzoate **245** (100 mg, 0.28 mmol) and NaH (60%, 12.1 mg, 0.30 mmol) in DMF (5 mL) at 0 °C and stirred for 16 h at rt, quenched with H_2O. The resulting precipitate was filtered to yield **387** as a white solid (102 mg, 78 %); δ_H (500 MHz, DMSO-d_6, 363K) 1.35 (3H, t, J = 7.0 Hz, CH_3), 2.80 (2H, t, J = 6.4 Hz, NC(O)CH_2), 3.70 (2H, t, J = 6.4 Hz, OC(O)CH_2), 4.35 (2H, q, J = 7.0 Hz, OCH_2), 4.95 (2H, s, SCH_2), 7.44 (1H, t, J = 7.6 Hz, C(8)H), 7.55 (1H, td, J = 7.6, 1.3 Hz, C(4')H), 7.61 (1H, t, J = 7.6 Hz, C(5')H), 7.72 (1H, d, J = 7.6 Hz, C(6')H), 7.78 (1H, td, J = 7.6, 1.3 Hz, C(7)H), 7.92 (1H, dd, J = 7.6, 1.3 Hz, C(3')H), 8.35 (1H, d, J = 7.6 Hz, C(6)H), 8.55 (1H, d, J = 8.3 Hz, C(9)H); δ_C (125 MHz, DMSO-d_6) 14.0 ($CH_2\underline{C}H_3$), 28.0 (C2''H_2), 33.0 (C3''H_2), 34.2 (SCH_2), 51.5 (*O*-C6''H_3), 61.0 (OCH_2), 117.2 (C6), 119.5 (C9b), 121.1 (C9), 125.8 (C8), 127.9 (C4'), 129.3 (C2'), 130.6 (C6'), 131.2 (5'), 132.0 (C3'), 132.5 (C7), 138.5 (C1'), 139.1 (C9b), 142.2 (C5a), 147.3 (C4a), 166.6 (C3), 167.6 (CO Phenyl ester), 172.3 (CO amide), 172.5 (CO ester); mp 206-208 °C (EZ Melt); *m/z* (ESI^+) 501 ($[M + Na]^+$, 100%); HRMS (ESI^+) $C_{24}H_{22}N_4NaO_5S$ ($[M+Na]^+$) requires 501.1203; found 501.1201; ν_{max} (solid) 2953 (aromatic C-H), 1725 (ester C=O), 1712 (NC=O), 1575, 1377, 1187; HPLC (Method 2) >95%, rt = 11.97 min

5*H*-[1,2,4]Triazino[5,6-*b*]indol-3-ol 388

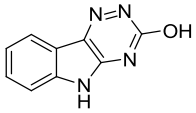

Thiosemicarbizide (2.30 g, 20.4 mmol) was added to a vigorously stirring suspension of isatin **135** (3.00 g, 20.4 mmol) and K_2CO_3 (4.20 g, 30.6 mmol) in H_2O (60 mL) and heated to reflux for 6 h. Suspension was acidified dropwise with glacial acetic acid and resulting precipitate was filtered to yield **388** as a yellow powder (200 mg, 5%); δ_H (500 MHz, DMSO-d_6, 363K) 6.91 (1H, d, *J* = 7.6 Hz, C(6)H), 7.06 (1H, app t, *J* = 7.6 Hz, C(8)H), 7.31 (1H, app t, *J* = 7.6 Hz, C(7)H), 7.59 (1H, d, *J* = 7.6 Hz, C(9)H); δ_C (125 MHz, DMSO-d_6) 111.7 (C6), 121.1 (C8), 121.2 (C9a), 123.1 (C7), 131.2 (C9), 131.9 (C9b), 142.3 (C5a), 155.9 (C4a), 163.6 (C3); mp >300 °C (EZ melt); *m/z* (ESI$^-$) 185 ([M - H]$^-$, 100%); HRMS (ESI$^-$) $C_9H_5N_4O^-$ ([M-H]$^-$) requires 185.0469; found 185.0457; ν_{max} (solid) 3468 (N-H), 3234, 2820 (O-H), 1701, 1465; HPLC (Method 2) >99%, rt = 7.84 min

3-Mercapto-6-methyl-1,2,4-triazin-5-ol 389

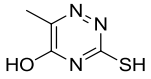

Pyruvic acid (120 mg, 1.73 mmol) was added to acetic acid (5 mL) and heated until homogeneous a solution formed. Thiosemicarbizide (204 mg, 2.25 mmol) was added and heated for 30 mins at reflux in a sealed vial in which the clear solution turned a faint yellow colour. The solution was cooled to rt and precipitate was filtered and dried *in vacuo* to yield **389** as a yellow solid (173 mg, 88 %); δ_H (500 MHz DMSO-d_6 363 K) 2.08 (3H, s, CH_3), 13.03 (1H, br s, SH), 13.27 (1H, br s, OH); δ_C (100 Hz, DMSO-d_6) 16.0 (CH_3), 148.4 (C6), 153.4 (C5), 173.4 (C3); mp 145-147 °C; *m/z* (ESI$^-$) 142 ([M - H]$^-$, 100%); HRMS (ESI$^-$) $C_4H_4N_3OS^-$ ([M-H]$^-$) requires 142.0081; found 142.0078; ν_{max} (solid) 3077 (S-H), 2928 (O-H), 1680, 1552, 1238; HPLC (Method 2) >97%, rt = 12.03 min

5,6-Diphenyl-1,2,4-triazine-3-thiol 390

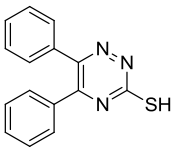

Benzil (200 mg, 0.95 mmol) was added to acetic acid (5 mL) and heated until a homogeneous solution formed. Thiosemicarbizide (116 mg, 1.27 mmol) was added and heated for 30 mins at reflux in a sealed vial. Vial was cooled to rt and precipitate was filtered and dried *in vacuo* to yield **390** as a yellow solid (201 mg, 79 %); δ_H (400 MHz DMSO-d_6 363 K) 7.31 - 7.50 (10 H, m, 10xAr-H), 15.17 (1 H, br s, SH); δ_C (100 Hz, DMSO-d_6) 128.1 (C3' and C5'), 128.3 (2C, C3'' and C5''), 128.7 (C2' and C6'), 129.4 (C4''), 129.5 (C4'), 129.7 (2C, C2'' and C6''), 133.6 (C1'), 134.8 (C1''), 146.3 (C6), 160.1 (C5), 179.2 (C3); mp 205-207 °C, lit 228-230[314]; *m/z* (ESI$^-$) 264 ([M - H]$^-$, 100%); HRMS (ESI$^+$) $C_{15}H_{11}N_3NaS$ ([M+Na]$^+$) requires 288.0566; found 288.0569; ν_{max} (solid) 3125 (N-H), 2875 (S-H), 1557, 1366, 1329, 1192

4,6,7,8-tetrahydrobenzo][1,2,4]triazine-3(2*H*)-thione 391[315]

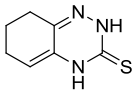

Thiosemicarbizide (812.5 mg, 8.9 mmol) was added to a solution of cyclohexadione (1.0 g, 8.9 mmol) and K_2CO_3 (2.46 g, 17.8 mmol) in H_2O (50 mL) and heated to reflux for 16 h in which the solution changed from light yellow brown. The solution was acidified with acetic acid and resulting precipitate was filtered to yield **391** as a brown solid (1.2 g, 80 %). δ_H (500 MHz, DMSO-d_6, 363K) 1.63 – 1.69 (2H, m, C(7)H), 2.08 – 2.13 (2H, m, C(6)H), 2.31 (2H, t, J = 6.8 Hz, C(8)H), 5.11 (1H, t, J = 4.6 Hz, C(5)H), 10.81 (1H, br s, NH), 11.27 (1H, br s, NH); δ_C (125 MHz, DMSO-d_6) 21.5 (C7), 23.9 (C6), 29.6 (C8),

104.7 (C5), 126.5 (C4a), 148.6 (C5a), 170.7 (C3); mp 164-167 °C; *m/z* (ESI⁻) 166 ([M - H]⁻, 100%); HRMS (ESI⁻) $C_7H_8N_3S^-$ ([M-H]⁻) requires 166.0444; found 166.00443; ν_{max} (solid) 3150 (N-H), 2937, 1551, 1214 (C=S)

2-(((5,6,7,8-tetrahydrobenzo[1,2,4])triazin-3-yl)thio)methyl)benzonitrile 392

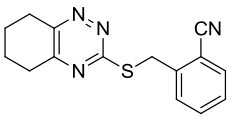

Following **General Procedure 3:** 2-cyanobenzyl bromide (70 mg, 0.36 mmol) was added to 4,6,7,8-tetrahydrobenzo][1,2,4]triazine-3(2*H*)-thione **391** (60 mg, 0.36 mmol) and Et_3N (74 µL, 0.54 mmol) in MeOH (5 mL) and stirred at rt for 16 h. The resulting precipitate was filtered and washed to give **392** as a faint yellow solid (46 mg, 46 %). δ_H (500 MHz, DMSO-d_6, 363K) 1.86 - 1.94 (4H, m, C(6)H_2 and C(7)H_2), 2.87 (2H, t, *J* = 6.1 Hz, C(5)H), 3.05 (2H, t, *J* = 6.3 Hz, C(8)H), 4.63 (2H, s, CH_2), 7.33 (1H, app td, *J* = 7.8, 1.3 Hz, C(5')H), 7.51 (1H, app td, *J* = 7.8, 1.3 Hz, C(4')H), 7.62 (1H, dd, *J* = 7.8, 1.3 Hz, C(6')H), 7.72 (1H, d, *J* = 7.8, C(3')H); δ_C (125 MHz, DMSO-d_6) 21.6, 22.0 (C6 and C7), 29.0 (C8), 31.3 (C5), 32.8 (CH_2), 113.0 (C2'), 117.5 (CN), 127.8 (C5'), 130.4 (C3'), 132.8 (C4'), 133.0 (C6'), 141.5 (C1'), 155.0 (C8a), 159.6 (C5a), 169.0 (C3); mp 101-102 °C; *m/z* (ESI^+) 305 ($[M + Na]^+$, 100%); HRMS (ESI⁻) $C_{15}H_{13}N_4S^-$ ([M-H]⁻) requires 281.0866; found 281.0860; ν_{max} (solid) 3061, 2947, 2225 (CN), 1506, 1286, 1316; HPLC (Method 2) >96%, rt = 10.69 min

2-Bromo-1-cyclopropylethanone 393[274]

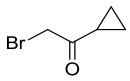

Cyclopropylmethyl ketone (0.5 g, 5.95 mmol) was diluted in MeOH (10 mL) and cooled to 0 °C and treated by dropwise addition of bromine (305 µL, 5.95 mmol). The solution was stirred for 2 hr followed by an addition of H_2O (5 mL) and stirred for 16 hr at rt. The resulting solution was diluted in H_2O (50 mL), extracted with Et_2O (50 mL), the organis layer was further washed with aq sat bicarb (50 mL), dried of $MgSO_4$, filtered and concentrated *in vacuo*.

6.4 Biological Procedures

6.4.1 Materials and Methods

Growth Factors

Recombinant human BMP-2 and BMP-4 were purchased from R&D systems and the protein was dissolved in sterile 4.0 mM HCl containing 0.1% bovine serum albumin (bsa) to a final concentration of 25 µg/mL.

Cell culture

HEK293T cells were grown in Dulbecco's modified eagle's medium (DMEM) supplemented with final concentrations of 10 % fetal bovine serum (FBS), 4.0 mM of L-glutamine, penicillin and streptomycin. Cells were incubated at 37 °C with 5 % CO_2.

6.4.1.1 Plasmids

Reporter plasmids

Smad 1, 5 and 8 expression vectors were prepared LR reaction in gateway cloning experiment following standard protocol (**Table 2**).[316] The LR reaction is a recombination reaction between the attL site on the entry clone and the attR site in the destination vector (Addgene) finally generating an expression clone. The entry vectors (Addgene) containing the respective smad gene, with attL sites on either side, were purchased from geneservice. The destination vector comprises of a pCDNA3 vector with a cytomegalovirus (CMV) promoter and the vector conversion kit (reading frame A) inserted into the EcoRV site. Before or after the conversion part, Rluc 8.1 or Rluc 8.2 were inserted. The resulting vectors were prepared by addition of the entry clone mixed with the appropriate Gateway® destination vector and LR Gateway® Clonase II from Invitrogen. This produced a total of 4 expression vectors for each smad insert (**Figure 1**).

Reagent	Quantity
Entry clone (300 ng)	1-11 µl
Destination vector (300 ng)	1-11 µl
5X LR Clonase™ Plus Reaction Buffer	4 µl
TE buffer, pH 8.0	to 16 µl

Table 2 Components of LR Gateway® reaction mixture

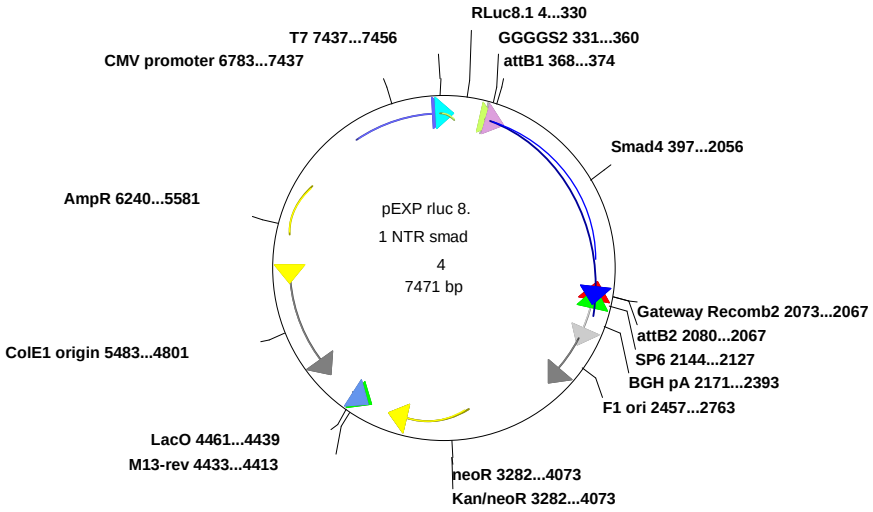

Figure 1 Example of the Expression vectors, with the smad insert with the att sites on either flanks, with the Rluc8.1 and CMV promoter in the vector.

Following the generation of expression vectors were firstly transformed into a bacterial stock by adding 1 µL of the relevant DNA plasmid to bacteria and cooled on ice for 30 min. Bacteria were heat shocked at 42 °C for 30 seconds and replaced on the ice immediately after. 200 µL of the bacterial suspension was added to LB medium to grow bacterial cultures and incubated at 37 °C for 1 h, followed by transfer onto an agar plate. Bacterial cultures are amplified and DNA extracted by mini/midi/maxi prep following manufacturers protocol (Quiagen). Enzymatic digests and sequencing were carried out on the expression vectors to confirm the presence of the intact plasmid.

BREluc construct

The BREluc plasmid was obtained from Peter Ten Dijke. It consisted of a PGL3 basics vector (Promega) and two BMP response elements (BRE), driving expression of the firefly luciferase (Fluc) gene (**Figure 2**).[131] BREs are smad complex binding sites taken from the mouse Id1 promoter.

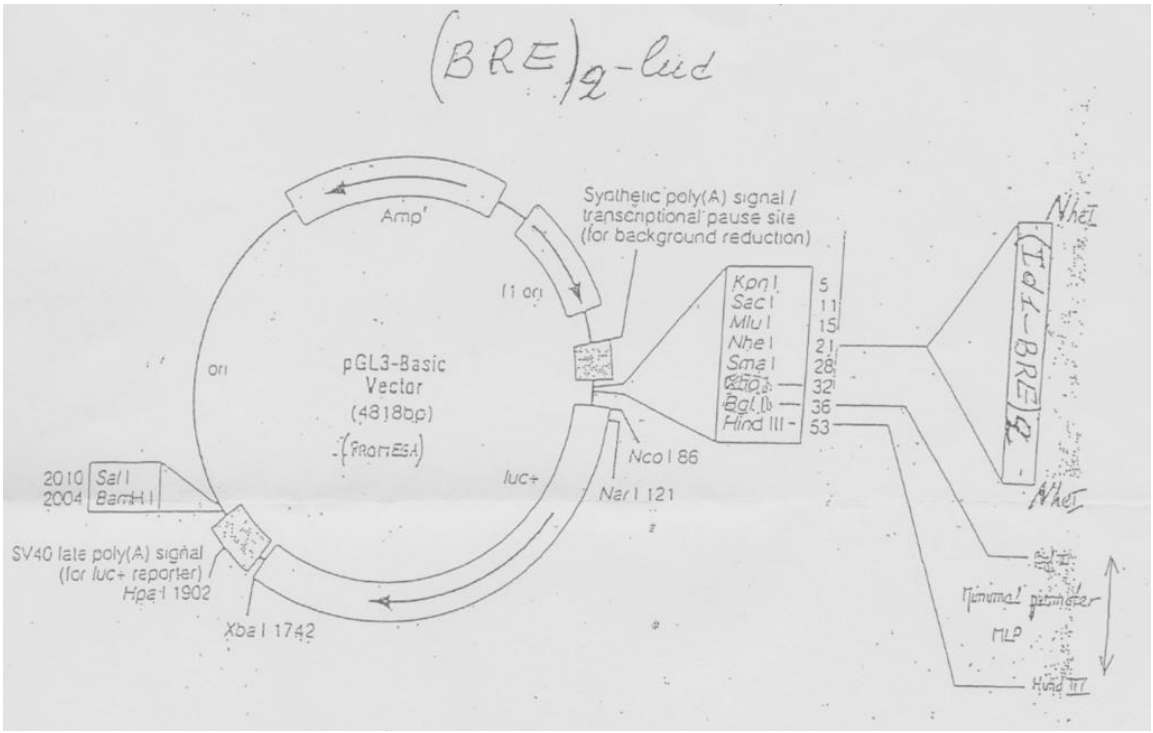

Figure 2 Circular BREluc plasmid map

RLuc Control Plasmid

The transfection control plasmid, which was cotransfected alongside the BREluc was renilla luciferase (Rluc). This consisted of a T7 promoter gene and the RLuc8 gene in a pcDNA vector (**Figure 3**).[317]

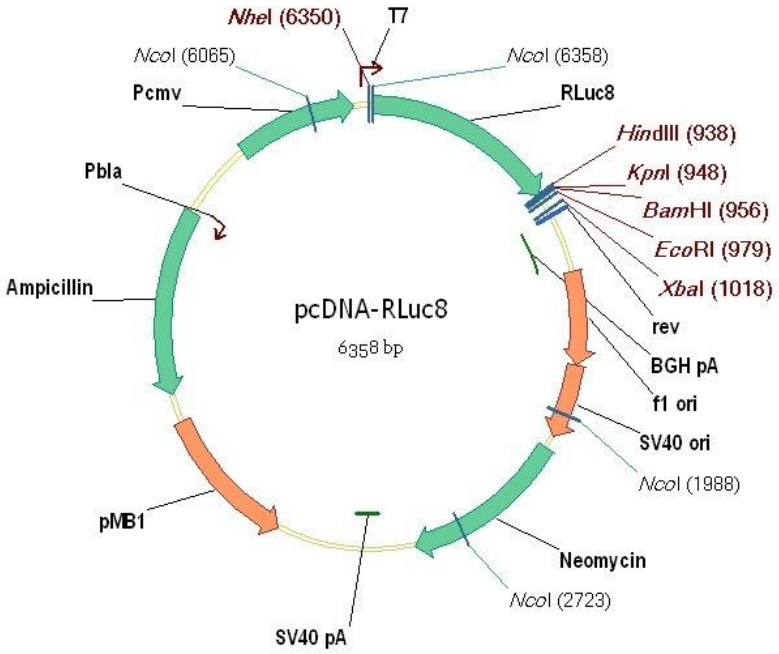

Figure 3 Circular RLuc8 plasmid

Transfection Protocol using Fugene HD[318]

1. To a sterile tube, add 90 – 98µl of Optim-MEM® medium pre-warmed to 37 °C so that the final volume after adding the DNA is 100 µL. Add 2 µg of plasmid DNA (0.2 – 1 µg/µL), and vortex. A 3:1 FuGENE® HD Transfection Reagent: DNA ratio was found to be most efficient where 6 µL of FuGENE® HD Transfection Reagent directly to medium, and mix immediately.

Note: Do not allow undiluted FuGENE® HD Transfection Reagent to contact the sides of the tube.

2. Incubate the FuGENE® HD Transfection Reagent/DNA mixture for 15 minutes at room temperature.
3. Add 2 – 10 µL of the FuGENE® HD Transfection Reagent/DNA mixture per well to a 96-well plate containing 100 µL of cells in growth medium and incubate cells.
4. After 24 hours incubation the medium was removed by aspiration and medium containing serum was applied.

5. Cells were stimulated with the corresponding dose of growth factors or chemicals compound and incubated for a further 24-48 hours.
6. Cells were washed and lysed (*vide infra*).
7. Luciferase assay was run measuring the luminescence produced by each well
8. Measure transfection efficiency using an assay appropriate for the reporter gene.

BREluc Stable Transfected Cell Line

Cells used in these experiments were the mouse derived myoblast cell line (C_2C_{12}). These cells were stably transfected with an expression construct (BREluc) containing a BRE driving expression of the Fluc reporter gene.[319] Activation of the BMP pathway in these cells led to an increase in luciferase gene expression and hence protein concentration and enzyme activity.

The BREluc C_2C_{12} stably transfected cell line was cultured in DMEM supplemented with 10% fetal bovine serum (FBS), 4 mM of L-glutamine, penicillin, streptomycin and 0.7 mg/mL geneticin sulphate (G418) for selectivity.

6.4.1.2 Biological Assays

6.4.1.2.1 Transactivation Assay

For the transactivation assay, $2x10^4$ HEK293T calls were seeded on a 96 well plate one day before transfection and cultured at 37 °C for 24h. The CMV-smad4 construct (20-80 ng) in combination with an R-smad construct of either CMV-smad1, 5 or 8 (20-80 ng) were cotransfected with the CMV-renilla plasmid (10 ng) using Fugene HD (Promega) following the manufacturer's protocol (*vide supra*). The cells were then incubated for 24h at 37 °C. After 6h serum starvation at 37 °C, the cells were washed with PBS and lysed for 20 min at rt using 100 µL lysis buffer (25 nM Tris Phosphate Buffer pH 7.8, 2 mM CDTA,

10 % glycerol and 1 % Triton X-100).[320] Firefly and renilla luminescence were measured sequentially. First, Fluc activity was measured using 10 µL of the lysate in 100 µL luciferase assay buffer (10 µg Potassium luciferin, 15 mM $MgSO_4$, 15 mM Potassium phosphate buffer pH 7.8, 4 mM EGTA pH 7.8, 20 µM ATP and 2 µM DTT). Luminescence was detected using a POLARstar Omega luminometer (BMG). Then renilla luciferase activity was measured by adding 100 µL of PBS containing 10 µM of benzyl coelenterazine and 25 mM of luciferase inhibitor I (Merck Chemicals) to inhibit the firefly luminescence. Fluc and Rluc activities were measured in relative light units (RLU) with the POLARstar omega luminometer (BMG). The values of the Fluc values were normalised for transfection efficiency using the Rluc activity values. Each experiment was performed once in triplicates. Numerical results were reported as averages with standard mean error.

6.4.1.2.2 Protein Complimentation Assay

In the PCA, the proteins of interest were fused to the first and second half of the Rluc using Gateway LR cloning. Both constructs (45 ng each) were cotransfected using HEK293T cell grown in 96-well plates using Fugene HD (Promega) following the manufacturers protocol. In addition, a transfection control plasmid, CMV-lacZ construct (10 ng) was also cotransfected to normalise for efficiency and cells number. After 24h incubation at 37 °C, the cells were washed with PBS and the renilla activity was measured in the living cells in 100 µL PBS by addition of another 100 µL PBS containing 10 µL of benzyl coelenterazine. The cells were then lysed at rt by adding 50 µL of 5x lysis buffer (125 mM Tris Phosphate buffer pH7.8, 10 mM CDTA, 50% glycerol and 5% Triton X-100) at rt for 20 min. The LacZ assay was performed using 10 µL of the lysate and adding 100 µL LacZ buffer (16 mM $Na_2HPO_4.7H_2O$, 40 mM $NaH_2PO_4.H_2O$, 10 mM KCl and 1 mM $MgSO_4$) containing 10 % of 10x OMPG and 0.27% Betamercaptoethanol. The lysate was incubated

at 37 °C shielded from light until the appearance of a yellow colour. The reaction was then blocked by adding 50 µL 1M Na_2CO_3. The absorbance was measured with a POLARstar Omega luminometer (BMG). The values of renilla luciferase were normalised for transfection efficiency using the LacZ absorbance values. Each experiment was performed once in triplicates. Numerical results were reported as averages with standard mean error.

6.4.2 Compound Testing

Transient Transfected Cells

For the compound testing using transiently transfected C2C12 cells, cells were incubated at 50% confluence one day before transfection and cultured at 37 °C for 24h. The BREluc reporter plasmid (90 ng) was cotransfected and rluc plasmid (10 ng) using Fugene, following the manufacturers protocol. The cells were washed with PBS and shaken in 100 µL lysis buffer (*vide supra*) for 20 min at rt. Fluc activity was measured using 5 µL lysate and 100 µL luciferase assay buffer (*vide supra*). Luminescence was detected using a POLARstar Omega luminometer (BMG). Then renilla luciferase activity was measured by adding 100 µL of PBS containing 10 µM of coelenterazine. The values of the Fluc values were normalised for transfection efficiency using the Rluc activity values. Each experiment was performed once in triplicates. Numerical results were reported as averages with standard mean error.

Stably Transfected Cells

The activity of the compounds was quantified in a luciferase assay where the light emitted by the luciferase-mediated transformation of luciferin was measured. Cells were plated in a 96 well plate at $5x10^3$ cells per well and incubated overnight at 37 °C. The final concentration of recombinant BMP-4 (R&D systems) used was 10 ng/mL. 1 µL of

compound stock solution (1 mM in DMSO) was added to the 100 µL of culture media to provide a final concentration of 10 µM. Fluc activity was measured using 10 µL of the lysate in 10 µL luciferase assay buffer. Luminescence was detected using a POLARstar Omega luminometer (BMG). Fluc activity was normalised using the absorbance value at 595 nm. %UpR of BMP activity was compared using BMP-4 stimulated cells as a 100% signal. Fluc values were normalised using the Bradford assay, following manufacturers protocol. Each experiment was performed once in triplicates and repeated for the results that showed changed activity. Numerical results were reported as averages with standard mean error.

6.4.3 Biological Assays

6.4.3.1 hCB_2R cAMP Assay[321]

The cAMP Hunter eXpress GPCR assay kit and cells used are from DiscoveRx Corporation (DiscoveRx Corporation, Birmingham, UK) and used according to the manufacturer's protocol. The CB_2R agonist HU-308 (Tocris Bioscience, UK) and CB_1R agonist Δ^9-THC (Sigma Aldrich) were used as positive controls. Briefly, $hCNR_2$ CHO-K_1 cells were plated in the provided medium (15000 cells per well) in half-area 96-well plates (Corning, UK) and placed overnight in an incubator 37°C 5% CO_2. Next day, the medium was aspirated and replaced with a 1:3 solution of anti-cAMP antibody in the provided buffer. In the presence of 20 μM forskolin, freshly reconstituted compounds or solvent alone (final concentration 0.2% DMSO) were added to the wells and incubated for 30 minutes at 37°C, 5 % CO_2. After the incubation, a mixture of provided lysis solution and substrates was added to the wells and incubated in the dark for one hour at room temperature. The provided detection reagent EA was then added to the wells and incubated in the dark for 3 hours at room temperature. The luminescence was then read using a standard luminometer (Perkin-Elmer, Seer Green, UK). The luminescence of the wells incubated only with forskolin and solvent (control wells) were normalised as 100% and the dose-response curves were expressed as a percentage of the control wells. The EC_{50} values shown are from pooling 3-4 independent experiments and were identified using GraphPad prism non-linear regression curve fit (4 PL parameters).

6.4.3.2 Radioligand Binding Assays for hCB_1R and hCB_2R[322,323]

Radioligand binding assays were contracted to CEREP (Celle l'Evescault, France) where membranes from CHO-cells expressing either hCB_1R or hCB_2R were used to assess binding to the two cannabinoid receptors. Competition binding studies were performed by

incubating membranes expressing hCB_1R or hCB_2R with the unlabelled compounds and tritiated CP-55940 (EC_{50} 0.5 nM) or WIN-55212 (EC_{50} 0.8 nM) respectively, for two hours at 37^{o}C. For CB_1R and CB_2R, non-specific binding was assessed using WIN-55212 at 10 and 5 μM respectively. Two hours later, the binding of tritiated ligands was assessed by scintillation counting. The competition binding data for each compound are expressed as the percentage of the remaining bound tritiated ligand after incubation of the compound with the membrane. K_i values (equilibrium dissociation constants for each compound) were calculated by CEREP using the Cheng-Prusoff equation and the K_d value (equilibrium dissociation constant for each radioligand).

6.4.3.3 Turbidimetric Solubility Assay[286]

The aqueous solubility assay was performed by Cyprotex using a high throughput turbidimetric assay. Initially, a stock DMSO solution was diluted in DMSO to produce a range of concentrations. These were then added to buffer, typically phosphate buffered saline at pH 7.4 (final test compound concentrations = 1 μM, 3 μM, 10 μM, 30 μM, 100 μM, final DMSO concentration = 1%, 7 replicates per concentration) and incubated for 2 h at 37 °C. At the end of the incubation period, the absorbance at 620 nm was read for each concentration and each replicate. The assay provided a precipitation range, where the mid-point was used as the estimated precipitation concentration and recorded in μM.

6.4.3.4 Microsomal Stability Assay[290]

The microsomal stability assay was performed by Cyprotex. The microsomes used were mouse liver microsomes and were incubated with the test compound at 37 °C in the presence of the co-factor, NADPH, which initiates the reaction. The reaction is terminated by the addition of methanol containing internal standard. Following centrifugation, the

supernatant is analysed on the LC-MS/MS. The disappearance of test compound is monitored over a 45 minute time period. Concentrations of compound were measured at 0, 5, 15 30, 45 min time points. Diazepam and Diphenhydramine were used as the positive controls which are

metabolised by the microsomes. Compound in the absence of the co-factor is measured at the 45 min time point.

Appendices

Appendix 1: HDAC selectivity profile for HDAC inhibitors

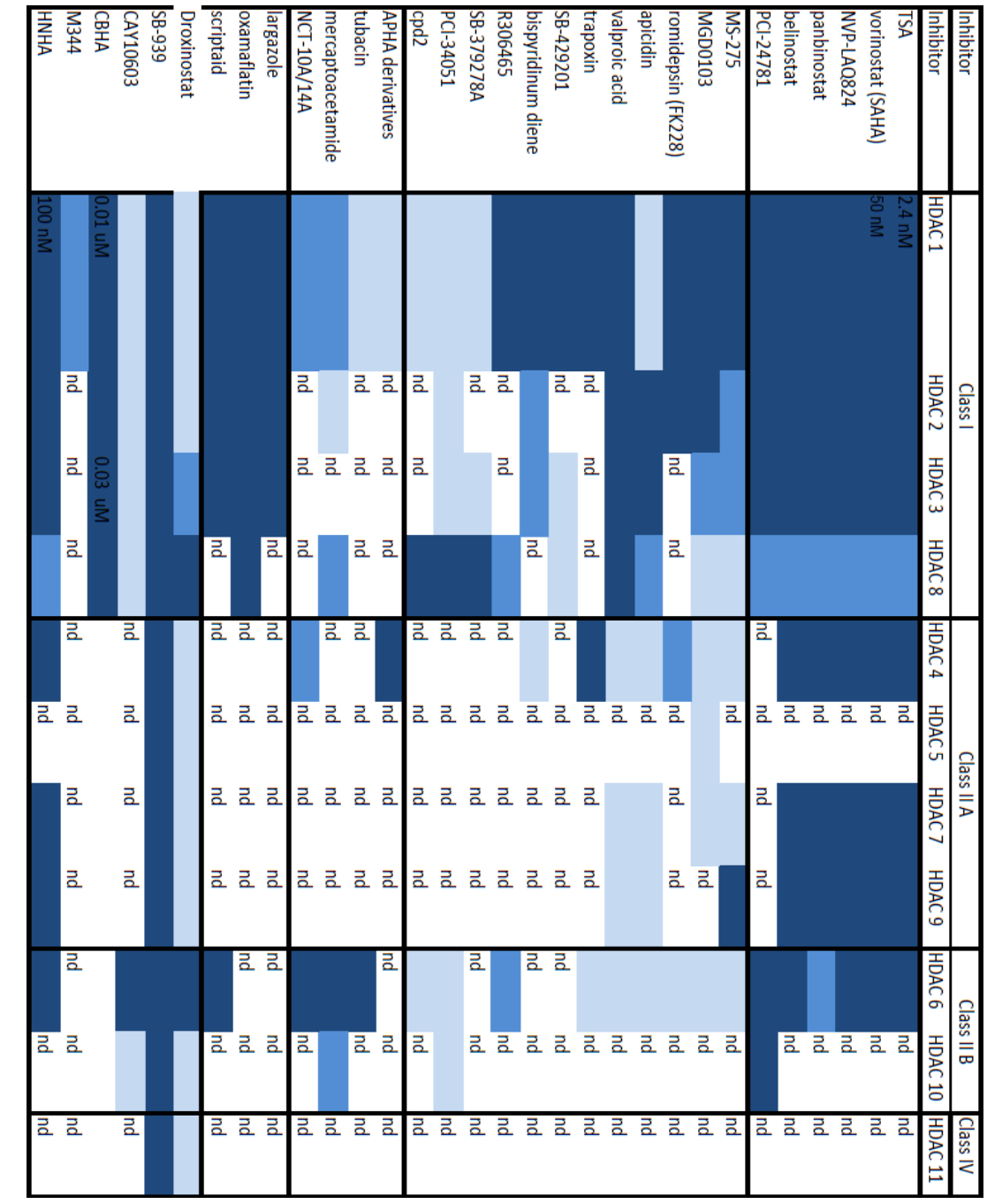

ıibitory potency of several pan-, class I selective, and class II selective compounds against HDAC's 1-11

t EC_{50} relative to most sensitive HDAC isoform)

EC_{50} relative to most sensitive HDAC isoform)

C_{50} relative to most sensitive HDAC isoform)

Appendix 2: Ligand Based Virtual Screen using HU-308 (226)

Rank	Structure	Tanimoto Score	Colour Score	Combo score	Activity at CB_2R	
					3 µM	1 µM
1	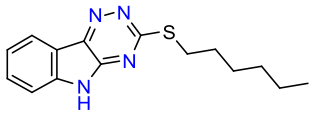	0.713	0.504	1.217	75.973	102.46
2	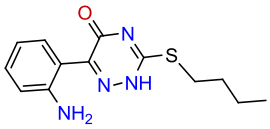	0.697	0.493	1.19	61.616	93.515
3	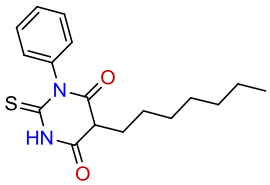	0.68	0.491	1.17	98.058	111.42
4	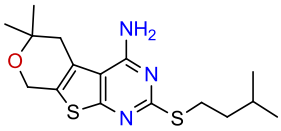	0.715	0.447	1.162	85.296	76.706
5	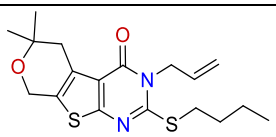	0.689	0.467	1.155	36.705	76.314
6	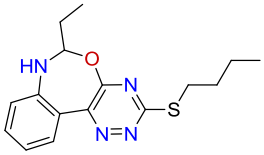	0.673	0.47	1.143	44.292	47.762
7	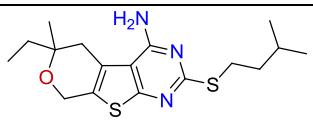	0.695	0.447	1.142	98.355	111.13
8	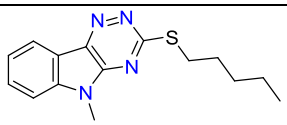	0.711	0.427	1.137	109.84	129.38
9	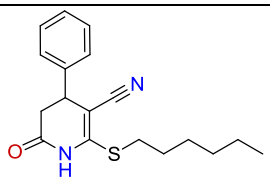	0.696	0.44	1.137	128.45	145.89
10	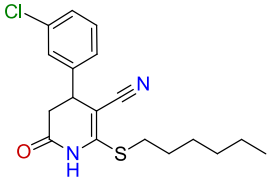	0.71	0.426	1.136	117.13	105.01

11	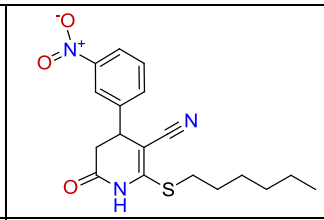	0.702	0.434	1.136	39.86	63.242
12	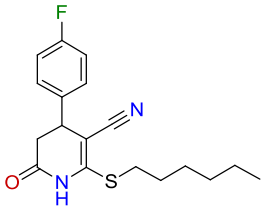	0.693	0.441	1.134	113.61	120.63
13	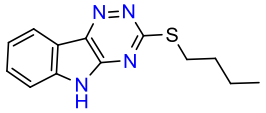	0.674	0.459	1.133	57.176	52.102
14	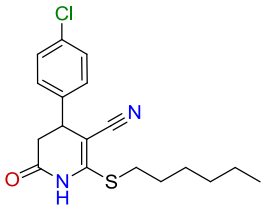	0.69	0.441	1.131	137.65	107.8
15	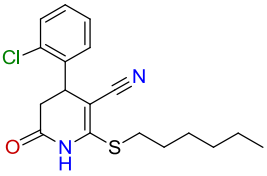	0.704	0.426	1.13	119.47	98.202
16	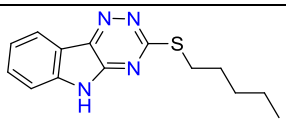	0.698	0.427	1.125	73.082	86.244

Figure A2 Top 16 compounds obtained from the virtual screen performed using ROCS programme with **226** (HU-308) as the template molecule. 40 conformers were generated of **226** to screen against the in-house library of 25,000 compounds providing a colour score and tanomoto score. The combination of the two presents the combo score, which the compounds are ranked by. Each compound was tested in a biological assay and tested at two concentrations (1 µM and 3 µM) to provide a measure of their activity.

Appendix 3: GPCR Screen of 236

Receptor	Receptor family	% of Control Agonist Response
A_{2A}	adenosine	0
A_3	adenosine	9
α_{1A}	adrenergic	-1
α_{2A}	adrenergic	2
β_1	adrenergic	0
β_2	adrenergic	0
D_1	dopamine	0
D_3	dopamine	1
H_1	histamine	1
H_2	histamine	0
H_3	histamine	10
MC_4	melanocortin	0
MT_1 (ML_{1A})	melatonin	21
M_1	muscarinic achetylcholine	1
M_4	muscarinic achetylcholine	-5
NK_1	neurokinin	1
κ (KOP)	opioid	14
μ (MOP)	opioid	11
5-HT_{1A}	serotonin	-21
5-HT_{1B}	serotonin	4
5-HT_{2B}	serotonin	0
5-HT_{4e}	serotonin	0
5-HT_6	serotonin	-3
sst_4	somastatin	6

Figure A3 GPCR screen of **236** for activity against a group of 23 representative GPCR's. Activity is demonstrated by their relative % agonist activity from the control. Biological assays using **236** were performed by Cerep SA, France.

Appendix 4: Kinase Screen of 236

Kinome Scan Gene Symbol	Gene Symbol	% Control
ABL1(E255K)-phosphorylated	ABL1	85
ABL1(T315I)-phosphorylated	ABL1	92
ABL1-nonphosphorylated	ABL1	86
ABL1-phosphorylated	ABL1	94
ACVR1B	ACVR1B	91
ADCK3	CABC1	95
AKT1	AKT1	85
AKT2	AKT2	93
ALK	ALK	72
AURKA	AURKA	100
AURKB	AURKB	100
AXL	AXL	65
BMPR2	BMPR2	90
BRAF	BRAF	94
BRAF(V600E)	BRAF	100
BTK	BTK	100
CDK11	CDK19	100
CDK2	CDK2	82
CDK3	CDK3	100
CDK7	CDK7	94
CDK9	CDK9	84
CHEK1	CHEK1	87
CSF1R	CSF1R	100
CSNK1D	CSNK1D	86
CSNK1G2	CSNK1G2	81
DCAMKL1	DCLK1	100
DYRK1B	DYRK1B	74
EGFR	EGFR	100
EGFR(L858R)	EGFR	100
EPHA2	EPHA2	87
ERBB2	ERBB2	94

ERBB4	ERBB4	74
ERK1	MAPK3	89
FAK	PTK2	98
FGFR2	FGFR2	91
FGFR3	FGFR3	88
FLT3	FLT3	84
GSK3B	GSK3B	100
IGF1R	IGF1R	91
IKK-alpha	CHUK	100
IKK-beta	IKBKB	100
INSR	INSR	88
JAK2(JH1domain-catalytic)	JAK2	100
JAK3(JH1domain-catalytic)	JAK3	93
JNK1	MAPK8	96
JNK2	MAPK9	90
JNK3	MAPK10	100
KIT	KIT	100
KIT(D816V)	KIT	75
KIT(V559D,T670I)	KIT	100
LKB1	STK11	87
MAP3K4	MAP3K4	100
MAPKAPK2	MAPKAPK2	82
MARK3	MARK3	93
MEK1	MAP2K1	95
MEK2	MAP2K2	87
MET	MET	87
MKNK1	MKNK1	98
MKNK2	MKNK2	95
MLK1	MAP3K9	98
p38-alpha	MAPK14	100
p38-beta	MAPK11	94
PAK1	PAK1	80
PAK2	PAK2	88
PAK4	PAK4	87

PCTK1	CDK16	100
PDGFRA	PDGFRA	94
PDGFRB	PDGFRB	91
PDPK1	PDPK1	91
PIK3C2B	PIK3C2B	95
PIK3CA	PIK3CA	100
PIK3CG	PIK3CG	100
PIM1	PIM1	90
PIM2	PIM2	75
PIM3	PIM3	74
PKAC-alpha	PRKACA	72
PLK1	PLK1	94
PLK3	PLK3	100
PLK4	PLK4	100
PRKCE	PRKCE	100
RAF1	RAF1	100
RET	RET	89
RIOK2	RIOK2	94
ROCK2	ROCK2	80
RSK2(Kin.Dom.1-N-terminal)	RPS6KA3	80
SNARK	NUAK2	93
SRC	SRC	100
SRPK3	SRPK3	75
TGFBR1	TGFBR1	100
TIE2	TEK	100
TRKA	NTRK1	98
TSSK1B	TSSK1B	100
TYK2(JH1domain-catalytic)	TYK2	96
ULK2	ULK2	94
VEGFR2	KDR	95
YANK3	STK32C	83
ZAP70	ZAP70	78

Figure A4 Kinase Screen of **236** against a set of 97 representative kinases. The activity was measured at 10 µM of **236** and is represented as a % from the control in each assay. The biological assays were carried out by Cerep SA, France.

References

1. I. Kola and J. Landis, *Nat Rev Drug Discov*, 2004, **3**, 711-716.
2. Y. Wang, *Pharm Med*, 2012, **26**, 91-96.
3. D. C. Swinney and J. Anthony, *Nat Rev Drug Discov*, 2011, **10**, 507-519.
4. J. P. Hughes, S. Rees, S. B. Kalindjian and K. L. Philpott, *Brit J Pharmacol*, 2011, **162**, 1239-1249.
5. A. Schuffenhauer, S. Ruedisser, A. Marzinzik, W. Jahnke, M. Blommers, P. Selzer and E. Jacoby, *Curr Top Med Chem*, 2005, **5**, 751-762.
6. H. Verheij, *Mol Div*, 2006, **10**, 377-388.
7. V. Purohit and A. K. Basu, *Chem Res Toxicol*, 2000, **13**, 673-692.
8. G. W. Bemis and M. A. Murcko, *J Med Chem*, 1996, **39**, 2887-2893.
9. G. W. Bemis and M. A. Murcko, *J Med Chem*, 1999, **42**, 5095-5099.
10. C. A. Lipinski, F. Lombardo, B. W. Dominy and P. J. Feeney, *Adv Drug Delivery Rev*, 1997, **23**, 3-25.
11. C. A. Lipinski, *J Pharmacol Toxicol Methods*, 2000, **44**, 235-249.
12. P. Leeson and B. Springthorpe, *Nat Rev Drug Discov*, 2007, **6**, 881-890.
13. A. P. Hill and R. J. Young, *Drug Discovery Today*, 2010, **15**, 648-655.
14. A. K. Ghose, V. N. Viswanadhan and J. J. Wendoloski, *J Comb Chem*, 1998, **1**, 55-68.
15. J. D. Hughes, J. Blagg, D. A. Price, S. Bailey, G. A. DeCrescenzo, R. V. Devraj, E. Ellsworth, Y. M. Fobian, M. E. Gibbs, R. W. Gilles, N. Greene, E. Huang, T. Krieger-Burke, J. Loesel, T. Wager, L. Whiteley and Y. Zhang, *Bioorg Med Chem Lett*, 2008, **18**, 4872-4875.
16. D. F. Veber, S. R. Johnson, H.-Y. Cheng, B. R. Smith, K. W. Ward and K. D. Kopple, *J Med Chem*, 2002, **45**, 2615-2623.
17. M. P. Gleeson, *J Med Chem*, 2008, **51**, 817-834.
18. S. J. Teague, A. M. Davis, P. D. Leeson and T. Oprea, *Angew Chem Int Ed*, 1999, **38**, 3743-3748.
19. J. Alper, *Science*, 1994, **264**, 1399-1401.

20. R. A. Fecik, K. E. Frank, E. J. Gentry, S. R. Menon, L. A. Mitscher and H. Telikepalli, *Med Res Rev*, 1998, **18**, 149-185.
21. D. Tan, *Nat Chem Biol*, 2005, **1**, 74-84.
22. D. E. Clark and S. D. Pickett, *Drug Discovery Today*, 2000, **5**, 49-58.
23. W. L. Jorgensen, *Science*, 2004, **303**, 1813-1818.
24. A. Carnero, *Clin Trans Oncol*, 2006, **8**, 482-490.
25. M. Simmons, *Mol Interventions*, 2005, **5**, 154-157.
26. S. Rajagopal, *Nat Rev Drug Discov*, 2013, **12**, 483-483.
27. J.-H. Zhang, T. D. Y. Chung and K. R. Oldenburg, *J Biomol Screening*, 1999, **4**, 67-73.
28. A. Dove, *Nat Meth*, 2007, **4**, 523-532.
29. S. Fox, S. Farr-Jones, L. Sopchak, A. Boggs, H. W. Nicely, R. Khoury and M. Biros, *J Biomol Screening*, 2006, **11**, 864-869.
30. W. L. Jorgensen, *Acc Chem Res*, 2009, **42**, 724-733.
31. D. C. Rees, M. Congreve, C. W. Murray and R. Carr, *Nat Rev Drug Discov*, 2004, **3**, 660-672.
32. M. J. Hartshorn, C. W. Murray, A. Cleasby, M. Frederickson, I. J. Tickle and H. Jhoti, *J Med Chem*, 2004, **48**, 403-413.
33. T. L. Blundell and S. Patel, *Curr Opin Pharmacol*, 2004, **4**, 490-496.
34. J. He, D. Wei, J. Wang and K. Chou, *Protein Peptide Lett*, 2011, **18**, 997-1001.
35. C. McInnes, *Curr Opin Chem Biol*, 2007, **11**, 494-502.
36. E. Garman and G. Laver, *Curr Drug Targets*, 2004, **5**, 119-136.
37. W. P. Burmeister, B. Henrissat, C. Bosso, S. Cusack and R. W. H. Ruigrok, *Structure*, 1993, **1**, 19-26.
38. M. Vonitzstein, W. Y. Wu, G. B. Kok, M. S. Pegg, J. C. Dyason, B. Jin, T. V. Phan, M. L. Smythe, H. F. White, S. W. Oliver, P. M. Colman, J. N. Varghese, D. M. Ryan, J. M. Woods, R. C. Bethell, V. J. Hotham, J. M. Cameron and C. R. Penn, *Nature*, 1993, **363**, 418-423.
39. J. N. Varghese, J. L. McKimmbreschkin, J. B. Caldwell, A. A. Kortt and P. M. Colman, *Proteins*, 1992, **14**, 327-332.
40. J. Black, *Postgraduate Medical Journal*, 1976, **52**, 11-13.
41. J. Black, L. Smith, R. Shanks, A. Crowther and A. Dornhorst, *Lancet*, 1964, **1**, 1081-&.
42. H. Konzett, Naunyn-Schmiedeberg's Arch Editon, 1940, **127**, 41-56.

43. C. E. Powell, I. H. Slater, L. LeCompte and J. E. Waddell, *J Pharmacol Exp Ther*, 1958, **122**, 480-488.
44. J. Black, in *Nobel Lecture*, King's College School for Medicine & Dentistry, Analytical Pharmacology Rayne Institute, London, England, 1988.
45. T. Raju, *Lancet*, 2000, **356**, 81-81.
46. R. Law, O. Barker, J. J. Barker, T. Hesterkamp, R. Godemann, O. Andersen, T. Fryatt, S. Courtney, D. Hallett and M. Whittaker, *J Comput Aided Mol Des*, 2009, **23**, 459-473.
47. C. W. R. Murray *et. al*., *Nat Chem*, 2009, **1**, 187-192.
48. M. Congreve, R. Carr, C. Murray and H. Jhoti, *Drug Discovery Today*, 2003, **8**, 876-877.
49. H.-J. Boehm, M. Boehringer, D. Bur, H. Gmuender, W. Huber, W. Klaus, D. Kostrewa, H. Kuehne, T. Luebbers, N. Meunier-Keller and F. Mueller, *J Med Chem*, 2000, **43**, 2664-2674.
50. T. Kenakin, *Trends Pharmacol Sci*, 2004, **25**, 186-192.
51. L. Enteen, J. Bauer, R. McLean, E. Wheeler, E. Huriaux, A. Kral and J. Bamberger, *J Urban Health*, 2010, **87**, 931-941.
52. R. Sink, S. Gobec, S. Pecar and A. Zega, *Curr Med Chem*, 2010, **17**, 4231-4255.
53. K. T. Weber, C. G. Brilla and J. S. Janicki, *Cardiovasc Res*, 1993, **27**, 341-348.
54. T. R. Cox and J. T. Erler, *Dis Models Mech*, 2011, **4**, 165-178.
55. W.-Z. Zhu, K. D. Hauch, C. Xu and M. A. Laflamme, *Transplantation Rev*, 2009, **23**, 53-68.
56. P. Kessler and B. Byrne, *Annu Rev Physiol*, 1999, **61**, 219-242.
57. N. Smart, S. Bollini, K. N. Dube, J. M. Vieira, B. Zhou, S. Davidson, D. Yellon, J. Riegler, A. N. Price, M. F. Lythgoe, W. T. Pu and P. R. Riley, *Nature*, 2011, **474**, 640-644.
58. N. Smart, C. A. Risebro, A. A. D. Melville, K. Moses, R. J. Schwartz, K. R. Chien and P. R. Riley, *Nature*, 2007, **445**, 177-182.
59. E. M. Zeisberg, O. Tarnavski, M. Zeisberg, A. L. Dorfman, J. R. McMullen, E. Gustafsson, A. Chandraker, X. Yuan, W. T. Pu, A. B. Roberts, E. G. Neilson, M. H. Sayegh, S. Izumo and R. Kalluri, *Nat Med*, 2007, **13**, 952-961.
60. T. Rando, *Nature*, 2006, **441**, 1080-1086.
61. B. Nadal-Ginard, J. Kajstura, A. Leri and P. Anversa, *Circ Res*, 2003, **92**, 139-150.

62. J. Hao, M. Daleo, C. Murphy, P. Yu, J. Ho, J. Hu, R. Peterson, A. Hatzopoulos and C. Hong, *Plos One*, 2008, **3**.

63. H. Sadek, B. Hannack, E. Choe, J. Wang, S. Latif, M. Garry, D. Garry, J. Longgood, D. Frantz, E. Olson, J. Hsieh and J. Schneider, *Proc Natl Acad Sci U.S.A.*, 2008, **105**, 6063-6068.

64. C. C. Hong and P. B. Yu, *Cytokine & Growth Factor Rev*, 2009, **20**, 409-418.

65. B. Hu, J. Weick, J. Yu, L. Ma, X. Zhang, J. Thomson and S. Zhang, *Proc Natl Acad Sci U.S.A.*, 2010, **107**, 4335-4340.

66. A. Raya, I. Rodriguez-Piza, G. Guenechea, R. Vassena, S. Navarro, M. Barrero, A. Consiglio, M. Castella, P. Rio, E. Sleep, F. Gonzalez, G. Tiscornia, E. Garreta, T. Aasen, A. Veiga, I. Verma, J. Surralles, J. Bueren and J. Belmonte, *Nature*, 2009, **460**, 53-61.

67. D.-W. Jung and D. R. Williams, *ACS Chem Biol*, 2012, **7**, 1773-1790.

68. Terri T. Ni, Eric J. Rellinger, A. Mukherjee, S. Xie, L. Stephens, Curtis A. Thorne, K. Kim, J. Hu, E. Lee, L. Marnett, Antonis K. Hatzopoulos and Tao P. Zhong, *Chem Biol*, 2011, **18**, 1658-1668.

69. K. W. Park, H. Waki, W.-K. Kim, B. S. J. Davies, S. G. Young, F. Parhami and P. Tontonoz, *Mol Cell Biol*, 2009, **29**, 3905-3914.

70. C. Xu, S. Police, N. Rao and M. K. Carpenter, *Circ Res*, 2002, **91**, 501-508.

71. G. Yang, J. Tian, C. Feng, L.-l. Zhao, Z. Liu and J. Zhu, *Cell Transplant*, **21**, 985-996.

72. T. Takahashi, B. Lord, P. C. Schulze, R. M. Fryer, S. S. Sarang, S. R. Gullans and R. T. Lee, *Circulation*, 2003, **107**, 1912-1916.

73. A. Wobus, K. Guan, S. Jin, M. Wellner, J. Rohwedel, G. Ji, B. Fleischmann, H. Katus, T. Hescheler and W. Franz, *J Mol Cell Cardiol*, 1997, **29**, 1525-1539.

74. J. L. Russell, S. C. Goetsch, H. R. Aguilar, H. Coe, X. Luo, N. Liu, E. van Rooij, D. E. Frantz and J. W. Schneider, *ACS Chem Biol*, 2012, **7**, 1077-1083.

75. H.-T. Yang, D. Tweedie, S. Wang, A. Guia, T. Vinogradova, K. Bogdanov, P. D. Allen, M. D. Stern, E. G. Lakatta and K. R. Boheler, *Proc Natl Acad Sci*, 2002, **99**, 9225-9230.

76. J. Massague, *Nat Rev Mol Cell Biol*, 2000, **1**, 169-178.

77. D. James, A. J. Levine, D. Besser and A. Hemmati-Brivanlou, *Development*, England, Editon, 2005, 132, 1273-1282.

78. J. F. Callahan, J. L. Burgess, J. A. Fornwald, L. M. Gaster, J. D. Harling, F. P. Harrington, J. Heer, C. Kwon, R. Lehr, A. Mathur, B. A. Olson, J. Weinstock and N. J. Laping, in *J Med Chem*, United States Editon, 2002, **45**, 999-1001.
79. X. Varelas, R. Sakuma, P. Samavarchi-Tehrani, R. Peerani, B. M. Rao, J. Dembowy, M. B. Yaffe, P. W. Zandstra and J. L. Wrana, in *Nat Cell Biol*, England Editon, 2008, **10**, 837-848.
80. K. Ogawa, A. Saito, H. Matsui, H. Suzuki, S. Ohtsuka, D. Shimosato, Y. Morishita, T. Watabe, H. Niwa and K. Miyazono, in *J Cell Sci*, England Editon, 2007, **120**, 55-65.
81. A. Schier and M. Shen, *Nature*, 2000, **403**, 385-389.
82. T. Watabe and K. Miyazono, in *Cell Res*, China Editon, 2009, **19**, 103-115.
83. S. T. Dougan, R. M. Warga, D. A. Kane, A. F. Schier and W. S. Talbot, *Development*, 2003, **130**, 1837-1851.
84. F. L. Conlon, K. M. Lyons, N. Takaesu, K. S. Barth, A. Kispert, B. Herrmann and E. J. Robertson, *Development*, 1994, **120**, 1919-1928.
85. D. Schade, M. Lanier, E. Willems, K. Okolotowicz, P. Bushway, C. Wahlquist, C. Gilley, M. Mercola and J. R. Cashman, *J Med Chem*, 2012, **55** (22), 9946-9957.
86. J. Zhang and L. Li, *Dev Biol*, 2005, **284**, 1-11.
87. P. ten Dijke, E. Korchynskyi, G. Valdimarsdottir and M. Goumans, *Mol Cell Encrinol*, 2003, **211**, 105-113.
88. B. L. Rosenzweig, T. Imamura, T. Okadome, G. N. Cox, H. Yamashita, P. Tendijke, C. H. Heldin and K. Miyazono, *Proc Natl Acad Sci U.S.A.*, 1995, **92**, 7632-7636.
89. S. Ross and C. Hill, *Int J Biochem Cell Biol*, 2008, **40**, 383-408.
90. T. Ogata, J. M. Wozney, R. Benezra and M. Noda, *Proc Natl Acad Sci U.S.A.*, 1993, **90**, 9219-9222.
91. A. Hollnagel, V. Oehlmann, J. Heymer, U. Rüther and A. Nordheim, *J Biol Chem*, 1999, **274**, 19838-19845.
92. N. Hartigan, L. Garrigue-Antar and K. E. Kadler, *J Biol Chem*, 2003, **278**, 18045-18049.
93. J. M. Wozney, V. Rosen, A. J. Celeste, L. M. Mitsock, M. J. Whitters, R. W. Kriz, R. M. Hewick and E. A. Wang, *Science*, 1988, **242**, 1528-1534.
94. P.-L. Kuo, Y.-T. Huang, C.-H. Chang and J.-K. Chang, *Biol Pharm Bull*, 2006, **29**, 119-124.

95. H.-f. Guo, H.-y. Shao, Z.-y. Yang, S.-t. Xue, X. Li, Z.-y. Liu, X.-b. He, J.-d. Jiang, Y.-q. Zhang, S.-y. Si and Z.-r. Li, *J Med Chem*, 2010, **53**, 1819-1829.

96. M. C. Fishman and E. N. Olson, *Cell*, 1997, **91**, 153-156.

97. M. Pera, J. Andrade, S. Houssami, B. Reubinoff, A. Trounson, E. Stanley, D. Ward-van Oostwaard and C. Mummery, *J Cell Sci*, 2004, **117**, 1269-1280.

98. M. Taha, M. Valojerdi and S. Mowla, *Intl J Cardiol*, 2007, **120**, 92-101.

99. C. Robin and C. Durand, *Int J Dev Biol*, Spain Editon, 2010, 54, 1189-1200.

100. T. L. Huber and L. I. Zon, in *Semin Immunol*, United States Editon, 1998, 10, 103-109.

101. B. L. M. Hogan, *Curr Opin Gene Dev*, 1996, **6**, 432-438.

102. G. Winnier, M. Blessing, P. A. Labosky and B. L. M. Hogan, *Gene Dev*, 1995, **9**, 2105-2116.

103. T. M. Schultheiss, J. B. Burch and A. B. Lassar, *Gene Dev*, 1997, **11**, 451-462.

104. S. Yuasa, Y. Itabashi, U. Koshimizu, T. Tanaka, K. Sugimura, M. Kinoshita, F. Hattori, S.-i. Fukami, T. Shimazaki, H. Okano, S. Ogawa and K. Fukuda, *Nat Biotech*, 2005, **23**, 607-611.

105. D. Hsu, A. Economides, X. Wang, P. Eimon and R. Harland, *Molecular Cell*, 1998, **1**, 673-683.

106. S. Piccolo, Y. Sasai, B. Lu and E. M. De Robertis, *Cell*, United States Editon, 1996, 86, 589-598.

107. P. B. Yu, C. C. Hong, C. Sachidanandan, J. L. Babitt, D. Y. Deng, S. A. Hoyng, H. Y. Lin, K. D. Bloch and R. T. Peterson, *Nat Chem Biol*, 2008, **4**, 33-41.

108. G. Zhou, R. Myers, Y. Li, Y. Chen, X. Shen, J. Fenyk-Melody, M. Wu, J. Ventre, T. Doebber, N. Fujii, N. Musi, M. F. Hirshman, L. J. Goodyear and D. E. Moller, *J Clin Invest*, 2001, **108**, 1167-1174.

109. W.-L. Yang, W. Perillo, D. Liou, P. Marambaud and P. Wang, *J Surg Oncol*, 2012, **106**, 680-688.

110. G. D. Cuny, P. B. Yu, J. K. Laha, X. Xing, J.-F. Liu, C. S. Lai, D. Y. Deng, C. Sachidanandan, K. D. Bloch and R. T. Peterson, *Bioorg Med Chem Lett*, 2008, **18**, 4388-4392.

111. J. H. Boergermann, J. Kopf, P. B. Yu and P. Knaus, *The Int J Biochem Cell Biol*, 2010, **42**, 1802-1807.

112. P. Yu, D. Deng, C. Lai, C. Hong, G. Cuny, M. Bouxsein, D. Hong, P. McManus, T. Katagiri, C. Sachidanandan, N. Kamiya, T. Fukuda, Y. Mishina, R. Peterson and K. Bloch, *Nat Med*, 2008, **14**, 1363-1369.
113. L. Zimmerman, J. DeJesusEscobar and R. Harland, *Cell*, 1996, **86**, 599-606.
114. C. L. Mummery, J. Zhang, E. S. Ng, D. A. Elliott, A. G. Elefanty and T. J. Kamp, *Circ Res*, 2012, **111**, 344-358.
115. C. Parng, W. Seng, C. Semino and P. McGrath, *Assay Drug Dev Technol*, 2002, **1**, 41-48.
116. D. P. Szeto and D. Kimelman, *Development*, 2004, **131**, 3751-3760.
117. F. Liu, M. Walmsley, A. Rodaway and R. Patient, *Curr Biol*, 2008, **18**, 1234-1240.
118. Q. Long, A. Meng, H. Wang, J. R. Jessen, M. J. Farrell and S. Lin, *Development*, 1997, **124**, 4105-4111.
119. E. M. Mandel, E. Kaltenbrun, T. E. Callis, X.-X. I. Zeng, S. R. Marques, D. Yelon, D.-Z. Wang and F. L. Conlon, *Development*, 2010, **137**, 1919-1929.
120. S. SchulteMerker, K. Lee, A. McMahon and M. Hammerschmidt, *Nature*, 1997, **387**, 862-863.
121. A. Russell, unpublished results
122. T. Kirsch, J. Nickel and W. Sebald, *EMBO J*, 2000, **19**, 3314-3324.
123. J. Nickel, M. K. Dreyer, T. Kirsch and W. Sebald, *J Bone Joint Surg Am*, 2001, **83-A Suppl 1**, S7-14.
124. http://www.eyesopen.com/rocs, *Openeye Scientific*.
125. R. Sheridan, G. McGaughey and W. Cornell, *J Comp Aided Mol Des*, 2008, **22**, 257-265.
126. T. S. Rush, J. A. Grant, L. Mosyak and A. Nicholls, *J Med Chem*, 2005, **48**, 1489-1495.
127. J. A. Grant, M. A. Gallardo and B. T. Pickup, *J Comp Chem*, 1996, **17**, 1653-1666.
128. W. Zhuang, N. Gathergood, R. G. Hazell and K. A. Jørgensen, *J Org Chem*, 2001, **66**, 1009-1013.
129. M. Abid and B. Török, *Tetrahedron: Asymmetry*, 2005, **16**, 1547-1555.
130. N. Kato and J. Jones, *Plant Dev Biol*, L. Hennig and C. Köhler, Humana Press Editon, 2010, **655**, 359-376.
131. O. Korchynskyi and P. ten Dijke, *J Biol Chem*, 2002, **277**, 4883-4891.
132. M. Furthauer, C. Thisse and B. Thisse, *Development*, 1997, **124**, 4253-4264.

133. S. A. Connors, J. Trout, M. Ekker and M. C. Mullins, *Development*, 1999, **126**, 3119-3130.

134. C. Brideau, B. Gunter, B. Pikounis and A. Liaw, *J Biomol Screening*, 2003, **8**, 634-647.

135. S.-i. Miura, Y. Kiya, H. Hanzawa, N. Nakao, M. Fujino, S. Imaizumi, Y. Matsuo, H. Yanagisawa, H. Koike, I. Komuro, S. S. Karnik and K. Saku, *PLoS ONE*, 2012, **7**, e37974.

136. M. Aghazadeh Tabrizi, P. G. Baraldi, G. Saponaro, A. R. Moorman, R. Romagnoli, D. Preti, S. Baraldi, C. Corciulo, F. Vincenzi, P. A. Borea and K. Varani, *J Med Chem*, 2013, **56**, 1098-1112.

137. E. S. H. El Ashry, E. S. Ramadan, H. M. A. Hamid and M. Hagar, *Synlett*, 2004, **2004**, 723,725.

138. V. J. Ram, *Arch Pharm*, 1980, **313**, 108-113.

139. J. Massagué, *Gene Dev*, 2003, **17**, 2993-2997.

140. M. P. de Caestecker, W. T. Parks, C. J. Frank, P. Castagnino, D. P. Bottaro, A. B. Roberts and R. J. Lechleider, *Gene Dev*, 1998, **12**, 1587-1592.

141. M. Buggisch, B. Ateghang, C. Ruhe, C. Strobel, S. Lange, M. Wartenberg and H. Sauer, *J Cell Sci*, 2007, **120**, 885-894.

142. H. Sauer, G. Rahimi, J. Hescheler and M. Wartenberg, *FEBS Lett*, 2000, **476**, 218-223.

143. A. Moustakas, *J Cell Sci*, 2002, **115**, 3355-3356.

144. K. Migita, K. Eguchi, Y. Kawabe, A. Mizokami, T. Tsakuda and S. Nagataki, *J Immunol*, 1994, **153**, 3457-3465.

145. A. Gazit, K. Yee, A. Uecker, F.-D. Böhmer, T. Sjöblom, A. Östman, J. Waltenberger, G. Golomb, S. Banai, M. C. Heinrich and A. Levitzki, *Bioorg Med Chem*, 2003, **11**, 2007-2018.

146. L. Ding, X. Liang and Y. Lou, *Acta Pharmacol Sin*, 2007, **28**, 634-642.

147. R. Schugar, P. Robbins and B. Deasy, *Gene Therapy*, 2008, **15**, 126-135.

148. D. Huangfu, R. Maehr, W. Guo, A. Eijkelenboom, M. Snitow, A. Chen and D. Melton, *Nat Biotechnol*, 2008, **26**, 795-797.

149. H. Sadek, B. Hannack, E. Choe, J. Wang, S. Latif, M. G. Garry, D. J. Garry, J. Longgood, D. E. Frantz, E. N. Olson, J. Hsieh and J. W. Schneider, *Proc Natl Acad Sci*, 2008, **105**, 6063-6068.

150. X. Wu, S. Ding, Q. Ding, N. S. Gray and P. G. Schultz, *J Am Chem Soc*, 2004, **126**, 1590-1591.
151. S. Chen, Q. Zhang, X. Wu, P. G. Schultz and S. Ding, *J Am Chem Soc*, 2003, **126**, 410-411.
152. K. Kirk, J. C. Ellory and J. D. Young, *J Biol Chem*, 1992, **267**, 23475-23478.
153. A. Sachinidis, S. Schwengberg, R. Hippler-Altenburg, D. Mariappan, N. Kamisetti, B. Seelig, A. Berkessel and J. Hescheler, *Cell Physiol Biochem*, 2006, **18**, 303-314.
154. I. Adcock and G. Caramori, *Immunol Cell Biol*, 2001, **79**, 376-384.
155. S. Flynn, R. Gristwood and D. Owen, *Brit J Pharmacol*, 1979, **65**, 127-137.
156. M. Cazzola and M. G. Matera, *Trends Pharmacol Sci*, 2000, **21**, 13-16.
157. F. H. Sarkar and Y. Li, *Mutat Res-Fund Mol M*, 2004, **555**, 53-64.
158. A. M. Wobus, G. Wallukat and J. Hescheler, *Differentiation*, 1991, **48**, 173-182.
159. D. Guo, I. J. Hildebrandt, R. M. Prins, H. Soto, M. M. Mazzotta, J. Dang, J. Czernin, J. Y. J. Shyy, A. D. Watson, M. Phelps, C. G. Radu, T. F. Cloughesy and P. S. Mischel, *Proc Natl Acad Sci*, 2009, **106**, 12932-12937.
160. J. M. Herbert, J. M. Augereau, J. Gleye and J. P. Maffrand, *Biochem Biophys Res Comm*, 1990, **172**, 993-999.
161. M. Kovács, J. Tóth, C. Hetényi, A. Málnási-Csizmadia and J. R. Sellers, *J Biol Chem*, 2004, **279**, 35557-35563.
162. P. A. Maher, *J Biol Chem*, 1993, **268**, 4244-4249.
163. N. Maeda, K. Kon, M. Sekiya and T. Shiga, *Biochem Pharmacol*, 1986, **35**, 625-629.
164. X. Wan, W. Zhang, L. Li, Y. Xie, W. Li and N. Huang, *J Med Chem*, 2013, **56**, 2619-2629.
165. J. C. Wong, R. Hong and S. L. Schreiber, *J Am Chem Soc*, 2003, **125**, 5586-5587.
166. L. Brault, C. Gasser, F. Bracher, K. Huber, S. Knapp and J. Schwaller, *Haematol-Hematol J*, 2010, **95**, 1004-1015.
167. A. Freitag, I. Wessler and K. Racké, *Eur J Pharmacol*, 1998, **354**, 67-71.
168. K. Gellynck, R. Shah, M. Parkar, A. Young, P. Buxton and P. Brett, *Bone*, 2013, **57**, 405-412.
169. D. Geiges, T. Meyer, B. Marte, M. Vanek, G. Weissgerber, S. Stabel, J. Pfeilschifter, D. Fabbro and A. Huwiler, *Biochem Pharmacol*, 1997, **53**, 865-875.
170. B. R. Stockwell, 2008, US2008/0299076 A1.

171. C. Yang, R. Madonna, Y. Li, Q. Zhang, W.-F. Shen, K. McNamara, Y.-J. Yang and Y.-J. Geng, *Vascular Pharmacology*, Online Nov, 2013

172. A. Endo, M. Kuroda and Y. Tsujita, *J Antibiot*, 1976 **29**, 1346-1348.

173. In-house research project led by post doc Dr. Alan Jones, Chemistry Department, Oxford.

174. J. M. Tinsley, R. J. Fairclough, R. Storer, F. J. Wilkes, A. C. Potter, S. E. Squire, D. S. Powell, A. Cozzoli, R. F. Capogrosso, A. Lambert, F. X. Wilson, S. P. Wren, A. De Luca and K. E. Davies, *PLoS ONE*, 2011, **6**, e19189.

175. H. F. Guo, H. Y. Shao, Z. Y. Yang, S. T. Xue, X. Li, Z. Y. Liu, X. B. He, J. D. Jiang, Y. Q. Zhang, S. Y. Si and Z. R. Li, *J Med Chem*, 2010, **53**, 1819-1829.

176. M. Quattrocelli, G. Palazzolo, I. Agnolin, S. Martino, M. Bouché, L. Anastasia and M. Sampaolesi, *J Cell Biochem*, 2011, **112**, 2006-2014.

177. R. P. Hebbel, G. M. Vercellotti, B. S. Pace, A. N. Solovey, R. Kollander, C. F. Abanonu, J. Nguyen, J. V. Vineyard, J. D. Belcher, F. Abdulla, S. Osifuye, J. W. Eaton, R. J. Kelm and A. Slungaard, *Blood*, 2010, **115**, 2483-2490.

178. M. Grunstein, *Nature*, 1997, **389**, 349-352.

179. S. Zhang, T. Fei, L. Zhang, R. Zhang, F. Chen, Y. Ning, Y. Han, X.-H. Feng, A. Meng and Y.-G. Chen, *Mol Cell Biol*, 2007, **27**, 4488-4499.

180. Testing carried out in collaboration with Dr Alexander Drakesmith at the John Radcliffe Hospital, Oxford.

181. S. A. Bustin, V. Benes, T. Nolan and M. W. Pfaffl, *J Mol Endocrinol*, 2005, **34**, 597-601.

182. Y. Gibert, V. J. Lattanzi, A. W. Zhen, L. Vedder, F. Brunet, S. A. Faasse, J. L. Babitt, H. Y. Lin, M. Hammerschmidt and P. G. Fraenkel, *PLoS ONE*, 2011, **6**, e14553.

183. T. Katagiri, M. Imada, T. Yanai, T. Suda, N. Takahashi and R. Kamijo, *Genes to Cells*, 2002, **7**, 949-960.

184. In collaboration with Dr Carole Bataille, Chemistry Department, Oxford.

185. T. Suzuki, T. Ando, K. Tsuchiya, N. Fukazawa, A. Saito, Y. Mariko, T. Yamashita and O. Nakanishi, *J Med Chem*, 1999, **42**, 3001-3003.

186. J. Y. Qin, L. Zhang, K. L. Clift, I. Hulur, A. P. Xiang, B. Z. Ren and B. T. Lahn, *PLoS One*, 2010, **5**, e10611.

187. S. Ehnert, J. Zhao, S. Pscherer, T. Freude, S. Dooley, A. Kolk, U. Stöckle, A. Nussler and R. Hube, *BMC Med*, 2012, **10**, 1-11.

188. H. Kang, J. Louie, A. Weisman, J. Sheu-Gruttadauria, B. N. Davis-Dusenbery, G. Lagna and A. Hata, *J Biol Chem*, 2012, **287**, 38656-38664.

189. C. Scholl, K. Weibetamuller, P. Holenya, M. Shaked-Rabi, K. Tucker and S. Wolfl, *BMC Genomics*, 2012, **13**, 298.

190. M. Shakèd, K. Weissmüller, H. Svoboda, P. Hortschansky, N. Nishino, S. Wölfl and K. L. Tucker, *PLoS ONE*, 2008, **3**, e2668.

191. M. S. Finnin, J. R. Donigian, A. Cohen, V. M. Richon, R. A. Rifkind, P. A. Marks, R. Breslow and N. P. Pavletich, *Nature*, 1999, **401**, 188-193.

192. A. Xie, B. Li, C. Liao, Z. Li, X. Lu, L. Shi and J. Zhou, *Acta Phys Chim Sin*, 2004, **20**, 569-572.

193. Q. C. Ryan, D. Headlee, M. Acharya, A. Sparreboom, J. B. Trepel, J. Ye, W. D. Figg, K. Hwang, E. J. Chung, A. Murgo, G. Melillo, Y. Elsayed, M. Monga, M. Kalnitskiy, J. Zwiebel and E. A. Sausville, *J Clin Oncol*, 2005, **23**, 3912-3922.

194. K. Mackie, *Annu Rev Pharmacol Toxicol*, 2006, **46**, 101-122.

195. R. G. Pertwee, *Br J Pharmacol*, 2009, **156**, 397-411.

196. J. Varani and P. A. Ward, *Shock*, 1994, **2**, 311-312.

197. L. Arnold, A. Henry, F. Poron, Y. Baba-Amer, N. van Rooijen, A. Plonquet, R. K. Gherardi and B. Chazaud, *J Exp Med*, 2007, **204**, 1057-1069.

198. C. Sunderkötter, T. Nikolic, M. J. Dillon, N. van Rooijen, M. Stehling, D. A. Drevets and P. J. M. Leenen, *J Immunol*, 2004, **172**, 4410-4417.

199. F. Geissmann, S. Jung and D. R. Littman, *Immunity*, 2003, **19**, 71-82.

200. F. K. Swirski, M. Nahrendorf, M. Etzrodt, M. Wildgruber, V. Cortez-Retamozo, P. Panizzi, J.-L. Figueiredo, R. H. Kohler, A. Chudnovskiy, P. Waterman, E. Aikawa, T. R. Mempel, P. Libby, R. Weissleder and M. J. Pittet, *Science*, 2009, **325**, 612-616.

201. P. Libby, P. M. Ridker and A. Maseri, *Circulation*, 2002, **105**, 1135-1143.

202. J. Regnstrom, J. Nilsson, P. Tornvall, A. Hamsten and C. Landou, *The Lancet*, 1992, **339**, 1183-1186.

203. R. Klingenberg and G. K. Hansson, *Eur Heart J*, 2009, **30**, 2838-2844.

204. C. Weber, A. Zernecke and P. Libby, *Nat Rev Immunol*, 2008, **8**, 802-815.

205. C. Auffray, M. H. Sieweke and F. Geissmann, *Annu Rev Immunol*, 2009, **27**, 669-692.

206. R. Ylitalo, O. Oksala, S. Yla-Herttuala and P. Ylitalo, *J Lab Clin Med*, 1994, **123**, 769-776.

207. P. Libby, *Nature*, 2002, **420**, 868-874.

208. M. Writing Group, V. L. Roger, A. S. Go, D. M. Lloyd-Jones, E. J. Benjamin, J. D. Berry, W. B. Borden, D. M. Bravata, S. Dai, E. S. Ford, C. S. Fox, H. J. Fullerton, C. Gillespie, S. M. Hailpern, J. A. Heit, V. J. Howard, B. M. Kissela, S. J. Kittner, D. T. Lackland, J. H. Lichtman, L. D. Lisabeth, D. M. Makuc, G. M. Marcus, A. Marelli, D. B. Matchar, C. S. Moy, D. Mozaffarian, M. E. Mussolino, G. Nichol, N. P. Paynter, E. Z. Soliman, P. D. Sorlie, N. Sotoodehnia, T. N. Turan, S. S. Virani, N. D. Wong, D. Woo and M. B. Turner, *Circulation*, 2012, **125**, e2-e220.

209. L. S. Whyte, L. Ford, S. A. Ridge, G. A. Cameron, M. J. Rogers and R. A. Ross, *Brit J Pharmacol*, 2012, **165**, 2584-2597.

210. T. W. Klein and *et. al.*, *J Leukoc Biol*, 2003, **74**, 486-496.

211. I. X. Zhu and *et. al.*, *J Immunol*, 2000, **165**, 373-380.

212. S. Steffens, N. R. Veillard, C. Arnaud, G. Pelli, F. Burger, C. Staub, M. Karsak, A. Zimmer, J. L. Frossard and F. Mach, *Nature*, 2005, **434**, 782-786.

213. M. Rinaldi-Carmona, F. Barth, J. Millan, J.-M. Derocq, P. Casellas, C. Congy, D. Oustric, M. Sarran, M. Bouaboula, B. Calandra, M. Portier, D. Shire, J.-C. Brelière and G. L. Fur, *J Pharmacol Exp Ther*, 1998, **284**, 644-650.

214. M. Gallant, C. Dufresne, Y. Gareau, D. Guay, Y. Leblanc, P. Prasit, C. Rochette, N. Sawyer, D. M. Slipetz, N. Tremblay, K. M. Metters and M. Labelle, *Bioorg Med Chem Lett*, 1996, **6**, 2263-2268.

215. M. Rinaldi-Carmona, F. Barth, M. Heaulme, D. Shire, B. Calandra and e. al, *FEBS Lett*, 1994, **350**, 240-244.

216. A. S. Plump and J. L. Breslow, *Annu Rev Nutr*, 1995, **15**, 495-518.

217. E. J. Schaefer, R. E. Gregg, G. Ghiselli, T. M. Forte, J. M. Ordovas, L. A. Zech and H. B. Brewer, *J Clin Invest*, 1986, **78**, 1206-1219.

218. W. A. Devane, F. A. Dysarz, M. R. Johnson, L. S. Melvin and A. C. Howlett, *Mol Pharmacol*, 1988, **34**, 605-613.

219. L. A. Matsuda, S. J. Lolait, M. J. Brownstein, A. C. Young and T. I. Bonner, *Nature*, 1990, **346**, 561-564.

220. S. Munro, K. L. Thomas and M. Abushaar, *Nature*, 1993, **365**, 61-65.

221. N. M. Clayton, C. T. O'Shaughnessy, F. Marshall and C. Bountra, *Brit J Pharmacol*, 2001, **134**.

222. A. C. Howlett, F. Barth, T. I. Bonner, G. Cabral, P. Casellas, W. A. Devane, C. C. Felder, M. Herkenham, K. Mackie, B. R. Martin, R. Mechoulam and R. G. Pertwee, *Pharmacol Rev*, 2002, **54**, 161-202.

223. H. P. Rang and M. Dale, *Churchill Livingstone*, 2007, 216.

224. R. Condie, H. , A., W. S. Koh, M. Lee and N. E. Kaminski, *J Biol Chem Sci*, 1996, **271**, 13175-13183.

225. S. D. McAllister and M. Glass, *Prostag Leukotr Ess*, 2002, **66**, 161-171.

226. R. Mechoulam and L. Hanus, *Chem Phys Lipids*, 2002, **121**, 35-43.

227. A. R. Schatz, M. Lee, R. B. Condie, J. T. Pulaski and N. E. Kaminski, *Toxicol Appl Pharmacol*, 1997, **142**, 278-287.

228. W. A. Devane, L. Hanus, A. Breuer, R. G. Pertwee, L. A. Stevenson and *et. al*., *Science*, 1992, **258**, 1946-1949.

229. R. Mechoulam, S. Ben-Shabat, L. Hanus, M. Ligumsky, N. E. Kaminski and *et. al*., *Biochem Pharmacol*, 1995, **50**, 83-90.

230. T. Sugiura, S. Kondo, A. Sukagawa, S. Nakane, A. Shinoda and *et. al.*, *Biochem Bioph Res Co*, 1995, **215**, 89-97.

231. T. Sugiura, S. Kondo, S. Kishimoto, T. Miyashita, S. Nakane, T. Kodaka, Y. Suhara, H. Takayama and K. Waku, *J Biol Chem*, 2000, **275**, 605-612.

232. M. J. McFarland and E. L. Barker, *Anandamide Transportation Pharmacology Therapy*, 2004, **104**, 117-135.

233. V. Di Marzo and S. Petrosino, *Curr Opin Lipodol*, 2007, **18**.

234. Y. Gaoni and R. Mechoulam, *J Am Chem Soc*, 1964, **86**, 1646-1647.

235. P. F. Smith and G.-G. Pharmaceuticals., *Curr Opin Investig Drugs*, 2004, **5**, 748-754.

236. J. S. Berman, C. Symonds and R. Birch, *Pain* 2004, **112**, 299.

237. D. T. Wade, P. Makela, P. Robson, H. House and C. Bateman, *Mult Scler*, 2004, **10**, 434–441.

238. A. Weissman, G. M. Milne and L. S. Melvin, *J Pharmacol Exp Ther*, 1982, **223**, 516-423.

239. L. S. Melvin, G. M. Milne, M. R. Johnson, B. Subramaniam, G. H. Wilken and A. C. Howlett, *Mol Pharmacol*, 1993, **44**, 1008-1015.

240. C. C. Felder, K. E. Joyce, E. M. Briley, J. Mansouri, K. Mackie, O. Blond, Y. Lai, A. L. Ma and R. L. Mitchell, *Mol Pharmacol*, 1995, **48**, 443-450.

241. A. Dyson, M. Peacock, A. Chen, J.-P. Courade, M. Yaqoob, A. Groarke, C. Brain, Y. Loong and A. Fox, *Pain*, 2005, **116**, 129-137.

242. R. Mechoulam, D. Panikashvii and E. Shohami, *Trends in Molecular Medicine*, 2002, **8**, 58-61.

243. J. Liu, H. Li, S. H. Burstein, R. B. Zurier and J. D. Chen, *Mol Pharmacol*, 2003, **63**, 983-992.

244. R. W. Foltin, M. W. Fischman and M. F. Byrne, *Appetite*, 1988, **11**, 1-14.

245. M. Rinaldi-Carmona, F. Barth, M. Héaulme, D. Shire, B. Calandra, C. Congy, S. Martinez, J. Maruani, G. Néliat, D. Caput, P. Ferrara, P. Soubrié, J. C. Brelière and G. Le Fur, *FEBS Lett*, 1994, **350**, 240-244.

246. G. G. Muccioli and D. M. Lambert, *Curr Med Chem*, 2005, **12**, 1361-1394.

247. S. R. Donohue, C. Halldin and V. W. Pike, *Bioorg Med Chem*, 2006, **14**, 3712–3720.

248. J. H. M. Lange and C. G. Kruse, *Drug Discovery Today*, 2005, **10**, 693-702.

249. R. Lan, Q. Liu, P. Fan, S. Lin, S. R. Fernando, D. McCallion, R. Pertwee and A. Makriyannis, *J Med Chem*, 1999, **42**, 769-776.

250. D. R. Haubrich, S. J. Ward, E. Baizman, M. R. Bell, J. Bradford, R. Ferrari, M. Miller, M. Perrone, A. K. Pierson and J. K. Saelens, *J Pharmacol Exp Ther*, 1990, **255**, 511-522.

251. D. R. Compton, L. H. Gold, S. J. Ward, R. L. Balster and B. R. Martin, *J Pharmacol Exp Ther*, 1992, **263**, 1118-1126.

252. M. Rinaldi-Carmona, F. Barth, M. Heaulme, D. Shire, B. Calandra and *et. al*., *FEBS Lett*, 1994, **350**, 240-244.

253. J.-M. Mussinu, S. Ruiu, A. C. Mulè, A. Pau, M. A. M. Carai, G. Loriga, G. Murineddu and G. A. Pinna, *Bioorg Med Chem*, 2003, **11**, 251-263.

254. R. A. Ross, H. C. Brockie, L. A. Stevenson, V. L. Murphy, F. Templeton, A. Makriyannis and R. G. Pertwee, *Brit J Pharmacol*, 1999, **126** 665-667.

255. Y. Gareau, C. Dufresne, M. Gallant, C. Rochette, N. Sawyer, D. M. Slipetz, N. Tremblay, P. K. Weech, K. M. Metters and M. Labelle, *Bioorg Med Chem Lett*, 1996, **5**, 189-194.

256. J. W. Huffman, S. Yu, V. Showalter, M. E. Abood, J. L. Wiley, D. R. Compton, B. R. Martin, R. D. Bramblett and P. H. Reggio, *J Med Chem*, 1996, **39**, 3875-3877.

257. A. Makriyannis and A. Khanolkar, *PCT Int Appl*, 2001, 33

258. L. Hanus and *et. al*., *Proc Natl Acad Sci U.S.A.*, 1999, **96** 14228-14233.

259. T. Ostenfeld, J. Price, M. Albanese, J. Bullman, F. Guillard, I. Meyer and *et. al.*, *Clin J Pain*, 2011, **27**, 668-676.
260. L. Di and E. H. Kerns, *Curr Opin Chem Biol*, 2003, **7**, 402-408.
261. R. Didziapetris, P. Japertas, A. Avdeef and A. Petrauskas, *J Drug Targeting*, 2003, **11**, 391-406.
262. M. Mahmoudian, *Journal of Molecular Graphics and Modelling*, 1997, **15**, 149-153.
263. X. Xie, J. Chen and E. Billings, *Proteins*, 2003, **53**, 307-319.
264. P. Markt, C. Feldmann, J. M. Rollinger, S. Raduner, D. Schuster, J. Kirchmair, S. Distinto, G. M. Spitzer, G. Wolber, C. Laggner, K.-H. Altmann, T. Langer and J. r. Gertsch, *J Med Chem*, 2008, **52**, 369-378.
265. N. Foloppe, N. Allen, C. Bentley, T. Brooks, G. Kennett, A. Knight, S. Leonardi, A. Misra, N. Monck and D. Sellwood, *Bioorg Med Chem Lett*, 2008, **18**, 1199-1206.
266. N. Foloppe, K. Benwell, T. D. Brooks, G. Kennett, A. R. Knight, A. Misra and N. J. T. Monck, *Bioorg Med Chem Lett*, 2009, **19**, 4183-4190.
267. M. Beltramo, N. Bernardini, R. Bertorelli, M. Campanella, E. Nicolussi, S. Fredduzzi and A. Reggiani, *Eur J Neuroscience*, 2006, **23**, 1530-1538.
268. L. Hanus and e. al, *Proc Natl Acad Sci U.S.A.*, 1999, **96**, 14228-14233.
269. http://www.eyesopen.com/omega, *Openeye Scientific*.
270. Testing carried out in collaboration with Prof Greaves labat the Sir William Dunn School of Pathology, Oxford.
271. http://www.discoverx.com/target-data-sheets/gpcr/cnr2.
272. A. B. Tomchin, O. Y. Uryupov, T. I. Zhukova, T. A. Kuznetsova, M. V. Kostycheva and A. V. Smirnov, *Pharmacol Chem J*, 1997, **31**, 125-133.
273. C. A. Hunter, *Angew Chem Int Ed*, 2004, **43**, 5310-5324.
274. V. J. Ram, *Arch Pharm*, 1980, **313**, 108-113.
275. M. Rinaldi-Carmona, B. Calandra, D. Shire, M. Bouaboula, D. Oustric, F. Barth, P. Casellas, P. Ferrara and G. Le Fur, *J Pharmacol Exp Ther*, 1996, **278**, 871-878.
276. S. Munro, K. L. Thomas and M. Abu-Shaar, *Nature*, 1993, **365**, 61-65.
277. Synthesis carried out in collaboration with an undergraduate student, Rebecca Cross, Chemistry Departmenr, Oxford.
278. G. A. Molander and D. L. Sandrock, *Curr Opin Drug Discov Devel*, 2009, **12** (6), 811-823.

279. M. Butters, J. N. Harvey, J. Jover, A. J. J. Lennox, G. C. Lloyd-Jones and P. M. Murray, *Angew Chem Int Ed*, 2010, **49**, 5156-5160.
280. G. A. Molander and B. Canturk, *Angew Chem*, 2009, **121**, 9404-9425.
281. Y. Miyauchi, S. Watanabe, H. Kuniyasu and H. Kurosawa, *Organometallics*, 1995, **14**, 5450-5453.
282. Q. Zhao, C. Li, C. H. Senanayake and W. Tang, *Chem-Eur J*, 2013, **19**, 2261-2265.
283. CambridgeSoft, 2010.
284. C. Abad-Zapatero and J. T. Metz, *Drug Discovery Today*, 2005, **10**, 464-469.
285. T. Ryckmans, M. P. Edwards, V. A. Horne, A. M. Correia, D. R. Owen, L. R. Thompson, I. Tran, M. F. Tutt and T. Young, *Bioorg Med Chem Lett*, 2009, **19**, 4406-4409.
286. Cyprotex, http://www.cyprotex.com/admepk/physicochemical-properties/turbidimetric-solubility/.
287. Y. Hajbi, F. Suzenet, M. Khouili, S. Lazar and G. Guillaumet, *Tetrahedron*, 2007, **63**, 8286-8297.
288. F. Desmoulin, V. Gilard, M. Malet-Martino and R. Martino, *Drug Metab Dispos*, 2002, **30**, 1221-1229.
289. G. B. Elion, *J Med Virol*, 1993, **41**, 2-6.
290. Cyprotex, http://www.cyprotex.com/admepk/in-vitro-metabolism/microsomal-stability/.
291. J. McLure, J. Miners and D. Birkett, *Brit J Clin Pharmaco*, 2000, **49**, 453-461.
292. Cyprotex, *Table 1,Classification of brain uptake using Cyprotex's MDR1-MDCK Permeability*, http://www.cyprotex.com/admepk/in-vitro-permeability/mdr1-mdck-permeability/.
293. E. Callegari, B. Malhotra, P. J. Bungay, R. Webster, K. S. Fenner, S. Kempshall, J. L. LaPerle, M. C. Michel and G. G. Kay, *Brit J Clin Pharmaco*, 2011, **72**, 235-246.
294. Testing carried out in collaboration with Prof Greaves lab at the Sir William Dunn School of Pathology, Oxford.
295. H. Xu, C. L. Cheng, M. Chen, A. Manivannan, L. Cabay, R. G. Pertwee, A. Coutts and J. V. Forrester, *J Leukocyte Biol*, 2007, **82**, 532-541.
296. M. C. Martellotta, G. Cossu, L. Fattore, G. L. Gessa and W. Fratta, *Neuroscience*, 1998, **85**, 327-330.
297. K. Laine, K. Järvinen and T. Järvinen, *Life Sciences*, 2003, **72**, 837-842.

298. Q. Zhang, P. Ma, M. Iszard, R. B. Cole, W. Wang and G. Wang, *Drug Metab Dispos*, 2002, **30**, 1077-1086.
299. A. Oussaid, F. Benyaqad, B. Oussaid and B. Garrigues, *Phosphorus, Sulfur, and Silicon and the Related Elements*, 2003, **178**, 1605-1616.
300. G. Németh, É. Rákoczy and G. Simig, *J Fluorine Chem*, 1996, **76**, 91-93.
301. P. He, Y. Lu, C.-G. Dong and Q.-S. Hu, *Org Lett*, 2006, **9**, 343-346.
302. F. Leonard and I. Ehrenthal, *J Am Chem Soc*, 1951, **73**, 2216-2218.
303. S. Miyamura, T. Satoh and M. Miura, *J Org Chem*, 2007, **72**, 2255-2257.
304. WO2006/117754, 2006.
305. B.-X. Tang, R.-J. Song, C.-Y. Wu, Y. Liu, M.-B. Zhou, W.-T. Wei, G.-B. Deng, D.-L. Yin and J.-H. Li, *J Am Chem Soc*, 2010, **132**, 8900-8902.
306. J. M. Z. Gladych, R. C. Stewart, Stanfiel.Fj, J. J. Boyle, R. Hornby, R. F. Haff, R. J. Ferlauto, D. Jack, J. H. Hunt and C. G. Kormendy, *J Med Chem*, 1972, **15**, 277-&.
307. S. M. Shelke and S. H. Bhosale, *Bioorg Med Chem Lett*, 2010, **20**, 4661-4664.
308. A. González, J. Quirante, J. Nieto, M. R. Almeida, M. J. Saraiva, A. Planas, G. Arsequell and G. Valencia, *Bioorg Med Chem Lett*, 2009, **19**, 5270-5273.
309. J. S. Yadav, B. V. S. Reddy, C. S. Reddy and A. D. Krishna, *Synthesis*, 2007, **2007**, 693,696.
310. L. Gupta, N. Sunduru, A. Verma, S. Srivastava, S. Gupta, N. Goyal and P. M. S. Chauhan, *European J Med Chem*, 2010, **45**, 2359-2365.
311. A. K. Singh, *Spectrochim Acta A Mol Biomol Spectrosc*, 2012, **85** (1), 1-6.
312. A. Monge, J. Palop, C. Ramirez, M. Font and E. Fernandez-Alvarez, *Eur J Med Chem*, 1991, **26**, 179-188.
313. W. Yao, L. Pan, Y. Zhang, G. Wang, X. Wang and C. Ma, *Angew Chem Int Ed*, 2010, **49**, 9210-9214.
314. L. C. March, G. S. Bajwa, J. Lee, K. Wasti and M. M. Joullie, *J Med Chem*, 1976, **19**, 845-848.
315. E. C. Taylor and J. E. Macor, *Tetrahedron Lett*, 1986, **27**, 431-432.
316. Invitrogen, http://tools.invitrogen.com/content/sfs/manuals/lrclonaseplus_man.pdf.
317. A. Loening, T. Fenn, A. Wu and S. Gambhir, *Protein Engineering Design & Selection*, 2006, **19**, 391-400.
318. Promega Corporation, http://www.promega.co.uk/~/media/Files/Resources/ProtCards/FuGENE%20HD%20Transfection%20Reagent%20Quick%20Protocol.pdf.

319. B. Herrera and G. Inman, *BMC Cell Biol*, 2009, **10**.

320. D. Logeart-Avramoglou, M. Bourguignon, K. Oudina, P. Ten Dijke and H. Petite, *Anal Biochem*, 2006, **349**, 78-86.

321. DiscoveRx Coorporation, http://www.discoverx.com/target-data-sheets/gpcr/cnr2.

322. CEREP http://www.cerep.fr/cerep/users/pages/catalog/Affiche_CondExp_Test.asp?test=36.

323. CEREP http://www.cerep.fr/cerep/users/pages/catalog/Affiche_CondExp_Test.asp?test=37.

324. K. Monzen, R. Nagai, I. Komuro, *Trends Cardiovasc Med*, 2002, **12**, 263-269

325. K. Monzen, Y. Hiroi, S. Kudoh, H. Akatawa, T. Oka, E. Takimoto, D. Hayashi, T. Hosoda, M. Kawabata, K., Miyazono, S. Ishii *et al*, *J Cell Biol*, 2001, **153**, 687-698